APAT
Agenzia per la Protezione dell'Ambiente e per i Servizi Tecnici
DIPARTIMENTO DIFESA DEL SUOLO
Servizio Geologico d'Italia
Organo Cartografico dello Stato (legge n. 68 del 2.2.1960)

MEMORIE
DESCRITTIVE DELLA
CARTA GEOLOGICA D'ITALIA
VOLUME LXIV

From seafloor to deep mantle: architecture of the Tyrrhenian backarc basin

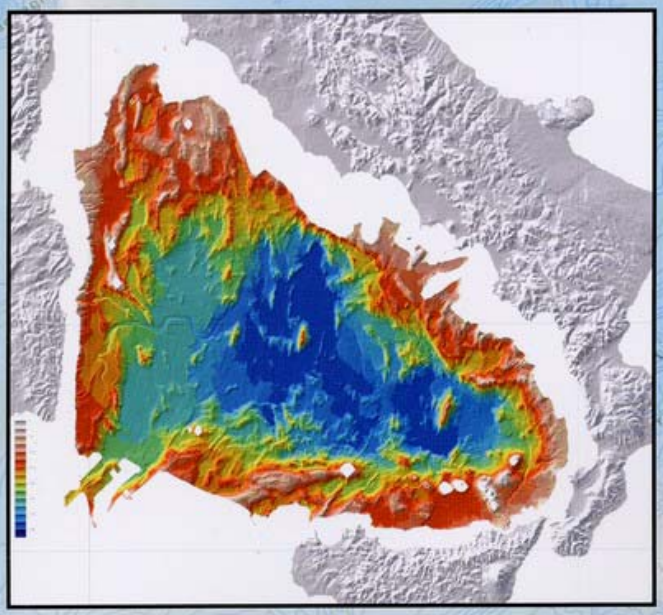

Editors
MARANI M. P.
GAMBERI F.
BONATTI E.

INDEX
INDICE

N. 4 PLATES in back pocket
N. 4 TAVOLE in tasca di copertina

In ricordo di

Luciano CASONI
Maurizio MENGOLI
Renzo SARTORI

APAT

Agenzia per la Protezione dell'Ambiente e per i Servizi Tecnici

DIPARTIMENTO DIFESA DEL SUOLO

Servizio Geologico d'Italia

Organo Cartografico dello Stato (Legge n°. 68 del 2-2-1960)

MEMORIE

DESCRITTIVE DELLA

CARTA GEOLOGICA D'ITALIA

VOLUME LXIV

FROM SEAFLOOR TO DEEP MANTLE: ARCHITECTURE OF THE TYRRHENIAN BACKARC BASIN

Dal fondale marino al mantello profondo:architettura del bacino Tirrenico

Authors

AOUDIA A., BERANZOLI L., CIMINI G.B., DE LORENZO S., DOGLIONI C., FACCENNA C., FAVALI P., FUNICIELLO F., FUNICIELLO R., GAMBERI F., GIARDINI D., INNOCENTI F., MARAMAI A., MARANI M. P., MONGELLI F., MORELLATO C., PANZA G. F., PECCERILLO A., PIROMALLO C.,PONTEVIVO A., PROCACCIANTI D., ROSSI P. L., ROSSETTI F., SARAÒ A., SCROCCA D., SERRI G., TRUA T., ZITO G.

Editors

Michael P. MARANI, Fabiano GAMBERI, Enrico BONATTI

SYSTEMCART

Roma - 2004

Direttore responsabile: **Leonello SERVA**

REDAZIONE a cura del Servizio Cartografico, Relazioni e Documentazione di Base
Dirigente: Normanno ACCARDI
Capo Settore: Domenico TACCHIA
Coordinatore Editoria: Marina COSCI
Coordinamento cartografico - editoriale: Marina COSCI, Maria Luisa VATOVEC
Allestimento testi: Alessia MARINELLI
Collaboratori: Mauro ROMA, Renato VENTURA

ROMA-2004

DIPARTIMENTO DIFESA DEL SUOLO
Servizio Geologico D'Italia

ISMAR
Sezione di Geologia Marina

Progetto CARG

Direttore del Dipartimento Difesa del Suolo: L. SERVA
Responsabile del Progetto GARG: F. GALLUZZO
Funzionario Delegato: P. MANETTI
Revisione Scientifica: S. D'ANGELO, V.EULILLI, F. FERRI
Coordinamento cartografico: D. TACCHIA, R. VENTURA
Coordinamento Editoriale e allestimento per la stampa: M. COSCI , M.L. VATOVEC
Gestione tecnico-amministrativa: M.T. LETTIERI

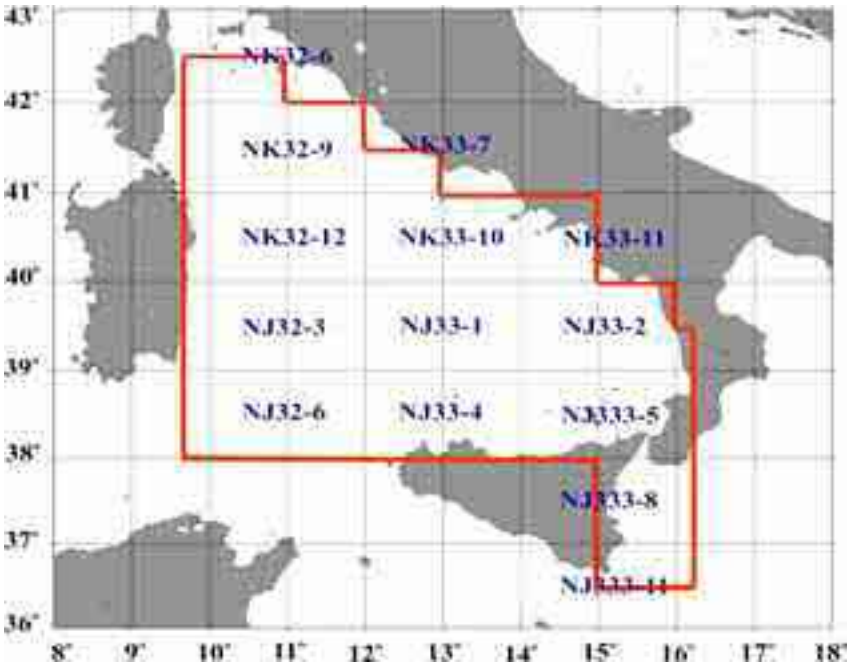

Scientific Comittee

A. FABBRI, F. INNOCENTI, P. MANETTI & R. SARTORI†

PRESENTATION

The official Italian geological mapping project (CARG), at scale 1:50000, promoted the importance of marine geology research in the knowledge of the complex geological structure of Italy.

The vast amount of data collected with the most modern technologies in the Tyrrhenian basin has been, in fact, very important to reconstruct the environmental and geodynamic evolution of the Italian peninsula. In particular the morpho-bathymetric, gravimetric and magnetometric data that resulted from the Tyrrhenian Project, provided the basis for a series of structural, volcanological and palaeo-climatologic studies.

Important achievements are, for example, the localization and the boundaries of the oceanic structures in the basin and in the surrounding areas, an accurate spotting of volcanic emission centres, a detailed map of the sediment entrainment toward the inner areas, the recognition of the gravitation instability zones.

All these data are important for the scientific community, but also for the Institutes, either public or not, surrounding the Tyrrhenian sea. This is why the Italian Geological Survey (now Land Resources and Soil Protection Department of the Italian Agency for the Protection of the Environment and Techinical Services, APAT) co-financed this project and is now publishing the results.

Il progetto di cartografia geologica di base (CARG) ha, fin dall'inizio, messo in luce quanto la conoscenza dettagliata della geologia dei mari italiani sia uno strumento fondamentale per la comprensione della complessa struttura geologica del Paese e, conseguentemente, per la valutazione del rischio geologico, vulcanico e sismico.

Per questo motivo, oltre a quanto previsto dal CARG, si è ritenuto importante acquisire con tecnologie moderne un complesso di dati di estremo dettaglio nel Bacino Tirrenico, strettamente legato all'evoluzione geodinamica della nostra penisola.

Il rilievo morfobatimetrico ad alta risoluzione, insieme ai dati gravimetrici e magnetometrici raccolti per il "Progetto Tirreno", ha dato il via ad una serie di studi di geologia strutturale, vulcanologia e paleoclimatologia che hanno visto convergere le conoscenze scientifiche della comunità internazionale.

La posizione e i limiti delle strutture oceaniche del bacino e delle zone circostanti, lo studio delle strutture tettoniche, la localizzazione dettagliata di centri di emissione lavica, la rappresentazione particolareggiata delle vie di trasporto sedimentarie verso le zone interne del bacino, il riconoscimento delle aree di instabilità gravitativa, sono informazioni di estrema importanza non solo per la comunità scientifica, ma anche per le altre Istituzioni, pubbliche o no, che con il Tirreno hanno a che fare.

Per tutti questi motivi il Servizio Geologico Nazionale (ora confluito nel Dipartimento Difesa del Suolo dell'APAT) ha co-finanziato il progetto e si è fatto carico della pubblicazione dei risultati.

Leonello SERVA

PREFACE
The Tyrrhenian Project

It gives me great pleasure to present this volume dedicated to the Tyrrhenian Sea, containing the results of years of scientific research on our small Mediterranean "ocean"; many of its secrets are finally revealed to us, starting with its morphology.

In 1996, Professor Enrico BONATTI, *director of the CNR Institute for Marine Geology (IGM), submitted a proposal to the CNR Committee for Geological and Mineral Resources for a study of the Tyrrhenian Sea; one of the objectives of this research proposal was the compilation of a morpho-bathymetric chart of the Tyrrhenian sea.*

I can remember his presentation of the project and his description of the results he expected to achieve by adopting a multi-beam. Even then, and things have not improved since, it was extremely difficult to obtain funds for such a complex and ambitious project. The Committee reported back to CNR recommending that the project should be included among the CNR "Strategic Projects", which meant that it would be allotted funds for a two-years period of research. This would suffice to cover part of the cost of chartering the ship fitted with the multi-beam, mission expenses, and the cost of analysing and processing the data. It was, however, a start, and allowed Bonatti to launch his project and begin the work.

Finding the financial resources to continue the project was just as difficult. Part of the money was taken from the yearly budget of the IGM, but a large injection of funds was to come from a research agreement between CNR and the National Technical Services – Geological Survey of Italy, thanks to the strong support given to the project by the Under-.Secretary for Civil Defence at that time, Professor Franco BARBERI, *who firmly believed that the "Tyrrhenian Project" would produce information of immense benefit to geological risk surveillance, especially as regards seismic and volcanic hazards. Additionally funding came from the Volcanology Group of Italy (GNV), whose activity includes the study of seismic and volcanic risks.*

As President of the Committee for Geological and Mineral Sciences, I signed the research agreement on behalf of CNR in 1998. I will spare you the details of the administrative and practical difficulties involved in implementing such an agreement, which included chartering a ship form the Russian Academy of Sciences. I would like to thank the director of the Geological Survey of Italy at that time, Andrea TODISCO, *his deputy-directors* Fernando PETRONE *and* Norman ACCARDI, *and the CARG project leader,* Fabrizio GALLUZZO, *whose support was instrumental in stipulating the agreement between CNR and the Geolgical Survey; but who also provided valuable assistance in solving problems that arose frequently during the research work. We are similarly indebted to* Pasquale SIDARI, Alessandro VOLPE *and* Maria Teresa LETTIERI, *for their help in overcoming the problems of a day-to-day nature, which were of no les importance to the success of the project. It is thanks to them what we were able to complete all the activities scheduled in the agreement.*

From the moment in which Enrico BONATTI *first illustrated his project, throughout the research activity and on to the final printing of this volume, many changes were to take place in our scientific community. The research institutions and universities have been repeatedly restructured and reorganised. The re-structuring of CNR that ensued from Act 19 to 30 January 1999 has been superseded by a new re-organisation dictated by legislation of 3 February 2003; similarly, the Geological Survey of Italy has now become an integral part of the Territorial Protection Department of the Agency for the Environmental and Technical Services (APAT).*

Despite such alarming and erratic background conditions, the researchers continued to work with the same dedication and enthusiasm, as demonstrated by the excellent results contained in this splendid edition of the Memorie descrittive della Carta Geologica d'Italia. This publication will become a major reference volume for scholar of the geology of Italy and the Mediterranean for many years to come.

Progetto Tirreno

Il Tirreno, questo piccolo "oceano" mediterraneo, ha finalmente un volume nel quale, dopo anni di ricerche, sono stati raccolti I dati scientifici che svelano molti dei suoi segreti a cominciare dalla sua morfologia.

Nel 1996 il Prof. Enrico BONATTI, direttore dell'Istituto di Geologia Marina (IGM) del CNR, sottopose al Comitato per le Scienze Geologiche e Minerarie del CNR un progetto riguardante lo studio del mar Tirreno che, tra gli altri obiettivi, proponeva l'elaborazione di una carta morfobatimetrica dei finali marini.

Ricordo la presentazione del progetto e l'illustrazione di quello che si poteva ottenere attraverso l'utilizzazione di un multibeam. Anche allora, come ora, i fondi necessari per il finanziamento di un progetto così complesso e ambizioso erano pochi. Il Comitato propose al CNR di inserire tale ricerca nei "Progetti Strategici" ottenendo così un finanziamento biennale che copriva solo in parte le spese di noleggio di una nave attrezzata con il multibeam, le spese di missione e quelle per l'analisi ed il trattamento dei dati raccolti. Era comunque una base finanziaria che permise il decollo del progetto e l'inizio dell'attività.

Trovare le risorse mancanti non fu certo cosa semplice e facile. Una parte fu reperita dalla dotazione ordinaria aell'IGM e una parte consistente arrivò attraverso un accordo di programma tra il CNR ed i Servizi Tecnici Nazionali – Servizio Geologico Nazionale e fortemente sostenuto dall'allora sottosegretario della Protezione Civile con delega per i Servizi Tecnici Nazionali, Pprof. Franco BARBERI che ritenne il "Progetto Tirreno" di grande interesse conoscitivo ai fini della prevenzione dei rischi geologici, soprattutto sismici e vulcanici. Inoltre il Gruppo Nazionale di Vulcanologia (GNV), la cui attività prevede lo studio di queste ultime tematiche, ha partecipato al progetto con un ulteriore contributo.

Il sottoscritto, quale Presidente del Comitato per le Scienze Geologiche e Minerarie, fu nominato dal CNR Funzionario Delegato per la stipula dell'Accordo di Programma che fu firmato nel 1998.

Enumerare le molte difficoltà di gestione di un accordo di programma che prevedeva il noleggio di una nave dell'Accademia delle Scienze russa il rispetto di tutte le procedure burocratiche e le molte scadenze amministrative sarebbe troppo lungo.

Devo ringraziare l'allora Direttore del Servizio Geologico d'Italia, Andrea TODISCO, i Vicari F. PETRONE e N. ACCARDI ed il responsabile del progetto CARG, Fabrizio GALLUZZO, che oltre a favorire l'attuazione dell'accordo tra il CNR ed il Servizio Geologico Nazionale hanno dato il loro prezioso aiuto anche per risolvere i problemi che si presentavano durante lo svolgimento delle attività di ricerca.

Per la risoluzione dei problemi "giornalieri", ma non per questo meno importanti, hanno ampiamente contribuito Pasquale SIDARI, Alessando VOLPE e Maria Teresa LETTIERI che hanno permesso di portare a termine tutte le attività previste nell'accordo di programma.

Dalla presentazione del "Progetto Tirreno", all'inizio delle ricerche ed infine alla stampa del volume, molte cose sono cambiate nel mondo della ricerca. Si sono susseguiti con ritmo notevole i cambiamenti nell'organizzazione e nelle finalità degli Enti Ricerca e delle Università. Con il decreto legislativo n. 19 del 30 gennaio 1999 è stato riordinato il CNR che attualmente sta per subire una nuova riorganizzazione in base al Decreto legislativo del 3 febbraio 2003 mentre il Servizio Geologico Nazionale è entrato a far parte del Dipartimento per la Difesa del Suolo dell'Agenzia per l'Ambiente ed i Servizi Tecnici (APAT).

Anche in presenza di queste continue riorganizzazioni il lavoro dei ricercatori è continuato con impegno e dedizione come dimostrano gli ottimi risultati scientifici presentati in questo bellissimo volume delle Memorie Descrittive della Carta Geologica d'Italia che rimarranno a lungo come punto di riferimento per gli studiosi che si occupano della Geologia dell'Italia e del Mediterraneo.

Piero MANETTI

PREFACE

The Tyrrhenian: a Project of the Institute of Marine Geology (now ISMAR) of the CNR

The Tyrrhenian is a sea shrouded in myth, legend and history since the rime of the Homeric poems. For a modern Earth Scientist, the Tyrrhenian Sea is a beautiful example of a young marginal basin within a structurally very complex region of our Planet. The study of the geology of the Tyrrhenian has been as intellectual challenge taken up first, almost half a century ago, by people such as Aldo Segre and then Raimondo Selli and coworkers.

It became increasingly clear that knowledge of the geology of the Tyrrhenian Sea floor is essential to understand the evolution of the entire circumtyrrhenian region, including the Italian territory. This knowledge is important also to understand the distribution of seismicity and volcanism in our region, and to assess risks due do subaerial and submarine processes, such as landslides, tsunamis, etc.

Development of new technologies, such as multibeam acoustic bathymetry, made clear a few years ago that our knowledge of the Tyrrhenian sea floor could achieve a quantum-jump if these technologies could be applied. The Institute of ;Marine Geology (IGM) of the Italian National Research Council (Istituto di Geologia Marina del CNR) took the lead in pushing forward a project for multibeam swath-mapping of the entire Tyrrhenian sea floor. A major problem was that Italy, although notoriously a country not only of poets and saints, but also of navigators, lacked a modern research ship equipped with multibeam technologies. We bypassed this problem obtaining at very low costs the use of two Russian research vessels, i.e. the R.V. Gelendzhik and the R.V. Akademic Strakhov, both equipped with modern, ocean-depth multibeam. We had already a good deal of experience with these vessels and with working together with scientists of the Russian Academy of Science, since we had carried out with them a number of expeditions in the central and southern Atlantic, part of a CNR-sponsored project on Mid Ocean Ridges.

Funds for this project were obtained mostly from the CNR, but also from the Italian Geological Survey and from GNV (National Group on Vulcanology). Scientists of IGM, now part of a larger Institute of Marine Sciences (ISMAR) of the CNR, have been active in various themes, from coastal geology and biogeochemistry to ocean geology.

Two expeditions were carried out planned, organized and led by researchers of IGM, with the collaboration of a number of other Institutions. In addition to 100% multibeam coverage, continuous seismic reflection, gravimetric and magnetometric data were acquired mostly with instrumentation of IGM. The large set of data that were acquired are being processed and interpreted at IGM: the entire scientific community will then be able to share there results. The maps presented in this volume are part of the first harvest produced by this project. The Tyrrhenian is less mysterious, but not less fascinating.

Enrico BONATTI
Mariangela RAVAIOLI

INTRODUCTION

From seafloor to deep mantle: architecture of the Tyrrhenian backarc basin

---

The western Mediterranean can be viewed as a single subduction zone, stretching from southern Spain to the northern Apennines, running parallel to the north African margin. During the last –30 Ma, slam retreat produced discreet intervals of back arc extension in the region, generally migrating from in time west to east, to the present Tyrrhenian back arc basin facing the narrow oceanic slab underlying the compact Calabrian arc.

Pioneering studies in the Tyrrhenian Sea carried out in the 1960's, first by A.Segre then by R.Selli, triggered the development of modern marine geology in Italy. Knowledge of the Tyrrhenian general structure, sedimentary depositional styles and submarine volcanism became well established in the following years, leading to the first ideas concerning the formation of the basin. Subsequent drilling surveys, first through the Deep Sea Drilling Project (DSDP) in 1975 and then through the Ocean Drilling Program (ODP) in 1986 gave new impetus to the understanding of the processes that played a part in the evolution of the Tyrrhenian sea.

Since then, however, innovative marine geology techniques were developed. In particular, the employment of swath bathymetric mapping as a remote sensing tool, augmented by steadily increasing ground truthing as a result of sampling and direct observations. Caused a forward thrust in our knowledge of seafloor geology.

As a consequence, a new research effort was undertaken in the with the objective of obtaining the detailed multibeam mapping of the Tyrrhenian seafloor. The "Tyrrhenian Project", (full title "The Tyrrhenian sea: High Resolution Morphology and Structure of a Back-arc Basin") initiated as a project of the Consiglio Nazionale delle Ricerche (CNR) and was completed with support also from the Gruppo Nazionale di Vulcanologia (GNV) and from the Servizi Tecnici dello Stato – Servizio Geologico Nazionale. In addition, the Istituto Idrografico della Marina provided shallow water data for several areas.

A full-ocean depth multibeam instrument was utilised to map the challenging topography of the Tyrrhenian basin. Continuous multibeam bathymetry was acquired from the deepest seafloor to an average of 350m below sea level. Four months of seagoing surveys, covering more than 60,000km, and many more months of processing the vast amount of collected data have resulted in the maps appended to this volume. Although of complete multibeam coverage was the priority of the surveys, contemporaneous collection of seismic reflection, magnetic and gravimetric data was also accomplished. The new maps have provided, moreover, base-line data for the planning of subsequent accurately targeted sampling and high resolution seismic reflection surveys.

In order to frame the new information within a wider scientific perspective, an effort was made to place our results within a wider geological and geophysical context. To meet this end. Invitations were issued to leading scientists of the field to summarise up to date results of studies pursued in the Tyrrhenian region. The response received from the invited authors has resulted in this volume. It is an opportunity to assemble together the diverse scientific disciplines that have been applied to improve our understanding of the Tyrrhenian region. Each of the papers collected in the volume offer the latest models and hypotheses aimed at understanding the subduction-backarc system of the Tyrrhenian region as a whole.

Papers in the volume have been ordered according to thematic groupings. The first two papers deal with the deep structure of the Tyrrhenian region.

Utilising a new three-dimensional P-wave velocity model obtained with a novel nonlinear inversion of high quality teleseismic data, CIMINI *highlights the complexity of the mantle structure beneath the Tyrrhenian-Apennnine area. Three basic types of lithosphere sinking are interpreted from the tomography data within the general geodynamic context of oceanic-continental subduction.* PANZA *et alii outline the mosaic of lateral variations in the upper mantle structure of the region trùhrough the integration of surface wave tomography maps with petrological and geochemical data from the Italian volcanic provinces.*

The Authors show how large-scale inhomogeneities in the lithosphere-asthenosphere structure are mirrored by large variation in the composition of magma types. In particular, the backarc volcanism the Southern Tyrrhenian Sea, is shown to be associated with a very shallow crust-mantle transition above a soft mantle that is related to 10% of partial melting.

The subsequent three papers focus on the geophysical and geological properties of the nature of the lithosphere in the region, namely seismicity, heat flow and petrology of submarine volcanism. A review of the seismicity-prone sectors of the Tyrrhenian region is offered by FAVALLI *et alii before discussing. with recent examples, the challenges and opportunities of extending the Italian seismological network offshore. The Authors present results of experiments involving marine seismological observations, emphasizing the significant improvements in the detection and accurate localisation of offshore events. Essential for unravelling the present-day geodynamics of the region.* MONGELLI *et alii suggest the necessity of migrating astenospheric intrusions to explain the high heat flow of the eastern Tyrrhenian region. They image the present heat flow as a transient wave migrating eastward in time.* TRUA *et alii present new geochemical and isotope analyses of recent seafloor samples and a useful summary of available submarine sampling data, to discuss the coexistence of Island Arc and Ocean Island Basalts in the southern Tyrrhenian region in order to map mantle structure and define the geodynamics of mantle flow in the region.*

The following three papers examine the geology of the Tyrrhenian Sea based on the new bathymetric data, specifically structure and tectonics, sedimentology and submarine volcanic landforms. MARANI *and* GAMBERI *describe the geodynamic provinces of the Tyrrhenian basin, providing focused maps to outline the structural trends that define the different sectors of the basin.* GAMBERI *and* MARANI *describe the present-day sedimentary processes and depositional system of the diverse portions of the Tyrrhenian Sea. The authors present examples of the reflection profiles acquired during the swath mapping surveys and their preliminary interpretations .Lastly,* MARANI *and* GAMBERI *present examples of the morphology of submarine volcanic landforms, highlighting the differences between the submerged arc volcanoes and the edifices constructed in the back-arc.*

Three final papers put forward models of the development of the Tyrrhenian region. Combining structural data and magmatism, DOGLIONI *et alii discuss the geodynamics of the Tyrrhenian region including unique explanations for uplift in different sectors of the region. The authors attribute the diversity of Quaternary volcanism in the southern Tyrrhenian to the interaction of an eastwards moving mantle wedge with a predominant contaminating component linked to altered oceanic crust in the Aeolian magmas or to sediments in the Campania province magmatism. The paper by* FACCENNA *et alii is based on a multidisciplinary approach combining surface geological data, mantle tomography images and tectonic reconstructions. The results of the integrated dataset, tested by laboratory experiments, suggest that the intermittent extension producing the opening of the Liguro-Provençal and of the Tyrrhenian basins can be explained by the interaction between the subducting slab and the 660-km discontinuity. The final paper by* MARANI *proposes the Marsili volcano in the Southern Tyrrhenian as a super inflated spreading ridge resulting from the up-rise of deep buoyant asthenosphere across lateral tears that develop at the sides of the subducting lithosphere. The author considers vertical accretion as the dominant mechanism acting within a restricted spreading environment.*

Michael P. Marani

Fabiano Gamberi

Enrico Bonatti

Mem. Descr. Carta Geol. d'It.
XLIV (2004), pp. 15-28
6 figg.

Tomographic studies of the deep structure of the Tyrrhenian-Apennine system

Studi tomografici della struttura profonda del sistema Tirreno-Appennino

CIMINI G. B. (*)

ABSTRACT - Since the beginning of the 1980s seismic tomography studies have helped to unravel the deep structure and to constrain the kinematic models of tectonic evolution of Italy. In this chapter I describe the main features of the upper mantle structure beneath the Tyrrhenian – Apennine system obtained by jointly analysing the tomographic results with the distribution of subcrustal earthquakes. A new three-dimensional P-wave velocity model is also presented to give the most recent advancement in this research field. The model is computed by applying a non linear inversion algorithm on an improved data set of high-quality teleseismic arrival times recorded at the National Seismic Network and by the stations of a temporary passive array deployed in southern Italy. The resulting picture indicates a remarkable along-strike complexity of the subduction system below the Tyrrhenian – Apennine region, with at least three basic types of lithospheric sinking. The recognized slabs are characterized by significant differences in the geometry, continuity at depth, velocity contrasts with respect to the surrounding mantle, and reology. In the uppermost mantle the seismic structure is furtherly complicated by the presence of prominent low – velocity regions interpreted as asthenospheric upwelling in front of the downgoing lithosphere.

KEY WORDS:seismic tomography, upper mantle, subduction, Tyrrhenian-Appennines

RIASSUNTO - Sin dall'inizio degli anni 80 gli studi di tomografia sismica hanno aiutato a dipanare la struttura profonda e a vincolare i modelli cinematici dell'evoluzione tettonica dell'Italia. In questo capitolo si descrivono le principali caratteristiche della struttura del mantello superiore al disotto del sistema Tirreno – Appennino, ottenute analizzando congiuntamente i risultati di studi tomografici con la distribuzione dei terremoti subcrostali. Si presenta, inoltre, un nuovo modello tridimensionale delle velocità delle onde P per fornire gli avanzamenti più recenti in questo campo di ricerche. Il modello è calcolato applicando un algoritmo di inversione non lineare su un dataset selezionato di tempi di arrivo di fasi telesismiche registrate dalla rete sismica nazionale e dalle stazioni di un array temporaneo installato nell'Italia meridionale. I risultati di questo studio mostrano una rimarchevole complessità del sistema di subduzione sotto la regione Tirreno – Appennino, con almeno tre tipi base di sprofondamento litosferico. Gli slabs ricostruiti sono caratterizzati da differenze consistenti nella geometria, continuità con la profondità, contrasti di velocità rispetto al mantello circostante e reologia della litosfera subdotta. Nella parte più superiore del mantello della regione la struttura sismica è ulteriormente complicata dalla presenza di estese zone di bassa velocità interpretate come risalita di materiale astenosferico di fronte alla litosfera in subduzione.

PAROLE CHIAVE: tomografia sisimica, mantello, subduzione, Tirreno-Appennini

(*)Istituto Nazionale di Geofisica e Vulcanologia, Rome, Italy

1. - INTRODUCTION

In the last two decades, many tomographic reconstructions of the seismic velocity field in the crust and upper mantle beneath the Tyrrhenian – Apennine system have been carried out in order to provide constraints on the geodynamic evolution of this part of the Mediterranean region (BABUSKA & PLOMEROVÁ, 1990; SPAKMAN, 1990; SCARPA, 1982; AMATO *et alii*, 1993a; AMATO *et alii*, 1993b; SPAKMAN *et alii,* 1993; CIMINI & AMATO, 1993; CIMINI & DE GORI, 1997; PIROMALLO & MORELLI, 1997; CIACCIO *et alii*, 1998; LUCENTE *et alii*, 1999; CIMINI, 1999; DI STEFANO *et alii*, 1999; CIMINI & DE GORI, 2001). From these investigations, characterized by the use of different datasets of seismic phase arrival times, inversion techniques, and Earth's parameterizations of the target volume, a common, although somewhat controversial result has emerged: the existence below the region of a complex, nearly continuous subduction system. This evidence, still matter of debate among Earth scientists for the implications it provides on the past tectonic processes, comes from the interpretation in terms of mantle structural features of the strong, broad high-velocity bodies imaged in the lithosphere – asthenosphere system of the Apennines and surrounding seas.

In regions of plate boundaries, deep tectonic processes, such as lithospheric subduction, continental collision, and magmatism generate strong thermal heterogeneities, the primary cause of anomalies in the propagation of seismic waves. Following the wide literature on seismic tomography, the existence of high velocity anomalies (HVA) in the upper mantle is generally interpreted as due to cold (dense) oceanic lithosphere which penetrates or sinks into a warm (soft) asthenosphere, characterized by lower velocity (HIRAHARA & HASEMI, 1993; LAY,1994; GRAND *et alii*, 1997).

In our region, however, despite the efforts undertaken to provide more and more reliable images of the deep structure, uncertanties still exist on the geometry, lateral extension and continuity with depth of the subducted lithosphere. Besides the intrinsic difficulty in reconstructing adequately the deep structure in complicated plate boundary zones, discrepancies between models arise also from the approximate experimental condition with which the tomographic inversions are usually performed, i.e. insufficient station coverage, poor data quality, and inhomogeneous and/or inadequate sampling of the target volume. Particularly the incomplete ray sampling may have severe consequences on the reliability of tomographic reconstructions, resulting in low resolution images of large regions of the study target. Lack of resolution can, for instance, lead to spurious mapping of the existing velocity anomalies with smearing in the predominant direction of illumination (EVANS & ACHAUER, 1993).

Another critical point in interpreting tomographic images is the type of lithosphere which has been involved in the subduction process. Below the Tyrrhenian – Apennine region, the presence of subducted lithosphere of both oceanic and continental-type have been hypothesized. In regions of continental collision, when the subduction zone reaches the continental lithosphere, the latter may be pulled down to a certain extent by the sinking oceanic lithosphere. The existence of lithospheric slabs in the upper mantle (either oceanic or continental) are supposed to cause higher velocities with respect to the surrounding asthenosphere, thus suitable to be recovered by seismic tomography methods provided a thermal contrast is mantained.

In this chapter, after briefly reviewing the basic ideas concerning the structural setting and evolution of the Tyrrhenian – Apennine system, I summarize the most recent results obtained with seismic tomography and deep seismicity studies. Then, a new three-dimensional P-wave velocity model for the upper mantle of the region is described, enhancing the main robust features displayed by the tomograms. Finally, I discuss the geodynamic implications of the tomographic reconstructions, in terms of active and past subduction processes.

2. - TECTONIC SETTING

The present-day tectonic setting of the Tyrrhenian-Apennine system is the result of a complex collision process between the African and Eurasian plates, active since at least 65 Ma (DERCOURT *et alii*, 1986; DEWEY *et alii*, 1989; PATACCA *et alii*, 1990). According to one of the most accreditated geodynamic models, the evolution of this system after the Alpine orogenesis was driven by the eastward migration of the Adriatic-Ionian lithosphere through a complex subduction system (MALINVERNO & RYAN, 1986; FACCENNA *et alii*, 1996). In the late Oligocene-early Miocene (~26 Ma), the estward retreat of subduction of Adriatic lithosphere produced rifting processes in the Hercinic crust of the European foreland and led to the opening of the Liguro-Provençal basin with a 25°- 30° counter-clockwise drifting of the Sardinia-Corsica block (MALINVERNO & RYAN, 1986; BECCALUVA *et alii*, 1989). During this tectonic phase calc-alkaline volcanism was widespread on Sardinia (BECCALUVA *et alii*, 1989) and the Apenninic accretionary wedge underwent shortening. In the Tortonian (10 Ma), the back arc related extensional phase migrated to the Tyrrhenian area while compression continued to affect the Apenninic accretionary prism. The opening of the newly formed Tyrrhenian basin produced wide crustal thinning along the western side of the Apenninic belt with normal faulting and graben tectonics. During Quaternary age, intensive magmatic activity developed along the Tyrrhenian rim of the Apennines, from Tuscany to Campania. The volcanoes show complex evolutionary histories, with high alkali-potassic content and a wide spectrum of silica percentages (WILSON & BIANCHINI, 1999). To the east of the volcanic area, three distinct sectors can be distinguished: the orogenic belt, the Bradanic foredeep and the Apulian foreland (fig. 1).

The orogenic belt, characterized by an extensional

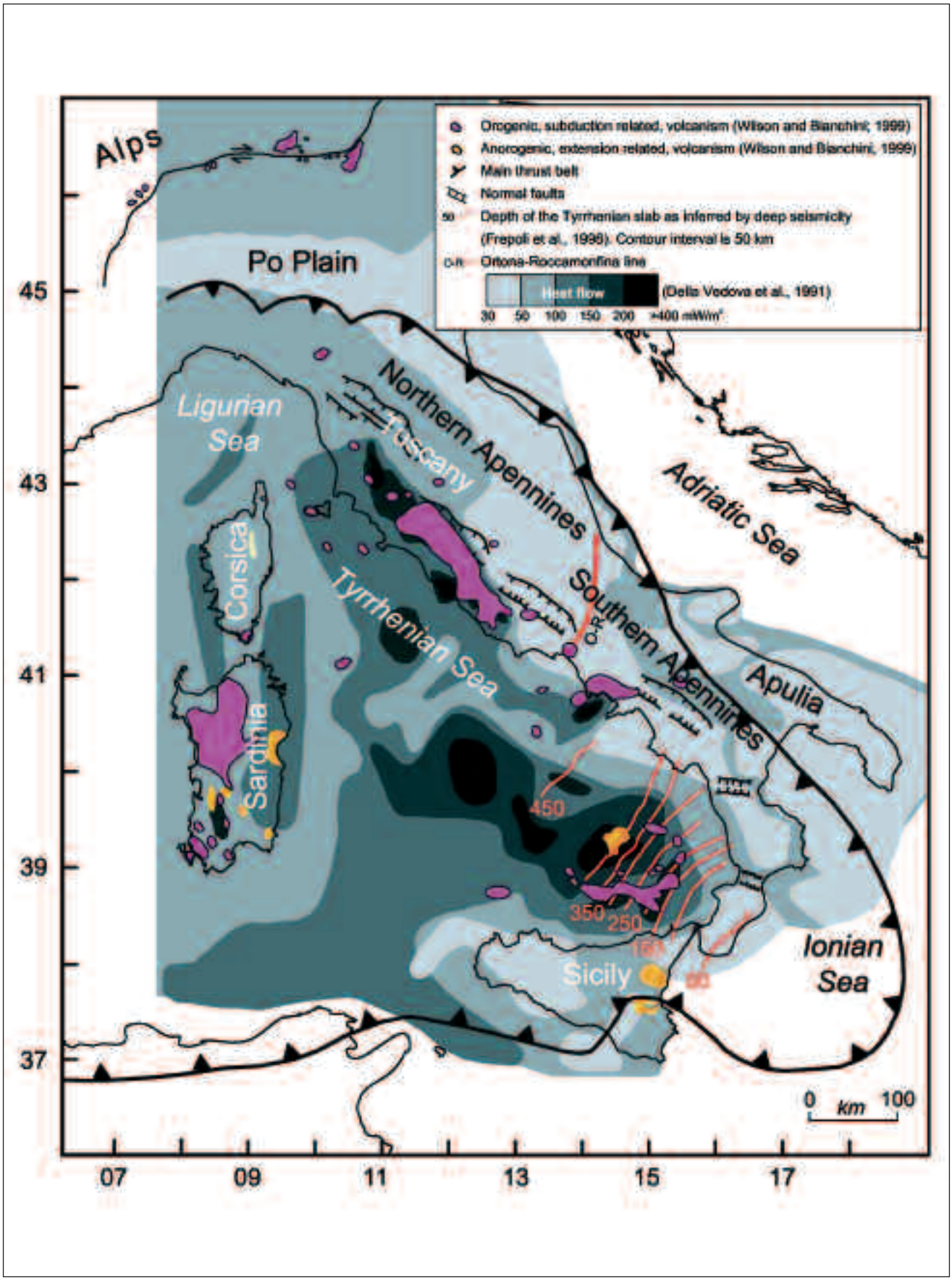

Fig. 1 - *Main tectonic features of the Italian peninsula (after* Jolivet *et alii, 1998).*

stress regime with the strongest normal faulting Apenninic earthquakes (AMATO & MONTONE, 1997), consists of several Adriatic vergent nappes, emplaced during the Miocene. The Bradanic foredeep, that extends from the Po plain to Sicily, is filled by 6-8 km of Plio- Quaternary sediments, and, according to ROYDEN *et alii* (1987), PATACCA & SCANDONE (1989), KRUSE & ROYDEN (1994), its considerable depth extension is related to the roll-back of the subducting slab beneath the belt rather than the lithostatic load of the orogen. The foreland, part of the Adria microplate, consists for the upper crust, of thick Meso-Cenozoic carbonate platform sequences, mostly undeformed during the compressive phases of the Alpine-Apenninic orogenesis (DOGLIONI *et alii*, 1994).

The present configuration of the Apennines consists of two major orogenic arcs, the Northern Apennine (NA) arc and the Southern Apennine (SA) arc, separated in the central Apennines by a ~ N-S trending fault zone (the Ortona-Roccamonfina line; O-R in fig. 1) that according to some authors is related to a deep lithospheric discontinuity (LOCARDI, 1982; PATACCA & SCANDONE, 1989). The SA arc is composed of two wings, the Southern Apennines wing to the north and the Calabrian arc to the south. As suggested by MALINVERNO & RYAN (1986), PATACCA & SCANDONE (1989), the different curvature of the two main arcs is an expression of a non-uniform retreat of the subducting slab beneath the belt, probably due to a strong lateral heterogeneity of the downgoing lithosphere. The more pronounced slab retreat beneath the northern Apennines and the Calabrian arc with respect to the southern Apennines produced, in this part of the belt, a tearing of the crust through a system of anti-Apenninic transfer faults that accommodates the differential movements between different sectors (PATACCA & SCANDONE, 1989).

3. - PREVIOUS TOMOGRAPHIC AND DEEP EARTHQUAKE STUDIES

The tomographic images together with the hypocentral distribution of crustal and subcrustal earthquakes, pose some of the tightest constraints to reconstruct the geodynamic evolution of our region. The study of the upper mantle structure using arrival times seismic tomography started only in the early 1980s, after the first reliable inversion technique was devoloped (AKI *et alii*, 1977). In this context it is worth recalling the first teleseismic tomography of Italy performed by SCARPA (1982), by using P and PKP data taken from seismic bulletins. He computed a velocity model of the upper mantle down to 360 km depth. The inversion revealed marked velocity contrasts especially in the deep structure of the southern Tyrrhenian Sea, although with a not satisfactory resolution. Further attempts with teleseisms were those of BABUSKA & PLOMEROVÁ (1990), that evidenced high velocities beneath the Alps and the northern Apennines, but still suffered from the use of poor quality data. The tomographic study by SPAKMAN *et alii*, (1993) is the first that investigates the 3-D P-wave velocity structure below the entire Mediterranean region, encompassing the mantle to a depth of 1400 km, by inverting a huge dataset of arrival times (~10^6) of both regional and teleseismic events. This study, based on P delay time data collected by the International Seismological Centre (ISC) from 18 years of observation, represents a considerable extension of earlier tomographic experiments.

Differently from SPAKMAN *et alii*, (1993), AMATO *et alii* (1993a), CIMINI & AMATO (1993) carried out their tomographic studies of the upper mantle below Italy by using a smaller teleseismic dataset (~10^3), but characterized by high precision in the estimate of the arrival times and a more homogeneous azimuthal coverage of the ray sampling. Compared to the use of noisy bulletin data, the use of accurately picked arrival times significantly improves the fit of the data, and the spatial resolution of the tomographic images (CIMINI & AMATO, 1993). Both these approaches, with some significative differences in the reconstruction of the velocity contrasts and in the geometry of lateral heterogeneities, found consistent high-velocity anomalies below peninsular Italy which were interpreted as related to remnants of subducted lithospheric slabs underlying the region.

More recent investigation of the deep structure of Italy are those by CIMINI & DE GORI (1997), PIROMALLO & MORELLI (1997), LUCENTE *et alii* (1999), DI STEFANO *et alii* (1999). In the study by CIMINI & DE GORI (1997), both direct (P and PKPdf) and secondary (pP, sP, PcP) P-wave arrival times were used to improve the sampling of the target volume and to reduce smearing effects. The tomographic model obtained by LUCENTE *et alii* (1999) extends the definition of the deep structures beneath both the Alps and the Apennines down to 800 km depth. The main finding is a nearly continuous pattern of high-velocity anomalies located between 250 and 670 km depth below the Apennines, shifting toward the Tyrrhenian basin with increasing depth. Finally, the paper by DI STEFANO *et alii* (1999) focuses on the P-wave velocity structure in the crust and uppermost mantle of Italy. They used a large dataset of arrival times of crustal earthquakes to retrieve the lateral heterogeneities at three depth levels located in the upper crust, lower crust, and beneath the Moho. The tomographic image for the lower crust (layer 2, 22 km depth) shows a pronounced low-velocity belt beneath the entire Apennines. This feature was interpreted by the authors as the effect of high temperatures caused by upwelling of asthenospheric material in front of the Adriatic slab.

In addition to seismic tomography, another important contribution to the delineation of the deep structure in regions of plate boundary comes from the distribution of intermediate and deep earthquakes foci. In peninsular Italy, subcrustal earthquakes are

observed beneath the southern Tyrrhenian Sea and the northern Apennines. Below the southern Tyrrhenian Sea, the occurrence of intermediate and deep hypocentres defines a continuous, well documented Wadati – Benioff zone from the surface down to at least 500 km depth (CAPUTO *et alii*, 1970; MCKENZIE, 1972; ANDERSON & JACKSON, 1987; GIARDINI & VELONÀ, 1991; among many others). The deep seismicity extends laterally for about 250 km and is mostly concentrated in depth range 50÷350 km (intermediate foci; fig. 2).

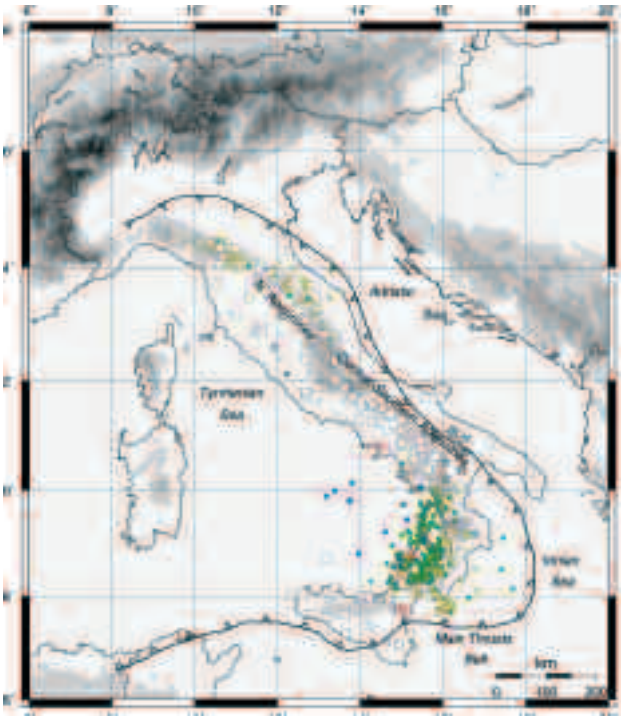

Fig. 2 - *Locations of the permanent and temporary seismic stations used for the tomographic analysis. White squares are the permanent short-period stations of the Istituto Nazionale di Geofisica e Vulcanologia (INGV) seismic network. Grey stars are the temporary three-component stations deployed for the SAPTEX passive array in southern Italy during the period 2001 – 2003. Circles indicate subcrustal seismicity selected from the INGV dataset in the period 1985 -2002: yellow circles are shallow foci (30 < h < 50 km); green circles are intermediate foci (50 < h < 350 km); blue circles are deep foci (h > 350 km). Note the absence of subcrustal seismicity below the central-southern Apennines and the northwestward migration of the deep seismicity (h > 350 km) of the southern Tyrrhenian subduction zone.*

The subcrustal earthquakes located beneath the Ionian Sea and the Calabrian Arc depict a subhorizontal seismic zone probably associated to the upper portion of the subduction zone delineated by seismic tomography (SELVAGGI & CHIARABBA, 1995; FREPOLI *et alii*, 1996; CIMINI, 1999). Below ~350 km depth the distribution appears to be shifted northwestward in the Tyrrhenian basin (blue circles in fig. 2), accordingly with the lateral deflection of the subducted lithosphere within the transition zone observed by CIMINI (1999).

In the northern Apennines, subcrustal earthquakes are observed down to 100 km (AMATO *et alii*, 1993b; SELVAGGI & AMATO, 1992). They are mainly located beneath the axis of the chain, following the bend of the northern Apenninic arc and apparently concentrated in two adjacent NW-SE trending zones (fig. 2). The distribution at depth delineates a ~45 dipping wedge from the Adriatic to the Tyrrhenian Sea, approximately coincident with the high-velocity anomaly detected by tomographic studies (AMATO *et alii*, 1993b; CIACCIO *et alii*, 1998).

Unlike the southern Tyrrhenian Sea and the northern Apennines, no subcrustal seismicity is currently observed beneath the central – southern Apennines (fig. 2). This evidence, along with the lack of clear high-velocity anomalies inferred from tomography in the uppermost mantle of the region, led various authors to suggest that the subduction has not been continuous beneath the whole Apenninic arc. This could be due either to the development of a slab window, as hypothesized by AMATO *et alii* (1993b) or to the presence of a detached slab as proposed by SPAKMAN *et alii* (1993), BIJWAARD & SPAKMAN (2000) A slab window may derive either by an irregular geometry of the two colliding plates or by a faster thermo-assimilation of the subducting lithosphere beneath the central part of the belt. The latter hypothesis is substantiated by the high heat-flow observed in the central Apenninic – Tyrrhenian margin (DELLA VEDOVA *et alii*, 1991; fig. 1). Moreover, a recent tomographic study by CIMINI & DE GORI (2001) shows a pronounced low-velocity zone ($\Delta Vp \cong -3 \div -5\%$) extending from the surface down to ~200 km in the upper mantle of the region. This feature is probably related to the presence of hot, high-attenuation asthenospheric material at uppermost mantle depths (MELE *et alii*, 1998), and has been proposed to affect the seismic structure of the downgoing Adriatic continental lithosphere, weakening its velocity signature.

4. - UPPER MANTLE STRUCTURE BELOW THE TYRRHENIAN - APENNINE REGION

In this section we show results from a new three-dimensional P-wave velocity model of the study region, computed with a modern teleseismic tomography procedure developed and previously applied by the author to the deep structure of southern Italy (CIMINI, 1999; CIMINI & DE GORI, 2001). This model differs from previous tomographic reconstructions (AMATO *et alii*, 1993a,b; CIMINI & AMATO, 1993; SPAKMAN *et alii*, 1993; CIMINI & DE GORI, 1997; LUCENTE *et alii*, 1999) by the use of an iterative inversion algorithm that incorporates a robust 3-D raytracer to compute more accurate ray paths in strongly heteregeneous media. By iterating, the velocity field is reconstructed gradually and larger data misfit reductions are usually achieved with respect to single step inversion (CIMINI & DE GORI, 2001). Furthermore, to better constrain the geometry of the

velocity anomalies, we used an improved dataset of high-quality teleseismic waveforms recorded by the seismic network of the Istituto Nazionale di Geofisica e Vulcanologia in the past 10 years, and by the stations of the SAPTEX array (CIMINI *et alii*, 2003) in southern Italy (fig. 2). The SAPTEX (Southern APpenines Tomography EXperiment) array is an ongoing deployment of temporary three-components digital stations, planned as a two-years passive experiment for high-resolution seismological studies of the southern Apennines.

For this nonlinear inversion we selected 140 teleseisms of magnitude $m_b \geq 5.5$ recorded by at least 30 stations. From the collected seismograms, the arrival times of 4765 P, and 1206 PKPdf phases were handpicked, giving a total of 5971 travel times. Figure 3 is a map of the great circle teleseismic ray paths showing the back azimuthal coverage of the region Since this kind of tomography inverts relative arrival times to estimate velocity perturbations, we used the 1-D velocity model ak135 (KENNETT *et alii*, 1995) to compute the predicted P-wave arrival times and, hence, the travel time residuals.

The tomography was performed by parameterizing the Earth structure beneath the Tyrrhenian –Apennines system with a three dimensional grid of nodes whith parameters are listed in table 1. The centre of the grid (x=0, y=0) corresponds to the geographic coordinates 40.5N, 14.0E, and, for ray paths computation, the bottom layer (600 km depth) is not inverted.

In figure 4 (a to c), six slices of the three-dimensional model are shown, from the uppermost mantle lithospheric layer (layer1, 50 km depth) down to 300 km (layer 6). The deepest part of the model, down to 500 km depth, is displayed subsequently in figure 5 by the three vertical sections across the Tyrrhenian – Apennine region.

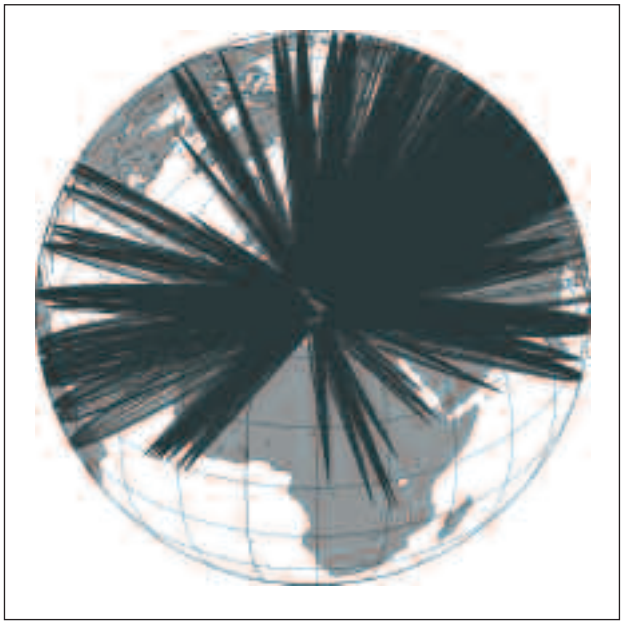

Fig. 3 - *Orthographic map showing the teleseismic ray sampling (great circle paths) of the deep structure beneath the study region. White circles represent the seismic stations of figure 2. The back azimuthal coverage is rather good, except from the south. The numerous ray crossing in the region significantly improve the resolution of the present tomographic model.*

The first two layers of the model (fig. 4a) show three main regions of high-velocity anomalies, located in the northern Apennines, Apulia region, and southern Tyrrhenian sea. The northern Apennines

TAB. 1 - *Grid model and reference P-wave velocities adopted for the iterative inversion.*

Layer	Depth km	Nodes in x	Nodes in y	Delta x km	Delta y Km	Vp km/s
0	0	Station layer - 110 recording sites				5.80
1	50	19	21	50	50	8.04
2	100	19	21	55	55	8.05
3	150	19	21	60	60	8.13
4	200	19	21	65	65	8.27
5	250	19	21	70	70	8.45
6	300	19	21	75	75	8.63
7	350	19	21	80	80	8.81
8	425	19	21	85	85	9.41
9	500	19	21	90	90	9.66
10	600	19	21	100	100	10.00

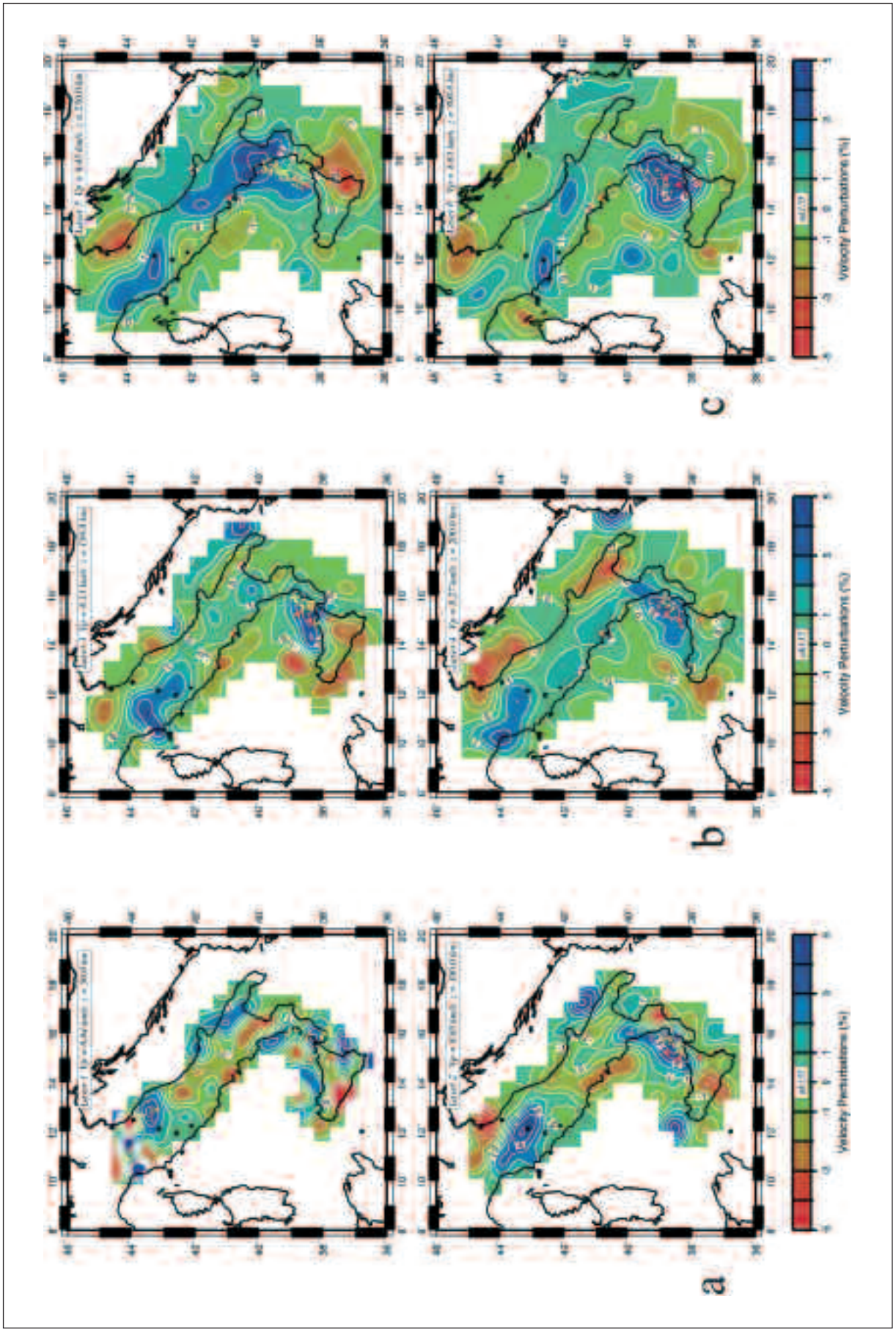

Fig. 4 - *Horizontal maps showing the 3-D P-wave velocity model for the upper mantle structure beneath the Tyrrhenian – Apennine system obtained by the nonlinear tomographic inversion after three iterations. a) layer1 (50 km), and layer2 (100 km); b) layer3 (150 km), and layer4 (200 km); c) layer5 (250 km), and layer6 (300 km). Note how the high-velocity regions, concentrated beneath the northern Apennines and the southern Tyrrhenian Sea at uppermost mantle depths (layer1 and layer 2), delineate a more continuous pattern at greater depths (particularly in layer 5, 250 km depth).*

HVA is very clear in the uppermost mantle at a depth of 100 km (fig. 4a, layer 2), where the velocity perturbations, as large as +4%, delineates a linear NW-SE anomalous body beneath the internal part of the chain. At shallower depths, the shape of the high velocity feature is strongly arcuate, suggesting that the slab curvature was acquired in the late stage of subduction (CIACCIO *et alii*, 1998). The subcrustal seismicity, which epicentral distribution closely follows the curvature of the northern Apenninic arc (fig. 2), appears mostly concentrated within the fast structures or at the border with the low-velocity zone reconstructed below the external front of the belt. Low-velocity anomalies are also found beneath the central-southern Apennines, the Campanian Tyrrhenian margin, and Sicily.

Figure 4b shows the P-wave velocity model for layers 3 and 4, set at 150 and 200 km depth, respectively. The main feature displayed by these tomograms is the nearly continuous pattern of high-velocity anomalies beneath the entire Apenninic chain and the southern Tyrrhenian sea. The largest positive perturbations are imaged in the southern Tyrrhenian area ($\Delta Vp \approx +3 \div +5\%$), consistently with the presence of a cold, dense oceanic-type subducted lithosphere (HIRAHARA & HASEMI, 1993). The resulting geometry delineates a SW-NE striking slab with thickness of about 100 km, lateral extent increasing with depth from ~200 km (layer 2) to ~400 km (layer 4), and that includes all the deep hypocenters. In central-southern Italy, between approximately 40N and 42N, the fast structures become weaker ($\Delta Vp \sim +1 \div +2\%$), thus confirming the along-strike difference in the HVA signature of the upper mantle below the Apennines pointed out by previous tomographic studies (AMATO *et alii*, 1993b; LUCENTE *et alii*, 1999; AMATO & CIMINI, 2001). Possible explanations are a heterogenous composition of the subducted lithosphere or a differential thermal assimilation of the slab at depth, or both. The prominent low-velocity anomaly recognized beneath the pery-Tyrrhenian area from the uppermost mantle (fig. 4a) below at least 150 km depth (fig. 4b, layer 3), suggests the presence of high temperature, probably partially melted, asthenospheric material in front of the Adriatic slab. This asthenospheric upwelling, as hypothesized by CIMINI & DE GORI (2001), may have promoted a more pronounced heating process and a faster termal assimilation of the downgoing slab.

The lateral heterogeneities in the P-wave velocity structure of the study region at greater upper mantle depths are displayed in figure 4c. The tomogram at 250 km depth (layer 5) shows a laterally continuous distribution of high-velocity anomalies from the northern Apennines to northeastern Sicily. The pattern is characterized by two main HVA regions ($\Delta Vp \geq +2\%$), separated in central Italy, around 42N, by an area of weaker perturbations marking the transition between the northern and the central-southern Apennines Two broad low-velocity anomalies are also reconstructed beneath the northern Adriatic sea-Po plain region and eastern Sicily. These slow features are visible from the uppermost mantle depths (figs. 4a,b), the latter probably related to the Mt. Etna volcanism. The horizontal map at 300 km depth (layer 6) depicts a more complex aspherical P-wave structure with respect to the previous one. The most prominent feature is still represented by the southern Tyrrhenian HVA that at this depth exibits the largest magnitude ($\Delta Vp \geq +5\%$) and the progressive shift toward the center of the Tyrrhenian basin, jointly with the NW migration of the deep seismicity (see also figs. 1, 2).

Figure 5 shows three vertical slices through the 3-D velocity model to better depict the different deep tectonic settings along peninsular Italy and surrounding seas.

Section AA' (upper panel) crosses the study region from Corsica, through the northern Apennines, to the Dinarides. Below the belt, the teleseismic image reveals a continuous HVA that extends from the uppermost mantle to at least 300 km depth. The slab is steeply dipping toward the back-arc region (Tuscany) and has a thickness of about 100 km. The maximum positive perturbations ($\Delta Vp = +4\%$) are reconstructed around 100 km depth, correspondently with the end of the subcrustal seismicity so far observed (SELVAGGI & AMATO, 1992). Section BB' (middle panel) is from the Tyrrhenian Sea, through the central Apennines, to the Dinarides. Here the velocity pattern shows a southwestward dipping HVA from about 200 km depth to the bottom of the present model. At uppermost mantle depths, the seismic structure is marked by a low-velocity region; this feature further enhances the difference in the deep structure between the Northern and Southern Apennines. Section CC' (lower panel) shows the upper mantle structure beneath the southern Tyrrhenian Sea and Calabria along a NW-SE profile. The high-velocity body depicting the subducting slab, steeply dipping from the Calabrian Arc to the northwest, is observed from the uppermost mantle down to 350 km. It includes all the intermediate and deep seismicity, which, in the present study, represents independent evidence for the geometry of the subduction zone. Below ~400 km, the tomogram displays a subhorizontal HVA, possibly detached from the highly seismic upper portion. This deep HVA may represent the oldest portion of the subducted lithosphere which is presently stagnant in the transition zone (CIMINI, 1999; LUCENTE *et alii*, 1999).

5. – DISCUSSION

Seismic tomography methods involve analysis of seismic waves that travel through the Earth to provide insights into the deep structure and tectonic evolution. High-velocity anomalies, where seismic waves speed-up, are comparatively common and correspond to regions where cold pieces of lithosphere have sunk into the mantle at the convergent margins of tectonic plates (subduction zones). Low-velocity anomalies are mainly explained as due to the effect of hot, low-Q

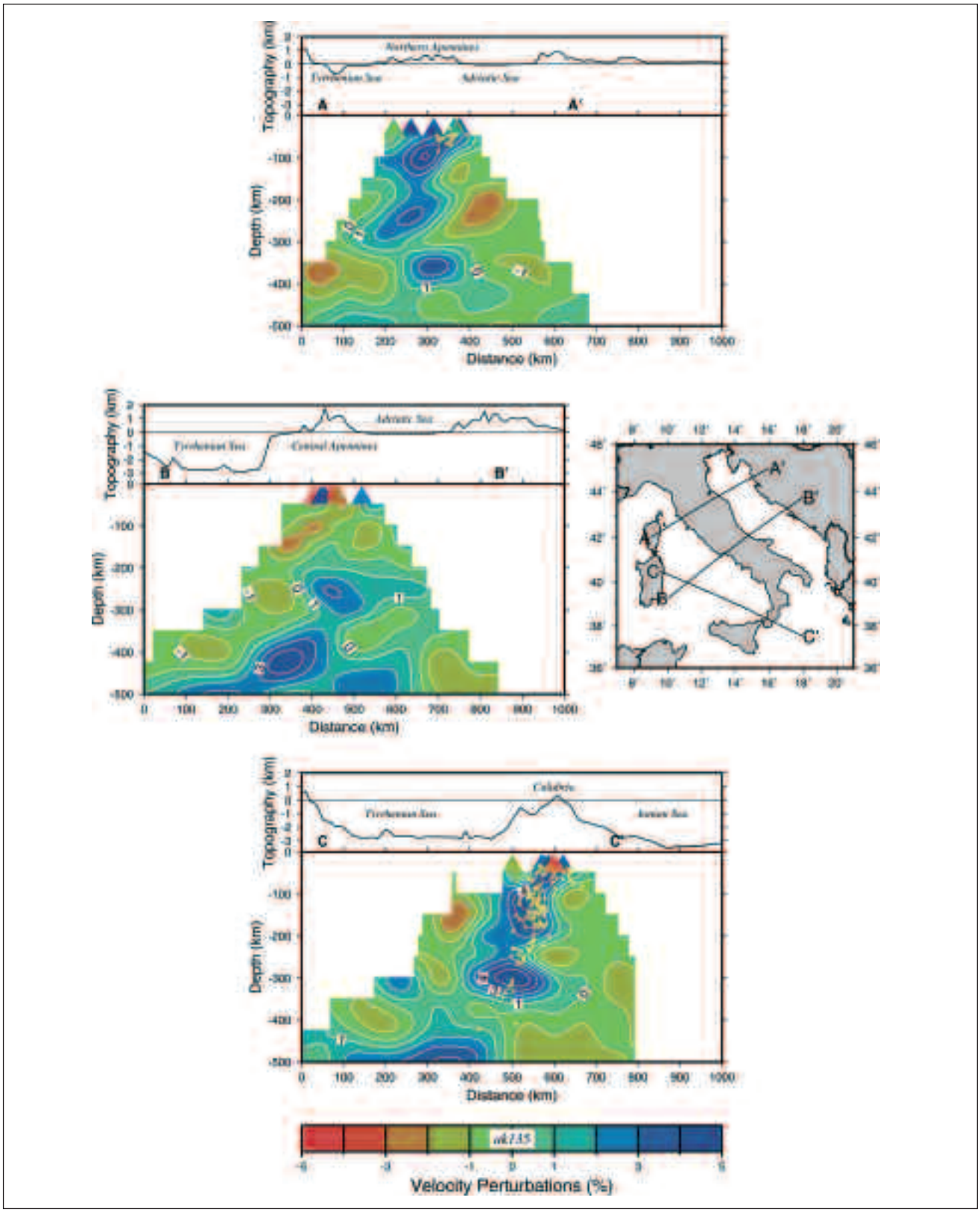

Fig. 5 - *Cross sections through the Tyrrhenian – Apennine region (see the panel for locations) showing the geometry of the subducted lithosphere and its relationship with the surrounding mantle. Yellow stars depict earthquake hypocenters located within 50 km of the vertical plane. A Beneath the northern Apennines a continuous high-velocity body characterized by positive perturbations as large as +4% is imaged between 50 and 300 km depth; B Beneath the central Apennines the downgoing slab is recognized from 200 km down to the bottom of the model. The fast structure, detached from the subcrustal high-velocity anomaly displayed in layer 1 (fig. 4a) at 50 km depth, is overlain by a pronounced low-velocity region extending from the uppermost mantle down to about 300 km below the central Tyrrhenian basin; C Deep velocity structure of the southern Tyrrhenian subduction zone along a NW-SE profile. The image delineates a main high-velocity seismic body from the uppermost mantle down to 350 km depth. Below this depth, a clear deflection of the subducted lithosphere to a nearly horizontal posture is observed.*

regions of upwelling asthenospheric material (hot spots, mid-ocean ridges, continental rift zones, etc.), or even, as in collision zone settings, associated to the subduction of continental crust (ROEKER, 1993). Within the spatial resolution limits previously pointed out (see section Introduction), seismic tomography tools can be used to visualize these mantle features because they produce strong temperature anomalies.

For the deep structure of the Italian region, the tomographic investigations carried out in the past twenty years enhance the presence of remnants of past subduction beneath the entire Apenninic belt.

The published models, although displaying significant differences both in the geometry and magnitude of the velocity contrasts between the subducted slabs and the surrounding mantle, all indicate a remarkable along-strike complexity of the subduction system below the Tyrrhenian – Apennine region. In particular, as also this study makes clear, the deep structures inferred from tomography depict three basic types of the Apenninic subduction, dividing the range into three segments. The main elements characterizing these different deep tectonic setting along the Apennines are summarized in figure 6, where the most reliable features reconstructed by the present nonlinear tomographic inversion are compared with surface tectonics, local seismicity, and regional Pn-wave studies.

The upper panel depicts the northern Apennines structure, in which the continuous slab determines the present subsidence of the foredeep, a still active compressional front and widespread extension in the back-arc region (FREPOLI & AMATO, 1997). No evidence for slab detachment are found in the depth range 150÷200 km, like the one reported by SPAKMAN *et alii* (1993) beneath the entire Apenninic belt. The arcuate shape of the high-velocity anomaly at uppermost mantle depths (fig. 4a, layer 1) reflects the arc curvature seen at the surface, repeating at smaller scale the arc migration model proposed for the earlier stages of the evolution of the Tyrrhenian – Apennine system (MALINVERNO & RYAN, 1986; DOGLIONI, 1991). This idea fits well with the post Miocene differential rotations observed along the outer thrust front from paleomagnetic data (SPERANZA *et alii*, 1997). At present, the subduction process in this area is probably close to the end because of the exhaustion of the oceanic lithosphere available in front of the trench and of the amount of continental lithosphere already subducted into the mantle. The geometry of the high-velocity anomalies depicted by the tomographic images (fig. 5, upper panel), suggest that the present-day configuration was reached through progressive slab roll-back, possibly determined by the older, deeper, oceanic lithosphere drawing from below. An alternative explanation of the steep dipping of the slab is the proposed E-W mantle flow that could increase the plunge of the subducting lithosphere in west-dipping subduction zones, like the Apennines (DOGLIONI, 1991).

The complex morphology of the subducted lithosphere beneath central-southern Apennines is outlined in the middle panel of figure 6. Below the Moho, MELE *et alii* (1996), MELE *et alii* (1998) found evidence for a broad low-Q, low-velocity zone of Pn phases. The high-attenuation feature was related to the presence of asthenospheric material at uppermost mantle depths. The prominent low-velocity anomaly imaged beneath the chain and the pery-Tyrrhenian area down to ~200 km depth (fig. 5, middle panel) strengthens this interpretation, featuring asthenospheric upwelling in front of the subducting lithosphere. Beneath the central Apennines, the slow structures join in a high-temperature mantle wedge that, as proposed by CIMINI & DE GORI (2001), may have been affecting the thermal and reological properties of the shallower, continental part of the Apenninic slab. A pronounced heating process of the downgoing lithosphere is consistent with the most recent (2-3 Ma) evolution of the Thyrrenian basin – Apenninic belt system, since the thick (~110 km) Apulian lithosphere reached the subduction hinge, slowing down (or even stopping) the eastward rollback and its penetration into the asthenosphere (MALINVERNO & RYAN, 1986; DOGLIONI *et alii*, 1994; AMATO & CIMINI, 2001). The lack of significant HVA observed in the ~50÷~200 km depth range (Fig. 4, layer 1 to layer 4) may then reflect a subducting lithosphere the seismic structure of which has been strongly modified by the long exposure to the uprising hot asthenosphere. A warmer, or less dense slab, could also explain the absence of active compression at the outer front suggested by present-day stress indicators (AMATO & MONTONE, 1997) and the diffuse uplift of the entire southern peninsula (WESTAWAY, 1993). Beneath ~200 km, the upper mantle structure is characterized by a clear SW-ward dipping high-velocity body, probably related to the past oceanic subduction. This portion could represent the lithosphere subducted before the collision of continental lithosphere in the central – southern Apennines, which most likely took place during the Messinian (6.5 Ma) as we can infer from paleomagnetic results (SPERANZA *et alii*, 1997).

The lower panel in figure 6 schematizes the southern Tyrrhenian subduction zone, enhancing the northwestward sinking of the Ionian oceanic lithosphere beneath Calabria. The oceanic nature of the slab was proposed by DE VOOGD *et alii* (1992), based on crustal thickness (~17 km in the Ionian area) and velocity profiles, as already hypothesized by BARBERI *et alii* (1973) based on volcanological data. The new teleseismic image (fig. 5, lower panel) shows two main fast structures depicting a ~650 km long slab. The broad low-velocity region reconstructed in front of the upper, steeply dipping HVA, may be due to a pronounced thermal anomaly induced by slab retreat and the subsequent rising of the asthenosphere in the Tyrrhenian basin. It is interesting to note that this feature appears to be the continuation at depth (not visible in cross-section CC', fig. 5) of the low-velocity zone imaged at 50 km depth below the Stromboli volcano (fig. 4a, layer 1). The deeper, almost

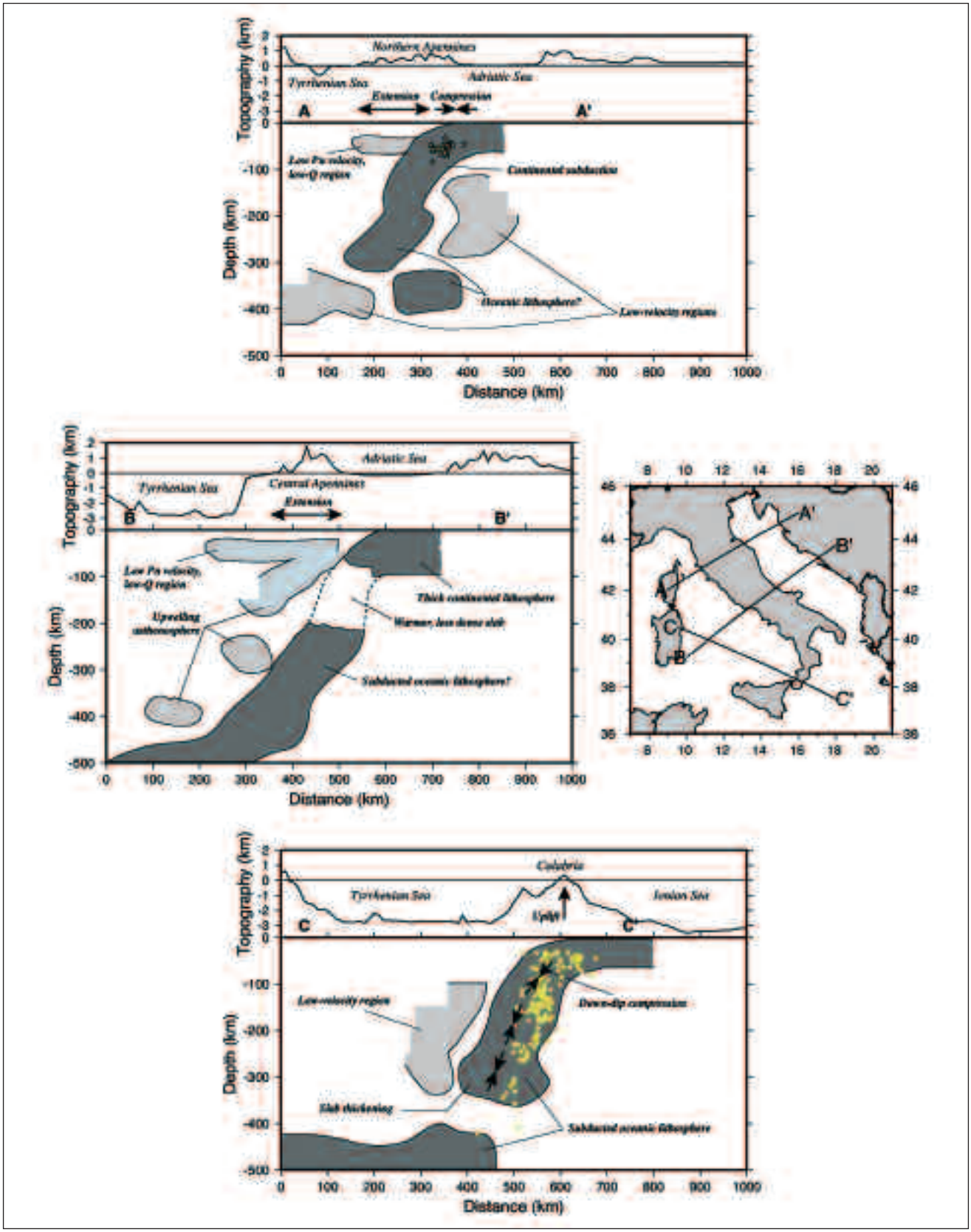

Fig. 6 - *Schematic diagrams along the same vertical planes of figure 5 summarizing the results of the present tomographic study of the Tyrrhenian – Apennine system. The main findings from some recent crustal and upper mantle studies of the region are also included in the maps for greater details and completeness. The Pn attenuation and low-velocity zones result from the study by* MELE *et alii,* 1998. *Deformation patterns are from earthquake fault plane solutions* (FREPOLI et alii, 1996; FREPOLI & AMATO, 1997) *and from borehole breakouts* (AMATO & MONTONE, 1997).

aseismic, portion of the slab lies subhorizontally in the transition zone, suggesting a difficult penetration into a high-strength lower mantle (CIMINI, 1999; LUCENTE *et alii*, 1999). The lateral deflection seen in the tomographic reconstructions is corroborated by the fault-plane geometries of intermediate and deep seismicity. This analysis enhances the shallowing of P-axes from dips of ~70°, found between 165 and 370 km depth, to subhorizontal dip observed for the deepest events located toward the central Tyrrhenian basin (FREPOLI *et alii*, 1996). Furthermore, it shows a diffuse down-dip compression within the upper portion of the subducted lithosphere (fig. 6), with the orientation of P-axes strikingly coinciding with the ~75° dipping seismogenic slab.

Another structural element characterizing the uppermost mantle geometry of the southern Tyrrhenian suduction zone is the increasing of lateral extent with depth. This observation, primarily reported by CIMINI (1999), can be related to the tectonic evolution undergone by the migrating Calabrian Arc in the last 2-3 Ma. During this period, the southeastward roll-back of the Apenninic subduction experienced, in the southern Tyrrhenian area, the highest rate of trench retreat (5-7 cm/yr), as witnessed by the rapid opening of the Marsili basin, forming the present-day shape of the arc (MALINVERNO & RYAN, 1986; FACCENNA *et alii*, 1996). The narrow lateral extent of the HVA depicting the shallower part of the slab, may reflect the narrow strip of oceanic lithosphere remaining after the continental collision took place at its eastern (southern Apennines) and western (Sicily) borders.

6. - CONCLUSIONS

Lateral heterogeneities, different thicknesses and a strongly irregular shape of the Ionian – Adriatic lithosphere have produced a complex subduction system beneath the Tyrrhenian – Apennine area. In this study, I summarized the contribution of seismic tomography to unravel the upper mantle structure of the region. The resulting picture, improved by the new tomographic images obtained with a modern nonlinear inversion of high-quality teleseismic data, shows different pieces of subducted slabs in a general geodynamic context of oceanic – continental subduction. This model is further complicated by along-strike variations that can be represented by at least three basic types of lithospheric sinking below peninsular Italy. Although no inferences can be made from the present results on the precise nature of the subducted lithosphere, we may consider the widespread evidence in collision zones of subducted thick crustal material to mantle depths (~50÷~150 km) to draw the following conclusive remarks. Beneath the northern Apennines the continental Adriatic lithosphere is attached to a deeper (>~150 km), probably oceanic, portion, forming a continuous, at least 300 km long, subducting slab. In the uppermost mantle of central – southern Apennines and central pery-Tyrrhenian area, low-velocity zones, laterally extending for about 300 km, interrupt the continuous HVA reconstructed below ~200 km depth. The slow structures, in good agreement with the observed high heat-flow, the thinning of the crust, and the presence of Quaternary volcanoes along the Tyrrhenian margin, form at depth a low-Q, high-temperature, mantle wedge lying above a heated, less dense slab. Beneath Calabria and the southern Tyrrhenian Sea, a long, seismically active, oceanic slab is subducting northwestward. The further and faster retreat experienced by this segment of the Apenninic subduction in the last few million years could have produced the apparent detachment of the deeper portion of the slab, which is presently stagnant in the upper mantle transition zone.

More investigations are still needed to better define the structure of the lithosphere-asthenosphere system beneath the Tyrrhenian - Apennine region. The most important seismological approaches to this goal include reconstruction of the Moho geometry from receiver function analysis, seismic anisotropy and attenuation studies, and both P- and S-wave tomographic models. Temporary passive deployments of three-components seismic arrays, like the ongoing SAPTEX array in southern Italy, have proved to be an essential tool for high-resolution studies, allowing to collect new data in areas characterized by paucity of permanent recording sites.

REFERENCES

AKI K., CHRISTOFFERSSON A. & HUSEBYE E.S. (1977) - *Determination of the three-dimensional seismic structure of the lithosphere*, J. Geophys. Res., **82**: 277-296.

AMATO A., ALESSANDRINI B. & CIMINI G.B. (1993a) - *Teleseismic wave tomography of Italy*, In: IYER H.M. & HIRAHARA K. (Eds.): *"Seismic Tomography: Theory and Practice"*. Chapman & Hall, London, 361-397.

AMATO A., ALESSANDRINI B., CIMINI G.B., FREPOLI A. & SELVAGGI G. (1993b) - *Active and remnant subducted slabs beneath Italy: evidence from seismic tomography and seismicity*, Annali di Geofisica, **36**: 201-214.

AMATO A. & CIMINI G.B. (2001) - *Deep structure from seismic tomography*, In: VAI G.B. & MARTINI I.P. (Eds.): "*Anatomy of an orogen: the Apennines and adjacent Mediterranean basins*". Kluwer Academic Publishers, Great Britain, 33-46.

AMATO A. & MONTONE P. (1997) - *Present-day stress field and tectonics in southern peninsular Italy,* Geophys. J. Int., **130**: 519-534.

ANDERSON H.J. & JACKSON J. (1987) - *The deep seismicity of the Tyrrhenian sea*, Geophys. Journ. Roy. Astr. Soc., **91**: 613-637.

BABUSKA V. & PLOMEROVÁ J. (1990) - *Tomographic studies of the upper mantle beneath the Italian region*, Terra Nova, **2**: 569-576.

BARBERI, F. GASPARINI P., INNOCENTI F. & VILLARI L. (1973) - *Volcanism of the Southern Tyrrhenian Sea and its geodynamic implications*, J. Geophys. Res., **78:** 5221-5231.

BECCALUVA L., BROTZU P., MACCIOTTA G., MORBIDELLI L., SERRI G. & TRAVERSA G. (1989) - *Cainozoic tectono-magmatic evolution and inferred mantle sources in the Sardo-Tyrrhenian Area*, In: BORIANI A. *et alii* (Eds.): *"The Lithosphere in Italy: Advances in Earth Science Research"*. Acc. Naz. Lincei, Rome,

229-248.

BIJWAARD H. & SPAKMAN W. (2000) - *Non-linear global P-wave tomography by iterated linearized inversion*, Geophys. J. Int., **141**: 71-82.

CAPUTO M., PANZA G.F. & POSTPISCHL D. (1970) - *Deep structure of the Mediterranean Basin*, J. Geophys. Res., **75**: 4919-4923.

CHIARABBA C. & AMATO A. (1996) - *Crustal velocity structure of the Apennines (Italy) from P-wave travel time tomography*, Annali di Geofisica, **39**: 1133-1148.

CIACCIO M.G., CIMINI G.B. & AMATO A. (1998) - *Tomographic images of the upper mantle high-velocity anomaly beneath Northern Apennines*, Mem. Soc. Geol. It., **52**: 353-364.

CIMINI G.B. (1999) - *P-wave deep velocity structure of the Southern Tyrrhenian Subduction Zone from nonlinear teleseismic traveltime tomography*, Geophys. Res. Lett., **26**: 3709-3712.

CIMINI G.B. & AMATO A. (1993) - P-*wave teleseismic tomography: contribution to the delineation of the upper mantle structure of Italy*, In: BOSCHI E., MANTOVANI E. & MORELLI A. (Eds.): *"Recent Evolution and Seismicity of the Mediterranean Region"*. Kluwer Academic Publishers, Dordrecht, 313-331.

CIMINI G.B. & DE GORI P. (1997) - *Upper mantle velocity structure benath Italy from direct and secondary P-wave teleseismic tomography*, Annali di Geofisica, **40**: 175-194.

CIMINI G.B. & DE GORI P. (2001) - *Nonlinear P-wave tomography of subducted lithosphere beneath central-southern Apennines (Italy)*, Geophys. Res. Lett., **28**: 4387-4390.

CIMINI G.B., DE GORI P. & FREPOLI A. (2003) - *Passive seismology in southern Italy: the SAPTEX array*, Annals of Geophysics, submitted.

DELLA VEDOVA B., MONGELLI F., PELLIS G., SQUARCI P., TAFFI L. & ZITO G. (1991) -*Heat-flow map of Italy*, Int. Ist. for Geoterm. Res., Pisa, Italy.

DERCOURT J., *et alii* (1986)- *Geological evolution of the Tethys Belt from the Atlantic to the Pamirs since the Lias*, Tectonophysics, **59**: 335-346.

DE VOOGD B. TRUFFERT C., CHAMOT-ROOKE N., HUCHON P., LALLEMANT S. & LE PICHON X. (1992) - *Two-ships deep seismic soundings in the basin of the eastern Mediterranean Sea (Pasiphae cruise),* Geophys. J. Int., **109**: 536-552.

DEWEY J.F., HELMAN M.L., TURCO E., HUTTON D.W.H. & KNOTT S.P. (1989) - *Kinematics of the western Mediterranean*, In: COWARD M.P., DIETRICH D. & PARK R.G. (Eds.): *"Alpine tectonics"*. Geol. Soc. London, Spec. Publ., **45**: 265-283.

DI STEFANO R., CHIARABBA C., LUCENTE F. & AMATO A. (1999) - *Crustal and uppermost mantle structure in Italy from the inversion of P-wave arrival times: geodynamics implications*, Geophys. J. Int*.*, **139**: 483-498.

DOGLIONI C. (1991) - *A proposal for the kinematic modelling of W dipping subductions – Possible applications to the Tyrrhenian – Apennines system*, Terra Nova, **3**: 423-434.

DOGLIONI C., MONGELLI F. & PIERI P. (1994) - *The Puglia uplift (SE Italy): An anomaly in the foreland of the Apenninic subduction due to buckling of a tick continental lithosphere*, Tectonics, **13**: 1309-1321.

EVANS J.R. & ACHAUER U. (1993) - *Teleseismic velocity tomography using the ACH method: theory and application to continental-scale studies*, In: IYER H.M. & HIRAHARA K. (Eds.): *"Seismic Tomography: Theory and practice*". Chapman & Hall, London, 319-360.

FACCENNA C., DAVY P., BRUN J.P., FUNICIELLO R., GIARDIN, D., MATTEI M. & NALPAS T. (1996) - *The dynamics of back-arc extension: an experimental approach to the opening of the Tyrrhenian Sea*, Geophys. J. Int., **126**: 781-795.

FREPOLI A., SELVAGGI G., CHIARABBA C. & AMATO, A. (1996) - *State of stress in the Southern Tyrrhenian subduction zone from fault-plane solutions*, Geophys. J. Int., **125**: 879-891.

FREPOLI A. & AMATO A. (1997) - *Contemporaneous extension and compression in the Northern Apennines from earthquake fault plane solutions*, Geophys. J. Int*.,* **125**: 879-891.

GIARDINI D. & VELONÀ M. (1991) - *The deep seismicity of the Tyrrhenian sea*, Terra Nova, **3**: 57-64.

GRAND S.P., VAN DER HILST R.D. & WIDIYANTORO S. (1997) - *Gloabal seismic tomography: a snaphot of convection in the Earth,* GSA Today, **7**: 1-7.

HIRAHARA K. & HASEMI A. (1993) - *Tomography of subduction zones using local and regional earthquakes and teleseisms*, In: IYER H.M. & HIRAHARA K. (Eds.): *"Seismic Tomography: Theory and practice"*. Chapman & Hall, London, 519-562

JOLIVET L., FACCENNA C., GOFFE, B., *et alii* (1998) - *Midcrustal shear zones in postorogenic extension: the Northern Tyrrhenian Sea case*, J. Geophys. Res., **88** (12): 123- 60.

KENNETT B.L.N., ENGDHAL E.R. & BULAND R. (1995) - *Constraints on seismic velocities in the Earth from traveltimes*, Geophys. J. Int., **126**: 555-578.

KRUSE S.E. & ROYDEN (1994) - *Bending and unbending of an elastic lithosphere: the Cenozoic history of the Apennine and Dinaride foredeep basins*, Tectonics, **13**: 278-302.

LAY T. (1994) - *Seismological structure of slabs*, DMOWSKA R. & SALTZMAN R. (Eds.) Academic Press, San Diego, 185 pp.

LOCARDI E.(1982) - *Neogene and Quaternary mediterranean volcanism: the Tyrrhenian example*, In: STANLEY D.J. & WEZEL F.C. (Eds.): *"Geological evolution of the Mediterranean basin*". Springer Verlag, New York, 273-291.

LUCENTE F.P., CHIARABBA C., CIMINI G.B. & GIARDINI D. (1999) - *Tomographic constraints on the geodynamic evolution of the Italian region*, J. Geophys. Res., **104** (20): 307-327.

MALINVERNO A. & RYAN W.B.F. (1986) - *Extension in the Tyrrhenian sea and shorthening in the Apennines as result of arc migration driven by the sinking of the lithosphere*, Tectonics, **5**: 227-245.

MCKENZIE D.P. (1972) - *Active tectonics of the Mediterranean region*, Geophys. J. Royal Astr. Soc., **30**: 109-185.

MELE G., ROVELLI A., SEBER D. & BARAZANGI M. (1996) - *Lateral variations of Pn propagation in Italy: evidence for a high-attenuation zone beneath the Apennines*, Geophys. Res. Lett*.,* **23**: 709-712.

MELE G., ROVELLI A., SEBER D., HEARN M.T. & BARAZANGI M. (1998) - *Compressional velocity structure and anisotropy in the uppermost mantle beneath Italy and surrounding regions*, J. Geophys. Res., **103** (12): 529-543.

PATACCA E. & SCANDONE P. (1989) - *Post-Tortonian mountain building in the Apennines. The role of the passive sinking of a relic lithospheric slab*, In: BORIANI A. *et alii* (Eds.): *"The Lithosphere in Italy: Advances in Earth Science Research"*, Acc. Naz. Lincei, Rome, 157-176.

PATACCA E., SARTOR R. & SCANDONE P. (1990) - *Tyrrhenian basin and Apenninic arcs: Kinematic relations since late Tortonian times*, Mem. Soc. Geol. It., **45**: 425-451.

PIROMALLO C. & MORELLI A. (1997) - *Imaging the Mediterranean upper mantle by P-wave travel time tomography*, Annali di Geofisica, **40**: 963-979.

ROEKER S.W. (1993) - *Tomography in zones of collision: practical considerations and examples*, In: IYER H.M. & HIRAHARA K. (Eds.): *"Seismic Tomography: Theory and practice"*. Chapman & Hall, London, 584-612

ROYDEN L., PATACCA E. & SCANDONE P. (1987) - *Segmentation and configuration of subducted lithosphere in Italy: An important control on thrust-belt and foredeep-basin evolution*, Geology, **15**: 714-717.

SCARPA R. (1982) *Travel-time residuals and three-dimensional velocity structure of Italy*, Pure Applied Geophysics, **120**: 83-606.

SELVAGGI G. & AMATO A. (1992) - *Intermediate-depth earthqauke in northern Apennines (Italy): evidence for a still active subduction?*,

Geophys. Res. Lett., **19**: 2127-2130.

SELVAGGI G. & CHIARABBA C. (1995) - *Seismicity and P-wave velocity image of the Southern Tyrrhenian subduction zone*, Geophys. J. Int., **121**: 818-826.

SPAKMAN W. (1990) - *Tomographic images of the upper mantle below central Europe and the Mediterranean*, Terra Nova, **2**, 542-552

SPAKMAN W., VAN DER LEE S. & VAN DER HILST R.D. (1993) - *Travel-time tomography of the European-Mediterranean mantle down to 1400 km*, Phys. Earth Planet Inter., **79**: 3-74.

SPERANZA F., SAGNOTTI L. & MATTEI M. (1997) - *Tectonics of the Umbria-Marche-Romagna arc (central-northern Apennines, Italy): new paleomagnetic constraints,* J. Geophys. Res., **102**: 3153-3166.

WESTAWAY R. (1993) - *Quaternary uplift of Southern Italy*, J. Geophys. Res., **98** (21): 741-772.

WILSON M. & BIANCHINI G. (1999) - *Tertiary-Quaternary magmatism within the Mediterranean and surrounding regions*, In DURAND B., JOLIVET L., HORVATH F. & SERRANE M. (Eds.): *"The Mediterranean Basins: Tertiary extension within the Alpine oroge"*. Geol. Soc., London, Spec. Publ., **156**: 141-168.

Mem. Descr. Carta Geol. d'It.
XLIV (2004), pp.29-56
7 figg.

Structure of the lithosphere-asthenosphere and volcanism in the Tyrrhenian Sea and surroundings

Struttura della litosfera-astenosfera e vulcanismo nel Mar Tirreno e regioni adiacenti

PANZA G.F. (*), PONTEVIVO A. (**), SARAÒ A. (***),
AOUDIA A. (****), PECCERILLO A. (*****)

ABSTRACT - The Italian peninsula and the Tyrrhenian Sea are some of the geologically most complex regions on Earth. Such a complexity is expressed by large lateral and vertical variations of the physical properties as inferred from the lithosphere-asthenosphere structure and by the wide varieties of Plio-Quaternary magmatic rocks ranging from tholeiitic to calcalkaline to sodium- and potassium-alkaline and ultra-alkaline compositions.
The integration of geophysical, petrological and geochemical data allows us to recognise various sectors in the Tyrrhenian Sea and surrounding areas and compare different volcanic complexes in order to better constrain the regional geodynamics. A thin crust overlying a soft mantle (10% of partial melting) is typical of the back arc volcanism of the central Tyrrhenian Sea (MAGNAGHI, VAVILOV & MARSILI) where tholeiitic rocks dominate. Similar lithosphere-asthenosphere structure is observed for Ustica, Vulture and Etna volcanoes where the geochemical signatures could be related to the contamination of the side intraplate mantle by material coming from either ancient or active roll-back. The lithosphere-asthenosphere structure and geochemical-isotopic composition do not change significantly when we move to the Stromboli-Campanian volcanoes, where we identify a well developed low-velocity layer, about 10-15 km thick, below a thin lid, overlain by a thin continental crust. The geochemical signature of the nearby Ischia volcano is characteristic of the Campanian sector and the relative lithosphere-asthenosphere structure may likely represent a transition to the back arc volcanism sector acting in the central Tyrrhenian. The difference in terms of structure beneath Stromboli and the nearby Vulcano and Lipari is confirmed by different geochemical signatures. The affinity between Vulcano, Lipari and Etna could be explained by their common position along the Tindari-Letoianni-Malta fault zone. A low velocity mantle wedge, just below the Moho, is present in all the regions related to the inactive recent volcanoes (Amiata, Vulsini, & Cimino, Vico, Sabatini, Albani Hills) in the Tuscany and Roman regions. A very thick rigid body is found in the upper mantle beneath the Ernici-Roccamonfina province that exhibits very distinct geochemical and isotopic compositions when compared with the Roman province.

KEY WORDS: lithosphere-asthenosphere system, geochemical-isotopic composition, Italian volcanic provinces, magma sources.

RIASSUNTO - La penisola italiana ed il Mar Tirreno sono alcune tra le regioni più complesse dal punto di vista geologico. Tale complessità è resa evidente da ampie variazioni verticali e laterali nelle proprietà fisiche della struttura litosfera-astenosfera e dalla grande varietà di rocce magmatiche del

(*) Dipartimento di Scienze della Terra, Università degli Studi di Trieste, Italy. (panza@dst.univ.trieste.it, aoudia)
The Abdus Salam International Centre for Theoretical Physics, SAND Group, Trieste, Italy.
(**) Dipartimento di Scienze della Terra, Università degli Studi di Trieste, Italy. (panza@dst.univ.trieste.it, aoudia)
now at the Geological Institute, University of Copenhagen, Denmark. (antonella@geo.geol.ku.dk)
(***) Dipartimento di Scienze della Terra, Università degli Studi di Trieste, Italy. (panza@dst.univ.trieste.it, aoudia.)
now at Osservatorio Vesuviano – INGV, Naples, Italy. (sarao@ov.ingv.it)
(****) Dipartimento di Scienze della Terra, Università degli Studi di Trieste, Italy. (panza@dst.univ.trieste.it, aoudia.)
The Abdus Salam International Centre for Theoretical Physics, SAND Group, Trieste, Italy.
(*****) Dipartimento di Scienze della Terra, Università degli Studi di Perugia, Italy. (pecceang@unipg.it)

periodo Plio-Quaternario, la cui composizione varia da toleitica a calcalcalina, da sodio- e potassio-alcalina ad ultra-alcalina.
L'analisi contestuale di dati geofisici, petrologici e geochimici ha permesso di riconoscere vari settori del mar Tirreno e delle aree circostanti e di mettere a confronto diversi complessi vulcanici con lo scopo di porre vincoli attendibili ai processi geodinamici regionali. La presenza di una crosta sottile che sovrasta un mantello soffice (10% di fusione parziale) è tipica del vulcanismo di retro-arco presente nel Tirreno centrale, dove predominano le rocce toleitiche. Una struttura litosfera-astenosfera simile è stata osservata in corrispondenza dei vulcani Ustica, Vulture ed Etna, dove le caratteristiche geochimiche possono essere legate alla contaminazione del mantello da parte di materiale derivante da processi di roll-back recenti o passati. La struttura litosfera-astenosfera e la composizione geochimica-isotopica non cambiano in modo significativo se si considerano Stromboli e i vulcani campani dove uno strato a bassa velocità ben sviluppato, dello spessore di 10-15 km, è presente sotto un sottile lid, sovrastato da una sottile crosta continentale. L'impronta geochimica del vicino vulcano di Ischia è caratteristica del settore campano e la relativa struttura litosfera-astenosfera può verosimilmente rappresentare una transizione al settore caratterizzato dal vulcanismo di retro-arco che è presente nel Tirreno centrale. La differenza, in termini di struttura, tra lo Stromboli ed i vicini Vulcano e Lipari è confermata dalle diverse caratteristiche geochimiche. L'affinità tra Vulcano, Lipari ed Etna può, invece, essere spiegata dalla loro comune posizione lungo la zona di faglia Tindari-Letoianni-Malta. Nella regione Toscana e nella provincia Romana, il mantello, a bassa velocità, affiora subito sotto la Moho in tutte le regioni in cui sono presenti vulcani recenti inattivi (Amiata, Vulsini, Cimino, Vico, Sabatini, Albani, Hills). Nel mantello superiore sotto la zona Ernici-Roccamorfina è stato identificato un corpo rigido e molto spesso che presenta composizioni geochimiche ed isotopiche ben distinte se paragonate con la provincia Romana.

PAROLE CHIAVE: sistema litosfera-astenosfera, composizione geochimica-isotopica, provincie vulcaniche italiane, sorgenti dei magmi

1. - INTRODUCTION

Volcanism is controlled by the lithosphere structure and architecture (e.g. MCNUTT, 1998; ANDERSON, 2000). The Italian peninsula and the Tyrrhenian Sea are some of the geologically most complex regions on Earth. Such a complexity is expressed by the strong heterogeneities of the crust-mantle system and the wide varieties of Plio-Quaternary magmatic rocks (e.g. PECCERILLO & PANZA, 1999). This setting is the result of the complex geodynamic evolution, of the Mediterranean during the Neogene and Quaternary times (e.g. DOGLIONI *et alii*, 1999). This generated a mosaic of compositionally and structurally distinct mantle domains that have undergone different evolutionary histories in terms of compositional and structural modifications.

The geodynamic evolution of the Mediterranean can be hardly unravelled when making use of models based on mono-disciplinary investigations. This is due to the complexity of the study area and to the intrinsic non-uniqueness of the inverse problem that is at the base of any geological model. In this paper we supply geophysical, petrological and geochemical data relative to different magmatic provinces recognised in Peninsular Italy and in the Tyrrhenian Sea. We combine the different datasets in order to better understand the genesis of the recent volcanism. Tying together geophysics, petrology and geochemistry we recognise various sectors in the Tyrrhenian Sea and surrounding areas and compare different volcanic complexes in order to better constrain the regional geodynamics.

2. - GEOPHYSICAL DATA AND METHOD

We determine the thickness and the vertical velocity distribution of the shear waves in the lithospheric layers for the area under investigation, represented in figure 1, using the surface-wave tomography regional study made by PONTEVIVO & PANZA (2002) and, where pertinent, the large-scale one by PASYANOS *et alii* (2001).

The available surface waves dispersion curves at regional scale (PONTEVIVO & PANZA, 2002; PANZA *et alii*, 2003), have been used to obtain tomography maps using the two-dimensional tomography algorithm developed by DITMAR & YANOVSKAYA (1987), YANOVSKAYA & DITMAR (1990). The lateral resolving power of the available dispersion data is of about 200 km (PONTEVIVO & PANZA, 2002); however the availability of a priori independent geological and geophysical information about the uppermost part of the crust improves the lateral resolving power and justifies the choice to perform the non-linear inversion of dispersion curves averaged over cells of a 1°x1° grid (PANZA *et alii*, 2003). Each cell of the grid is characterised by average dispersion curves of group velocity, $V_g(T)$ (in the period range of 10-35 s), and of phase velocity, $V_{ph}(T)$ (in the period range of 25-100 s). Each mean velocity is the average of the values read from the relevant tomography maps of PONTEVIVO & PANZA (2002) at the four nodes of each 1°x1° cell. The dispersion relations computed in such a way are listed in table 1. In the same table are shown the errors considered in the inversion, at each period. Following PANZA *et alii* (2003), each single point error (ρ_g, ρ_{ph}) associated to group and phase velocity values of a cell, is the quadratic sum of the measurement error (ρ'_g, ρ'_{ph}) and of the standard deviation (σ_g, σ_{ph}) of the average cellular velocities ($V_g(T)$, $V_{ph}(T)$).

At each period, the measurement error associated to the group velocity is estimated from the difference

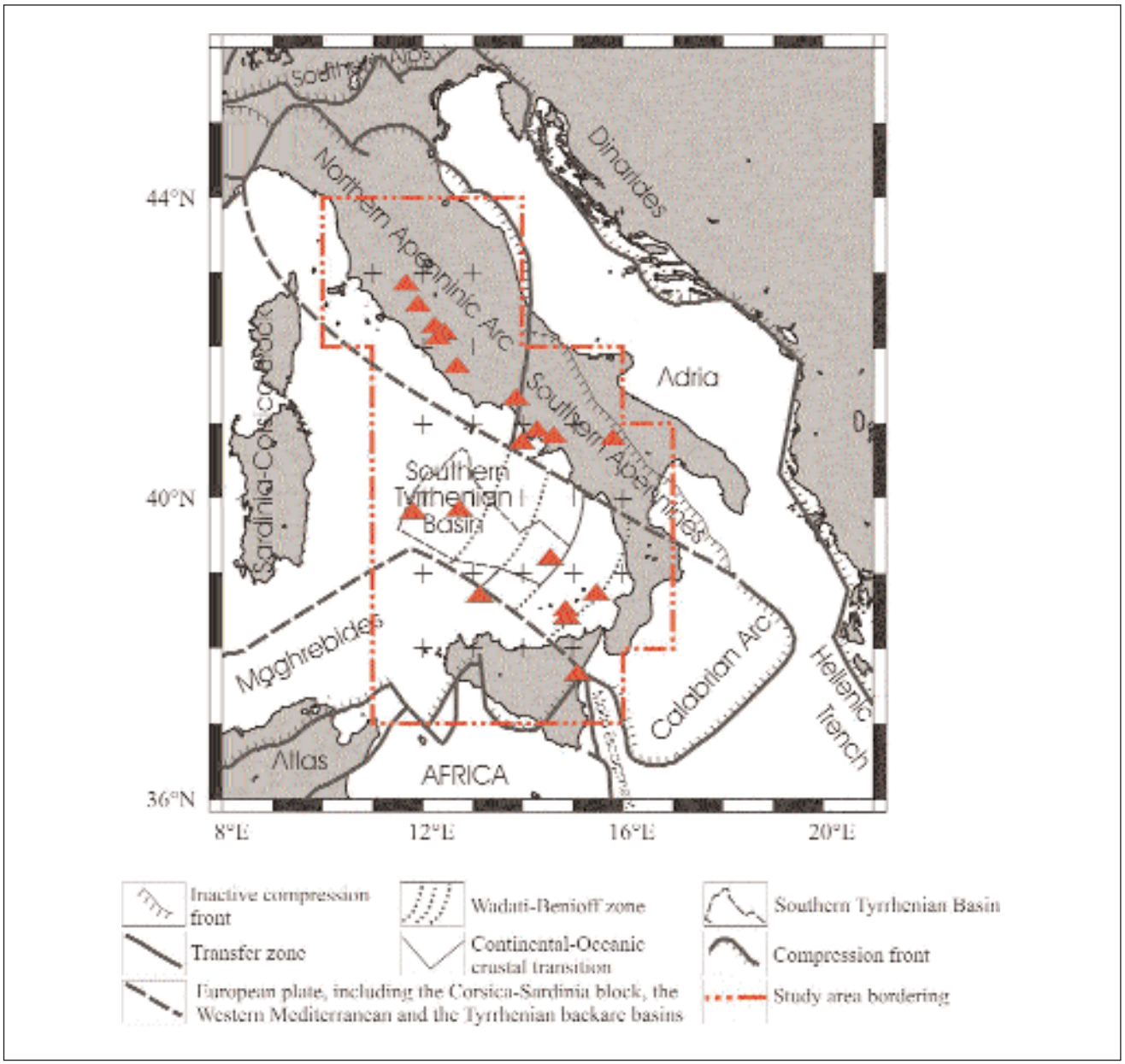

Fig. 1. - *Structural and kinematic sketch of Italy and surrounding areas, modified from* MELETTI *et alii* (2000). *The recent (active and not active) volcanoes in the study area (see the legend) are indicated by triangles.*

in the group velocity values determined along similar paths crossing similar areas, and is considered to be the same, ρ'_g, in all the cells well covered by the source-receiver paths. For the cells with a low path-coverage, the assumed error in the inversion is $2\rho'_g$. The measurement error associated to the phase velocity, ρ'_{ph}, is fixed accordingly to typical values published in the literature (BISWAS & KNOPOFF, 1974; CAPUTO *et alii*, 1976) for cells with a good path-coverage, and it is $2\rho'_{ph}$ elsewhere.

The parametrization of the structure to be inverted is chosen taking into account the resolving power of the data (KNOPOFF & PANZA, 1977; PANZA 1981) and relevant petrological information (e.g. RINGWOOD, 1966; GRAHAM, 1970; AHRENS, 1973; BOTTINGA & STEINMETZ, 1979; DELLA VEDOVA *et alii*, 1991). In such a way we have fixed the upper limit of V_S, for the sub-Moho mantle, at 4.9 km/s, and the lower limit of V_s at 4.0 km/s for the asthenosphere at depths greater than about 60 km. Average models of the lower crust and of the upper mantle are retrieved by the non-linear inversion method called Hedgehog (VALYUS *et alii*, 1969; VALYUS, 1972; KNOPOFF, 1972; PANZA, 1981). Following this procedure, the structure is modeled as a stack of N homogeneous isotropic layers in the elastic approximation, and each layer is

Tab. 1 - *Group (Vg) and phase (Vph) velocity values at different periods (from 10 s to 35 s and from 25 s to 100 s, respectively) with the single point error (g, ph) and the r.m.s. values for each cell. All phase velocities have been corrected for sphericity following* BOLT & DORMAN (1961).

	Cell c0 (10.5; 43.5)				**Cell c1 (11.5; 43.5)**				**Cell c2 (12.5; 43.5)**				**Cell c3 (13.5; 43.5)**				**Cell b0 (10.5; 42.5)**			
Period	V_g	ρ_g	V_{ph}	ρ_{ph}	V_g	ρ_g	V_{ph}	ρ_{ph}	V_g	ρ_g	V_{ph}	ρ_{ph}	V_g	ρ_g	V_{ph}	ρ_{ph}	V_g	ρ_g	V_{ph}	ρ_{ph}
(s)	(km/s)	(km/s)	(km/s)	(km/s)	(km/s)	(km/s)	(km/s)	(km/s)	(km/s)	(km/s)	(km/s)	(km/s)	(km/s)	(km/s)	(km/s)	(km/s)	(km/s)	(km/s)	(km/s)	(km/s)
10	1.96	0.20			2.01	0.10			2.09	0.10			2.18	0.11			2.15	0.21		
15	2.17	0.16			2.13	0.09			2.16	0.08			2.22	0.10			2.52	0.20		
20	2.43	0.16			2.38	0.08			3.38	0.07			2.42	0.08			2.81	0.19		
25	2.66	0.16	3.53	0.11	2.61	0.07	3.50	0.11	2.61	0.07	3.51	0.11	2.63	0.08	3.56	0.11	2.99	0.18	3.54	0.11
30	2.96	0.17	3.61	0.09	2.89	0.09	3.60	0.09	2.86	0.08	3.62	0.09	2.85	0.08	3.67	0.09	3.24	0.18	3.63	0.09
35	3.14	0.33	3.67	0.08	3.11	0.17	3.67	0.08	3.06	0.16	3.69	0.08	3.01	0.16	3.73	0.08	3.42	0.33	3.68	0.08
50			3.81	0.06			3.81	0.06			3.83	0.06			3.86	0.06			3.82	0.06
80			3.94	0.06			3.94	0.06			3.95	0.06			3.95	0.06			3.92	0.06
100			3.97	0.06			3.97	0.06			3.97	0.06			3.98	0.06			3.97	0.06
r.m.s.		0.12		0.055		0.07		0.055		0.07		0.055		0.07		0.055		0.13		0.055
	Cell b1 (11.5; 42.5)				**Cell b2 (12.5; 42.5)**				**Cell b3 (13.5; 42.5)**				**Cell a1 (11.5; 41.5)**				**Cell a2 (12.5; 41.5)**			
Period	V_g	ρ_g	V_{ph}	ρ_{ph}	V_g	ρ_g	V_{ph}	ρ_{ph}	V_g	ρ_g	V_{ph}	ρ_{ph}	V_g	ρ_g	V_{ph}	ρ_{ph}	V_g	ρ_g	V_{ph}	ρ_{ph}
(s)	(km/s)	(km/s)	(km/s)	(km/s)	(km/s)	(km/s)	(km/s)	(km/s)	(km/s)	(km/s)	(km/s)	(km/s)	(km/s)	(km/s)	(km/s)	(km/s)	(km/s)	(km/s)	(km/s)	(km/s)
10	2.17	0.21			2.21	0.12			2.23	0.11			2.40	0.21			2.47	0.21		
15	2.39	0.19			2.32	0.12			2.26	0.11			2.82	0.20			2.73	0.20		
20	2.63	0.18			2.51	0.10			2.46	0.09			3.04	0.19			2.88	0.18		
25	2.80	0.17	3.54	0.11	2.67	0.09	3.55	0.11	2.60	0.08	3.56	0.11	3.13	0.17	3.58	0.22	2.95	0.17	3.60	0.11
30	3.13	0.18	3.63	0.09	3.01	0.11	3.63	0.09	2.89	0.09	3.64	0.09	3.38	0.17	3.65	0.18	3.26	0.17	3.66	0.09
35	3.32	0.33	3.68	0.08	3.19	0.16	3.68	0.08	3.06	0.17	3.70	0.08	3.53	0.32	3.69	0.16	3.41	0.33	3.69	0.08
50			3.82	0.06			3.83	0.06			3.86	0.06			3.82	0.12			3.83	0.06
80			3.94	0.06			3.95	0.06			3.96	0.06			3.93	0.12			3.94	0.06
100			3.97	0.06			3.97	0.06			3.98	0.06			3.98	0.12			3.98	0.06
r.m.s.		0.13		0.055		0.07		0.055		0.07		0.055		0.13		0.09		0.13		0.055

segue Tab. 1

	Cell a3 (13.5; 41.5)				**Cell a4 (14.5; 41.5)**				**Cell a5 (15.5; 41.5)**				**Cell A1 (11.5; 40.5)**				**Cell A2 (12.5; 40.5)**			
Period	V_g	ρ_g	V_{ph}	ρ_{ph}	V_g	ρ_g	V_{ph}	ρ_{ph}	V_g	ρ_g	V_{ph}	ρ_{ph}	V_g	ρ_g	V_{ph}	ρ_{ph}	V_g	ρ_g	V_{ph}	ρ_{ph}
(s)	(km/s)	(km/s)	(km/s)	(km/s)	(km/s)	(km/s)	(km/s)	(km/s)	(km/s)	(km/s)	(km/s)	(km/s)	(km/s)	(km/s)	(km/s)	(km/s)	(km/s)	(km/s)	(km/s)	(km/s)
10	2.47	0.12			2.36	0.11			2.28	0.10			2.53	0.20			2.60	0.10		
15	2.56	0.14			2.38	0.09			2.31	0.08			3.07	0.16			2.99	0.08		
20	2.71	0.12			2.57	0.08			2.56	0.07			3.29	0.15			3.14	0.08		
25	2.75	0.12	3.61	0.11	2.63	0.08	3.59	0.11	2.66	0.08	3.58	0.11	3.31	0.15	3.63	0.11	3.17	0.08	3.64	0.11
30	3.07	0.12	3.67	0.09	2.94	0.10	3.66	0.09	2.93	0.09	3.66	0.09	3.45	0.16	3.67	0.09	3.36	0.08	3.67	0.09
35	3.23	0.18	3.71	0.08	3.09	0.17	3.71	0.08	3.03	0.16	3.72	0.08	3.59	0.32	3.71	0.08	3.51	0.16	3.70	0.08
50			3.84	0.06			3.87	0.06			3.88	0.06			3.82	0.06			3.81	0.06
80			3.95	0.06			3.96	0.06			3.95	0.06			3.92	0.06			3.93	0.06
100			3.98	0.06			3.98	0.06			3.98	0.06			3.98	0.06			3.98	0.06
r.m.s.		0.08		0.055		0.07		0.055		0.07		0.055		0.12		0.055		0.07		0.055
	Cell A3 (13.5; 40.5)				**Cell A4 (14.5; 40.5)**				**Cell A5 (15.5; 40.5)**				**Cell A6 (16.5; 40.5)**				**Cell B1 (11.5; 39.5)**			
Period	V_g	ρ_g	V_{ph}	ρ_{ph}	V_g	ρ_g	V_{ph}	ρ_{ph}	V_g	ρ_g	V_{ph}	ρ_{ph}	V_g	ρ_g	V_{ph}	ρ_{ph}	V_g	ρ_g	V_{ph}	ρ_{ph}
(s)	(km/s)	(km/s)	(km/s)	(km/s)	(km/s)	(km/s)	(km/s)	(km/s)	(km/s)	(km/s)	(km/s)	(km/s)	(km/s)	(km/s)	(km/s)	(km/s)	(km/s)	(km/s)	(km/s)	(km/s)
10	2.55	0.11			2.36	0.20			2.25	0.11			2.20	0.12			2.51	0.10		
15	2.74	0.12			2.45	0.17			2.33	0.08			2.31	0.09			2.95	0.10		
20	2.89	0.11			2.63	0.15			2.53	0.07			2.51	0.08			3.16	0.10		
25	2.96	0.10	3.65	0.11	2.76	0.15	3.64	0.11	2.70	0.08	3.62	0.22	2.77	0.09	3.61	0.11	3.28	0.08	3.68	0.11
30	3.22	0.10	3.69	0.09	3.06	0.16	3.69	0.09	2.99	0.08	3.68	0.18	3.04	0.09	3.68	0.09	3.40	0.09	3.71	0.09
35	3.37	0.17	3.72	0.08	3.20	0.32	3.73	0.08	3.13	0.17	3.73	0.16	3.21	0.17	3.73	0.08	3.52	0.16	3.74	0.08
50			3.83	0.06			3.85	0.06			3.86	0.12			3.87	0.06			3.83	0.06
80			3.94	0.06			3.94	0.06			3.94	0.12			3.93	0.06			3.92	0.06
100			3.98	0.06			3.98	0.06			3.98	0.12			3.98	0.06			3.99	0.06
r.m.s.		0.07		0.055		0.12		0.055		0.07		0.09		0.07		0.055		0.07		0.055

segue Tab. 1

	Cell B2 (12.5; 39.5)				**Cell B3 (13.5; 39.5)**				**Cell B4 (14.5; 39.5)**				**Cell B5 (15.5; 39.5)**				**Cell B6 (16.5; 39.5)**			
Period	V_g	ρ_g	V_{ph}	ρ_{ph}	V_g	ρ_g	V_{ph}	ρ_{ph}	V_g	ρ_g	V_{ph}	ρ_{ph}	V_g	ρ_g	V_{ph}	ρ_{ph}	V_g	ρ_g	V_{ph}	ρ_{ph}
(s)	(km/s)	(km/s)	(km/s)	(km/s)	(km/s)	(km/s)	(km/s)	(km/s)	(km/s)	(km/s)	(km/s)	(km/s)	(km/s)	(km/s)	(km/s)	(km/s)	(km/s)	(km/s)	(km/s)	(km/s)
10	2.53	0.10			2.47	0.11			2.34	0.11			2.19	0.10			2.11	0.10		
15	2.85	0.11			2.69	0.10			2.50	0.09			2.36	0.09			2.27	0.08		
20	3.02	0.10			2.85	0.09			2.68	0.08			2.56	0.08			2.47	0.07		
25	3.16	0.08	3.68	0.11	3.02	0.08	3.68	0.11	2.89	0.08	3.67	0.11	2.78	0.08	3.66	0.11	2.73	0.07	3.65	0.22
30	3.30	0.08	3.70	0.09	3.21	0.09	3.70	0.09	3.11	0.08	3.70	0.09	3.05	0.08	3.70	0.09	3.02	0.08	3.70	0.18
35	3.44	0.16	3.73	0.08	3.36	0.16	3.73	0.08	3.28	0.16	3.74	0.08	3.24	0.16	3.75	0.08	3.25	0.16	3.75	0.16
50			3.81	0.06			3.82	0.06			3.84	0.06			3.85	0.06			3.86	0.12
80			3.92	0.06			3.93	0.06			3.93	0.06			3.92	0.06			3.92	0.12
100			3.99	0.06			3.99	0.06			3.98	0.06			3.98	0.06			3.98	0.12
r.m.s.		0.07		0.055		0.07		0.055		0.07		0.055		0.07		0.055		0.07		0.09
	Cell C1 (11.5; 38.5)				**Cell C2 (12.5; 38.5)**				**Cell C3 (13.5; 38.5)**				**Cell C4 (14.5; 38.5)**				**Cell C5 (15.5; 38.5)**			
Period	V_g	ρ_g	V_{ph}	ρ_{ph}	V_g	ρ_g	V_{ph}	ρ_{ph}	V_g	ρ_g	V_{ph}	ρ_{ph}	V_g	ρ_g	V_{ph}	ρ_{ph}	V_g	ρ_g	V_{ph}	ρ_{ph}
(s)	(km/s)	(km/s)	(km/s)	(km/s)	(km/s)	(km/s)	(km/s)	(km/s)	(km/s)	(km/s)	(km/s)	(km/s)	(km/s)	(km/s)	(km/s)	(km/s)	(km/s)	(km/s)	(km/s)	(km/s)
10	2.44	0.20			2.41	0.20			2.34	0.11			2.25	0.11			2.16	0.10		
15	2.73	0.17			2.63	0.17			2.52	0.10			2.45	0.08			2.39	0.08		
20	2.91	0.15			2.80	0.15			2.71	0.08			2.66	0.07			2.62	0.07		
25	3.19	0.14	3.74	0.11	3.10	0.14	3.73	0.11	3.01	0.08	3.72	0.11	2.93	0.07	3.70	0.11	2.87	0.07	3.68	0.22
30	3.34	0.16	3.75	0.09	3.25	0.16	3.74	0.09	3.17	0.08	3.73	0.09	3.11	0.08	3.72	0.09	3.07	0.08	3.72	0.18
35	3.48	0.32	3.78	0.08	3.41	0.32	3.77	0.08	3.34	0.16	3.76	0.08	3.28	0.16	3.76	0.08	3.26	0.16	3.75	0.16
50			3.84	0.06			3.83	0.06			3.83	0.06			3.84	0.06			3.85	0.12
80			3.93	0.06			3.92	0.06			3.92	0.06			3.92	0.06			3.92	0.12
100			3.99	0.06			3.99	0.06			3.99	0.06			3.98	0.06			3.98	0.12
r.m.s.	0.12		0.055		0.12		0.055	0.12		0.07		0.055		0.07		0.055		0.07		0.09

segue Tab. 1

	Cell C6 (16.5; 38.5)				Cell D1 (11.5; 37.5)				Cell D2 (12.5; 37.5)			
Period	V_g	ρ_g	V_{ph}	ρ_{ph}	V_g	ρ_g	V_{ph}	ρ_{ph}	V_g	ρ_g	V_{ph}	ρ_{ph}
(s)	(km/s)	(km/s)	(km/s)	(km/s)	(km/s)	(km/s)	(km/s)	(km/s)	(km/s)	(km/s)	(km/s)	(km/s)
10	2.12	0.10			2.38	0.20			2.33	0.20		
15	2.32	0.08			2.61	0.16			2.54	0.16		
20	2.54	0.07			2.80	0.14			2.74	0.14		
25	2.80	0.07	3.67	0.22	3.18	0.14	3.77	0.11	3.13	0.14	3.76	0.11
30	3.03	0.08	3.71	0.18	3.32	0.16	3.78	0.09	3.27	0.16	3.77	0.09
35	3.25	0.16	3.76	0.16	3.50	0.32	3.81	0.08	3.46	0.32	3.80	0.08
50			3.85	0.12			3.86	0.06			3.86	0.06
80			3.92	0.12			3.93	0.06			3.92	0.06
100			3.98	0.12			3.99	0.06			3.99	0.06
r.m.s.		0.07		0.09		0.12		0.055		0.12		0.55
	Cell D3 (13.5; 37.5)				Cell D4 (14.5; 37.5)				Cell D5 (15.5; 37.5)			
Period	V_g	ρ_g	V_{ph}	ρ_{ph}	V_g	ρ_g	V_{ph}	ρ_{ph}	V_g	ρ_g	V_{ph}	ρ_{ph}
(s)	(km/s)	(km/s)	(km/s)	(km/s)	(km/s)	(km/s)	(km/s)	(km/s)	(km/s)	(km/s)	(km/s)	(km/s)
10	2.27	0.20			2.22	0.20			2.18	0.20		
15	2.47	0.16			2.44	0.16			2.45	0.16		
20	2.70	0.14			2.70	0.15			2.71	0.14		
25	3.07	0.15	3.74	0.22	3.03	0.16	3.71	0.22	2.99	0.15	3.70	0.22
30	3.23	0.16	3.75	0.18	3.19	0.17	3.74	0.18	3.16	0.16	3.72	0.18
35	3.40	0.32	3.78	0.16	3.34	0.32	3.77	0.16	3.31	0.32	3.77	0.16
50			3.85	0.12			3.85	0.12			3.85	0.12
80			3.92	0.12			3.92	0.12			3.92	0.12
100			3.98	0.12			3.98	0.12			3.98	0.12
r.m.s.		0.12		0.09		0.12		0.09		0.12		0.09

defined by V_p, V_s, density and thickness (h). Each parameter of the structure can be independent (the parameter is variable and can be well resolved by the data), dependent (the parameter has a fixed relationship with an independent parameter) or fixed (the parameter is held constant during the inversion, accordingly with independent geophysical evidences). For the cells with a low path-coverage, both in phase and group velocity, we have adopted a parametrization with a number of independent parameters lower than elsewhere. The adopted parameterization for each cell is given in table 2.

3. - AVERAGE CELLULAR LITHOSPHERIC MODELS FROM GEOPHYSICAL DATA

The available interpretations of the seismic profiles that cross most of the peninsula and adjacent seas together with other information available from literature (Bally *et alii,* 1986; Calcagnile *et alii*, 1982; Catalano *et alii*, 1996 and 2001; Cernobori *et alii*, 1996; Chimera *et alii*, 2003; Cristofolini *et alii*, 1985; De Gori *et alii*, 2001; Della Vedova *et alii,* 1989 and 1991; De Matteis *et alii*, 2000; De Voggd *et alii*, 1992; Doglioni *et alii*, 2001; Ferrucci *et alii*, 1991; Finetti, 1982; Finetti & Del Ben, 1986; Finetti *et alii*, 2001; Improta *et alii*, 2000; Kern & Schenk, 1988; Mantovani *et alii*, 1985; Marson *et alii*, 1995; Morelli, 1998; Monstaanpour, 1984; Pepe *et alii*, 2000; Pialli *et alii*, 1995; Scarascia & Cassinis, 1992; Scarascia *et alii*, 1994; Venisti *et alii*, 2003) are used to fix h and V_P of the uppermost crustal layers, assuming that they are formed by Poissonian solids. In table 2 the fixed V_p, V_s and h of the upper crustal layers are reported for each cell. The thickness of the water layer is chosen accordingly with standard bathymetric maps. The density of all the layers is in agreement with the Nafe-Drake relation, as reported by Ludwig *et alii* (1970): one and the same relation between V_p, V_s and density has been used for all the dependent parameters in the inversion, in most of the cells of the study area. The deviations from this rule can be seen in table 2. The structure below the

Tab. 2 - *Parametrization used in the non-linear inversion. Grey area: h (thickness), V_s and V_p of each layer. The uppermost layers are fixed on the base of available literature* (BALLY *et alii*, 1986; CALCAGNILE *et alii*, 1982; CATALANO *et alii*, 1996 and 2001; CERNOBORI *et alii*, 1996; CHIMERA *et alii*, 2003; CRISTOFOLINI *et alii*, 1985; DE GORI *et alii*, 2001; DELLA VEDOVA *et alii,* 1989 and 1991; DE MATTEIS *et alii*, 2000; DE VOGGD *et alii*, 1992; DOGLIONI *et alii*, 2001; FERRUCCI *et alii*, 1991; FINETTI, 1982; FINETTI & DEL BEN, 1986; FINETTI *et alii*, 2001; IMPROTA *et alii*, 2000; KERN & SCHENK, 1988; MANTOVANI *et alii*, 1985; MARSON *et alii*, 1995; MORELLI, 1998; MONSTAANPOUR, 1984; PEPE *et alii*, 2000; PIALLI *et alii*, 1995; SCARASCIA & CASSINIS, 1992; SCARASCIA *et alii*, 1994; VENISTI *et alii*, 2003). *The variable parameters are Pi, with i= 1, … 5 for thickness and i= 6, … 10 for V_s when the parameters are 10, and Pi, with i= 1, … 4 for thickness and i= 5, … 8 for V_s when the parameters are 8. White area: step (δPi) and variability range for each parameter Pi. The inverted velocities have always the second decimal value equal to 0 or 5. This rule is not in the fixed upper crust. The range of variability of the parameters h and V_s for each layer of the chosen solutions are deducible from this table.*

Cell c0 (10.5; 43.5)			**Cell c1 (11.5; 43.5)**			**Cell c2 (12.5; 43.5)**			**Cell c3 (13.5; 43.5)**			**Cell b0 (10.5; 42.5)**			**Cell b1 (11.5; 42.5)**		
h	V_S	V_P	h	V_S	V_P	h	V_S	V_P	h	V_S	V_P	h	V_S	V_P	h	V_S	V_P
(km)	(km/s)	(km/s)	(km)	(km/s)	(km/s)	(km)	(km/s)	(km/s)	(km)	(km/s)	(km/s)	(km)	(km/s)	(km/s)	(km)	(km/s)	(km/s)
4	2.20	3.80	4	2.20	3.80	0.5	1.60	2.65	1.1	1.55	2.65	0.5	0.00	1.52	0.25	3.00	5.50
1	2.65	4.60	1	2.65	4.60	1	2.30	3.60	2.4	2.08	3.60	0.5	3.00	5.50	0.75	3.50	6.10
3	3.00	5.20	3	3.00	5.20	1	3.00	5.50	1.5	3.18	5.50	6	2.65	5.00	6	2.65	5.00
P1	P6	P6x1.73	P1	P6	P6x1.73	1.5	3.50	6.10	1	3.50	6.10	P1	P6	P6x1.73	P1	P6	P6x1.73
P2	P7	P7x1.73	P2	P7	P7x1.73	P1	P6	P6x1.73	P1	P6	P6x1.73	P2	P7	P7x1.73	P2	P7	P7x1.73
P3	P8	P8x1.73	P3	P8	P8x1.73	P2	P7	P7x1.73	P2	P7	P7x1.73	P3	P8	P8x1.73	P3	P8	P8x1.73
P4	P9	P9x1.73	P4	P9	P9x1.73	P3	P8	P8x1.73	P3	P8	P8x1.73	P4	P9	P9x1.73	P4	P9	P9x1.73
P5	P10	P10x1.73	P5	P10	P10x1.73	P4	P9	P9x1.73	P4	P9	P9x1.73	P5	P10	P10x1.73	P5	P10	P10x1.73
						P5	P10	P10x1.73	P5	P10	P10x1.73						
h	Step	Range	h	Step	Range	h	Step	Range	h	Step	Range	h	Step	Range	h	Step	Range
(km)	(km)	(km)	(km)	(km)	(km)	(km)	(km)	(km)	(km)	(km)	(km)	(km)	(km)	(km)	(km)	(km)	(km)
P1	4	4-16	P1	8	6-14	P1	5	4-19	P1	4	5.5-17.5	P1	10	10-20	P1	5	5-20
P2	20	20-40	P2	10	10-30	P2	5	5-25	P2	6	5-29	P2	20	15-35	P2	30	15-45
P3	20	15-35	P3	10	15-35	P3	10	25-45	P3	5	10-50	P3	30	20-50	P3	20	20-60
P4	60	60-120	P4	65	50-135	P4	25	60-110	P4	10	20-110	P4	50	60-110	P4	60	30-90
P5	60	60-120	P5	60	60-120	P5	60	60-120	P5	30	40-130	P5	55	70-125	P5	50	70-120
V_S	Step	Range	V_S	Step	Range	V_S	Step	Range	V_S	Step	Range	V_S	Step	Range	V_S	Step	Range
(km/s)	(km/s)	(km/s)	(km/s)	(km/s)	(km/s)	(km/s)	(km/s)	(km/s)	(km/s)	(km/s)	(km/s)	(km/s)	(km/s)	(km/s)	(km/s)	(km/s)	(km/s)
P6	0.20	2.70-3.90	P6	0.10	2.30-3.80	P6	0.10	2.10-3.40	P6	0.05	2.35-4.25	P6	0.30	2.20-4.30	P6	0.30	2.20-3.10
P7	0.20	3.50-4.50	P7	0.20	3.50-4.40	P7	0.20	2.35-4.55	P7	0.10	3.30-4.50	P7	0.40	3.35-4.55	P7	0.40	2.80-4.40
P8	0.25	3.75-4.75	P8	0.30	3.55-4.45	P8	0.15	3.40-4.60	P8	0.20	3.35-4.75	P8	0.30	3.6-4.8	P8	0.40	3.65-4.45
P9	0.40	4.00-4.80	P9	0.20	4.00-4.80	P9	0.20	4.00-4.80	P9	0.10	4.00-4.80	P9	0.25	4.00-4.75	P9	0.20	4.00-4.80
P10	0.40	4.00-4.80	P10	0.40	4.00-4.80	P10	0.30	4.00-4.90	P10	0.20	4.00-4.80	P10	0.30	4.00-4.90	P10	0.25	4.00-4.75

segue Tab. 2

Cell b2 (12.5; 42.5)			**Cell b3 (13.5; 42.5)**			**Cell a1 (11.5; 41.5)**			**Cell a2 (12.5; 41.5)**			**Cell a3 (13.5; 41.5)**			**Cell a4 (14.5; 41.5)**		
h	V_S	V_P	h	V_S	V_P	h	V_S	V_P	h	V_S	V_P	h	V_S	V_P	h	V_S	V_P
(km)	(km/s)	(km/s)	(km)	(km/s)	(km/s)	(km)	(km/s)	(km/s)	(km)	(km/s)	(km/s)	(km)	(km/s)	(km/s)	(km)	(km/s)	(km/s)
1.2	1.60	2.65	1.2	1.55	2.65	1	0.00	1.52	1	0.00	1.52	3	1.87	3.25	2.6	2.13	3.70
0.8	2.30	3.60	0.8	2.13	3.70	2.7	1.33	2.30	2.7	1.32	2.30	2	2.19	3.80	2.5	2.45	4.25
1.5	3.00	5.50	1.5	3.10	5.35	1	2.90	5.00	1	3.06	5.30	3	3.26	5.65	2.9	3.06	5.30
1	3.50	6.10	1	3.61	6.25	2	3.30	5.70	2	3.25	5.60	2	3.45	6.00	3	4.15	5.50
P1	P6	P6x1.73	P1	P6	P6x1.73	P1	P5	P6x1.73	P1	P6	P6x1.73	P1	P6	P6x1.73	P1	P6	P6x1.73
P2	P7	P7x1.73	P2	P7	P7x1.73	P2	P6	P7x1.73	P2	P7	P7x1.73	P2	P7	P7x1.73	P2	P7	P7x1.73
P3	P8	P8x1.73	P3	P8	P8x1.73	P3	P7	P8x1.73	P3	P8	P8x1.73	P3	P8	P8x1.73	P3	P8	P8x1.73
P4	P9	P9x1.73	P4	P9	P9x1.73	P4	P8	P9x1.73	P4	P9	P9x1.73	P4	P9	P9x1.73	P4	P9	P9x1.73
P5	P10	P10x1.73	P5	P10	P10x1.73				P5	P10	P10x1.73	P5	P10	P10x1.73	P5	P10	P10x1.73
h	Step	Range	h	Step	Range	h	Step	Range	h	Step	Range	h	Step	Range	h	Step	Range
(km)	(km)	(km)	(km)	(km)	(km)	(km)	(km)	(km)	(km)	(km)	(km)	(km)	(km)	(km)	(km)	(km)	(km)
P1	6	9-21	P1	4	3-19	P1	20	20-40	P1	10	15-35	P1	5	11-26	P1	6	5.5-23.5
P2	10	15-25	P2	5	8-28	P2	20	5-45	P2	10	15-25	P2	4	10-18	P2	6	5-35
P3	15	15-30	P3	15	15-45	P3	50	50-100	P3	30	15-45	P3	20	15-35	P3	10	6-56
P4	50	50-100	P4	30	65-125	P4	60	60-120	P4	60	40-100	P4	60	60-120	P4	15	40-100
P5	60	40-160	P5	40	40-120				P5	70	60-130	P5	30	70-130	P5	30	30-120
V_S	Step	Range	V_S	Step	Range	V_S	Step	Range	V_S	Step	Range	V_S	Step	Range	V_S	Step	Range
(km/s)	(km/s)	(km/s)	(km/s)	(km/s)	(km/s)	(km/s)	(km/s)	(km/s)	(km/s)	(km/s)	(km/s)	(km/s)	(km/s)	(km/s)	(km/s)	(km/s)	(km/s)
P6	0.15	2.35-3.85	P6	0.10	2.20-4.10	P5	0.20	3.50-4.10	P6	0.30	3.05-4.25	P6	0.20	2.95-4.15	P6	0.05	2.40-4.40
P7	0.25	2.40-4.40	P7	0.10	3.20-4.40	P6	0.45	3.70-4.60	P7	0.30	3.50-4.40	P7	0.30	3.35-4.55	P7	0.10	3.25-4.75
P8	0.30	3.55-4.75	P8	0.15	3.60-4.65	P7	0.80	4.00-4.80	P8	0.80	3.85-4.65	P8	0.15	3.60-4.65	P8	0.10	3.40-4.70
P9	0.30	4.05-4.95	P9	0.10	4.00-4.80	P8	0.80	4.00-4.80	P9	0.40	4.00-4.80	P9	0.20	4.00-4.80	P9	0.05	4.00-4.80
P10	0.20	4.00-4.80	P10	0.20	4.00-4.80				P10	0.40	4.00-4.80	P10	0.40	4.00-4.80	P10	0.10	4.00-4.80

segue Tab. 2

Cell A6 (16.5; 40.5)			**Cell B1 (11.5; 39.5)**			**Cell B2 (12.5; 39.5)**			**Cell B3 (13.5; 39.5)**			**Cell B4 (14.5; 39.5)**			**Cell B5 (15.5; 39.5)**		
h	V_S	V_P	h	V_S	V_P	h	V_S	V_P	h	V_S	V_P	h	V_S	V_P	h	V_S	V_P
(km)	(km/s)	(km/s)	(km)	(km/s)	(km/s)	(km)	(km/s)	(km/s)	(km)	(km/s)	(km/s)	(km)	(km/s)	(km/s)	(km)	(km/s)	(km/s)
1.1	1.50	2.65	3	0.0	1.52	3	0.0	1.52	3.2	0.0	1.52	2.5	0.0	1.52	0.9	0.0	1.52
2.4	2.10	3.60	0.7	1.2	2.05	0.7	1.2	2.05	0.5	1.2	2.05	0.5	1.3	2.24	1.9	1.15	1.98
1.5	2.90	5.00	1	3.45	6.0	1	3.45	6.0	1	3.45	6.0	2	3.45	6.0	3	2.9	5.0
4	3.49	6.05	2	4.0	6.9	2	4.0	6.9	2	4.0	6.9	1.5	4.0	6.9			
P1	P6	P6x1.73	P1	P6	P6x1.73	P1	P6	P6x1.73	P1	P6	P6x1.73	P1	P6	P6x1.73	P1	P6	P6x1.73
P2	P7	P7x1.73	P2	P7	P7x2.00	P2	P7	P7x2.00	P2	P7	P7x2.00	P2	P7	P7x2.00	P2	P7	P7x1.73
P3	P8	P8x1.73	P3	P8	P8x2.00	P3	P8	P8x2.00	P3	P8	P8x2.00	P3	P8	P8x2.00	P3	P8	P8x1.73
P4	P9	P9x1.73	P4	P9	P9x2.00	P4	P9	P9x2.00	P4	P9	P9x2.00	P4	P9	P9x2.00	P4	P9	P9x1.73
P5	P10	P10x1.73	P5	P10	P10x2.00	P5	P10	P10x2.00	P5	P10	P10x2.00	P5	P10	P10x2.00	P5	P10	P10x1.73
h	Step	Range	h	Step	Range	h	Step	Range	h	Step	Range	h	Step	Range	h	Step	Range
(km)	(km)	(km)	(km)	(km)	(km)	(km)	(km)	(km)	(km)	(km)	(km)	(km)	(km)	(km)	(km)	(km)	(km)
P1	2.5	4.5-12	P1	4.5	6.5-20	P1	4	2-18	P1	3	3.5-12.5	P1	4	5-21	P1	2	5-29
P2	10	10-40	P2	10	11-31	P2	7	8-29	P2	4	6-18	P2	10	10-30	P2	10	5-25
P3	30	15-45	P3	40	11-51	P3	20	20-60	P3	20	30-70	P3	40	25-65	P3	20	20-60
P4	70	50-120	P4	60	45-105	P4	50	45-95	P4	70	35-105	P4	30	35-95	P4	20	15-95
P5	60	60-120	P5	70	60-130	P5	80	55-135	P5	70	60-130	P5	55	15-130	P5	45	35-125
V_S	Step	Range	V_S	Step	Range	V_S	Step	Range	V_S	Step	Range	V_S	Step	Range	V_S	Step	Range
(km/s)	(km/s)	(km/s)	(km/s)	(km/s)	(km/s)	(km/s)	(km/s)	(km/s)	(km/s)	(km/s)	(km/s)	(km/s)	(km/s)	(km/s)	(km/s)	(km/s)	(km/s)
P6	0.20	2.40-4.40	P6	0.3	3.1-4.6	P6	0.2	3.1-4.5	P6	0.15	3.60-4.65	P6	0.1	2.4-4.6	P6	0.05	2.5-4.6
P7	0.30	3.40-4.60	P7	0.3	2.8-4.6	P7	0.25	2.80-4.55	P7	0.2	2.5-4.1	P7	0.3	3.25-4.75	P7	0.2	3.2-4.6
P8	0.35	3.45-4.85	P8	0.25	3.40-4.65	P8	0.4	3.3-4.5	P8	0.1	3.7-4.7	P8	0.1	3.5-4.7	P8	0.1	3.45-4.85
P9	0.30	4.00-4.90	P9	0.35	4.0-4.7	P9	0.3	4.0-4.9	P9	0.25	4.00-4.75	P9	0.4	4.0-4.8	P9	0.1	4.0-4.8
P10	0.40	4.00-4.80	P10	0.3	4.0-4.9	P10	0.3	4.0-4.9	P10	0.3	4.0-4.9	P10	0.3	4.0-4.9	P10	0.1	4.0-4.8

segue Tab. 2

Cell A6 (16.5; 40.5)			**Cell B1 (11.5; 39.5)**			**Cell B2 (12.5; 39.5)**			**Cell B3 (13.5; 39.5)**			**Cell B4 (14.5; 39.5)**			**Cell B5 (15.5; 39.5)**		
h	V_S	V_P	h	V_S	V_P	h	V_S	V_P	h	V_S	V_P	h	V_S	V_P	h	V_S	V_P
(km)	(km/s)	(km/s)	(km)	(km/s)	(km/s)	(km)	(km/s)	(km/s)	(km)	(km/s)	(km/s)	(km)	(km/s)	(km/s)	(km)	(km/s)	(km/s)
1.1	1.50	2.65	3	0.0	1.52	3	0.0	1.52	3.2	0.0	1.52	2.5	0.0	1.52	0.9	0.0	1.52
2.4	2.10	3.60	0.7	1.2	2.05	0.7	1.2	2.05	0.5	1.2	2.05	0.5	1.3	2.24	1.9	1.15	1.98
1.5	2.90	5.00	1	3.45	6.0	1	3.45	6.0	1	3.45	6.0	2	3.45	6.0	3	2.9	5.0
4	3.49	6.05	2	4.0	6.9	2	4.0	6.9	2	4.0	6.9	1.5	4.0	6.9			
P1	P6	P6x1.73	P1	P6	P6x1.73	P1	P6	P6x1.73	P1	P6	P6x1.73	P1	P6	P6x1.73	P1	P6	P6x1.73
P2	P7	P7x1.73	P2	P7	P7x2.00	P2	P7	P7x2.00	P2	P7	P7x2.00	P2	P7	P7x2.00	P2	P7	P7x1.73
P3	P8	P8x1.73	P3	P8	P8x2.00	P3	P8	P8x2.00	P3	P8	P8x2.00	P3	P8	P8x2.00	P3	P8	P8x1.73
P4	P9	P9x1.73	P4	P9	P9x2.00	P4	P9	P9x2.00	P4	P9	P9x2.00	P4	P9	P9x2.00	P4	P9	P9x1.73
P5	P10	P10x1.73	P5	P10	P10x2.00	P5	P10	P10x2.00	P5	P10	P10x2.00	P5	P10	P10x2.00	P5	P10	P10x1.73
h	Step	Range	h	Step	Range	h	Step	Range	h	Step	Range	h	Step	Range	h	Step	Range
(km)	(km)	(km)	(km)	(km)	(km)	(km)	(km)	(km)	(km)	(km)	(km)	(km)	(km)	(km)	(km)	(km)	(km)
P1	2.5	4.5-12	P1	4.5	6.5-20	P1	4	2-18	P1	3	3.5-12.5	P1	4	5-21	P1	2	5-29
P2	10	10-40	P2	10	11-31	P2	7	8-29	P2	4	6-18	P2	10	10-30	P2	10	5-25
P3	30	15-45	P3	40	11-51	P3	20	20-60	P3	20	30-70	P3	40	25-65	P3	20	20-60
P4	70	50-120	P4	60	45-105	P4	50	45-95	P4	70	35-105	P4	30	35-95	P4	20	15-95
P5	60	60-120	P5	70	60-130	P5	80	55-135	P5	70	60-130	P5	55	15-130	P5	45	35-125
V_S	Step	Range	V_S	Step	Range	V_S	Step	Range	V_S	Step	Range	V_S	Step	Range	V_S	Step	Range
(km/s)	(km/s)	(km/s)	(km/s)	(km/s)	(km/s)	(km/s)	(km/s)	(km/s)	(km/s)	(km/s)	(km/s)	(km/s)	(km/s)	(km/s)	(km/s)	(km/s)	(km/s)
P6	0.20	2.40-4.40	P6	0.3	3.1-4.6	P6	0.2	3.1-4.5	P6	0.15	3.60-4.65	P6	0.1	2.4-4.6	P6	0.05	2.5-4.6
P7	0.30	3.40-4.60	P7	0.3	2.8-4.6	P7	0.25	2.80-4.55	P7	0.2	2.5-4.1	P7	0.3	3.25-4.75	P7	0.2	3.2-4.6
P8	0.35	3.45-4.85	P8	0.25	3.40-4.65	P8	0.4	3.3-4.5	P8	0.1	3.7-4.7	P8	0.1	3.5-4.7	P8	0.1	3.45-4.85
P9	0.30	4.00-4.90	P9	0.35	4.0-4.7	P9	0.3	4.0-4.9	P9	0.25	4.00-4.75	P9	0.4	4.0-4.8	P9	0.1	4.0-4.8
P10	0.40	4.00-4.80	P10	0.3	4.0-4.9	P10	0.3	4.0-4.9	P10	0.3	4.0-4.9	P10	0.3	4.0-4.9	P10	0.1	4.0-4.8

segue Tab. 2

Cell B6 (16.5; 39.5)			**Cell C1 (11.5; 38.5)**			**Cell C2 (12.5; 38.5)**			**Cell C3 (13.5; 38.5)**			**Cell C4 (14.5; 38.5)**			**Cell C5 (15.5; 38.5)**		
h	V_S	V_P	h	V_S	V_P	h	V_S	V_P	h	V_S	V_P	h	V_S	V_P	h	V_S	V_P
(km)	(km/s)	(km/s)	(km)	(km/s)	(km/s)	(km)	(km/s)	(km/s)	(km)	(km/s)	(km/s)	(km)	(km/s)	(km/s)	(km)	(km/s)	(km/s)
4	2.45	4.25	1.5	0.0	1.52	1	0.0	1.52	2	0.0	1.52	2.2	0.0	1.52	1	0.0	1.52
9	2.8	4.85	0.9	1.1	1.9	1.4	1.1	1.9	0.4	1.1	1.9	0.2	1.0	1.75	2	2.6	4.5
			0.4	2.31	4.0	0.4	2.31	4.0	0.4	2.31	4.0	0.4	2.31	4.0			
			4.2	2.90	5.0	3.2	2.9	5.0	3.2	2.9	5.0	3.2	3.55	6.15			
P1	P6	P6x1.73	P1	P6	P6x1.73	P1	P6	P6x1.73	P1	P6	P6x1.73	P1	P6	P6x1.73	P1	P6	P6x1.73
P2	P7	P7x1.73	P2	P7	P7x1.73	P2	P7	P7x1.73	P2	P7	P7x1.73	P2	P7	P7x1.73	P2	P7	P7x1.73
P3	P8	P8x1.73	P3	P8	P8x1.73	P3	P8	P8x1.73	P3	P8	P8x1.73	P3	P8	P8x1.73	P3	P8	P8x1.73
P4	P9	P9x1.73	P4	P9	P9x1.73	P4	P9	P9x1.73	P4	P9	P9x1.73	P4	P9	P9x1.73	P4	P9	P9x1.73
P5	P10	P10x1.73	P5	P10	P10x1.73	P5	P10	P10x1.73	P5	P10	P10x1.73	P5	P10	P10x1.73	P5	P10	P10x1.73
h	Step	Range	h	Step	Range	h	Step	Range	h	Step	Range	h	Step	Range	h	Step	Range
(km)	(km)	(km)	(km)	(km)	(km)	(km)	(km)	(km)	(km)	(km)	(km)	(km)	(km)	(km)	(km)	(km)	(km)
P1	8	12-20	P1	9	12-30	P1	10	14-34	P1	2	7-25	P1	2	5-19	P1	4	2-22
P2	12	12-36	P2	30	15-45	P2	30	20-50	P2	5	5-30	P2	4	10-34	P2	4	4-28
P3	20	25-45	P3	30	40-70	P3	25	25-75	P3	20	20-80	P3	5	20-50	P3	10	5-35
P4	50	45-95	P4	40	40-80	P4	40	45-85	P4	30	25-85	P4	15	25-100	P4	50	60-110
P5	60	65-125	P5	55	45-100	P5	40	50-90	P5	60	55-115	P5	35	20-125	P5	60	70-130
V_S	Step	Range	V_S	Step	Range	V_S	Step	Range	V_S	Step	Range	V_S	Step	Range	V_S	Step	Range
(km/s)	(km/s)	(km/s)	(km/s)	(km/s)	(km/s)	(km/s)	(km/s)	(km/s)	(km/s)	(km/s)	(km/s)	(km/s)	(km/s)	(km/s)	(km/s)	(km/s)	(km/s)
P6	0.4	2.8-4.4	P6	0.4	3.35-4.55	P6	0.3	3.15-4.65	P6	0.1	2.55-4.35	P6	0.05	2.45-4.55	P6	0.15	2.30-4.25
P7	0.8	2.9-4.5	P7	0.5	3.2-4.7	P7	0.25	3.25-4.5	P7	0.05	3.05-4.55	P7	0.2	3.05-4.55	P7	0.4	3.15-4.75
P8	0.4	3.5-4.7	P8	0.3	3.7-4.6	P8	0.6	3.4-4.6	P8	0.1	3.6-4.8	P8	0.1	3.3-4.7	P8	0.2	3.1-4.7
P9	0.4	4.0-4.8	P9	0.2	4.0-4.8	P9	0.2	4.0-4.8	P9	0.2	4.0-4.8	P9	0.05	4.0-4.8	P9	0.2	4.0-4.8
P10	0.8	4.0-4.8	P10	0.4	4.0-4.8	P10	0.4	4.0-4.8	P10	0.4	4.0-4.8	P10	0.1	4.0-4.8	P10	0.25	4.00-4.75

segue Tab. 2

Cell C6 (16.5; 38.5)			**Cell D1 (11.5; 37.5)**			**Cell D2 (12.5; 37.5)**			**Cell D3 (13.5; 37.5)**			**Cell D4 (14.5; 37.5)**			**Cell D5 (15.5; 37.5)**		
h	V_S	V_P	h	V_S	V_P	h	V_S	V_P	h	V_S	V_P	h	V_S	V_P	h	V_S	V_P
(km)	(km/s)	(km/s)	(km)	(km/s)	(km/s)	(km)	(km/s)	(km/s)	(km)	(km/s)	(km/s)	(km)	(km/s)	(km/s)	(km)	(km/s)	(km/s)
4	2.5	4.3	0.5	0.00	1.52	0.25	0.00	1.52	2.5	1.73	3.00	3	1.73	3.00	2.5	0.0	1.52
9	2.85	4.9	2.5	1.73	3.00	2.75	1.85	3.20	2.5	2.60	4.50	2	2.60	4.50	1.6	2.25	3.9
			2	2.90	5.00	2	2.65	4.60	5	2.90	5.00	5	2.90	5.00	1.1	2.35	4.05
			5	3.45	6.00	5	2.95	5.10	P1	P5	P6x1.73	P1	P5	P6x1.73	2.8	3.35	5.8
P1	P6	P6x1.73	P1	P6	P6x1.73	P1	P6	P6x1.73	P2	P6	P7x1.73	P2	P6	P7x1.73	P1	P6	P6x1.73
P2	P7	P7x1.73	P2	P7	P7x1.73	P2	P7	P7x1.73	P3	P7	P8x1.73	P3	P7	P8x1.73	P2	P7	P7x1.73
P3	P8	P8x1.73	P3	P8	P8x1.73	P3	P8	P8x1.73	P4	P8	P9x1.73	P4	P8	P9x1.73	P3	P8	P8x1.73
P4	P9	P9x1.73	P4	P9	P9x1.73	P4	P9	P9x1.73							P4	P9	P9x1.73
P5	P10	P10x1.73	P5	P10	P10x1.73	P5	P10	P10x1.73							P5	P10	P10x1.73
h	Step	Range	h	Step	Range	h	Step	Range	h	Step	Range	h	Step	Range	h	Step	Range
(km)	(km)	(km)	(km)	(km)	(km)	(km)	(km)	(km)	(km)	(km)	(km)	(km)	(km)	(km)	(km)	(km)	(km)
P1	4	4-16	P1	20	15-35	P1	10	5-25	P1	5	15-35	P1	10	5-35	P1	10	15-25
P2	15	2.5-32.5	P2	15	10-25	P2	10	15-35	P2	30	25-55	P2	30	25-55	P2	15	20-35
P3	10	10-30	P3	40	15-55	P3	30	25-55	P3	40	60-100	P3	80	40-120	P3	25	20-45
P4	60	65-125	P4	50	50-100	P4	50	50-100	P4	80	60-140	P4	60	60-120	P4	40	70-110
P5	70	60-130	P5	60	60-120	P5	40	80-120							P5	60	65-125
V_S	Step	Range	V_S	Step	Range	V_S	Step	Range	V_S	Step	Range	V_S	Step	Range	V_S	Step	Range
(km/s)	(km/s)	(km/s)	(km/s)	(km/s)	(km/s)	(km/s)	(km/s)	(km/s)	(km/s)	(km/s)	(km/s)	(km/s)	(km/s)	(km/s)	(km/s)	(km/s)	(km/s)
P6	0.3	2.7-4.5	P6	0.20	3.15-4.35	P6	0.20	3.05-4.25	P5	0.10	3.20-4.40	P5	0.20	3.20-4.40	P6	0.25	3.0-4.5
P7	0.5	3.4-4.4	P7	0.40	3.50-4.30	P7	0.20	3.20-4.40	P6	0.30	3.45-4.65	P6	0.10	3.85-4.65	P7	0.4	3.3-4.5
P8	0.5	3.1-4.6	P8	0.20	3.85-4.65	P8	0.30	3.75-4.65	P7	0.40	4.00-4.80	P7	0.40	4.00-4.80	P8	0.35	3.45-4.85
P9	0.2	4.0-4.8	P9	0.40	4.00-4.80	P9	0.40	4.00-4.80	P8	0.80	4.00-4.80	P8	0.80	4.00-4.80	P9	0.4	4.0-4.8
P10	0.25	4.00-4.75	P10	0.40	4.00-4.80	P10	0.40	4.00-4.80							P10	0.8	4.0-4.8

inverted layers is the same for all the considered cells and it has been fixed accordingly with already published data (DU *et alii*, 1998).

In figure 2 (a & b) we plot all the solutions of the inversion, that is V_s versus depth, from the surface to 250 km, and the explored parameter's space (shadowed area).

For each cell we indicate the depth of the Mohorovicic discontinuity (M) and the solution that we select (bold line) following, as in PANZA *et alii* (2003), the criterion that a simple solution is preferable to one that is unnecessarily complicated (DEGROOT-HEDLIN & CONSTABLE, 1990). The structural models chosen for all the cells, whose uncertainty can be inferred from direct inspection of figure 2, satisfy (within the r.m.s. value used in our inversions, see tab. 1) the additional condition to be consistent, at periods greater than 35 s, with the group velocity values given by PASYANOS *et alii* (2001).

3.1. - THE CRUST

Cells c0-c3 and b0-b3 (see fig. 2a) are characterized by the presence of a relatively high velocity layer (V_s 3.0 km/s) in the uppermost crust, followed by one at low velocity (2.60 V_s 2.95 km/s) and less than about 10 km thick. In these cells the model in the uppermost 10 km is fixed according to the results obtained by CHIMERA *et alii* (2003), which use CROP-03 profile to define the sequence of the stratigraphic units, their density and V_p. The structures of cells b0-b3 and c3 are obtained considering the phase velocity data ranging from 25 s to 100 s and not from 30 s to 100 s as in CHIMERA *et alii* (2003) for the same area. The differences between our structures and those of CHIMERA *et alii* (2003) are negligible, and the use of a larger period range of the phase velocity dispersion confirms the findings of CHIMERA *et alii* (2003). In this Apenninic area, the lower crust above the Moho has the V_s in the range 3.1-4.0 km/s. More to the South, in cells a1-a5 (fig. 2a), a positive velocity gradient is present in the crust, reaching the velocity of about 3.75-3.95 km/s in the lower crust.

In cells A1-A3 (fig. 2a) and B1-B4 (fig. 2b) the sedimentary layer is very thin and it is followed by a layering consistent with standard schematic oceanic crustal models (e.g. PANZA, 1984). In A5-A6 a low velocity layer appears in the upper crust and it is just above the Moho in A4, C4 and D5 with the V_s in the range 2.75-3.25 km/s. All the other cells are characterized by a thick crust, where the velocity of the sediments increases with increasing depth. With the exception of cells b2, C3-C5 and D5, all the cells in the continental region and in the Tyrrhenian offshore of Sicily, are characterized by a layer, just above the Moho, with V_s in the range 3.5-4.0 km/s. The location of the Moho depth in each cell is defined within a few kilometres.

3..2. - THE MOHO AND THE UPPERMOST UPPER MANTLE.

In the Northern Apenninic area (cells from c0 to c3 and from b1 to b3) and in cell b0, which contains Elba island, the Moho depth falls in the range 28-39 km with the maximum value in c1 and the minimum value in cells b0-b2 (fig. 2a). In the structures of c0-c3, b0 and b3 cells, the lid just below the Moho is characterized by relatively high V_s, in the range 4.35-4.60 km/s. The velocity of the lid increases with the depth in cells c2-c3 and b3, reaching values between 4.6 km/s and 4.8 km/s. In cells c1-c3 and b3 the asthenosphere starts below this high velocity layer at the depth of about 130-175 km. In cell c0, instead, the lid has a thickness of about 35 km. In cells b1 and b2, below the Moho, a relatively low velocity layer ($4.05 \leq V_s \leq 4.15$ km/s) and 15-20 km thick is present. This layer defined mantle wedge (layer with V_s less than about 4.2 km/sec in the uppermost mantle that overlies a high velocity lid with V_s greater than about 4.5 km/sec) by PANZA *et alii* (2003), with a percentage of partial melting of about 1-2% accordingly with BOTTINGA & STEINMETZ, 1979) could be associated to the presence of the inactive recent volcanoes of Amiata, Vulsini in b1 and Cimino, Vico, Sabatini in b2. The structural model of cell b0 is different from that of the neighbouring cells for the presence of a lid about 50 km thick and with a V_s of about 4.5 km/s. Going towards the South, the Moho in cells a1-a5 falls in the depth range from 26 to 42 km. A mantle wedge is seen in cells a1-a3. It is characterized by variable V_s, in the range 3.95-4.15 km/s, and its thickness (about 10 km in cell a3) increases going towards west (about 45 km). Cell a3 is characterized by the thinnest mantle wedge (with a percentage of partial melting of about 2-3%, accordingly with BOTTINGA & STEINMETZ, 1979) of this northernmost study area and it could be associated to the inactive recent volcano of Roccamonfina; similarly the low velocity layer of cell a2 (with a percentage of partial melting less than 2%) can be correlated with the inactive volcanoes of Albani Hills. In cell a4 a relatively low velocity layer is also present, with V_s around 4.2 km/s, and less than 10 km thick. A high velocity layer ($4.65 \leq V_s \leq 4.80$ km/s) is surmounted by the mantle wedge layer in cells a1-a4 and its thickness varies from about 35 km to 100 km. Cell a5, on the contrary, has the uppermost mantle structure rather similar to that of cell b3.

Cell A1 mimics the structure geometry of cell a1, but with a lower velocity both for the mantle wedge (V_s around 4.05 km/s) and the layer below it (V_s about 4.5 km/s). Similarly, cells A5 and A6 well resemble the structural characteristics of the uppermost mantle of cells a4 and a5, respectively, but with the lowermost lid at a velocity of about 4.6 km/s and reaching a depth of about 130-170 km.

In the central area of the Tyrrhenian Sea study area (cells A2, A3 and B1-B4), the average Moho is very shallow (about 7 km deep) and the lid thickness is less than about 15 km. Below this thin and strongly laterally variable lid (V_s in the range 4.0-4.4 km/s), there is a very well developed low velocity layer (V_s in the range 2.90-3.85 km/s) with variable thickness (in the range 8-33 km) and centred at a depth of about 20 km (uppermost asthenosphere). A similar layering is found in the uppermost 30 km of cell A4, the main difference being a deeper Moho, at a depth of about 15 km.

The V_s in the uppermost upper mantle of cells A2-A4 and B1-B4 is consistent with a high percentage of partial melting (about 10% accordingly with BOTTINGA & STEINMETZ, 1979). This regional feature, in cells B1-B4, is well compatible with the presence of anomalous shallow mantle materials reported by TRUA *et alii* (2002) in correspondence of the huge volcanic structures like the Vavilov-Magnaghi and the Marsili Seamounts; the shallow partial melting in cells A3 and A4 can be associated to Ischia, Phlegraean Fields and Vesuvio active volcanoes.

In cells A2-A4 the top of the high velocity lid (V_s about 4.45-4.55 km/s) is at a depth of about 30-40 km. In the other cells (B1-B3), the V_s just below the very low velocity layer in the uppermost asthenosphere, is in the range 4.10-4.15 km/s. In cell B4, the asthenosphere is perturbed by a layer with relatively high velocity (V_s about 4.4 km/s) and centred at a depth of about 120 km.

Going towards East (cells B5-B6) the Moho is as deep as about 27-33 km. In B5 the lid velocity increases with increasing depth and the lithosphere is about 110 km thick; in cells B6 the lid is characterized by high V_s and reaches depths of about 100 km.

The structural models of cells C1-C5 (fig. 2b) are markedly different from those of cells B1-B4. In fact, the Moho depth varies from about 13 km to 34 km and the smaller value is reached in correspondence of the active Aeolian volcanic islands (cells C4 and C5). In cells C2-C3 the V_s gradient in the lid, which is about 70-90 km thick, is stronger than the gradient that characterizes the sub-Moho materials in cell C1. In C4, the V_s immediately below the Moho can be as low as 3.85 km/s (about 3-4% of partial melting, accordingly with BOTTINGA & STEINMETZ, 1979), while the high velocity lid is found at a depth larger than about 40 km. In C5 the relatively soft lid extends only to about 17 km of depth and it is on top of a low velocity (V_s about 3.5 km/s) layer, the mantle wedge (about 10% of partial melting, accordingly with BOTTINGA & STEINMETZ, 1979), which overlies a lithospheric root (V_s around 4.6 km/s) reaching about 140 km of depth. The large amount of partial melting (where V_s in the upper mantle is less than 4.0 km/s) in C4 and C5 correlates well with the presence of the Aeolian volcanic islands (Lipari and Vulcano in C4 and Stromboli in C5).

The structural properties change abruptly in cell C6. Below a crust about 25 km thick, and a very thin lid, there is a low velocity (V_s around 3.6 km/s) layer about 10 km thick, on top of a layer with V_s around 4.6 km/s that reaches a depth of about 100 km. These features (not imposed a priori in the inversion scheme) can be interpreted as a lithospheric doubling and the deeper Moho can be seen about 38 km deep.

In Sicily, cells D1-D4 (fig. 2b) show a Moho that deepens from West to East from about 25 km to 35 km, while in the Etna area (cell D5) the Moho is only about 23 km deep. In cells D1-D2 the lid thickness varies between 80 km and 40 km and the V_s increases with increasing depth, about 4.20-4.65 km/s. Cells D3 and D4 have a high velocity lid with V_s 4.65 km/s, reaching a depth of about 90 km.

In cells C5 and C6, below the high velocity lid of about 4.60 km/s, there is a layer characterized by a V_s around 4.25 km/s. PANZA *et alii* (2003) suggest that the structural setting depicted by the models for cells C5-C6 and the area East of them indicate the subduction of a rifted continental Ionian lithosphere, formed during the Jurassic extensional phase.

In cell D5 a mantle wedge (V_s about 4.1 km/s) is detected just below the Moho and it overlies a high velocity lid (V_s about 4.5 km/s) that reaches the velocity of 4.8 km/s and the depth of about 160 km. The V_s around 4.1 km/s implies that, in the mantle wedge, the partial melting is around 1-2% (BOTTINGA & STEINMETZ, 1979).

3.3. - THE ASTHENOSPHERE.

The properties below the uppermost upper mantle change significantly going from Sicily, through the Tyrrhenian Sea and towards the Apennines. In fact, the depth of the top of the asthenosphere is very variable and its bottom is not always detected at about 200-250 km of depth.

In c0-c2 (fig. 2a) the asthenosphere has a V_s of about 4.3-4.4 km/s, and it starts at a depth of about 170 km in c1-c2 and of about 70 km in c0. Cells c3 and b0-b3 are characterized by an asthenosphere with V_s varying in the range 4.00-4.25 km/s whose top is at the depth of about 80 km in b0 and between 135-160 in b1-b3 and c3. The estimated thickness of the asthenosphere is about 100 km in c3, b0, b2 and 70 km in b1, and not detectable in b3 (as in the cells c0-c2). In cells b1-b2 and a1-a4, the shallow mantle wedge is separated from the asthenosphere by a high velocity lid, very variable in thickness. In cells b1 and a1 the asthenosphere is only about 60-70 km thick and centred at an average depth of about 160 km. In b2 it

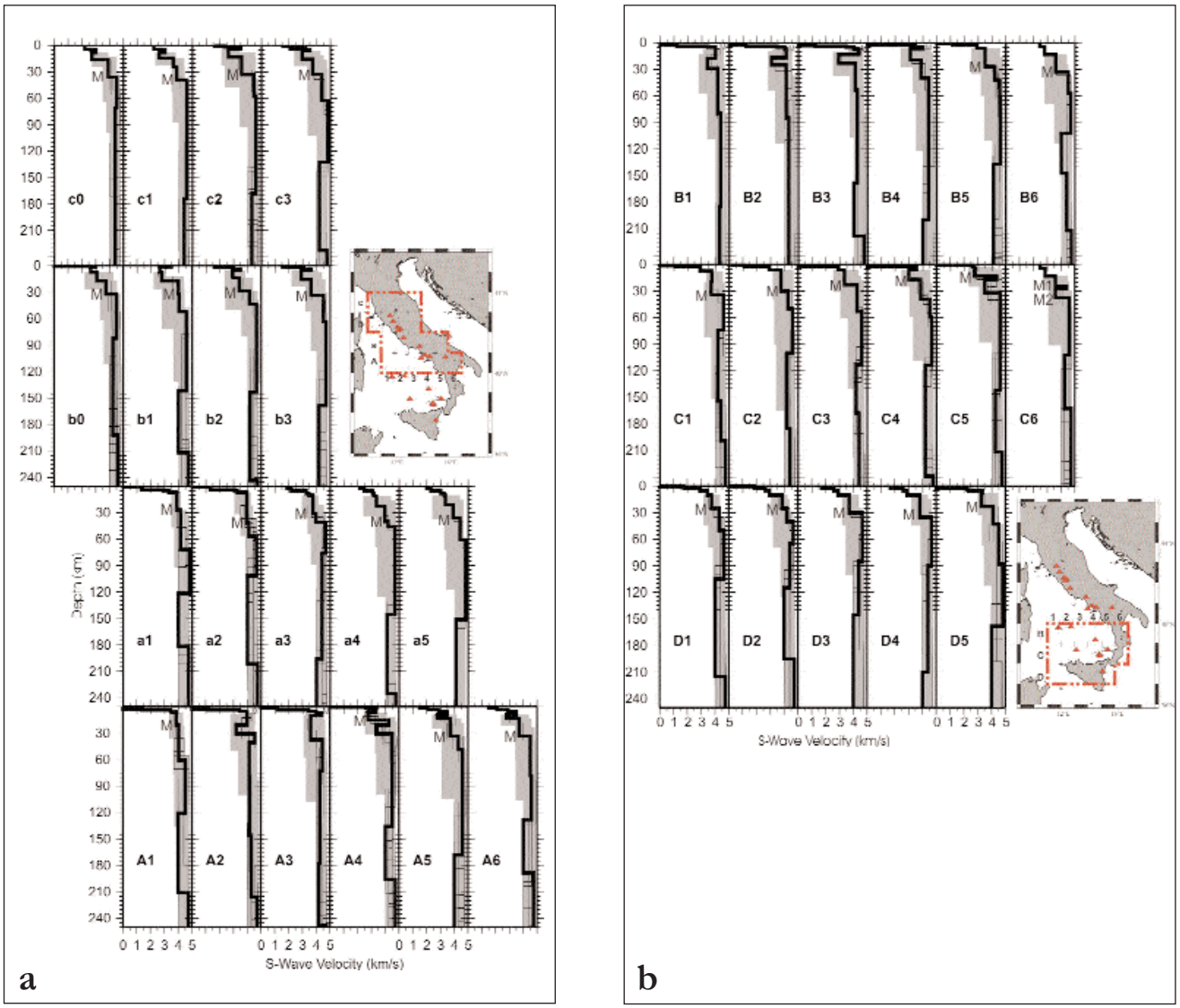

Fig. 2. - *(a and b) The set of solutions (thin lines) obtained through the non–linear inversion of the dispersion relations of each cell in the evidenced area (indicated in the insert). The investigated parameter's space (grey zone) and the chosen solution (bold line) are shown as well. The Moho is marked with M. M1 and M2, in cell C6, indicate the lithospheric doubling.*

is deep as in b1 and has a thickness of about 100 km. In cell A1 the asthenosphere, with V_s around 4.0 km/s, starts around the depth of 120 km and ends at the depth of about 210 km. Going from cell a2 to cell a5, the asthenospheric layer is very different. In cell a2 the top of the asthenosphere is at a depth of about 100 km, with a thickness of about 100 km. The asthenospheric V_s in a3 ranges from 4.4 km/s to 4.0 km/s. Finally, in a4-a5 the asthenosphere is characterized by V_s around 4.2 km/s and in a5 it reaches a depth larger than 250 km.

In the central part of the Tyrrhenian Sea study area, the asthenosphere is as shallow as about 10 km and, between the Tyrrhenian and Ionian basins (see PANZA *et alii*, 2003), the asthenosphere is interrupted by a seismogenic high velocity body dipping towards NW (cells C5 and C6, fig. 2b).

In cells A2-A4 the high velocity lid is surmounted by a mantle wedge (V_s about 3.35-4.25 km/s) originally detected by CALCAGNILE & PANZA (1981), PANZA *et alii* (1980) and confirmed by the geochemical analysis of LOCARDI (1986). A similar situation is seen in cells C4 and C5, where the V_s in the wedge is in the range 3.50-4.35 km/s. In the cells, A2-A3 and B1-B3, V_s reaches the maximum velocity of about 4.35 km/s in the lower asthenosphere. The lower bound of the asthenosphere is at a depth of about 215 km in A2 and B3, 245 km in A3 and deeper than 250 km in B1-B2. In cells A4-A6 the asthenosphere is very pronounced (V_s about 4.0 km/s), it starts at a depth variable in the range from 130 to 170 km and reaches the depth of about 190 km in A4 and A6 and larger

than 250 km in A5. In cells A4 and A5, the relatively low velocity layer could have the same origin as in cells C5 and C6.

In B4, where the asthenosphere is perturbed by a layer with relatively high velocity at about 4.4 km/s, and B5 the V_s at the low velocity asthenospheric layer varies in the range 4.00-4.10 km/s and the bottom of the low velocity layer reaches a depth larger than 250 km.

In A6 and B6 the asthenosphere starts at a depth of about 130 km and 100 km, respectively, and extends for 60-100 km with V_s about 4.0 km/s in A6 and ranging from 4.0 km/s to 4.4 km/s in B6. In cells C1-C4, going towards East, the asthenosphere is as deep as about 75 km reaching a maximum depth of about 115 km. The V_s is in the range 4.20-4.40 km/s in C1-C3 and is about 4.20 km/s in C4, with the bottom of the low velocity layer detectable at depth exceeding 200 km only in C1 and C4. The cells C6 and C5 are characterized by a low velocity layer about 60-70 km thick and with V_s about 4.25 km/s, deeper in C5 than in C6. The asthenospheric low velocity layer is well developed in cells D1-D5 (with the minimum V_s about 4.0 km/s) with the top varying in the depth range from 65 to160 km. In D5 a relatively high velocity body (V_s in the range 4.5-4.8 km/s) separates the asthenosphere from the shallow mantle wedge with V_s around 4.10 km/s.

4. - PETROLOGICAL DATA AND METHOD

The study of primary (i.e., not modified by evolution processes) or near-primary magmatic rocks is able to furnish a wealth of information on the composition of their source zones. Since basaltic magmas come from the upper mantle, their study can provide important information on mantle composition and evolution.

The major element composition of primary magmas depends on the type and proportion of the phases that enter into the melt during anatexis. This can be better understood by the use of phase diagrams, which can be constructed either experimentally or on the basis of free energy values of various phases at different P-T conditions. Phase diagrams are able to furnish information on the stability fields of mineral phases, the proportions of the phases that enter into the melt, the major element composition and the degree of silica saturation of the melts, and the modification of melt compositions with changing degrees of anatexis.

Trace elements give additional and complementary information on melt composition and their source. The equation that describes the variation of trace elements during equilibrium batch melting is:

$$C_l/C_0 = 1/(D(1-F)+F) \quad (1)$$

where Cl is the concentration of a given trace element in the magma, C0 is the concentration of the same element in the source rock, D (partition coefficient) is the ratio between the abundance of the element in the residual minerals and in the coexisting melt; F is the degree of partial melting.

Some elements, known as *incompatible,* strongly prefer to enter the liquid phase during partial melting (i.e. D~0). For the mantle rocks, incompatible elements include Th, U, Ta, Nb, Rb, Ba, Light Rare Earth Elements (LREE), Zr, etc. When D = 0 equation (1) becomes:

$$C_l/C_0 \sim 1/F \quad (2)$$

Equations (1) and (2) demonstrate that the concentration of an incompatible element in the magma depends on the concentration of the element in the source rock, and increases with decreasing degrees of partial melting.

However, ratios of incompatible elements are largely independent of the degrees of partial melting and reflect source composition. Therefore, different ratios of highly incompatible elements in basaltic magmas suggest distinct values for the source rocks. These, in turn, reveal different evolutionary histories of the mantle sources. Study of incompatible element ratios in mantle-derived magmas is helpful for reconstructing the nature of these modifications.

The isotopic ratios of several elements (e.g. $^{87}Sr/^{86}Sr$, $^{143}Nd/^{144}Nd$, $^{206}Pb/^{204}Pb$, $^{207}Pb/^{204}Pb$, $^{208}Pb/^{204}Pb$, $^{16}O/^{18}O$) are not significantly modified during equilibrium partial melting; primary magmas inherit the isotope signatures of their sources. Therefore, isotope composition of basaltic rocks is of key importance to understand the composition and evolution of mantle rocks.

One of the main problems in investigating the mantle composition, through the study of basaltic rocks, is that magmas erupted at the surface rarely represent unmodified primary melts. In most cases, they undergo geochemical diversification by fractional crystallisation, assimilation, and mixing, or, more commonly, by a combination of these processes. However, closed-system fractional crystallisation produces strong variations in major and trace element abundances, but leaves incompatible element ratios and isotopic signatures unaffected. On the contrary, assimilation and mixing may generate dramatic modification of the element abundances and ratios, and of the isotope signatures. Therefore, a golden rule for studies of mantle compositions through studies of the magmatism is to focus on the most primitive rocks

(e.g. those with the highest Ni, Cr, MgO and Mg# = Mg/(Mg+Fe^{+2}) atomic ratio). Primary mantle-equilibrated magmas have Mg# around 70, Ni = 250-300 ppm and Cr = 500-600 ppm. Therefore, basalts with high Mg#, Ni and Cr are the closest representatives of their mantle-equilibrated parents and furnish the maximum of information on mantle composition and processes.

5. - REGIONAL LITHOSPHERIC MODELS FROM PETROLOGICAL-GEOCHEMICAL DATA

Petrological and geochemical data of mafic rocks can be used to place constraints on the composition of the upper mantle beneath the Italian Peninsula and the Tyrrhenian see floor. Figure 3 is a classification diagram based on ΔQ vs. K_2O/Na_2O relationships (PECCERILLO, 2001a). ΔQ is the algebraic sum of normative quartz (Q), minus nepheline (ne), leucite (lc), kalsilite (ks) and forsterite; it measures the degree of silica saturation of magmas: ΔQ<0 means undersaturated magmas, whereas ΔQ>0 reveals silica oversaturated magmas.

It can be noticed that the Italian mafic volcanics range from tholeiitic and calcalkaline to Na-alkaline, shoshonitic, potassic and ultrapotassic. This is a strong regional variation of magma types. For instance, Na-alkaline rocks occur in Sicily; calcalkaline and shoshonitic rocks are concentrated in the Aeolian arc; potassic and ultrapotassic rocks represent the main magma types along the Italian peninsula. However, the potassic and ultrapotassic rocks from Umbria and Tuscany have different composition than other K-rich rocks from central Italy, and the Vulture rocks are strongly undersaturated in silica and have variable K_2O/Na_2O ratios.

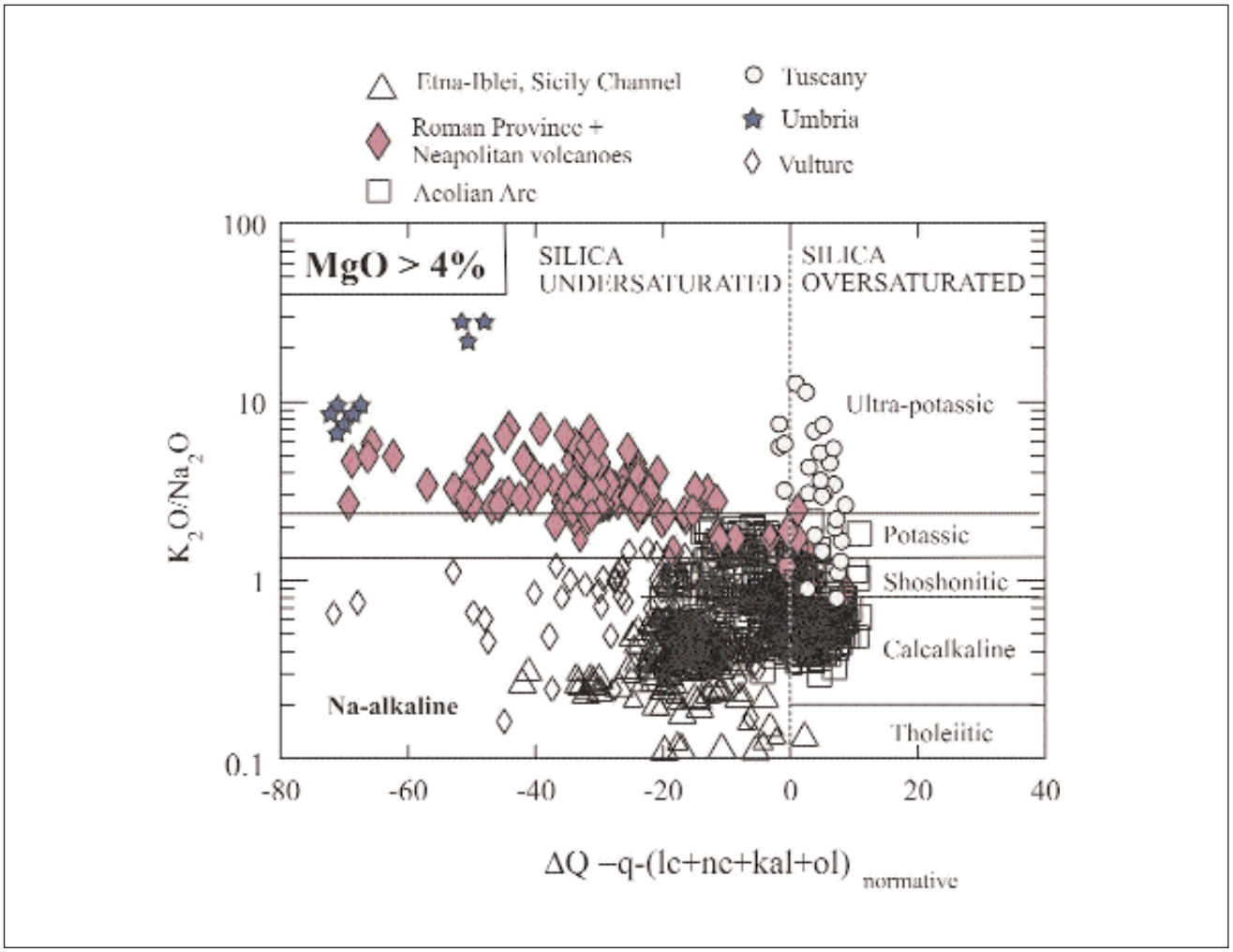

Fig. 3. - *Classification diagram based on ΔQ vs. K2O/Na2O for Plio-Quaternary mafic rocks (MgO > 4 wt%) from Italy. ΔQ is the algebraic sum of normative quartz (Q), minus leucite (lc), nepheline (ne), kalsilite (kal) and olivine (ol); it measures the degree of silica saturation of rocks. Silica oversaturated rocks have ΔQ> 0, whereas silica undersaturated rocks have ΔQ < 0. Modified after* PECCERILLO (2001a).

Other differences among various potassic rocks are found for Na_2O, Al_2O_3, CaO concentrations. Tuscany ultrapotassic rocks are depleted in Na_2O, CaO and Al_2O_3: this particular type of ultrapotassic rocks are known as *lamproites*. The rocks from Umbria are low in Na_2O and Al_2O_3 but have high CaO: these ultrapotassic rocks are known as ultrapotassic *kamafugites* (PECCERILLO *et alii*, 1988).

Most mafic rocks in Italy have higher Na_2O, Al_2O_3, CaO than lamproites, and variable potassium contents. These rocks are known as Roman-type potassic (KS) and ultrapotassic (HKS) rocks (FOLEY *et alii*, 1987). KS rocks are moderately rich in potassium and are nearly saturated in silica; HKS rocks have $K_2O > 3$ and $K_2O/Na_2O > 2.5$, and are strongly undersaturated in silica. KS and HKS form the large volcanic complexes of Vulsini, Vico, Sabatini and Alban Hills, the Ernici and Roccamfonfina centres, and the Campania volcanoes (i.e. Ischia, Vesuvio and Phlegraean Fields).

Major elements and the degree of silica saturation give important clues as to the genesis of the various groups of Italian mafic rocks. The low Ca, Na and Al of lamproites indicate a generation in an upper mantle that was depleted in Ca- and Na- bearing phases such as clinopyroxene. Therefore, a harzburgite source, i.e. a rock mainly formed of orthopyroxene and olivine, is inferred for lamproites. The silica oversaturated nature of lamproitic magmas suggests melting at low pressure (FOLEY, 1992). However, the high K_2O content of these rocks require a K-rich phase (e.g., phlogopite, pargasite) in the mantle. In summary, lamproites reveal the occurrence of a phlogopite-rich harzburgitic mantle at low pressure beneath southern Tuscany.

The high CaO of kamafugites require abundant clinopyroxene; moreover, high K points to phlogopite bearing upper mantle. Therefore, the kamafugite source may be represented by a phlogopyre clinopyroxenite. Kamafugites occur in Umbria, and this points to the presence of clinopyroxenite upper mantle beneath this region.

The high Al, Ca, K, and Na of Roman-type rocks suggest that mantle sources were represented by a phlogopite- clinopyroxene- bearing peridotite. The variable enrichment in potassium of KS and HKS likely relates to different degrees of partial melting and/or to a variable quantity of phlogopite in the mantle.

A particular type of alkaline rocks, rich in both Na and K, occur at Mount Vulture (DE FINO *et alii*, 1986). High alkalis make the rocks in this volcano distinct from any other potassic rocks from central-southern Italy. However, the origin of these rocks is still poorly understood.

The calcalkaline and shoshonitic rocks have comparable Al, Ca and Na contents as the Roman-type rocks, but display comparable to lower potassium contents. The major element chemistry suggests a genesis in lherzolitic sources, but with low amounts of potassium-rich phases. Moreover, the CA magmas require hydrous conditions during partial melting (e.g. WENDLANDT & EGGLER, 1980). Therefore, petrological data suggest the presence of a hydrated lherzolitic upper mantle beneath the Aeolian arc.

Thus, the major element data suggest that the volcanism of central southern Italy has been generated in petrologically heterogeneous mantle sources. Since various types of magmas are concentrated in different regions, the obvious implication is that the upper mantle beneath Italy is a mosaic of mineralogically different peridotitic rocks.

Trace element and isotope geochemistry can furnish additional constraints on the nature of the upper mantle beneath Italy. Variations of key incompatible element ratios and isotopes are shown in figure 4 and figure 5.

It can be noticed that mafic rocks from various volcanic areas define different trends or plot in different areas, which calls for geochemically different mantle sources. In particular, it can be noted that the volcanic rocks from Naples area plot in the same field as Stromboli. These rocks show strong compositional differences as Tuscany and Roman areas. Moreover, the rocks from Roccamonfina and Ernici Mts. partially plot with Neapolitan volcanoes and partly with Roman volcanics. Therefore, the Ernici Mts.-Roccamonfina region is characterised by the coexistence of two geochemically and isotopically distinct rocks suites.

In conclusion, major element, trace element and isotopic data on mafic rocks suggest that Italian volcanism can be subdivided into different magmatic provinces, which were generated by petrologically and geochemically distinct mantle sources. These zones are shown in figure 6 (PECCERILLO, 1999; PECCERILLO & PANZA, 1999).

5.1. - SOUTHERN TUSCANY PROVINCE

The province extends from southern Tuscany and the Tuscan archipelago to the Tolfa-Manziana zone. It is formed by an association of mantle-derived mafic magmas and crustal anatectic acid rocks. Mafic rocks have variable enrichment in potassium, but have peculiar incompatible trace element ratios and isotope signatures. Lamproitic rocks occur in this region, which suggest a phlogopite-bearing harzburgitic upper mantle at low pressure. All the mafic rocks have crustal-like isotopic signatures (e.g., $^{87}Sr/^{86}Sr$ around 0.712-0.717; POLI *et alii*, 1984; CONTICELLI & PECCERILLO, 1992; CONTICELLI *et alii*, 2001). Acid crustal anatectic intrusive and effusive rocks (e.g. Roccastrada, Elba, etc.) associated with mafic magmas are likely related to intra-crustal anatexis induced by isotherm uprise during mafic magma emplacement.

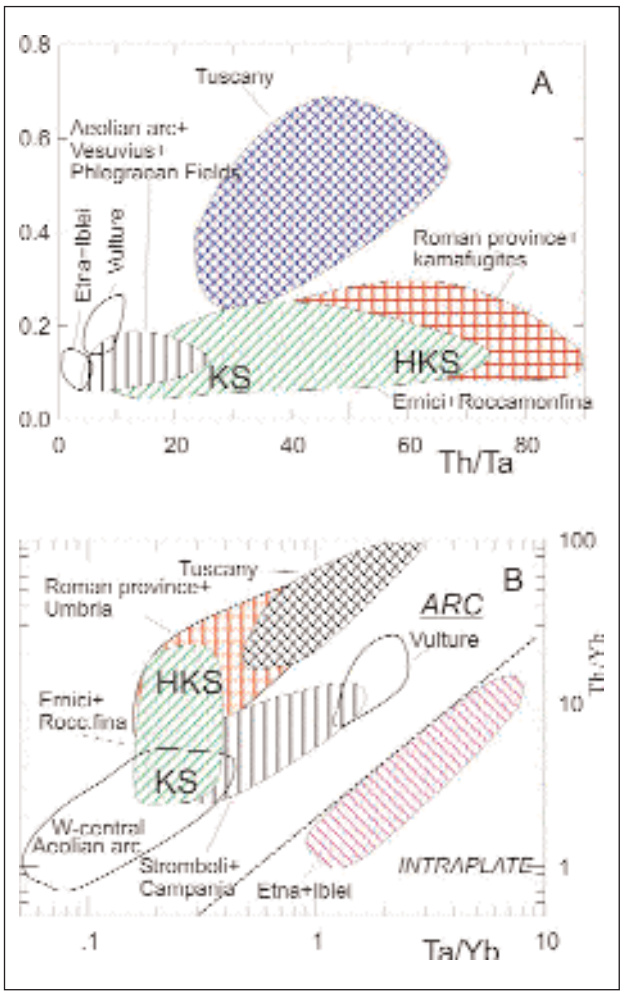

Fig. 4. - *Variation of trace element ratios in the Plio-Quaternary mafic rocks (MgO > 4 wt%) from Italy. Note that: 1) rocks from the various zones plot in different fields; 2) Stromboli and Neapolitan volcanoes plot along the same trend; 3) the Ernici and Roccamonfina potassic rocks (KS) plot with Campania-Stromboli, whereas ultrapotassic rocks (HKS) plot in the filed of the Roman Province.*

5.2. - Roman Province s.s.

The province includes the Vulsini Mts., Vico, Sabatini and the Alban Hills. It is formed by KS and HKS rocks with variable degree of evolution. Trace element ratios are different from those of Tuscany rocks; moreover isotope compositions are less extreme than in Tuscany (e.g. $^{87}Sr/^{86}Sr$ is typically around 0.710; e.g., Conticelli & Peccerillo, 1992). The high CaO, Al_2O_3, Na_2O and K_2O contents of Roman province reveal the presence of phlogopite-bearing lherzolitic mantle sources beneath the Roman area.

5.3. - Umbria province

The province is formed by kamafugitic rocks, which have incompatible element ratios and isotopic signatures similar as those of the Roman province. However, the low Na and Al and the very high CaO and K_2O suggest the presence of a phlogopite-clinopyroxenite mantle source for these magmas, which is distinct from the Roman province.

5.4. - Ernici-Roccamonfina

The province consists of potassic and ultrapotassic (KS and HKS) rocks that display distinct enrichment in potassium and incompatible elements, and isotopic signatures. KS rocks are similar to Neapolitan volcanoes and Stromboli, whereas HKS resemble Roman rocks. This testifies to the occurrence of a compositionally zoned upper mantle beneath Ernici-Roccamonfina, which is peculiar of this area.

5.5 - Campania Province- Stromboli

Campania volcanoes are represented by the active volcanoes of Naples area (Vesuvio, Phlegraean Fields and Ischia) and by slightly older volcanic rocks found by borehole drilling (Di Girolamo, 1978). Stromboli consists of calcalkaline, shoshonitic and potassic rocks, which show strong compositional similarities with the Campanian volcanoes (Peccerillo, 2001b). However Vesuvio shows an ultrapotassic composition, which is not found at Stromboli, Ischia and Phlegraean Fields.

5.6. - Aeolian arc.

Two sectors can be distinguished in the Aeolian arc. The western Aeolian arc basically consists of CA volcanics with low $^{87}Sr/^{86}Sr$ (= 0.7035-0,7045). The eastern sector (Panarea and Stromboli) consists of calcalkaline to KS rocks with Sr isotope ratios of about 0.704 to 0.707 (i.e. from the low values typical of the western arc to those typical of Campania volcanoes; De Astis *et alii*, 2000).

5.7. - Mount Vulture

The alkaline rocks are enriched in both Na and K, and hauyne rather than leucite is the most typical feldspathoidal mineral. Vulture rocks have major and trace element composition that is distinct from other Italian volcanics, which indicates a different mantle source

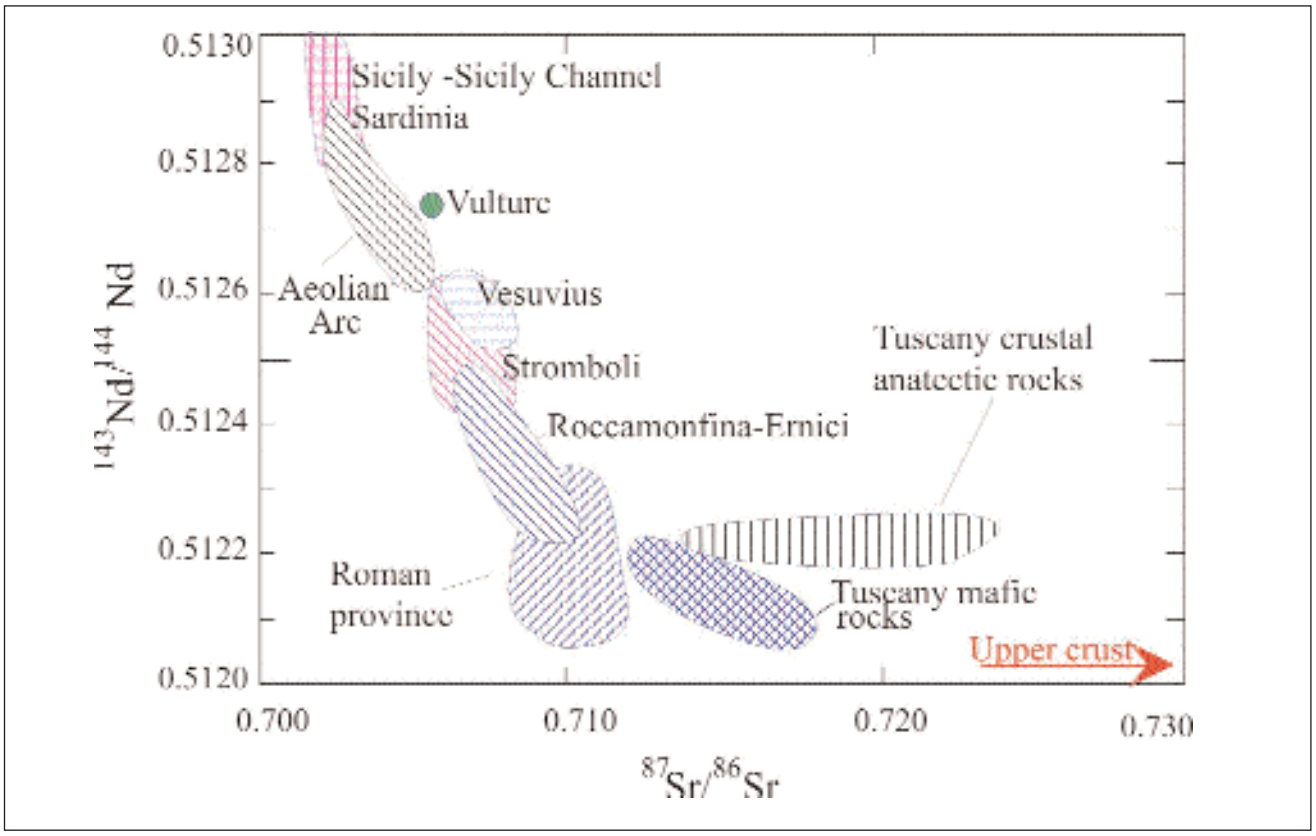

Fig. 5. - *Plot of $^{87}Sr/^{86}Sr$ vs. $^{143}Nd/^{144}Nd$ in the Plio-Quaternary mafic rocks (MgO > 4 wt%) from Italy.*

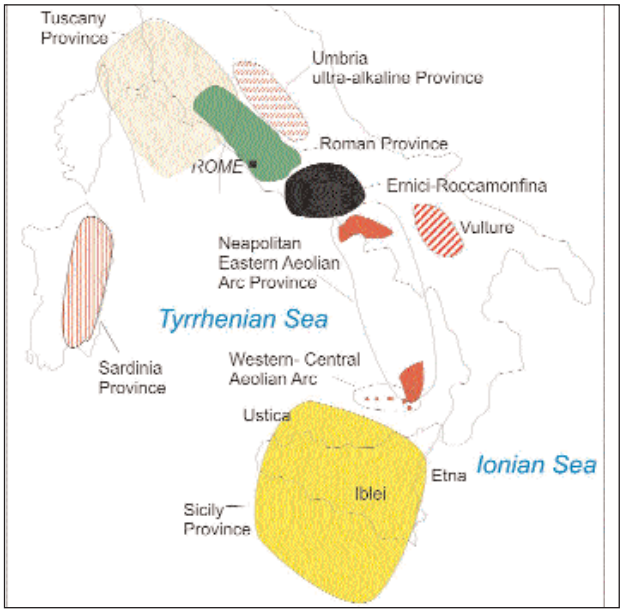

Fig. 6. - *Plio-Quaternary magmatic provinces in Italy. Modified after* Peccerillo & Panza (1999).

5.8. - Sicily Province

The province consists of tholeiitic and Na-alkaline rocks (Etna, Iblei, Sicily Channel) with distinct trace element and isotopic composition as the other provinces. All these centres display typical intraplate geochemical affinity.

5.9. - Tyrrhenian Sea

A large volume of volcanic rocks are hidden below the Tyrrhenian Sea. The few data available on the Tyrrhenian seamounts indicate a compositional variability. Tholeiitic rocks seem to prevail among the younger products. Ages range from Miocene to Pliocene and increase in age going westward toward the Oligocene-Miocene calcalkaline and shoshonitic belt of Sardinia. This magmatism is the result of the SE migration of subduction processes and of asthenospheric mantle uprise behind the volcanic arc (e.g. Beccaluva *et alii*, 1989; Locardi, 1988 and 1993; Locardi & Nicolich, 1988).

6. - THE MODELS TYING PETROLOGICAL AND GEOPHYSICAL DATA

In figure 7 the selected solutions for the 10x10 cells containing recent volcanism are shown. On the base of the discussed data it is possible to recognize the following groups:

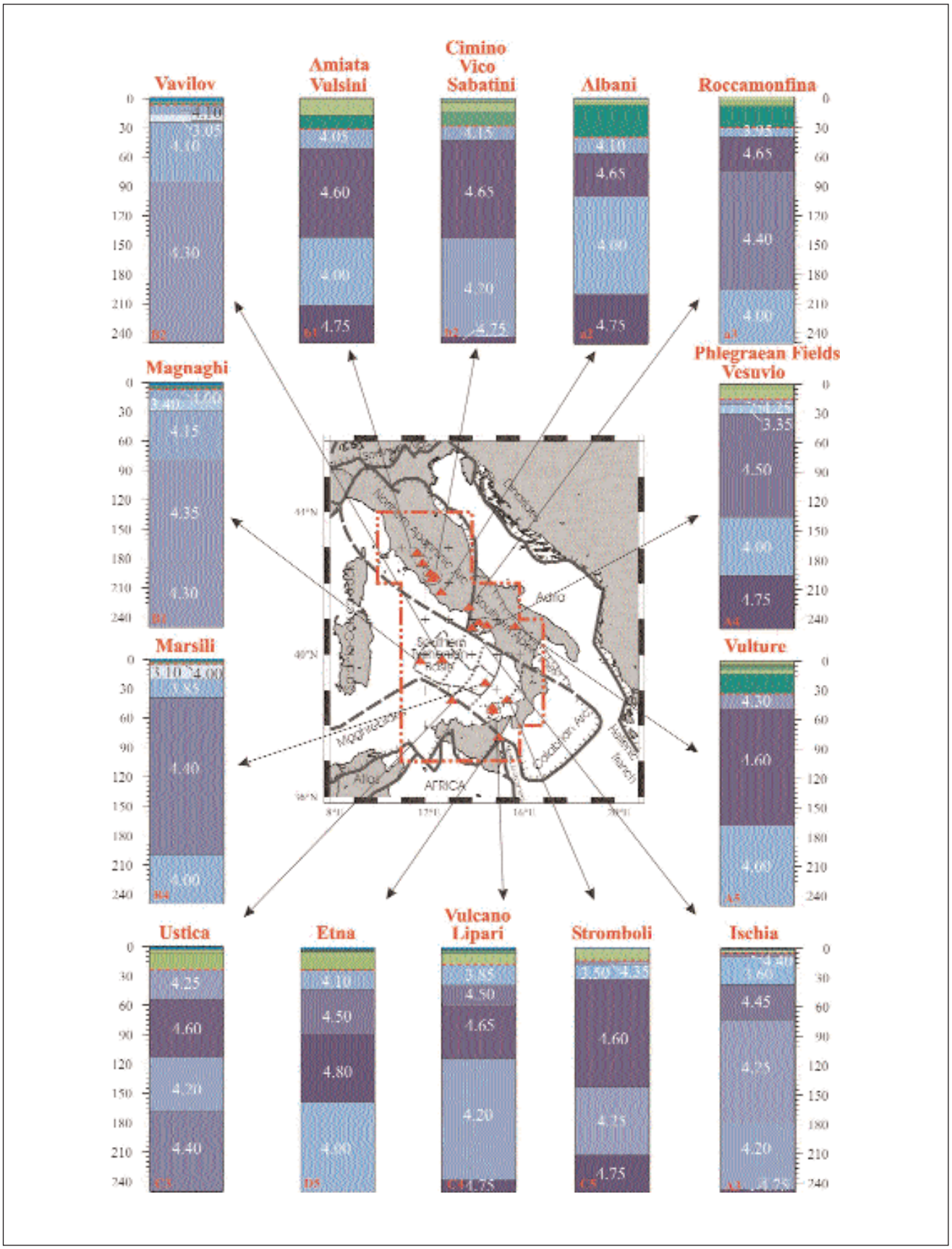

Fig. 7. - *The chosen structure (the solution of each set indicated by bold line in fig. 2) of the cells (indicated in red) containing the recent volcanoes (indicated by red triangles in the central frame): Amiata-Vulsini (b1), Cimino-Vico-Sabatini (b2), Albani (a2), Roccamonfina (a3), Phlegraean Fields-Vesuvio (A4), Vulture (A5), Ischia (A3), Stromboli (C5), Vulcano-Lipari (C4), Etna (D5), Ustica (C3), Marsili (B4), Magnaghi (B1), Vavilov (B2).*

6.1. - Magnaghi, Vavilov and Marsili

Magnaghi, Vavilov and Marsili are characterized by a thin crust sitting on a very thin lid bounding a very low velocity layer in the mantle. This low velocity in the uppermost mantle can be interpreted as the indication of the existence of large amounts of melt. These seamounts represent back arc volcanoes with a dominant tholeitic petrochemical affinity, which requires a genesis at low pressure by high degree (some 10%) of partial melting in the mantle. Therefore this uppermost mantle low velocity layer seems to be the source of the back arc volcanism in the Tyrrhenian.

6.2. – Ustica, Etna and Vulture

Ustica, Etna and Vulture are characterized by a continental crust with thickness variable from about 23 to about 33 km, that overlies a mantle whose uppermost part, up to a depth of about 50 km, has V_s in the range from about 4.1 km/s (Etna) to about 4.3 km/s (Vulture); below this layer, the lid (V_s about 4.5-4.8 km/s) extends to depths between 115-170 km. The three volcanoes have variable geochemical signatures. Etna and Ustica have Na-alkaline affinity, similar trace elements and Sr isotopic compositions, which fall in the range of the intraplate volcanoes, even if evidence for a subduction related geochemical component has been found (Cristofolini *et alii*, 1987; Cinque *et alii*, 1988). The Vulture volcano results from the interaction between intraplate and subduction related reservoirs, but the subduction component is much stronger that at Etna and Ustica. In spite of the variable petrological, geochemical and isotopic signatures, subduction and intraplate components have played a role in the genesis of these volcanoes. The unifying elements of these volcanoes are: (a) their lateral position with respect to the active subduction, (b) the coexistence of subduction and intraplate related geochemical signatures, (c) similar structure of the lithosphere-asthenosphere system. Thus, the structure of the magma sources and the geochemical signatures could be related to the contamination of the side intraplate mantle by material coming from the either active (the case of Etna) or ancient (the cases of Ustica and Vulture) roll back.

6.3. – Stromboli, Phlegraean Fields and Vesuvio

Stromboli, Phlegraean Fields and Vesuvio are characterized by a thin continental crust (about 15 km thick). Below the crust there is a mantle wedge with V_s as low as about 3.35-3.50 km/sec in its deeper part and about 4.25-4.35 km/s just below the Moho (the lid). In correspondence of the Phlegraean Fields and Vesuvio, the layering under the wedge is consistent with the presence of a subducted lithospheric slab (Ionian/Adria slab), seismically active at depth larger than 300 km, and the crust contains a well developed low velocity layer, about 10 km thick and centred at a depth of about 10 km. The strong similarity in the geochemical and isotopic composition between Stromboli and Phlegraean Fields and Vesuvio matches well the similarity in the lithospheric structural models. The anomalous K enrichment in Vesuvio magmas could be a feature acquired either by melting of higher proportion of a K-rich phase or may be related to low pressure magma evolution.

6.4. – Vulcano and Lipari

Vulcano and Lipari are in a thin continental crust, less than 20 km thick, that overlies a very soft upper mantle (V_s ~ 3.85 km/s). In the mantle the V_s reaches about 4.65 km/sec and about 115 km of depth. This lithospheric structural setting has relevant affinities with the models described for Etna and Ustica rather than to the one of the nearby Stromboli. The structural difference between Vulcano and Stromboli lithosphere is not surprising considering the different geochemical signatures. On the other side, the affinity between Vulcano, Lipari and Etna could be explained by the common position along the Tindari-Letoianni-Malta fault zone. The clear difference in V_s distribution, between the Eastern (Stromboli) and the Central-Western (Vulcano and Lipari) sectors of the arc, could have been partly masked by a different positioning of the 10x10 cells, therefore the geochemical data are a strong support for our findings. Zanon *et alii* (2003), Frezzotti *et alii* (2003), in their model of the Vulcano island and Aeolian arc magmatic evolution, suggest the existence of a deep accumulation reservoir, at about 18-21 km, and of a shallow accumulation level in the upper crust, at a depths of 1.5-5.5 km. Petrological and geochemical data of Gauthier & Condomines (1999), Francalanci *et alii* (1999) show that the magma of the volcano has properties that are characteristic of magma chambers located at different depths. It is possible to associate the layer with V_s at about 3.85 km/sec, just below the Moho, to the deepest magma reservoir found by Zanon *et alii* (2003), Frezzotti *et alii* (2003), while the resolution of our data does not allow us to sort out the uppermost (crustal) accumulation zone.

6.5. – Ischia

Ischia is geochemically and petrologically belonging to the other Campanian volcanoes. Therefore the quite remarkable difference in the structural lithospheric

model, with respect to the Phlegraean Fields and Vesuvio, could be partly related to the resolving power of our geophysical data and, however, it could reveal a transition to the Tyrrhenian domain.

6.6. – Amiata, Vulsini, Cimino, Vico, Sabatini, Albani, Roccamonfina

Amiata, Vulsini, Cimino, Vico, Sabatini, Albani, Roccamonfina sit on a continental crust about 30 km thick (40 km for Albani) and the V_s below the Moho is rather low (in the range 3.95-4.15 km/sec). The main differences are seen below the high velocity lid (about 4.6 km/s). The asthenospheric "low" velocity layer (V_s < 4.4 km/s) is very deep (it starts at about 200 km of depth) under Roccamonfina, while it is about 145 km deep in Cimino-Vico-Sabatini and Amiata-Vulsini, and 100 km deep in Albani. The region from Vulsini to Albani Hills is rather homogenous from a petrological point of view, being mainly formed by ultrapotassic rocks with poorly variable geochemical and isotopic signatures. On the other side, the Roccamonfina area differs significantly form the northern Latium volcanoes because of the occurrence of both potassic and ultrapotassic rocks with very distinct geochemical and isotopic compositions. Also in this case the differentiation of the provinces of Roccamonfina and Latium finds a correspondence in the upper mantle structure.

7. - CONCLUSIONS

In the Tyrrhenian Sea area, large-scale inhomogeneities in the lithosphere-asthenosphere structure are reflected by large variations in the composition of magma types.

The main features identified by our geophysical study are: (1) a low velocity mantle wedge, just below the Moho, as the common feature detected in all the cells containing inactive recent volcanoes (Amiata, Vulsini, and Cimino, Vico, Sabatini, Albani Hills and Roccamonfina) in the Tuscany and Roman regions; (2) a very thick rigid body in the upper mantle beneath the Ernici-Roccamonfina province that exhibits a distinct geochemical and isotopic compositions when compared with the Roman province; (3) a shallow and very low V_s layer in the mantle in the areas of Aeolian islands, Vesuvio, Ischia and Phlegraean Fields, which represents their shallow-mantle magma source; (4) a very shallow crust-mantle transition in the Southern Tyrrhenian Sea and very low V_s just below a very thin lid in correspondence of the submarine volcanic bodies (Magnaghi, Marsili & Vavilov); (5) a shallow mantle wedge, below Etna's crust, consistent with the hypothesis of the presence of an asthenospheric window feeding the volcano; (6) the subduction of the Ionian lithosphere towards NW below the Tyrrhenian Basin; (7) the subduction of the Adriatic/Ionian lithosphere underneath the Vesuvio and Phlegraean Fields.

Petrology and geochemistry reveal rocks ranging in composition from tholeiitic to calcalkaline to sodium- and potassium-alkaline and ultra-alkaline. Scrutiny of the relevant data allows us to recognize several magmatic provinces, which display distinct major and/or trace element and/or radiogenic isotope signatures: Tuscany, Latium (Roman Province), Umbria (kamafugitic province), Ernici-Roccamonfina, Campania Province, Stromboli, Vulture, Aeolian arc, Sicily and Sicily Channel, Tyrrhenian Sea and Sardinia. The rocks from the Aeolian arc and the Italian Peninsula range from calcalkaline to ultrapotassic, and display trace element ratios (e.g., Th/Ta, La/Nb etc.), which fall into the field of subduction-related (i.e., orogenic) magmatic suites. On the contrary, Sicily, the Sicily Channel and Sardinia rocks have intraplate, (anorogenic) geochemical characteristics.

The combined analysis of petrological, geochemical and geophysical data reveals a surprisingly close match between geophysical characteristics of the lithosphere-asthenosphere and the compositions of magmatic rocks erupted at the surface in the various regions. This suggests that variations of seismic wave velocity in the mantle could be related to compositional modifications of peridotite. The present paper, therefore, provides important constrains that must be considered by geodynamic models for the evolution of the Alpine-Apennines systems.

Aknowledgements

Part of this research is funded by Italian MIUR Cofin *(2001: Subduction and collisional processes in the Central Mediterranean; 2002: A multidisciplinary monitoring and multiscale study of the active deformation in the Northern sector of the Adria plate),* GNDT *(2000: Determinazione dello stile di deformazione e dello stato di sforzo delle macrozone sismogenetiche italiane) and* INGV *(Eruptive Scenarios from Physical Modeling and Experimental Volcanology). The research on Italian magmatism has been funded by* CNR, GNV-INGV *and by the* University of Perugia.

REFERENCES

Ahrens T.J. (1973) - *Petrologic properties of the upper 670 km of the Earth's mantle; geophysical implications.* Phys. Earth Planet. Inter., **7**: 167-186.

Anderson D.L. (2000) - *The thermal state of the upper mantle; no role for mantle plumes.* Geophys. Res. Lett., **27**: 3623-3626.

Bally A.W., Burbi L., Cooper C., & Ghelardoni R. (1986) - *Balanced sections and seismic reflection profiles across the Central Apennines.* Mem. Soc. Geol. It., **35**: 257-310.

Beccaluva L., Macciotta G., Morbidelli L., Serri G. &

TRAVERSA G. (1989) - *Cainozoic tectono-magmatic evolution and inferred mantle sources in the Sardo-Tyrrhenian area*. In: BORIANI A., BONAFEDE M., PICCARDO G.B. & VAI G.B. (Eds.): "*The lithosphere in Italy*". Atti Convegni Lincei, **80**: 229-248.

BISWAS N.N. & KNOPOFF L. (1974) - *The structure of the Upper Mantle under the U.S. from the dispersion of Rayleigh waves*. Geophys. J. R. Astr. Soc., **36**: 515-539.

BOLT B.A. & DORMAN J. (1961) - *Phase and Group velocity of Rayleigh waves in a spherical gravitating earth*. Journal of Geophysical Research, **66**: 2965-2981.

BOTTINGA Y. & STEINMETZ L. (1979) - *A geophysical, geochemical, petrological model of the sub-marine lithosphere*. Tectonophysics, **55**: 311-347.

CALCAGNILE G. & PANZA G.F. (1981) - *The main characteristics of the lithosphere-astenosphere system in Italy and surrounding regions*. Pure Appl. Geophys., **119**: 865-879.

CALCAGNILE G., D'INGEO F., FARRUGIA P. & PANZA G.F. (1982) - *The lithosphere in the central-eastern Mediterranea area*. Pure Appl. Geophys., **120**: 389-406.

CAPUTO M., KNOPOFF L., MANTOVANI E., MUELLER S. & PANZA G.F. (1976) - *Rayleigh waves phase velocities and upper mantle structure in the Apennines*. Ann. Geof., **29**: 199-214.

CATALANO R., DI STEFANO P., SULLI A. & VITALE F.P. (1996) *Paleogeography and structure of the central Mediterranean: Sicily and its offshore area*. Tectonophysics, **260**: 291-323.

CATALANO R., DOGLIONI C. & MERLINI S. (2001) - *On the Mesozoic Ionian Basin*. Geophys. J. Int., **144**: 49-64.

CERNOBORI L., HIRN A., MCBRIDE J.H., NICOLICH R., PETRONIO L., ROMANELLI M. & STREAMERS/PROFILES WORKING GROUPS (1996) - *Crustal image of the Ionian basin and its Calabrian margin*. Tectonophysics, **264**: 175-189.

CHIMERA G., AOUDIA A., SARAO' A. & PANZA G.F. (2003) - *Active Tectonics in Central Italy: constraints from surface wave tomography and source moment tensor inversion*. Phys. Earth Planet. Inter., **138**: 241-262.

CINQUE A., CIVETTA L., ORSI G. & PECCERILLO A. (1988) - *Geology and geochemistry of the Island of Ustica (Southern Tyrrhenian Sea)*. Boll. Soc. Ital. Miner. Petrol., **43**: 987-1002.

CONTICELLI S. & PECCERILLO A. (1992) - *Petrology and geochemistry of potassic and ultrapotassic volcanism from Central Italy: inferences on its genesis and on the mantle source evolution*. Lithos, **28**: 221-240.

CONTICELLI S., D'ANTONIO M., PINARELLI L., CIVETTA L. (2001) - *Source contamination and mantle heterogeneity in the genesis of Italian potassic and ultrapotassic rocks: Sr-Nd-Pb isotope data from Roman Province and southern Tuscany*. Mineral. Petrol., **74**: 189-222.

CRISTOFOLINI R., GHISETTI F., SCARPA R. & MEZZANI L. (1985) - *Character of the stress field in the Calabrian Arc and Southern Apennines (Italy) as deduced by geological, seismological and volcanological information*. In: EVA, C. PAVONI, N (Eds.): *"Seismotectonics"*. TECTONOPHYSICS, **117**: 39-58.

CRISTOFOLINI R., MENZIES M.A., BECCALUVA L. & TINDLE A. (1987) - *Petrological notes on the 1983 lavas at Mount Etna, Sicily, with reference to their REE and Sr-Nd isotopic composition*. Bull. Volcanol., **49**: 599-607.

DE ASTIS G., PECCERILLO A., KEMPTON P.D., LA VOLPE L. & WU T.W. (2000) - *Transition from calcalkaline to potassium-rich magmatism in subduction environments: geochemical and Sr, Nd, Pb isotopic constraints from the Island of Vulcano (Aeolian arc)*. Contrib. Mineral. Petrol., **139**: 684-703.

DE FINO M., LA VOLPE L., PECCERILLO A., PICCARRETA G. & POLI G. (1986) - *Petrogenesis of Monte Vulture volcano (Italy): inferences from mineral chemistry, major and trace element data*. Contrib. Miner. Petrol., **92**: 135-145.

DE GORI P., CIMINI G.B., CHIARABBA C., DE NATALE G., TROISE C. & DESCHAMPS A. (2001) - *Teleseismic tomography of the Campanian volcanic area and surrounding Apenninic belt. J. Volc.* Geoth. Res., **109**: 55-75.

DEGROOT-HEDLIN C. & CONSTABLE S. (1990) - *Occam's inversion to generate smooth, two-dimensional models from magnetotelluric data*. Geophysics, **55**: 1613-1624.

DELLA VEDOVA B., PELLIS G. & PINNA E. (1989) - *Studio geofisico dell'area di transizione tra il Mar Pelagico e la piana abissale dello Ionio*. Atti 8° Convegno Annuale G.N.G.T.S., Roma, 543-558.

DELLA VEDOVA B., MARSON I., PANZA G.F. & SUHADOLC P. (1991) - *Upper mantle properties of the Tuscan-Tyrrhenian area: a framework for its recent tectonic evolution*. Tectonophysics, **195**: 311-318.

DE MATTEIS R., LATORRE D., ZOLLO A. & VIRIEUX J. (2000) - *1D P-velocity models of Mt. Vesuvio Volcano from the Inversion of TomoVes96 first arrival time data*. Pure Appl. Geophys., **157**: 1643-1661.

DE VOGGD B., TRUFFERT C., CHAMOT-ROOKE N., HUCHON P., LALLERMANT S. & LE PICHON X., (1992) - *Two-ship deep seismic soundings in the basins of the Eastern Mediterranean Sea (Pasiphae cruise)*. Geophys. J. Int., **109**: 536-552.

DI GIROLAMO P. (1978) - *Geotectonic setting of Miocene-Quaternary in and around the eastern Tyrrhenian Sea border (Italy) as deduced from major element geochemistry*. Bull. Volcanol., **41**: 229-250.

DITMAR P.G. & YANOVSKAYA T.B. (1987) - *A generalization of the Backus-Gilbert method for estimation of lateral variations of surface wave velocity*. Izv. AN SSSR, Fiz. Zemli (Physics of the Solid Earth), **23** (6): 470-477.

DOGLIONI C., HARABAGLIA P., MERLINI S., MONGELLI F., PECCERILLO A. & PIROMALLO C. (1999) - *Orogens and slabs vs. their direction of subduction*. Earth Sci. Review, **45**: 167-208.

DOGLIONI C., INNOCENTI F. & MARIOTTI G. (2001) - *Why Mt. Etna?* Terra Nova, **13**: 25-31.

DU Z.J., MICHELINI A. & PANZA G.F. (1998) - *EurID: a regionalised 3-D seismological model of Europe*. Phys. Earth Planet. Inter., **105**: 31-62.

FERRUCCI F., GAUDIOSI G., HIRN A. & NICOLICH R. (1991) - *Ionian Basin and Calabrian Arc: some new elements from DSS data*. Tectonophysics, **195**: 411-419.

FINETTI I. (1982) - *Structure, stratigraphy and evolution of central Mediterranean*. Boll. Geof. Teor. Appl., **24**: N. 96.

FINETTI I. & DEL BEN A. (1986) - *Geophysical study of the Tyrrhenian opening*. Boll. Geofis. Teor. Appl., **28**, 110: 75-156.

FINETTI I.R., BOCCALETTI M., BONINI M., DEL BEN A., GELETTI R., PIPAN M. & SANI F. (2001) - *Crustal section based on CROP seismic data across the North Tyrrhenian - Northern Apennines - Adriatic Sea*. Tectonophysics, **343**: 135-163.

FOLEY S.F. (1992) - *Vein-plus-wall-rock melting mechanisms in the lithosphere and the origin of potassic alkaline magmas*. Lithos, **28**: 435-453.

FOLEY S.F., VENTURELLI G., GREEN D.H. & TOSCANI L. (1987) - *The ultrapotassic rocks: characteristics, classification and constraints for petrogenesis*. Earth Sci. Rev., **24**: 81-134.

FRANCALANCI L., TOMMASINI S., CONTICELLI S. & (1999) - *Sr isotope evidence for short magma residence time for the 20th century activity at Stromboli volcano, Italy*. Earth and Planet. Sc. Lett., **167**, 1-2: 61-69.

FREZZOTTI ML., PECCERILLO A., BONELLI R. (2003) -

Magma ascent rates and depths of magma reservoirs beneath the Aeolian volcanic arc (Italy): inferences from fluid and melt inclusions in crustal xenoliths. In R.J. BODNAR & B. DE VIVO (Eds.): "*Melt inclusions in volcanic systems*". Elsevier, Amsterdam,185-206.

GAUTHIER P.J. & CONDOMINES M. (1999) *210Pb–226Ra radioactive disequilibria in recent lavas and radon degassing: inferences on the magma chamber dynamics at Stromboli and Merapi volcanoes*. Earth and Planet. Sc. Lett., **172**, 1-2: 111-126.

GRAHAM E.K. (1970) - *Elasticity and composition of the upper mantle*. Geophys. J. R. Astr. Soc., **20**: 285-302.

IMPROTA L., IANNACCONE G., CAPUANO P., ZOLLO A. & SCANDONE P. (2000) - *Inferences on the upper crustal structure of Southern Apennines (Italy) from seismic refraction investigations and surface data*. Tectonophysics, **317**: 273-297.

KERN H. & SCHENK V. (1988) - *A model of velocity structure beneath Calabria, southern Italy, based on laboratory data*. Earth and Planet. Sc. Lett., **87**: 325-337.

KNOPOFF L. (1972) - *Observations and inversion of surface-wave dispersion*. In: RITSEMA A.R. (Ed.): "*The Upper Mantle*". Tectonophysics, **13** (1-4): 497-519.

KNOPOFF L. & PANZA G.F. (1977) - *Resolution of Upper Mantle Structure using higher modes of Rayleigh waves*. Annales Geophysicae, **30**: 491-505.

LOCARDI E. (1986) - *Tyrrhenian volcanic arcs: volcano-tectonics, petrogenesis and economic aspects*. In: F.C. WEZEL (Ed.): "*The origin of the arcs*". Elsevier, 351-373.

LOCARDI E. (1988) - *The origin of the Apenninic arc*. In: WEZEL, F.C. (Ed.): "*The Origin and Evolution of the Arcs*". Tectonophysics, **146**: 105-123.

LOCARDI E. (1993) - *Dynamics of deep structures in the Tyrrhenian-Apennines area and its relation to neotectonics*. Il Quaternario, **6**: 59-66.

LOCARDI E. & NICOLICH R. (1988) - *Geodinamica del Tirreno e dell'Appennino centro-meridionale: la nuova carta della Moho*. Mem. Soc. Geol. It., **41**: 121-140.

LUDWIG W.J., NAFE J.E., DRAKE C.L. (1970) - *Seismic refraction*. In: WILEY-INTERSCI. *The Sea*, New York. Vol. 4, Part 1: 53-84.

MANTOVANI E., NOLET G. & PANZA G.F. (1985) - *Lateral heterogeneity in the crust of the Italian region from regionalized Rayleigh-wave group velocities*. Annales Geophysicae, **3**: 519-530.

MARSON I., PANZA G.F. & SUHADOLC P. (1995) - *Crust and upper mantle models along the active Tyrrhenian rim*. Terra Nova, **7**: 348-357.

MCNUTT M.K. (1998) - *Superswells*, Rev. Geophys. **36**: 211-244.

MELETTI C., PATACCA E. & SCANDONE P. (2000) - *Construction of a Seismotectonic Model: The Case of Italy*. Pure Appl. Geophys., **157**: 11-35.

MORELLI C. (1998) - *Lithospheric structure and geodynamics of the Italian peninsula derived from geophysical data: a review*. Mem. Soc. Geol. It., **52**: 113-122.

MOSTAANPOUR M.M. (1984) - Einheitliche Auswertung krustenseismicher daten in Westeuropa. Darstellung von Krustenparametern und Laufzeitanomalien. Verlag von Dirtrich Reimer in Berlin.

PANZA G.F. (1980) - *Evolution of the Earth's lithosphere. NATO Adv. Stud. Inst. Newcastle, 1979*. In: DAVIES P.A. & RUNCORN S.K. (Eds.): "*Mechanisms of Continental Drift and Plate Tectonics*". Academic Press: 75-87.

PANZA G.F. (1981) - *The resolving power of seismic surface waves with respect to crust and upper mantle structural models*. In: CASSINIS R. (Ed.): "*The solution of the inverse problem in geophysical interpretation*". Plenum Publ. Corp.: 39-77.

PANZA G.F. (1984) *Contributi geofisici alla geologia: stato attuale dell'arte e prospettive future*. In: "*Cento anni di geologia italiana*". Vol. giub. I Centenario S.G.I., 363-376, Bologna.

PANZA G.F., CALCAGNILE G., SCANDONE P. & MUELLER S. (1980) - *La struttura profonda dell'area mediterranea*. Le Scienze, **141**: 60-69.

PANZA G.F., PONTEVIVO A., CHIMERA G., RAYKOVA R. & AOUDIA A. (2003) - *The lithosphere-asthenosphere: Italy and surroundings*. Episodes, **26**: 169-174.

PASYANOS M.E., WALTER W.R. & HAZLER S.E. (2001) - *A surface wave dispersion study of the Middle East and North Africa for Monitoring the Compressive Nuclear-Test-Ban Treaty*. Pure Appl. Geophys., 158: 1445-1474.

PECCERILLO A. (1999) - *Multiple mantle metasomatism in central-southern Italy: geochemical effects, timing and geodynamic implications*. Geology, **27**: 315-318.

PECCERILLO A. (2001a) - *Geochemistry of Quaternary magmatism in central-southern Italy: genesis of primary melts and interaction with crustal rocks*. Geochemistry International, **39**: 521-535.

PECCERILLO A. (2001b) - *Geochemical affinities between Vesuvius, Phlegraean Fields and Stromboli volcanoes: petrogenetic, geodynamic and volcanological implications*. Mineral. Petrol., **73**: 93-105.

PECCERILLO A. & PANZA G.F. (1999) - *Upper mantle domains beneath Central-Southern Italy: petrological, geochemical and geophysical constraints*. Pure Appl. Geophys., **156**: 421-443.

PECCERILLO A., POLI G. & SERRI G. (1988) - *Petrogenesis of orenditic and kamafugitic rocks from Central Italy*. Canad. Mineral., **26**: 45-65.

PEPE F., BERTOTTI G., CELLA F. & MARSELLA E. (2000) - *Rifted margin formation in the south Tyrrhenian Sea: a high-resolution seismic profile across the north Sicily passive continental margin*. Tectonics, **19**, 2: 241-257.

PIALLI G., ALVAREZ W. & MINELLI G. (1995) - *Geodinamica dell'Appennino settentrionale e sue ripercussioni nella evoluzione tettonica miocenica*. Studi geol. Camerti, Volume speciale 1995/1: 523-536.

POLI G., FREY F.A. & FERRARA G. (1984) - *Geochemical characteristics of the south Tuscany (Italy) volcanic province: constraints on lava petrogenesis*. Chem. Geol., **43**: 203-221.

PONTEVIVO A. & PANZA G.F. (2002) - *Group Velocity Tomography and Regionalization in Italy and bordering areas*. Phys. Earth Planet. Inter., **134**: 1-15.

RINGWOOD A.E. (1966) - *Mineralogy of the mantle*. In: P.M. HURLEY (Ed.): "*Advances in Earth Science*". MIT Press, 357-399.

SCARASCIA S. & CASSINIS R. (1992) - *Profili sismici a grande angolo esplorati in prossimità del tracciato del profilo Crop01: una raccolta dei risultati e qualche revisione*. Studi geol. Camerti, volume speciale CROP 1-1A: 17-26.

SCARASCIA S., LOZEJ A. & CASSINIS R. (1994) - *Crustal structures of the Ligurian, Tyrrhenian and Ionian Seas and adjacent onshore areas interpreted from wide-angle seismic profiles*. Boll. Geof. Teor. Appl., **36**: 141-144.

TRUA T., SERRI G., MARANI M.P., RENZULLI A. & GAMBERI F. (2002) - *Volcanological and petrological evolution of Marsili Seamount (Southern Tyrrhenian Sea)*. J. Volcanol. Geotherm. Res., **114**: 441-464.

VALYUS V.P. (1972) - *Determining seismic profiles from a set of observations*. In: KEILIS-BOROK (Ed.): "*Computational Seismology*". Consult. Bureau, New-York: 114-118.

VALYUS V.P., KEILIS-BOROK V.I. & LEVSHIN A. (1969) - *Determination of the upper-mantle velocity cross-section for Europe*. Proc. Acad. Sci. USSR, **185**, 3.

VENISTI N., CALCAGNILE G., PONTEVIVO A. & PANZA G.F.

(2003) - *Surface wave and body wave tomography combined study of the Apulian Plate*. Submitted to PAGEOPH.

WENDLANDT R.F. & EGGLER D.H. (1980) - *The origin of potassic magmas: stability of phlogopite in natural spinel lherzolite an in the KAlSiO4-MgO-SiO2-H2O-CO2 at high pressures and high temperatures*. Amer. J. Sci., **280**: 421-458.

YANOVSKAYA T.B. & DITMAR P.G. (1990) - *Smoothness criteria in surface-wave tomography*. Geophys. J. Int., **102**: 63-72.

ZANON V., FREZZOTTI M. & PECCERILLO (2003) - *Magmatic feeding system and crustal magma accumulation beneath Vulcano Island (Italy): evidence from CO2 fluid inclusions in quartz xenoliths* . Geophys. J. Res., **108**, B6, In press.

Mem. Descr. Carta Geol. d'It.
XLIV (2004), pp.57-70
7 figg.

Review of the Tyrrhenian Sea seismicity: how much is still to be known?

Esame della sismicità del Mar Tirreno: quanto deve essere ancora conosciuto?

FAVALI P. (*), BERANZOLI L. (**), MARAMAI A. (**)

ABSTRACT - The Tyrrhenian basin extends in the central part of the Mediterranean sea and is of major importance in the frame of the general convergence of Eurasia and Africa plates. The southernmost sector, comprising the Aeolian Islands, the southern cost of the Italian peninsula and the northern Sicily cost, is the place of frequent, intense and, differently from the other regions of the basin, deep seismicity. This peculiarity has attracted many seismologists explaining the large amount of papers dealing with it.
We present a detailed description of the seismicity of the Tyrrhenian basin, including the Ligurian Sea, based on historical and instrumental data also dwelling on zones that are considered so far of scarce interests by most of the authors because of rare and weak activity. Large areas of the basin, generally the furthest from the coast, appear to be affected by very scarce seismicity with low energy events even in recent periods, when new conceived equipment's with high sensitivity were made available to the monitoring. The results of experiments of seafloor monitoring carried out in the Tyrrhenian and Ionian Seas in the last two decades are taken as examples of the present limits of the investigation capacity of land-based monitoring networks and, consequently, of the still persistent incompleteness of the knowledge of the basin seismicity.

KEY WORDS: historical and instrumental siesmicity, Tyrrhenian Sea, Ligurian Sea, seafloor monitoring

RIASSUNTO - Il Bacino Tirrenico occupa la parte centrale del Mediterraneo e riveste grande importanza nel quadro generale della convergenza delle pacche continentali Eurasiatica e Africana. Il settore più meridionale del bacino, che comprende l'arco insulare delle Eolie, le coste meridionali dell'Italia peninsulare e le coste settentrionali della Sicilia, è luogo di sismicità intensa, frequente e, al contrario di altre regioni del bacino, profonda. Tali caratteristiche, che hanno attratto l'interesse di molti sismologi, giustificano l'abbondante letteratura al riguardo.
In questo articolo presentiamo una descrizione dettagliata della sismicità del bacino Tirrenico, includendo anche il Mar Ligure, sulla base di dati storici e strumentali, soffermandoci ad esaminare anche zone considerate di scarso interesse perché sedi di debole e sporadica attività sismica. Estese aree del bacino, generalmente le più lontane dalle coste, sono caratterizzate da sismicità scarsa e di bassa energia anche in periodi recenti, da quando nuova strumentazione con elevata sensibilità è stata messa a disposizione del monitoraggio sismologico.
I risultati di esperimenti di monitoraggio dei fondali marini del Tirreno e dello Ionio effettuati negli ultimi due decenni sono portati ad esempio dei limiti attuali del monitoraggio sismologico, basato esclusivamente su punti di osservazione a terra, e della conseguente incompletezza della conoscenza della sismicità del bacino Tirrenico.

PAROLE CHIAVE: sismicità storica e strumentale, bacino Tirrenico, Mar Ligure, monitoraggio dei fondali marini

(*)Istituto Nazionale di Geofisica e Vulcanologia (INGV), Roma 2 Dept., Roma (Italy)
Università "G. D'Annunzio" (UDA), Chieti Scalo (Italy)
(**)Istituto Nazionale di Geofisica e Vulcanologia (INGV), Roma 2 Dept., Roma (Italy)

1. - INTRODUCTION

The Mediterranean Sea, one of the most studied regions of the world for its geodynamic and tectonic relevance, is the site of a complex system of continental blocks, oceanic basins and orogenic belts marking the boundary of the stable parts of the European and African converging plates. The Tyrrhenian Sea, a back-arc basin with a maximum depth of around 3600 m that progressively opened starting from about 10 Ma ago (KASTENS *et alii*, 1988) (CARTER *et alii*, 1972), is bordered by the orogenic belt of the Apennines on the north and east, and by the Corsica-Sardinia block and Sicily on the west and south respectively (fig. 1).

Fig. 1 - *Map of the Tyrrhenian basin and surroundings. The isobaths of 200, 1000, 2000 and 3000 m are shown. Most of the geographic names used in the text are also reported, other names are included in the next figures.*

The opening of the Tyrrhenian basin has been related to the sinking of the lithosphere with a roll-back mechanism (e.g., MALINVERNO & RYAN, 1986; ROYDEN *et alii*, 1987; PATACCA & SCANDONE, 1989). Its morphology is complex but similar to larger ocean basins in having an abyssal plain, seamounts, and well-developed continental shelves. Two main structural domains are recognised, respectively N and S of a prominent E-W lineament, named "41st N Parallel" (SERRI, 1990; FAVALI *et alii*, 1993a; b and references therein) running from northern Sardinia to Campania, evidenced also by E-W striking magnetic (CHIAPPINI *et alii*, 2000) and free-air gravity anomalies (MORELLI, 1970). North and south of this parallel, extension rates should have been markedly different if only in the south they were so high as to generate oceanic lithosphere (PATACCA *et alii*, 1993). The northern sector has a continental crust (about 20 km thick) while some basins (Magnaghi-Vavilov and Marsili) in the southern sector are underlain by thin oceanic crust (6-10 km thick, STEINMETZ *et alii*, 1983; BRUNO *et alii*, 2000). More in general, strong lateral heterogeneities affect the Tyrrhenian lithosphere (MORELLI *et alii*, 1975; CALCAGNILE *et alii*, 1979; 1982; CALCAGNILE & PANZA, 1981; SCARPA, 1982; STEINMETZ *et alii*, 1983; PANZA *et alii*, 1990; AMATO *et alii*, 1993; CIMINI, this volume, PANZA *et alii,* this volume), whose main features are the thickening of both the crust and LID from the abyssal plain of the central part of the southern sector to the Calabrian Arc. This thickening accompanies a decrease of heat flow (EL ALI & GIESE, 1978; LODDO & MONGELLI, 1979; MONGELLI *et alii*, 1989) and gravity anomaly values (MORELLI, 1970; 1981; COLOMBI *et alii*, 1973; MONGELLI *et alii*, 1975; MORELLI *et alii*, 1975). Refraction and reflection experiments have shown that the bathial plain has an oceanic crust with a thickness of only about 8 km, underlying surficial, 1.5 km thick sediments (FINETTI & MORELLI, 1973; MALINVERNO 1981, STEINMETZ *et alii*, 1983; RECQ *et alii*, 1984; DUSCHENES *et alii*, 1986; FINETTI & DEL BEN, 1986; PASCUCCI *et alii*, 1999). A noticeably different crustal structure has been found under the Tyrrhenian shelf along the southern Apennines, Calabria and Sicily where "continental" velocity structures accompany a crust with a thickness of 18-20 km (MORELLI *et alii*, 1975). Onshore within only few kilometres from the coast, the crustal thickness increases abruptly to 45-50 km in places (MORELLI *et alii*, 1975; CASSINIS, 1981; NICOLICH, 1989).

One of the peculiarities of the Tyrrhenian area is the presence, in the basin and eastern adjacent areas, of volcanoes among the most important in Europe. Some of the Tyrrhenian seamounts are still very poorly explored in spite of their dimensions: as an example, the activity of the Marsili seamount, with an extension of around (70 x 30) km^2 and an elevation of around 3000 m from the sea bottom (MARANI, this volume), is still debated and remains largely unknown. In addition, Vesuvius and Etna, large volcanoes adjacent to the basin, are known to extend their roots in marine areas, contributing to the underwater volcanic, seismological and hydrothermal activity of the border of the basin with not well-investigated implications. Notably, rocks typical of continental crust have been dredged from seamounts in part of the Tyrrhenian Sea (HEEZEN *et alii*, 1971), thought as remnants of extremely stretched continental material that are floating on an oceanic crust.

Other seamounts, the largest ones of the central Tyrrhenian, namely Marsili and Vavilov, are basaltic (BARBERI *et alii*, 1973; TRUA *et alii*, 2003). Basalt has also been recovered from Deep Sea Drilling Project (DSDP) Core Site 373-A from the Tyrrhenian seafloor (DIETRICH *et alii*, 1978). According to some Authors (SARTORI, 1990; BECCALUVA *et alii*, 1994; KASTENS *et alii*, 1988; ZITO *et alii*, 2003) the age of these rocks is

estimated 4.1 and 1.8 Ma for the Magnaghi-Vavilov and the Marsili basins respectively, indicating a relatively young age for the formation of the central Tyrrhenian crust, progressively younger toward the S-SE.

A considerable spread of opinions still exists about the geodynamic evolution and present tectonic setting of this zone. The seismicity is undoubtedly one of the most basic elements to be explained in the geodynamic framework of the region. Many studies yielded important information bearing on our understanding of the specific features of the basin. However, in spite of a constant development of the telemetered Italian seismic network and the operation of local networks over the last 20 years, the knowledge of the Tyrrhenian basin seismicity is still incomplete and restricted to the southern Italian coasts and the Aeolian island arc. This limitation is mainly due to the inability, even at present, of the land-based monitoring networks to detect and localise earthquakes, especially of medium and weak energy, in many parts of the basin. The peculiar shape of the Italian peninsula has constrained the geometry of the land-based monitoring networks. In addition, from the beginning of their development, the seismological networks have been firstly considered as a tool for civil protection and consequently concentrated in deemed highly hazardous areas.

The recent technological advances in scientific marine instrumentation and communication systems, have produced modules and observatories for the seismological monitoring at seabed able to operate both autonomously and cabled. The adoption of this new investigation equipment, nowadays obtainable with relatively accessible resources, is essential to make a significant step forward in the seismological observation in marine zones that are still excluded from systematic monitoring.

As a result, most of the studies on seismicity are addressed to the southernmost sector, namely the Calabrian Arc, Sicily, the Tyrrhenian coasts and Aeolian Islands, which is considered to have a key role in the comprehension of the geodynamic evolution of the central Mediterranean.

The occurrence of destructive earthquakes and, differently from most of the other Italian regions, the presence of intermediate and deep seismicity related to the subduction were attractive elements for many geophysicists. The Ligurian Sea and restricted coastal areas of Tuscany and Latium, where weaker seismicity than the southernmost sector occurs, were also studied.

The Italian region, together with the Greek one, is considered the most exposed to tsunami risk in the Mediterranean, having experienced a relevant number of destructive and minor tsunamis. From 79 b.C. to 2002, 68 tsunamis have been identified (Tinti & Maramai, 1996; Tinti *et alii*, 2004). According to these Authors, the most frequent source of tsunamis is represented by earthquakes occurring along the coasts. Volcanic activity and gravitational sliding are recognised, although to a lesser extent, as tsunamigenic events. In particular, the Tyrrhenian coasts have been the site of a large number of tsunamis, 70% of which occurred in the south-eastern sector and related to the volcanic activity of the Vesuvius, Campi Flegrei and Aeolian Islands. The two most destructive tsunamis so far known are related to seismic activity and they respectively took place along the Calabrian coast in 1783 (I_0 =IX-X MCS, m_b =6.3) and in the area of the Messina Strait during the 1908 Messina earthquake (I_0=XI MCS, m_b =7.2)

This paper presents a review of the Tyrrhenian seismicity mostly addressed to offshore areas and the narrow coastal belt of few kilometres, with the aim to highlight how much knowledge is still lacking concerning the seismicity of large portions of this basin.

2. - SEISMICITY

2.1. - Ligurian and Northern Tyrrhenian Seas

The Ligurian Sea is an oceanic basin originated in the Oligocene-Miocene by the counter-clockwise rotation of the Sardo-Corsican block respect to the European plate (De Voogd *et alii*, 1991; Makris *et alii*, 1999: Speranza *et alii*, 2002). A system of shallow normal faults extends alongside the Ligurian coast and the NW sector is steep and incised with canyons transversal to the strike of the fault system (Chaumillon *et alii*, 1994). The Moho depth under the basin is in the order of 20 km (Ginzburg *et alii*, 1986; Pasquale *et alii*, 1997; Eva *et alii*, 2001). Gravitational sliding, over- and under-thrusting, which could have caused crustal thickening and embryonic subduction, are mechanisms proposed in the literature to explain the regional tectonics of the Ligurian margin (Rehault & Bethoux, 1984; Cassinis *et alii*, 1990; de Franco *et alii*, 1998; Makris *et alii*, 1999; Contrucci *et alii*, 2001).

The seismic activity is related to two distinct structural systems: one located in the western part of the Ligurian Sea and the other on land, between the Nice-Savona coast and the Maritime Alps (Issel, 1887; Mercalli & Taramelli; 1888; Cattaneo *et alii*, 1987).

The seismicity distribution appears asymmetric as it is mainly concentrated in the western part, on the northern margin of the sphenochasm of the Sardo-Corsica block (fig. 3) (Bethoux *et alii*, 1992). Seismicity is characterised by a low number of events with some large shocks with magnitude greater than 5.0 and one event (1887) reaching magnitude 6.2 (Gruppo di Lavoro CPTI, 1999). Figure 2 shows the epicentral locations of the most relevant events, while figure 3 shows the instrumental seismicity (1983-2003; INGV, 2004). All the on land earthquakes have very shallow focal depth (within 6 km) while the offshore hypocentres, related to the structures in front of Imperia, are usually located at larger depths. The focal mechanisms related to the two structural systems are

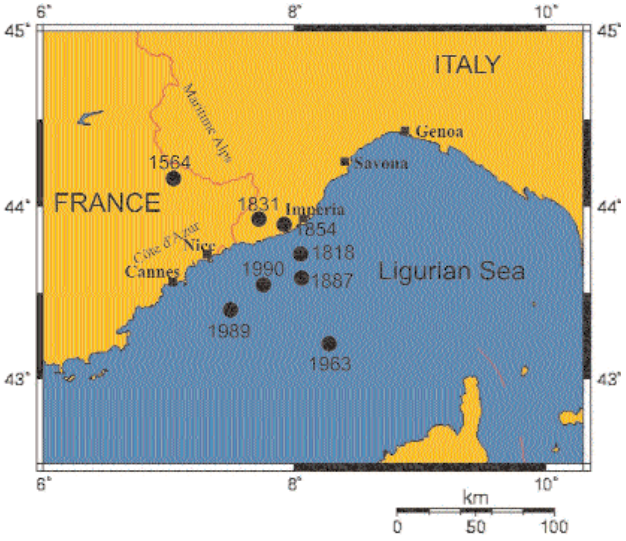

Fig. 2 - *Seismicity of the Ligurian Sea, the most relevant events in term of magnitude (4.2 = M_L = 6.2) are shown in the period 1564 to 1990.*

also different: the events of the western Liguria-Maritime Alps domain have mainly transtensive mechanisms, while a compressive regime dominates the offshore earthquakes (CATTANEO *et alii*, 1987). Offshore seismicity is rare and a gap of seismicity appears roughly coincident with a high heat-flow region (80-100 mW m^{-2}) in the central Ligurian Sea (PASQUALE *et alii*, 1995; 1997; EVA *et alii*, 2001).

BETHOUX *et alii* (1988; 1992) suggest that the northern margin of the Ligurian Sea is affected by to a general compressive regime which results from the tectonic setting of the area and hypothesise the closing of the Ligurian Sea as a consequence of the lateral expulsion of the south-western Alps along the south-western sidewall of the Apulian indenter (TAPPONNIER, 1977; VIALON *et alii*, 1989). The compressive focal mechanisms of some of the major recent seismic events seem to confirm this hypothesis; the 1963, 1989 and 1990 earthquakes occurred offshore in front of the Italian-French border, with the principal horizontal stress vector lying in the NW-SE direction (EVA & SOLARINO, 1998).

As far as concerns tsunamis, the two contiguous areas of Liguria and Côte d'Azur can be assumed as a unique single tsunamigenic-source zone, even if within this area the exact source location for some events is rather uncertain. Along these coasts, ten events affected Liguria from 1564 to 1979, involving in many cases also the French coasts. The most relevant tsunami is the February 1887 tsunami, associated to a destructive shock (I_0=X MCS) with epicentre in the Ligurian Sea (MERCALLI & TARAMELLI, 1888). The tsunami, recorded by tide-gauge stations at Genoa and Nice, hit a large portion of the coast with an initial sea withdrawal followed by

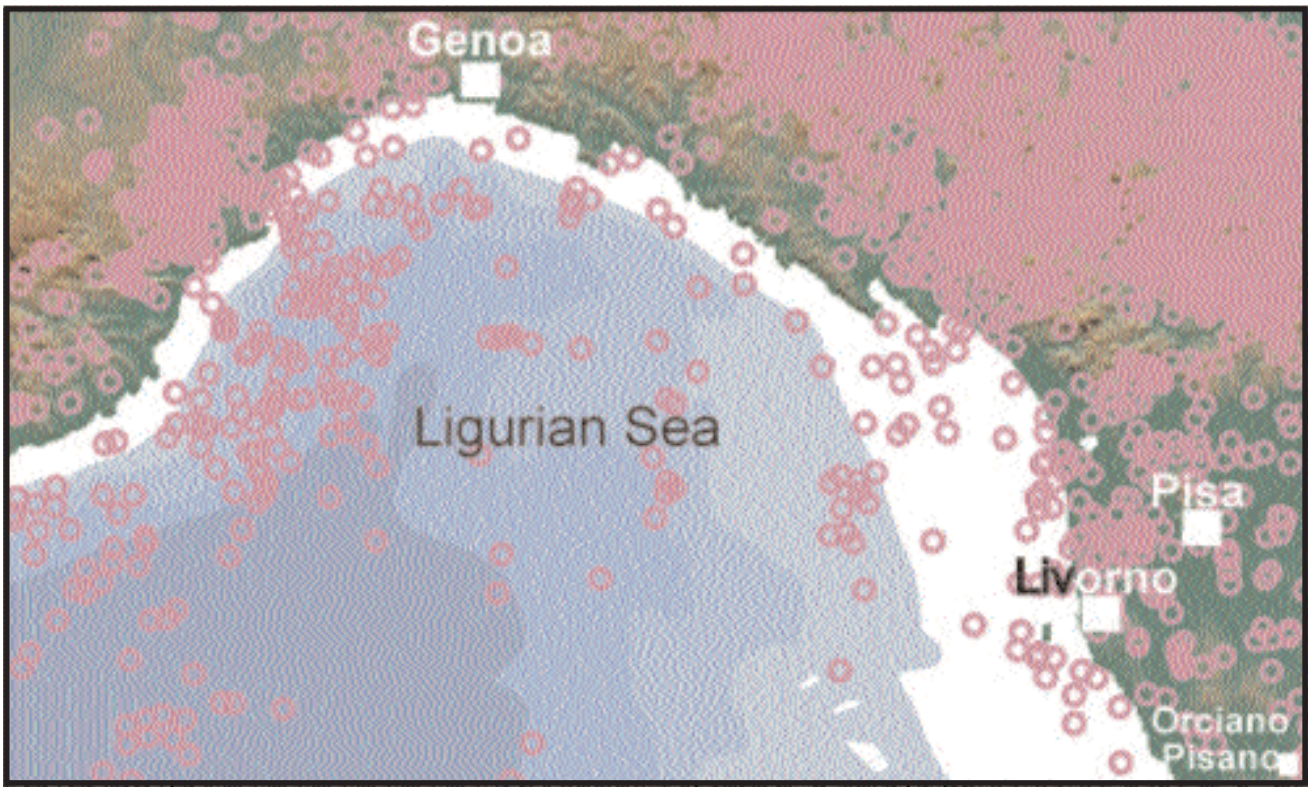

Fig. 3 - *Map of the seismicity of the Ligurian Sea (1983-2003; INGV,2004).*

an inundation. The maximum run-up of 1,5 metres was measured at Imperia. Excluding the 1887 event, all the other tsunamigenic earthquakes of this area are located in land roughly close to the coasts, some of these having small magnitude (ranging from 3.2 to 4.0). The capability of those weak earthquakes to generate tsunamis can be explained by the triggering of submarine landslides in very unstable sediments of the Ligurian Sea canyons.

To the south, of note is the northern Tyrrhenian basin along the coastal area of Tuscany where seismicity is related to extensional tectonics. From the analysis of the historical and instrumental seismicity it is possible to identify two different areas of seismic activity, one located offshore in front of Pisa and Livorno and the other on land some kilometres south of Livorno (fig. 3). The offshore seismic activity is characterised by events with shallow depths and low energy with effects in coastal villages rarely reaching an intensity of VII MCS, like in the case of the 1646 Livorno earthquake. On land, scattered seismicity characterises the area south of Livorno, where some historical relevant events occurred (1742, 1771, 1846) reaching a maximum intensity of VIII-IX MCS (Maramai & Tertulliani, 1994; Boschi *et alii*, 1997). Only two weak tsunamis, affecting Livorno with small run-up, can be associated with shocks that occurred in this area in 1646 and 1742 (I_0=V-VI MCS). Associated with the inland-scattered seismicity located south of Livorno, only one tsunami event certainly occurred on the occasion of the most relevant shock of August 1846 in Orciano Pisano (I_0=IX MCS).

2.2. - Central Tyrrhenian Sea

Many studies have been carried out on the evolution of the Tyrrhenian basin (e.g., Malinverno & Ryan, 1986; Mantovani *et alii*, 1990; 1996) but without fully considering the evolution of the central part of the basin. Only few studies on tectonics and seismicity are available in the literature.

Historical catalogues and modern instrumental databases do not report relevant seismic events located in the central Tyrrhenian Sea. This characteristic, although excluding medium-high levels of seismic activity, does not give sufficient elements to consider this area lacking in seismicity.

The Campania-Latium Tyrrhenian margin is characterised by NW-SE elongated structural depressions, limited by WNW-ESE to NW-SE and by NE-SW striking faults (Bruno *et alii*, 2000). From a geodynamic point of view the Latium Tyrrhenian margin presents a system of basins oriented both NW-SE and NE-SW and created by the activity of normal

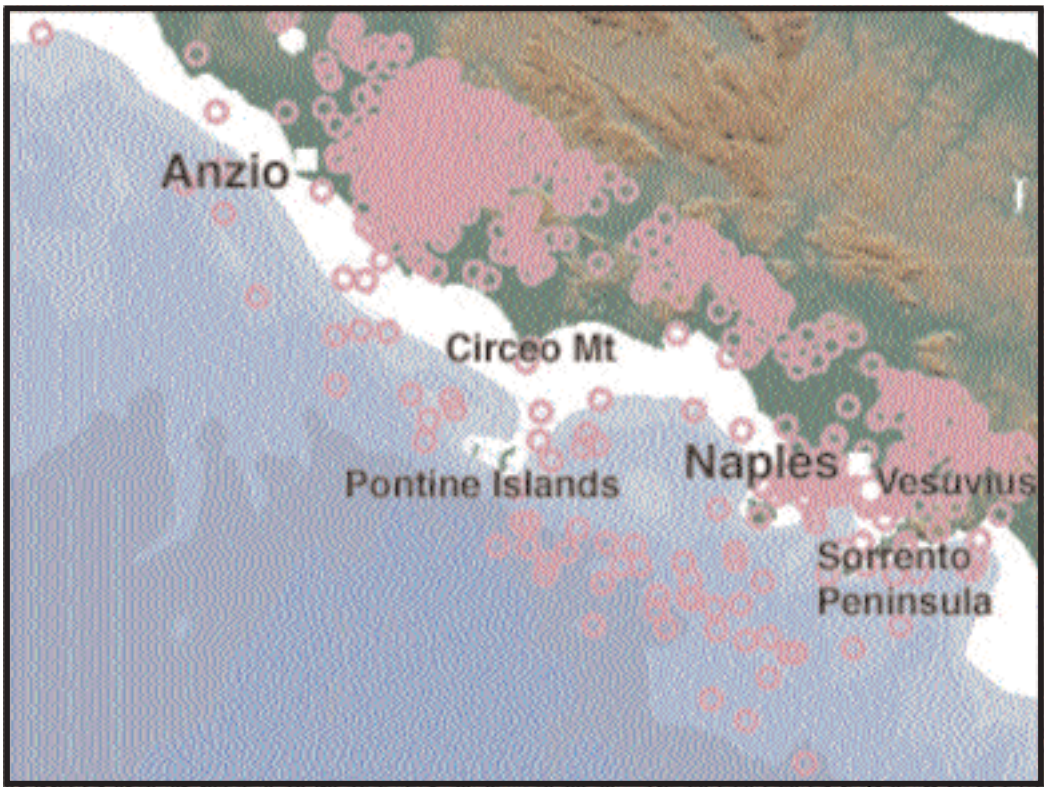

Fig. 4 - *Map of the instrumental seismicity located along the Italian coasts of the northern and central Tyrrhenian Sea (1983-2003; INGV, 2004).*

faults from Messinian to early Pleistocene (FACCENNA *et alii*, 1994). Offshore, the Latium area is separated from Campania by the eastern propagation of the E-W magnetic and free-air gravimetric anomaly of the 41st parallel (BRUNO *et alii*, 2000; CHIAPPINI *et alii*, 2000). Extensional tectonics, generally pertaining to the whole Tyrrhenian margin of the Italian Peninsula, is associated to the presence of the volcanic systems in the Latium area.

On the basis of historical and instrumental data, it emerges that the Latium area is characterised by low seismic activity both in occurrence and energy (for instrumental seismicity see fig. 4).

Nevertheless two distinct areas can be identified: the first one is located offshore and includes the Pontine Islands, a Pleistocene volcanic complex built on the continental slope in front of the Circeo promontory (fig. 4). This area is characterised by frequent weak earthquakes, which reached the maximum felt intensity with the 1781 April 13 earthquake (VII MCS). The second area includes the Latium coast south of Rome characterised by small to moderate, rare seismic events (fig. 4). The largest known earthquake, referred in literature as the "Anzio earthquake", in this area occurred in 1919 (M=5.0), with epicentre located offshore about 20 km from the coast. TERTULLIANI *et alii* (2003) make a careful revision of this shock, underlining that seismic events appear only at the end of 1800s, becoming more frequent after 1980. This is due both to the recent development of the Italian seismic network and to the lack of sources before the 1800s for the uninhabited territory. On the basis of historical data, the southernmost part of Latium coast was supposed to be almost a-seismic, with very few weak events with maximum intensity V MCS (MOLIN & PACIELLO, 1995). On the contrary, from the analysis of instrumental data the presence of rare seismic activity with low magnitude and focal depth roughly ranging between 5 and 10 km has been observed (CAPOCECERA *et alii*, 1995). The coasts of Latium are believed to be almost exempt from tsunamis. TINTI (1991) shows that only one event, and moreover very doubtful, could have occurred in this area, with description of sea withdrawal at the Tevere mouth during the February 1703 shock (I_0=X-XI MCS) that occurred in the central Apennines. No tsunami events are associated with the offshore seismicity of the Pontine Islands.

The western border of the Tyrrhenian basin, from the Ligurian Sea to the Sardinian-Tunisian strait along the eastern coasts of Corsica and Sardinia Islands, is reported in literature as an area affected by scarce and moderate seismicity. In fact, the analysis of the French database on historical seismicity for Corsica and Sardinia islands put in evidence that since the XVIII century only three seismic events have reached intensity greater then or equal to VI EMS98 (BGRM, 2004). In particular, the maximum earthquake occurred along the western coast of Corsica in 1775 (I_0=VII EMS98). Another interesting event took place on November 1948 (I_0=VI EMS98), with epicenter located in the sea close to the northern Sardinian coast. This shock caused light damages in some villages in Sardinia, while it was felt in southern Corsica (PERONACI, 1953). As far as concerns the seismicity of the last 20 years for the Sardinia-Corsica zone, the available instrumental data report about 200 events with maximum magnitude reached in the Bonifacio strait area (June 2000, M_L=4.6; EOST, 2004); moreover, this area has to be considered the most seismically active of the whole Sardinia-Corsica block. Finally, only one relevant event has been localised in the Sardinia channel. The CMT focal mechanism of this shock, that occurred in August 1977 (m_b=5.1), shows a compressive trend (GIARDINI et alii, 1984).

2.3. - SOUTHERN TYRRHENIAN SEA

The southern part of the Tyrrhenian basin has attracted the interests of many Authors given its complex tectonics, large scale geodynamic deformations and high-frequency and deep seismicity. Frepoli et alii (1996) summarises the main geodynamic features as follows: i) subduction of the Ionian oceanic lithosphere beneath the Calabrian Arc (MALINVERNO & RYAN; 1986, ROYDEN *et alii*, 1987; PATACCA & SCANDONE, 1989; DOGLIONI, 1991; SELVAGGI & CHIARABBA, 1995); ii) recent opening (post-Tortonian) of the Tyrrhenian basin (BARBERI *et alii*, 1973; 1978; CARMINATI *et alii*, 1998); iii) present uplift of the Calabrian Arc (WESTAWAY, 1993; BORDONI & VALENSISE, 1998); iv) high heat-flow (HUTCHISON *et alii*, 1985; DELLA VEDOVA *et alii*, 1991; MONGELLI & ZITO, 1994; 2000); v) volcanic activity of the Aeolian islands linked to the subducting slab (BARBERI *et alii*, 1973; SERRI, 1990; BECCALUVA *et alii*, 1994). The whole Southern Tyrrhenian region is characterised by shallow to deep seismicity (e.g., CAPUTO *et alii*, 1970; 1973; ANDERSON & JACKSON, 1987; GIARDINI & VELONÀ, 1991; CACCAMO *et alii*, 1996).

The models at different scales proposed in the last thirty years witness the still continuing debate on the geodynamic evolution and present tectonics of the southern Tyrrhenian region. The existence of subduction processes and the consequent key role of the basin in Mediterranean geodynamics has been recognised starting from the early seventies (e.g., CAPUTO *et alii*, 1970; 1973) on the basis of seismological data from teleseismic and regional stations. BARBERI *et alii* (1973) also suggested a subduction process probably active beneath the Southern Tyrrhenian Sea, with a trench zone close to the Ionian coast of Calabria and a W-NW slab immersion. In this context, the southern Tyrrhenian Sea is assumed to be a back-arc basin. The model would explain the arc structure, the location of seismicity, and the volcanism of the Aeolian Islands. The Etna and the Ustica extensional volcanism marks the southern limit of the compressive tectonic sector,

while the Tyrrhenian abyssal plain is interpreted as a marginal basin (NERI *et alii*, 1991). The Wadati-Benioff zone, formerly identified by CAPUTO *et alii* (1970; 1973) dipping from the Calabrian arc to the NNW, has been interpreted by GASPARINI *et alii* (1982; 1985), PATACCA *et alii* (1990) as a relic of a subducted lithosphere. SCANDONE & PATACCA (1984) interpret the Tyrrhenian area as a fragment inside a large and partially ductile belt separating the stable margins of the African and European plates. These Authors hypothesise the presence of a passive subduction of the residual slab and spreading mechanisms probably still acting in the southern Tyrrhenian region. MANTOVANI *et alii* (1985; 1990; 1996) suggest that the kinematics of the Adriatic microplate, with anticlockwise rotation with respect to the European plate, play a relevant role in the evolution of the Tyrrhenian basin.

Recently, the improvement in seismological station coverage has allowed to refine the analysis of event records, leading to the identification of a WNW-oriented Benioff zone down to 500 km of depth (NERI *et alii*, 1991; FREPOLI *et alii*, 1996; LUONGO & MAZZARELLA, 1997). The upper part of the slab, dipping around 70° above 250 km and around 50° below, should intersect the Earth's surface near the Ionian coasts of Calabria (NERI *et alii*, 1991; SELVAGGI & CHIARABBA, 1995; FREPOLI *et alii*, 1996).

The southern Tyrrhenian subduction zone is the Italian region with highest seismic energy release given the yearly occurrence of many $m_b \sim 5$ earthquakes (AMATO *et alii*, 1997). Figure 5 shows all the instrumental seismicity localised by INGV in the period 1983-2003 (INGV, 2004).

Differently from most of the other Italian areas which experience crustal seismicity, the southern Tyrrhenian basin is characterised by the occurrence of shallow, intermediate and deep earthquakes, with maximum depth estimated at about 400 km. In the last decade the geometry of the seismogenic volume interested by the deep seismicity has been studied by many Authors, also through tomographic techniques. A discussion on the most recent results is given in this volume (see CIMINI; PANZA *et alii*).

Due to the presence of an intense seismic activity and of remarkable volcanic processes, the southern Tyrrhenian basin is of great interest also with respect to tsunami genesis. Here we can identify five coastal zones where most of the Italian tsunamis and all the strongest events are concentrated, respectively Campania, Tyrrhenian Calabria, Aeolian islands, northern Sicily and Messina Straits (TINTI & MARAMAI, 1996; TINTI *et alii*, 2004).

Two tsunami events that occurred in June 1760 and in July 1805 are associated with earthquakes not related with the Vesuvius activity. The first shock (M=

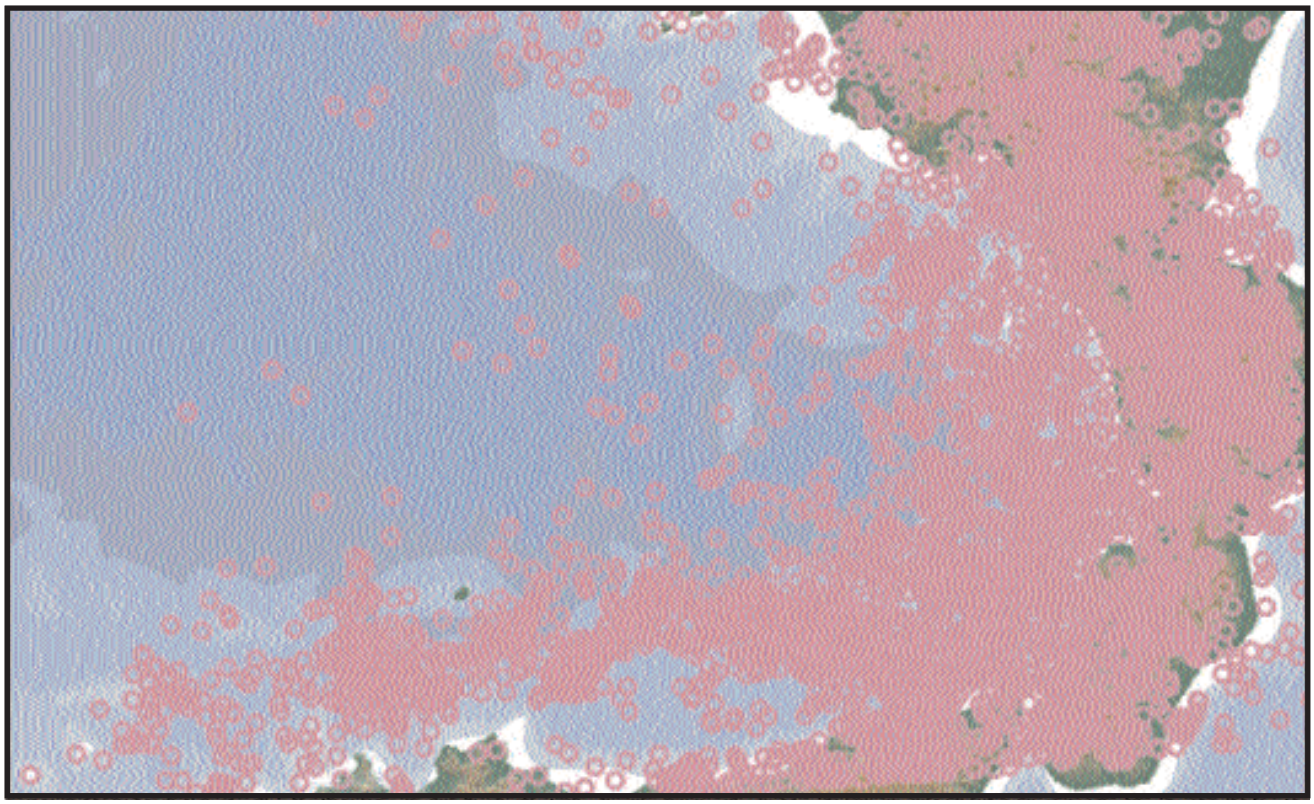

Fig. 5 - *Map of seismicity of the southern Tyrrhenian Sea (1983-2003; INGV, 2004).*

4.3) was located offshore and caused a very large withdrawal in the Portici harbour (nearby Naples) that remained dried for a few minutes. The second one was a destructive event (M= 6.6) causing more than 5,000 victims and generating a tsunami involving the coast from the Sorrento peninsula to southern Latium with sea level rising up to 3 metres in some coastal villages.

The Tyrrhenian Calabria and the Messina Straits coastal zones are the regions with the highest tsunamigenic potential from the point of view of the largest tsunami waves observed. In Tyrrhenian Calabria, eight tsunamis occurred from 1638 to 1905, related with seismic shocks located on land close to the coast. Most of them are strong and one is the catastrophic tsunami that occurred in February 1783, caused by a huge earthquake-induced rock fall: a portion of the Monte Pacì (south-western side of the Scilla beach) collapsed suddenly into the sea, triggering a violent tsunami with maximum run-up of about 9 metres, causing about 1500 victims at Scilla and also involving the coast of Sicily. Two rather strong tsunamis occurred on November 1894 and September 1905, related to violent seismic shocks in southern Italy, the first one along the Calabrian Tyrrhenian coast and the second in the north-eastern Sicilian coast. In both cases the sea receded, then flooded the shore causing severe damage to vessels and rising up to 6 metres.

The northern Sicily zone is the source area of two tsunamigenic events, both located offshore in front of Palermo. The earthquake that occurred on September 1726 caused a strong sea withdrawal in Palermo and in many other places. For the December 1823 shock, tsunami effects were observed along the whole coast between Cefalù (60 km east of Palermo) and Palermo. Investigations carried out after the earthquake that occurred on September 6, 2002, located offshore between Ustica and Alicudi (not far from the source of the 1823 event), pointed out that anomalous sea behaviour had been observed in the northern coast of Sicily, particularly in areas adjacent to Cefalù.

In the Messina Straits area two minor events (only causing some damage to ships) occurred in 1649 and in 1784 while the strongest tsunami recorded in Italy took place in this zone on December 28, 1908, associated to the catastrophic earthquake causing the destruction of Messina, Reggio Calabria and many other localities in Calabria and Sicily. The generated tsunami hit the Calabrian and the whole eastern Sicily coasts provoking severe damage and many victims. The maximum tsunami intensity was reached in the Calabrian coast (maximum run-up 13 m) and in north-eastern Sicily (maximum run-up 12 m).

The Aeolian islands zone is, together with Liguria-Côte d'Azur, the region with the highest tsunamigenic potential from the point of view of the number of the events: seven tsunamis occurred in the last century, from 1916 to 1988. All events are related to volcanic activity and they are mainly due to explosions and/or earthquakes associated with volcanic episodes as well as to gravitational landslides. The analysis of the Italian tsunami catalogue (TINTI & MARAMAI, 1996) underlines that Stromboli, the most active volcano in the area, is responsible for most of the tsunamis, both in number and in intensity, also causing severe destruction in the villages of the island. Some events with minor effects are also generated at Salina and Vulcano islands. A new strong tsunami, caused by two episodes of submarine slide, occurred in Stromboli Island at the end of 2002 (TINTI *et alii*, 2004).

3. - DISCUSSION AND CONCLUSIONS

The results, over the years, of research concerning the Tyrrhenian basin seismicity, have led to a very inhomogeneous knowledge of the area. This is mostly due to the impossibility of investigating wide offshore areas without the aid of appropriate technology. Some offshore sectors, in proximity of observation sites, have captured the attention of many Authors involved in assessing the role of the basin in central-Mediterranean geodynamics. Other parts were studied because of the great relevance of earthquakes and tsunamis that had occurred, which in some cases determined heavy casualties and destruction over large areas. Nonetheless, a reliable reconstruction of the seismological past of the Tyrrhenian basin is limited by the deficiency of historical information in remote areas, for example the islands, with fragmentary descriptions of the observed events. An example can be represented by the case of the Aeolian Islands: the available seismological catalogues only account for events that have occurred in the last century.

The transition to modern seismological sensors has helped in the identification of seismogenic marine areas. For example in the Ligurian Sea, the hypocentres of the recent events that occurred at sea, likely generated by the same marine structures that originated the historical ones, are localised farther and farther from the coast. This advance in the event localisations can be explained by the enhanced characteristics of the present-day monitoring systems (e.g., broad-band sensors, 24-bits digitisers), the improvement of hypocentre computation algorithms, and, at times, the assumption of more appropriate structure models based on the progress in the knowledge of the lithosphere.

In recent times, numerous marine geophysical campaigns (e.g., GAMBERI *et alii*, 1997) have once again put in light the presence of important seismogenic structures together with the persistence of terrestrial structures, more deeply investigated, toward the sea.

In spite of these latter advances, the study of the seismicity and of its relationship with other phenomena associated with marine structures is still at a very early stage, notwithstanding the key role attributed to the Tyrrhenian basin in regional geodynamics. As an example, nothing is known of the importance, the distribution also with depth, the temporal evolution and associated phenomena (e.g., volcanic activity, hydrothermalism, degassing) of the

seismicity of south western sectors of the basin, supposed to be weaker than the remaining sectors. To neglect these additional features results in a limited view of the geodynamic framework of the Tyrrhenian area and of its relationships with neighbouring sectors.

The monitoring systems presently operating on land all around the basin, although very dense in some areas and based on modern technology, are still inadequate for an efficient monitoring of marine regions. The major critical aspects relate to the detection capacity and localisation accuracy. The extent of the basin and the scarcity of seismological stations in Sardinia and Corsica islands, represent obstacles for the complete and systematic detection of events of medium and low magnitude and of course of micro-seismicity. The localised seismicity available from the INGV bulletin for the central sector of the Tyrrhenian basin is reported in table 1 (INGV, 2004).

The low number of localised events (20) over a period of around 20 years and the depths, in the majority fixed at 5 and 10 km, reveals the difficulty of application of the localisation procedures. In addition to the inhomogeneous distribution of the network stations, the unfavourable large lateral velocity variations of the lithosphere below the basin, determine large location errors. Estimates of probable errors in the location of offshore and coastal events can be over 50 km with respect to the mislocation of the terrestrial events that is typically 5-10 km (Di Giovambattista & Barba, 1997).

Some experiments of seafloor monitoring have allowed a rough quantification of the undetected seismicity by the land-based monitoring at least for

Tab. 1 - *Localisations of seismic events in the central sector of the Tyrrhenian Sea from instrumental catalogue (INGV, 2004). Only 20 events were recorded over 18 years. Most of the localisations are estimated keeping the depth fixed (5 or 10 km) due to the instability of the solutions.*

N.	Date	Time	Lon	Lat	Depth	M_d	M_L
1.	1983-04-21	04:32:03	12.714	40.640	*10.000	31	—
2.	1983-10-10	22:01:59	13.470	39.698	*10.000	—	—
3.	1984-04-02	21:47:08	11.658	40.910	*10.000	31	—
4.	1986-01-09	18:51:08	12.881	40.293	*10.000	34	—
5.	1988-04-03	07:47:16	13.259	39.501	*10.000	31	24
6.	1989-07-03	14:54:07	12.926	40.659	* 5.000	40	34
7.	1989-07-09	10:58:55	12.752	40.339	*10.000	30	—
8.	1989-08-02	14:27:21	12.946	40.367	*10.000	27	25
9.	1991-03-27	09:49:22	11.648	41.485	*10.000	38	32
10.	1991-06-30	03:17:13	10.906	39.751	*10.000	34	33
11.	1992-05-08	16:50:36	13.535	39.578	*10.000	30	25
12.	1992-10-08	18:46:17	13.431	39.452	*10.000	27	24
13.	1993-09-20	17:47:31	12.554	39.376	* 5.000	29	26
14.	1996-01-21	12:16:54	13.394	39.984	611.046	32	34
15.	1996-08-19	22:48:20	12.436	39.464	*10.000	29	22
16.	1996-12-21	08:45:35	13.188	39.878	681.422	40	43
17.	1998-12-13	22:57:46	13.585	39.497	646.026	—	46
18.	1999-09-07	07:13:30	12.062	39.333	*10.000	29	26
19.	2000-04-27	22:04:18	10.638	40.788	*10.000	28	—
20.	2001-04-21	17:31:41	10.540	40.995	*10.000	34	28

(*): depth kept fixed during the localisation procedure

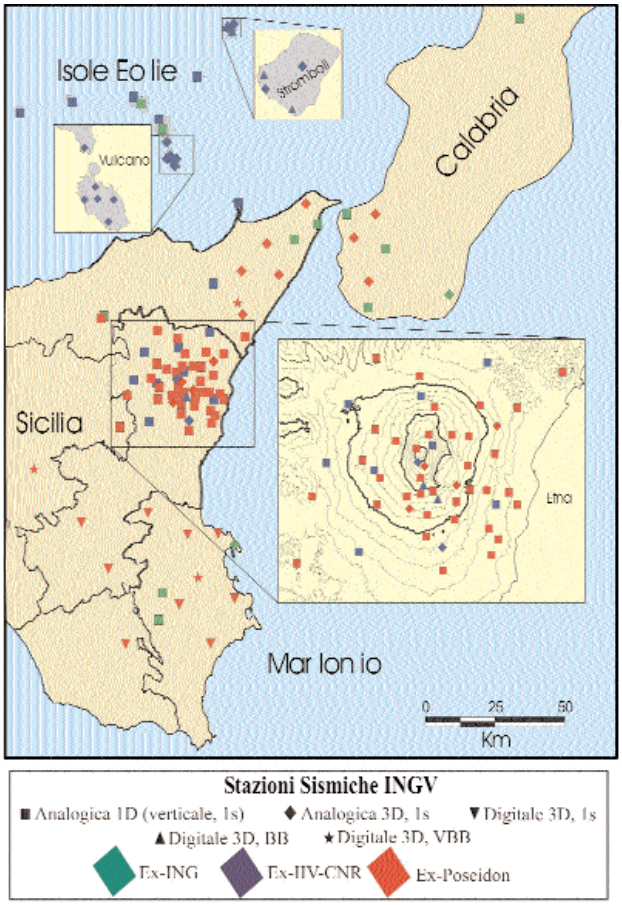

Fig. 6 - *Map of the seismic stations in Eastern Sicily, Etna volcano, Aeolian Islands and part of Calabria managed by INGV.*

some sectors of major interest. In 1987 an experiment was carried out in the Southern Tyrrhenian Sea at a depth range of 1000-2800 m. The experiment used five Ocean Bottom Seismometers (OBS) and land-based stations opportunely thickened with temporary stations (SOLOVIEV *et alii*, 1990). Over only 12 days of operation, about 200 local shocks with M_L=3, approximately concentrated beneath sub-sea volcanic seamounts and located offshore the central Calabria coast, were recorded exclusively by the OBS network. The experiment pointed out that land-stations, regardless of their number, are unable to record the numerous minor earthquakes occurring in the crust because of the low energy of these events, the attenuation of the seismic signals and the level of noise. The seismic activity within the crust in the Tyrrhenian basin is thus underestimated if determined from land station records only. A further experiment was conducted in 1996 in the framework of co-operation among INGV, Tokyo and Chiba Universities (BERANZOLI *et alii*, 1997). In the experiment ten OBS were deployed for around eighteen days in a depth range from 1500 to 3400 m in the southern Tyrrhenian Sea, northwest of the Aeolian islands. During the experiment, more than 150 crustal events with Md=3.5 were recorded mostly at the OBS closest to the Aeolian volcanic arc. Most of these events were neither localised nor detected by the on land network, due mainly to their low energy.

In the period December 2000-May 2001 a new experiment, the TYrrhenian Deep Experiment (TYDE) conducted by INGV, and the German institutes of GEOMAR and Forschungsgemeinschaft-Hamburg Universitaet, made use of 14 ocean bottom instrumented modules equipped with seismometers and hydrophones (OBS/H), deployed in water depth of 1500 to 3500 m in the southern Tyrrhenian Sea (DAHM *et alii*, 2002). More than 350 events, exclusively recorded by the OBS/H, could be localised (Sgroi, personal communication) revealing once again the inadequacy of the land-based monitoring to efficiently cover the area.

In the period October 2002-May 2003 the multidisciplinary seafloor observatory SN-1, built up and operated in the framework of a project coordinated by INGV and funded by the Italian National Group for the Defence against Earthquakes (GNDT), was deployed in the western Ionian Sea around 25 km off Catania town (eastern Sicily) at a depth of 2105 m (BERANZOLI *et alii*, 2003). The seismicity of the area is generally considered sufficiently guaranteed by a very dense coverage of land seismological stations (see fig. 6).

In table 2 the monitoring efficiency reached through the integration of the land-based networks and the SN-1 seafloor observatory data reveal an increment of up to 78% in a monthly period (10 November-10 December 2002) with a consistent amount of very local events. Figure 7 represents the position on the sea bottom of SN-1 observatory during the experiment, the two circles indicate the distance of 35 and 100 km respectively according to table 2.

In addition, 25 events became localisable due to the availability of arrival times at SN-1. Basically, it can be concluded that all the sea experiments carried out till now have demonstrated that seafloor observations can improve the event detection from 50% to 75%

Fig. 7 - *Map of Eastern Sicily, the red dot represents the position of SN-1 observatory on the sea bottom during the 2002-2003 experiment. The2 circles indicate the distance of 35 km (internal circle) and of 100 km (external circle) from the observatory (see tab. 2).*

Tab. 2 - *Number of events registered by the on-land Italian networks operating in the western Ionian area and by SN-1 seafloor observatory in the period 10 November-10 December 2002. The category of the events (Very Local, Local, Regional and Teleseismic) is set on the basis of the distance from SN-1 site (see Fig. 7). The number of events detected simultaneously by the Italian national centralised seismological network (RSNC), by the local monitoring network of Eastern Sicily (CT) and by SN-1 is compared to the number of events detected exclusively by SN-1 and not observed at the other stations. The number in bold (25) is the increment in the number of events that became localisable thanks to the detections of SN-1. The increment of efficiency in Very Local, and Local event detection through the inclusion of SN-1 data is around 78%, while 25 among the Very Local and Local events (around 25 %) become localisable thanks to SN-1 data.*

Event category	RSNC, CT, SN-1	Only SN-1
Very Local (Dist. ≤ 35 km)	12	78
Local (35 < Dist. ≤ 100 km)	90	34
Regional (100 < Dist. ≤ 3000 km)	32	19
Teleseismic (Dist. >3000 km)	2	-
TOTAL	136	131

25

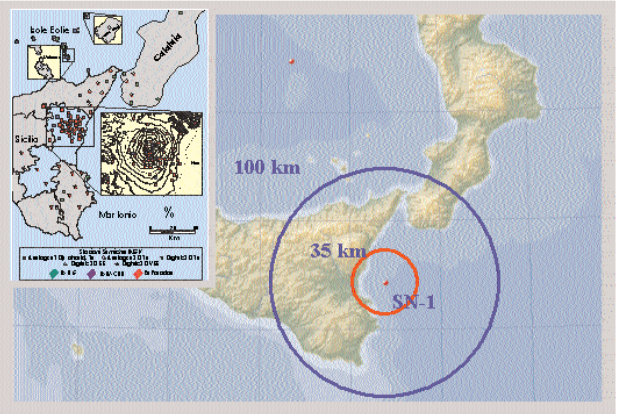

with an increase in the number of localisable events of more than 20%.

The progress of marine monitoring and communication systems and the increasing synergy between science and technology are favourable conditions to undertake scientific-technological programs addressed to the development of seafloor observation networks integrated to the land-based ones. The study of Earth structures in offshore zones of the Italian and the Mediterranean regions can largely benefit from these opportunities.

REFERENCES

Amato A., Alessandrini B., Cimini G., Frepoli A. & Selvaggi G. (1993) - *Active and remnant subducted slabs beneath Italy: evidence from seismic tomography and seismicity.* Annali di Geofisica, **36**:201-214.

Amato A., Chiarabba C. & Selvaggi G. (1997) - *Crustal and deep seismicity in Italy (30 years after).* Annali di Geofisica, **40**:981-993.

Anderson H. & Jackson J. (1987) - *Active tectonics of the Adriatic region*, Geophys. J. R. Astr. Soc., **91**:937-983.

Barberi F., Gasparini P., Innocenti F. & Villari L. (1973) - *Volcanism of the Southern Tyrrhenian Sea and its geodynamic implications.* J. Geophys. Res., **78**:5221-5232.

Barberi F., Bizouard H., Capaldi G., Ferrara G., Gasparini P., Innocenti F., Joron J.L., Lambert B., Treuil M. & Allegre C. (1978) - *Age and nature of basalts from the Tyrrhenian abyssal plain.* In: Hsü K.J (Ed.). Init. Rep. DSDP, **42**:509-514.

Beccaluva L., Coltorti M., Galassi B., Macciotta G. & Siena F., (1994) - *The Cainozoic calc-alkaline magmatism of the western Mediterranean and its geodynamic significance.* Boll. Geof. Teor. Appl., **36**:293-308.

Beranzoli L., Aoyagi Y., Braun T., Calcara M., Etiope G., Favali P., Frugoni F., Murayama T., Shinohara M., Smriglio G. & Suyehiro K. (1997) - *Microseismicity of the southern Tyrrhenian basin monitored by an Ocean Bottom Seismometer network (October 15 - November 3, 1996).* Appendix Atti del 16° Convegno Nazionale GNGTS (on CD).

Beranzoli L., Favali P., Gasparoni F. & Gerber H. (2003) - *SN-1 observatory: the first node of the Italian geophysical and environmental monitoring network.* InterRidge News, **12**:21-26.

Bethoux, N., Cattaneo M., Delpech P.Y., Eva C. & Rehault J.P. (1988) - *Mècanismes au foyer de seismes en Mer Ligure et dans le Sud del Alpes Occidentales: rèsultats et interpretations. Focal mechanisms obtained for earthquakes of the Ligurian Sea and south-western Alps; results and interpretations.* Comptes Rendus de l'Academie des Sciences, Serie 2, Sciences de l'Univers, Sciences de la Terre, **307**:71-77.

Bethoux N., Fréchet J., Guyoton F., Thouvenot F., Cattaneo M., Eva C., Nicolas M. & Granet M. (1992) - *A closing Ligurian Sea?* Pageoph., **139**:179-194.

Bordoni P. & Valensise G. (1998) - *Deformation of the 125 ka marine terrace in Italy; tectonic implications.* In: Stewart I.S. & Vita-Finzi C. (Eds.): "*Coastal tectonics*". Geol. Soc. of London, Spec. Publ., **146**:71-110.

Boschi E., Guidoboni E., Ferrari G., Valensise G. & Gasperini P. (1997) - *Catalogue of the strong earthquakes in Italy from 461 b.C. to 1990 (in Italian).* ING-SGA, pp.973, Bologna.

BRGM (2004) - French database SisFrance on Historical Seismicity (internal file).

Bruno P.P., Di Fiore V. & Ventura G. (2000) - *Seismic study of the "41st Parallel" fault system offshore the Campanian-Latial continental margin, Italy.* Tectonophysics, **324**:37-55.

Caccamo D., Neri G., Sarao A. & Wyss M. (1996) - *Estimates of stress directions by inversion of earthquake fault-plane solutions in Sicily.* Geophys. J. Int., **125**:857-868.

Calcagnile G., Panza G.F. & Knopoff L. (1979) - *Upper-mantle structure of north-central Italy from the dispersion of Rayleigh waves.* Tectonophysics, **56**:51-63.

Calcagnile G., & Panza G.F. (1981) - The main characteristics of the lithosphere-asthenosphere system in Italy surrounding regions. Pageoph., **119**:865-879.

Calcagnile G., D'Ingeo F., Farruggia P., & Panza G.F. (1982) - *The lithosphere in the central-eastern Mediterranean area.* Pageoph., **120**:389-406.

Capocecera P., Carbonara S. & Verrubbi V. (1995) - *Lazio Meridionale. Sintesi delle ricerche geologiche multidisciplinari. "Elaborazione ed interpretazione dei risultati".* ENEA-Serie Studi e Ricerche, Rome: 237-243.

CAPUTO M., PANZA G.F. & POSTPISCHL D. (1970) - *Deep structure of the Mediterranean Basin*. J. Geophys. Res., **75**:4919-4923.

CAPUTO M., PANZA G.F. & POSTPISCHL D. (1973) - *New evidences about the deep structure of the Lipari arc*. Tectonophysics, **15**:219-231.

CARMINATI E., WORTEL M.J.R., SPAKMAN W. & SABADINI R., (1998) - *The role of slab detachment processes in the opening of the western-central Mediterranean basins: some geological and geophysical evidence,* Earth. Planet. Sci. Lett., **160**:651-665.

CARTER T.G., FLANAGAN J.P., REED-JONES C., MARCHANT F.L., MURCHISON R.R., REBMAN J.H., SYLVESTER J.H. & WHITNEY J.C. (1972) - *A new bathymetric chart and physiography of the Mediterranean Sea.* In: STANLEY D.J. (Ed.): "*The Mediterranean Sea: A Natural sedimentation Laboratory*". Dowden, Hutchinson and Ross, London.

CASSINIS R. (1981) - *The structure of the Earth's crust in the Italian region*. In: WEZEL F.C. (Ed.): "*Sedimentary basins of Mediterranean margins*". Proceedings/C.N.R. International conference held at Urbino University, Pitagora, Bologna.

CASSINIS R., LOZEJ A., TABACCO I., GELATI R., BIELLA G., SCARASCIA S. & MAZZOTTI A. (1990) - *Reflection and refraction seismics in areas of complex geology. An example in the Northern Apennines*. Terra Res., **2**:351-362.

CATTANEO M., EVA C., MERLANTI F. & PASTA M. (1987) - *Analisi della sismicità della Liguria occidentale dal 1982 al 1986*. Atti del 6o Convegno Nazionale GNGTS, **1**:295-305.

CHAUMILLON E., DEVERCHÈRE J., RÉHAULT J.P. & GUEGUEN E. (1994) - *Réactivation tectonique et flexure continentale Ligure (Méditerranée Occidentale).* C.R. Acad. Paris, **319**:675-682.

CHIAPPINI M., MELONI A., BOSCHI E., FAGGIONI O., BEVERINI N., CARMISCIANO C. & MARSON I. (2000) - *Shaded relief magnetic anomaly map of Italy and surrounding marine areas,* Annali di Geofisica, **43**:983-989.

COLOMBI B., GIESE P., LUONGO G., MORELLI C., RIUSCETTI M., SCARASCIA S., SCHÜTTE K.G., STROWALD J. & DE VISENTINI G. (1973) - *Preliminary report on the seismic refraction profile Gargano-Salerno-Pantelleria*. Boll. Geof. Teor. Appl., **15**:225-254.

CONTRUCCI I., NERCESSIAN A., BETHOUX N., MAUFFRET A. & FERRANDINI J. (2001) - *A Ligurian (Western Mediterranean Sea) geophysical transect revisited*. Geophys. J. Int., **146**:74-97.

DAHM T., THORWART M., FLUEH E.R., BRAUN TH., HERBER R., FAVALI P., BERANZOLI L., D'ANNA G., FRUGONI F. & SMRIGLIO G. (2002) - *Ocean bottom seismometers deployed in the Tyrrhenian Sea.* EOS Trans. AGU, **83**:309, 314-315.

DE FRANCO R., BIELLA G., CORSI A., CAEILTI G., MAUFFRET A. & CONTRUCCI I. (1998) - *Crustal structure of the Northern Tyrrhenian from reflection-refraction data*. Annales Geophysicae, **16**:119.

DELLA VEDOVA B., MONGELLI F., PELLIS G., SQUARCI P., TAFFI L. & ZITO G. (1991) - *Heat flow map of Italy*. Int. Inst. For Geothermal Research Pubbl., Pisa.

DE VOOGD B., NICOLICH R., OLIVET J.L., FANNUCCI F., BURRUS J. & ECORS-CROP Working Group (1991) - *First Deep Seismic Reflection Transect from the Gulf of Lions to Sardinia (ECORS-CROP Profiles in Western Mediterranean)*. In: MEISSNER R.O., BROWN L.D., DÜRBAUM H.J., FRANKE W. & FUCHS K. (Eds.): "*Continental Lithosphere Seismic Reflection*". Geodyn. Ser. **22**, 265-274.

DIETRICH V.; EMMERMANN R.; PUCHELT H.; KELLER J. (1978) - *Oceanic basalts from the Tyrrhenian Basin*, DSDP Leg 42A, Hole 373A. In: HSÜ K. J.; MONTADERT L.; GARRISON R. E.; FABRICIUS F. H.; MUELLER C.; CITA M. B.; BIZON G.; WRIGHT R. C.; ERICKSON A. J.; BERNOULLI D.; MELIERES F.; KIDD R. B.; WORSTELL P. J. (Eds.). Initial Reports of the Deep Sea Drilling Project **42** Part 1, Ocean Drilling Program, ISSN: 0080-8334 CODEN: IDSDA6:515-530.

DI GIOVAMBATTISTA R. & BARBA S. (1997) - *An estimate of hypocentre location accuracy in a large network: possible implications for tectonic studies in Italy.* Geophys. J. Int., **129**:124-132.

DOGLIONI C. (1991) - *A proposal for the kinematic modelling of W-dipping subduction: possible applications to the Tyrrhenian-Apennines system*. Terra Nova, **3**:423-434.

DUSCHENES J., SINHA M.C. & LOUDEN K.E. (1986) - *A seismic refraction experiment in the Tyrrhenian Sea*. Geophys. J. R. Astr. Soc., **85**:139-160.

EL ALI H. & GIESE P. (1978) - *A geothermal profile between the Adriatic and Tyrrhenian Seas.* In: CLOSS H., ROEDER D. & SCHMIDT R. (Eds.). Inter-Union Commission on Geodynamics Scientific Report **38**:324-327.

EOST- Ecole et Observatoire des Sciences de la Terre de Strasbourg (2004) - RéNaSS (Résau National de Surveillance Sismique (internal file).

EVA E. & SOLARINO S. (1998) - V*ariations of stress directions in the western Alpine arc*. Geophys. J. Int., **135**:438-448.

EVA E., SOLARINO S. & SPALLAROSSA D. (2001) - *Seismicity and crustal structure beneath the western Ligurian Sea derived from local earthquake tomography.* Tectonophysics, **339**:495-510.

FACCENNA C., FUNICIELLO R. & MATTEI M. (1994) - *Late Pleistocene N-S shear zones along the Latium Tyrrhenian margin: structural characters and volcanological implications*. Boll. Geof. Teor. Appl., **36**:141-144.

FAVALI P., FUNICIELLO R., MATTIETTI G., MELE G. & SALVINI F. (1993a) - *An active margin across the Adriatic Sea (central Mediterranean Sea)*. Tectonophysics, **219**:109-117.

FAVALI P., FUNICIELLO R. & SALVINI F. (1993b) - *Geological and seismological evidence of strike-slip displacement along E-W Adriatic-Central Apennine belt*. In: BOSCHI E., MANTOVANI E. & MORELLI A. (Eds.): "*Recent evolution and seismicity of the Mediterranean region*", NATO ASI Series C, **402**:333-346, Kluwer Acad. Publ., Netherlands.

FINETTI I. & MORELLI C. (1973) - G*eophysical exploration of the Mediterranean Sea*. Boll. Geof.. Teor. Appl., **15**:263-340.

FINETTI, I. & DEL BEN A. (1986) - *Geophysical study of the Tyrrhenian opening*. Boll. Geof. Teor. Appl., **28**:75-156.

FREPOLI A., SELVAGGI G., CHIARABBA C. & AMATO A. (1996) - S*tate of stress in the Southern Tyrrhenian subduction zone from fault-plane solutions*. Geophys. J. Int., **125**:879-891.

GAMBERI F., MARANI M. & SAVELLI C. (1997) - *Tectonic, volcanic and hydrothermal features of a submarine portion of the Aeolian arc (Tyrrhenian Sea)*. Mar. Geol., **140**:167-181.

GASPARINI C., IANNACCONE G., SCANDONE P. & SCARPA R. (1982) - *Seismotectonics of the Calabrian Arc*. Tectonophysics, **84**:267-286.

GASPARINI C., IANNACCONE G., SCANDONE P. & SCARPA R. (1985) - *Fault plane solutions and seismicity of the Italian peninsula*. Tectonophysics, **117**:59-78.

GIARDINI D., DZIEWONSKI A.M., WOODHOUSE J.H. & BOSCHI E. (1984) - *Systematic analysis of the seismicity of the Mediterranean region using the centroid moment tensor method*. Boll. Geof. Teor. Appl., **26**:103-121.

GIARDINI D. & VELONÀ, M. (1991) - *The deep seismicity of the Tyrrhenian Sea*. Terra Nova, **3**:57-64.

GINZBURG A., MAKRIS J. & NICOLICH R. (1986) - *European geotraverse: a seismic refraction profile across the Ligurian Sea*. Tectonophysics, **126**:85-97.

Gruppo di Lavoro CPTI (1999) - Catalogo Parametrico dei Terremoti Italiani. ING, GNDT, SGA, SSN. Bologna,

92 pp.

HEEZEN B.C., GRAY C., SEGRE A.G. & ZARUDZKI E.F.K. (1971) - *Evidence of foundered continental crust beneath the central Tyrrhenian Sea*. Nature, **229**:327-329.

HUTCHISON I., VON HERZEN R.P., LOUDEN K.E., SCLATER J.G. & VERNON F.L. (1994) - *Heat flow in the Balearic and Tyrrhenian basins, western Mediterranean*. J. Geophys. Res., **90**:685-701.

KASTENS K., MASCLE J., AUROUX C., BONATTI E., BROGLIA C., CHANNELL J., CURZI P., EMEIS K.C., GLACON G., ASEGAWA S., HIEKE W., MASCLE G., MCCOY F., MCKENZIE J., MENDELSON J., MULLER C., RÉHAULT J.P., ROBERTSON A., SARTORI R., SPROVIERI R. & TORII M. (1988) - *ODP Leg 107 in the Tyrrhenian Sea: insights into passive margin and back-arc basin evolution*. Geol. Soc. Am. Bull., **100**:1140-1156.

ISSEL A. (1887) - *Il terremoto del 1887 in Liguria*. Suppl. Boll. R. Com. Geol. d'Italia. pp.190, Tipografia Nazionale, Roma.

INGV- Istituto Nazionale di Geofisica e Vulcanologia (2004) - Instrumental seismic catalogue (internal file).

LODDO M. & MONGELLI F. (1979) - *Heat flow in Italy*. Pageoph., **117**:135-149.

LUONGO G. & MAZZARELLA A. (1997) - *On the clustering of seismicity in the Southern Tyrrhenian area*. Annali di Geofisica, **40**:1303-1309.

MAKRIS J., EGLOFF F., NICOLICH R. & RIHM R. (1999) - *Crustal structure from the Ligurian Sea to the Northern Apennines - a wide angle seismic transect*. Tectonophysics, **301**:305-319.

MALINVERNO A. (1981) - *Quantitative estimates of age and Messinian paleobathymetry of the Tyrrhenian Sea after seismic reflection, heat flow and geophysical models*. Boll. Geof. Teor. Appl., **23**:159-171.

MALINVERNO A. & RYAN W.B.F. (1986) - *Extension in the Tyrrhenian Sea and shortening in the Apennines as result of arc migration driven by sinking of the lithosphere*. Tectonics, **5**:227-245.

MANTOVANI E., BABBUCCI D. & FARSI F. (1985) - *Tertiary evolution of the Mediterranean region: major outstanding problems*. Boll. Geof. Teor. Appl., **105**:67-90.

MANTOVANI E., BABBUCCI D., ALBARELLO D. & MUCCIARELLI M. (1990) - *Deformation pattern in the Central Mediterranean and behaviour of the African/Adriatic promontory*. Tectonophysics, **179**:63-79.

MANTOVANI E., ALBARELLO D., TAMBURELLI C. & BABBUCCI D. (1996) - *Evolution of the Tyrrhenian basin and surrounding regions as a result of the Africa-Eurasia convergence*. J. Geodynamics, **21**: 35-72.

MARAMAI A. & TERTULLIANI A. (1994) - *Some events in Central Italy: are they all tsunamis? A revision for the Italian tsunami catalogue*. Annali di Geofisica, **37**:997-1008.

MERCALLI G. & TARAMELLI T. (1888)- *Il terremoto ligure del 23 febbraio 1887*. Annali Uff. Cent. Meteor. e Geodin., Serie II, Vol.VIII, Parte IV, Roma.

MOLIN D. & PACIELLO A. (1995) - *Lazio Meridionale. Sintesi delle ricerche geologiche multidisciplinari. "Caratteri della sismicità storica"*. ENEA-Serie Studi e Ricerche, 215-222.

MONGELLI F., LODDO M. & CALCAGNILE G. (1975) - *Some observations on the Apennines gravity field. Earth Planet*. Sci. Lett., **24**:385-393.

MONGELLI F., ZITO G., CIARANFI N. & PIERI P. (1989) - *Interpretation of heat flow density of the Apennine chain, Italy*. Tectonophysics, **164**:267-280.

MONGELLI F. & ZITO G. (1994) -*Thermal aspects of some geodynamical models of Tyrrhenian opening*. Boll. Geof. Teor. Appl., **36**:21-28.

MONGELLI F. & ZITO G. (2000) - *The thermal field in a basin after a sudden passive pure shear lithospheric extension and sublithospheric mechanical erosion: the case of the Tuscan Basin (Italy)*. Geoph. J. Int., **142**:142-150.

MORELLI C. (1970) - *Physiography, gravity and magnetism of the Tyrrhenian Sea*. Boll. Geof. Teor. Appl., **12**:275-311.

MORELLI C. (1981) - *Gravity anomalies and crustal structures connected with the Mediterranean margins*. In: WEZEL F.C.(Ed.): "*Sedimentary Basins of Mediterranean Margins*", C.N.R. Italian Project of Oceanography, Tecnoprint, Bologna, 33-53.

MORELLI C., GIESE P., CASSINIS R., COLOMBI B., GUERRA I., LUONGO G., SCARASCIA S. & SCHUTTE K.G. (1975) - *Crustal structure of southern Italy. A seismic refraction profile between Puglia-Calabria-Sicily*. Boll. Geof. Teor. Appl., **17**:182-210.

NERI G., CACCAMO D., COCINA O. & MONTALTO A. (1991) - *Shallow earthquake features in the Southern Tyrrhenian region: geostructural and tectonic implications*. Boll. Geof. Teor. Appl., **129**:47-60.

NICOLICH R. (1989) - *Crustal structure from seismic studies in the frame of the European Geotraverse (southern segment) and CROP project*. In: BORIANI A., BONAFEDE M., PICCARDO G.B. & VAI G.B. (Eds.): "*The lithosphere in Italy. Advances in Earth Science Research*". Atti Convegni dei. Lincei, **80**, 41-61.

PANZA G.F., PROZOROV A.G. & SUHADOLC P. (1990) - *Lithosphere structure and statistical properties of seismicity In Italy and surrounding regions*. J. Geodynamics, **12**:189-215.

PASCUCCI V., MERLINI S. & MARTINI P. (1999) - *Seismic stratigraphy of the Miocene-Pleistocene sedimentary basins of the Northern Tyrrhenian Sea and western Tuscany (Italy)*. Basin Res., **11**:337-356.

PASQUALE V., VERDOYA M. & CHIOZZI P. (1995) - *Rifting and thermal evolution of the Northwestern Mediterranean*. Annali di Geofisica, **38**:43-53.

PASQUALE V., VERDOYA M., CHIOZZI P. & RANALLI G. (1997) - *Rheology and seismotectonic regime in the northern central Mediterranean*. Tectonophysics, **270**:239-257.

PATACCA E. & SCANDONE P. (1989) - *Post-Tortonian mountain building in the Apennines: the role of the passive sinking of a relic lithospheric slab*. In: BORIANI A., BONAFEDE M., PICCARDO G.B. & VAI G.B. (Eds.): "*The lithosphere in Italy: Advances in Earth Science Research*". Atti Convegni Lincei, **80**:157-176.

PATACCA E., SARTORI R. & SCANDONE P. (1990) - *Tyrrhenian basin and Apenninic arcs: kinematics relations since late Tortonian times*. Mem. Soc. Geol. It., **45**:425-451.

PATACCA E., SARTORI R. & SCANDONE P. (1993) - *Tyrrhenian basin and Apennines, kinematic evolution and related dynamic constraints*. In: BOSCHI E., MANTOVANI E. & MORELLI A. (Eds.): "*Recent evolution and seismicity of the Mediterranean region*". NATO ASI Series C, **402**, 161-171, Kluwer Acad. Publ., Netherlands.

PERONACI F. (1953) - *Il terremoto Sardo del 13 novembre 1948*. Annali di Geofisica, **6**:1-11.

RECQ M., REHAULT J.P., STEINMETZ L. & FABBRI A. (1984) - *Amincissement de la croute et accretion au centre du bassin Tyrrhenien d'apres la sismique refraction*. Mar. Geol., **55**:411-428.

REHAULT J.P. & BETHOUX N. (1984) - *Earthquake relocation in the Ligurian Sea (Western Mediterranean): Geological interpretation*. Mar. Geol., **55**:447-477.

ROYDEN L., PATACCA E. & SCANDONE P. (1987) - *Segmentation and configuration of subducted lithosphere in Italy: an important control on thrust-belt and foredeep basin evolution*. Geology, **15**:714-717.

SARTORI R. (1990) - *The main results of ODP Leg 107 in the frame of Neogene to recent geology of peri-Tyrrhenian areas*. In: KASTENS K., MASCLE J., AUROUX C., BONATTI E.,

BROGLIA C., CHANNELL J., CURZI P., EMEIS K.C., GLACON G., ASEGAWA S., HIEKE W., MCCOY F., MCKENZIE J., MASCLE G., MENDELSON J., MULLER C., RÉHAULT J.P., ROBERTSON A., SARTORI R., SPROVIERI R. & TORII M. (Eds.). Proceedings of the Ocean Drilling Program, **107**:715-730.

SCANDONE P. & PATACCA E. (1984) - T*ectonic evolution of the central Mediterranean area*. Annales Geophysicae, 2:139-142.

SCARPA R. (1982) - *Travel-time residuals and three dimensional velocity structure of Italy*. Pageoph., **120**:583-606.

SELVAGGI G. & CHIARABBA C. (1995) - *Seismicity and P-wave velocity image of the Southern Tyrrhenian subduction zone*. Geophys. J. Int., **121**:818-826.

SERRI G. (1990) - *Neogene-Quaternary magmatism of the Tyrrhenian region: characterisation of the magma sources and geodynamics implications*. Mem. Soc. Geol. It., **41**:219-242.

SOLOVIEV S.L., KUZIN I.P., KOVACHEV S.A., FERRI M., GUERRA I. & LUONGO G. (1990) - *Micro-earthquakes in the Tyrrhenian Sea as revealed by joint land and sea-bottom seismographs*. Mar. Geol., **94**:131-146.

SPERANZA F., VILLA I.M., SAGNOTTI L., FLORINDO F., CASENTINO D., CIPOLLATI P. & MATTEI M. (2002) - *Age of the Corsica-Sardinia rotation and Liguro-Provençal basin spreading: new paleomagnetic and Ar/Ar evidence*. Tectonophysics, **347**:231-251.

STEINMETZ L., FERRUCCI F., HIRN A., MORELLI C., & NICOLICH R. (1983) - *A 550 km long Moho transverse in the Tyrrhenian Sea by OBS recorded Pn waves*. Geophys. Res. Lett., **94**:5637-5649.

TAPPONNIER P. (1977) - *Evolution tectonique du systeme alpine en Mediterranée. Poinçonnement et ecrasement rigide-plastique*. Bull. Soc. Geol. Fr., **19**:437-460.

TERTULLIANI A., ROSSI A. & DI GIOVAMBATTISTA R. (2003) - *Reappraisal of the October 1919 Central Italy Earthquake*. Bull. Seis. Soc. Am., **93**:1298-1305.

TINTI S. (1991) -*Assessment of tsunami hazard in the Italian seas*. Natural Hazards, **4**: 267-283.

TINTI S. & MARAMAI A. (1996) - *Catalogue of tsunamis generated in Italy and in Côte d'Azur, France: a step towards a unified catalogue of tsunamis in Europe*. Annali di Geofisica, **39**:1253-1299.

TINTI S., MARAMAI A. & GRAZIANI L. (2004) - The new catalogue of Italian tsunamis. Natural Hazards (in press).

TRUA T., SERRI G. & MARANI M.P. (2003) - *Lateral flow of African mantle below the nearby Tyrrhenian plate: geochemical evidence*. Terra Nova, **15**:433-440.

VIALON P., ROCHETTE P. & MÈNARD G. (1989) - *Indentation and rotation in the western Alpine arc*. In: COWARD M.P., DIETRICH D. & PARK R.G. (Eds.): "*Alpine Tectonics*". Geol. Soc. of London, Spec. Publ., **45**:326-338.

WESTAWAY R. (1993) - *Quaternary uplift of southern Italy*. J. Geophys. Res., **98**:741-772.

ZITO G., MONGELLI F., DE LORENZO S. & DOGLIONI C. (2003) - *Heat flow and geodynamics in the Tyrrhenian Sea*. Terra Nova, **15**:425-432.

Mem. Descr. Carta Geol. d'It.
XLIV (2004), pp71-82
12 figg.

Geodynamic interpretation of the heat flow in the Tyrrhenian Sea
Interpretazione geodinamica del flusso di calore nel Mar Tirreno

MONGELLI F. (*), ZITO G. (*), DE LORENZO S. (*), DOGLIONI C. (**)

ABSTRACT - The higher heat flow in the eastern Tyrrhenian Sea supports both the notion of a migrating rift and an eastward migrating asthenosphere underneath the basin. Punctuation of the Tyrrhenian backarc extension in lithopheric boudins is accompanied by increase in heat flow generated by asthenospheric intrusions progressively moving eastward. The rifting developed in a pre-existing thickened lithosphere by the Alpine orogeny. The present heat flow should then be imaged as a transient wave of values migrating eastward in time.

KEY WORDS: heat flow, asthenospheric intrusions, eastwards migration, Tyrrhenian Sea

RIASSUNTO - La mappa del flusso di calore nel Mar Tirreno mostra un valore regionale molto alto di 120 mW m^{-2} e due forti massimi locali di 143 e 245 mW m^{-2} in aree di recente attività tettonica e vulcanica.
Il rifting che ha generato il bacino di retro-arco tirrenico iniziò nellOligocene superiore (19-15 Ma) generando il bacino Ligure-Provenzale. Il rifting saltò ad est del blocco Sardo-Corso, procedendo a salti e generando nel Tirreno meridionale due bacini principali: Vavilov (7-3.5 Ma) e Marsili (1.7-1.2 Ma) caratterizzati dai due omonimi vulcani. L'alto valore regionale del flusso di calore viene interpretato come conseguenza dell'assottigliamento litosferico mentre i due massimi locali vengono spiegati come intrusioni astenosferiche. Questa interpretazione supporta l'idea di un rift e di una astenosfera migranti entrambi verso est, accompagnate da intrusioni astenosferiche che si succedono l'una all'altra nella stessa direzione.

PAROLE CHIAVE: flusso di calore, intrusioni astenosferiche, migrazione verso est, Mar Tirreno

1. - INTRODUCTION

The Tyrrhenian Sea is an area of great interest from a geothermal point of view because the observed heat flow is one of the highest in the world.

ERICKSON (1970) carried out the first measurements of heat flow in the Tyrrhenian basin in 12 stations. The average value of the best 10 sites was 147.5 mW m^{-2}.

SCLATER (1972) studied the relationship between heat flow and elevation of the marginal basins of the western Pacific, and LODDO & MONGELLI (1974) pointed out that Erickson's value was too high with respect to the elevation, denoting an anomalous state of the basin.

MALINVERNO (1981) & MALINVERNO *et alii* (1981) interpreted the existing data by supposing that the Tyrrhenian basin was created behind an eastward migrating trench system by the stretching of the lithosphere.

HUTCHISON *et alii* (1985) produced new heat flow data and applied the simple stretching model of MCKENZIE (1978) to the western Tyrrhenian (HF=1348±8 mW m^{-2}) and obtained a very high stretching factor (β=6). They maintain that, when stretching is long and continuous, oceanic crust is created in the central rift. They modeled this phase in the southern Tyrrhenian where the heat flow was 151±10 mW m^{-2}, with the oceanic plate model of PARSONS & SCLATER (1977) which corresponds to β=×.

DELLA VEDOVA *et alii* (1991) compiled a heat flow

(*) Dipartimento di Geologia e Geofisica, Università di Bari, Italy
(**) Dipartimento di Scienze della Terra, Università "La Sapienza", Roma, Italy

DELLA VEDOVA *et alii* (1991) compiled a heat flow map of the Tyrrhenian Sea and surrounding areas based both on pre-existing data and new measurements. This map (fig. 1) shows a very high regional value of 120 mW m^{-2} and two strong local maxima of 143 mW m^{-2} and 245 mW m^{-2} in areas of recent tectonic and volcanic activity and of probable convective water movements.
Since new geological and geophysical knowledge has accumulated on the basin, we propose an updated geodynamic interpretation of the heat flow..

2. - GEOLOGICAL AND GEOPHYSICAL SETTING

Research about the geological history of the Tyrrhenian Sea has greatly improved due to some DSDP and ODP wells, seismic reflection profiles, sampling and volcanological studies (e.g., ZITELLINI *et alii*, 1986; ELLAM *et alii*, 1988; KASTENS *et alii*, 1988; FRANCALANCI *et alii*, 1993; PASCUCCI *et alii*, 1999). Several papers proposed geophysical and geodynamic models on the opening of the basin (e.g., SCANDONE, 1980; MALINVERNO *et alii*, 1981; MANTOVANI, 1982;

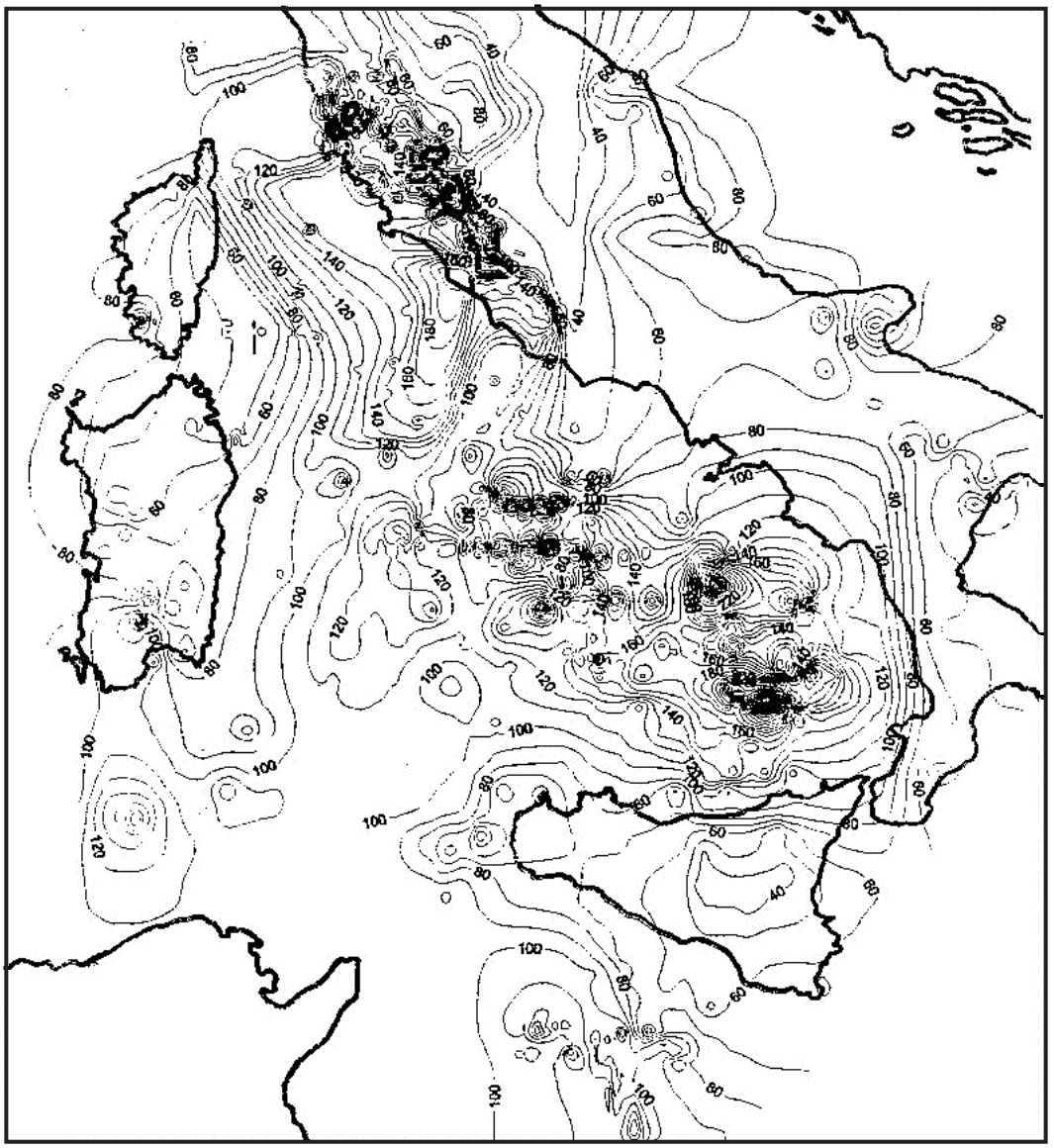

Fig. 1 – *Heat flow density (mW m-2) in the Italian Peninsula and surrounding areas (Contour lines equidistance: 10 mW m-2)*

FINETTI & DEL BEN, 1986; MALINVERNO & RYAN, 1986; PATACCA & SCANDONE, 1989; MONGELLI & ZITO, 1994; GUEGUEN *et alii* 1997; CELLA *et alii*, 1998). Here we summarize some important results that are useful for our study.

The Adriatic microplate subduction initiated in the Late Oligocene-Early Miocene and developed to the East of the former Alpine Chain. The Apenninic accretionary prism formed in sequence at the front of the pre-existing Alpine back-thrust belt. The Apenninic back-arc extension migrated eastward and boudinated the former Alpine nappe stack (DOGLIONI *et alii*, 1998). Kinematics and geophysical data support the presence of an eastward migrating asthenospheric wedge at the subduction hinge of the rolling-back Adriatic plate (GUEGUEN *et alii*, 1997).

Rifting initiated in the Upper Oligocene in the Liguro-Provençal basin to the west of Corsica-Sardinia, floored by oceanic crust 19-15 Ma ago. The rifting jumped east of Corsica and Sardinia proceeding by steps and generating in the southern Tyrrhenian two major basins, i.e., the Vavilov basin (7-3.5 Ma) and the Marsili basin (1.7-1.2 Ma) marked by the two homonymous volcanoes Vavilov and Marsili (fig. 2).

Basalts at the Mt Vavilov are OIB-MORB type with an age of 4.1 Ma (SARTORI, 1989), while the basalts of Mt. Marsili are calc-alcaline (BECCALUVA *et alii*, 1990), and the upper-lying sediments have an age of 1.8 Ma (KASTENS *et alii*, 1988) indicating a very young basaltic crust.

Subduction of the southern Adriatic plate is demonstrated by the existence of a well-defined Benioff plane under the Tyrrhenian Sea. Many authors (GASPARINI *et alii*, 1982; ANDERSON & JACKSON, 1987; GIARDINI & VELONÀ, 1991; AMATO *et alii*, 1991, 1993; SELVAGGI & CHIARABBA, 1995; CIMINI, 1999; SELVAGGI, 2001) have attempted to define the geometry of the subducted slab by different seismological methods. SELVAGGI & CHIARABBA (1995) described a continuous slab having a gentle slope down to 50 km of depth, then a rapid increase at the hinge, where the slope reaches 70° that remains constant down to 500 km.

CALCAGNILE & PANZA (1981) defined the lithosphere thickness of the Tyrrhenian area by the dispersion of surface waves; they found that the lithosphere is thinned up to 30 km in the central sector of the area. Recently PONTEVIVO & PANZA (2002) found that the thickness is about 20 km in the southernmost sector of the basin (fig. 3). The structure of the Tyrrhenian crust has been studied at length by gravimetric methods (MORELLI, 1970, 1981; MORELLI *et alii*, 1975) and seismic exploration (FINETTI & DEL BEN, 1986; PASCUCCI *et alii*, 1999).

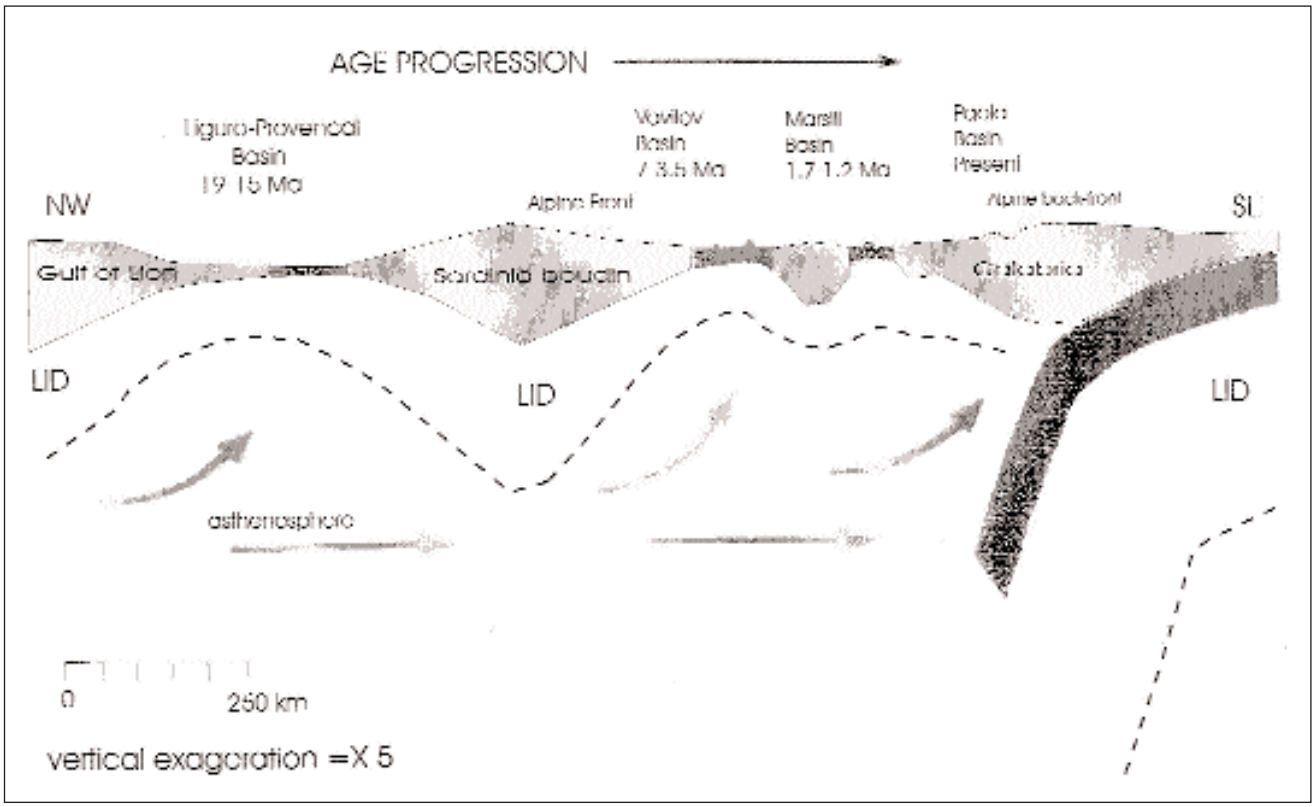

Fig. 2 – *The progressive boudinage and deformation of the Alpine belt by the back-arc extension of the Apenninic subduction* (*by* GUEGUEN *et alii*, 1999)

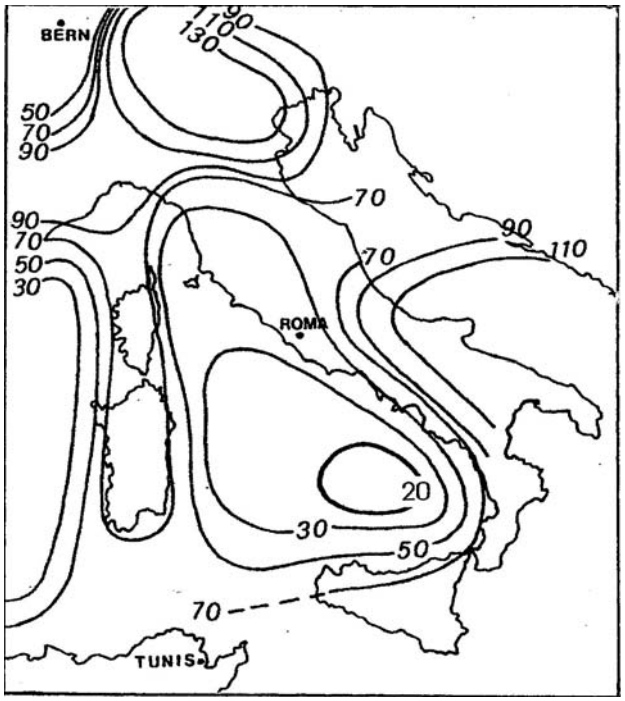

Fig. 3 – *Lithospheric thickness (km) in Italian territory and surrounding areas* (CALCAGNILE & PANZA, 1980, *modified after the results of* PONTEVIVO & PANZA, 2002)

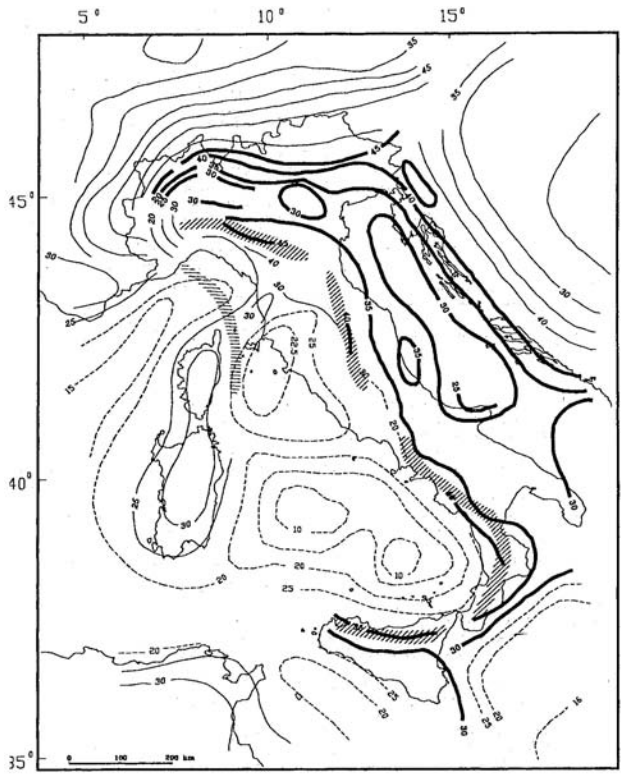

Fig. 4 – *Moho isobaths (km) in Italian territory and surrounding areas. Different contour lines are ascribed to the Adriatic plate -thick lines-; the European plate -thin lines- and the stretched continental crust -dashed lines-* (after LOCARDI & NICOLICH, 1988, *modified*).

The Tyrrhenian Sea is the site of an intense Bouguer anomaly (>250 mGal); its interpretation (CELLA *et alii*, 1998) by assuming density values constrained by the results of the seismic exploration, confirms the existence of a very thin crust (fig.4).

The map of the depth of the Moho (LOCARDI & NICOLICH, 1988 modified by MORELLI, 1995) shows values lower than 15-20 km for the batial plane, and two minima of 10 km centered on the Vavilov and Marsili basins. It is worthwhile to note that these minima coincide with the highest values of the heat flow. The lithospheric boudinage proposed by GUEGUEN *et alii* (1997) and shown as figure 2 is suggested to be slightly asymmetric by the gravimetric reconstruction of CELLA *et alii* (1998), the continental roots of Corsica-Sardinia being shifted to the east with respect to the higher topography. This would confirm the presence of a migrating asthenosphere from west to east.

3. - THE MODEL OF THE TYRRHENIAN SEA FORMATION

3.1. - GEODYNAMIC MODEL

Let suppose that during Oligocene time, the European and Adriatic plates are sutured by the Alpine orogen giving a thickened lithosphere h_L, ideally composed of two sectors BC and CD, to the East of a sector AB of the Alpine foreland with thickness L (fig. 5).

In early Miocene time, between 19 and 15 Ma ago, sector AB first stretched by a factor β so that it thinned to L/β. Further stretching caused the laceration of the thinned lithophere favouring the passive rising at the surface of an asthenopheric body wide a. As a consequence, blocks BC+CD rifted by AB $(\beta\text{-}1)+a$.

During Late Miocene-Early Pliocene times between 7 and 3.5 Ma ago, sector BC stretched by the factor β_1, and thinned to h_L/β_1. At 3.5 Ma ago, further stretching caused the laceration of the thinned lithosphere favoring the passive rising of an asthenospheric body, wide b. As a consequence, block CD further rifted by BC $(\beta_1\text{-}1)+b$.

During Pleistocene times, between 1.7 and 1.2 Ma ago, block CD stretched by the factor β_2 and thinned to h_L/β_2. At 1.2 Ma ago further stretching caused the laceration and the rising of an other asthenospheric body, wide c. Point D further rifted by CD $(\beta_2\text{-}1)+c$. These last two extensions formed the southern Tyrrhenian Sea.

At present, the distance BD is about 550 km, that is the distance between Sardinia and Calabria.

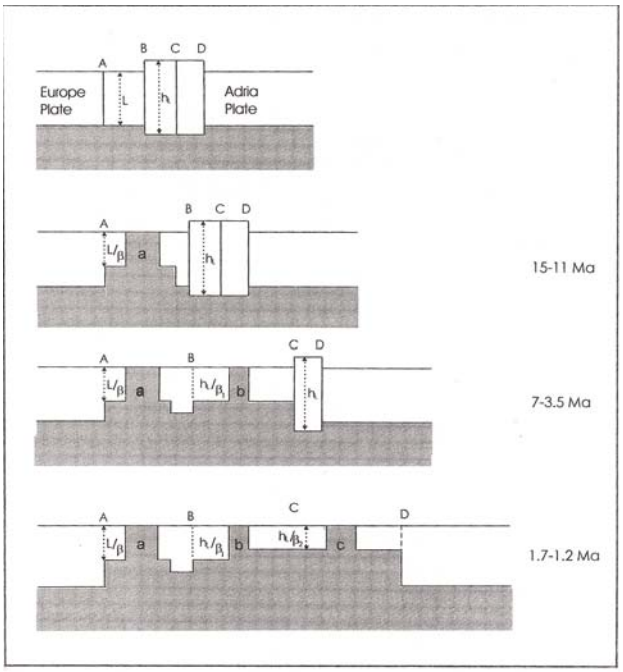

Fig. 5 – *Diagrammatic illustration of the time evolution of the lithospheric extension and thinning, since Oligocene to Pleistocene. See text for explanation.*

3.2. - THERMAL MODEL

Figure 6 shows the heat flow map of the Tyrrhenian Sea, which has been smoothed to eliminate small local anomalies. This map is the result of the superimposition of the effects of the lithospheric extension and of local asthenospheric intrusions in two different areas: the older Vavilov basin, where heat flow reaches the value of 140 mW m^{-2}, and the younger Marsili basin, with values of 240 mW m^{-2}.

From a thermal point of view, we have to consider the mantle, the radioactive components of the heat flow, and the intrusion effects.

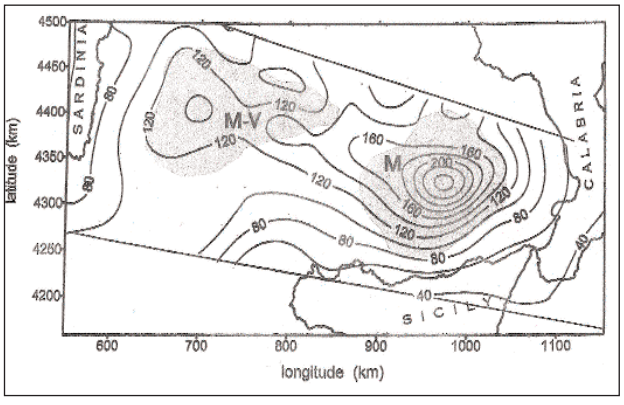

Fig. 6 – *The smoothed heat flow density map (in mW m-2) of the Southern Tyrrhenian Sea.*

3.2.1 - *Mantle component*

MC KENZIE (1978) showed that the mantle component of the temperature and heat flow in a basin after a sudden passive pure shear extension, taking the surface temperature equal to zero, are respectively:

$$T(z,t) = T_1\left\{1 - \frac{z}{h_L} + \frac{2}{\pi}\sum_{n=1}^{\infty}\frac{(-1)^{n-1}}{n}\left[\frac{\beta}{n\pi}\sin\left(\frac{n\pi}{\beta}\right)\right]\sin\left(\frac{n\pi}{h_L}z\right)\exp\left(-\frac{n^2 t}{\tau}\right)\right\} \quad (1)$$

$$q_m = \lambda\frac{T_1}{h_L}\left[1 + 2\sum_{n=1}^{\infty}\left[\frac{\beta}{n\pi}\sin\left(\frac{n\pi}{\beta}\right)\right]\exp\left(-\frac{n^2 t}{\tau}\right)\right] \quad (2)$$

where the thermal conductivity of the lithosphere
T_1 the temperature at the base of the lithosphere
h_L the thickness of the lithosphere before thinning
β the thinning factor of the lithosphere

$$\tau = \frac{h_L^2}{\pi^2\kappa}$$

κ the thermal diffusivity of the lithosphere
τ the time after the thinning
$\lambda T_1/h_L$ is the mantle heat flow before thinning.

We assume that before the extension phase the lithosphere had the same structure as the present Alpine Chain (because it was part of this chain): a lithosphere 130 km thick (CALCAGNILE & PANZA, 1980) and a crust 45-50 km thick (LOCARDI & NICOLICH, 1988; MORELLI, 1995).

To calculate values in both basins we use the numerical relation (MONGELLI, 1991) which expresses the rethickening after stretching

$$\frac{h_i - h}{h_i} = 0.0109 + \left(1 - \frac{1}{\beta}\right)0.99\exp\left(-\frac{10t}{\beta\tau}\right) \quad (3)$$

where h is the lithospheric thickness at the time t after extension.

We obtain β_1=*6.3* for the older extension and β_2=*7.0* for the younger.

We assume T_a = 1330°C, k= 25.3 $km^2\ Ma^{-1}$, λ= 2.5 $Wm^{-1}\ K^{-1}$ (ZITO *et alii*, 1993). The mantle contribution to the heat flow before thinning is 25.6 mW m^{-2}.

Figure 7 shows the mantle component of the geotherms to both extensions at present. Figure 8 shows the evolution of the heat flow; it is possible to see that at present, the value relative to the first extension is 135 mW m^{-2}, while that relative to the second extension is 205 mW m^{-2}.

3.2.2 - *Radioactive component*

The radioactive component of the heat flow in the Tyrrhenian basin can be deduced from the crust structure of the Alps. As the result of continent-

continent underthrusting, the crust under the Alps is a doubled crust (PFINNER, 1990; YE & ANSORGE, 1990).

CERMAK & BODRI (1991, 1996) modeled the thermal evolution of the Alps by assuming an exponential distribution of heat production in each crust component. As the total crust is 50 km thick, we assume each crust component 25 km thick. This crust under the central Tyrrhenian sea is reduced, by extension, to 15 km thick by a factor β_c=3.3, and each crust component to H_r=7.5 km.

In the southernmost sector the crust is reduced to 10 km by a factor of β_c=5 and each crust component to H_r=5 km. As a consequence, the contribution of radioactivity to the surface heat flow is strongly reduced. We retain that, in a short time the contribution is near the equilibrium. For simplicity, we calculate the thermal contribution of the radioactivity of this thinned crust in steady state.
We solve the equation:

$$\frac{d^2T_r}{dz^2} = -\frac{A(z)}{\lambda} \qquad (4)$$

where:

$$A(z) = \frac{A_0}{\beta_c}\exp\left(-\frac{z}{D}\right) \qquad 0 < z < H_r$$

$$A(z) = \frac{A_0}{\beta_c}\exp\left(-\frac{z-H_r}{D}\right) \qquad H_r < z < \frac{h_L}{\beta}$$

that is we assume that the pre-extension radioactive heat production A_0=3.15 μWm^{-3} is depleted by the factor β_c. Moreover D=8 km, h_L/β_1= 30 km, H_r=7.5 km for the older basin, and h_L/β_2=20 km and H_r=5 km for the younger.

With the boundary conditions:

$$T_1(z=0) = T_r\left(z=\frac{h_L}{\beta}\right) = 0°C$$

$$T_r(z=H_r^-) = T_r(z=H_r^+)$$

$$\left.\frac{dT_r}{dz}\right|_{z=H_r^-} = \left.\frac{dT_r}{dz}\right|_{z=H_r^+}$$

we have the solution given in Appendix (A1).
Figure 9 shows the radioactive component of the geotherms relative to both extensions. From the solution (A3) in the Appendix, we have the surface heat flow given by:

$$\lambda\left.\frac{dT_r}{dz}\right|_{z=0} = \frac{A_0Dz_1}{\beta_1 z_2}\left\{\exp\left(-\frac{z_1}{D}\right)-1\right\} + \frac{A_0D^2}{\beta_1 z_2}\left[\exp\left(-\frac{(z_2-z_1)}{D}\right)+\exp\left(-\frac{z_1}{D}\right)-2\right] + \frac{A_0D}{\beta_1}\left\{2-\exp\left(-\frac{z_1}{D}\right)\right\} \qquad (5)$$

Thus, the contribution to the surface heat flow is 7.95 mWm^{-2}, for the older and 6.2 mWm^{-2} for the younger basin.

As a consequence the calculated surface heat flow of the first extension is about 143 mWm^{-2}, and that of the second extension is about 213 mWm^{-2}. It is worthwhile to remember that the present value of the heat flow in the area of the first extension is more than 140 mWm^{-2} whereas it is more than 240 mWm^{-2} in the eastward younger Marsili basin (fig.6). These values are attributable to the asthenospheric intrusions and seems to confirm that when β>6 laceration of the lithosphere occurs.

3.2.3 - *Thermal effect of asthenospheric intrusion*

We suppose that the asthenospheric intrusion reaches the surface and cools down. The magma has a melt temperature Tm at which the phase change from liquid to solid occurs. The position of the phase change boundary z_m moves downward as solidification proceeds and, moreover, at this interface latent heat of fusion L is liberated. This is the Stefan problem. The solution, in one dimension, is (TURCOTTE & SCHUBERT, 1982):

$$\frac{T_1(z,t)-T_0}{T_m-T_0} = \frac{erf\left(\frac{z}{2\sqrt{kt}}\right)}{erf\lambda_1} \qquad (6)$$

where T_0 is the surface temperature,

$$\lambda_1 = \frac{z_m}{2\sqrt{kt}} \qquad (7)$$

and λ_1 is determined by the transcendental equation:

$$\frac{\exp(-\lambda_1^2)}{\lambda_1 erf\lambda_1} = \frac{L\sqrt{\pi}}{c(T_m-T_0)} \qquad (8)$$

where c is the specific heat.
The surface heat flow is:

$$\lambda\left.\frac{dT_1}{dz}\right|_{z=0} = \frac{\lambda}{\sqrt{\pi kt}}\frac{T_m}{erf\lambda_1} \qquad (9)$$

We retain that the second extension is so recent (1.2 Ma) that the one-dimension Stefan model may be applied to the central part of the basin.

We assume T_0=0°C, T_m=1330 °C, c=1 kJkg^{-1}°K^{-1} L=400 kJkg^{-1} and for ultrabasic rocks at 1300 °C thermal conductivity λ=1.45 Wm^{-1}°K^{-1} (ZOTH & HAENEL, 1988) and the thermal diffusivity κ=21.5 km^2 Ma^{-1} (ZITO *et alii*, 1993).

From eq. (8) we obtain λ_1 = 0.932 Wm^{-1}°K^{-1} and *erf*(λ_1)=0.812 figure 10 shows the geotherm in the second intrusion case. Figure 11 shows the variation of the surface heat flow in time, on which the value relative to the second intrusion is well fitted.

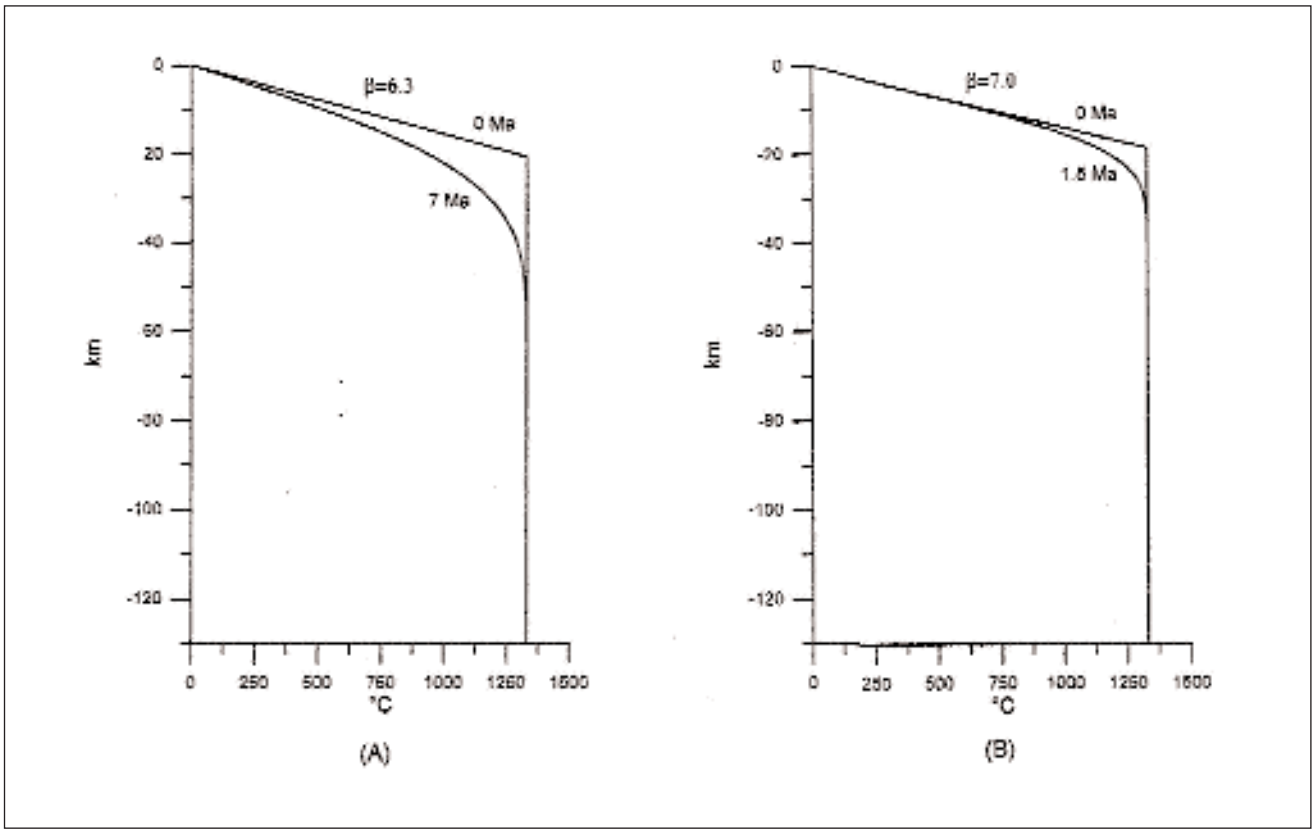

Fig. 7 – *Present mantle component of the geotherms for the first (a) and second (b) extension.*

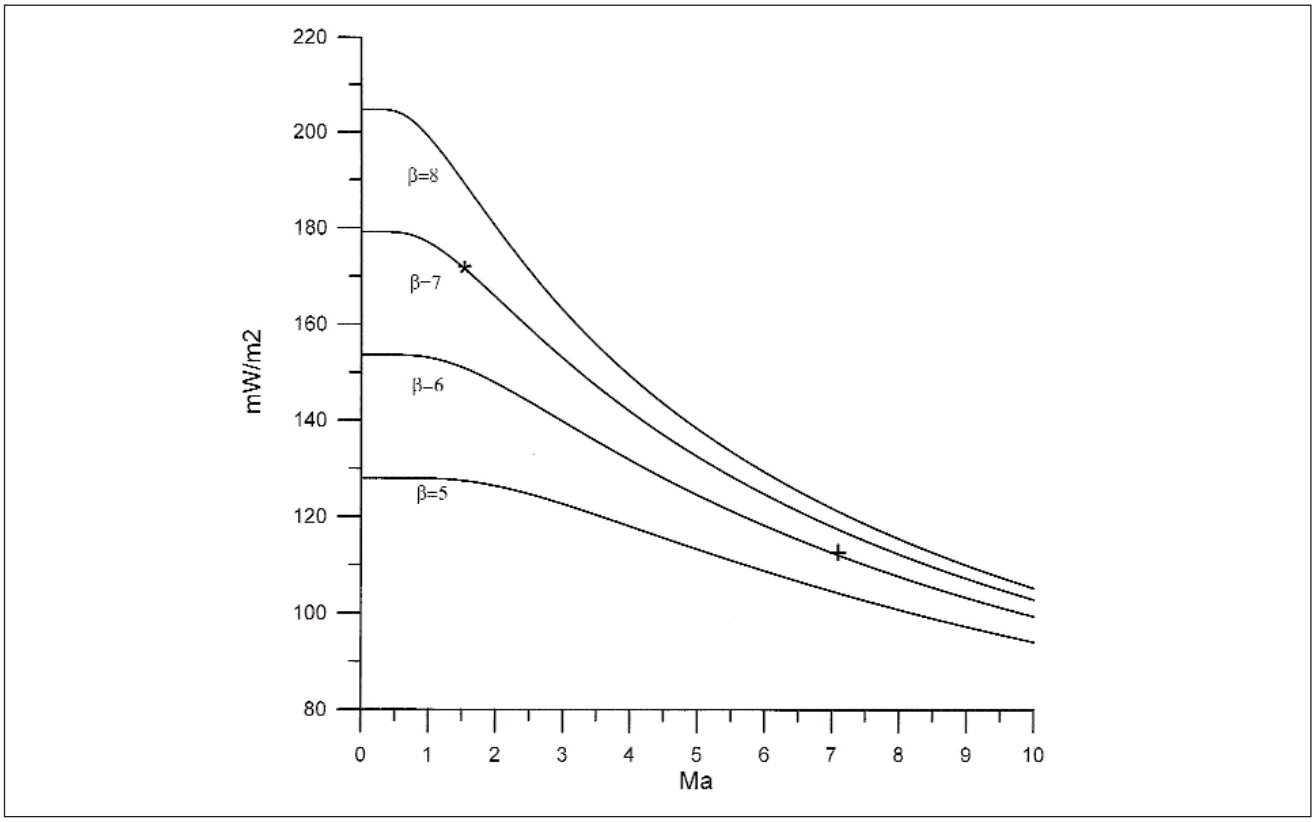

Fig. 8 – *Time variation of the surface heat flow density (mW m-2) of a lithosphere stretched by different factor . Cross refers to the first extension; asterisk to the second extension.*

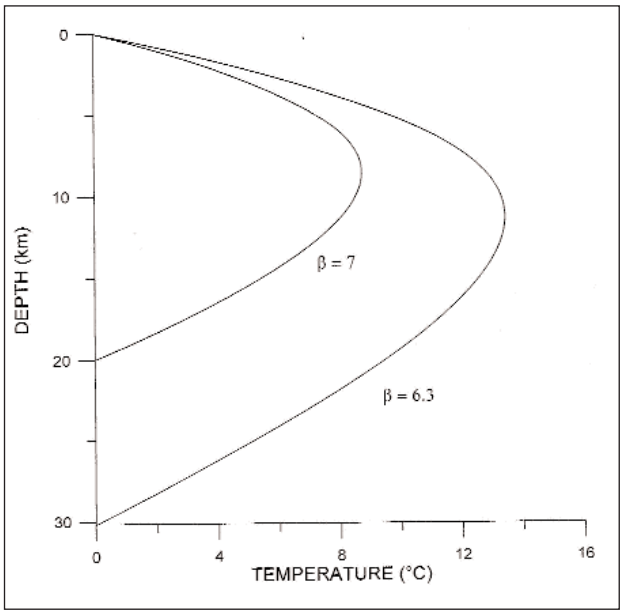

Fig. 9 – *Radioactive component of the geotherms*

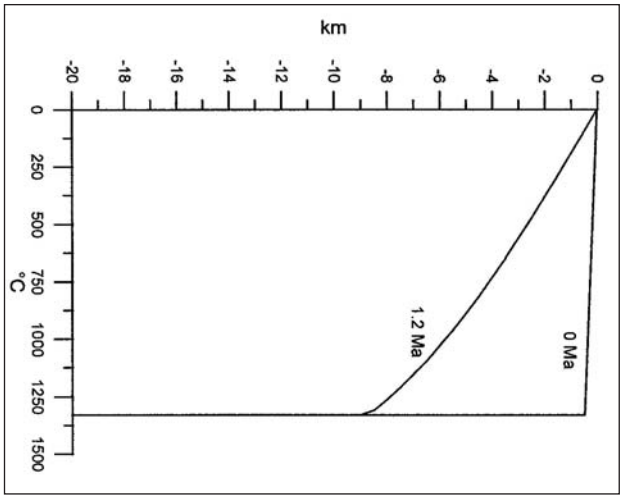

Fig. 10 – *Present geotherm in the second intrusion beneath the Marsili basin.*

From eq.(5), taking k=0.7 mm2/s we obtain z_m=7.0 km. This is the thickness of the newly created lithosphere. Moreover, the contour 10 km below the Marsili basin in figure 4 indicates the thickness of the lithosphere.

The intrusion below the Vavilov basin is older, thus the new lithosphere is thicker. By assuming approximately the one-dimension solution, we obtain z_m =11.2 km. Because the lateral loss of heat of the older intrusion, z_m is surely more than 11.2 km, we expect that within the new lithosphere, new thin oceanic crust is differentiated. In this case we retain that the contour of 10 km in figure 4 below the Vavilov basin indicates effectively the Moho depth.

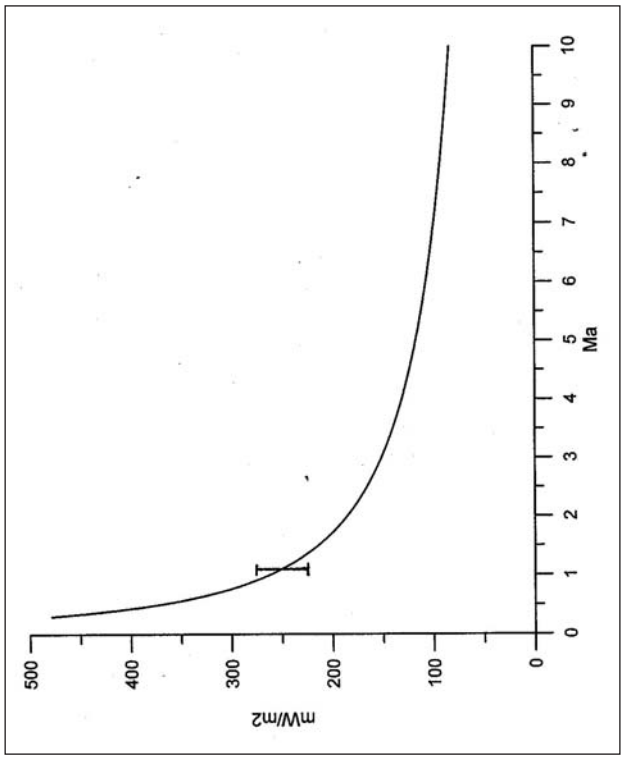

Fig. 11– *Time variation of the surface heat flow (mW m-2) of an asthenospheric body according to the Stefan's equation (9). Error bar refers to the second intrusion under the Marsili basin*

4. - CONCLUSION

Figure 12 shows the thickness of the lithosphere along the sector of figure 6 and the geotherms in each sector calculated by using eqs. (1), A1 and (6).
It is worthwhile to underline some interesting results deriving from this study:

- the opening of the southern Tyrrhenian basin occurred by two rapid and separate episodes which stretched the lithosphere by the factor β=6.
- further stretching generates the laceration of the lithosphere allowing the sudden passive rise of the asthenospheric materials which cools, liberates the latent heat of fusion and solidifies.
- new lithosphere is formed within the intrusion whose thickness is defined by the depth of the solidification boundary.
- the Moho depth in the Tyrrhenian basin has different origin: in the continental areas it is due to the stretching of the primitive crust-lithosphere, whereas within the intrusion it is a new oceanic one, formed by differentiation of the asthenospheric material.

It is generally accepted that extensional thinning of the lithosphere is due to stresses generated by boundary forces related to slab pull (e.g. FORSYTH & UYEDA, 1975; ANGELIER & LE PICHON, 1979) or to differential drag exerted by an eastward migrating

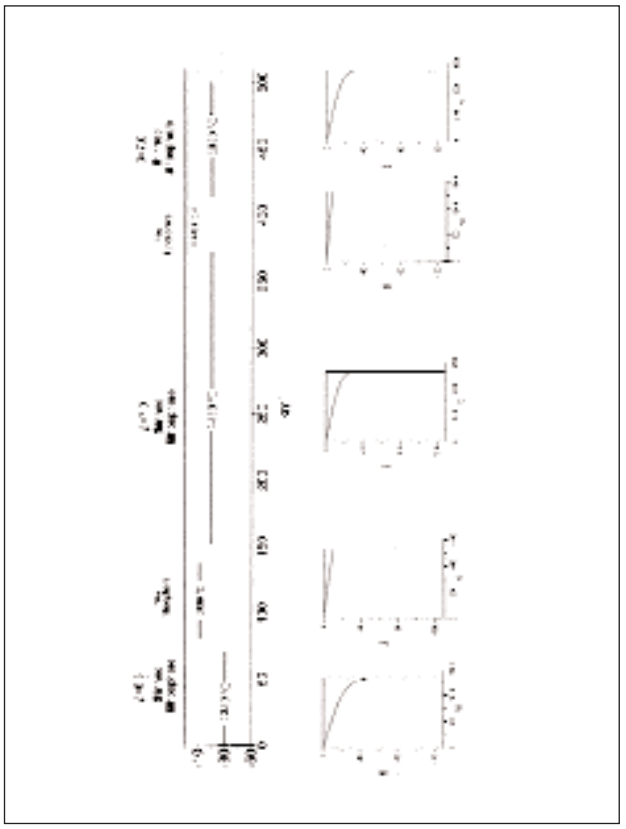

Fig. 12 – *Present lithospheric thicknesses along the given profile and the respective geotherms.*

mantle (DOGLIONI *et alii*, 1998). In these cases, extension may be related to the rate of subduction. Episodic backarc extension of the Tyrrhenian basin induces us to retain that the subduction rate is not continuous, or that stretching in the backarc is not continuous during a steady state subduction process. In fact, while the average rate deduced by the extension of the subducted slab (about 500 km) and its age (about 20 Ma) is about 2.5 cm/a, PATACCA *et alii*, (1990) estimated a rate of about 5 cm/a for the last Ma probably related to the second intrusion.

APPENDIX

The solution of the steady state heat conduction equation:

$$\frac{d^2T}{dz^2} = -\frac{A(z)}{\lambda}$$

where:

$$A(z) = \frac{A_0}{\beta_1}\exp\left(-\frac{z}{D}\right) \qquad 0 < z < z_1$$

$$A(z) = \frac{A_0}{\beta_1}\exp\left(-\frac{z - z_1}{D}\right) \qquad z_1 < z < z_2$$

with the following boundary conditions:

$$T_1(z=0) = T_2(z=L) = 0°C$$

$$T_1(z=H_1^-) = T_2(z=H_1^+)$$

$$\left.\frac{dT_1}{dz}\right|_{z=H_1} = \left.\frac{dT_2}{dz}\right|_{z=H_1^+}$$

is given by:

$$T(z) = \frac{A_0 D^2}{\beta_1 \lambda}\left[1 - \exp\left(-\frac{z}{D}\right)\right] + \frac{A_0 D z_1}{\beta_1 \lambda z_2} z\left\{\exp\left(-\frac{z_1}{D}\right) - 1\right\} +$$
$$\frac{z}{z_2}\frac{A_0 D^2}{\beta_1 \lambda}\left[\exp\left(-\frac{(z_2 - z_1)}{D}\right) + \exp\left(-\frac{z_1}{D}\right) - 2\right] + \qquad \text{(A1)}$$
$$+\frac{A_0 D z}{\beta_1 \lambda}\left\{1 - \exp\left(-\frac{z_1}{D}\right)\right\} \qquad 0 < z < z_1$$

$$T(z) = -\frac{A_0 D^2}{\beta_1 \lambda}\exp\left[-\frac{(z - z_1)}{D}\right] + \frac{A_0 D z_1}{\beta_1 \lambda z_2} z\left[\exp\left(-\frac{z_1}{D}\right) - 1\right] +$$
$$\frac{z}{z_2}\frac{A_0 D^2}{\beta_1 \lambda}\left[\exp\left(-\frac{(z_2 - z_1)}{D}\right) + \exp\left(-\frac{z_1}{D}\right) - 2\right] +$$
$$+2\frac{A_0 D^2}{\beta_1 \lambda}\left[2 - \exp\left(-\frac{z_1}{D}\right)\right] + \frac{A_0 D z_1}{\beta_1 \lambda}\left[1 - \exp\left(-\frac{z_1}{D}\right)\right] \qquad z_1 < z < z_2$$

$$\frac{dT}{dz} = \frac{A_0 D}{\beta_1 \lambda}\left[\exp\left(-\frac{z}{D}\right)\right] + \frac{A_0 D z_1}{\beta_1 \lambda z_2}\left\{\exp\left(-\frac{z_1}{D}\right) - 1\right\} +$$
$$\frac{A_0 D^2}{\beta_1 \lambda z_2}\left[\exp\left(-\frac{(z_2 - z_1)}{D}\right) + \exp\left(-\frac{z_1}{D}\right) - 2\right] + \qquad \text{(A2)}$$
$$+\frac{A_0 D}{\beta_1 \lambda}\left\{1 - \exp\left(-\frac{z_1}{D}\right)\right\} \qquad 0 < z < z_1$$

and the gradient is:

$$\frac{dT}{dz} = \frac{A_0 D}{\beta_1 \lambda}\exp\left[-\frac{(z - z_1)}{D}\right] + \frac{A_0 D z_1}{\beta_1 \lambda z_2}\left[\exp\left(-\frac{z_1}{D}\right) - 1\right] +$$
$$\frac{A_0 D^2}{\beta_1 \lambda z_2}\left[\exp\left(-\frac{(z_2 - z_1)}{D}\right) + \exp\left(-\frac{z_1}{D}\right) - 2\right] + \qquad z_1 < z < z_2$$

The surface gradient (z=0) is:

$$\left.\frac{dT}{dz}\right|_{z=0} = \frac{A_0 D z_1}{\beta_1 \lambda z_2}\left\{\exp\left(-\frac{z_1}{D}\right) - 1\right\} + \frac{A_0 D^2}{\beta_1 \lambda z_2}\left[\exp\left(-\frac{(z_2 - z_1)}{D}\right) + \exp\left(-\frac{z_1}{D}\right) - 2\right] +$$
$$+\frac{A_0 D}{\beta_1 \lambda}\left\{2 - \exp\left(-\frac{z_1}{D}\right)\right\} \qquad \text{(A3)}$$

REFERENCES

AMATO A., CIMINI C., ALESSANDRINI B. (1991) - *Struttura del sistema litosfera–astenosfera nell'Appennino Settentrionale da dati di tomografia sismica*. Studi Geologici Camerti, Vol. Spec. (1991/1), 83–90.

ANDERSON H. & JACKSON J. (1987) - *The deep seismicity of the Tyrrhenian Sea*. Geophysical Journal of Royal Astronomical Society, v.91, pp. 613-637.

ANGELIER J. & LE PICHON X. (1979) - *The Hellenic Arc and Trench system: a key to the tectonic evolution of the eastern Mediterranean*. Tectonophysics, **60**: 1-40.

BECCALUVA L., BONATTI E., DUPUY C. *et alii* (1990) - *Geochemistry and mineralogy of volcanic rocks from the ODP*

sites 650, 651, 655 and 654 in the Tyrrhenian sea. Proceedings of the ODP, *Scientific Result*s, **107**: 49–74.

CALCAGNILE G. & PANZA G.F. (1980) - *Upper mantle structure of the Apulian plate from Rayleigh waves*, Pure appl. Geophys., **118**: 823-830.

CALCAGNILE G. & PANZA G.F. (1981) - *The main characteristics of the Lithosphere Asthenosphere System in Italy and surrounding regions*. Pageoph, v.119, pp. 865-879.

CELLA F., FEDI F., FLORIO G. & RAPOLLA A. (1998) - *Optimal gravity modelling of the litho-asthenosphere system in Central Mediterranean*. Tectnophysics. Vol. 287, Nos. 1-4, 117-138.

CERMAK V. & BODRI L. (1991) - *A heat production model of the crust and upper mantle*. Tecttonophysics, **194**: 307-323.

CERMAK V. & BODRI L.(1996) - *Time dependent deep temperature modelling: Central Alps*. Tectonophysics, **257**: 7-24.

CIMINI G.B. (1999) - *P-wave deep velocity structure of the southern Tyrrhenian subduction zone from non-linear teleseismic travel time tomography*. Geoph. Res. Let., **26** (24): 3709-3712.

DELLA VEDOVA B., MONGELLI F., PELLIS G. & ZITO G. (1991) - *Campo regionale del flusso di calore nel Tirreno*. Ati 10° Convegno GNGTS, Esagrafico, Rora, 817-825.

DOGLIONI C., MONGELLI F. & PIALLI G.P. (1998) - *Boudinage of the Alpine belt in the Apenninic back-arc*. Mem. Soc. Geol. It., **52**: 457-468.

ELLAM R.M. *et alii* (1988) - *The transition from calc-alkaline to potassic orogenic magmatism in the Aeolian Islands, Southern Italy*. Bull. Volcanol., **30**: 386-398.

ERICKSON A.J. (1970) - *Heat flow measurements in the Mediterranean, Black and Red Seas*. Oh. D. Thesis, M.I.T., Cambridge.

FINETTI M. & DEL BEN A. (1986) - *Geophysical study of the Tyrrhenian opening*. Boll. Geofis. Teor e Appl., V.28, pp. 75-156.

FORSYTH D. & UYEDA S. (1975) - *On the relative importance of the driving forces of plate motions*. Geophys. J. R. Astr. Soc., **43**: pp.163-200.

FRANCALANCI L., TAYLOR S.R., MCCULLOCH M.T. & WOODHEAD J. (1993) - *Petrological and geochemical variations in the calc-alkaline rocks of Aeolian arc (Southern Tyrrhenian Sea, Italy)*. Contrib. Mineral. Petrol., **113**: 300-313

GASPARINI C., IANNACCONE G., SCANDONE P. & SCARPA R. (1982) - *Seismotectonics of the Calabrian Arc*. Tectonophysics, **84**: 267-286.

GIARDINI D. & VELONÀ M. (1991) - *The deep seismicity of the Tyrrhenian Sea*. Terra Nova, **3**: 57-64.

GUEGUEN E., DOGLIONI C. & FERNANDEZ M. (1997) - *Lithospheric boudinage in the Western Mediterranean back-arc basins*. Terra Nova, **9**, 4, 184-187.

HUTCHINSON I., VON HERZEN R.P., LOUDEN K.E., SCLATER J.G. & JEMSEK J. (1985) - *Heat flow in the Balearic and Tyrrhenian basins, Western Mediterranean*. Journal of Geophysical Research, v.90, pp.685-702.

KASTENS K, MASCLE J., AUROUX C., BONATTI E., BROGLIA C., CHANNELL J., CURZI P., EMEIS K.C., GLACON G., ASEGAWA S., HIEKE W., MASCLE G., MCCOY F., MCKENZIE J., MENDELSON J., MULLER C., RÉHAULT J.P., ROBERTSON A., SARTORI R., SPROVIERI R. & TORII M., (1988) - *ODP Leg 107 in the Tyrrhenian Sea: Insights into passive margin and back-arc basin evolution*. Geological Society of American Bulletin, v.100, pp.1140-1156.

LOCARDI E. & NICOLICH R. (1988) – *Geodinamica del tirreno e dell'Appennino Centro-Meridionale: la nuova carta della Moho*. Memorie Società Geologica Italiana, **41**: 121-140

LODDO M. & MONGELLI F. (1974) – *Heat Flow in southern Italy and surrounding seas*. Boll. Geof. Teor. Appl., 115-122.

MALINVERNO A. & RYAN W.B.F. (1986) - *Extension in Tyrrhenian Sea and shortening in the Appennines as a result of arc migration driven by sinking of the lithosphere*. Tectonics, **5**: 2, pp. 227-245.

MALINVERNO A., CAFIERO M., RYAN W.B.F. & CITA M.B. (1981) - *Distribution of Messinian sediments and erosional surfaces beneath the Tyrrhenian Sea: geodynamical implications*. Oceanol. Acta, **4**: 489-496.

MALINVERNO A. (1981) - *Quantitative estimates of age and Messinian paleobathymetry of the Tyrrhenian Sea after seismic reflection, heat flow and geophysical models*. Boll.Geof. Teor. Appl., **23**: 159-171.

MANTOVANI E. (1982) - *Some remarks on the driving forces in the evolution of the Tyrrhenian basin and Calabrian Arc*. Earth Evol. Sci. 3,266-170.

MCKENZIE D. P. (1978) - *Some remarks on the development of sedimentary basins*. Earth Planet. Sci. Lett., **40**: 25-32.

MONGELLI F. (1991) - *Rethickening of the lithosphere after simple stretching in the Tuscan-Latial pre-apenninic belt*. Boll. Geof. Teor. Appl., XXXIII, **129**: 61-67.

MONGELLI F. & ZITO G. (1994) - *Thermal aspects of some geodynamical models of Tyrrhenian opening*. Boll. Geof. Teor. e Appl., Vol. XXXVI, 141-144, pp. 21-28.

MORELLI C., PISANI M. & GANTAR C. (1975) - *Geophysical anomalies and tectonics in the Strait of Sicily and of the Ionian Sea*. Boll. Geof. Teor. e Appl., v. XVII, **67**: pp. 211-249.

MORELLI C. (1970) - *Physiography, Gravity and magnetism of the Tyrrhenian Sea*. Boll. Geof. Teor. e Appl., v. XII, n. **48**: pp. 275-311.

MORELLI C. (1981) - *Gravity anomalies and crustal structures connected with the Mediterranean margins*. In: WEZEL F.C. (Ed): "*Sedimentary Basins of Mediterranean Margins"*. C.N.R. Italian Project of Oceanography, Tecnoprint, Bologna, 33-53.

MORELLI C. (1995) - *Ulteriori vincoli geofisici, petrografici e geodetici alla geodinamica del Mediterraneo centrale*. Atti XIII Conv. Naz. del GNGTS, Vol.1, 27-43.

PARSONS B. & SCLATER J.G. (1977) - *An analysis of the variation of ocean floor bathymetry and heat flow with age*. J. Geoph. Res., **82**: 803-827.

PASCUCCI V., MERLINI S., MARTINI P. (1999) - *Seismic stratigraphy of the Miocene-Pleistocene sedimentary basins of the Northern Tyrrhenian Sea and western Tuscany (Italy)*. Basin Res., **11**: 337-356.

PATACCA E., SARTORI R. & SCANDONE P. (1990) - *Tyrrhenian basin and Appenninic Arcs: Kinematic relations since Late Tortonian times*. Memorie della Società Geologica Italiana., v.45, pp.453-462.

PATACCA E. & SCANDONE P. (1989) - *Post-Tortonian mountain building in the Apennines. The role of the passive sinking of a relic lithospheric slab*. In BORIANI A., BONAFEDE M., PICCARDO G.B. & VAI G.B. (Eds.): "*The Lithosphere in Italy*". Accademia Nazionale Lincei, **80**: 157-176.

PONTEVIVO A. & PANZA G.F. (2002) - *Group velocity tomography and regionalization in Italy and bordering areas*. Phys. Earth Plan. Int., **134**: 1-15.

PFINNER O.A. (1990) - *Crustal shortening of the Alps along the EGT profile*. In FREEMAN R., GIESE P. & MUELLER ST. (Eds): "*The European Geotransverse: Integrative studies"*. Eur. Sci. Found., Strasbourg, pp. 255-262

SARTORI R. (1989) - *Evoluzione neogenico-recente del bacino tirrenico ed I suoi rapporti con la geologia delle aree circostanti*. Gior. Geol., **3**: 51/2, 1-39.

SCANDONE P. (1980) - *Origin of the Tyrrhenian Sea and Calabrian Arc*. Bollettino Società Geologica Italiana, **98**: 27-34.

SCLATER J.G. (1972) – *Heat flow and elevation of the marginal basins of the western Pacific*. J. Geoph. Res., **77**: 5075-5083.

SELVAGGI G. & CHIARABBA C. (1995) – *Seismicity and P-wave velocity image of the Southern Tyrrhenian subduction zone.*

Geophys. J. Int., **121**: 818-826.

SELVAGGI G. (2001) – *Strain pattern of the Southern Tyrrhenian slb from moment tensors of deep earthquakes: implications on the down-dip velocity*. Ann. Geof., **44** (1): 155-165.

TURCOTTE D.L. & SCHUBERT G. (1982) - *Geodynamics. Application of continuum Physics to geological problems*. John Wiley, New York.

YE S. & ANSORGE J. (1990) – *A crustal section through the Alps derived from the EGT seismic refraction data*. In FREEMAN R., GIESE P. & MUELLER ST. (Eds): "*The European Geotransverse: Integrative studies"*. Eur. Sci. Found., Strasbourg, pp. 221-236

ZITELLINI N., TRINCARDI F., MARANI M., TRAMONTANA M. & BARTOLE R. (1986) - *Neogene tectonics of the Northern Tyrrhenian Sea*. Giorn. Geol., **48**: 25-40.

ZITO G., MONGELLI F. & LODDO M. (1993) – *Temperature dependence of the thermal parameters of some rocks*. Boll. Geof. Teor. Appl., **140**: 437-445.

ZOTH G. & HAENEL R. (1988) *Appendix of the Handbook of terrestrial heat-flow density determination*. HAENEL R., RYBACH L. & STEGENA L. (Eds). Kluwer Academic Publisherrs, Dordecht (Holland), 499-453.

Mem. Descr. Carta Geol. d'It.
XLIV (2004), pp.83-96
7 figg.

Coexistence of IAB-type and OIB-type magmas in the southern Tyrrhenian back-arc basin: evidence from recent seafloor sampling and geodynamic implications

Coesistenza di magmi di tipo IAB e di tipo OIB nel bacino di retro-arco del Tirreno meridionale

TRUA T. (*), SERRI G. (*), ROSSI P.L. (**)

ABSTRACT - We present a review of petrological data on the submarine volcanic samples up to now recovered from the Southern Tyrrhenian basin. This area represents one example of an active arc/back-arc system where IAB- and OIB-type magmas coexist. IAB-type magmatism is the most common, in both arc and back-arc settings, whereas OIB-type magmas are restricted to few areas. We show how the geochemistry and isotopic characteristics of the more basic Southern Tyrrhenian submarine lavas, especially the volcanic samples recently recovered from Marsili seamount and Prometeo lava field, provide constraints on the mantle sources of the Southern Tyrrhenian submarine magmatism. The geochemical and isotopic features of these basic lavas are used to map mantle structure beneath the Southern Tyrrhenian basin thus providing an important insight into the possible geodynamic scenario able to explain the coexistence of IAB and OIB magmas in this area.

KEYWORDS: Southern Tyrrhenian, calc-alkaline magmas, alkaline magmas

RIASSUNTO - In questo lavoro viene presentata una revisione dei dati petrologici relativi alle vulcaniti sottomarine fino ad oggi recuperate dal bacino meridionale del Tirreno. Quest'area rappresenta un esempio di sistema "arco vulcanico attivo/bacino di retro-arco" dove coesistono magmi di tipo IAB e OIB. I magmi IAB sono i più diffusi, sia in ambiente di arco che di retro-arco, mentre i magmi OIB si rinvengono in poche aree. Le caratteristiche geochimiche ed isotopiche delle lave sottomarine più basiche del Tirreno meridionale, ed in particolare quelle recuperate durante le recenti campionature del vulcano sottomarino Marsili e dal campo lavico Prometeo, permettono di caratterizzare le sorgenti mantelliche dei magmi IAB e OIB di quest'area. Le caratteristiche geochimiche ed isotopiche di queste lave basiche sono usate per definire la struttura del mantello al di sotto del bacino meridionale del Tirreno e forniscono una importante introspezione sul possibile scenario geodinamico che ha controllato la co-esistenza in quest'area di magmi IAB e OIB.

PAROLE CHIAVE: Tirreno meridionale, magmi calcalcalini, magmi alcalini

(*) Dipartimento di Scienze della Terra, Università degli Studi di Parma, Parco Area delle Scienze, 157A, I-43100 Parma, Italy
(**)Dipartimento di Scienze della Terra e Geologico-Ambientali, Piazza di Porta S. Donato 1, I 40126 Bologna, Italy

1. - INTRODUCTION

The southern Tyrrhenian basin represents an example of an active volcanic arc/back-arc system where there is the coexistence of Island Arc Basalt (IAB)-type and Ocean Island Basalt (OIB)-type magmas (fig. 1). In the last decade several authors focused their attention on the geochemical and petrological characteristics of this magmatism with the aim to unravel its geodynamic significance (BECCALUVA *et alii*, 1982, 1985; ELLAM *et alii*, 1989; SERRI, 1990; FRANCALANCI & MANETTI,1994; PECCERILLO, 2001; SERRI *et alii*, 2001; CALANCHI *et alii*, 2002). However, most of these studies focused on the emerged part of this magmatism whereas the knowledge of the submerged part is still mottled and incomplete, being referred to the pioneer seafloor explorations of this area carried out between the 70s-80s (SELLI *et alii*, 1977; BARBERI *et alii*, 1978; COLANTONI *et alii*, 1981; BECCALUVA *et alii*, 1985; ROBIN *et alii*, 1987; BECCALUVA *et alii*, 1990).

In the southern Tyrrhenian region, IAB-type lavas are widespread, occurring in the Aeolian volcanic arc, the Marsili and Aeolian seamounts and as seamount remants and lava flows flooring the basement of the Marsili and Vavilov Basins. By contrast, the few OIB-type lavas are represented by isolated volcanic centres or lava flows (*i.e.,* Magnaghi, Vavilov and Aceste seamounts; Ustica island; rocks drilled, dredged and cored in the East Sardinia rifted margin and the

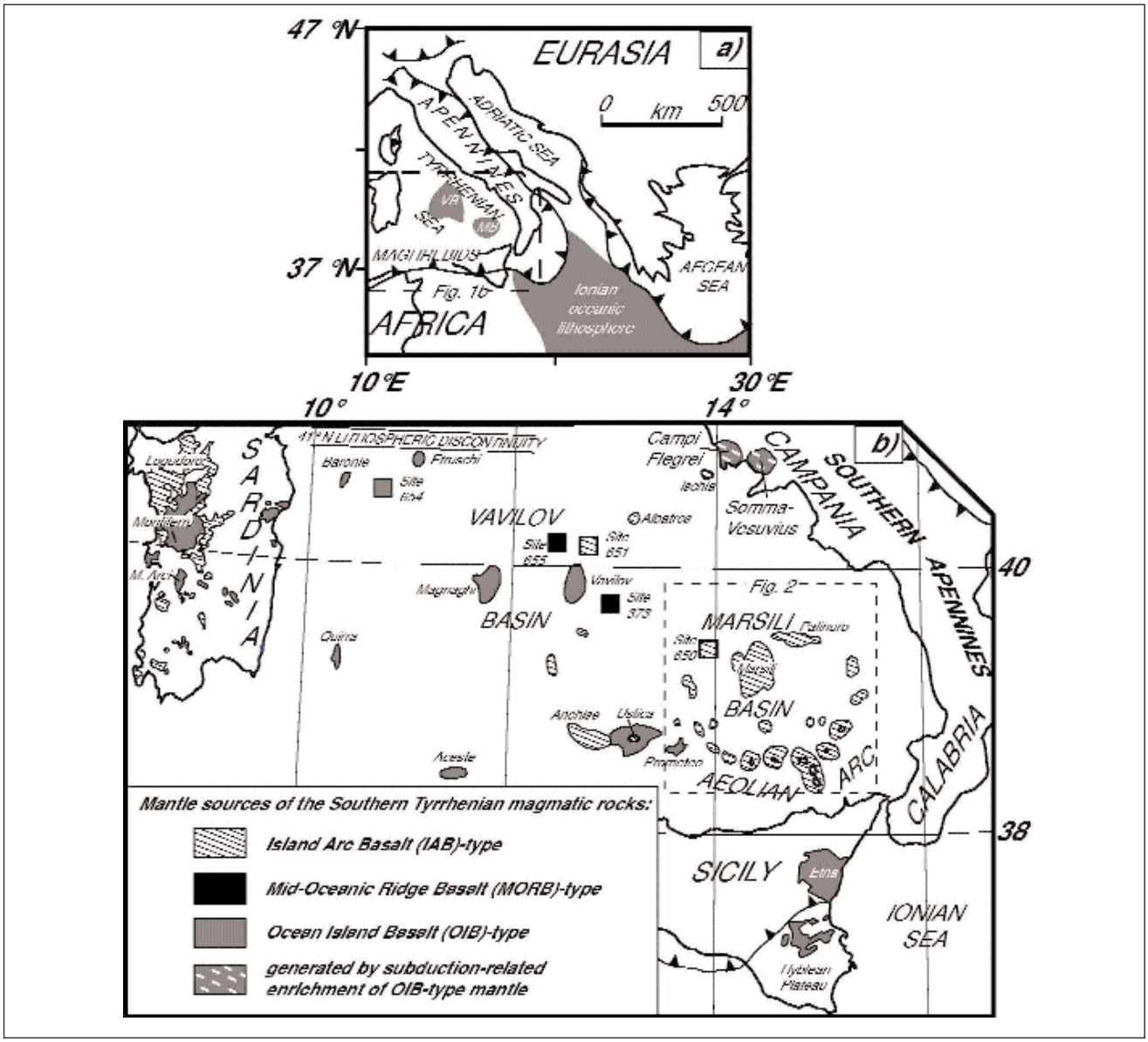

Fig. 1 – *a) Schematic outline showing the main thrust fronts (barbed line) that bound Neogene fold and thrust belts of the central Mediterranean region (modified after* MARANI & TRUA, 2002). *VB, Vavilov basin. MB, Marsili basin. b) Schematic map of the Cenozoic magmatic rocks of the southern Tyrrhenian region according to their inferred dominant magma sources (modified after* SERRI *et alii*, 2001).

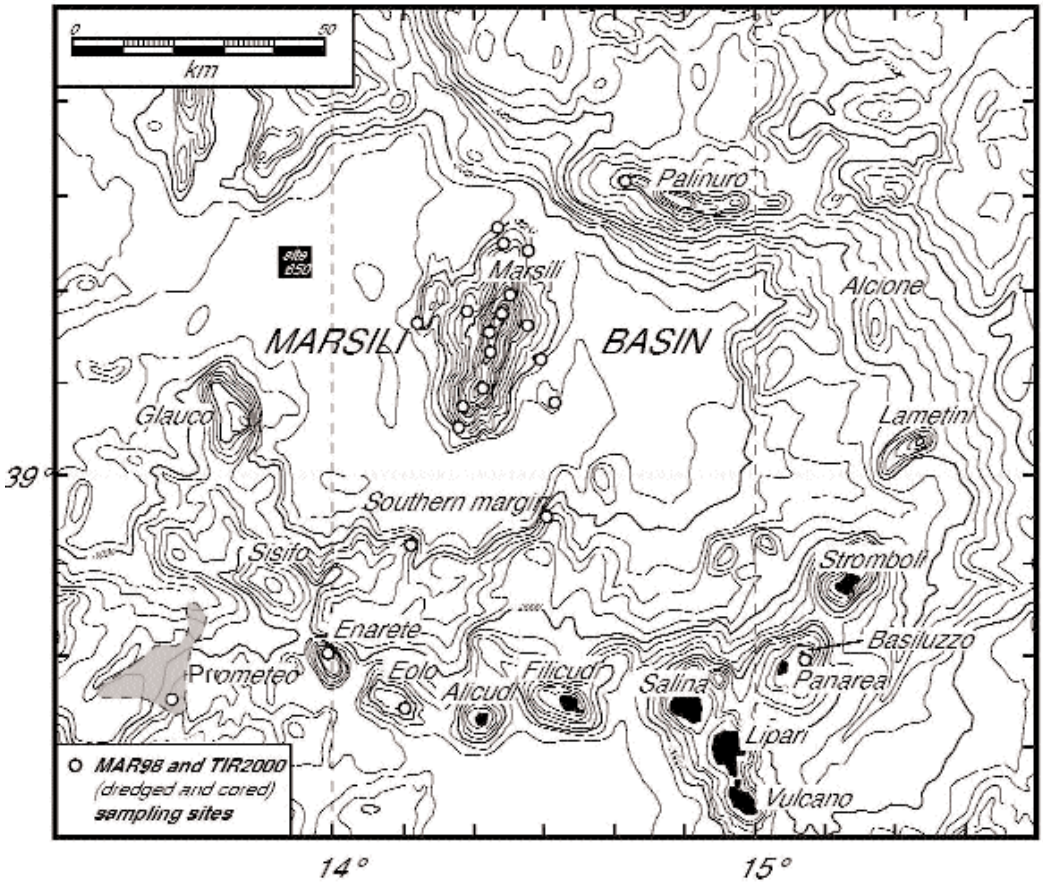

Fig. 2 – *Sampling areas of MAR98 and TIR2000 cruises discussed in the text (modified after* MARANI *et alii*, 1999). *Isobaths every 200 m.*

recently discovered (TRUA *et alii*, 2003) Prometeo submarine lava field) (fig. 1). There is a general consensus in considering the IAB-type magmatism of this area related to northwestward subduction of the narrow Mesozoic Ionian oceanic slab occurring within a general context of Africa and Euroasia convergence (SERRI *et alii*, 2001 and references therein). By contrast, the occurrence of the OIB-type magmatism in this complex subduction-related environment is a still matter of discussion (GVIRTZMAN & NUR, 1999; SERRI *et alii*, 2001; TONARINI *et alii*, 2001a; GASPERINI *et alii*, 2002; MARANI & TRUA, 2002; TRUA *et alii*, 2003).

During the MAR98 and TIR2000 cruises, on board the Consiglio Nazionale delle Ricerche (CNR) ship R/V Urania, a large number of submarine samples of volcanic rocks from the southern Tyrrhenian basin were recovered (fig. 2). Owing to their location and their elevated number, these samples represent a potential reservoir of petrogenetic information on the submarine volcanism which took place in the last 2 Ma in this region.

In this paper, we present petrological and geochemical data on newly collected samples and compare them with available literature data on the Neogene-Quaternary magmatism of the southern Tyrrhenian basin. We show how the recent, more detailed study of the submarine magmatism provides a breakthrough to understand (i) the relationships between areal distribution and petrogenetic affinity of magmatism and (ii) the geotectonic processes which are still active in this complex area.

2. - GEOLOGICAL SETTING AND REGIONAL VARIATION OF NEOGENE-QUATERNARY SUBDUCTION-RELATED MAGMATISM

Since Early Miocene, a fragment of the Hercynian Alpine orogenic belt began to separate from the Corsica-Sardinia area leading to the opening of the Tyrrhenian Sea basin (GUEGUEN *et alii*, 1998) which occurred differently in its northern and southern sector (SERRI *et alii*, 2001 and references therein). In the northern Tyrrhenian, rifting and crustal thinning developed entirely within a continental realm (SERRI *et alii*, 1993), whereas, in the southern Tyrrhenian, rifting gave way to seafloor spreading which was first focused in the western sector to form the Vavilov back-arc basin (4.3-2.6 Ma) and then in the eastern sector to form the Marsili back-arc basin (2.0-1.8 Ma) (KASTENS *et alii*, 1990) (fig. 1). Most authors agree that the diachronous opening of the Marsili and Vavilov basins was related to the very rapid acceleration in the subduction roll-back of the Ionian oceanic lithosphere below the

southern Tyrrhenian (KASTENS *et alii*, 1988, 1990; SARTORI, 1990; GUEGUEN *et alii*, 1998; SERRI *et alii*, 2001).

In step with back-arc basin development, the subduction related magmatism of the southern Tyrrhenian basin migrated from west to south-east, from Sardinia (32-13 Ma) to the currently active Aeolian island arc (SERRI *et alii*, 2001 and references therein) (fig. 1). This magmatism is characterized by the coeval eruptions of IAB-and OIB-type magmas. IAB-type magmatism is by far the most common. Calc-alkaline (CA) and shoshonite (SHO) suites characterize both the submarine and subaerial magmatism of this region, notably Marsili (site 650) and Vavilov (site 651) basins and Marsili seamount, Anchise seamount, Aeolian islands and related seamounts. Arc tholeiites (A-Th) have been only recovered from Lametini seamount and they seem to be present also along the lowermost northern Aeolian slope, interpreted by MARANI *et alii* (1999) as the faulted southern margin of the Marsili basin. Transitional Mid Oceanic Ridge Basalts (T-MORB) were recovered from Vavilov basin (sites 655 and 373). Both A-Th and T-MORB are absent among the subaerial rocks. Potassic rocks (KS) occur in two Aeolian volcanoes (*i.e.,* Vulcano and Stromboli) and along the eastern margin of the southern Tyrrhenian Sea (*i.e.,* Phlegrean Fields and Mt. Somma-Vesuvius volcano). Unlike the widespread IAB-type magmas, OIB-type magmas are restricted to few areas: Magnaghi, Vavilov and Aceste seamounts; rocks drilled (site 654), dredged and cored in the East Sardinia rifted margin, Ustica island and Prometeo submarine lava field (figs. 1,2).

3. - RESULTS OF RECENT SEAFLOOR SAMPLING

The submarine volcanic samples recovered during the recent oceanographic cruises (MARANI *et alii*, 1999; TRUA *et alii*, 1999; TRUA *et alii*, 2002a,b,c) include samples from Marsili, Palinuro, Eolo and Enarete seamounts, the Basiluzzo area and the faulted southern margin of the Marsili basin (fig. 2). Moreover, some samples derive from Prometeo, a recently discovered lava flow (TRUA *et alii*, 2003) located between Ustica and Alicudi (figs. 1,2)

3.1. - MARSILI SEAMOUNT

Marsili seamount is located in the central, youngest part of the Marsili back-arc basin (fig. 1). The newly collected volcanic rocks (TRUA *et alii*, 2002a,b,c) were dredged/cored from several sites covering the entire depth range of the volcano (fig. 2). Both recent and newly collected samples (SAVELLI & GASPAROTTO, 1994; TRUA *et alii*, 2002a,b,c) reveal that Marsili volcano is entirely made up of CA volcanic rocks (fig. 4) which range from basalts to basaltic andesites to trachyandesites in terms of Total Alkalis *vs.* Silica (TAS) diagram (fig. 3). On the K2O *vs.* SiO2 diagram (fig. 4), the basalts plot within the medium-K CA series whereas the basaltic andesites range between medium-K and high-K CA fields; the evolved trachyandesites, only erupted from small cones on the summit axis zone of the volcano, plot within the high-K CA andesite field.

Petrological and geochemical characteristics of the least differentiated Marsili CA basalts reveal that at least two types of magmas have been erupted on the volcano (TRUA *et alii*, 2002a,b,c): *group 1* basalts have plagioclase and olivine as dominant phases (tab. 1) and show lower Al, Ca, K, Ba, Rb, Sr and higher Fe, Na, Ti, Zr with respect to *group 2* basalts, which reveal the presence of clinopyroxene as additional phenocryst phase (tab. 1).

Geochemically, both types of magmas are enriched in large-ion lithophile elements (LILE) relative to high field strength elements (HFSE) typical of IAB lavas, but they show very different LILE/HFSE ratios (*i.e., group 1* basalts have Ba/Nb=20 whereas *group 2* basalts have Ba/Nb which ranges from 30 to 80) (fig. 5a). Nevertheless, only *group 2* basalts display primitive-mantle normalized patterns similar in shape, but enriched in all the incompatible elements, in respect to the low-lying CA oceanic crust (site 650) of Marsili basin (fig. 5a).

Sr-Nd isotope ratios of Marsili lavas range from 0.7358 to 0.70493 and 0.51267 to 0.51289 respectively, with the two varieties of Marsili IAB magmas representing the two end-members of Marsili Sr-Nd isotopic range (TRUA *et alii*, 2002a,b) (fig. 6). Notably, the least differentiated *group 2* Marsili basalt has Sr-Nd isotopic compositions similar to the less radiogenic composition of Stromboli basic IAB lavas field, whereas the least differentiated *group 1* Marsili basalt displays less radiogenic Sr isotopic composition and higher $^{143}Nd/^{144}Nd$ values, resulting isotopically similar to Alicudi lavas, which represent the least radiogenic composition of the whole Aeolian Arc (fig. 6).

The Marsili high-K andesites display primitive-mantle normalized patterns similar in shape to the *group 2* basalts, but enriched in all the incompatible elements (fig. 5a). Moreover, these evolved rocks have Sr-Nd isotopic ratios similar to *group 2* basalts (TRUA *et alii*, 2002 a,b). Therefore one could envisage a derivation of andesites from *group 2* basalts mainly by fractional crystallization. Geochemical modelling, based on correlation between trace elements and isotopic compositions, are required to test quantitatively the validity of this hypothesis. However, it is to note that preliminary fractional crystallization calculations obtained from MELTS (GHIORSO & SACK, 1995) reveal that the evolved andesites can only exclusively be derived from a low-pressure fractionation of magmas compositionally similar to the least evolved *group 2* basalts (TRUA *et alii*, 2002c).

3.2. - VAVILOV BASIN AND SEAMOUNTS

Data obtained on igneous rocks drilled on the basement of Vavilov basin (BARBERI *et alii*, 1978; BECCALUVA *et alii*, 1990) show a complex petrogenetic frame, typical of back-arc basins floored with oceanic

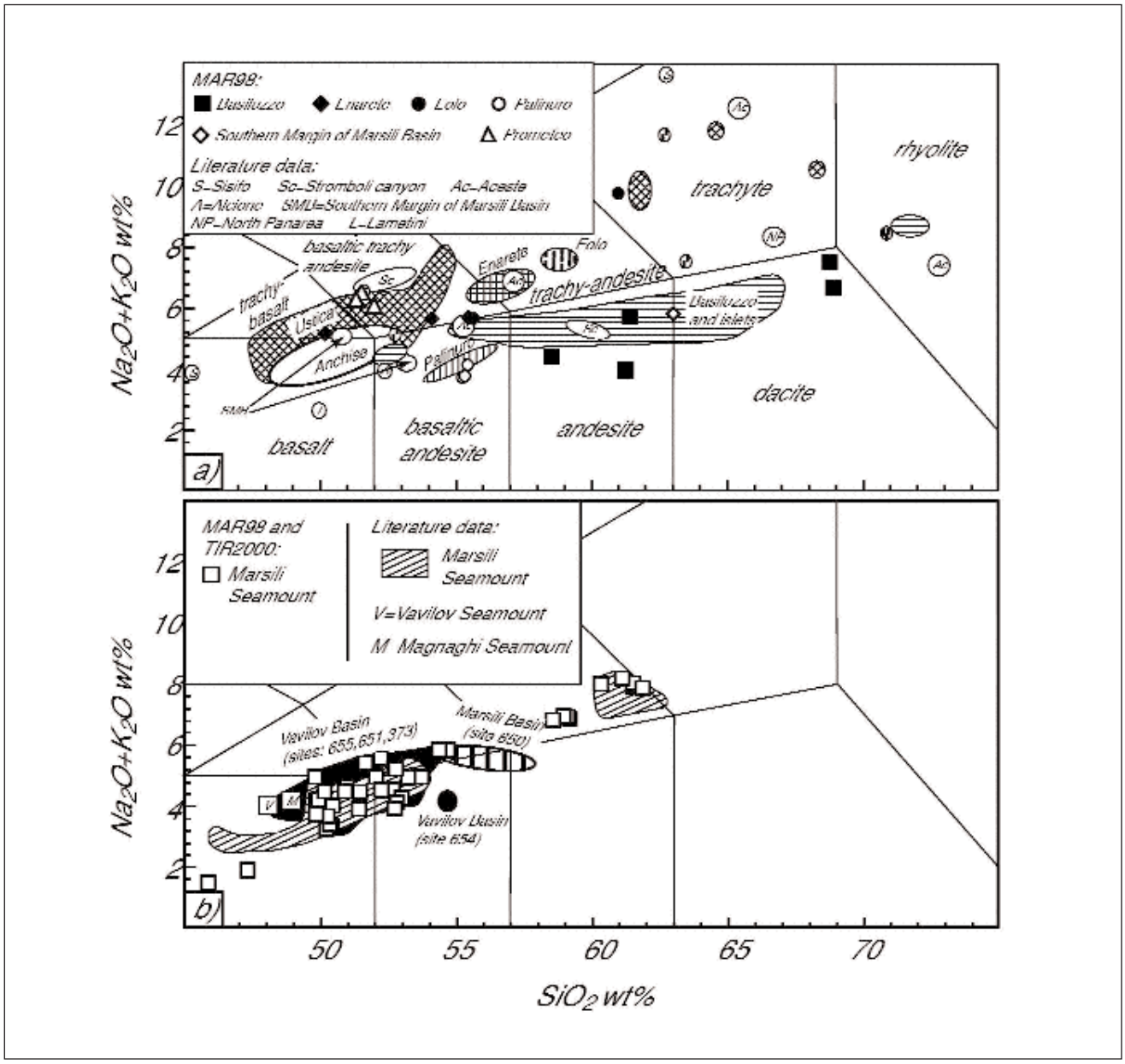

Fig. 3 – *Total alkalis-silica diagram* (Le Bas *et alii*, 1986) *for the Neogene-Quaternary southern Tyrrhenian volcanic rocks. MAR98 and TIR2000 data are from* Trua *et alii* (1999, 2002c). *Literature data: Sisifo, Alcione, Lametini, Stromboli canyon, southern margin of Marsili basin, Enarete and Eolo* (Beccaluva *et alii*, 1985); Palinuro (Colantoni *et alii*, 1981; Beccaluva *et alii*, 1985); *Aceste* (Beccaluva *et alii*, 1984); *Ustica* (Calanchi *et alii*, 1984; Cinque *et alii*, 1988; Trua *et alii*, 2003); *Vavilov and Magnaghi seamounts* (Selli, 1977; Robin *et alii*, 1987; Serri, 1990); *Marsili seamount* (Selli, 1977; Savelli & Gasparotto, 1994); *Anchise* (Calanchi *et alii*, 1984); *Vavilov basin, sites: 373, 651, 654 and 655* (Barberi *et alii*, 1978; Beccaluva *et alii*, 1982; Beccaluva *et alii*, 1990; Serri, 1990; Gasperini *et alii*, 2002); *Marsili basin, site 650* (Beccaluva *et alii*, 1990); *Basiluzzo and islets* (Calanchi *et alii*, 1999). *Note that Marsili basin, Sisifo and southern margin of Marsili basin samples, although reported in this classification digram, are too altered (i.e., LOI>3 wt%) to be classified according to these chemical parameters.*

crust. Most of the Vavilov basin samples (*i.e.,* Sites 373, 651, 655) have suffered a variable degree of hydrothermal alteration that prevent to derive their magmatic affinity from TAS or K2O *vs.* SiO2 diagrams (figs. 3,4). However, least altered samples have ratios of elements, whose secondary mobilization is negligible (*i.e.*, Ti, Zr, Hf, Nb, Ta, Y, Rare Earth Elements (REE)), that can be used for this purpose (Barberi *et alii*, 1978; Beccaluva *et alii*, 1982; Beccaluva *et alii*, 1990; Serri, 1990).

Basalts which show T-MORB type geochemical (in terms of light REE enrichment and Zr/Nb ratio: $1<(La/Sm)_N<1.5$, normalizing values for chondrite from Sun & McDonough, 1989; $16<Zr/Nb<25$) and isotopic features have been so far recovered at Sites 655 and 373 (high-Ti basalts) (figs. 5b,6). Only one sample from site 655, having the lowest Zr/Nb ratio (=16), shows relatively little tendency for light REE depletion ($(La/Sm)_N=0.88$) approaching normal

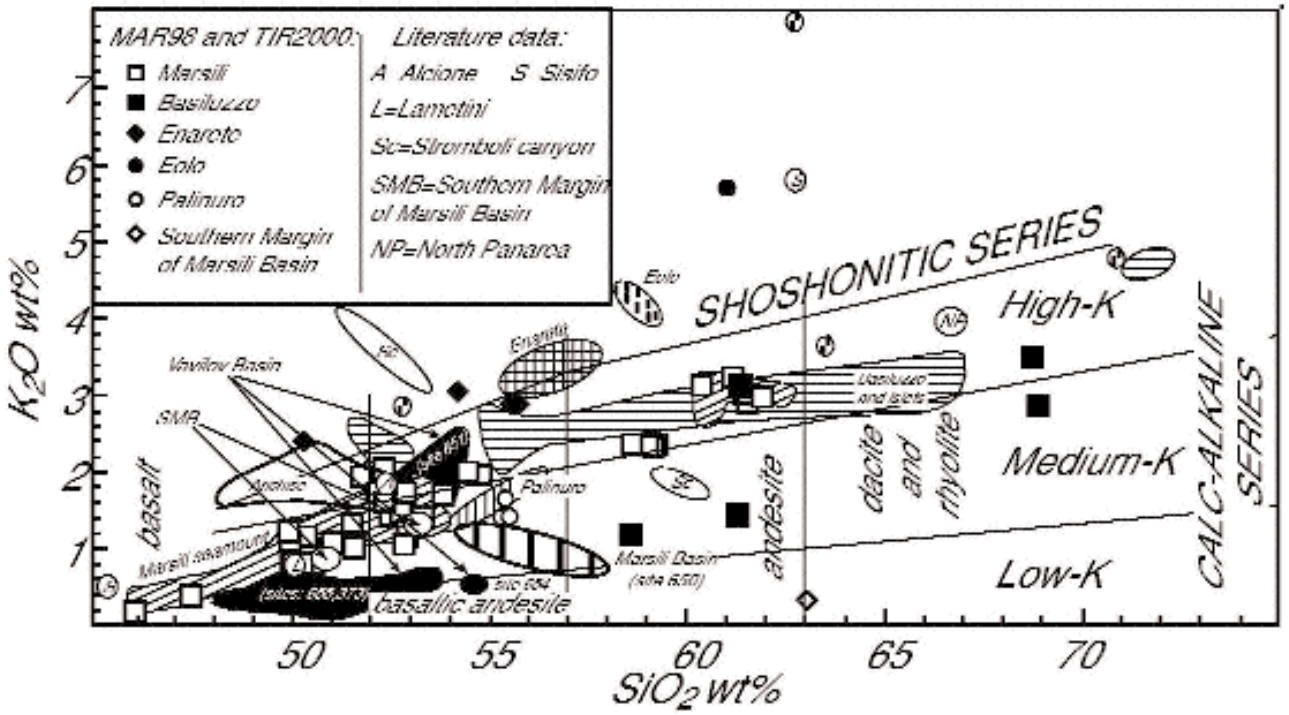

Fig. 4 – *K2O vs SiO2 diagram, showing the major subdivision of the island-arc volcanic rock suites* (WILSON, 1989), *for the Neogene-Quaternary southern Tyrrhenian volcanic rocks. Data source as in figure 3.*

MORB more than any other Tyrrhenian sea basalt (BECCALUVA *et alii*, 1990). Moreover, these basalts show distinct incompatible element pattern (fig. 5b) with positive anomalies for elements partitioned into the fluid phase (such as Cs, Ba, Th, U, K, Pb and light REE) and a depletion in Nb and Ta compared to average E-MORB of SUN & MCDONOUGH (1989). The geochemical features of Site 373-low Ti basalts as well as that of basic rocks from Site 651 (high K-CA basaltic andesites, fig. 4) are best explained with the addition of a small amount of subducted slab fluids to a T-MORB type mantle source akin to that of Sites 655 and 373 (high-Ti) basalts (BECCALUVA *et alii*, 1982, 1990). The Sr-Nd isotopic compositions of Sites 655 and 651 rocks are distinct from the rest of the southern Tyrrhenian primitive rocks (MgO>5 wt%) (fig. 6). According to BECCALUVA *et alii* (1990), hydrothermal alteration suffered by these samples does not affect their Nd isotopic composition which approaches that of Mid Atlantic Ridge E-MORB, whereas their Sr isotopic ratio was modified by basalt/seawater interaction (fig. 6). A similar process has also been invoked to explain the genesis and alteration of the oceanic crust of the Marsili basin (Site 650) which shows a medium K-CA basaltic andesites composition (figs. 4,5a).The two large central volcanoes of Vavilov basin, Magnaghi (3.0-2.7 Ma) and Vavilov (Late Pliocene - 0.1 Ma) seamounts, were built after cessation of the seafloor-spreading tectonic regime (ROBIN *et alii*, 1987; KASTENS *et alii*, 1988, 1990; SAVELLI, 1988). Few samples recovered from these seamounts reveal a basaltic composition (SELLI *et alii*, 1977; ROBIN *et alii*, 1987) and show incompatible trace element patterns indicating a derivation by partial melting of typical OIB-source (SERRI, 1990 and references therein) (fig. 5b).

A derivation from an OIB-type mantle source has been also suggested for the basaltic andesite rocks recovered from the eastern Sardinia rifted margin (Site 654) in spite of their tholeiitic affinity (figs. 3,4,5b) (SERRI, 1990).

3.3. - AEOLIAN SUBMARINE VOLCANISM: EOLO AND ENARETE SEAMOUNTS AND BASILUZZO AREA

Eolo and Enarete together with Sisifo represent volcanic seamounts oriented in a NW-SE direction and located to the west of the emerged Aeolian arc (MARANI *et alii*, 1999; MARANI & TRUA, 2002) (fig. 1).

Following the K2O *vs.* SiO2 diagram, most of the samples recently recovered from Enarete seamount plot in the SHO field and range from shoshonitic basalts to shoshonites, with some intermediate rocks displaying a high-K CA affinity and a basaltic andesite composition (fig. 4). Also samples recovered from Eolo seamount belong to the SHO series but they show a more evolved composition (latite) if compared to Enarete products. Several samples have been recovered from Basiluzzo area. All of them have a CA affi-

Tab. 1 – *Synthetic petrographic features of dredged and cored magmatic rocks from the Southern Tyrrhenian Basin during MAR98-TIR2000 cruises and comparison with literature data.*

Locality	Magma series (1)	Rock type (2)	Phenocrysts and micro-phenocrysts (3)	Age (Ma) (4)	Reference
Marsili seamount	CA	MK-/HK- B and BA	*group 1:* pl, ol, opq *group 2:* pl, ol, cpx, opq	0.7-<0.1	SELLI *et alii*, 1977; SERRI, 1990; SAVELLI & SCHREIDER, 1991; SAVELLI & GASPAROTTO, 1994; TRUA *et alii*, 2002c
		HKA	pl, cpx, opq ±opx ±ol		
Eolo seamount	SHO	B	pl, cpx, ol, ap	0.85-0.66	BECCALUVA *et alii*, 1985; TRUA *et alii*, 1999
		S	pl, cpx, bt, opx, ol, opq, ap		
		L	pl, cpx, ol, opq, ap ±bt ±opx		
		T	pl, bt, ap, opq		
	CA	HKD	pl, hb, cpx, bt, opx, opq, ap		
		R	pl, bt, cpx, opq, ap		
Enarete seamount	SHO	B	pl, bt, cpx	0.78-0.67	BECCALUVA *et alii*, 1995; TRUA *et alii*, 1999
		S	pl, bt, cpx ±opx, ±opq, ±ap		
Basiluzzo and islets	CA	MK-/HK-A	pl, cpx, opx, hb, opq	0.05	CALANCHI *et alii*, 1999 TRUA *et alii*, 1999
		MK-/HK-D	pl, cpx, opx, hb, opq		
		KHR	pl, cpx, hb		
Palinuro seamount	CA	MK-BA	pl, cpx, opx, ol, opq	0.35	COLANTONI *et alii*, 1981; TRUA *et alii*, 1999
Southern margin	TH	B	pl, cpx, ol	n.a.	BECCALUVA *et alii*, 1985; TRUA *et alii*, 1999
	CA	tonalite	qz, pl, opq		
Prometeo	A	Mug	pl, ol, cpx, opq	n.a.	TRUA *et alii*, 1999; TRUA *et alii*, 2003
Ustica	A	B	pl, ol, cpx	0.75-0.13	CALANCHI *et alii*, 1984; CINQUE *et alii*, 1988; SERRI, 1990; DE VITA *et alii*, 1998
		Haw	pl, ol, cpx		
		Mug	pl, ol, cpx, opq		

(1) A= alkaline; CA= calcalkaline; TH= tholeiitic; SHO= shoshonitic. (2) LK-= low K; MK-= medium K; HK-= high K; B= basalt, BA= basaltic andesite; A= andesite; D= dacite; R= rhyolite; S=shoshonite; L=latite; T=trachyte; Haw= hawaiite; Mug= mugearite. (3) ol=olivine, opx=orthopyroxene; cpx=clinopyroxene, pl=plagioclase, bt=biotite, hb=hornblende, opq=opaque, ap=apatite, qz=quartz. (4) n.a.=not available.

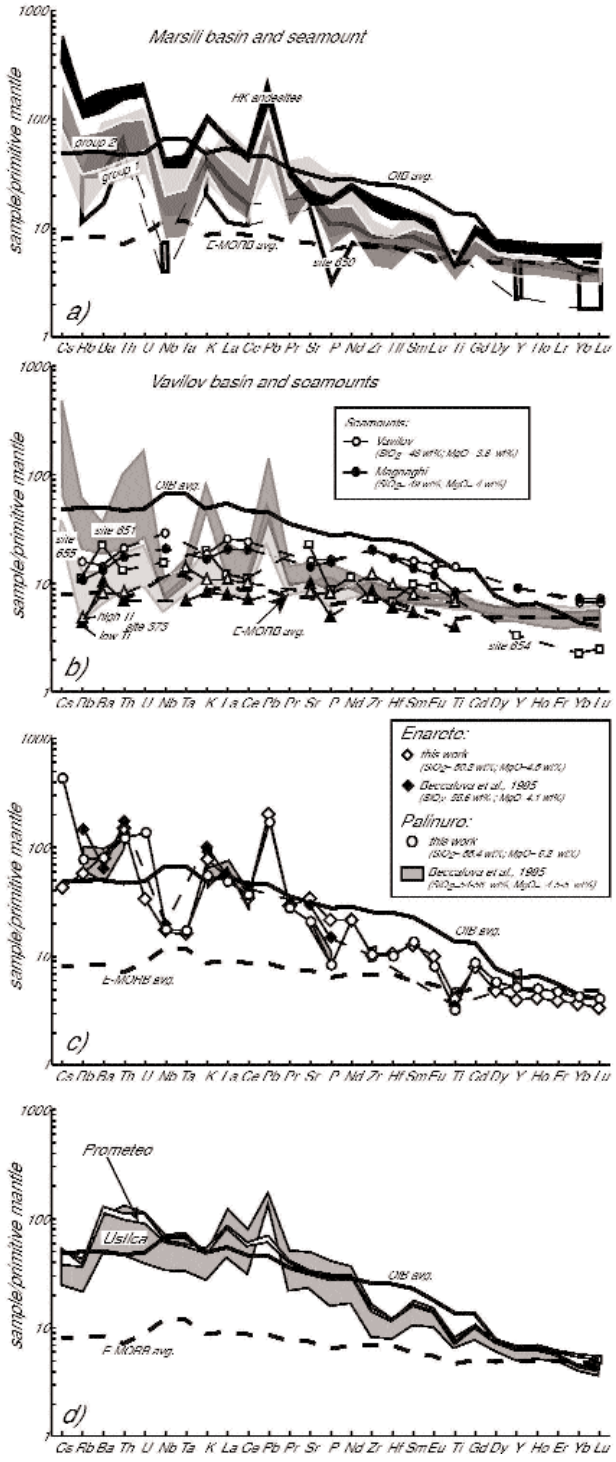

Fig. 5 – *Primordial mantle normalized incompatible element variation diagrams (normalizing values from* SUN & MACDONOUGH, 1989*). Trace element pattern for: a) Marsili basin and seamount lavas); b) Vavilov basin and seamounts lavas; c) Enarete and Palinuro seamounts; d) Prometeo lava field samples and Ustica lavas. Southern Tyrrhenian data source as in figure 3. Average OIB and E-MORB from* SUN & MACDONOUGH (1989).

nity and range from medium-K andesites up to medium- or high-K dacites in composition (fig. 4).

Eolo, Enarete and Basiluzzo samples are strictly

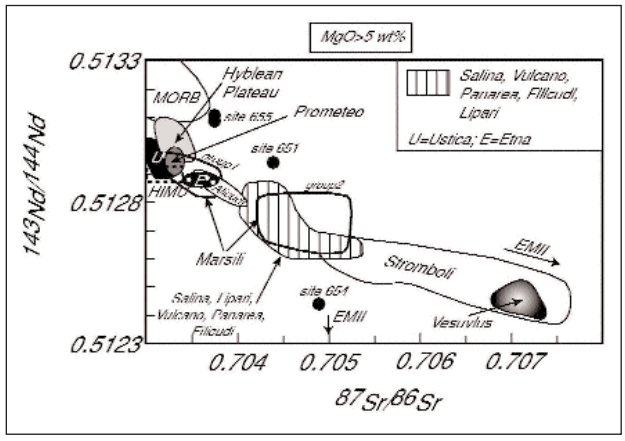

Fig. 6 – *$^{87}Sr/^{86}Sr$ vs. $^{143}Nd/^{144}Nd$ diagram for Neogene-Quaternary southern Tyrrhenian and African foreland lavas (MgO>5 wt%). Marsili* (TRUA *et alii*, 2002a,b); *Vavilov basin: sites 651, 654, 655* (BECCALUVA *et alii*, 1990); *Prometeo and Ustica* (TRUA *et alii*, 2003); *Alicudi, Filicudi, Salina, Lipari, Vulcano, Panarea and Stromboli* (ELLAM *et alii*, 1988, 1989; FRANCALANCI *et alii*, 1993; PECCERILLO *et alii*, 1993; DE ASTIS *et alii*, 2000; CALANCHI *et alii*, 2002); *Hyblean OIB-type alkaline rocks* (TRUA *et alii*, 1998); *recent Etnean lavas* (TONARINI *et alii*, 2001a); *Vesuvius* (AYUSO *et alii*, 1998; SOMMA *et alii*, 2001). *MORB field* (WILSON, 1989). *HIMU, EMI and EMII: OIB end-member mantle components* (ZINDLER & HART, 1986).

comparable, both in petrographical and geochemical characteristics, to previous samples recovered from these areas (tab. 1; figs. 3,4). However, it is worth to note that among the samples dredged from Enarete seamount by the MAR98 cruise there is a fragment of lava which resulted the most primitive basalt so far recovered from the seamount (figs. 3,4). The primitive mantle-normalised trace element pattern of this sample is very similar to that of the least differentiated Enarete sample studied by BECCALUVA *et alii* (1985). Both these samples display troughs at Nb, Ta and Ti and high LILE/HFSE ratios which are distinct features of island arc magmas (fig. 5c).

3.4. - PALINURO SEAMOUNT

Palinuro seamount is a volcanic complex consisting of five coalesced edifices straddling the eastern margin of the southern Tyrrhenian Sea in a W-E direction (MARANI *et alii*, 1999). It is located in a crucial position between the oceanic-crust floored Marsili basin and the Campanian-Calabrian continental slope (fig. 1). Despite the fact that it represents one of the main volcanic complex in the Tyrrhenian basin, it is still poorly studied from a petrological point of view.

Among the few samples recovered from the seamount during previous seafloor explorations, only two have been chemically studied (COLANTONI *et alii*, 1981). Furthermore, only three volcanic samples were recovered from the summit and in the south-eastern flank of the Palinuro volcanic complex (fig. 2) during the MAR98 cruise, since the principal target of that cruise was to sample hydrothermal deposits from this

volcanic area (MARANI *et alii*, 1999). These newly collected volcanic samples from Palinuro belong to the CA series and show a basaltic andesite composition similar to that observed in previously studied rocks (fig. 4). Also their petrographic features are strictly comparable to previous samples recovered by COLANTONI *et alii* (1981) from this area (tab. 1). Moreover, Palinuro samples have IAB-type pattern which results very similar to that also displayed by the western Aeolian seamounts (*e.g.,* Enarete) (fig. 5c).

3.5. - SOUTHERN MARGIN OF THE MARSILI BASIN

Few dredge hauls were made during MAR98 cruise in this still poorly studied area (fig. 2). Fragments of volcanic microbreccia, basic lavas and intrusive (tonalite, tab. 1) rocks have been recovered. Both lavas and the tonalite are affected by a strong degree of hydrothermal alteration, petrographically and chemically evidenced by the presence of abundant secondary minerals and high (from 4 up to 13 wt%) LOI respectively. The less altered sample (tonalite, LOI=4wt%) shows geochemical features similar to the low-K CA andesites (fig. 4).

From this area BECCALUVA *et alii* (1985) recovered two samples of basalts which suffered a strong degree of hydrothermal alteration. According to these authors, the petrochemical characteristics of these basalts are analogous to those of tholeiitic basalts, with IAB affinity. These samples would represent together with the tholeiitic basalt recovered from the north Lametini seamount, the only A-Th rocks so far recovered from the southern Tyrrhenian basin (fig. 4).

3.6. - PROMETEO LAVA FIELD

Few samples recovered during the MAR98 cruise derive from a lava flow located between Ustica and Alicudi islands (figs. 1,2) and erupted from a submarine eruptive centre recently discovered through the interpretation of multibeam reflectivity data (MARANI *et alii*, 1999). This previously unknown submarine lava field was named Prometeo by TRUA *et alii* (2003).

Prometeo samples are Na-alkaline basic rocks with a mugearite composition (fig. 3) and result petrographically and geochemically similar to the mugearites of Ustica island (tab. 1; fig. 3) (TRUA *et alii*, 2003). Prometeo mugearites show distinct patterns, with positive anomalies for elements partitioned into the fluid phase (*i.e.,* Ba, Th, U, Pb and La) and a relative depletion in less incompatible elements (from Zr to Ti) compared to average OIB-magmas (fig. 5d). In this respect, Prometeo lavas are similar to the OIB-type lavas from the nearby Ustica island (fig. 5d).

Prometeo and Ustica lavas have Sr and Nd isotopic compositions that are more consistent with OIB-type magmas than their trace-element concentrations (fig. 6). These lavas have a small range in $^{87}Sr/^{86}Sr$ (0.70304-0.70329) and 143Nd/144Nd (0.51291–0.51300) isotopic ratios approaching the isotopic composition of HIMU (high-μ) OIB-type basalts (Weaver, 1991). Interestingly, an HIMU-type component is also present in the source of the Plio-Pleistocene Hyblean and the most recent (post-1970) Etna OIB-type magmas (BECCALUVA *et alii*, 1998; TRUA *et alii*, 1998; SCHIANO *et alii*, 2001; TONARINI *et alii*, 2001a) (fig. 6), both erupted on the side of the African plate adjacent to the subduction-related Aeolian island arc (fig. 1).

We will discuss below how this observation provides strong useful geochemical tracers that can infer mantle structure beneath the southern Tyrrhenian basin.

4. – DISCUSSION

The geochemical complexities of southern Tyrrhenian volcanic rocks exemplify an important, debated issue of active volcanic arc systems: why do OIB-type basalts erupt in subduction related environments?

The coexistence of OIB and IAB magmatism is a long-standing petrological problem of the southern Tyrrhenian magmatism and has important implications not only for models of magma generation in this complex area but also for understanding its geodynamic evolution. The generation of OIB-type magmas in a volcanic arc system can occur where pristine asthenospheric material replaces mantle domains previously modified by subduction processes. The mechanisms proposed to explain this replacement are arc rifting (LEEMAN *et alii*, 1990; MARQUEZ *et alii*, 1999), slab window opening (HOLE *et alii*, 1991) or tear development along the subducting slab (TURNER & HAWKESWORTH, 1998). Alternatively, OIB-like signatures of some rocks occurring in arc environments may simply be related to low degree of partial melting of mantle wedge material that had undergone a low degree of contamination by slab components (REINERS *et alii*, 2000).

In the southern Tyrrhenian, IAB-type volcanic activity is widespread, being represented in the Vavilov and Marsili basins, Marsili seamount, Aeolian volcanic arc and related seamounts, whereas OIB-type magmatism is restricted to few areas (fig. 1): Magnaghi, Vavilov and Aceste seamounts; rocks drilled (site 654), dredged and cored in the East Sardinia rifted margin; Ustica island and Prometeo submarine lava field.

The petrological study of samples recently recovered from the southern Tyrrhenian will provide a much-needed insight into the relative role of OIB-type and IAB-type mantle sources in determining the unusual magmatic scenario offered by this region. In the following sections we discuss the petrological implications of preliminary geochemical and isotopic data for these samples, taking into account the key Marsili IAB-type seamount and Prometeo OIB-type volcanic rocks, and compare them with the literature data from the other volcanic areas in and around the southern Tyrrhenian region.

4.1. - Upper mantle structure beneath the southern Tyrrhenian: geochemical and isotopic constrains.

In the last decade it has become well established that geochemical tracers that distinguish between the sources of magmas (OIB, MORB, IAB) may provide a useful tool for mapping upper-mantle structure. Here we use incompatible element ratios coupled with isotope compositions of the most primitive southern Tyrrhenian rocks (MgO>5.0 wt%) to constrain variation in the magmas source composition of this region. Our arbitrary cut off of 5.0 wt% MgO was chosen to maximize the available data.

Pearce & Parkinson (1993), Pearce & Peate (1995) have advocated the use of graph of the type M (=conservative element)/Yb *vs.* Nb/Yb, where Yb is used as the normalising element to minimize the effects of partial melting and fractional crystallization, to estimate the mantle source composition of arc basalts, prior to its modification by slab-derived components. Both Nb and Zr may be considered as conservative elements for southern Tyrrhenian IAB-type magmas because the great majority of them plot within the MORB array in the Zr/Yb *vs.* Nb/Yb diagram, suggesting a derivation from sources enriched with respect to an average normal MORB and broadly comparable to T-/E-MORB sources (fig. 7a).

It is to be noted that only Stromboli samples have Zr/Yb ratios comparable with E-MORB lavas, thus approaching that of literature OIB-type lavas (Weaver, 1991). Moreover, according to these ratios, Stromboli and *group-2* Marsili basalts have the strongest OIB affinity among the southern Tyrrhenian IAB-lavas, resulting similar to that of the OIB-lavas of Prometeo, Ustica and Vesuvius. These observations suggest that the southern Tyrrhenian mantle wedge is laterally inhomogeneous and that such heterogeneity was present prior to modification related to subduction processes.

The involvement of OIB-like mantle in the genesis of southern Tyrrhenian subduction-related magmatism was previously suggested by several studies (Beccaluva *et alii*, 1982; Ellam *et alii*, 1988, 1989; Serri, 1990; 1997; De Astis *et alii*, 2000; Serri *et alii*, 2001; Tonarini *et alii*, 2001b; Calanchi *et alii*, 2002; Gasperini *et alii*, 2002).

We will show below that differences in incompatible element and isotopic ratios of the most primitive

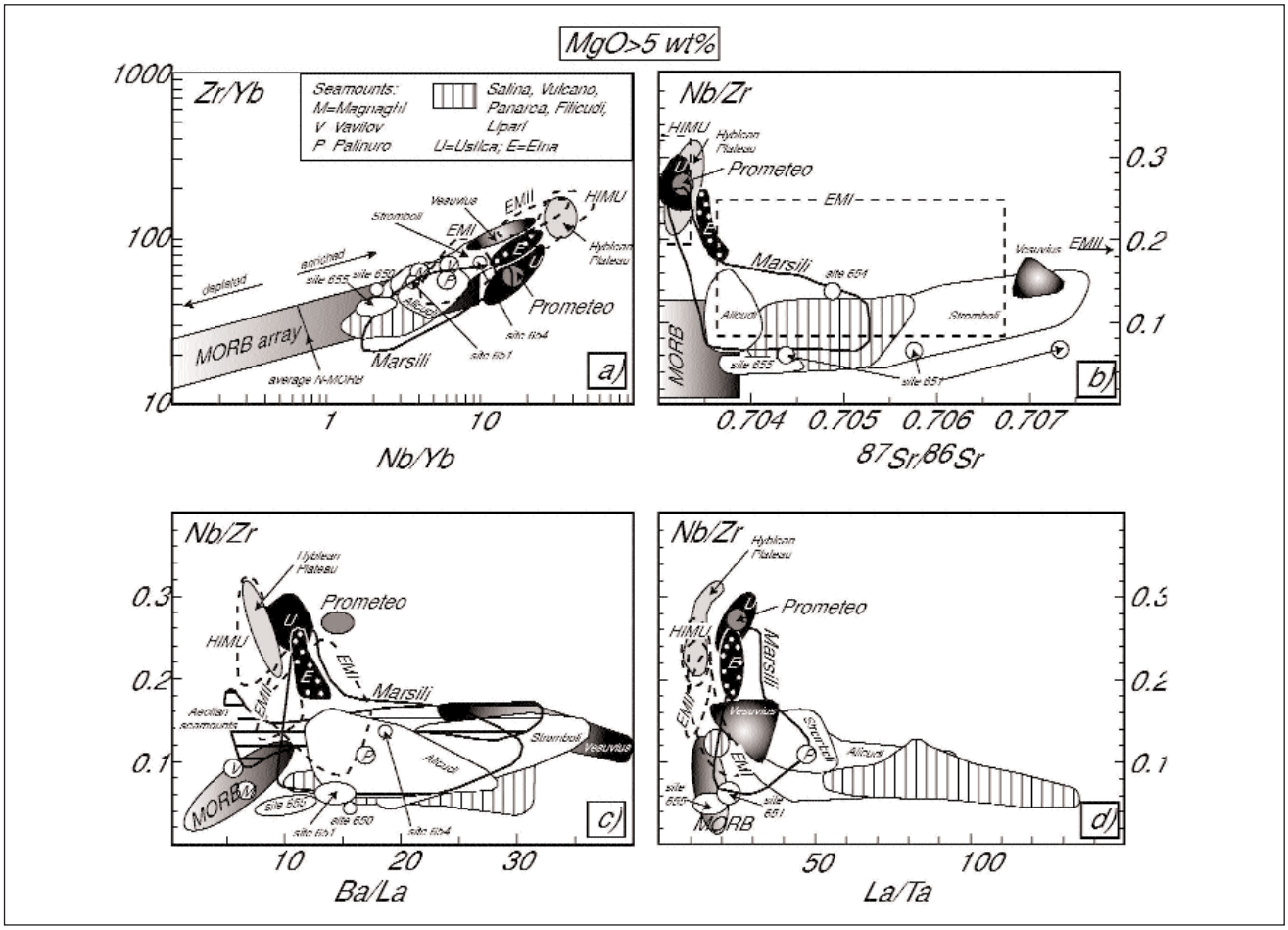

Fig. 7 – *Regional variation of some key incompatible trace element ratios and $^{87}Sr/^{86}Sr$ ratios in mafic rocks (MgO >5 wt%) from the Neogene-Quaternary southern Tyrrhenian and African foreland volcanic areas. MORB array in Zr/Yb vs. Nb/Yb diagram* (Pearce & Parkinson, 1993); *HIMU, EMI and EMII OIB fields* (Weaver, 1991; Zindler & Hart, 1986*). Aeolian seamounts* (Beccaluva *et alii*, 1985). *Other data source as in figures. 3 and 6.*

(MgO>5wt%) southern Tyrrhenian IAB-type lavas, especially those from Marsili seamount, reflect the presence of two distinct OIB-type components in the mantle wedge above the subducting Ionian slab.

These rocks are characterised by a wide range of Sr and Nd isotopic signatures (fig. 6). Notably, Marsili seamount and Aeolian IAB-type rocks have radiogenic isotope signatures that plot along a continuous trend extending from Ustica-Prometeo OIB-type magmatism to potassic rocks from Vesuvius. Two important observations arise from this diagram.

1) Unlike the Aeolian arc, Marsili seamount magmas erupted on oceanic crust and it is likely that they preserved the geochemical and isotopic characteristics of mantle-derived primitive melts. Thus, the Sr-Nd isotopic similarity between Marsili seamount and Aeolian rocks suggest that the main compositional differences between primitive Aeolian magmas are mostly inherited from an heterogeneous mantle source, akin to that involved in the genesis of Marsili seamount magmas, instead of acquired during shallow-level magma contamination.

2) Several studies have pointed that the potassic rocks from Stromboli and Vesuvius are derived from an originally OIB-type mantle metasomatized by subduction-related fluids or melts (Serri, 1990; Beccaluva *et alii*, 1991; Peccerillo, 2001). Thus, if we accept this interpretation, the variations in Sr-Nd isotopes encountered within the southern Tyrrhenian IAB-type magmatism could reflect the interaction between two distinct OIB-type components: one akin to that involved in the genesis of Ustica/Prometeo magmas (HIMU-like) and one more similar to that involved in the genesis of potassic magmas from Vesuvius (Vesuvius-like). These two OIB-like components were added to the pre-existing mantle wedge which had T-MORB isotopic signature, as evinced by the isotopic compositions of the samples drilled from the basement of the Vavilov basin (sites 373 and 655).

Combined evaluation of Sr isotope and ratios between some highly incompatible trace elements brings a further strong argument in support of the involvement of different mantle-derived components (OIBs HIMU-like and Vesuvius-like, T-MORB) as the cause of geochemical and isotopic variations in the most primitive southern Tyrrhenian magmas. Note that, for the most primitive rocks (MgO>5wt%) within each volcanic area of the southern Tyrrhenian basin, the chosen incompatible element ratios are constant with decrease of MgO content. Therefore, in absence of crustal contamination processes, they closely reflect those of their source.

From the previous discussion, we can assume that Nb/Zr ratio in the southern Tyrrhenian IAB-lavas is mantle-derived (fig. 7a). Different Nb/Zr ratios are generally interpreted in terms of variations in source composition or changes in degree of partial melting of the mantle. Since variable Nb/Zr ratio amongst these lavas nicely correlates with $^{87}Sr/^{86}Sr$, it can not be the consequence of variable partial melting of a single mantle source, but it requires that three different kinds of mantle-derived components were implicated in the genesis of southern Tyrrhenian magmatism (fig. 7b). Systematic variations in La/Ta (Ba/Nb and La/Nb, not shown) and Ba/La (Ba/Zr, not shown) ratios against Nb/Zr among the southern Tyrrhenian mafic lavas (fig. 7 c,d) further supply a straightforward test for this hypothesis and give fundamental information on the nature and possible origin of the three distinct mantle components involved in the genesis of the southern Tyrrhenian primitive magmas: (1) a depleted mantle wedge with T-MORB geochemical and isotopic signatures, probably somewhat modified by the incorporation of sedimentary and subduction-related material (mostly evident in Site 651 volcanics from Vavilov Basin); (2) a high Nb/Zr, low LREE/HFSE, Ba/La, Ba/Zr and $^{87}Sr/^{86}Sr$ OIB-type mantle component best developed in Ustica an Prometeo lavas; (3) an intermediate Nb/Zr, high LREE/HFSE, Ba/La, Ba/Zr and $^{87}Sr/^{86}Sr$ OIB-type mantle component best developed in Stromboli and Vesuvius lavas.

However, it is to note that in these trace element ratio diagrams the involvement of Vesuvius OIB-type mantle beneath the southern Tyrrhenian region may mask the contribution from the addition of Ionian subduction-related components (*i.e.,* fluids or melts derived from oceanic crust and subducted sediments) that several studies have documented to have occurred in both OIB (Trua *et alii*, 2003) and IAB (Serri, 1997; Tonarini *et alii*, 2001b) mantle sources of this region. This does not happen only for lavas from the central Aeolian arc (*i.e.,* Vulcano, Lipari, Salina and Panarea) that derived from more fluid-rich metasomatized mantle sources (Francalanci *et alii*, 1993; De Astis *et alii*, 2000; Tonarini *et alii*, 2001b). Geochemical modelling involving both incompatible trace element ratios and isotopic ratios is able to discriminate between the contribution from the various mantle reservoirs recognised beneath the southern Tyrrhenian basin and their interaction with Ionian slab-derived sediments and fluids. But this interaction represents a second-order process in the petrogenesis of the southern Tyrrhenian magmatism which, in terms of geochemical and isotopic components, reflects the presence of two distinct OIB-type components in the T-MORB mantle wedge prior to the addition of subduction-related components.

4.2. - Geodynamic implications

The geochemical tracers discussed in the previous section can be used to map mantle structure in the southern Tyrrhenian basin and represent an important contribution to the debate on the recent geodynamics of mantle flow in this region (Gvirtzman & Nur, 1999; Doglioni *et alii*, 2001; Gasperini *et alii*, 2002; Marani & Trua, 2002, Trua *et alii*, 2003).

Gvirtzman & Nur (1999) suggested that several geological features of the southern Tyrrhenian basin could be explained by suction of intraplate mantle from the African plate margin into the mantle wedge

above the subducting Ionian slab. According to Gvirtzman and Nur's model, Etna and Vesuvius magmatism would be a main surface effect of the African asthenospheric inflow along the southern and the northern tear of the subducted Ionian plate, respectively. The evidence here discussed reveals that GVIRTZMAN & NUR's (1999) hypothesis could effectively account for the presence of distinct OIB-type components in the mantle wedge of the southern sector of the southern Tyrrhenian basin (MARANI & TRUA, 2002).

The OIB HIMU-like components seem to be restricted to a roughly NW-SE trending belt across the Sicilian Maghrebide orogen which is composed of Ustica, Prometeo and Etna volcanoes (fig. 1) (TRUA *et alii*, 2003). According to MARANI & TRUA (2002) the volcanic alignment defined by these OIB-type volcanoes is the surface evidence of the southern slab tear of the Ionian subducted slab. It is noteworthy that BECCALUVA *et alii* (1982) were the first to raise the issue that OIB-type magmas from Ustica could be associated with a first order lateral discontinuity of the subducted Ionian slab. The authors based their hypothesis mainly on the similar geochemical characteristics shared by Ustica and Etna OIB-type lavas. The finding of Prometeo HIMU-type submarine lava field along the same NW-SE volcanic alignment defined by Ustica and Etna strongly supports this idea.

The similarity between most of the geochemical features of the primitive potassic magmas from Stromboli and Vesuvius in terms of geochemical and isotopic signatures likely points to compositionally similar mantle sources (SERRI, 1990; PECCERILLO, 2001 and references therein). These mantle sources, which define the OIB Vesuvius-like component (figs. 5, 6), consist of a mixture of an OIB-type and slab-derived components. However, unlike the HIMU OIB-type component, the origin of the OIB Vesuvius-like component in this sector of the southern Tyrrhenian is still unclear. A detailed petrological study on the poorly known submarine volcanic areas (e.g., Palinuro, Aceste, Anchise, Albatros, Alcione and Lametini) are required to better define the mantle dynamics and magma-generation processes occurring in southern Tyrrhenian back-arc basin.

Acknowledgments

This work was financially supported by grants from MURST-COFIN *and* CNR (G.S.).*We wish to thank* A. RENZULLI *for his thoughtful review.*

REFERENCES

AYUSO R.A., DE VITO B., ROLANDI G., SEAL II R.R. & PAONE A. (1998) – *Geochemical and isotopic (Nd-Pb-Sr-O) variations bearing on the genesis of volcanic rocks from Vesuvius, Italy*. Journal of Volcanology and Geothermal Research, **82**: 53-78.

BARBERI F., BIZOUARD H., CAPALDI G., FERRARA G., GASPARINI P., INNOCENTI F., JORON J.L., LAMBERT B., TREUIL M. & ALLÈGRE C. (1978) - *Age and nature of basalts from the Tyrrhenian Abyssal Plain*. In: HSU K., MONTADERT L. *et alii* (Eds.): "*Initial Reports of the Deep Sea Drilling Project*". Washington, **42**: 509-514.

BECCALUVA L., ROSSI P.L. & SERRI G. (1982) - *Neogene to Recent volcanism of the Southern Tyrrhenian-Sicilian area: Implications for the geodynamic evolution of the Calabrian arc*. Earth Evolutionary Sciences, **3**: 222-238.

BECCALUVA L., MORLOTTI E. & TORELLI L. (1984) – *Notes on the geology of the Elimi Chain area (Southwestern margin of the Tyrrhenian Sea)*. Mem. Soc. Geol. It., **27**: 213-232.

BECCALUVA L., GABBIANELLI G., LUCCHINI F., ROSSI P.L. & SAVELLI C. (1985) - *Petrology and K/Ar ages of volcanics dredged from the Aeolian seamounts: implications for geodynamic evolution of the Southern Tyrrhenian basin*. Earth and Planetary Science Letters, **74**: 187-208.

BECCALUVA L., BONATTI E., DUPUY C., FERRARA G., INNOCENTI F., LUCCHINI F., MACERA P., PETRINI R., ROSSI P.L., SERRI G., SEYLER M. & SIENA F. (1990): *Geochemistry and mineralogy of volcanic rocks from ODP sites 650, 651, 655 and 654 in the Tyrrhenian Sea*. In: KASTERNS K & MASCLE J. (Eds.): "*Proceeding of the ODP*". Scientific Results, **107**:' 49-74.

BECCALUVA L., DI GIROLAMO P. & SERRI G. (1991) – *Petrogenesis and tectonic setting of the Roman volcanic province*. Lithos, **26**: 191-221.

BECCALUVA L., SIENA F., COLTORTI M., DI GRANDE A., LO GIUDICE A., MACCIOTTA G., TASSINARI R. & VACCARO C. (1998) – *Nephelinitic to tholeiitic magma generation in a transtensional tectonic setting: an integrated model for the iblean volcanism, Sicily*. Journal of Petrology, **39**: 1547-1576.

CALANCHI N., COLANTONI P., GABBIANELLI G., ROSSI P.L. & SERRI G. (1984) – *Physiography of Anchise Seamount and of the submarine part of Ustica Island (south Tyrrhenian): petrochemistry of dredged volcanic rocks and geochemical characteristics of their mantle sources*. Miner. Petrogr. Acta, **XXVIII**, 215-241.

CALANCHI N., TRANNE C.A., LUCCHINI F., ROSSI P.L. & VILLA I.M. (1999) – *Explanatory notes to the geological map (1:10,000) of Panarea and Basilizzo islands (Aeolian Arc, Italy)*. Acta Vulcanologica, **11**(2): 223-243.

CALANCHI N., PECCERILLO A., TRANNE C.A., LUCCHINI F., ROSSI P.L., KEMPTON P., BARBIERI M. & WU T.W. (2002) - *Petrology and geochemistry of volcanic rocks from the island of Panarea: implications for mantle evolution beneath the Aeolian island arc (southern Tyrrhenian sea)*. Journal of Volcanology and Geothermal Research, **115**: 367-395.

CINQUE A., CIVETTA L., ORSI G. & PECCERILLO A. (1988) - *Geology and geochemistry of the island of Ustica (Southern Tyrrhenian Sea)*. Rendiconti della Società Italiana di Mineralogia e Petrologia, **43**: 987-1002.

COLANTONI P., LUCCHINI F., ROSSI P.L., SARTORI R. & SAVELLI C. (1981) - *The Palinuro Volcano and magmatism of the south-eastern Tyrrhenian Sea (Mediterranean)*. Marine Geology **39**: M1-M12.

DE ASTIS G., PECCERILLO A., KEMPTON P., LA VOLPE L. & WU T.W. (2000) - *Transition from calc-alkaline to potassium-rich magmatism in subduction environments: geochemical and Sr, Nd, Pb isotopic constraints from the island of Vulcano (Aeolian arc)*. Contribution to Mineralogy and Petrology, **139**: 684-703.

DE VITA S., LAURENZI M.A., ORSI G. & VOLTAGGIO M. (1998) – *Application of $^{40}Ar/^{39}Ar$ and ^{230}Th dating methods to the chronostratigraphy of Quaternary basaltic volcanic areas: the Ustica Island case history*. Quaternary International, **47/48**, 117-127

DOGLIONI C., INNOCENTI F. & MARIOTTI G. (2001) - *Why Mt. Etna?* Terra Nova, **13**: 25-31.

ELLAM R.M., MENZIES M.A., HAWKESWORTH C.J., LEEMAN W.P., ROSI M. & SERRI G. (1988) - *The transition from calc-alkaline to potassic orogenic magmatism in the Aeolian Islands, Southern Italy*. Bullettin of Volcanology, **50**: 386-398.

ELLAM R.M., HAWKESWORTH C.J., MENZIES M.A. & ROGERS N.W. (1989) – *The volcanism of Southern Italy: role of subduction and the relationship between potassic and sodic alkaline magmatism*. Journal of Geophysical Research, **94**: 4589-4601.

FRANCALANCI L., TAYLOR S.R., MCCULLOCH M.T. & WOODHEAD J.D. (1993) - *Geochemical and isotopic variations in the calc-alkaline rocks of Aeolian arc, southern Tyrrhenian Sea, Italy: constraints on magma genesis*. Contribution to Mineralogy and Petrology, **113**: 300-313.

FRANCALANCI L. & MANETTI P. (1994) – *Geodynamic models of the Southern Tyrrhenian region: constraints from the petrology and geochemistry of the Aeolian volcanic rocks*. Bollettino di Geofisica Teorica ed Applicata, **XXXVI**, 141-144, 283-292.

GASPERINI D., BLICHERT-TOFT J., BOSCH D., DEL MORO A., MACERA P. & ALBEREDE F. (2002) - *Upwelling of deep mantle material through a plate window: evidente from the geochemistry of Italian basaltic volcanics*. Journal of Geophysical Research, **107**: B12, 2367, doi: 10.1029/2001JB000418.

GHIORSO M.S. & SACK R.O. (1995) - *Chemical transfer in magmatic processes IV. A revised and internally consistent thermodynamic model for the interpolation and extrapolation of liquid-solid equilibria in magmatic systems at elevated temperatures and pressures*. Contribution to Mineralogy and Petrology **119**: 197-212.

GUEGUEN E., DOGLIONI C. & FERNANDEZ M. (1998) - *On the post-25 Ma geodynamic evolution of the western Mediterranean*. Tectonophysics, **298**: 259-269.

GVIRTZMAN Z. & NUR A. (1999) - *The formation of Mount Etna as the consequence of slab rollback*. Nature, **401**: 782-785.

HOLE M.J., ROGERS G., SAUNDERS A.D. & STOREY M. (1991) - *Relation between alkalic volcanism and slab-window formation*. Geology, **19**: 657-660.

KASTENS K.A. *et alii* (1988) - *ODP Leg 107 in the Tyrrhenian Sea: insights into passive margin and back-arc basin evolution*. Geological Society of America Bullettin, **100**, 1140-1156.

KASTENS K.A. *et alii* (1990) - *The geological evolution of the Tyrrhenian Sea: an introduction to the scientific results of ODP Leg 107*, In: KASTENS K.A., MASCLE J. *et alii* (Eds.): "*Proceedings of the ODP*". Scientific Results **107**: 3-26.

LE BAS M.J., LE MAITRE R.W., STRECKEISEN A. & ZANETTIN B. (1986) - *A chemical classification of volcanic rocks based on the total alkali-silica diagram*. Journal of Petrology, **27**: 745-750.

LEEMAN W.P., SMITH D.R., HILDRETH W., PALACI Z. & ROGERS N. (1990) - *Compositional diversity of Late Cenozoic basalts in a transect across the southern Washington Cascades: implications for subduction zone magmatism*. Journal of Geophysical Research, **95**: 19,561-19,582.

MARANI M.P. & TRUA T. (2002) - *Thermal constriction and slab tearing at the origin of a superinflated spreading ridge: Marsili volcano (Tyrrhenian Sea)*. Journal of Geophysical Research, 107(B9): 2188, doi: 10,1029/ 2001JB000285.

MARANI M.P., GAMBERI F., CASONI L., CARRARA G., LANDUZZI V., MUSACCHIO M., PENITENTI D., ROSSI L. & TRUA T. (1999) - *New rock and hydrothermal samples from the southern Tyrrhenian sea: the MAR-98 research cruise*. Giornale di Geologia, **61**: 3-24.

MARQUEZ A., OYARZUM R., DOBLAS M. & VERMA S.P. (1999) - *Alkalic (ocean-island basalt type) and calc-alkalic volcanism in the Mexican volcanic belt: a case for plume-related magmatism and propagating rifting at an active margin?* Geology, **27**: 51-54.

PEARCE J.A. & PEATE D.W. (1995) – *Tectonic implications of the composition of volcanic arc magmas*. Annu. Rev. Earth Planet. Sci., **23**: 251-285.

PEARCE J.A. & PARKINSON I.J. (1993) – *Trace element models for mantle melting: application to volcanic arc petrogenesis*. Geol. Soc. London Spec. Publ., **76**: 373-403.

PECCERILLO A., KEMPTON P.D., HARMON R.S., SANTO A.P., BOYCE A.J. & TRIPODO A. (1993) - *Petrological and geochemical characteristics of the Alicudi Volcano, Aeolian Islands, Italy: implications for magma genesis and evolution*. Acta Vulcanologica, **3**: 235-249.

PECCERILLO A. (2001) – *Geochemical similarities between the Vesuvius, Phlegraean Fields and Stromboli Volcanoes: petrogenetic, geodynamic and volcanological implications*. Mineralogy and Petrology, **73**: 93-105.

REINERS P.W, HAMMOND P.E., MCKENNA J.M. & DUNCAN R.A. (2000) - *Young basalts of the central Washington Cascades, flux melting of the mantle, and trace element signatures of primary arc magmas*. Contribution to Mineralogy and Petrology, **138**: 249-264.

ROBIN C., COLANTONI P., GENNESSEAUX M. & REHAULT J.P. (1987): *Vavilov seamount: a mildly alkaline quaternary volcano in the Tyrrhenian Basin*. Marine Geology, **78**: 125-136.

SARTORI R. (1990) – *The main results of ODP Leg 107 in the frame of Neogene to Recent geology of perityrrhenian areas*. In: KASTENS K.A., MASCLE J. *et alii* (Eds.): "*Proceedings of the ODP*". Scientific Results **107**: 715-730.

SAVELLI C. & GASPAROTTO G. (1994) - *Calc-alkaline magmatism and rifting of the deep-water volcano of Marsili (Aeolian back-arc, Tyrrhenian Sea)*, Marine Geology, **119**: 137-157.

SAVELLI C. & SCHRIEDER A.A. (1991) - *The opening processes in the deep Tyrrhenian basins of Marsili and Vavilov, as deduced from magnetic and chronological evidence of their igneous crust*. Tectonophysics **189**: 1-13.

SAVELLI C. (1988) – *Late Oligocene to Recent episodes of magmatism in and around the Tyrrhenian Sea: implications for the processes of opening in a young inter-arc basin of intra-orogenic (Mediterranean) type*. Tectonophysics, **146**: 163-181.

SCHIANO P., CLOCCHIATTI R., OTTOLINI L. & BUSÀ T. (2001) - *Transition of Mount Etna lavas from a mantle-plume to an island-arc magmatic source*. Nature, **412**: 900-904.

SELLI R., LUCCHINI F., ROSSI P.L., SAVELLI C. & DEL MONTE M. (1977) - *Dati geologici, petrochimici e radiometrici sui vulcani centro-tirrenici*. Giornale di Geologia **42**: 221-246.

SERRI G. (1990) - *Neogene-Quaternary magmatism of the Tyrrhenian region: characterization of the magma sources and geodynamic implications*. Mem. Soc. Geol. It. **41**: 219-242.

SERRI G., INNOCENTI F. & MANETTI P. (1993) – *Geochemical and petrological evidence of the subduction of delaminated Adriatic continental lithosphere in the genesis of the Neogene-Quaternary magmatism of central Italy*. Tectonophysics, **223**: 117-147.

SERRI G. (1997) - *Neogene-Quaternary magmatic activity and its geodynamic implications in the Central Mediterranean region. Annali di Geofisica*, **XL**, 3, 681-703.

SERRI G., INNOCENTI F. & MANETTI P. (2001) - *Magmatism from Mesozoic to Present: petrogenesis, time-space distribution and geodynamic implications*. In: VAI G.B. & MARTINI P.I. (Eds.): "*Anatomy of a mountain: the Apennines and the adjacent Mediterranean Basins*". Kluwer Academic Publishers (Great Britain), 77-104.

SOMMA R., AYUSO R.A., DE VIVO B. & ROLANDI G. (2001) – *Major, trace element and isotope geochemistry (Sr-Nd-Pb) of interplinian magmas from Mt. Somma-Vesuvius (Southern Italy)*. Mineralogy and Petrology, **73**: 121-143.

SUN S.S. & MCDONOUGH W.F. (1989) - Chemical and isotopic systematics of oceanic basalts: implications for mantle composition and processes. In: SAUNDERS A.D. & NORRY M.J. (Eds.): "*Magmatism in the ocean basins*". Geological Society of London Special Publication, **42**: 313-345.

TONARINI S., ARMIENTI P., D'ORAZIO M. & INNOCENTI F. (2001a) - *Subduction-like fluids in the genesis of Mt. Etna magmas: evidence from boron isotopes and fluid mobile elements*. Earth and Planetary Science Letters, **192**: 471-483.

TONARINI S., LEEMAN W.P. & FERRARA G. (2001b) - *Boron isotopic variations in lavas of the Aeolian volcanic arc, South Italy*. Journal of Volcanology and Geothermal Research, **110**: 155-170.

TRUA T., ESPERANCA S. & MAZZUOLI R. (1998) - *The evolution of the lithospheric mantle along the N. African Plate: geochemical and isotopic evidence from the tholeiitic and alkaline volcanic rocks of the Hyblean plateau, Italy*. Contribution to Mineralogy and Petrology, **131**: 307-322.

TRUA T., SERRI G., RENZULLI A., MARANI M. & GAMBERI F. (1999) - *The volcanism in and around the Marsili basin (southern Tyrrhenian Sea): geochemical characteristics of new dredged rocks*. Geoitalia, 2° Forum FIST, Riassunti, **1**: 193-194.

TRUA T., SERRI G., DENIEL C., MARANI M., RENZULLI A. & GAMBERI F. (2002a) - Marsili volcano: an active calcalkaline seamount along the spreading axis of the southern Tyrrhenian backarc basin. *Montagne Pelee 1902-2002 – Explosive volcanism in subduction zones, Saint-Pierre, Martinique, May 12-16, 2002*. Abstracts volume, pag.63.

TRUA T., SERRI G., DENIEL C., MARANI M., RENZULLI A. & GAMBERI F. (2002b) - An active calcalkaline seamount along the quaternary to recent spreading axis of the southern Tyrrhenian backarc basin: the Marsili volcano. *82° Congresso Nazionale S.I.M.P., Cosenza, 18-20 settembre 2002*. Plinius, pag. 283-284.

TRUA T., SERRI G., MARANI M., RENZULLI, A. & GAMBERI F. (2002c) - *Volcanological and petrological evolution of Marsili seamount (southern Tyrrhenian Sea)*. Journal of Volcanology and Geothermal Research, **114**: 441-464.

TRUA T. , SERRI G. & MARANI M. (2003) - *"Lateral flow of African mantle below the nearby Tyrrhenian plate: geochemical and isotopic evidence"*. Terra Nova, doi: 10.1046/j.1365-3121.2003.00509.x.

TURNER S. & HAWKESWORTH C. (1998) - *Using geochemistry to map mantle flow beneath the Lau Basin*. Geology, **26**: 1019-1022.

WEAVER B.L. (1991) - *Trace element evidence for the origin of ocean-island basalts*. Geology, **19**: 123-126.

WILSON M. (1989) – *Igneous petrogenesis. Harper Collins Academic*, London, pp. 466.

ZINDLER A. & HART S. (1986) – *Chemical geodynamics*. Ann. Rev. Earth Planet. Sci., **14**: 493-571.

Mem. Descr. Carta Geol. d'It.
XLIV (2004), pp.97-108
5 figg.

Structural framework of the Tyrrhenian Sea unveiled by seafloor morphology

Struttura del Mar Tirreno svelata dalla morfologia del fondale

MARANI M.P. (*), GAMBERI F. (*)

ABSTRACT - A review is made of the principal morphological characteristics of the Tyrrhenian basin from a structural point of view. On this basis, four geodynamic provinces are defined: the basin and range province of the northern Tyrrhenian, the passive margin province of the Sardinia block, the active Apenninic margins of the eastern and southern Tyrrhenian and the ocean floored deep central basins.
The four provinces are characterised by distinct development of structural elements both from a stress state point of view and their timing.

KEY WORDS: seafloor morphology, structural provinces, tectonic activity, Tyrrhenian Sea

RIASSUNTO - E' presentato un quadro generale delle principali caratteristiche strutturali del Tirreno da un punto di vista morfologico. Sono state distinte quattro province geodinamiche: la provincia *basin and range* del nord Tirreno, la provincia di margine passivo della Sardegna, la provincia Appenninica attiva del Tirreno orientale e meridionale e la provincia di crosta oceanica del Tirreno centrale.
Le quattro province possiedono caratteri distinti sia dal punto di vista del campo di stress originario che dalla loro età di attività.

PAROLE CHIAVE: morfologia del fondale, province strutturali, attività tettonica, Mar Tirreno

1. - INTRODUCTION

The Tyrrhenian Sea, the youngest back-arc basin of the Mediterranean, has been entirely surveyed by means of multibeam swath bathymetry, from 400 metres water depth up to its deeper portions. The resulting data set provides baseline morphological information to corollary research in portions of the Tyrrhenian involving rock sample collection and deep-towed side scan sonar surveys and acquisition of high resolution seismic data.

Detailed seafloor morphology in evolving arc/back-arc settings offers the opportunity of revealing surface features that, for the most part, result from the deeper geological processes that act in the region. It is evident that deep-seated events influence the pattern of structural styles, the development of volcanism and even the occurrence of large sedimentary transport and depositional systems. Therefore, a comprehensive characterization of the surface morphology offers a means to define the properties, structure and dynamics of its ultimate source region, the mantle.

In some cases, as this paper attempts to show, the effects of events occurring as deep as within the asthenosphere or at the asthenosphere-lithosphere boundary are largely revealed through surface morphology.

(*)ISMAR - CNR, Sezione di Geologia Marina, Via Gobetti 101, 40129 Bologna.

2. - REGIONAL SETTING

The formation of the Tyrrhenian Sea occurs within the overall context of slow convergence between the African and Eurasian plates, which presently characterises the Mediterranean (DEWEY *et alii*, 1989; ARGUS *et alii*, 1989; DE METS *et alii*, 1990; WARD, 1994). Bordered to the east and south by the Apennine-Maghrebides mountain belt and to the west by the passive Sardinian margin, the Tyrrhenian basin formed as a consequence of rifting and back-arc extension of the Alpine/Apennine suture above the north-westerly-subducting Ionian oceanic slab, (KASTENS *et alii*, 1988; KASTENS, MASCLE *et alii*, 1990; SARTORI, 1990; JOLIVET, 1991).

E-W directed rifting in the northern Tyrrhenian in lower-mid Miocene (~15 Myr) and along the western margin of Sardinia in Tortonian (~11 Myr) (ZITELLINI *et alii*, 1986; KASTENS, MASCLE *et alii*, 1990) marks the initial opening of the Tyrrhenian basin leading to the formation of oceanic domains in the Central and Southern Tyrrhenian. First, production of ocean crust occurred westward, during the Pliocene spreading of the Vavilov basin (4.3-2.6 Myr), (KASTENS, MASCLE *et alii*, 1990) accompanied by the thermal subsidence of the thinned western margin crust. A subsequent change to ESE-directed extensional stress in Late Pliocene-Quaternary resulted in the emplacement of basaltic crust southeastwards, generating the Marsili backarc basin (2 Myr), (KASTENS, MASCLE *et alii*, 1990).

The most widely accepted mechanism to account for the migration in space and time of rifting, volcanism and ocean crust emplacement links the eastwards migration of crustal thinning and oceanic accretion to the passive rollback of the Ionian plate (MALINVERNO & RYAN, 1986; SAVELLI, 1988; ARGNANI & SAVELLI, 1999). Since Early Miocene, time of the Alpine/Apennine collisional suture in the future Tyrrhenian area (BECCALUVA *et alii*, 1994), most of the pre-existing Mesozoic oceanic lithosphere in the western and central Mediterranean had been consumed, with the exception of the remnant Ionian ocean, delimited to the southwest by its ancient margin, the Malta escarpment

The Tyrrhenian opening, induced by the rollback of the remnant slab, was matched by the eastward and southward radial growth of the Apennine-Maghrebides fold and thrust belt on the Italian peninsula and Sicily (SARTORI *et alii*, 1989). In step with backarc basin development, the subduction-related island arc volcanism of the southern Tyrrhenian basin migrated from west to south-east, from Sardinia (32-13 Ma) to the currently active Aeolian island arc (SERRI 1997 and references therein), developing the present-day arc/backarc configuration of the southern Tyrrhenian region.

The deep-water, ocean crust floored, central and southern Tyrrhenian Sea is surrounded by different geodynamic margin settings. The western Tyrrhenian margin represents a typical passive continental margin while the eastern and southern margins are associated with high seismicity, active volcanism and elevated rates of uplift of land areas represented by the Apennine-Maghrebid mountain chain.

3. - GEODYNAMIC PROVINCES OF THE TYRRHENIAN BASIN

Due to the young age of the Tyrrhenian Sea, tectonic and associated volcanic processes exert a strong control on the seafloor make-up. Consequently, simple examination of the morpho-bathymetry of the basin consents a primary subdivision (fig. 1) of the region on the basis of its morphology: the northern Tyrrhenian zone; the eastern Sardinia margin; the eastern Tyrrhenian margin of peninsular Italy and Sicily and the deep, central and southeastern abyssal plains. This classification based on purely morphological features, which undeniably derives from the history of the basin, is substantiated, however, by distinctive geological and geophysical information that characterizes each zone. As a result, the morphology of the Tyrrhenian seafloor matches the distribution of four principal geodynamic provinces related to its formation and development.

3.1. - BASIN AND RANGE PROVINCE: THE NORTHERN TYRRHENIAN

Bordered to the north by the Tuscan Archipelago and to the south by the conjunction of Baronie seamount and the Pontine Islands, this sector is

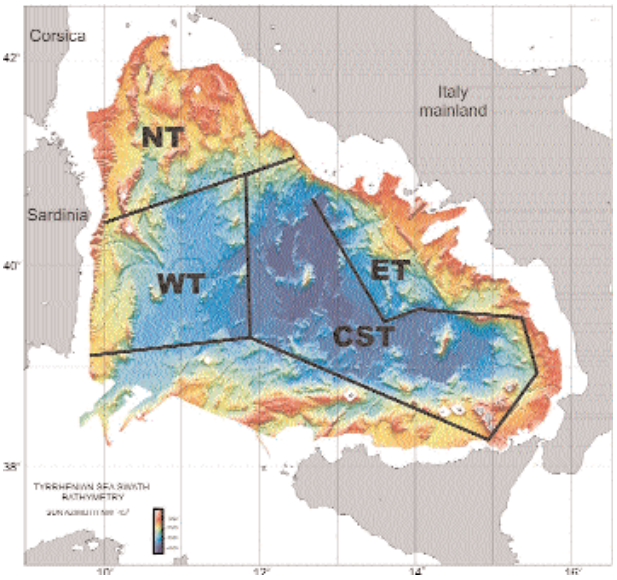

Fig. 1. - *Shaded relief bathymetric map of the Tyrrhenian Sea showing the surveyed region. Depths are colour-coded, illumination from the NW. Black lines divide the four geodynamic provinces discussed in text: NT, Northern Tyrrhenian Basin and Range province; WT, Western Tyrrhenian passive margin province; ET, Eastern Tyrrhenian active margin province and CST, Central and Southern Tyrrhenian ocean crust floored province.*

roughly triangle-shaped and extends between 42° N, (northern edge of survey) and 40°30' N (fig. 2).

Previous work in the region, based on single channel seismic reflection profiles, has shown the extensional nature of the northern Tyrrhenian terrain (ZITELLINI *et alii*, 1986; MARANI & ZITELLINI, 1986; BARTOLE 1995), composed of a series of rotational normal faults resulting in a tectonic framework of tilted blocks, half-graben and graben-horst structures.

Extensional thinning of the significantly thickened crust resulting from the Alpine/Apennine collisional suture that previously occupied this region began in early-mid Miocene (CARMIGNANI & KLIGFIELD, 1990; JOLIVET *et alii*, 1991; PASCUCCI *et alii* 1999). Extension with accompanied magmatic activity gets younger from east to west (BECCALUVA *et alii*, 1989; SERRI *et alii*, 1993; CARMIGNANI *et alii*, 1995), from ~15/20 Myr in the Corsica Basin to the presently active normal faults in the northern Apennines. The Northern Tyrrhenian is presently characterized by relatively thin crust (SCARASCIA *et alii*, 1994) in the order of 22 km and a shallow asthenosphere, 50 km deep (SUHALDOC & PANZA, 1989; SERRI *et alii*, 1993; FINETTI *et alii*, 2001). Bathymetrically, the northern Tyrrhenian principally develops as a series of N-S and NNW-SSE trending structural highs and adjacent, relatively flat-lying basins. On average, the structures have a length of ~40 km and are set 20/25 km apart. The bathymetric base level of the region, corresponding to the basin depths, is ~1500 meters in the northern portion of the region and reaches 2000 meters only in the southernmost part of it. The major structures (fig.2), such as the Etruschi samount in the West and the Civitavecchia Valley in the East, have a continuity of more than 70 km and the average elevation of the highs, with respect to the basin lows, is of more than 1000 meters with the summits reaching 300/400 meters below sea level.

Detailed seafloor bathymetry thus furnishes a comprehensive picture of the array of extensional features that affected a thickened crustal wedge in the 200 km wide northern Tyrrhenian marine region. The overall surface topography of this broad extensional system reveals a striking similarity to areas of diffuse continental extension such as the Basin and Range province of the western United States. This comparison between structural styles, based only on morphological grounds, is also however supported by the finding of low angle detachment faults and core complexes in Corsica and Tuscany (CARMIGNANI & KLIGFIELD, 1990; JOLIVET *et alii*, 1991), by the extensive block faulting and by the diachronous development of extension and magmatism. In effect, all these traits are common to the Basin and Range province, namely extension involving low angle extensional faults coupled to high angle, rotational block faults and the documented migration in time and space of extension and magmatism (WERNICKE, 1981; LISTER & DAVIS, 1989; SURPLESS *et alii*, 2002).

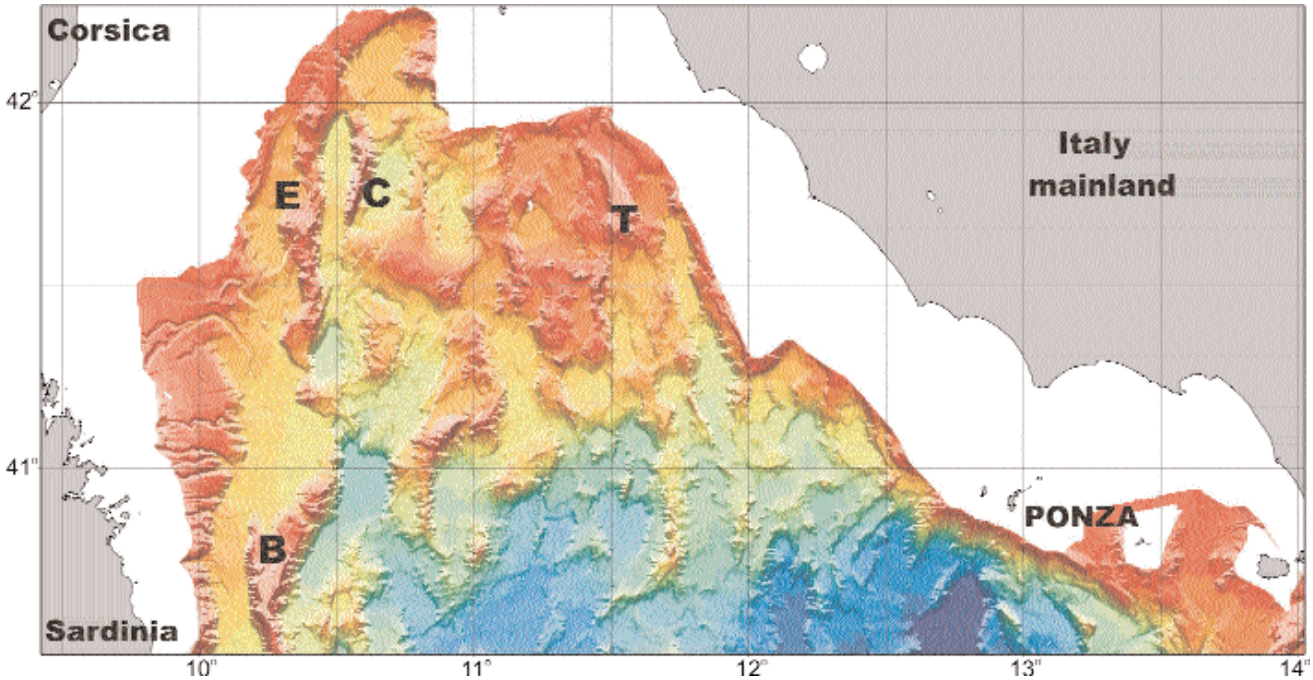

Fig. 2. - *North Tyrrhenian Province. Colour code and illumination as in figure 1. The relatively shallow base-level of the seafloor is interrupted by mostly N-S trending structural highs and intervening basins. Major seamounts are Etruschi (E) Cialdi (C) and Tiberino (T). Baronie seamount (B) to the west and Ponza offshore structures to the east delimit the region to the south. Refer to text for further discussion.*

3.2. - Passive Margin Province: the eastern Sardinia margin

The eastern Sardinia province is delimited to the north by the Baronie Seamount at 40°30'N and to the south at 39°N, covering the marine area westwards to 11°30E (fig. 3). Baronie seamount, the largest structural high in the Tyrrhenian Sea, with a length of over 120 km is the morphological link between the northern Tyrrhenian Basin and Range province and the Passive margin province of western Sardinia. Moreover, from a geodynamic point of view, Baronie seamount represents the tectonic boundary between the two provinces, being made up of Alpine units, analogous to those outcropping in eastern Corsica, and Alpine foreland units that make up most of the islands of Corsica-Sardinia (Structural model of Italy, 1991). South of Baronie Seamount, in fact, only the latter units seem to persist, according to rather extensive seafloor sampling.

The initiation of tectonic activity in this sector has been established by the drilling results of ODP Leg 107 (Kastens & Mascle *et alii*, 1990.). A date of mid-upper Miocene (Tortonian ~10myr) is established from hole 654. However, due to the fact that undatable conglomerates make up the base of the sequence, one cannot rule out that the age of inception of the activity could be older.

Thus, the Sardinia slope area morphology records the rifting episode that resulted in the subsequent formation of the ocean crust floored deep Tyrrhenian basin domain. During this latter period, the Sardinia slope area began to represent the passive margin geodynamic province of the basin. Crust thickness is a clear record of this process, thinning from ~30 km beneath Sardinia to less than 10 km in the Vavilov basin (Panza & Suhaldoc, 1989, Scarascia *et alii*, 1994).

The margin consists broadly of 2 distinct physiographic belts parallel to the Sardinia coastline and with increasing water depth. At a regional depth of ~1000-1500 meters, an upper slope belt, about 50 km wide, of sediment-filled, flat lying intraslope basins develops, bounded seawards by a series of structural highs. The basins, generally termed the Sardinia basin (SB) are delimited landwards by the outer continental shelf and slope dissected by numerous canyons (fig. 3). These promote basin filling but also contribute to the development of the larger-

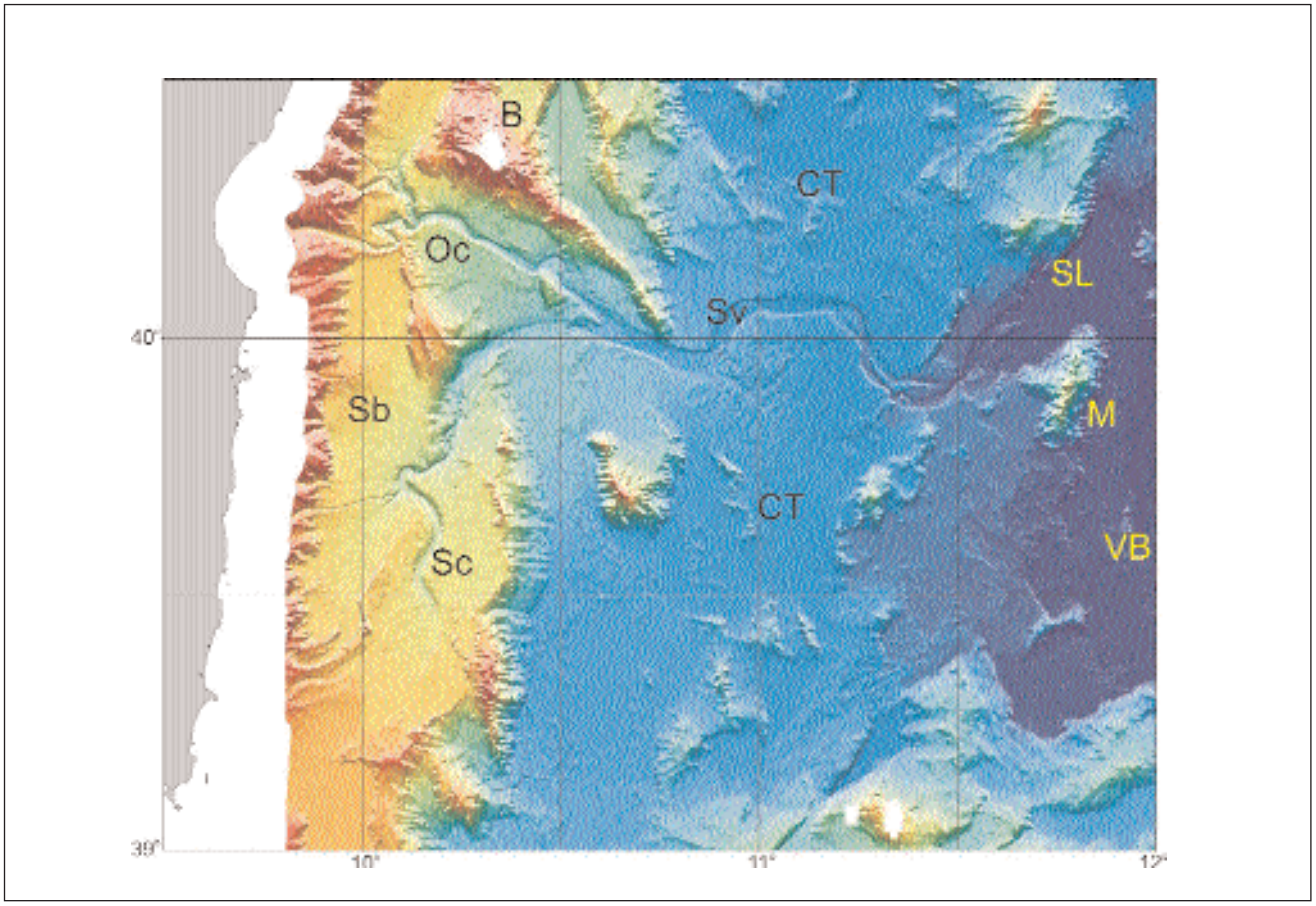

Fig. 3. - *Western Tyrrhenian Province. Colour code and illumination as in figure 1. The region is subdivided into two separate physiographic zones by the outcropping morphological highs: the Sardinia basin (Sb) and the Cornaglia Terrace (CT). The trend of the southern portion of Baronie seamount (B) allows breaching of the Sarrabus (Sc) and Orosei (Oc) canyons seaward where they merge to form the Sardinia Valley (Sv). The western province is delimited eastwards by the Selli Line (SL) which drops down into the deep Vavilov basin (VB). Magnaghi seamount is one of the two volcanoes that characterise the VB. Refer to text for further discussion.*

scale Sarrabus and Orosei canyon systems that merge at a breach in the bounding structural highs, in proximity to the southern Baronie seamount, to continue to the deeper ocean as the Valley of Sardinia (fig. 3).

The Valley of Sardinia extends within the second belt, the Cornaglia Terrace (CT), which is also morphologically well defined. This consists of a relatively flat lying deep-water plain (~2500-2800 meters water depth), extending about 70 km seawards. The plain is bounded eastwards by a NE-SW-trending fault scarp, the Selli Line that separates the Sardinia margin from the Vavilov abyssal plain (fig. 3).

Apart from the Baronie seamount, the structural highs that bound the SB display a subdued topography. Numerous seismic reflection studies in the region show that the structural highs are actually the uplifted footwall leading edges of large tilted blocks, formed by the development of rotational faults generally dipping eastwards, with the half-grabens formed by block tilting now practically filled in by the SB sediments. Similar structures underlie the CT, although the thinner sediment cover does not register block tilting as adequately as in the SB.

3.3. - Active Margin Province: the eastern Tyrrhenian

For the purpose of this paper, the eastern Tyrrhenian margin is defined as the continental slope region between the Pontine Archipelago and the Palinuro seamount. It has variable width, between a minimum of a few kilometers to about 60 km and runs parallel to peninsular Italy, in a NW-SE direction (fig. 4). The southern Apennine chain represents the emergent area to the East of the margin.

Morphologically, the limits of the area are well revealed. To the north, a series of ~25 km long fault scarps that develop in a NE-SW direction west and south of Ponza Island are seen to clearly separate the structural trends of the eastern Tyrrhenian margin from the northern basin portion. The western limits of the area are the flat lying, deep-water, Vavilov and Marsili abyssal plains (fig. 4).

Differently from the passive margin geodynamic province the structures in this region are morphologically distinct, despite the undoubtedly large sediment supply due to the proximity to the Apennine mountain chain, implying a very recent or on-going

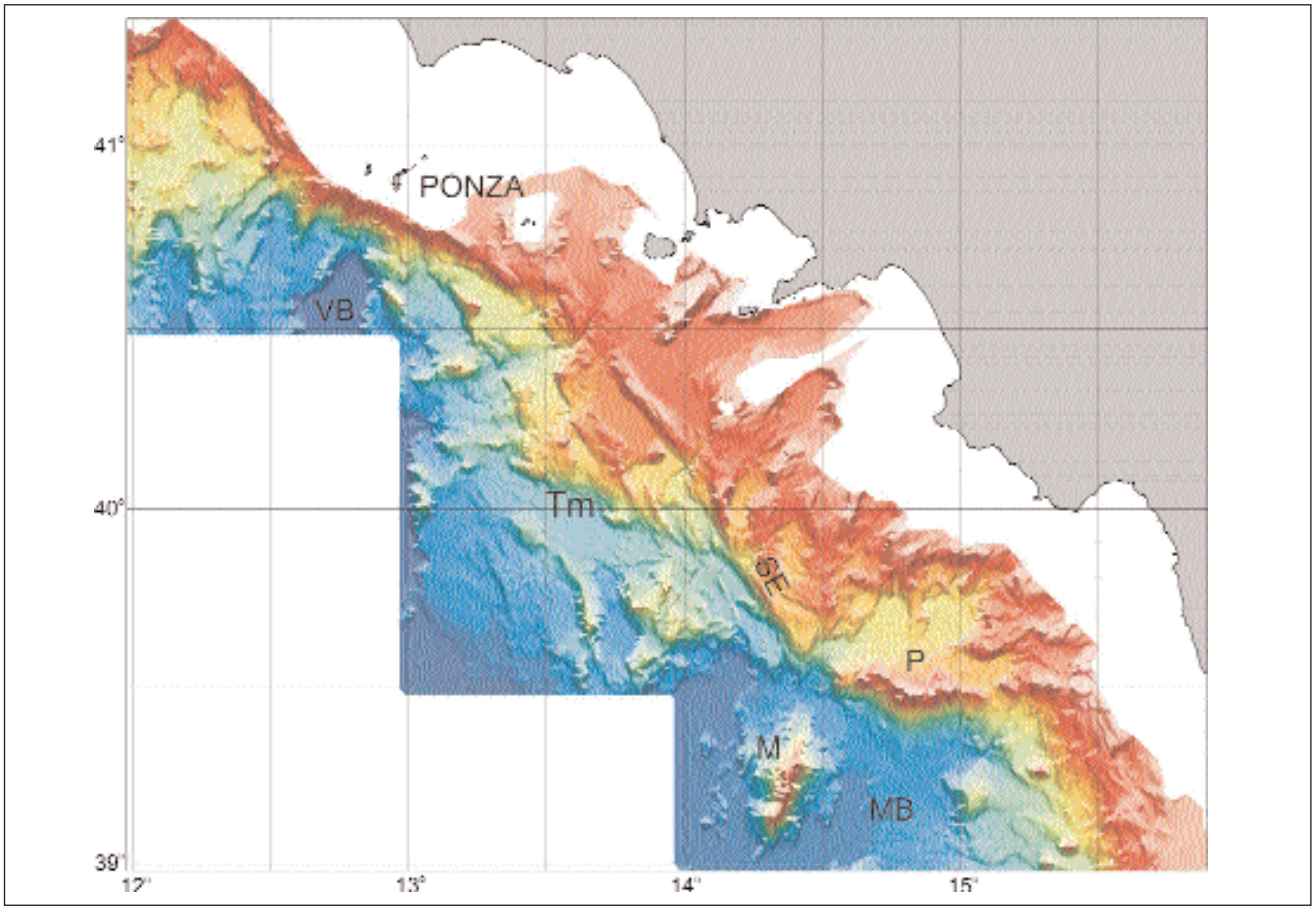

Fig. 4. - *Eastern Tyrrhenian Province. Colour code and illumination as in figure 1. The outstanding feature of the region is the Sartori Escarpment (SE) that separates the structurally diverse upper ("Apenninic" type margin, Am) and lower ("Tyrrhenian" type margin, Tm) slopes of the area. Also visible are the Palinuro volcanic complex (P) forming the southern boundary to the province, the Marsili volcano (M) within the Marsili basin (MB) and the northern extension of the Vavilov basin (VB) offshore Ponza Island. Refer to text for further discussion.*

tectonic activity. On the basis of its morphology, the eastern Tyrrhenian margin can be structurally subdivided into two sectors roughly corresponding to the upper (<2000 m depth) and lower (>2000 m depth) continental slope regions.

Structural partitioning of the margin is brought about by a NNW-SSE trending, 80 km long normal fault system (fig. 4). The system basically consists of a 330° directed, west-dipping master fault with displays increasing throw southwards, from ~400 meters to over 1 km. Adjacent to the southern portion of the master fault, an east-dipping 60 km long conjugate fault develops with a 340° trend and a throw in the order of 300 meters. The resulting graben consequently has southward increasing widths, from ~5 km in the north to ~ 12 km in the south. Between the two faults, three NW-SE faults develop with 200-meter throw, producing three steps, distanced roughly 15 km, within the graben. Based on its overall morphological characteristics, the fault system, named the Sartori Escarpment (SE) (CURZI *et alii*, 2003) has been interpreted to be a left lateral transtensive system (MUSACCHIO *et alii*, 1999). The southern termination of the SE is in proximity of the conjunction between the Palinuro and Marsili volcanic seamounts.

The upper slope region is characterized by numerous relatively short, 100 to 250 meter high fault scarps (fig. 4). Fault orientation falls within the N-S quadrant mostly in the seaward portion of the region while mostly NE-SW trends are present to the East. The scarps extend on average 20 km and dissect the region into several small, N-S/NE-SW trending horsts and grabens, each on average about 8 km wide.

The development of these upper slope structures occurs exclusively to the north of the SE, they are not present to the east of the SE southern termination. Moreover, the southern terminations of the structures are directly juxtaposed to the major SE hanging wall. This seems to indicate that there may well be a structural connection between these two tectonic regimes.

A distinctive morphological characteristic prevails within the lower slope of the Eastern Tyrrhenian margin, west of the SE system. The striking morphological differentiation from the upper slope region is brought about by the development of a number of linear fault scarps that closely follow the trend of the SE. The faults affect the entire lower slope area, up to the limits of the deep-water abyssal plain. Average fault length is in the order of 35 km with down-to-the-West variable throw between 100 and 400 meters. The SE trend is dominant, with virtually the only exception being the N-S fault bounding Flavio Gioia seamount.

The SE in point of fact bounds a lower slope affected by extensional structures directly linked to the generation of the deeper portion of the Tyrrhenian basin, or a "Tyrrhenian-type" lower slope, and an "Apenninic-type" upper slope area that can only be loosely associated to this event. South of Palinuro seamount, a remarkable change occurs in morphology and structure style since it is both the northern limit of the ocean floored Marsili basin and the associated active Aeolian volcanic arc

A deep-seated cause can be advanced to better comprehend these structural differences. Considering that the seismicity related to subduction beneath the southeastern Tyrrhenian Sea is rather well delimited by the entire length of the SE, occurring practically only to the West of it, mantle stress gradients generated by slab rollback and sinking may have propagated to superficial crustal levels to form structural divides, such as the SE, approximately aligned along the deep slab edge (MARANI & TRUA, 2002). In this sense, this region is defined as the active margin geodynamic province, notwithstanding that, since at least mid-Pleistocene, the inner portions of the Apennine fold and thrust belt bordering this sector are affected by normal faulting, the compressional front having migrated to the Adriatic Sea.

3.4. - OCEANIC TERRAIN PROVINCE: CENTRAL/SOUTHERN TYRRHENIAN BACK-ARC AND ARC

The central and south-eastern, deep-water (>3000 m) portions of the Tyrrhenian Sea are floored by oceanic crust produced during two distinct episodes of accretion, first in the central Tyrrhenian Vavilov backarc basin (VB), followed by a shift to the south-east to the Marsili backarc basin (MB). Generation of the VB and MB are dated 4.3-2.6 Myr and <2 Myr respectively. Regional lithosphere models for both basins concur with their oceanic nature giving crustal thicknesses of <10 km and a 30 km LID.

Outstanding morphological features of the otherwise flat lying, turbidite-filled abyssal plains are the large seamounts that occupy the central parts of the VB and MB (figs. 5, 6). The submerged portion the Aeolian Island volcanic arc associated to the development of the MB, moreover, is well developed both to the West and East of the islands.

The deep plains of the Vavilov basin have roughly a triangular shape, delimited to the West by the Selli Line and to the east by the lower slope of the southeastern Tyrrhenian active margin and the MB (fig.5). The vertex of the triangle, the northernmost limit of the VB, occurs only a few km south of Ponza Island, forming one of the highest gradient slopes (from 0 to -3500 m) in the Tyrrhenain Sea. The southern border of the VB occurs in a region of complex, sediment capped topography north of western Sicily.

Several large seamounts, along with seamount chains and linear trending fault scarps complicate the morphology of the VB. Extensive previous (Structural model of Italy, 1991) and recent (GAMBERI *et alii*, in press) seafloor sampling shows that the structural features are related either to basement terrains or to the development of large submarine volcanoes.

Outcropping "Corsica-type" alpine units and Upper Miocene rocks characterise the scarp of the NE-SW Selli Line (SL). It is morphologically distinct for about 80 km and has on average 250/300 m.

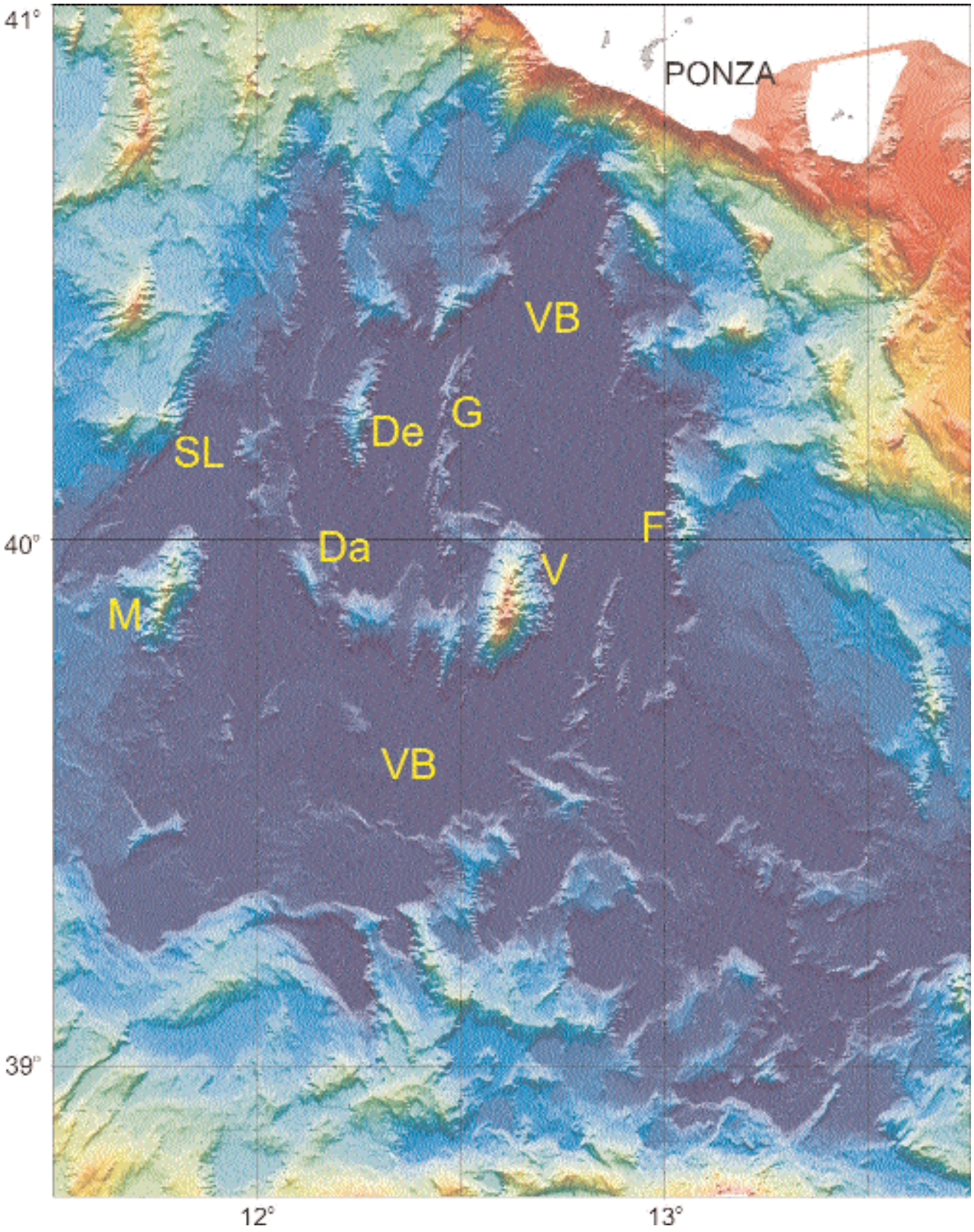

Fig 5. - *Vavilov Basin Province. Colour code and illumination as in figure 1. The deep Vavilov basin (VB) plain is interspersed with diverse morphological elements. These are the Selli Line (SL), fault, the De Marchi (De) and Flavio Gioia (F) tilted blocks, the Gortani (G) and D'Ancona (Da) ridges and the large volcanoes Vavilov (V) and Magnaghi (M). Refer to text for detailed discussion of each feature.*

throw, dropping down to the VB abyssal plain. Fault throw is variably distributed along close spaced splays in some cases connected by relay ramps. The SL is a fault system of significant structural importance, dividing the passive margin province from the Tyrrhenian oceanic domain.

Within the northern part of the VB, two seamounts represent a second and probably definite boundary between the oceanic crust of the basin and the surrounding thinned crustal blocks. These are the western De Marchi and the eastern Flavio Gioa seamounts. They are 80 km apart, both are N-S trending and characterised by a distinct asymmetry, the former presenting a steep eastwards dipping fault scarp and gentler western slope, the latter being a mirror image, with a steep westwards dipping fault scarp and gentler eastern slope. Both have an elevation of 1200 m, rising from the ~3600 m deep VB plain. The seamounts, composed of metamorphic units related to Alpine Corsica in the case of De Marchi and to Calabride units in that of Flavio Gioia, in effect represent the final trace of rotational crustal blocks within the VB.

The Gortani Ridge, a ~40 km linear morphological high with a maximum elevation in the order of 300/400 meters is positioned between the two tilted blocks, about 20 km from De Marchi seamount and 60 km from Flavio Gioia seamount. ODP drill-site 655 showed this feature to be made up of T-MORB basalt flows, considered by KASTENS & MASCLE, 1990 to be the earliest evidence (~4 Myr) for emplacement of oceanic crust in the VB.

The central VB is more intricate from a morphological point of view. The major feature is the axially located Vavilov volcano. It is positioned just south and midways between the De Marchi and Flavio Gioia seamounts. Vavilov volcano is elongated NNE/SSW for 40 km, is on average about 10 km wide and stands 2800 meters above the abyssal plain with summit depth at 730 meters. Its distinctive asymmetry, displayed by a steep, smooth western flank and a gentler eastern flank, where satellite cones develop, presupposes a probable collapse event of the western flank of the volcano. Deep-tow side scan sonar data along the base of the western flank do not definitely clarify this hypothesis since the areal extension of the isolated patches of large blocks that have been found to crop out cannot be verified due to the area being mostly sediment covered (MARANI *et alii*, 2003). However, reflection seismic data along the western base region show a very shallow acoustic basement respect to the eastern base, which could correspond to infilling of rock avalanche deposits.

One other large volcano, Magnaghi seamount dominates the western part of the central VB, in proximity to the SL. It has approximately the same trend of the Vavilov, with a length of ~25 km and a summit height of 1470 meters.

Both Vavilov and Magnaghi volcanoes are made up of tholeitic to alkalic basalts (ROBIN *et alii*, 1987; SAVELLI, 1988) of Late Pliocene age (KASTENS, MASCLE *et alii*, 1990; SAVELLI, 1988). These Authors therefore conclude that the large volcanoes of the VB were formed after the bulk of the low standing basaltic crust of the basin had been generated.

The final morphological feature of the central VB casts some doubt on the actual position of the boundary between continental and oceanic crust in this portion of the basin. The D'Ancona ridge is an arcuate high-standing feature that initiates in the region between the SL and the De Marchi seamount and terminates against the southern tip of the Vavilov volcano. The structure is made up of a series of highs, with elevations reaching even 800 meters but on average with heights between 200 and 400 meters. In proximity to the Vavilov volcano, the D'Ancona ridge is formed by sharply defined N-S striking linear features, similar to the trend of the volcano and to the trend of the linear, subdued ridge to the east of the Vavilov seamount. Recently acquired high resolution air-gun seismic reflection data (MARANI *et alii*, 2003) show that the central portion of the D'Ancona ridge positioned between the Magnaghi and Vavilov seamounts possesses a sedimented (~250 meter thick) cover, faulted basement with a seismic facies more akin to continental basement, very different from the strongly reflective, basaltic crust. Although Vavilov seamount has been recently extensively sampled (GAMBERI *et alii*, in press), no samples were collected from the nearby linear part of the D'Ancona ridge which could, due its morphological character and proximity to the volcano, be of a volcanic nature. However, the continental basement type characters of that portion of the D'Ancona ridge lying between the Magnaghi and Vavilov volcanoes demonstrates that the alleged geodynamic setting of the northern VB does not apply to the central VB. The differentiation could be simply brought about by the presence of isolated rafted blocks of continental crust within the basaltic basement of the central VB, which did not develop in its northern portion. Alternatively, the D'Ancona ridge could play a more important role as a strong demarcation in crustal nature in some way involving the development of the two large volcanoes that characterise this region.

To the southeast, across a region of subdued seafloor topography corresponding to a saddle of ~15 km thick crust (SCARASCIA 1994, PANZA & SUHALDOC, 1989), the Vavilov basin passes to the more recent Marsili basin (fig. 6) where crustal thickness returns to less than 10 km. This small, ~2 Myr-old near-circular backarc basin stands at 3500 meters water depth. Kilometre-scale fault scarps, which develop at the southern part of the basin, delimit the upper slope area in which the Aeolian volcanic arc develops. To the north, the Palinuro volcanic complex bounds the deep basin plain. More subdued topography characterises the eastern boundary of the MB along the course of the Stromboli Canyon as it reaches the abyssal plain. Most of the MB is occupied by the homonymous Marsili volcano, which is practically the only morphological element of relevance. The volcano

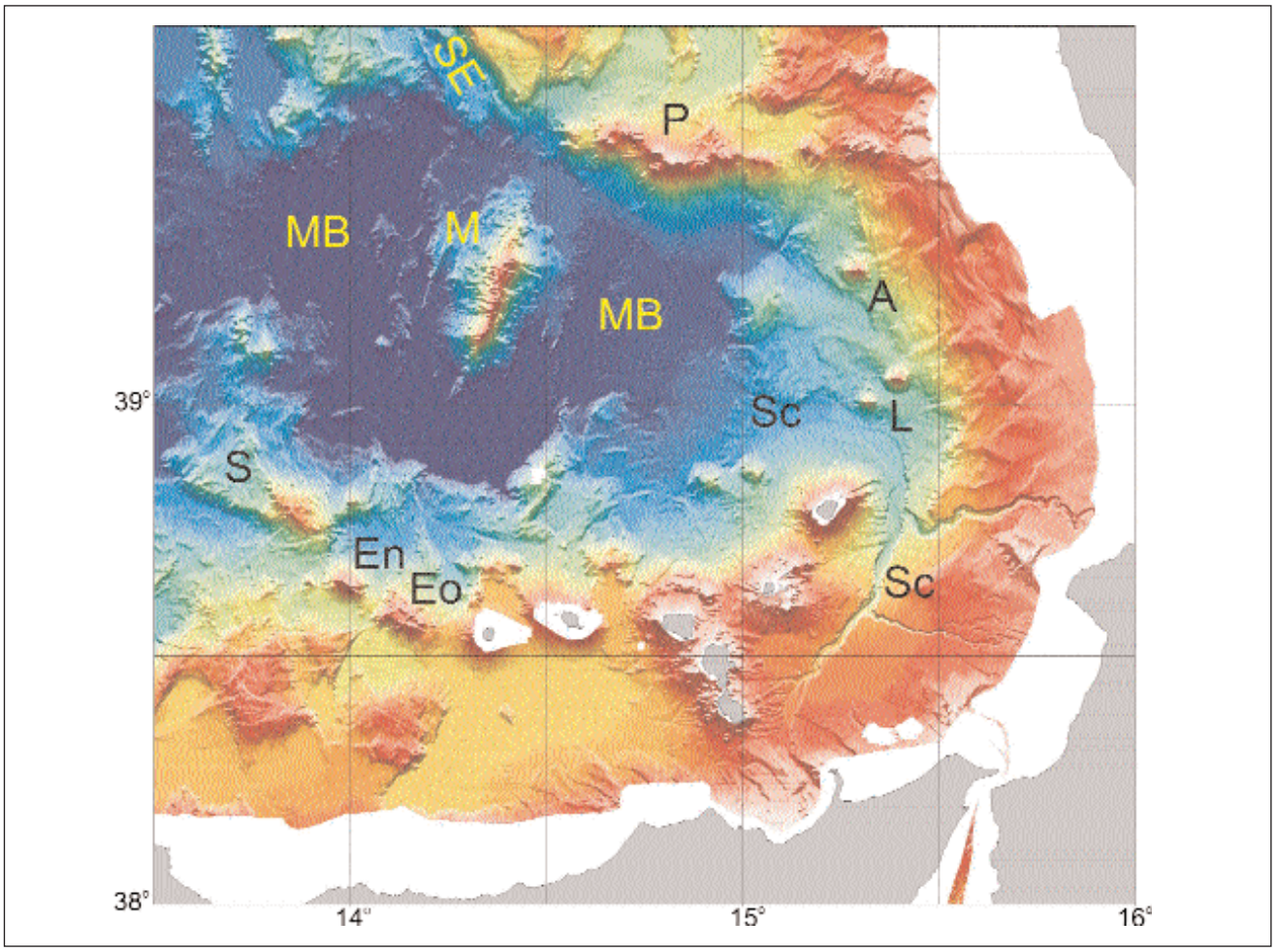

Fig. 6. - *Marsili basin Province. Colour code and illumination as in figure 1. Marsili basin (MB) is the recent-most ocean crust floored basin, characterised by the large, axially located Marsili volcano (M). The deep basin is delimited by the Palinuro volcanic complex (P) and by the Aeolian volcanic arc located on the upper slope which is cut by the Stromboli Canyon (Sc). Submarine extensions to the arc are represented by the Lametini seamounts (L) and Alcione volcano (A) to the east and Eolo (Eo), Enarete (En) volcanoes and the Sisifo volcanic (S) ridge to the west. Refer to text for detailed discussion of each feature.*

rises 3000 metres from the deep plain of Marsili basin to a minimum depth of 489 metres, and is elongated NNE-SSW with a length in the order of 50 km and a mean width of 16 km. It is flanked by a series of linear basin-floor fault scarps that form a symmetrical horst and graben structure at its sides (fig. 6). In its summit region the volcano is characterised by a marked linearity formed by coalesced or single elongated cones. The development of fields of small volcanoes with mostly flat tops, and several with breached craters, characterise its lower flanks.

Sampling data (MARANI *et alii*, 1999; TRUA *et alii*, 2002) show that the volcanoes of the cone fields and the lower flanks of the volcano are composed of calc-alkaline basalts while evolved high-K andesites were recovered only in the summit cones. Moreover, modelling results (TRUA *et alii*, 2002) indicate that the formation of the andesites is compatible with the differentiation of the type of basalts found in the lower reaches of the volcano, indicating a possible upper magma chamber within the volcano. The age of the volcano is estimated at ~0.7 Ma, based on the magnetic anomaly pattern of the edifice (FAGGIONI *et alii*, 1995) which indicates that the bulk of the volcano erupted within the normal polarity geomagnetic chron C1 (Bruhnes). Radiometric dating of rocks collected from near the summit area (SELLI *et alii*, 1977) furnish ages of ~0.1 Ma. The volcano has been interpreted to result from a strong thermal pulse of asthenospheric material produced by a rapid phase of slab rollback during Mid Pleistocene (MARANI & TRUA, 2002).

The islands and submarine volcanoes comprising the active volcanic arc associated to the Marsili backarc basin occupy the upper slope of the southeastern Tyrrhenian Sea. Submarine volcanoes, developed since 0.8 Ma (BECCALUVA *et alii*, 1985), form an extension to the emerged islands both eastwards and westwards. The arc is well delimited to the north by the 50 km E-W development of the ~0.35 Ma old (COLANTONI *et alii*, 1981) Palinuro composite basaltic andesite volcano. The volcano morphology is made up of at least 6 distinct volcanic

cones developed at a base level in the order of 1400 metres in the slope margin between the active margin geodynamic province to the north and the MB oceanic terrain to the south. In fact, the southern flank of the Palinuro volcanic complex drops more than 3 km to the MB abyssal plain (fig. 6).

The complex morphology and the key location of Palinuro volcano, at the boundary between two wholly distinct geodynamic provinces, point to an important role played by this structure during the recent evolution of the southeastern Tyrrhenian Sea. Its structural importance may be followed also through its extension to the emerged areas of the Italian peninsula, where the boundary between the Apennine terrains and the Calabride complex occurs.

South of Palinuro volcano the three submarine volcanoes that form the eastern extension of the Aeolian arc, Alcione volcano and the twin cones of the Lametini seamount are morphologically distinct (fig. 6). The submerged western extension of the arc is formed by the NW-SE alignment of the Eolo and Enarete volcanoes and the Sisifo volcanic ridge.

4. - QUATERNARY MANTLE DYNAMICS IN THE SOUTHEASTERN TYRRHENIAN SEA

The preceding account has attempted to show the geological development of the Tyrrhenian Sea by way of the present-day seafloor morphology. It is evident that seafloor makeup furnishes more immediate information the more recent are the geological events that contribute to its creation. The Marsili basin is thus the region of the Tyrrhneian Sea where a possible link between seafloor morphology and deep structure can be established. In fact this recent backarc basin is underlain by a steeply dipping subducting slab of Mesozoic oceanic crust and contains or is surrounded by some of the major shallow seated structures described in this paper. If one extends a view to the surrounding southern Apennine chain and Calabrian arc, the geological overall picture becomes of geodynamic importance.

Recently, various authors have put forward models relating deep mantle dynamics induced by rollback of the Ionian slab to the coupled effects observable at the seafloor. Gvirtzman & Nur, 1999, based on crustal modeling studies, link the formation of Etna volcano to sideways asthenospheric flow induced by slab decoupling beneath Calabria, giving also rise to the uplift of Calabria itself. Based on the morphology of the southern Tyrrhenian seafloor, its structural makeup and with the support of petrographical studies of recently sampled rocks (Trua *et alii*, in press), Marani & Trua, 2002 suggest that dip-directed tears at the sides of the slab induce the rise of deep asthenospheric material to the Marsili basin area and surroundings, and recognise the surface traces of the tears.

This paper has endeavoured to show that seafloor morphology can serve a variety of functions in regions of recent formation. Particularly in cases where detailed topographic data may indirectly reveal the surficial effects of deep-seated processes, the same information becomes the baseline data for subsequent research, for instance seafloor sampling and petrological studies or geophysical surveys that can be undertaken to substantiate the surface observations.

REFERENCES

Argnani A. & Savelli C. (1999) - *Cenozoic volcanism and tectonics in the southern Tyrrhenian Sea: space-time distribution and geodynamic significance*. Geodynamics, **27**: 409-432.

Argus D.F., Gordon R.G., De Mets C., Stein S. (1989) - *Closure of the Africa-Eurasia-North America plate motion circuit and tectonics of the Gloria Fault*. J. Geophys. Res., **94** : 5,585-5,602.

Bartole R. (1995) - *The north Tyrrhenian-Northern Apennines post-collisional system: constrain for a geodynamic model*. Terra Nova, 7-30.

Beccaluva L., Brotzu P., Macciota G., Morbidelli L., Serri G., Traversa G. (1989) - *Cainozoic tectono-magmatic evolution and inferred mantle sources in the Sardo-Tyrrhenian area*. In: Boriani A., Bonafede M., Piccardo G.B., Vai G.B. (Eds.): "*The lithosphere in Italy*". Accad. Naz. Lincei, Rome, 229-248.

Beccaluva L., Coltorti M., Galassi B., Maciotta G., Siena F. (1994) - *The Cainozoic calcalkaline magmatism of the western Mediterranean and its geodynamic significance*. Boll. Geof. Teor. App., **XXXVI**, 141-144, 293-308.

Beccaluva L., Gabbianelli G., Lucchini F., Rossi P.L., Savelli C. (1985) - *Petrology and K/Ar ages of volcanics dredged from the Eolian seamounts: implications for geodynamic evolution of the southern Tyrrhenian basin*. Earth Planet. Sci. Lett., **74**: 187-208.

Carmignani L., Decandia F.A., Disperati L., Fantozzi P.L., Lazzarotto A., Liotta D., Oggiano G. (1995) - *Relationships between the Tertiary structural evolution of the Sardinia-Corsica-Provençal domain and the northern Apennines*. Terra Nova, **7**: 128-137.

Carmignani L. & Kligfield R. (1990) - *Crustal extension in the northern Apennines: the transition from compression to extension in the Alpi Apuane complex*. Tectonics, **9**: 1275-1305.

Colantoni P., Lucchini F., Rossi P.L., Sartori R. & Savelli C. (1981) - *The Palinuro Volcano and magmatism of the south-eastern Tyrrhenian Sea (Mediterranean)*. Marine Geology **39**: M1-M12.

Curzi P.V., Castellarin A., Vai G.B., Zitellini N., Selli R. & Sartori R. (2003) - *Una staffetta generazionale della Geologia Marina Italiana*. In: Extended Abstracts, Convegno in Memoria di Raimaondo Selli e Renzo Sartori, La Geologia del Mar Tirreno e degli Appennini, Bologna, 11-12 Dec.

De Mets C., Gordon R.G., Argus D.F., Stein S. (1990) - *Current plate motions*. Geophys. J. Int., **101**: 425-478.

Dewey J.F., Helman M.L., Turco E., Hutton D.H.W., Knott S.D. (1989) - *Kinematics of the western Mediterranean*. In: Coward M.P. & Dietrich D. (Eds.): "*Alpine Tectonics*". Geol. Soc. Spec. Pubbl., **45**: 265-283.

Faggioni O., Pinna E., Savelli C., Schreider A.A. (1995) - *Geomagnetism and age study of Tyrrhenian seamounts,* Geophys. J. Int., **123**: 915-930.

Finetti I.R., Boccaletti M., Bonini M., Del Ben A.,

GELETTI R., PIPAN M., SANI F. (2001) - *Crustal section based on CROP seismic data accross the North Tyrrhenian-Northern Apennines-Adriatic Sea*. Tectonophysics, **343**: 135-163.

GAMBERI F., MARANI M., LANDUZZI W., MAGAGNOLI A., PENITENTI D., ROSI M., PERTAGNINI P., DI ROBERTO A. (in press) - *Sedimentologic and volcanologic investigations in the deep Tyrrhenian Sea*. Ann. Geoph.

GVIRTZMAN Z. & NUR A. (1999) - *The formation of Mount Etna as the consequence of slab rollback*. Nature, **401**: 782-785.

JOLIVET L. (1991) - *Extension of thickened continental crust, from brittle to ductile deformation: examples from Alpine Corsica and Aegean Sea*. Ann. Geofis., **36**: 139-153.

KASTENS K.A. *et alii* (1988) - *ODP Leg 107 in the Tyrrhenian Sea: insight into passive margin and backarc basin evolution*. Geol. Soc of America Bull., **100**: 1,140-1,156.

KASTENS K.A. & MASCLE J. *et alii* (1990) - *The geological evolution of the Tyrrhenian Sea: an introduction to the scientific results of ODP Leg 107*. In: KASTENS K.A., MASCLE J. *et alii* (Eds.): "*Proceedings of the ODP*". Scientific Results, **107**: 3-26.

LISTER G.S. & DAVIS G. A. (1989) - *The origin of metamorphic core complexes and detachment faults formed during Tertiary continental extension in the northern Colorado River region, U.S.A.* Journ. Struct. Geol., **1/2**, 65-94.

MALINVERNO A. & RYAN W.B.F. (1986) - *Extension in the Tyrrhenian Sea and shortening in the Apennines as result of arc migration driven by slab sinking in the lithosphere*. Tectonics, **5**: 227-245.

MARANI M.P., GAMBERI F., IVANOV M. AND SHIP-BOARD PARTY (2003) - *Introduction and main objectives of TTR-12 Leg IV - Tyrrhenian Sea.*, IOC, Technical Series, **67**, 72-90

MARANI M.P., GAMBERI F., CASONI L., CARRARA G., LANDUZZI V., MUSACCHIO M., PENITENTI D., ROSSI L., TRUA T. (1999) - *New rock and hydrothermal samples from the southern Tyrrhenian sea: the MAR-98 research cruise*. Giorn. Di Geologia, **61**: 3-24.

MARANI M.P. & T. TRUA (2002) - *Thermal constriction and slab tearing at the origin of a superinflated spreading ridge: Marsili volcano (Tyrrhenian Sea)*. Journal of Geophysical Research, **107**(B9): 2188, doi:10,1029/2001JB000285.

MARANI M., ZITELLINI N. (1986) - *Rift structures and wrench tectonics along the continental slope between Civitavecchia and C. Circeo*. Mem. Soc. Geol. Ital., **35**: 453-457.

MARANI M.P., GAMBERI F., IVANOV M. AND SHIPBOARD SCIENTIFIC PARTY OF TTR-12 (2003) - *Tyrrhenian Sea (Leg 4), Interdisciplinart Geoscience Research on the NorthEast Atlantic Margin, Mediterranean Sea and Mid-Atlantic Ridge*, I.O.C. Technical Series, UNESCO.

MUSACCHIO M., CARRARRA G., GAMBERI F., MARANI M. (1999) - *Tectonic setting of the eastern Tyrrhenian margin*. Geoitalia, 2° Forum FIST, Riassunti, **1**: 184-185.

PASCUCCI V., MERLINI S., MARTINI I.P. (1999) - *Seismic stratigraphy of the Miocene-Pleistocene sedimentary basins of the Northern Tyrrhenian Sea and western Tuscany (Italy)*. Basin Res., **11**: 337-356.

ROBIN C., COLANTONI P., GENNESSEAUX M., REHAULT J.P. (1987) - *Vavilov seamount: a mildly alkaline Quaternary volcano in the Tyrrhenian basin*. Mar. Geol., **78**: 122-136.

SARTORI R & ODP LEG 107 SCIENTIFIC STAFF, DRILLINGS OF ODP LEG 107 IN THE TYRRHENIAN SEA (1989) - *Tentative basin evolution compared to deformations in the surrounding chains*. In: BORIANI A., BONAFEDE M., PICCARDO G.B., VAI G.B. (Eds.): "*The lithosphere in Italy*". Accad. Naz. Lincei, Rome, 139-156.

SARTORI R. (1990) - *The main results of ODP Leg 107 in the frame of Neogene to Recent geology of peri-Tyrrhenian areas*. In: KASTENS K.A., MASCLE J. *et alii* (Eds.): "*Proceedings of the ODP*". Scientific Results, **107**: 715-730.

SAVELLI C. (1988) - *Late Oligocene to recent episodes of magmatism in and around the Tyrrhenian Sea: implications for the processes of opening in a ypung inter-arc basin of intra-orogenic (Mediterranean) type*. Tectonophysics, **146**: 163-181.

SCARASCIA S., LOZEJ A., CASSINIS R. (1994) - *Crustal structures of the Ligurian, Tyrrhenian and Ionian Seas and adjacent onshore areas interpreted from wide-angle seismic profiles*. Boll. Geof. Teor. Appl., **36**: n. 141-144, 4-19.

SELLI R., LUCCHINI F., ROSSI P.L., SAVELLI C., DEL MONTE M. (1977) - *Dati geologici, petrochimici e radiometrici sui vulcani centro-tirrenici*. Gionale di Geologia, XLII, 221-246.

SERRI G. (1997) - *Neogene-Quaternary magmatic activity and its geodynamic implications in the central Mediterranean region*. Ann. Geophys., **40** (3): 681-703.

SERRI G., INNOCENTI F., MANETTI P. (1993) - *Geochemical and petrological evidence of the subduction of delaminated Adriatic continental lithosphere in the genesis of the Neogene-Quaternary magmatism of central Italy*. Tectonophysics, **223**: 117-147.

SUHALDOC P. & PANZA G.F 1989 ( ) - *Physical properties of the Lithosphere-Asthenosphere system in Europe from geophysical data*. In: BORIANI A., BONAFEDE M., PICCARDO G.B., VAI G.B. (Eds.): "*The lithosphere in Italy*". Accad. Naz. Lincei, Rome, 15-40.

SURPLESSB.E., STOCKLI D.K., DUMITRU T.A., MILLER E.L. (2002) - *Two-phase westward encroachment of Basin and Range extension into the northern Sierra Nevada*. Tectonics, **21**: 1, 10.1029/2000TC001257, 2002.

TRUA T., SERRI G., MARANI M. ( ) - *Lateral flow of African mantle below the nearby Tyrrhenian plate: geochemical and isotopic evidence*. Terra Nova, in press.

TRUA T., SERRI G., RENZULLI A., MARANI M., GAMBERI F. (2002) - *Volcanological and petrological evolution of Marsili seamount (southern Tyrrhenian Sea)*. J. Volcanol. Geotherm. Res., **114**: 441-464.

WERNICKE B. (1981) - *Low-angle normal faults in the Basin and Range province: nappe tectonics in an extending orogen*. Nature, **291**: 645-648.

WARD, S.N. (1994) - *Constraints on the seismotectonics of the central Mediterranean from Very Long Baseline Interferometry*. Geophys. J. Int., **117**: 441-452.

WESTAWAY, R. (1993) - *Quaternary uplift of southern Italy*, J. Geophys. Res., **98** : 21,741-21,772.

WILSON M. (1989) - Igneous Petrogenesis (Harper Collins Academic, London), pp. 466.

ZITELLINI N., TRINCARDI F., MARANI M., FABBRI A., (1986) - *Neogene tectonics of the northern Tyrrhenian Sea*. Giorn. Geol., **48**: 1/2, 25-40.

Mem. Descr. Carta Geol. d'It.
XLIV (2004), pp.109-126
15 figg.

Distribution and nature of submarine volcanic landforms in the Tyrrhenian Sea: the arc vs the backarc

Distribuzione e natura della morfologia del vulcanismo sottomarino nel Mar Tirreno: l'arco e retro-arco

MARANI M.P. (*), GAMBERI F. (*)

ABSTRACT - Based on morphological characters, different varieties of submarine volcanic landforms typify the arc and back-arc portions of the Tyrrhenian Sea. The arc volcanoes. develop both to the northeast and west of the emergent Aeolian Islands are isolated, more or less longlived vent centres as shown by the geochemical variety of collected rock types. Primarily cone shaped, several of the volcanoes display morphologies related to incipient flank instability. Stronger, more developed instability is found in the easternmost volcano of the Palinuro volcanic complex.
In contrast, the back-arc basins of the Tyrrhenian are characterised by the development of large volcanic complexes that occupy their axial parts. The flanks of the volcanoes display a variety of volcanic constructs including flat topped and conical seamounts, volcanic terraces and, less commonly cratered edifices.
It is shown that the morphologies of the volcanoes can offer clues to their origin and subsequent development.

KEY WORDS: seafloor morphology, submarine volcanoes, arc and backarc edifices, Tyrrhenian Sea

RIASSUNTO - Dal punto di vista morfologico, esiste una netta diversità di forma fra i vulcani sottomarini di arco e quelli di retroarco nel Mar Tirreno. I vulcani sommersi che si sviluppano sia a nord-est sia ad ovest delle isole dell'arco Eoliano sono centri di alimentazione isolata, come evidenziato dalle differenze geochimiche delle rocce costituenti e hanno principalmente forma conica. Alcuni dei vulcani di arco mostrano morfologie riconducibili ad incipienti eventi di instabilità. Questi eventi sono invece in fase matura nell'edificio all'estremità orientale del complesso vulcanico di Palinuro.
I bacini di retroarco del Tirreno sono caratterizzati dallo sviluppo di grandi complessi vulcanici posizionati nelle loro porzioni assiali. I fianchi di questi vulcani presentano una varietà di morfologie vulcaniche, fra i quali edifici a sommità piatta, edifici conici, terrazzi di lava ed alcuni vulcani con crateri.
Sulle basi della sola morfologia, si dimostra comunque che possono essere avanzate alcune ipotesi circa l'origine dei vulcani sottomarini ed il loro successivo sviluppo.

PAROLE CHIAVE: morfologia dei fondali, edifici vulcanici sottomarini, arco e retro-arco, Mar Tirreno

1. - INTRODUCTION

Submarine volcanic landforms have been shown to result, in part, from processes similar to those commonly observed in terrestrial volcanic settings. All land-based lava flow morphologies have been recognized in the marine environment, while the products of the range of explosive eruption styles have been documented; even from the deep ocean at >3000 metres water depth (HEAD & WILSON, 2003).

However, submarine conditions dictate the development of unique lava flow morphologies and landforms that are absent from terrestrial counterparts. Higher lava viscosity or lower extrusion rates at the seafloor give rise to the ubiquitous pillow or tube lavas that form small edifices and ridges, observed in all submarine geological settings, and also in the fossil

(*) ISMAR - CNR, Sezione di Geologia Marina, Via Gobetti 101, 40129 Bologna.

record (GREGG & FINK, 1995). Landforms typical only to the submarine environment are low aspect ratio flat top volcanic seamounts, the origin and modes of formation of which are much less understood. In part explained by the faster cooling rates, varying eruption styles and greater pressure ranges of the marine ambient (CLAGUE *et alii*, 2000; BRIDGES, 1997), much data is lacking in terms of the controlling parameters due to the impossibility of directly observing their formation.

Volcanism at subducting plate boundaries represents about 25% of the Earth's magma production (SIGURDSSON, 2000), mainly developed within the volcanic arc environment. Convergent settings characterised by the subduction of ancient, dense oceanic lithosphere result in an extensional volcanic island arc due to the rollback of the oceanic slab and, ultimately, to the generation of further magmatism and new lithosphere in back arc basin (BAB) spreading environments. Thus, subduction zones are characterised by the development of large volcanic edifices both in island arc and backarc basin environments hosting 80% of the currently active volcanoes of the planet (CHESTER, 1993). Much of the volcanism occurs in the submarine environment.

This has been shown to be true by the increasing coverage worldwide of high resolution swath bathymetry targeting the development of submarine volcanism and associated processes. Recent examples include innovative studies of the morphology of submerged volcanoes carried out in the Mariana arc (BLOOMER *et alii*, 1989) and in the submerged sectors of Hawaii (PARFITT *et alii*, 2002; GREGG & SMITH, 2003). The use of swath bathymetric mapping as a remote sensing tool, augmented by steadily increasing ground truthing by means of sampling and direct observations, has profoundly increased our knowledge about the unique characters of submarine volcanism, concerning both edifice morphology and the structural instability of volcanic constructs inherent to the underwater environment.

A similar mapping effort has been undertaken in the Tyrrhenian Sea, a young backarc basin characterised by active arc volcanoes, where the primary morphologies of submarine arc and backarc volcanoes are preserved, and can thus contribute to the understanding of submarine volcanic processes.

2. – SETTING

The Tyrrhenian Sea, bordered to the east and south by the Apenninic-Maghrebides mountain belt and to the west by the passive Sardinian margin, formed as a consequence of rifting and backarc extension of the Alpine/Apennine suture above the north-westerly-subducting Ionian oceanic slab, (KASTENS *et alii*, 1988; KASTENS *et alii*, 1990; SARTORI, 1990; JOLIVET, 1991). An eastwards migration of crustal thinning and oceanic accretion affected the Tyrrhenian area since lower-mid Miocene (~15 Myr). E-W directed rifting in the northern Tyrrhenian and along the western margin of Sardinia (ZITELLINI *et alii*, 1986; KASTENS *et alii*, 1990) marks the initial opening of the Tyrrhenian basin leading to the formation of oceanic domains and associated volcanism in the Southern Tyrrhenian. First, production of oceanic crust occurred westward, during the Pliocene spreading of the Vavilov basin (4.3-2.6 Myr), where the large centrally located Vavilov volcano developed (KASTENS *et alii*, 1990). A subsequent change to ESE-directed extensional stress in Late Pliocene-Quaternary resulted in the emplacement of basaltic crust southeastwards, generating the Marsili backarc basin (2 Myr) also containing a large axial volcano, Marsili seamount, (KASTENS *et alii*, 1990).

To account for the eastwards migration of backarc basin development and active volcanism is the passive rollback of the Ionian plate (MALINVERNO & RYAN, 1986; SAVELLI, 1988). In step with backarc basin development, the subduction-related island arc volcanism of the southern Tyrrhenian basin migrated from west to south-east, from Sardinia (32-13 Ma) to the currently active Aeolian island arc (SERRI 1997 and references therein), developing the present-day arc-backarc configuration of the southern Tyrrhenian region (fig. 1).

The Aeolian arc consists of seven islands and a number of submarine volcanoes west and northeast of the emerged arc. The Aeolian arc, together with the Agean arc, represent the only still active island arcs of the Mediterranean. Available chronological data (BECCALUVA *et alii*, 1985) show that the beginning of activity took place in the Quaternary (~1-1.3 Ma) at Sisifo seamount and Filicudi. From ~0.8 Ma to the Present, dominantly shoshonitic and calcalkaline lavas, mainly consisting of basalts and basaltic andesites to rhyolites, were erupted in the different submarine and emerged edifices.

The northeastern submerged portion of the arc, positioned on the Calabrian margin, consists of isolated cones and the large, Palinuro volcanic complex. To the west of the emergent islands a number of submerged arc volcanoes are located on the Sicilian margin. The following discussion will describe the morphology of the submarine arc volcanoes and provide a provisional analysis of their origin. Subsequently, the large, axially located backarc volcanoes, Marsili and Vavilov, will be illustrated in the same manner.

3. - THE SUBMERGED AEOLIAN ARC

3.1. - NORTHEASTERN ARC VOLCANOES

Three volcanoes, Alcione and the twin cones of the Lametini seamounts (fig. 2), lie in the Calabrian slope delimited by the Palinuro volcanic complex to the north and Stromboli Island to the south. The volcanoes develop in the westerly deepening lower slope at a depth in the order of 2000 m. At this depth, the slope gradient decreases to form a relatively lower

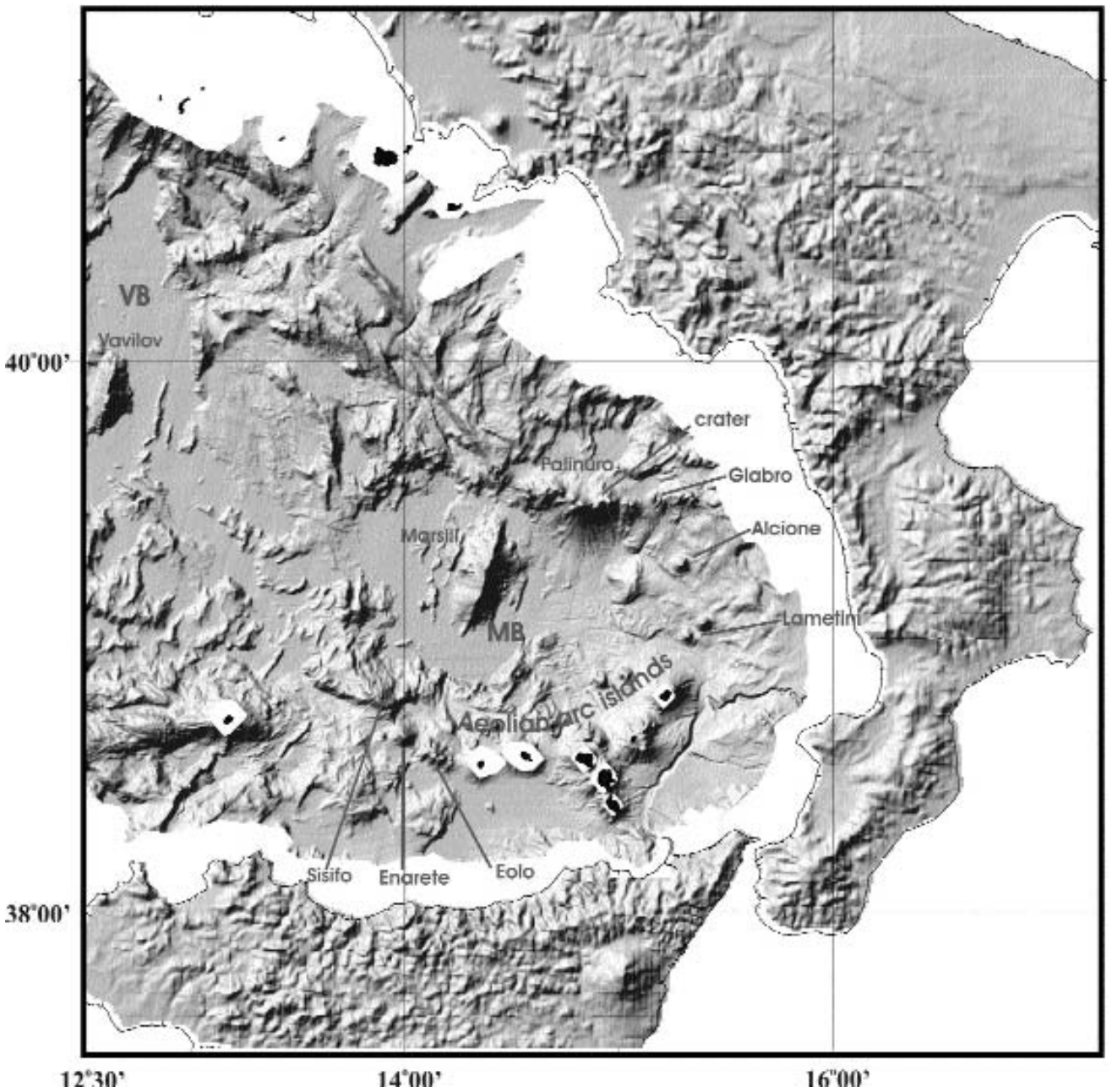

Fig. 1. - *Shaded relief bathymetry (illum. from NW) of the central-southern Tyrrhenian Sea with features discussed in the text. MB and VB, Marsili Basin and Vavilov Basin respectively.*

gradient bench (LAMETINI-ALCIONE flat, GAMBERI & MARANI, this volume) on which the volcanoes arise.

3.1.1 - *Alcione.*

Dredge hauls indicate a calc-alkaline basaltic composition for the seamount (BECCALUVA *et alii*, 1985). Measurement of the height of the volcano is dependant on the sloping bench on which it is situated. Summit heights vary from 900 m to 1200 m for the eastern summit and from 825 m to 1125 m for the western one determined on whether the heights are taken from the eastern base of the volcano or from the deeper western base of the volcano respectively (tab. 1). This ~1000 m high volcano is a textbook example of primary edifice gravitational instability. It's general conical shape is dissected by NNW-SSE trending, 100 m relief arcuate scarp (fig.3) that displaces downwards the western (seaward) half of the edifice. The top of the volcano is characterised by two summit areas, separated by the scarp: an eastern one, directly flanked by the scarp, elongated along the scarp trend and a western conical summit,

Tab. 1 - *Summary table of the dimensions of the submarine Aeolian arc volcanoes. h1 and h2 refer to volcano heights taken respectively from the upper slope and lower slope directions when the edifices bases are located on sloping seafloor; for the Palinuro crater these refer to maximum and minimum crater wall heights. d1 refers to water depths of volcano summits (in the case of Alcione, d2 refers to the water depth of the second summit). Volumes have been estimated by averaging summit heights when two summits are present. Note the comparatively large volumes of Eolo and Enarete.*

	Morphology	h_1 m.	h_2 m.	d_1 m.	d_2 m.	D_{iam} km.	A_{base} km²	V km³
Alcione	conical	1125/1200	825/900	850	925	6.3	33	11
Lametini N	conical	1300	900	900		6.0	24.5	10
Lametini S	conical	850	650	1450		4.2	14	3.5
PVC Hshoe	cratered	290	180	500		2.7		~0.58
Glabro W	split cone	670		830		4		2.85
Glabro E	irregular	450		870				~1.2
Eolo	flat summit	900		775		8 x 10	80	~40
Enarete	conical	1700		300		9.8	75	42

located 500 m from the scarp and 75 m deeper than the former.

The distinguishing morphological features of Alcione are to some extent similar to analogue models involving basement fault activation beneath a volcanic edifice (VIDAL & MERLE, 2000) or differential flank creep and spreading (WALTER & TROLL, 2003) although not all the morphological elements seen in the model runs are present on the volcano.

3.1.2 - *Local structure of Alcione region.*

A summary analysis of the basement structure around the volcano furnishes an indication to verify which, if any, of the above-mentioned modelled processes are active on Alcione. Surrounding seafloor morphology shows two steep, N-S trending, 400m high fault scarps located north and east of Alcione and a NW-SE scarp west of its base. The northern scarp intersects the northern flank of the volcano, the eastern one makes up the slope buttress to the eastern flank of the edifice and is sidestepped to the right by ~4 km. The scarp to the west delimits the flat area on which the volcano develops. If the scarps are the surface expression of a fault system, the volcano could be located in the relay ramp area linking the two N-S faults. E-W seismic profiles crossing the edifice show seismic basement dropping ~600 m, from 2400 m depth East of the volcano to 3000 m depth west of it and sediment fill increasing from ~400 m to ~700 m across the drop. The seismic signal beneath the volcano is obscured but it is reasonable to assume the existence of a fault system in this position. It is however significant to note that the analysis of seismic profiles in the Alcione region illustrate that faults do not affect the sedimentary cover, indicating that tectonic activity probably ceased in the past. Thus, the direct influence of an active fault on the volcano structure can be realistically ruled out. Moreover, analogue modelling results demonstrate that volcano deformation due to basement fault activation provides an accurate estimate of fault trend, in the case of Alcione this should be NNE-SSW and no structures with this trend are observed to directly affect the volcano. Flank creep due to differential spreading of the western portion of Alcione is, on the other hand a possible mechanism considering the E-W asymmetry of the volcano base, the basement drop beneath it and the thicker sediment pile to its west. Spreading or creep should be towards WSW, perpendicular to the edifice-cutting scarp with a deep-seated decollement plane probably located within the weaker sedimentary material.

3.1.3 - *Lametini seamounts*

The two conical edifices of the Lametini seamounts are located 20 km due south of Alcione on the same gently sloping bench area (fig. 4). They are aligned in a NE-SW direction 3 km apart. The NE volcano (LamN) is larger than the SW one (LamS). Dredge samples from LamN (BECCALUVA *et alii*, 1985) recovered basalts. Both volcanoes display E-W asymmetry due to the sloping bench, LamN having heights between 1300 m and 900 m and LamS between 850 m and 650 m measured along the western and eastern flanks respectively (tab. 1). Apart from its size, a distinctive characteristic of LamN, is a prominent slide scar on its western flank (fig. 5). It initiates as a 600 wide scar at the summit and broadens to 1500 m at the base of the edifice. Scarp walls are in the order of 100/150 metres high at the top, diminishing downwards. Interestingly, a feature with positive relief, within the lower part of the scar, from 1600 m depth to the base of the cone at 2100 m, possibly represents the proximal portion of the slide material still lying on the volcano flanks. There is no indication, however, of slide deposits on the adjacent seafloor, at the base of the volcano.

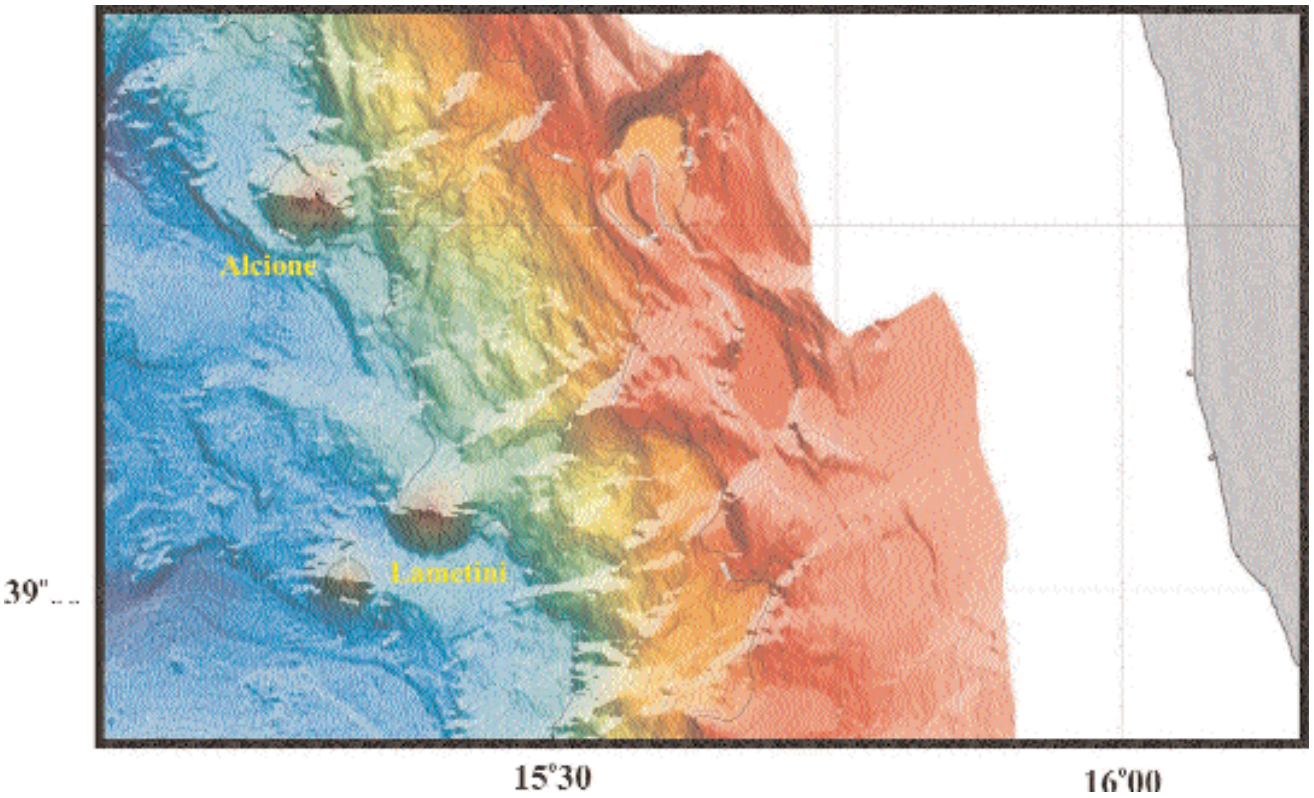

Fig. 2. - *Colour-coded relief bathymetry (illum from N) of the Calabrian slope and location of the submerged eastern Aeolian arc volcanoes. Note the position of Alcione and the Lametini volcanoes on the slope bench. Contour interval 50 m.*

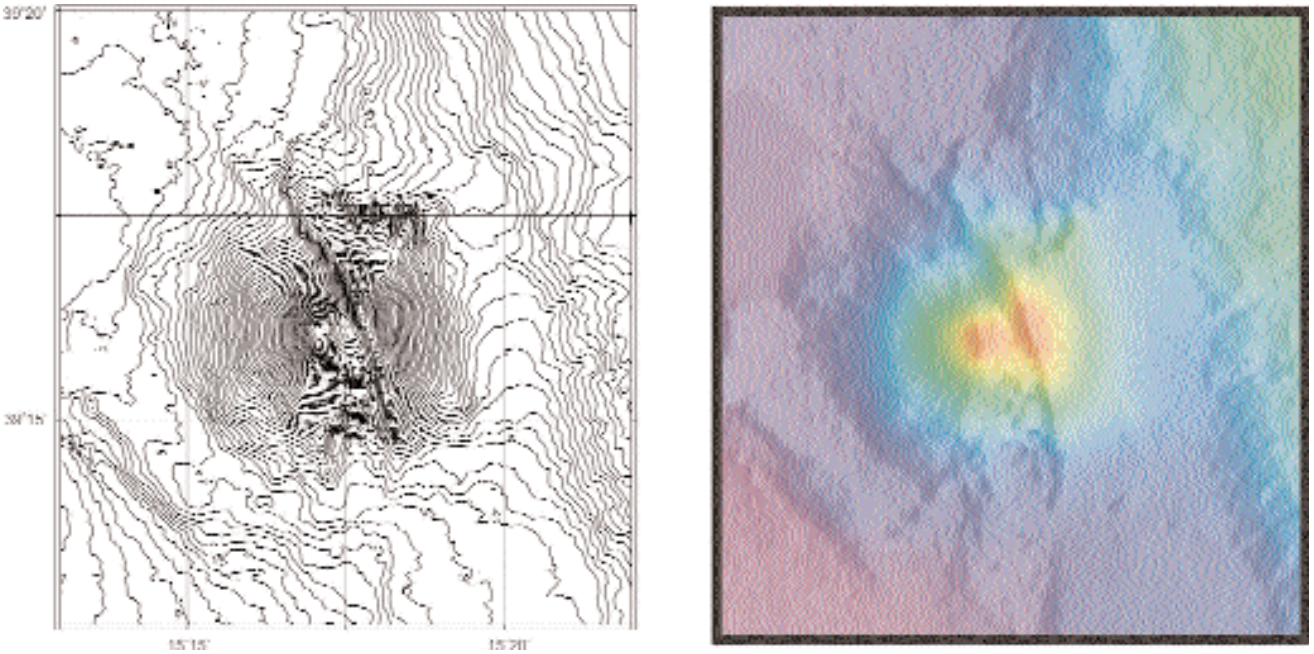

Fig. 3. - *Alcione volcano. Left: bathymetry, contour interval 25m; Right: colour-coded relief (illum from E). Note the scarp cutting across the edifice. Contour interval 25 m. For discussion refer to text.*

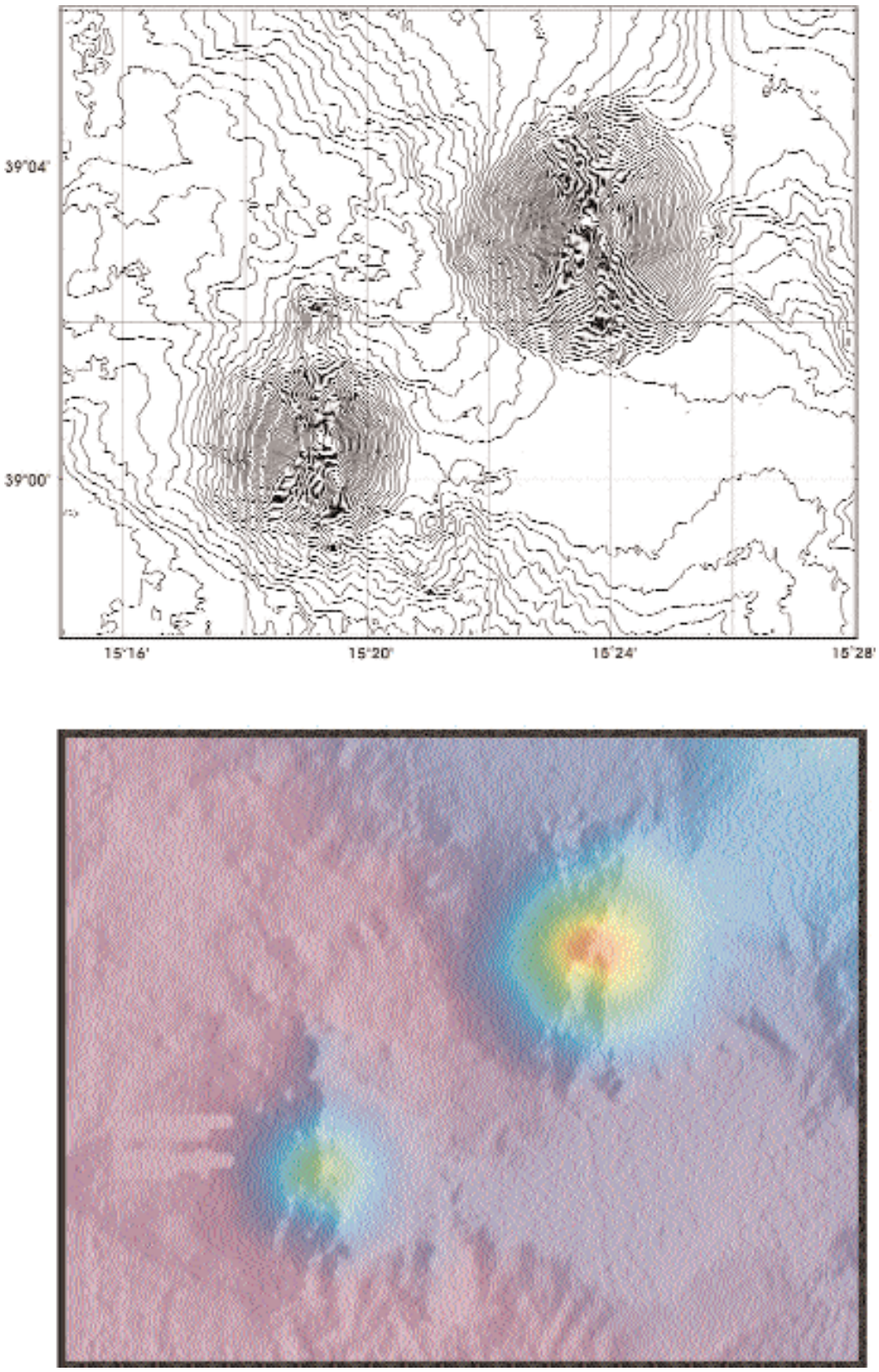

Fig. 4. - *Lametini Seamounts. . Top: bathymetry, contour interval 25m; Bottom: colour-coded relief (illum from* E*). Refer to figure 5 for details of the larger cone. See text for discussion.*

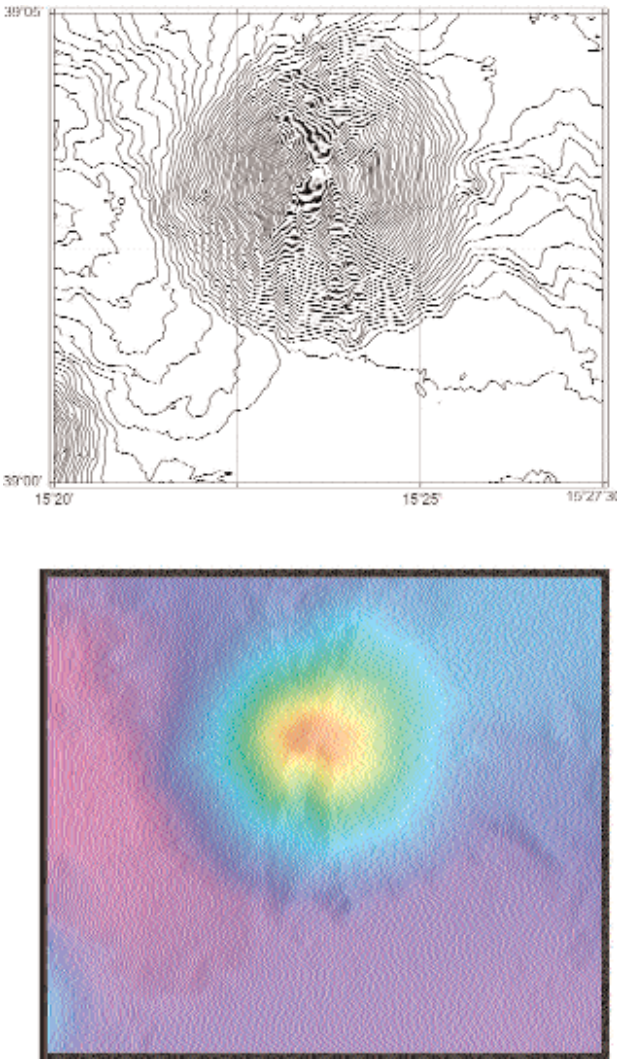

Fig. 5. - *Largest Lametini cone (LamN in text). Top: bathymetry, contour interval 25m; Bottom: colour-coded relief (illum from E). Note the large scar affecting the southern flank of the cone and the positive relief at its base, possibly representing the proximal portion of the failed material.*

3.1.4 - *Local structure of the Lametini region*

Although scarce, seismic data in the Lametini region indicate variations in basement depth, which could be related to the location and alignment of the two volcanoes. Basement depth, in fact, is 2800 m north of the cones, dropping to 3250 m south of them. Available data however preclude any accurate estimate of the direction of the structure affecting the basement.

As to the slide scar on LamN, the feature is most probably related to a mass-wasting event along a shallow-seated detachment plane, evidence of gravitational instability due to the sloping (~15°) flanks of the volcano and not associated to any form of deep-seated source.

3.2. - Palinuro

Palinuro is made up of basalts and basaltic andesites and has been dated to 0.35 Ma (Beccaluva *et alii*, 1985). The composite Palinuro volcanic complex (PVC) stretchs E-W for 75 km. It stands between the lower slope at 2000 m water depth to its north and the deep Marsili basin (3400 m depth) to its south. The PVC delimits the north-western extent of Aeolian arc volcanism. At least eight single volcanic edifices can be recognised along the PVC (fig. 6), their bases coalescing to form a near continuous volcanic ridge. Shallow water depths characterise the central portion of the PVC, with two volcanoes between 14°45' and 14°50' reaching 175 m and 70 m depths. They display flat tops, mostly due to emersion during glacial times.

To the west of the two shallower volcanoes, clusters of small cones surround a depressed area (14°40'-14°45') bordered by an arcuate northwestern ridge and smooth slope. This morphology could be related to a caldera-forming gravitational collapse event of a pre-existing volcanic edifice, followed by the creation of resurgent domes; the linear scarp bordered by the smooth slope could be the sole remainder of the original volcano flank.

To the east, adjacent to the central area (14°50'-15°00'), a series of smaller cones develop, mostly exhibiting horseshoe morphology and cratered summits. Further east, the PVC is affected by tectonic structures that are very prominent in the morphology of the last volcano, Glabro (centred on 15°10'), isolated from the PVC by a narrow moat.

Rather than describing the Palinuro complex as a whole, the features of two of its components have been chosen as examples to illustrate the differences in genesis and post-edifice construction diversity.

3.2.1 - *Cratered volcano (14o53'-14o55')*

The volcano is a small cone characterised by an asymmetric crater located at a minimum water depth of 500 m (fig. 7). Based on the difference in slope of its eastern flank and the flat seafloor to the west, the base of the cone lies at ~800 m water depth. Crater walls have a maximum height of 290 m, diminishing to 180 m at its western rim. The floor of the crater is at 130 m above the base of the volcano. No data are available about the rock composition. Assumptions may be made for the generation of this feature that range from explosive activity (wholly possible at this depth, Head & Wilson, 2003) or lava drain-back and/or lava lake formation.

3.2.2 - *Glabro*

This easternmost volcano from the PVC is treated for fairly obvious reasons given its outstanding morphology (fig. 8). No samples are available for

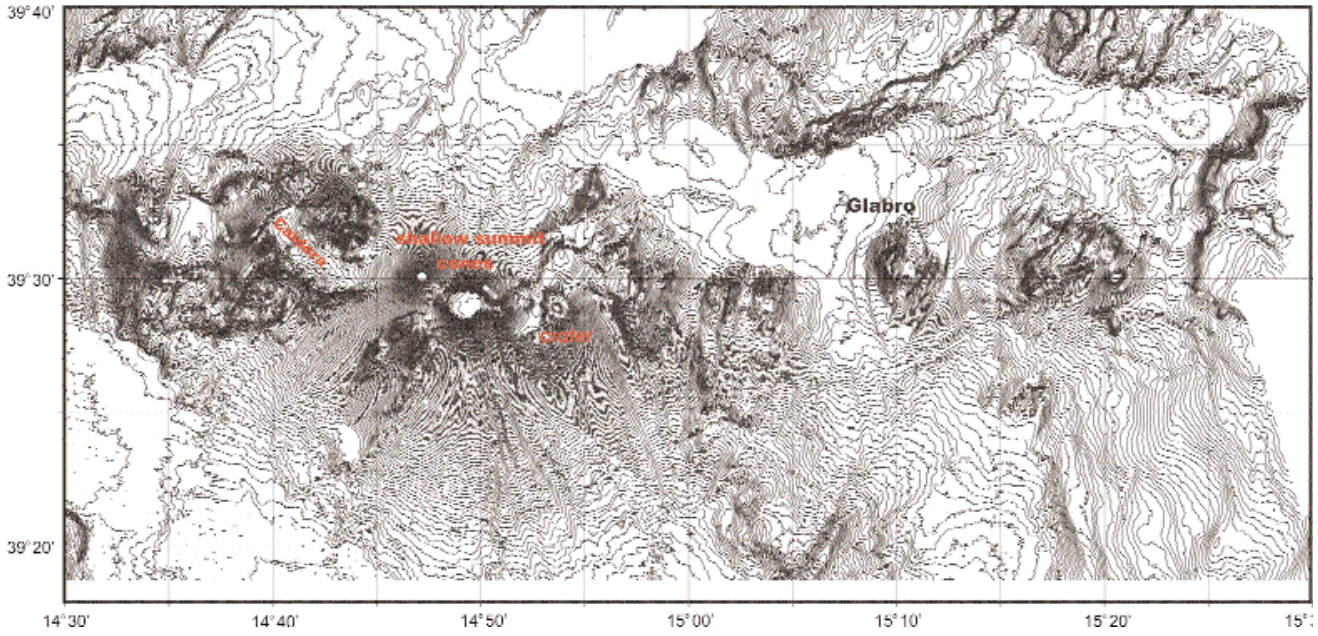

Fig. 6. - *25m interval bathymetry of the Palinuro Volcanic Complex (PVC), with main features described in text labeled. See text for discussion of details of the crater and Glabro volcanoes.*

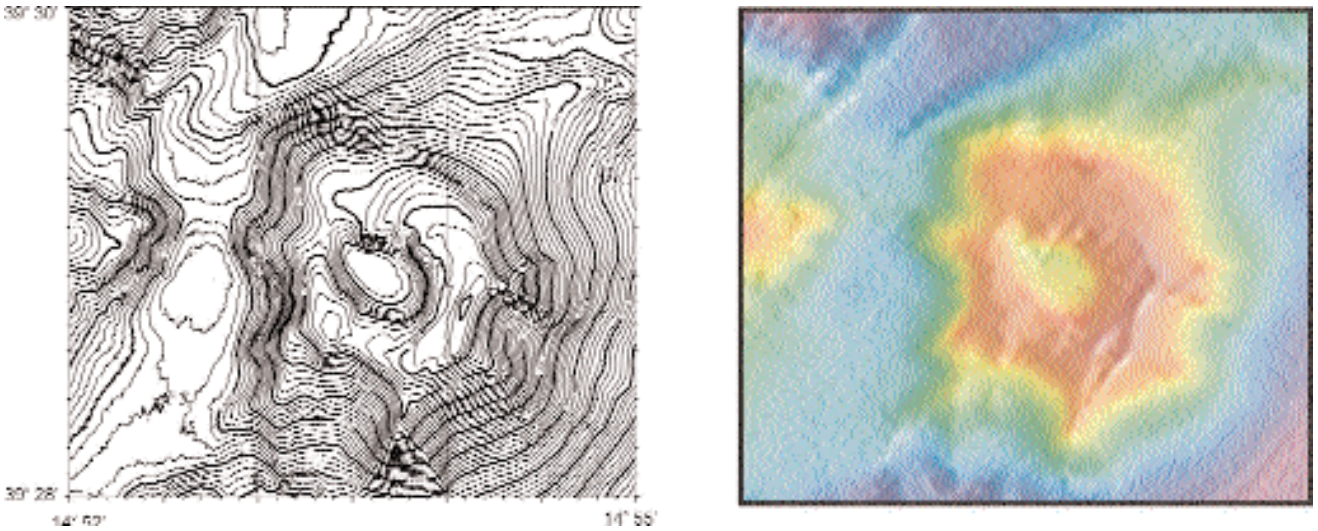

Fig. 7. - *Details of the cratered volcano on the PVC. Left: 10m contour interval bathymetry of the cone, Right: colour coded relief and contours. Note that the crater wall heights are asymmetric, nearing breach conditions to NW. This morphology is common for other cratered cones as well.*

Glabro. The volcano is dissected by a series of arcuate fault scarps into two separate parts characterised by N-S elongated, linear summit zones. Very steep internal scarps delimit the western (830 m water depth) and eastern (870 m water depth) summit portions of Glabro, separated by a 1.8km wide saddle lying at a water depth of 1100m. The western portion of Glabro is larger, higher (tab.1) and has a shape very similar to a smooth-flanked elongated cone split vertically into half. The flanks of the smaller, eastern portion are morphologically irregular, and its resulting shape is more complex. Surrounding perimeter faults also characterise the adjacent seafloor of Glabro. All perimeter fault scarps are west dipping, two intersecting the seafloor to the west of the edifice and one to the east.

The faults that have dissected Glabro, both the internal and perimeter features, have two distinctive properties. Firstly, all scarps are arcuate but with trends that fall into the N-S quadrant, elements with cross-cutting attributes are in fact lacking. Secondly, all the faults affect solely the area contiguous to the

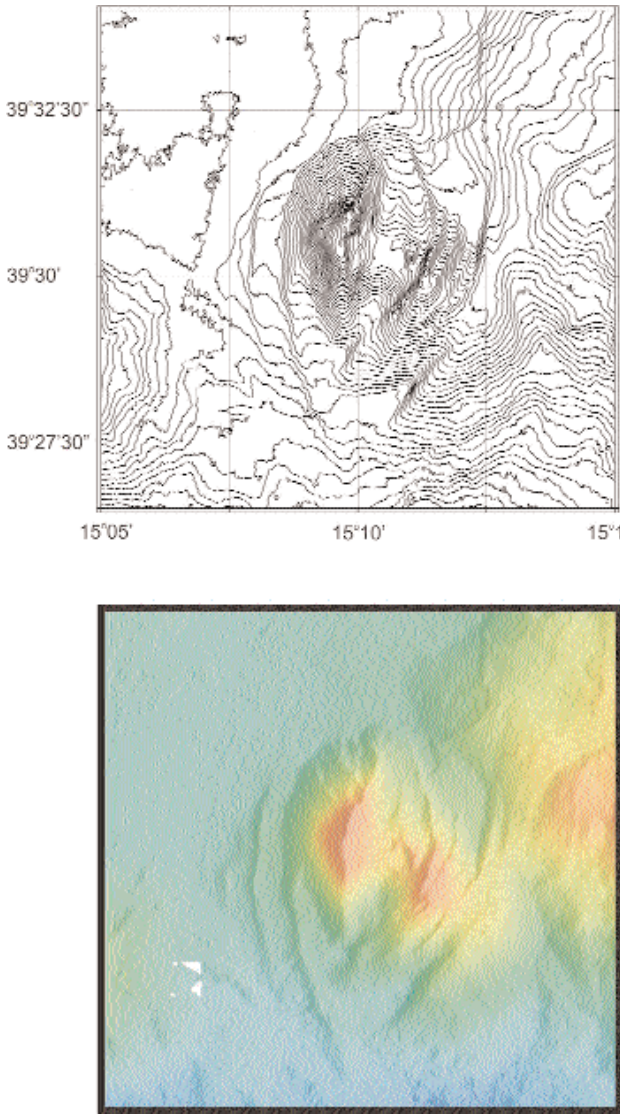

Fig 8. - *Glabro Volcano. Top: bathymetry, contour interval 25m; Bottom: colour-coded relief (illum from E). Glabro is made up of two summit areas bounded by striking internal and perimeter scarps. Note the diminishing throw of perimeter scarps away from the volcano. See text for discussion.*

volcano, conspicuously diminishing in height until terminating at the immediate external perimeter of the edifice. These elements lead to the conclusion that the observed volcano-tectonics is intimately linked to, and the surface expression of the destabilising processes that have affected Glabro.

3.2.3 - *Local Structure of the Glabro region*

Seismic reflection lines available in the vicinity of Glabro once again show that the volcanic structure is positioned on a ~800 m high basement step. In fact, to the northwest of the structure, the basement at a depth of around 2200 m is overlain by the 600 m thick sedimentary fill of an intraslope basin, ahile to the East and South of Glabro, the basement is at a depth of only 1200 to 1400 m. The basement data seem to fit with the structural elements described so far, in that the distribution of the volcano portions and directions of the faults point to an E-W or NE-SW trend of destabilisation. With regard to the processes at the origin of destabilisation, a first possibility is a thorough dissection of the volcano by normal faulting. A problem with this assumption is that since the faults are linked only to the volcano, some other process must have been at work to focus the faulting. A more credible process is directional gravitational spreading towards the E-NE. In effect, some of the elements characterising Glabro seem to have development close to the morphological characteristics of volcanic spreading described by the analogue modelling results of MERLE & BORGIA, 1996 and the numerical modelling of VAN WYK DE VRIES & MATELA, 1998. In the spreading case, the western scarps could be the surface expression of compression due to a slide surface underlying the entire edifice, probably initiating at the inward facing eastern fault. Movement along the decollement surface would cause destabilisation and dissection of the volcano summit, originating the two steep inward- facing collapse scars delimiting the two summit areas, developing as the flanks of a central leaf graben.

3.3. - WESTERN ARC VOLCANOES

Located on the seaward portion of the Cefalù basin, and west of the Island of Alicudi, the submerged portion of the western Aeolian arc is aligned in a NW direction and consists of Eolo and Enarete seamounts and the volcanic range comprising Sisifo seamount. Eolo, Enarete and the Islands of Filicudi and Alicudi are positioned at the northern margin of the Cefalu basin (fig. 9), flanking the 1500 m deep, flat-lying seafloor of the basin and bounded by a 500 m to 1000 m seawards-facing scarp to the north.

3.3.1 - *Eolo*

Eolo is located 20km due west of Alicudi Island. The volcano is generally characterised by irregular flanks, and a wide, 3 km by 2 km, relatively flat summit area, ~800 m deep, elongated in a NW-SE direction (figs. 10, 11). The flat summit is roughly square shaped and bounded by linear highs (75 to 125 m high) on 3 sides except to the SW (fig. 11). In this latter side, the southwestern portion of the summit area terminates at a 300 m deep scarp surrounded by 3 small cones (350 m, 250 m and 175 m high) which thus form a closed depression.

Dredge hauls from Eolo have included basalts, dacites and rhyolites, dated between 0.85-0.77 Ma (BECCALUVA *et alii*, 1985). The more silica-rich rocks characterise the small cones that surround the southwestern depression, suggesting a second episode

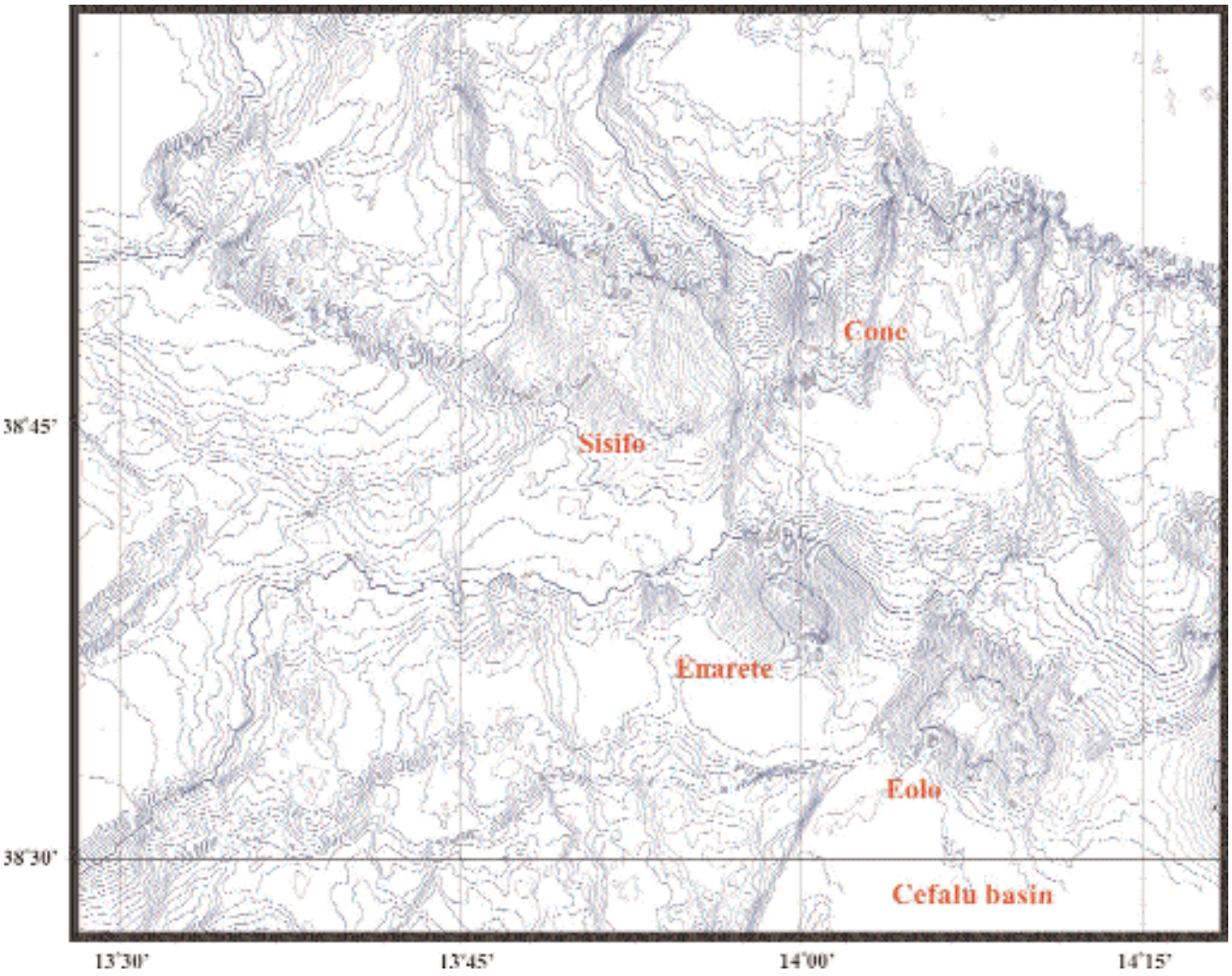

Fig. 9. - *Bathymetry (interval 50 m) of the western submerged Aeolian arc. Features discussed in text are labeled.*

of volcanism and cone emplacement following gravitational collapse of this flank of Eolo. The wide irregular base area of Eolo does not seem proportional to its present morphology. A conjecture could interpret the flat lying summit surrounded by delimiting highs as a filled caldera, implying the destruction of a previously larger edifice.

3.3.2 - *Enarete*

Enarete lies 10 km to the NW of Eolo. This volcano, from which basalt rocks, dated 0.78-0.67 Ma, were dredged (BECCALUVA *et alii*, 1985), has the morphology of a near perfect cone, slightly elongated with NW-SE trend (figs. 9, 10). It is asymmetric in height, ranging between 1700 m and 1450 m, given that its northern flank terminates at greater depth. About 3 km west from the base of Enarete, a small, 500 m high cone rises from the flat seafloor (fig. 10).

NW of Enarete lies the complex and irregular morphology of Sisifo seamount (fig. 9) which lies upon a WNW-ESE directed, 40 km long ridge. Made up of basalts and trachytes, dated 1.3-0.9 Ma, this edifice holds the oldest age data so far available for the Aeolian Arc. Younger volcanism, however, has been active in the region as shown by the morphological expression of a regular 1000 m high, conical volcano (fig. 9) located north of Enarete, at the southeastern margin of the Sisifo ridge.

3.3.3 - *Local Structure of the Eolo/Enarete/Sisifo region*

Both Eolo and Enarete are positioned above the seaward-facing border fault of the northern part of the Cefalù basin. The southern border of the Sisifo ridge, however, having the same trend as the Cefalù border fault, is characterised by a 500 m morphologically evident landward-facing scarp.

A significant volumetric difference emerges when comparing the western submarine volcanoes with the

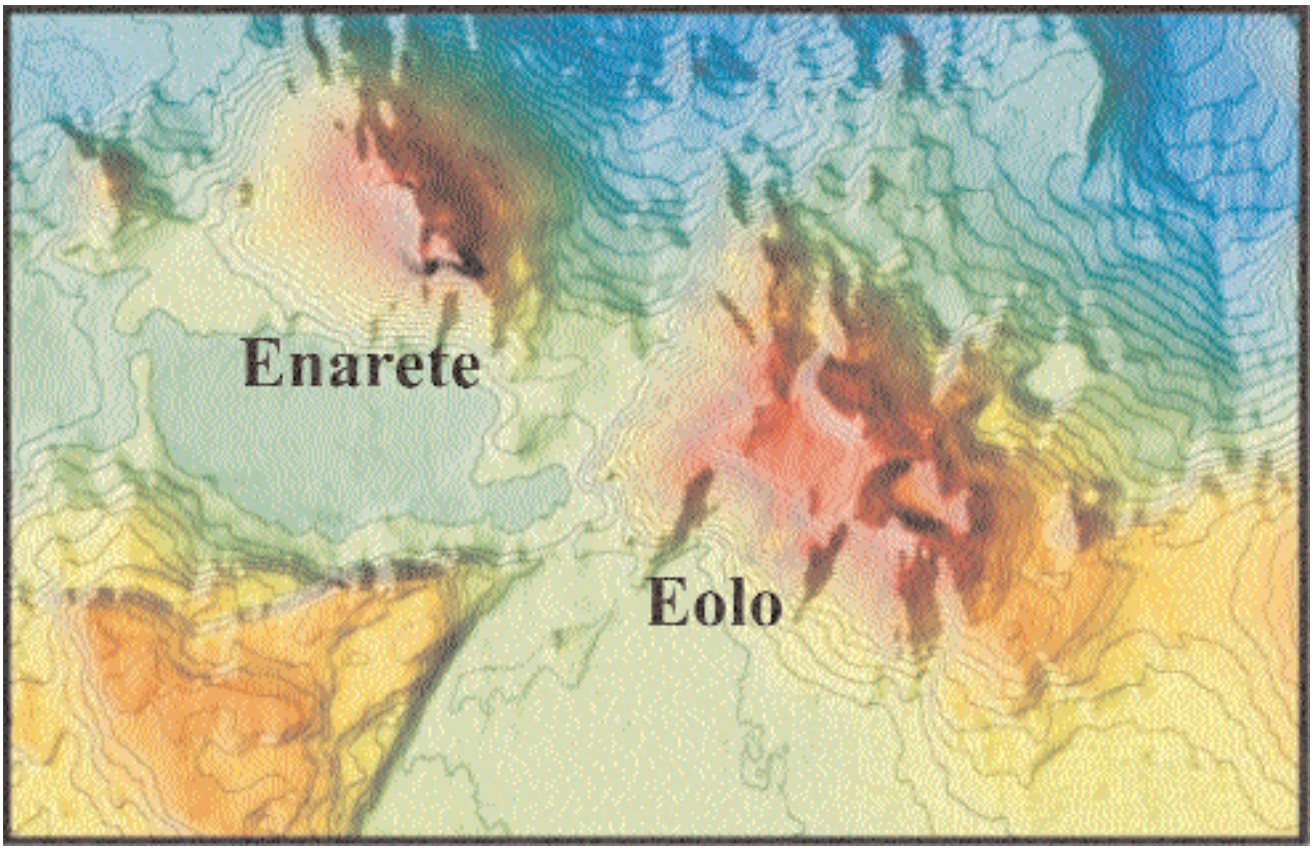

Fig. 10. - *Colour coded relief map of Eolo and Enarete volcanoes. Flat seafloor to southwest of the volcanoes is the Cefalù basin. For details of Eolo see figure 10.*

ones to the east. Enarete alone has a volume (tab. 1) that is close to double of the volumes of Alcione and the Lametini seamounts summed together. This is reflected in a comparison of the basal areas as well (tab.1), with both Eolo and Enarete having base areas close to the ones characterising the emerged volcanoes of Alicudi and Filicudi. In spite of the lack of age data for the eastern arc volcanoes, a simple difference in timing of formation cannot be ruled out, older volcanoes being larger, since an eastwards younging trend is evident, at least in the Recent. On the other hand, if one considers Palinuro as part of the northeastern arc, volume distribution could be more comparable.

4. - BACKARC VOLCANOES

4.1. - MARSILI

Marsili volcano rises 3000 metres from the Marsili basin seafloor to a minimum depth of 489 metres. It is elongated ~ 60 km NNE-SSW with mean width of 16 km. A narrow, 1 km wide linear region of lower gradient, approximately bounded by the 1000 metre isobath, marks the summit zone that stretches 20 km along the main axis of the volcano. On the lower flanks of the volcano, particularly to the NW and SE, numerous seamounts develop while the adjacent basin areas to the west and to the east of the Marsili edifice are characterised by large fault scarps (fig. 12).

The volcano summit axis zone and tip regions are characterised by the development of linear structures arranged in segments generated mainly by the alignment of narrow, linear cone ridges, or by the linear arrangement of several circular-based cones (MARANI & TRUA, 2002). Segment locations show that the central portion of the volcano is the main site of stress release and ensuing volcanic activity. These features, along with other morphological characteristics of the volcano and adjacent regional geology, led MARANI & TRUA, 2002 to interpret Marsili volcano as a super-inflated spreading ridge, constructed due to robust volcanism during the last 0.7Ma. In this paper we will deal with the small-scale volcanic features that occur on the NW flanks of the main volcano, in comparison and in contrast to the volcanoes of the volcanic arc.

4.1.1 - *North-western Flank seamounts*

Numerous small seamounts grow on the flanks of Marsili volcano, being most developed on its northern tip. The cones have circular bases with diameters up to 1500 metres and heights up to 300 metres (fig. 13).

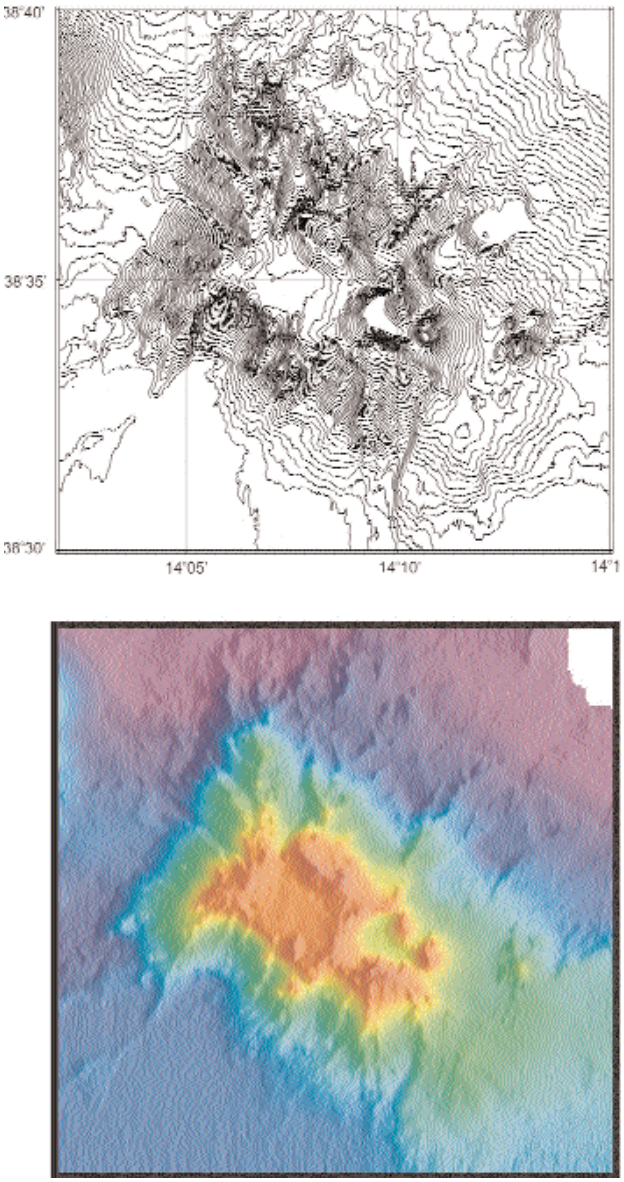

Fig. 11. - *Eolo volcano. Top- bathymetry, contour interval 25m; Bottom - colour-coded relief (illum from E). Note the broad, flat lying summit zone and the wide irregular base of the edifice. For discussion see text.*

Several are characterised by very low gradient, flat tops and a few display summit craters. In addition, a number of volcanic constructs form flat topped, semi-circular terraces, formed by up-slope buttressing on the inclined flanks of Marsili volcano. Similar features have been reported from the submarine Puna Ridge offshore Hawaii (ZHU *et alii*, 2002). Essentially, terraces can be considered a morphological variant of typical submarine flat topped volcanoes that are constructed on sloping terrain, forming flat steps with semicircular, steep down-slope flanks. On the contrary, cones are volcanic constructs characterised by a circular base, that add significant (~50 m) vertical relief to the slope and identified bathymetrically by enclosing contours. The morphology of cones nevertheless display asymmetry, with higher relief in the down-slope direction. Slope gradient, taking lava production and eruptive products constant, could thus be the discriminating parameter between the formation of the two morphologies. Cones would develop in lower gradient sectors while terraces would characterise higher gradient portions of the Marsili volcano. Examples of the former include the cone 1 (fig. 13) that develops in the distal slope area adjacent to the flat-lying Marsili basin floor (summit depth 3050 m). The cone has a flat top (base diameter ~1750 m; summit diameter ~1250 m), which culminates in a dome like feature. Morphologically, the cone is asymmetric, displaying a height of 240 m in the down slope direction and a relief of only ~60 m towards the saddle separating it from the sloping Marsili flanks. About 3 km south of cone 1, a series of terraces, characterised by typical semi circular steeply sloping flanks bounding flat seafloor (fig. 13), develop from 2800 metres depth. Dimensions are variable, widths of the flat summits averaging ~600 m and flanks ~100-150 m high. The pre-existing volcano flank slope profile, estimated from terrace morphologies is in the range of 10-12°, sharply contrasting with terrace flanks which reach 30° slopes.

A final, particular volcano morphology is displayed by three cones trending NW-SE at ~2400 m depth southeast of cone 1 (fig. 13). The three cones are a striking example of the evolution of cratered edifices. The most southern cone is characterised by horseshoe morphology, open to the southeast, with entirely enclosing, variable height crater walls. Crater depth is ~100 m, taken from the highest standing portion of the wall, the diameter is in the order of 1 km. The middle cone also displays horseshoe morphology with similar crater depth and diameter but is fully breached northeastwards, towards the northernmost cone. This latter, in reality consists of only the 150 m high western flank of what could have been a structure similar to the previous ones, the lacking portion of the original edifice located to the east. Thus, by following the morphology of the three cones northwards, one can trace the possible fate of these singular edifices. At the moment, it is difficult to make assumptions to explain the origin and characteristics of these volcanoes. If the increasing asymmetry is due to failures of the crater walls, it is difficult to explain the different trends, mostly away from the steeper slopes of Marsili. On the contrary, an eruptive origin to explain the features would be in line with random near-breach or breach directions but leaves open the question of why this process should affect only these volcanoes. A third possibility is that the volcanoes have been affected by extreme lava drawback due to intersection of younger magma conduits basically feeding new constructs in adjacent regions.

4.2. - VAVILOV

Vavilov volcano has a length of ~30 km, elongated in a N-S direction with a maximum width of ~14 km. It rises 2800 m from the flat Vavilov basin floor 3600 m

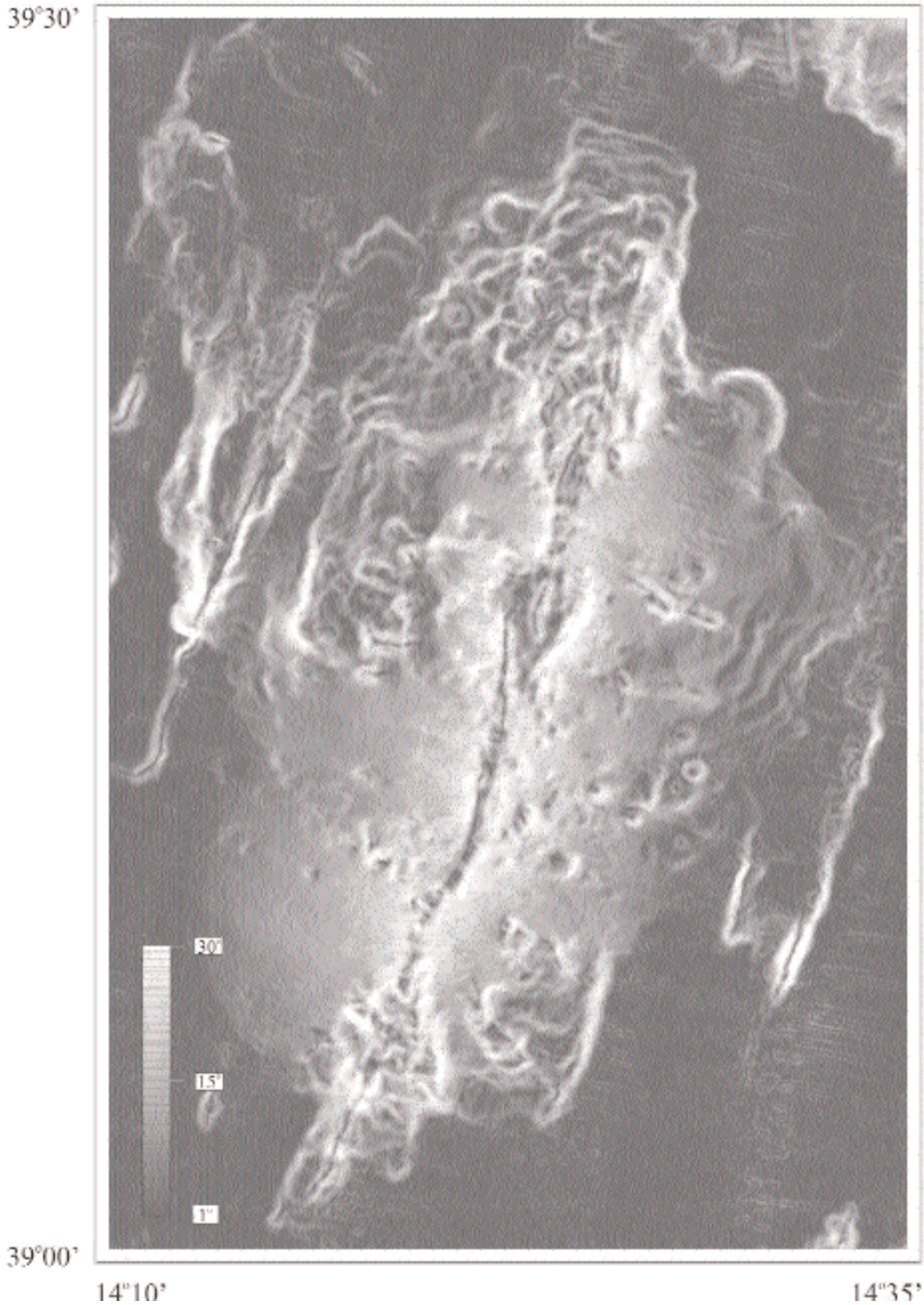

Fig. 12. - *Grey shaded gradient map of Marsili volcano. Steeper slopes are white, flat lying areas are black. Note development of numerous cones on the NW flank of the volcano.*

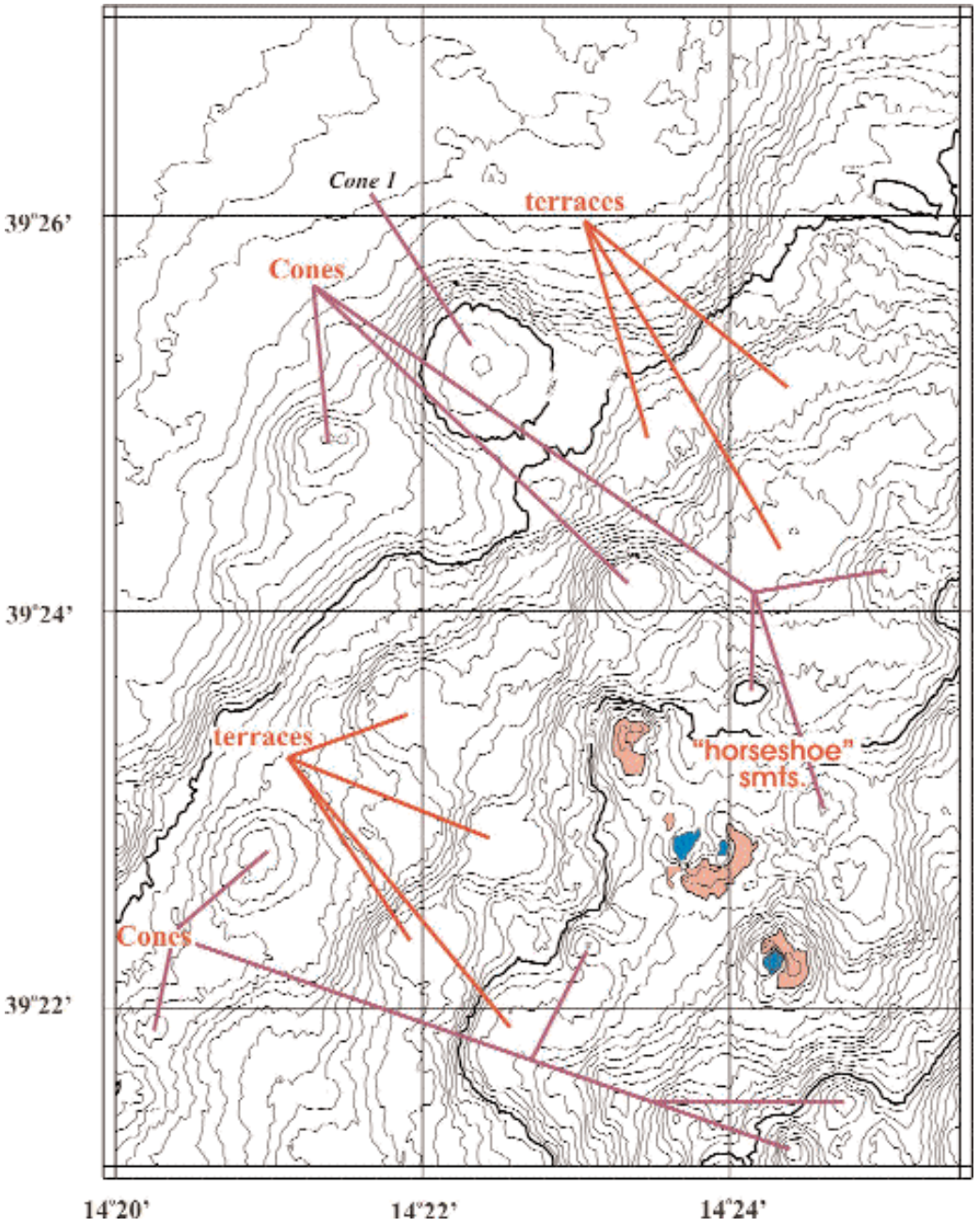

Fig. 13. - *25m interval bathymetry of the northwestern flank of Marisli volcano. Features discussed in detail in the text are labeled. Note that both cones and terraces develop on the flanks.*

deep to minimum water depth of 800m. Vavilov is a mature volcano, its formation occurring at the time of oceanisation of the Vavilov backarc basin at about 3Ma (KASTENS *et alii*, 1988). The summit area, however, seems to have been subsequently active (ROBIN *et alii*, 1987) at 0.4 to 0.1Ma.

The overall morphology of Vavilov volcano is dominated by the strong asymmetry between its eastern and western flanks (figs.14, 15). While the eastern flank, dipping on average 15°, displays irregular "volcanic" topography due to small cones, restricted terraces and ridges, a large portion of the western flank is steeply dipping (from >30° above 2800 m depth to 20° along the lower flanks) and is remarkably smooth, displaying a complete lack of small scale topography. Considering the arcuate scar that bounds the high gradient western flank, it is likely that this portion of the volcano has been affected either by one or more flank collapses or by faulting that has resulted in the removal of a large volume of the pre-existing edifice.

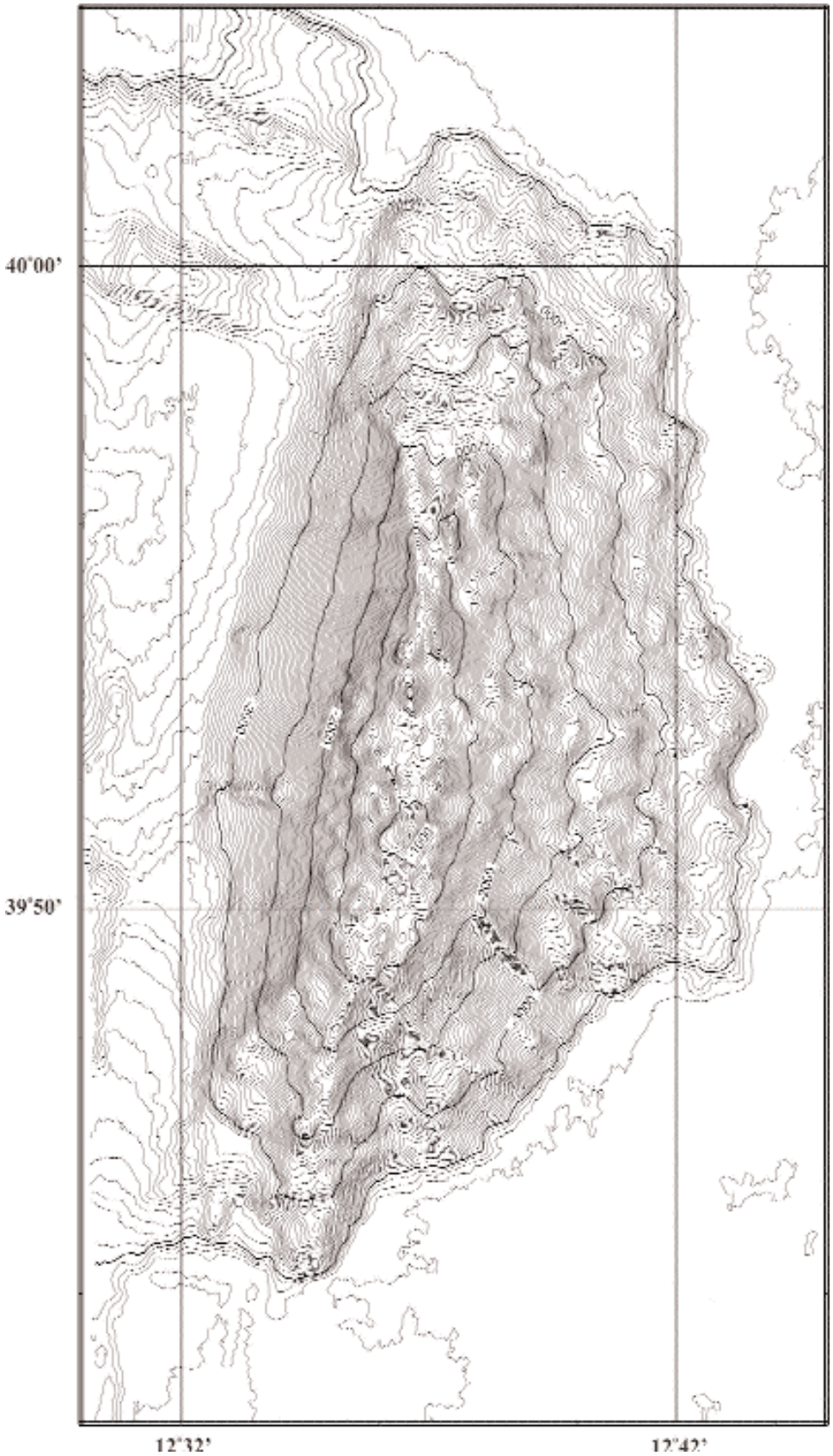

Fig. 14. - *Vavilov volcano. Bathymetry, contour interval 50m. The asymmetry of the volcano is evident as well as the range of features occurring on the volcano flanks, including terraces and small conical volcanoes.*

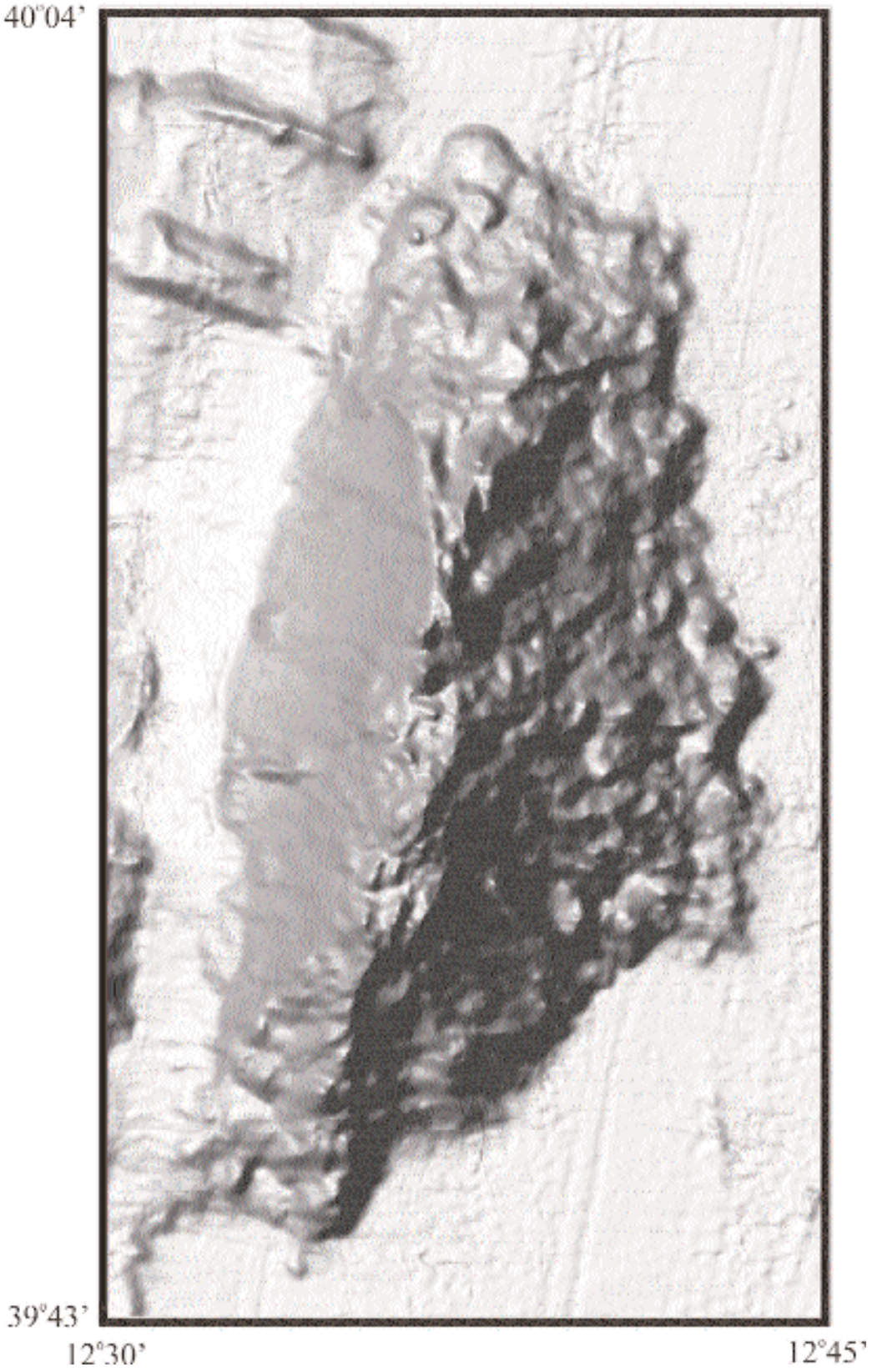

Fig. 15. - *Shaded relief bathymetry (illum. from E) of Vavilov volcano showing the marked morphological asymmetry of the edifice, both in terms of gradient variation and smaller-scale topography. For discussion see text.*

The summit of the volcano is composed of a relatively low gradient area occupied by two large 250 m high, circular cones and a number of smaller edifices. In general the morphology of the flanks of the Vavilov seamount has a more subdued character in comparison with the Marsili edifice most probably due to sediment blanketing. Both the southern and northern flanks of the volcano are traversed by 100-150 m high ridges, some characterised by the development of small cones, that originate at the summit tips and continue to the base of the volcano. Particularly on the northern flank, interruption of the ridges by steep transverse scarps gives rise to terrace-like morphologies. Apart from the summit cones, Vavilov volcano is the site of a number of circular based cones that, however, are located for the major part, on the lower slope portions, between 2500 m and 3500 m depth.

An interesting feature related to the bulk of the volcano is that the eastern base is consistently at least 100 m (in the central part ~300 m) deeper than the western one. Since the base level of the basin flanking the Vavilov seamount is for all practices the same, the shallower depth of the basin adjacent to the western flank could be due to the accumulation of the material derived from the assumed collapse. The lack of rugged topography on the basin floor could be related to sediment blanketing, thus indirectly indicating a timing of the event.

5. - DISCUSSION AND CONCLUSION

Although based exclusively on morphological grounds, the brief and non-exhaustive descriptions given above illustrate the diversity of the submarine volcanism of the Tyrrhenian basin. All volcanoes of the Aeolian arc are conical except for Eolo seamount that has a wide, flat summit area. Rough volume estimates show that the western submarine arc sector is the site of major production, with Enarete having near double the volume of the northeastern edifices summed together. The different edifices demonstrate that more or less long lived stationary magma vents are at the origin of the volcanoes. The vents are essentially isolated, as shown by the variations of geochemical signatures of the products between adjacent volcanoes, and may tap portions of a heterogenous mantle beneath the arc, most probably affected by different degrees of contamination from the subducted slab. A probable exception is the Palinuro volcanic complex. Although complicated by a range of volcanic morphologies, its linearity given by the uninterrupted merging of its vents could be indicative of the stability of magma supply along a major crustal discontinuity. Moreover, its trend and location, together with it being the limit of arc volcanism in this sector, are distinctive characters that differentiate Palinuro from the other submerged Aeolian volcanoes, and make it more similar to the two major backarc seamounts.

Backarc volcanoes of the Tyrrhenian are characteristically large reaching relatively shallow water depths (500-800 m) with bases at ~3500 m water depth. Both Marsili and Vavilov display satellite cones and terraces on their flanks, and relatively lower gradient summits characterised by a series of cones. The younger Marsili exhibits a range of flank seamount morphologies from flat top volcanoes, deeply cratered cones, elongated cone ridges and well developed terraces. The differentiating parameters of these various morphologies is still unclear but merit further study. Vavilov displays a more subdued topography probably due to sediment draping, but nevertheless shows the development of similar features described for Marsili.

A variety of instability processes have affected several of the described volcanoes. In the arc sectors, these processes are linked to the ubiquitous basement faults that underlie the volcanoes. In particular, since the analysis of seismic lines seems to rule out present-day activity of these faults, it is the basement step that provokes instability, with the volcano straddling a shallow, stable basement on one side and a sequence of weaker sedimentary layers on the other. This framework could favour gravitational spreading, which causes the most outstanding morphological transformation in the arc. It may be incipient in the case of Alcione and in a mature stage in the case of Glabro. If these two examples represent the end members of the spreading case, it follows that this process takes place by slow movement along the sliding surface, demonstrated by the development of the two cone summits on Alcione and the integrity, albeit disjointed, of the Glabro edifice. On the contrary to deep-seated spreading, the northern Lametini seamount displays a relatively large flank slide scar, most probably related to the failure along a slide surface limited to the edifice and due to the high gradient of the flanks. This type of instability evolves within a much more restricted time frame than that of gravitational spreading. Vavilov volcano is the most representative candidate for this style of gravitational instability, in this case leading to large-scale catastrophic sector collapse. The asymmetrical morphology of Vavilov, in fact, may be the result of a landslide scar that occupies almost its entire western sector. Although no estimate can be made regarding the possibility of multiple events forming the scar, the sector failure would have been to all effects instantaneous.

In addition to morphological adaptation to the general case of gravitational stress, a series of volcanoes display modification due to particular eruptive styles that result in cratered volcanoes. Examples include those described on Palinuro and Marsili volcanoes. The observed cratered volcanoes commonly exhibit asymmetrical crater wall heights, thus having a horseshoe shape in plan view. Some are entirely breached, having no positive relief bounding the crater in one sector. All are relatively small, 150-250 m high with a basal diameter of ~1 km and crater depths of 100 m on average. Less common than conical or flat top volcanoes, cratered cones however have particular morphologies that suggest two opposing models for their origin. A first case considers the interior dynamics of magma flux, in which reduction of supply results in

magma withdrawal from the vent, the formation of the crater depression and ensuing instability and failure of part of the crater walls. Reduction in magma flux could be a general phenomenon or be induced by intersection of a later conduit leading to the development of parasite volcanism in the vicinity of the cratered edifice.

A conjecture may be made for the case of Marsili volcano, in which the cratered cones may have fed or be linked to the generation of the surrounding lava terraces. The second case involves the explosive expulsion of lava and the formation of a pyroclastic cone around an explosive vent. In the Palinuro case, the ~500 m water depth poses no limit to submarine explosive activity. However, the Marsili cratered cones lie at ~2400 m water depth. Although explosive volcanism has been shown to be possible at these depths, a necessary requirement for submarine pyroclastic eruptions is that the feeding magma possesses a high volatile content allowing gas exsolution and lava disruption and/or gas pressure build-up in the reservoir. Thus, in both the Palinuro and Marsili cases, the cratered cones would have been necessarily fed by a unique magma, with different characteristics than the one at the origin of the regular or flat top cones and terraces that occupy their immediate vicinity.

A significant case involves Eolo seamount. The volcano is 900 m high, its broad, 3 km-wide flat lying summit reaching depths of 800 m, and is characterised by a large, irregular base area. Perimeter scarps partly enclose the summit area seemingly representing relics of a former edifice suggesting perhaps the formation of a caldera structure due to the explosive destruction of the previous high-standing volcano.

Recalling the particular nature of swath bathymetry as a remote sensing tool for the exploration of the seabed, together with the advantages and disadvantages specific of such a method, it is however noteworthy that the morphology alone of many of the landforms described provides clues to their origin and evolution. This is especially true in the marine realm in which the direct observation of actively forming volcanic constructs is precluded.

REFERENCES

Beccaluva L., Gabbianelli G., Lucchini F., Rossi P.L. & Savelli C. (1985) - *Petrology and K/Ar ages of volcanics dredged from the Aeolian seamounts: implications for geodynamic evolution of the Southern Tyrrhenian basin*. Earth and Planetary Science Letters, **74**: 187-208

Bloomer S.H., Stern R.J., Smoot N.C. (1989) - *Physical volcanology of the submarine Mariana and Volcano arcs*, Bull.of Volcanol., **51**: 210-224.

Bridges N.T. (1997) - *Ambient effects on basalt and rhyolite lavas under Venusian, subaerial and subagueous conditions*, Jour. Geophys. Res., **102**: E4, 9243-9255.

Chester D. (1993) - *Volcanoes and Society*, Arnold, London, 1-351.

Clague D.A., Moore J.G., Reynolds J.R. (2000) - *Formation of submarine flat-topped volcanic cones in Hawai'i*, Bull. Volcanol., **62**: 214-223.

Gregg T.K.P. & Fink J.H. (1995) - *Quantification of lava flow morphology through analog experiments*, Geology, **23**, 73-76.

Gregg T.K.P, Smith D.K. (2003) - *Volcanic investigations of the Puna Ridge, Hawai'i: relations of lava flow morphologies and underlying slopes*, J. Volcanol.Geoth. Res., **126**: 63-77.

Head J.W., Wilson L. (2003) - *Deep submarine pyroclastic eruptions: theory and predicted landforms and deposits*, J. Volcanol. Geotherm. Res., **121**: 155-193.

Kastens K.A. *et alii* (1988) - *ODP Leg 107 in the Tyrrhenian Sea: insight into passive margin and backarc basin evolution*, Geol. Soc of America Bull., **100**: 1,140-1,156.

Kastens K.A. *et alii* (1990) - *The geological evolution of the Tyrrhenian Sea: an introduction to the scientific results of ODP Leg 107*, Proc. Ocean Drill. Program Sci. Results, **107**: 3-26.

Jolivet L. (1991) - *Extension of thickened continental crust, from brittle to ductile deformation: examples from Alpine Corsica and Ageab Sea*, Ann. Geofis., **36**: 139-153.

MalinvernoA., Ryan W.B.F. (1986) - *Extension in the Tyrrhenian Sea and shortening in the Apennines as a result of arc migration driven by slab sinking in the lithosphere*, Tectonics, **5**: 227-245.

Marani M.P., Trua T. (2002) - *Thermal constriction and slab tearing at the origin of a superinflated spreading ridge: Marsili volcano (Tyrrhenian Sea)*, J. Geophys. Res., **107**: B9, doi: 10.1029/2001JB000285.

Merle O., Borgia A. (1996) - *Scaled experiments of volcanic spreading*, J. Geophys. Res., **101**: B6, 13805-13817.

Parfitt E.A., Gregg, T.K.P., Smith D.K. (2002) - *A comparison between subaerial and submarine eruptions at Kilauea volcano, Hawai'i: implications for the thermal viability of feeder dikes*, J. Volcanol.Geoth. Res., **113**: 213-242.

Robin C., Colantoni P., Gennesseaux M., Rehault J.P. (1987) - *Vavilov seamount: a mildly alkaline Quaternary volcano in the Tyrrhenian Sea*, Mar. Geology, **78**: 125-136.

Sartori R. (1990) – The main results of ODP Leg 107 in the frame of Neogene to Recent geology of perityrrhenian areas. In: Kastens K.A., Mascle J. *et alii* (Eds.): "*Proceedings of the ODP*". Scientific Results **107**: 715-730.

Savelli C. (1988) – *Late Oligocene to Recent episodes of magmatism in and around the Tyrrhenian Sea: implications for the processes of opening in a young inter-arc basin of intra-orogenic (Mediterranean) type*. Tectonophysics, **146**: 163-181

Serri G. (1997) - *Neogene-Quaternary magmatic activity and its geodynamic implications in the Central Mediterranean region*. Annali di Geofisica, Vol. XL, N. 3, 681-703

Sigurdsson H. (2000) - *Encyclopedia of Volcanoes*, Academic Press, Florida, U.S.A., 1-1417.

Smith D.K., Cann J.R (1997) - *Constructing the upper crust of the mid-Atlantic ridge: a reinterpretation based on the Puna ridge, Kilauea volcano*, J. Geophys. Res., **104**: B11, 25379-25399.

Vidal N. & Merle O. (2000) - *Reactivation of basement faults beneath volcanoes: a new model of flank collapse*, J. Volcanol. Geotherm. Res., **99**: 9-26.

Walter T. R. & Troll V. R. (2003) - *Experiments on rift zone evolution in unstable volcanic edifices*, J. Volcanol. Geotherm. Res., **127**: 107-120.

van Wyk de Vries B. & Matela R. (1998) - *Styles of volcano-induces deformation: numerical models of substratum flexure, spreading and extrusion*, J. Volcanol. Geotherm. Res., **81**: 1-18.

Zhu W., Smith D.K., Montesi L.G.J. (2002) - *Effects of regional slope on viscous flows: a preliminary study of lava terrace emplacement at submarine volcanic rift zones,* J. Volcanol. Geotherm. Res., **119**: 145-159.

Zitellini N., Trincardi F., Marani M., Fabbri A. (1986) - *Neogene tectonics of the northern Tyrrhenian Sea*, Giorn. Geol., **48**: 1/2, 25-40.

Mem. Descr. Carta Geol. d'It.
XLIV (2004), pp.127-146
18 figg.

Deep-sea depositional systems of the Tyrrhenian basin
Sistemi deposizionali di mare profondo del bacino Tirrenico

GAMBERI F. (*), MARANI M. P. (*)

ABSTRACT - The multibeam and seismic data acquired during 1996 and 1999 by the Institute for Marine Geology of Bologna tied with the already available seismic lines have been interpreted for the understanding of the present-day depositional systems of the Tyrrhenian Sea. A variety of sedimentary processes and related depositional environments characterizes the different portions of the Tyrrhenian Sea. Major differences are evident between the intraslope basins stretching along the Latium-Campanian, Calabrian and Sicilian active margins and those of the Sardinian passive one. In addition, a high variability of active sedimentary processes emerges also for adjacent sectors of single intraslope basins.

KEY WORDS: sedimentary processes, intraslope basins, depositional system distribution, Tyrrhenian Sea

RIASSUNTO - I dati sismici e batimetrici di dettaglio acquisiti nel 1996 e 1999 dall'Istituto per la Geologia Marina di Bologna sono stati interpretati allo scopo di ricostruire la distribuzione e le caratteristiche dei sistemi deposizionali di mare profondo del Mar Tirreno. Una grande variabilità caratterizza i processi sedimentari e gli ambienti deposizionali del bacino. Differenze sostanziali sono state evidenziate tra i bacini di intrascarpata dei margini attivi Laziale-Campano, Calabro e Siciliano e quelli sviluppati lungo il margine passivo Sardo. Inoltre, una grande variabilità dei processi sedimentari attivi è stata rilevata anche in settori adiacenti dei singoli bacini di intrascarpata.

PAROLE CHIAVE: processi sedimentari, bacini di intrascarpata, distribuzione sistemi deposizionali, Mar Tirreno

1. - INTRODUCTION

The significant increase in the exploration of deep-water reservoirs has recently led to a renewed interest in the study of deep-sea depositional systems (WEIMER *et alii* 2000). Moreover, the growing development of seafloor communication networks, the need for a safe development of deep-sea oilfields and the strong exploitment of coastal areas has stimulated the studies of sedimentary processes capable of marine geohazards (STOCKER *et alii* 1998; LOCAT & MEINERT 2003). As a consequence, an intense worldwide seafloor and sub-seafloor mapping effort is underway that, also thanks to the always expanding resolution potential of the techniques of marine investigations, has led to the formulation of new concepts about the deep-sea sedimentary environment. In particular, the analysis of the deep-sea depositional systems is focused in recognizing, interpreting and delineating the process-oriented submarine geomorphic elements (GALLOWAY 1998) that are conveniently imaged by a detailed bathymetric coverage of the seafloor. Multibeam bathymetric mapping with the capacity of providing an unprecedented resolution of morphosedimentary features, is therefore one of the tools that has been recently extensively used in the study of present-day deep-sea depositional systems. In addition, the integration of seismic stratigraphy and seismic geomorphology in the interpretation of

(*) ISMAR – CNR, Sezione di Geologia Marina, Via Godetti 101, 40129 Bologna

seismic lines, have led to new details about the processes that govern the evolution and the history of deep-sea depositional systems (POSAMENTIER 2003; POSAMENTIER & KOLLA 2003).

The last comprehensive researches regarding the Tyrrhenian deep-sea depositional environments date back to the 70's and 80's when, in the frame of the project "Oceanografia e Fondi Oceanici" launched by the Consiglio Nazionale delle Ricerche, seismic lines and seafloor samples were extensively collected over the basin. The acquired data led to the individuation of the single basins and of the main geomorphic elements that characterize the different portions of the Tyrrhenian Sea. In particular, the numerous intraslope basins that stretch along the Italian, Sicilian and Sardinian margins and the Marsili and Vavilov abyssal plains that centre the basin were evidenced. (WEZEL *et alii* 1981; NICOLICH 1986). Following studies have only dealt with specific research themes in particular sectors of the Tyrrhenian Sea.

The multibeam and seismic data acquired during 1996 and 1999 by the Institute for Marine Geology of Bologna tied with the already available seismic lines and seafloor samples offer therefore the possibility of advancing the understanding of the present-day depositional systems and of their temporal evolution in the Tyrrhenian Sea in the light of the new ideas about the deep-sea environment. A brief review of this issue is presented in this paper through the integrated interpretation of the recently acquired multibeam and seismic data in the different sectors of the basin (fig. 1, Plates 1,2).

2. - LATIUM-CAMPANIAN MARGIN

This margin is characterized by a complex slope sector that flanks to the east the 3500 m deep Vavilov abyssal plain and constantly widens southward from the area of the Pontine islands, where it is only 20 km large, to the area of the Palinuro volcanic complex, where it reaches a width of 150 km (fig. 2). To the

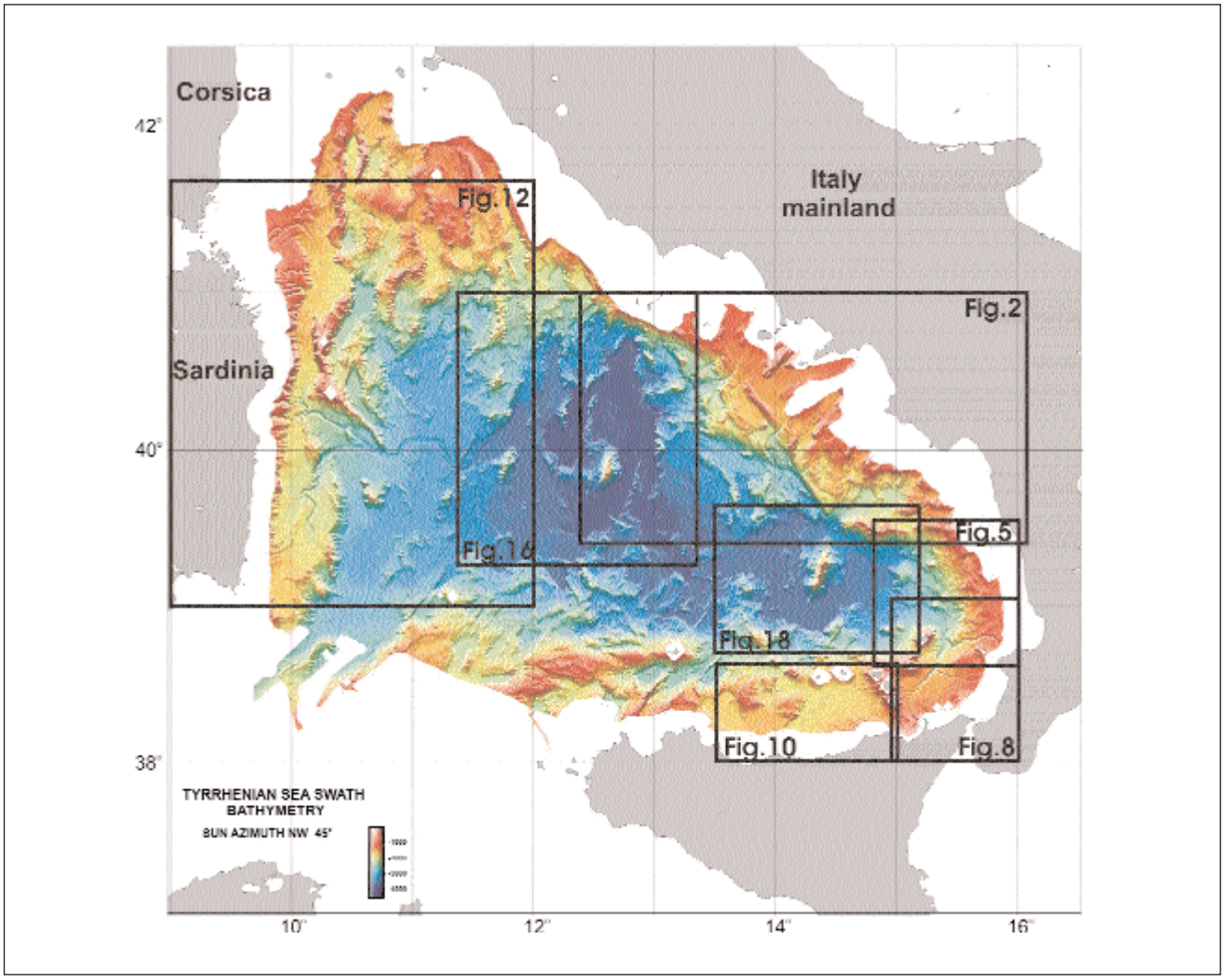

Fig. 1. – *Colour-shaded bathymetric map of the Tyrrhenian Sea from multibem data. Boxes correspond to the detailed maps of the distinct basin sectors presented in this paper. Colour depth intervals are shown in the left corner of figure.*

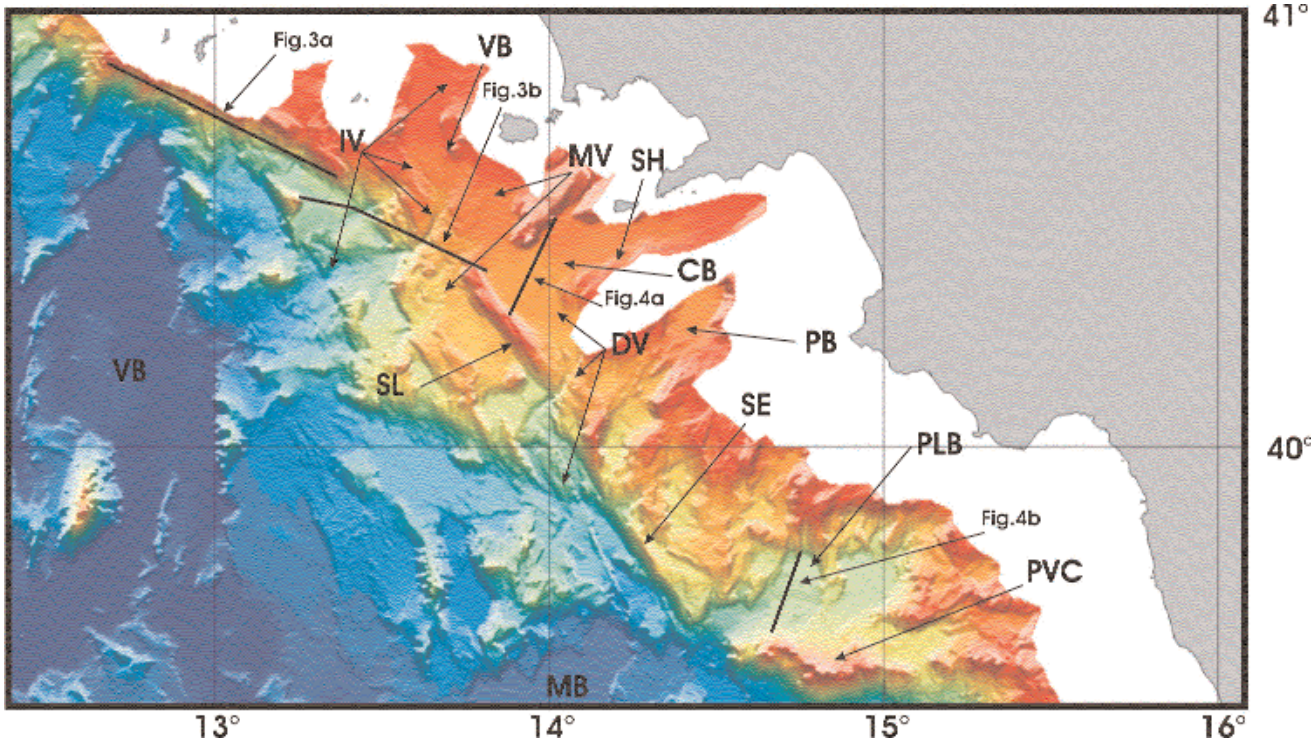

Fig. 2. - *Colour-shaded bathymetric map of the Latium-Campanian margin (IV = Ischia valley; VB= Ventotene intraslope basin; MV = Magnaghi valley; SL = Sirene lineament; SH = Sele high; CB = Capri intraslope basin; DV = Dhorn valley; PB = Paestum intraslope basin; SE = Sartori escarpment; PLB = Palinuro intraslope basin; PVC = Palinuro volcanic complex; VB = Vavilov basin; MB = Marsili basin).*

north, a single slope sector is responsible for the deepening of the margin from the platform surrounding the volcanic island of Ponza to the 3500 m deep Vavilov basin (fig. 2); here, due to the high slope gradient, canyons and associated slump scars dominate and originate a dendritic pattern of slope erosion (fig 3a) as also imaged with deep-towed sidescan sonar data by CHIOCCI *et alii* 2003.

An array of closely spaced extensional faults and fault-bounded basement highs, mainly oriented in a NNW-SSE direction, characterizes the area between Ponza Island and the Sele high and results in a down-to-the-west stepping margin morphology (fig. 2). The recent age of the tectonics that originated the basement highs has not allowed their mantling by slope sediments; as a consequence, the main loci of deposition are intraslope basins developed over the basement depressions. The intraslope basins are mainly narrow, NNW-SSE elongated troughs; apart from the Ventotene and the Capri basins, in fact, the close spacing of the fault-bounded highs does not allow the formation of large intraslope basins (fig. 2). Some portions of the intraslope basins are completely isolated from the upslope sectors; hemipelagite drapings and mounded bodies with a transparent seismic facies resulting from mass-wasting degradation of the adjacent highs, prevail (fig. 3b). Other portions of the intraslope basins are on the contrary characterized by complex submarine drainage networks that connect successive deeper intraslope basins. Some of the drainage networks originate in the upper slope portion and, crossing the entire slope, represent throughgoing sedimentary pathways that link the upper margin with the deep abyssal plain. The course, the morphology, and the depositional or erosional character of the different trunks of the submarine drainage networks are strongly influenced by the distribution of the intraslope highs. The range of the downslope variations in the character of a drainage network as a function of the margin morphology and of the changing slope gradient, in turn controlled by the tectonic structures, is illustrated by the Ischia valley (fig. 2). It starts as gullies in the upper slope north of Ischia Island and then evolves into small scale depositional channels running in a low-relief valley in the eastern portion of the Ventotene basin. It then turns parallel to and finally breaches the edge of the Sirene fault-block becoming a narrow, around 1 km wide, v-shaped deeply incised canyon. (fig. 3b). Downslope of the Sirene lineament, the Ischia valley is again very large attaining a width of 12 km (fig. 2); beside sediments fed from the upslope segment of the drainage network, it receives the sedimentary contribution from the undercutting of the margins of the valley itself, where frequent mass wasting scars are present. Finally the Ischia valley enters the eastern portion of the Vavilov basin where a small fan with a radius of around 5 km is developed. South of Ischia valley another system of gullies is present in the slope

of the Ischia Island originating the Magnaghi valley that evolves to a depositional channel in the eastern portion of the Ventotene basin (fig. 3b) and joins the Ischia valley further downslope of the Sirene lineament (fig. 2).

The Dhorn canyon is another drainage system that crosses the entire slope and reaches the deep Tyrrhenian basin plain, in this case the Marsili basin (fig. 2). The bathymetric coverage, starting in the Capri intraslope basin does not image its upper reaches that consists of two single canyons that connect north of Capri Island (MILIA & TORRENTE 1999); in the Capri intraslope basin however, a very narrow and shallow depositional channel associated with a fan is evident (fig. 4a). The Dohrn canyon becomes again strongly erosive as it crosses the southern tip of the Sirene high. It is then structurally forced to run in the area east of the Sartori escarpment (CURZI *et alii* 2003)

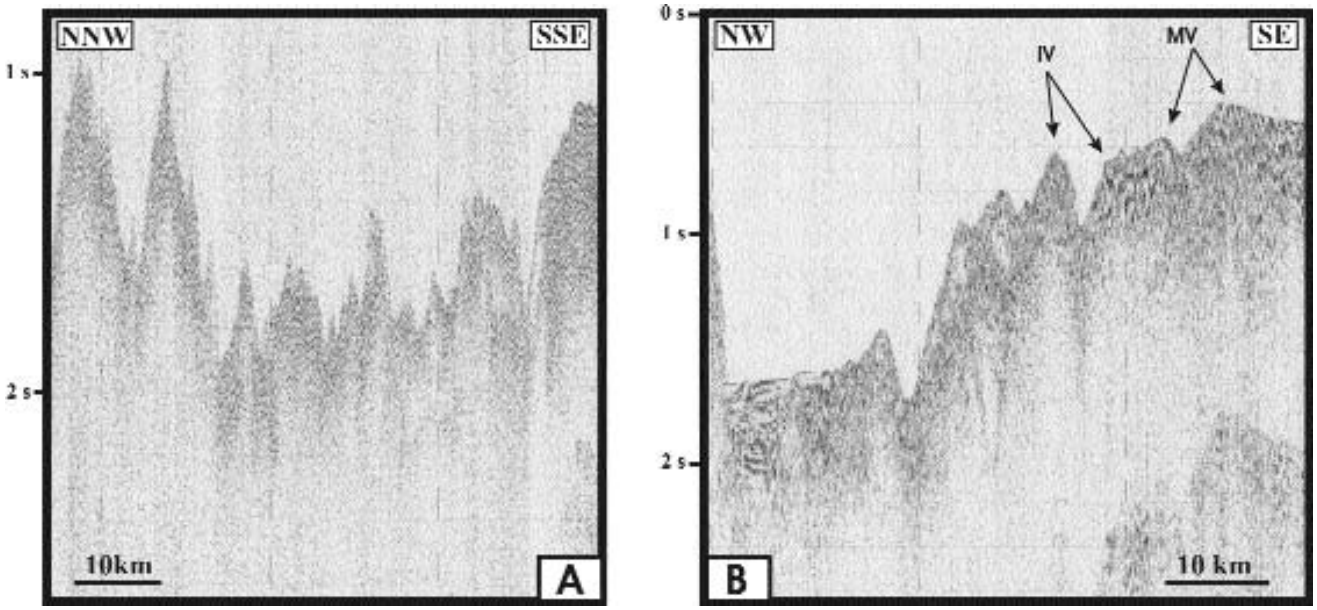

Fig.3. – *a) Seismic line T9964 crossing the Latial slope offshore Ponza island. The upper slope portion (left in figure) is characterized by narrow and deep canyons that evolve downslope into larger areas of seafloor erosion originating a dendritic pattern of slope erosion. b) Seismic line T9962 crossing the Ischia (IV) and Magnaghi (MV) sea valleys. Note the mainly erosional segment of the Ischia valley in the crossing of the Sirene lineament at variance with the depositional segment of the Magnaghi Sea valley in the eastern portion of the Ventotene basin. At the base of the Sirene lineament a further erosional fairway is evident. The filling of the intraslope basin at the foot of the Sirene lineament mainly consists of hemipelagites; however, thin transparent mounded bodies due to mass-wasting processes affecting the adjacent highs are evident.*

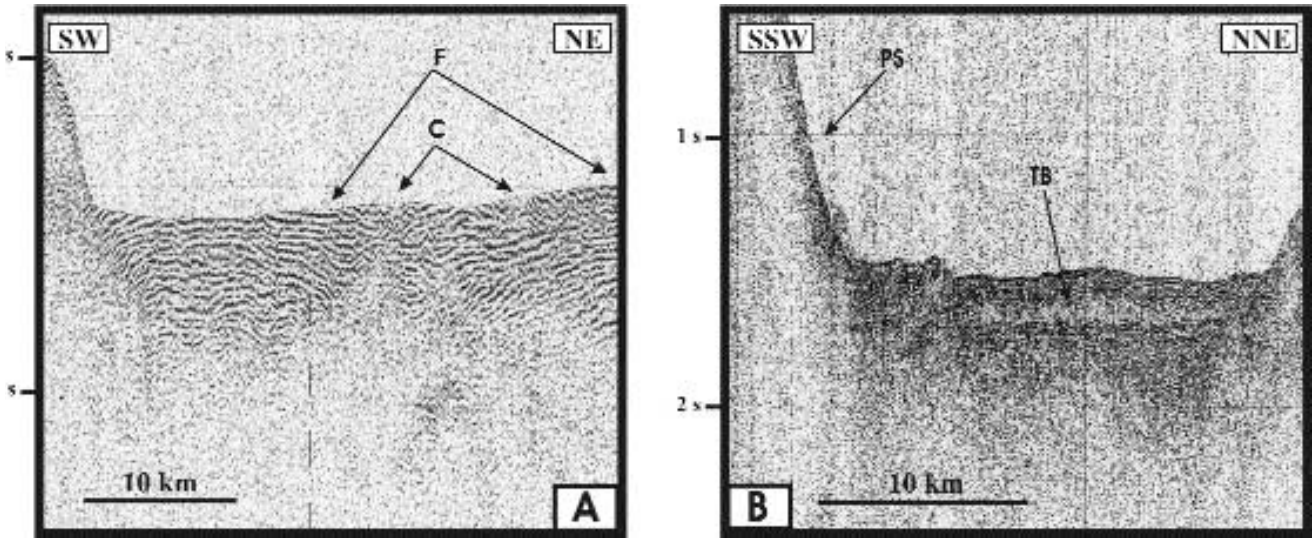

Fig. 4. – *a) Seismic line T96186 crossing the Capri intraslope basin. A fan (F) characterized by highly discontinuos reflections and mounded geometry makes up the recentmost basin infill; very low-relief channels (C) represent the fan-feeding elements. b) Seismic line T9681 over the western portion of the Palinuro basin. A transparent body (TB) with a thickness of around 100 m is imaged in the basin infill at the base of the Palinuro volcanic complex (PS) (see text for further details).*

where it branches into a series of canyons running in a SSE direction within a graben; the structural control results in its distal course being parallel to the margin for a length of 70 km entering the Marsili basin 150 km south of its initiation in the Naples Gulf (fig. 2).

South of the Sele high, both NNW-SSE and NE-SW trending extensional faults result in a complex margin morphology and in mainly completely confined small intraslope basins; the Paestum and the Palinuro basins are the only intraslope basins that have a considerable areal extent (fig. 2). Predominantly erosional processes in the form of dendritic submarine drainage systems are evident in the slope surrounding the Paestum and the Palinuro basins. Mass-wasting deposits over the western portion of the Palinuro basin (fig. 4b) can be the result of instability of the surrounding slopes or alternatively they could be a record of the evolution of the nearby Palinuro volcanic complex.

3. - NORTHERN CALABRIAN MARGIN

South of the Palinuro volcanic complex and north of the submarine extension of Capo Vaticano, the Calabrian margin consists of the upper slope, the

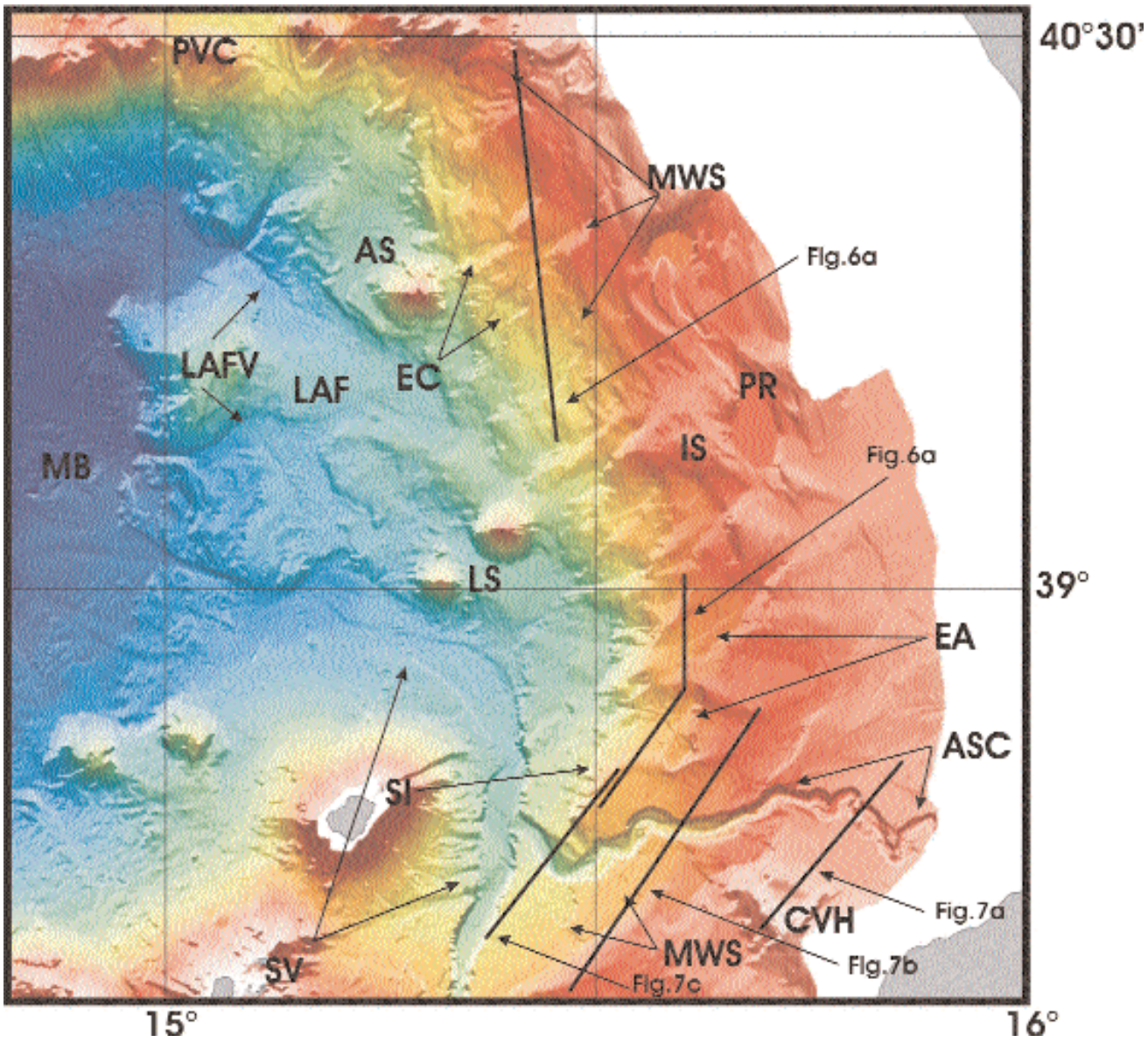

Fig. 5. – *Colour-shaded map of the Calabrian margin (PVC = Palinuro volcanic complex; MWS = mass-wasting scars; AS = Alcione Seamount; EC = embryonic canyons; LAF = Lametini-Alcione flat; LAFV = Lametini-Alcione flat valleys; LS = Lametini seamounts; IS = Intermediate slope; PR = Paola ridge; EA = erosional areas; SI = linear scarp with seafloor instability; ASC = Angitola slope channel; CVH = submarine extension of Capo vaticano high; SV = Stromboli valley; MB = Marsili basin).*

Paola intraslope basin, an intermediate slope, the Lametini flat and a further slope that marks the boundary with the Marsili basin (fig. 5). The upper slope and the Paola basin whose axis lies at a depth of around 700 m (GALLIGNANI 1982) were not investigated during the two cruises of data acquisition. Since an elevated ridge, topping at around 600 m, bounds the Paola basin seaward (ARGNANI & TRINCARDI 1993), the intermediate slope is not directly connected to the emerged areas; only in the southern portion of this margin sector, north of Capo Vaticano high, in fact, does the Angitola drainage network originate in the upper slope (GALLIGNANI 1982), and runs in the intermediate slope before connecting with the Stromboli canyon (fig. 5).

The intermediate slope spans the margin with a width of around 40 km down to depth of around 2000 m (fig. 5). In the seismic lines, the structural grain of this slope sector is evident as basement culminations and depressions (fig. 6a); however, a mantling of slope deposits has almost obliterated the resulting topography as evidenced by the very subdued morphologic expression in the bathymetric map (fig. 5). North of the Lametini seamounts, the main characteristics of the intermediate slope are mass-wasting scars and associated packages of downslope translated deformed sediments that straddle almost the whole slope (figs. 5, 6a); in addition, in the lower sector, flat-bottomed upslope narrowing elongated areas of focussed erosion occur on the surface of the displaced sediments that could represent embryonic canyons (fig. 5).

To the south of the Lametini seamounts, seafloor instability is concentrated along a linear, NNE to N trending scarp that coincides with a step in the basement and represents the western limit of the intermediate slope (fig. 5). From the linear scarp, however, seafloor instability propagates upslope. The linear mass-wasting dominated escarpment is in fact connected upslope to a large amphitheatre shaped erosional area with a width of around 15 km and with bounding scarps as high as 100 m and to a 2 km wide 20 km long erosional area that spans the whole intermediate slope, indenting the ridge that bounds the Paola basin seaward (figs. 5; 6b).

Although known as a canyon in the literature, the Angitola submarine conduit presents some segments that have a morphology more akin to slope channels (fig. 5). The upper segment of the Angitola slope channel presents in fact a meandering planform and a negative relief of around 100 m; oxbows and lateral accretion packages are the evidence of the swinging and sweeping of the channel within a larger channel-belt (fig. 7a). Downslope from the high that bounds seaward the Paola basin and of the submarine extension of the Capo Vaticano high, the Angitola slope channel has a straighter planform, is more incised reaching a negative relief of around 200 m, and is characterized by the development of inner terraces (figs. 7b, c). Along the whole course of the Angitola slope channel, outer levees are in general very narrow and have low relief over the adjacent slope areas (fig 7b). Mass-wasting scars and slump deposits are present in the flanks of the channel and the surrounding slope sediments, particularly in the lower reach of the channel (figs. 5, 7c). In the Lametini-Alcione flat, two low relief valleys, around 15 km large, bottomed by several smaller scale channels are present; they are likely originated by sediment gravity flows that originate owing to the widespread instability processes that characterize the intermediate slope (fig. 5). The lower reach of the Stromboli valley runs in the southern part of this sector of the Calabrian margin (fig. 5); however, since it originates in the Gioia Basin it will be described in the following section.

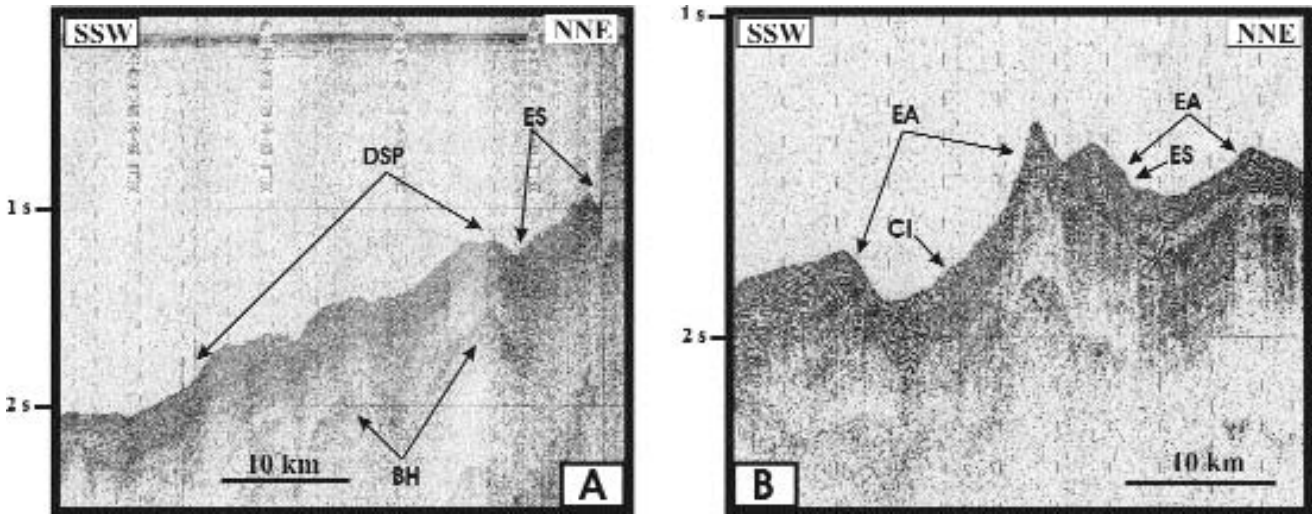

Fig. 6. – *a) Seismic line T9672 crossing the intermediate slope of the Calabrian margin. See text for further explanations (ES = evacuation surface; DSP = packages of deformed downslope translated sediments; BH = basement high). b) Seismic line T9666 over the areas of focussed erosion in the lower intermediate slope (EA = erosional areas; ES = evacuation surface; CI = chaotic infill).*

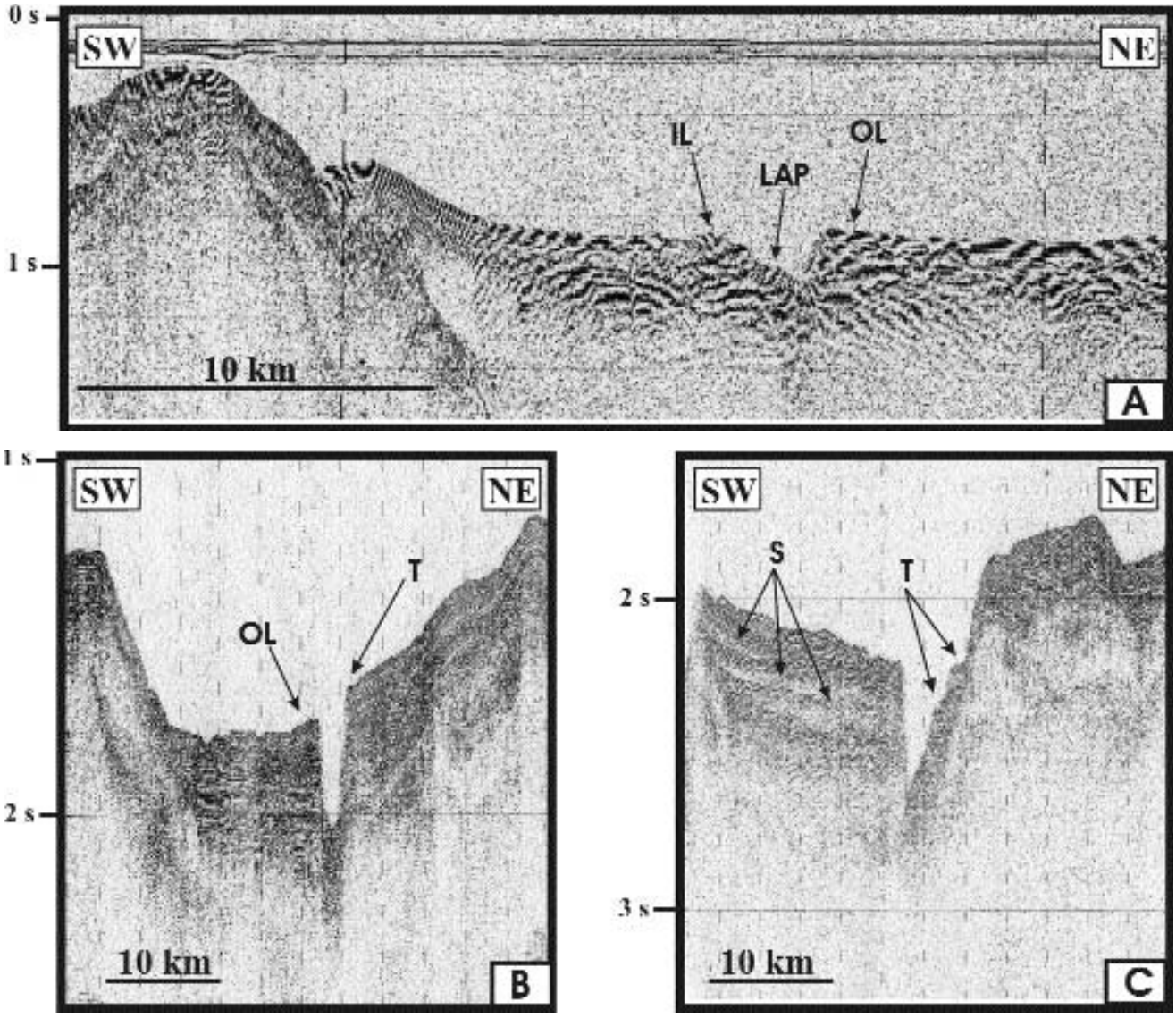

Fig. 7. – *Seismic lines showing the downslope variations in the Angitola slope channel.* ***a)*** *Upper, meandering segment of the Angitola slope channel (line T99221). The asymmetry of the channel is due to outer bend erosion and deposition of lateral accretion packages (LAP) on the inner bend (OL = outer levee; IL = inner levee).* ***b)*** *Intermediate segment of the Angitola slope channel (line T9664). Note the very low-relief and small areal extent of the outer levee (OL) on the southern side of the channel (T = terrace).* ***(c)*** *Lower reach of the Angitola slope channel (line T9666) showing inner terraces developed in the left side of the channel. Transparent packages (S) in the surrounding slope are slump bodies due to instability likely fostered by the canyon dynamics.*

4. - GIOIA BASIN

Gioia Basin is a SW-NE trending trough enclosed between Sicily and Calabria to the SE and the Aeolian Island arc to the NW (fig. 8). It has a length of about 80 km and a width that increases from 40 to 80 km northeastward; the basin axis that is the site of the Stromboli canyon deepens northeastward from to 1000 to 1500 m (fig. 8). Gioia Basin was formed as a result of the extensional tectonics that affected the circum-Tyrrhenian regions from late Miocene (FABBRI *et alii* 1980) Different slope and base-of-slope depositional systems, each characterized by specific sedimentary environments and processes, co-exist along the Gioia basin margin (figs. 8, 9a) (GAMBERI & MARANI 1998). The Milazzo and the Niceto canyons are developed in the southwestern slope sector; in particular, the Milazzo canyon is an up to 400 m deep erosional feature. The canyons pass downslope to leveed-channels with an average width of around 2 km and levees that elevate up to 100 m from the channel floor and display at times sediment waves (fig. 9a). The leveed-channels coalesce into a prograding channel-levee system that spans the Sicilian margin for a total width of 20 km (figs. 8, 9a). To the northeast of the channel-levee system, a destructional slope is present; the recent Villafranca mass-transport complex, with an average width of 10 km and a length of around 25

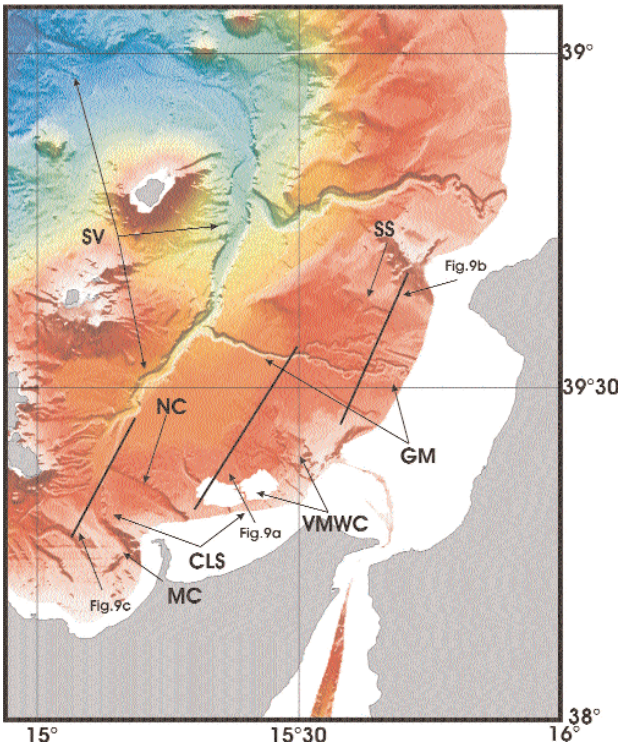

Fig. 8. – *Colour-shaded map of the Gioia basin (MC = Milazzo canyon-channel; NC = Niceto canyon-channel; CLS = Channel-levee system; VMWC = Villafranca mass-wasting complex; GM = Gioia-Mesima slope channel; SS = slump scars; SV = Stromboli valley).*

km occupies in fact the whole slope and basin plain down to the Stromboli valley. Mass-wasting is widespread also in other sectors of the basin and in deeper stratigraphic levels as evidenced by transparent and chaotic mounded bodies at different heights in the Gioia basin infill (fig. 9a). The Gioia-Mesima slope channel occupies the northern portion of the Gioia basin (fig. 8). It starts in the Gioia Tauro coastal area (COLANTONI *et alii* 1992) and has been imaged in the bathymetric data from a depth of around 600 m. In the upper part it comprises various channels with both meandering and straight planforms and with a negative relief of around 20 m running within a wide channel-belt (figs. 8, 9b); some of the straight channel segments are flanked by abandoned meander loops that are likely the evidence of a temporal progression from meandering to straight channels (fig. 8). The various channels join at a depth of around 1000 into a single trunk that deepens downslope to reach a negative relief of around 200 m in its distal part close to the junction with the Stromboli valley (figs. 8, 9a). The channel is v-shaped and a narrow levee is developed in its right side (fig. 8).

In the southwestern portion of the Gioia basin, the Milazzo, the Niceto channels and numerous chutes and valleys that run in the Vulcano volcaniclastic apron (GAMBERI 1998) join to originate the Stromboli axial sea valley. This valley runs in the central portion of the Gioia basin and after a turn to E-W strike, north of Stromboli Island, reaches the Marsili back-arc basin. Along its course it receives numerous tributaries from the Sicilian and Calabrian margin and from the Aeolian volcanic slope (fig. 8). The proximal segment of the Stromboli valley is flat-bottomed with a maximum width of around 6 km and is flanked on its right side by a depositional levee (fig. 9c). A first morphologic change occurs where the valley crosses a basement step located at the base of the Panarea volcanic edifice; here the valley is 400 m deep and only 2,5 km wide and slump scars, terraces and gullies characterize its flank. At a depth of around 1900 the Stromboli valley resumes a flat-bottomed morphology and a wider cross-sectional area and is characterized by a meandering thalweg running in the valley floor; in this area the valley has an aggradational character as evidenced by a thick chaotic infill above the erosional margin of the valley and by the seafloor sedimentary features (GAMBERI & MARANI 2003). After the turn north of Stromboli Island the valley maintains a large width (up to 10 km) is characterized by braiding thalwegs and retains a mainly aggradational character down to its debouching into the Marsili basin.

5. - CEFALU BASIN

The Cefalu basin, with a length of around 150 km, is located along the northern Sicilian margin (fig. 10). The basin was originated through various phases of extensional tectonics of mainly Pliocene age. Tectonic structures were oriented with NE-SW and NW-SE and E-W direction (FABBRI *et alii* 1981; PEPE *et alii* 2000). The interaction of the various trends of the tectonic structures resulted in the Finale intrabasinal high that separates the Cefalu basin into the Orlando Basin to the east and the Palermo basin to the west (WEZEL *et alii* 1981).

The Orlando basin is around 50 km in width and 80 km in length and is completely confined to the north by the ridge of the Aeolian volcanic arc; the basin plain is flat and lies at a depth of around 1500 m (fig. 10). The Orlando basin was investigated by multibeam swath bathymetry up to depth of around 500 m and as a consequence the bathymetric data cover the slope, the base-of-slope and the basin plain (fig. 10). In the eastern sector, that is directly connected with the emerged areas, a system of canyons that evolves downslope into a channel-levee system is evident. The channels have a NW-trending course and are as much as 6 km wide; they are mainly flat-bottomed and are flanked by levees that elevate up to 100 m from the adjacent channel floor (fig. 11a). Seismic lines evidence that the channels migrate toward the west in time and that as a whole the channel-levee system is prograding with a NW trend over the basin-plain deposits (fig. 11b). This evolution appears to reflect the location of the main sediment entry points in the Milazzo and the Aeolian arc areas.

The western portion of the Orlando basin is on the contrary flanked to the south by the Palermo basin and as a consequence it is not directly connected to

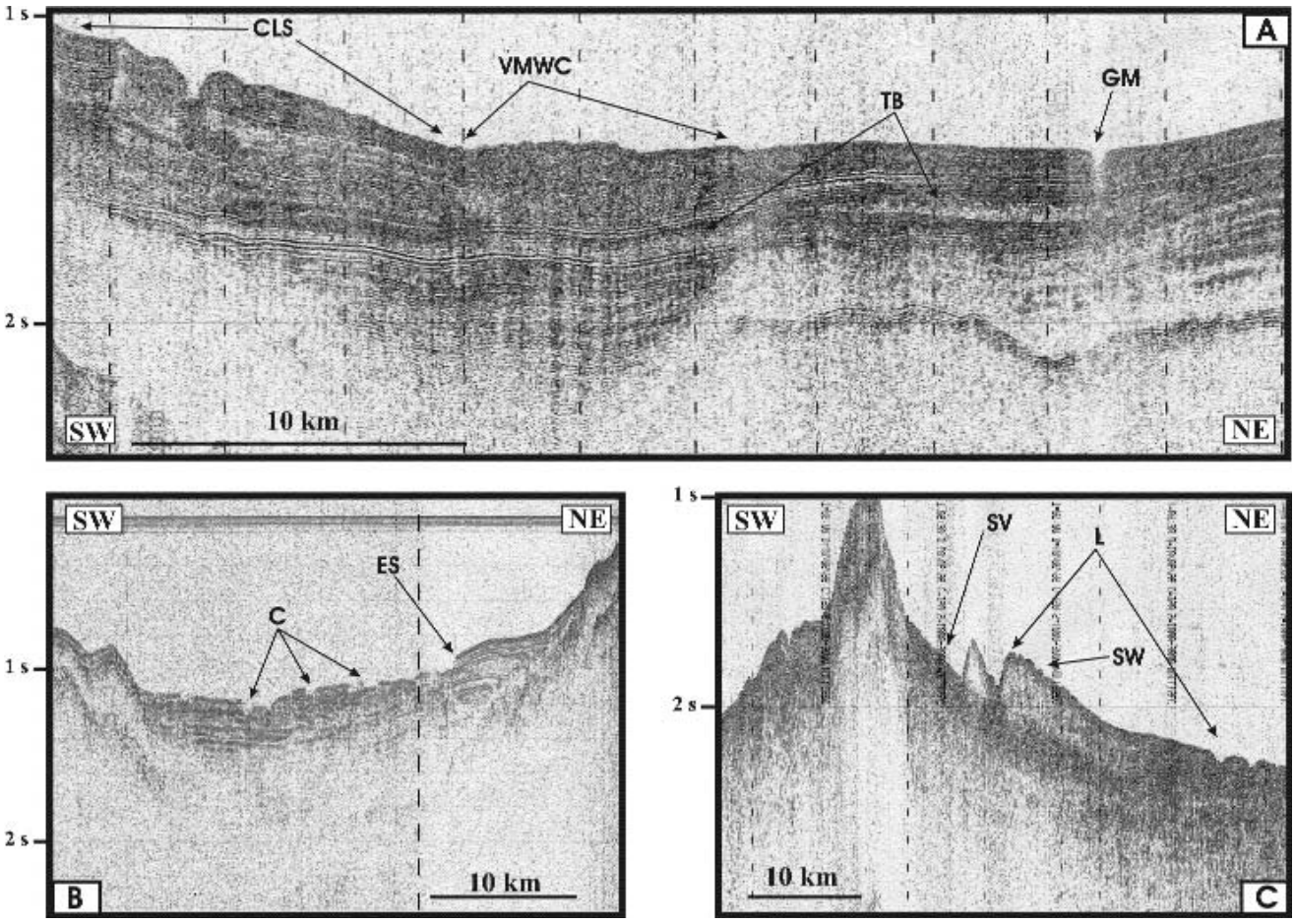

Fig. 9. – *a) Seismic line T9662 crossing the different sectors of the Gioia basin. The channel-levee system (CLS) is visible in the southern side of the line and is flanked in the centre by the Villafranca mass-wasting complex (VMWC), a thick package of transparent and chaotic reflections. Laterally, smaller scale slump bodies (TB) are present within the Gioia basin infill. In the northern portion, the distal segment of the Gioia- Mesima submarine conduit (GM) is evident. b) Seismic line over the upper segment of the Gioia-Mesima slope channel (C = channel; ES = evacuation surface). c) Seismic line T9966 running along the Stromboli Valley (SV), showing the coarse-grained high reflective infill of its upper trunk and its right levee with sediment waves (SW) displaying downslope decreasing height. The levee deposits (L) present a thickness that diminishes downslope to completely disappear where the canyon is a mainly erosional feature.*

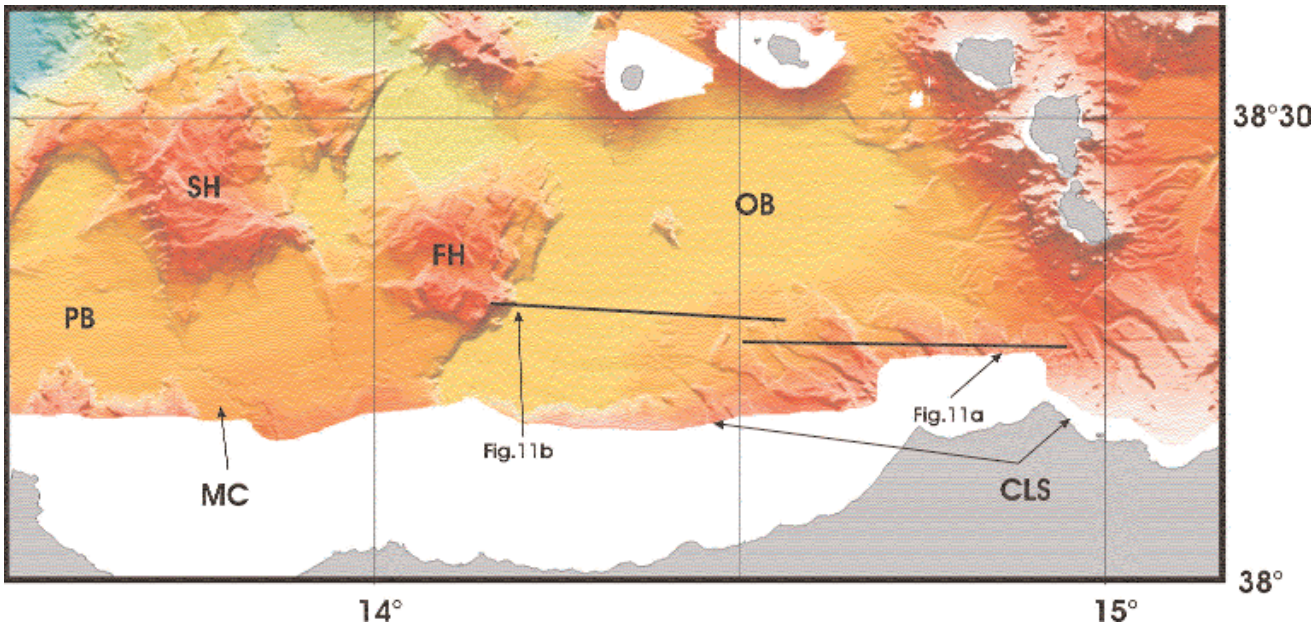

Fig. 10. – *Colour-shaded map of the Cefalù basin (OB = Orlando basin; PB = Palermo basin; FH = Finale high; SH = Solunto high; CLS = channel-levee system; MC = meandering channel).*

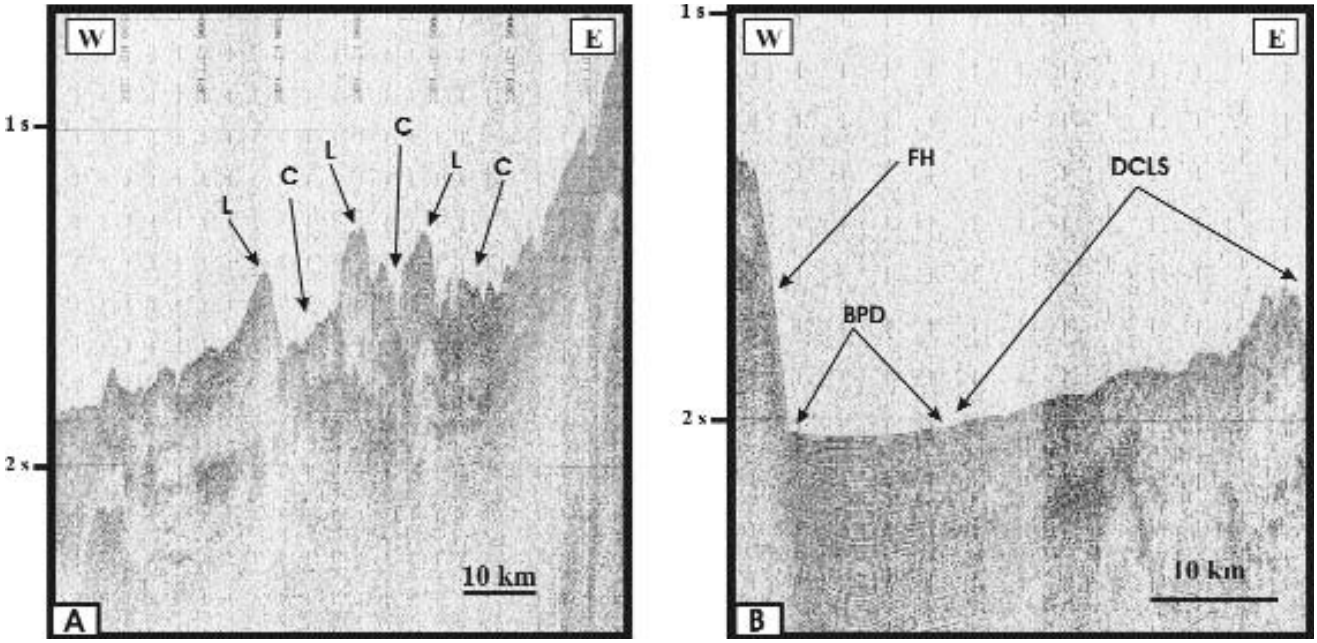

Fig. 11. - *Seismic lines over the Cefalu' Basin. a) Proximal part of the channel-levee system in the Orlando basin. See text for further details (C = channel; L = levee). b) Distal part of the channel levee-system (DCLS) and transition to basin plain deposits (BPD) with continuous parallel reflections indicative of distal sheet turbidites onlapping the Finale high (FH).*

emerged areas. Due to reduced sediment input destructional processes characterize the slope that in the seismic lines is onlapped by the basin-plain deposits. Sediments are fed to the Orlando basin also from the slope of the Alicudi and Filicudi volcanoes; a volcaniclastic apron consisting of thick packages with chaotic seismic facies mantles in fact the submarine portions of the edifices and interfingers with the distal basin plain sediments.

The Palermo basin is directly connected to the emerged areas only to the east and west; in its central portion in fact the Termini basin is interposed between the Sicilian platform and the Palermo basin (PEPE *et alii* 2003). The resultant basin morphology consists therefore of a narrow 20 km wide trough elongated in WNW-ESE. Few data have been acquired over the slopes that surround the Palermo basin; the main interesting feature that emerges from the combination of multibeam bathymetric data and seismic lines is a basin axis fan fed by a shallow meandering channel (fig. 10).

6. - SARDINIAN MARGIN

The Sardinian margin is characterized by the upper slope, various intraslope basins elongated parallel to the margin with a depth variable between 1500 and 1700 m and the Cornaglia Terrace that lies at a depth comprised between 2500 m and 3000 m. A basement step at a depth of around 3000 m separates the Cornaglia Terrace from the western portion of the Vavilov basin. To the north, the Etruschi and the Baronie ridges bound seaward the Olbia and the Baronie basins; further elevated basement blocks and intervening confined basins, the largest of which are the Tavolara and the Vercelli ones, are developed between the Etruschi and the Baronie highs and the Cornaglia Terrace (fig. 12). To the south, on the contrary, a single elevated ridge that spans northward from the Quirra seamount marks the deepening from the Ogliastra and Sarrabus-Ichnusa intraslope basins to the Cornaglia Terrace (fig. 12). The Sardinian margin was formed during extensional tectonics of mainly post-Messinian age (SARTORI *et alii* 2001). The tectonic structures are mainly oriented in N-S to NNE-SSW and E-W directions (SARTORI *et alii* 2001). The present-day morphologic differences between the southern and northern sectors reflect the progressive eastward rift migration in the northern area at variance with a stable rifting locus in the southern area (SARTORI *et alii* 2001).

The Olbia basin is the northernmost intraslope basin; being flanked by a 20 km large platform and by a very large slope with a width of around 50 km it lies at a distance of around 70 km from the coastline (fig. 12). The Olbia basin has a length of around 70 km and a maximum width of around 30 km. The slope is incised by single canyons and by canyon systems consisting of various upper slope trunks that connect downslope into single canyons (fig. 12). The Caprera is the largest canyon system and consists of two tributaries in the upper slope that join in a single, 2.5 km wide canyon, at a depth of around 1000 m (figs. 12, 13a). An abandoned canyon is still morphologically expressed in the bathymetry presenting a passive infill consisting of plane parallel reflections (fig. 13a). It has a deeper level of incision than the presently active canyons (fig. 13a).

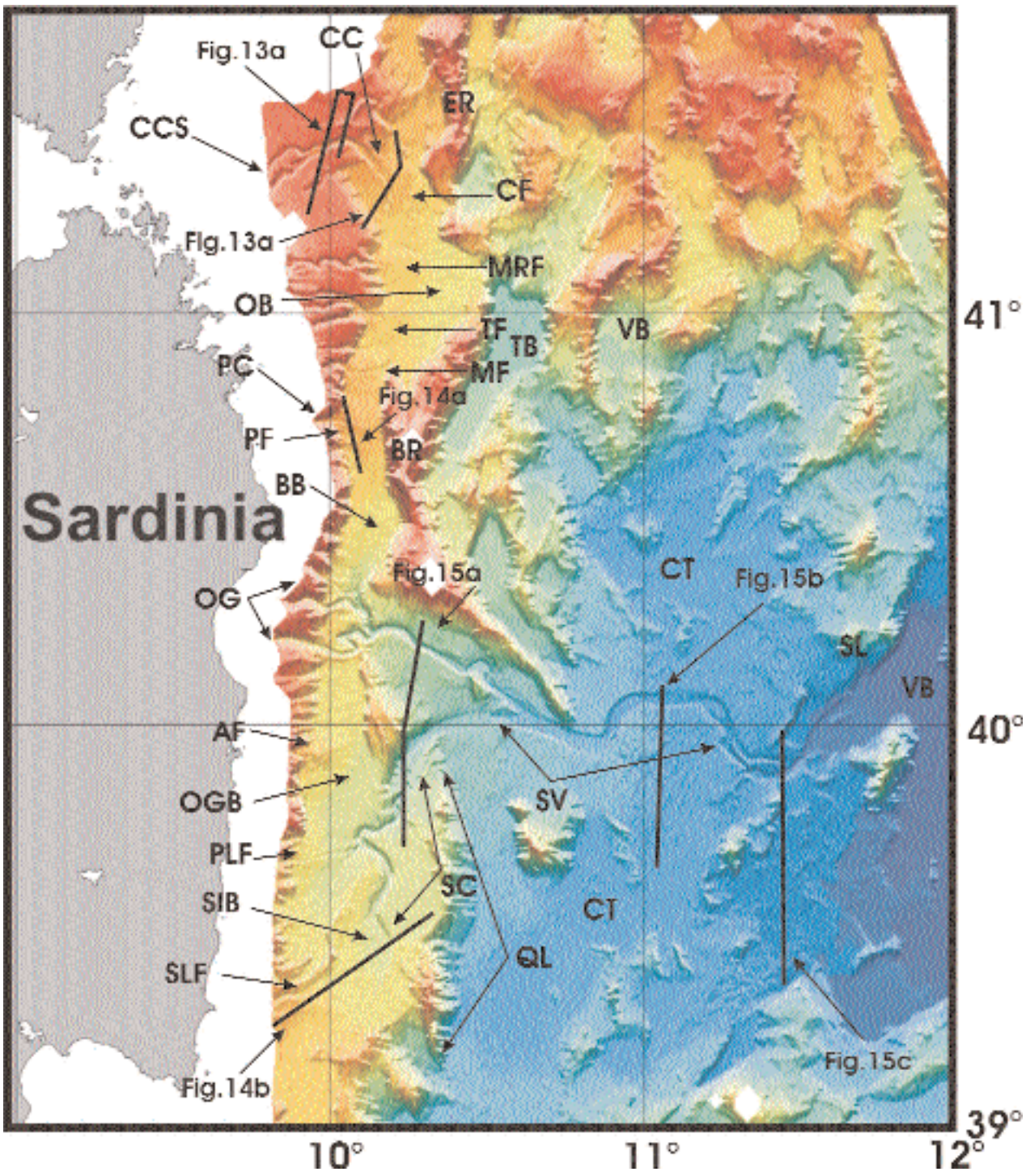

Fig. 12 . – *Colour-shaded map of the Sardinian margin (CC = Caprera channel; CCS = Caprera canyon system; ER = Etruschi ridge; CF = Caprera fan; MRF = Mortorio fan; OB = Olbia basin; TF = Tavolara fan; TB = Tavolara basin; MF = Molara fan; VB = Vercelli basin; PC = Posada canyon; PF = Posada fan; BR = Baronie ridge; BB = Baronie intraslope basin; OG = Orosei-Gonone canyon system; AF = Arbatax fan; OGB = Ogliastra intraslope basin; PLF = Pelau fan; SIB = Sarrabus-Ichnusa intraslope basin; SLF = San Lorenzo fan; SC = Sarrabus canyon; QL = Quirra lineament; CT = Cornaglia terrace; SV = Sardinia valley; SL = Selli line; VB = Vavilov basin).*

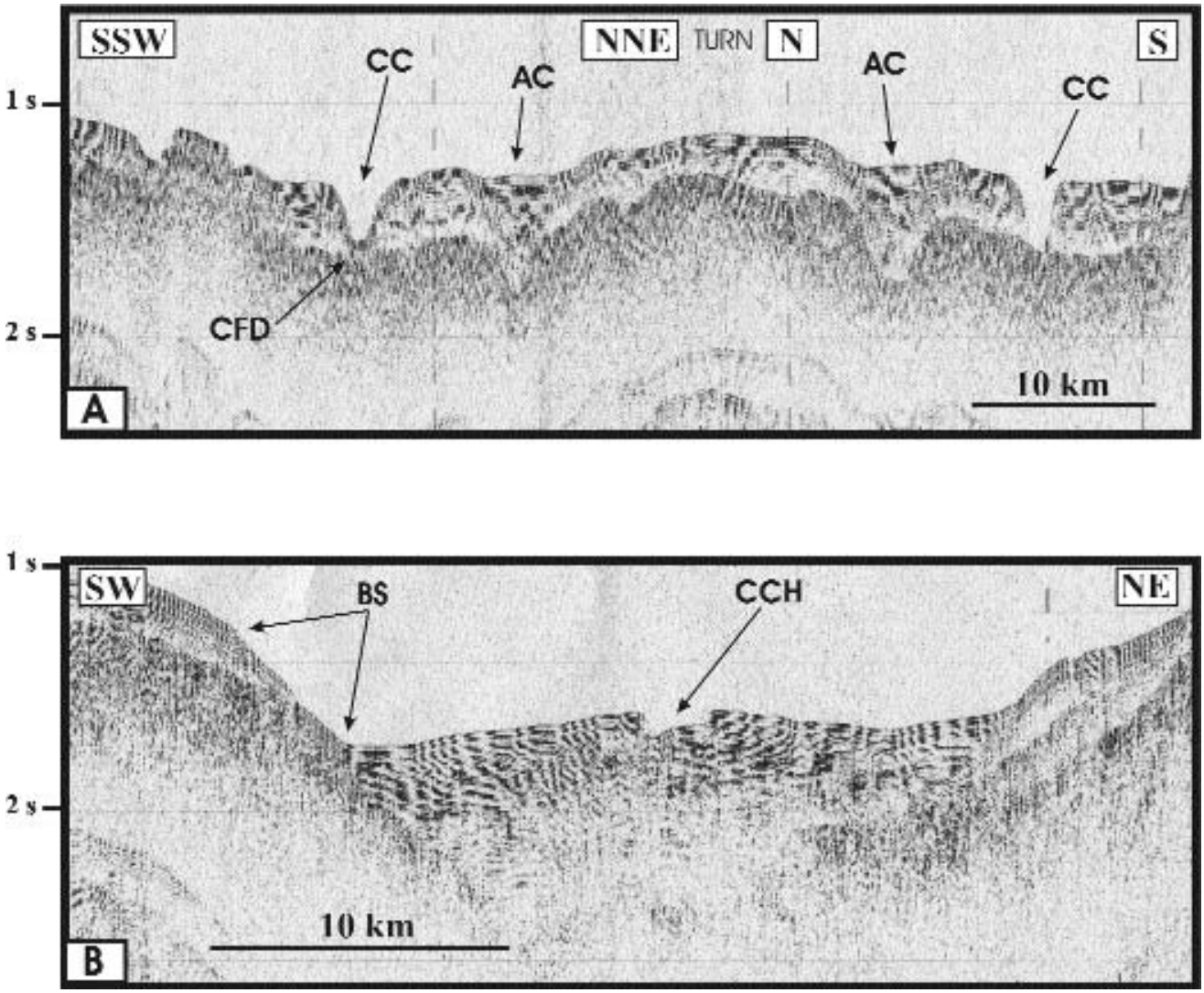

Fig. 13. – *a) Two crossings (lines T99101 and T99102) of the Olbia Basin slope and of the Caprera canyon system. The lines cross the single trunk segment of the Capreera canyon (CC); downslope variations in the sediment-gravity flows result in the presence of a thin high amplitude reflection in the canyon floor (CFD) that is not present in the downslope following line. Note an abandoned canyon (AC) that incises the slope to a deeper level than the present-day one. b) Line T99105 crossing the northern portion of the Olbia Basin site of the Caprera leveed-channel (CCH). A small inner thalweg is present in the southern side of the channel. Note that the lower slope of the Olbia basin (BS) is mainly affected by sediment bypass.*

At the base-of-slope the Caprera canyon evolves into a leveed channel with a width of 2 km with levees that elevate up to 100 m above the channel floor (fig. 13b). Further downslope, in the axis of the basin, the Caprera channel gives way to small relief channels that run on the surface of the Caprera fan spanning much of the northern portion of the Olbia basin (fig. 12). The fan surface is characterized by bifurcating channels that become shallower downslope. In the southern basin portion, smaller scale canyon-mouth fans with a radius in the order of 5 km face the Mortorio, Tavolara and Molara canyons (fig. 12). The Baronie basin is a narrow, 10 km wide and around 60 km long, trough that deepens southward from 1300 m to 1800 m, bounded seaward by the Baronie ridge that tops at around 80 m below sealevel (fig. 12). The northern slope portion of the basin is incised by the up to 400 m deep Posada canyon, while the Orosei-Gonone canyon system represents the southern margin of the basin. The slope between the Posada and the Orosei-Gonone canyon system presents the unique tract in the Sardinain margin of being completely devoid of canyons (fig. 12). At the base-of-slope the Posada canyon evolves into a leveed channel and further downslope into a branching channel pattern running on the surface of a fan with an along basin length of around 10 km, spanning the whole basin transversally (fig. 14a). Channels with a negative relief in the order of 20 m continue beyond the extent of the fan and run in the axial part of the basin with a braiding pattern between depositional longitudinal bars. At the southern end of the basin they connect into a single erosional feature with an erosional relief uf up to 100 m that then joins the Orosei-Gonone canyon system.

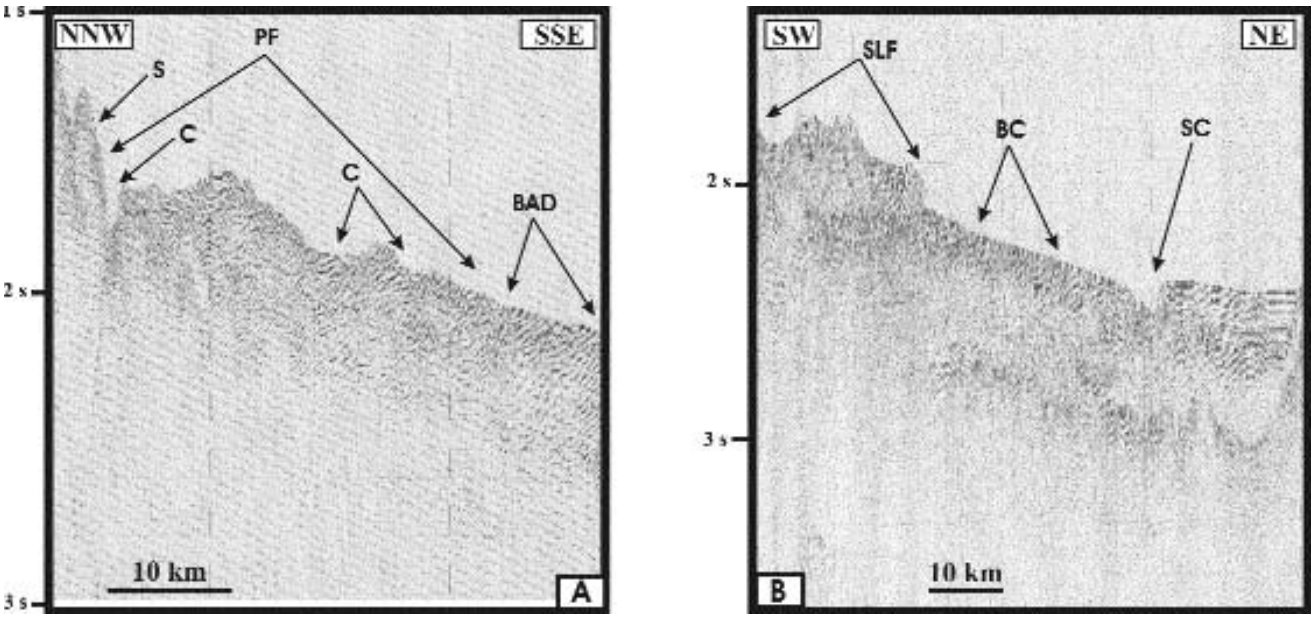

Fig. 14. – *a) Strike seismic line (T9916) over the Posada fan (PF). A major channel (C) scours the northern side of the fan at the base-of slope (S); smaller-scale channels (C) are however evident further downslope. Note the abrupt termination of the fan over basin axis deposits (BAD). b) Dip seismic line (T9929) over the San Lorenzo Fan (SLF); a network of braiding channels (BC) is present downslope of the fan, connecting with the Sarrabus canyon (SC).*

The Orosei-Gonone system spans the Sardinian margin for a length of around 20 km and consists of 3 canyons (fig.12). The Gonone canyon incises the slope at a depth of around 500 m. At the base-of-slope the various canyon of the system evolve into leveed channels that connect in a single trunk at a depth of around 1800 m. The levees are very narrow. Downslope of the junction, the Gonone-Orosei system is straight, has a levee in the right side while slumping dominates the left side adjacent to the southern tip of the Baronie ridge (fig. 15a); an abrupt turn of the channel at a depth of 2300 m (fig. 12) corresponds to the obstruction of a salt diapir that pierces the seafloor. The Ogliastra and the Sarrabus-Ichnusa intraslope basins develop south of the Gonone Orosei drainage system and are separated by a very subdued intraslope high. Canyons that incise the slope and canyon-mouth channelized fans are the main features of the Ogliastra basin. The Arbatax fan is the largest fan and having around 15 km length, occupies much of the basin with its distal portions adjacent to the Quirra high (fig. 12). The proximal part of the Arbatax fan is scoured by a single, up to 50 m deep meandering channel that loses relief downslope and repeatedly branches into numerous low-relief channels. A smaller-scale fan is developed at the mouth of the Pelau canyon; the Pelau channel that runs in its surface continues beyond the fan as a single v-shaped 50 m deep feature that connects with the Sarrabus canyon (fig. 12). At the southern limit of the investigated slope portion, in the Sarrabus-Ichnusa basin, the Picocca submarine drainage network originates the San Lorenzo fan characterized by a complex morphology that likely reflects the control of basement highs over depositional processes (figs. 12, 14b). The main morphologic feature of the Ichnusa-Sarrabus basin is the axial Sarrabus canyon that runs in the axis of the basin (fig. 12). It nucleates as a single evident erosional feature at a depth of around 1700 m but appears to be connected upslope to a braided valley consisting of a widespread area of less focused seafloor erosion (fig. 14b). The Sarrabus canyon gradually enlarges and widens downslope within the axis of the basin (fig. 12); however, a striking increase in both relief and width is evident where the canyon crosses the Quirra tectonic lineament. Here the canyon is up to 400 m deep and up to 8 km large; much of the morphologic change appears to be related to undercutting and related slumping of the slope deposits flanking the erosional fairway (fig. 15a).

The Sarrabus Canyon and the Orosei-Gonone system connect at a depth of around 2600 forming the Sardinia Valley that crosses the whole Cornaglia Terrace and reaches the Vavilov abyssal plain (fig. 12). The Sardinia valley is mainly flat bottomed with an average width of around 5 km and a floor that lies around 100 m below the surrounding basin plain (fig. 15b). A breach in the right, outer valley flank coincides with a northward turn of the valley at a depth of around 2800 m (fig. 12); it could represent an avulsion point as also shown by the sedimentary features of the Cornaglia Terrace downslope of the breaching point (fig. 15b). In the crossing of the Selli Line, the Sardinia Valley becomes strongly erosive with a v-shaped profile and a depth of more than 200 m (fig.15c). In addition, a recent southward shift has occurred in this area; an abandoned fairway is in fact visible hanging north over the present-day active Sardinia Valley (fig.12).

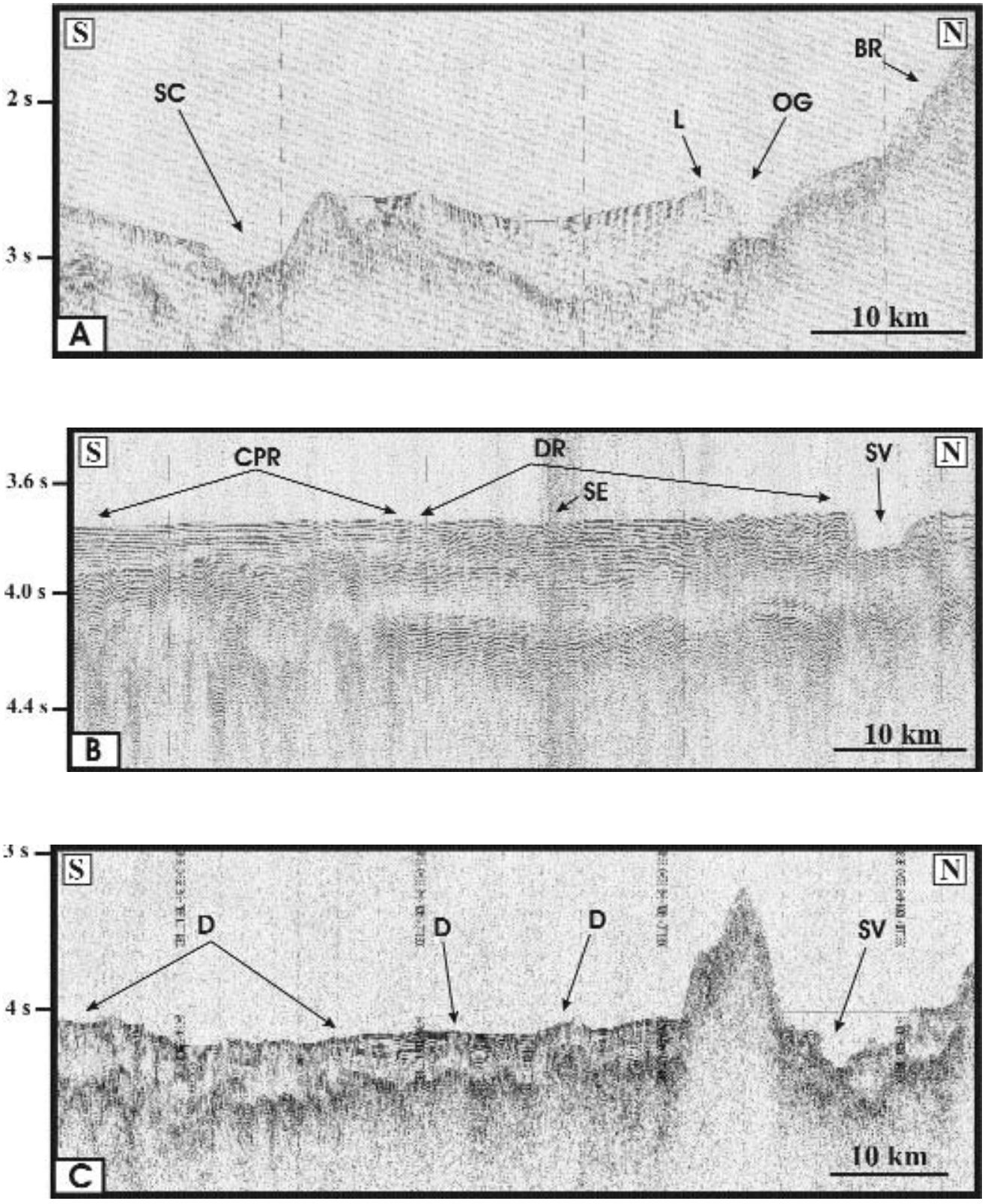

Fig. 15. – *a) Seimic line T9916 crossing the distal portion of the Sarrabus canyon (SC); the erosional conduit is much more incised in the surrounding slope deposits than in figure 14b. The distal portion of the Orosei-Gonone canyon system (OG) is imaged to the north at the base of the Baronie ridge (BR); a small levee (L) is developed in the right side of the conduit. b) Seismic line T9925crossing the Sardinia valley (SV). Note the seafloor erosion (SE) in the centre of the line that is underlied by highly discontinuos reflections (DR) at variance with the continuous parallel reflections (CPR) further south ; it could represent a conduit developed in the Cornaglia terrace as a consequence of avulsion of the Sardinian valley in correspondence of a tight northward turn. c) In correspondence of the Selli line the Sardinia Valley (SV) resumes an highly erosive character. South of the Sardinian Valley, the Cornaglia Terrace is the site of salt diapirs (D); some of them pierce the whole sedimentary package and are evident at the seafloor.*

7. - VAVILOV BASIN

The Vavilov basin, dating back to 6 Ma is the oldest back arc basin of the Tyrrhenian region (KASTENS & MASCLE 1990). The D'Ancona ridge and the Vavilov volcanic seamount separate the Vavilov basin into two distinct areas: the Gortani basin to the northeast and the Magnaghi basin to the southwest (fig. 16).

The distal portion of the Sardinia Valley, the main submarine sedimentary pathway that collect siliciclastic sediments from the Sardinian passive margin runs in the Magnaghi basin south of the D'Ancona ridge (fig. 16). It is a very low-relief channels that does not terminate with any evident depositional body; likely because much of the coarse-grained sedimentary load of the Sardinia valley is deposited in the Cornaglia terrace and only high-efficencies flows reach the deep basin. In the Gortani basin, adjacent to the base of the Campanian slope, recently acquired high resolution seismic data show that a depositional fan with a very low areal extent (radius of around 5 km) is present at the mouth of the Ischia Valley (GAMBERI *et alii* 2003). The main seismic characteristic of the sedimentary infill of both the Gortani and Magnaghi basins is that of continuous parallel reflections evidence of distal turbidites with a basin-wide areal extent (fig 17a). This pattern is interrupted however by a thick acoustic transparent layer (ATL) at a depth of around 50 m (fig. 17a). As a matter of fact, recently acquired chirp data have shown that at least 4 ATLs are present within the recentmost basin infill (GAMBERI *et alii* 2003). The thickness and areal extent of the deeper, thicker ATL, shown in figure 17, leads to a volume of around 150 km^3.

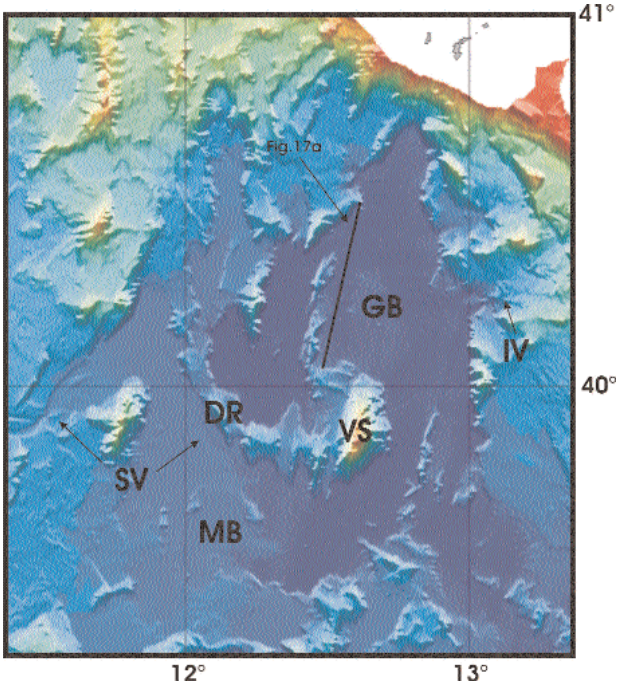

Fig . 16. – *Colour-shaded map of the Vavilov basin (GB = Gortani basin; MB = Magnaghi basin; VS = Vavilov seamount; DR = D'Ancona ridge; SV = distal segment of sardinia valley; IV = distal segment of Ischia valley).*

8. - MARSILI BASIN

The Marsili basin occupies the deepest portion of the southeastern Tyrrhenian Sea and lies at a depth of around 3300 m. The Stromboli valley funnels to the eastern portion of the Marsili basin a large input of siliciclastic and volcaniclastic material. As a consequence, a deep-sea fan is developed, with apex in the eastern basin margin and distal portions that reach the base of the Marsili seamount (fig. 18) The fan has a length of 40 km and a width of 20 km, and is fed by various branching channels that scour the surface of the fan down to its distal part (figs. 17b, 18). Lobes are developed at the mouth of the channels that at times display the development of outer levees and intra-channel longitudinal bars (GAMBERI *et alii* 2003). The resulting seismic facies consists of highly discontinuos reflection arranged in lens-shaped bodies and frequent erosional surfaces.

A markedly different depositional environment characterizes the western portion of the basin sheltered by the Marsili seamount from the main sediment entry points (fig. 18). Here, distal turbidites with continuos, basin-wide parallel reflections are evident; sedimentation rate is however very high with a thickness of quaternary deposits of 650 m (HIEKE *et alii* 1990).

Besides the Stromboli valley, the surrounding steep slopes feed sediments to the basin. In particular, a volcaniclastic input to the northeastern portion of the basin occurs through chutes and channels that develop on the southern slope of the Palinuro volcanic complex and on the northern slope of the Aeolian volcanic arc (fig.18).

9. - CONCLUSIONS

The present-day morphosedimentary features and the character and distribution of depositional systems within the Tyrrhenian Sea reflect the recent geological evolution of the area consisting of distinct, eastward migrating episodes of extensional tectonics and backarc basin opening. Numerous intraslope basins, bounded seaward by fault blocks, are located along the rifted Latium-Campanian, Calabrian, Sicilian and Sardinian margins that surround the two abyssal plains of Vavilov and Marsili, where extensional tectonics has progressed up to back-arc basin formation. Due to the variability in age and style of the tectonics that have shaped the different margins and of the present-day geodynamic setting of the adjacent emerged areas, however, contrasting sedimentary processes are active and are responsible for the distinct depositional

settings of the intraslope basins.

A striking difference emerges for example between the depositional architecture of the Sardinian passive margin and that of the Cefalu and Gioia basins located along the Sicilian active margin. While both margins have slopes with numerous canyons, they show a markedly different setting of deposition at the base-of–slope. The Sardinian intraslope basins (Olbia, Baronie, Ogliastra and Ichnusa-Sarrabus) are in fact characterized by the development of distinct mounded depositional bodies with circular or elongated planform and dimensions up to 15 km consisting of small fans developed at the mouth of the main canyons. In the Cefalu and in the Gioia basins, on the contrary, canyons pass downslope to leveed channels that at the base-of slope build a prograding wedge of channel-levee deposits forming a constructional depositional apron elongated along the basin margin. Different sedimentary processes are also responsible for the destructional slope sectors that characterise both the Sardinian and the Sicilian margin. In the Gioia basin in fact a 20 km wide slope sector is affected by seafloor instability that results in the Villafranca mass-wasting complex straddling transversally the whole basin. In the Sardinian margin, on the contrary, slope destruction occurs through erosion focused along canyon systems that in the case of the Orosei-Gonone system affect a slope sector with a longitudinal dimension of 20 km.

In spite of a general fundamental homogeneity of the depositional tracts of the single margins, major differences do however still arise when comparing single intraslope basins along the same margin. Variations in canyon morphology and distribution are evident in the slope of the Sardinian margin intraslope basins. In the Olbia basin slope, isolated, widely-spaced canyons or canyon systems are present; in the Ogliastra basin a network of closely spaced canyons, at times with merging flanks, dissect the slope; the Baronie basin slope is completely devoid of canyons

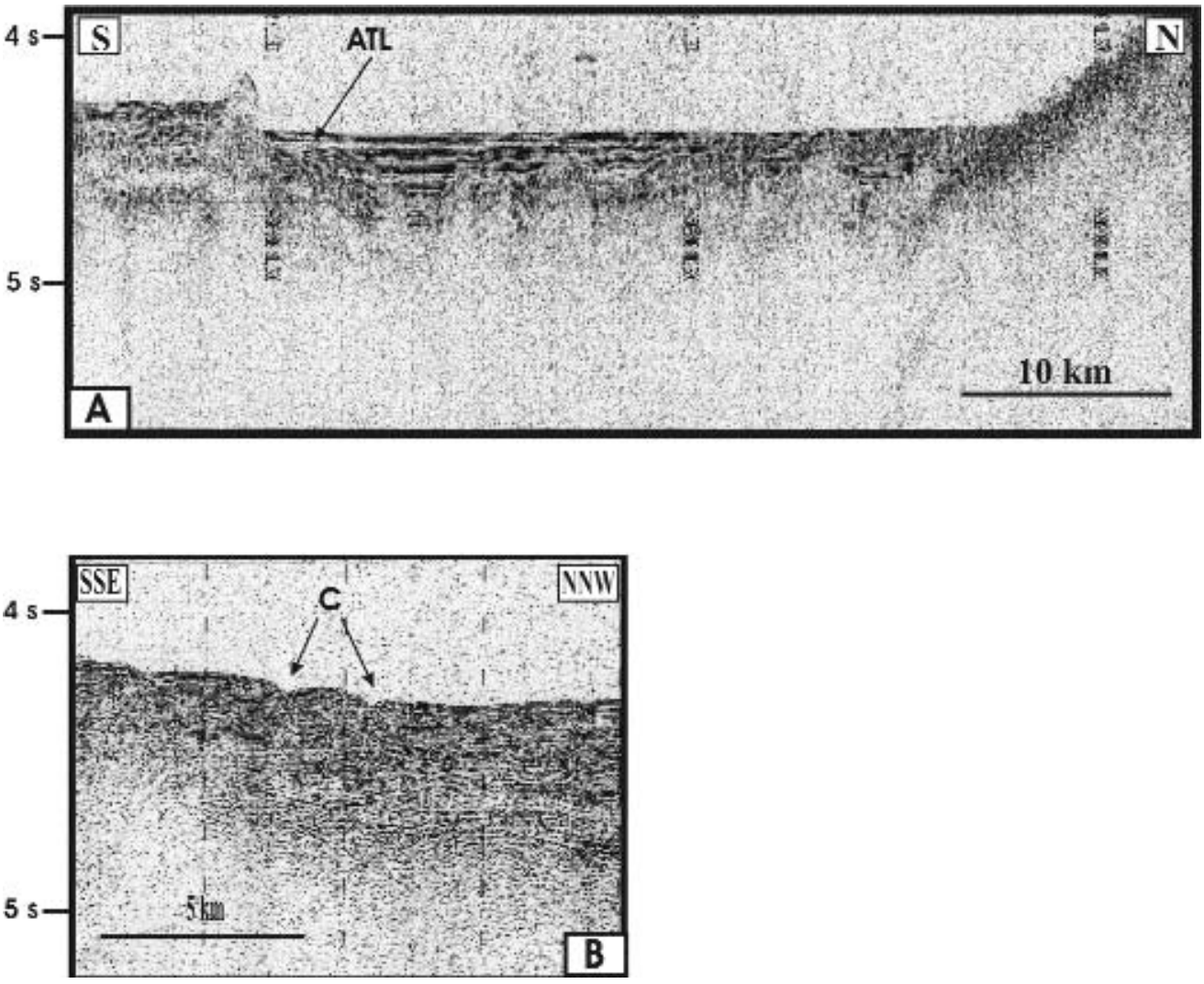

Fig. 17. – *a) Seismic line over the Gortani Basin showing the continuous and parallel character of the reflections within the basin infill; however a transparent layer (ATL) is evident in the upper portion of the basin infill. b) Seismic line crossing the Marsili basin deep-sea fan; channels (C) are evident on the surface of the fan.*

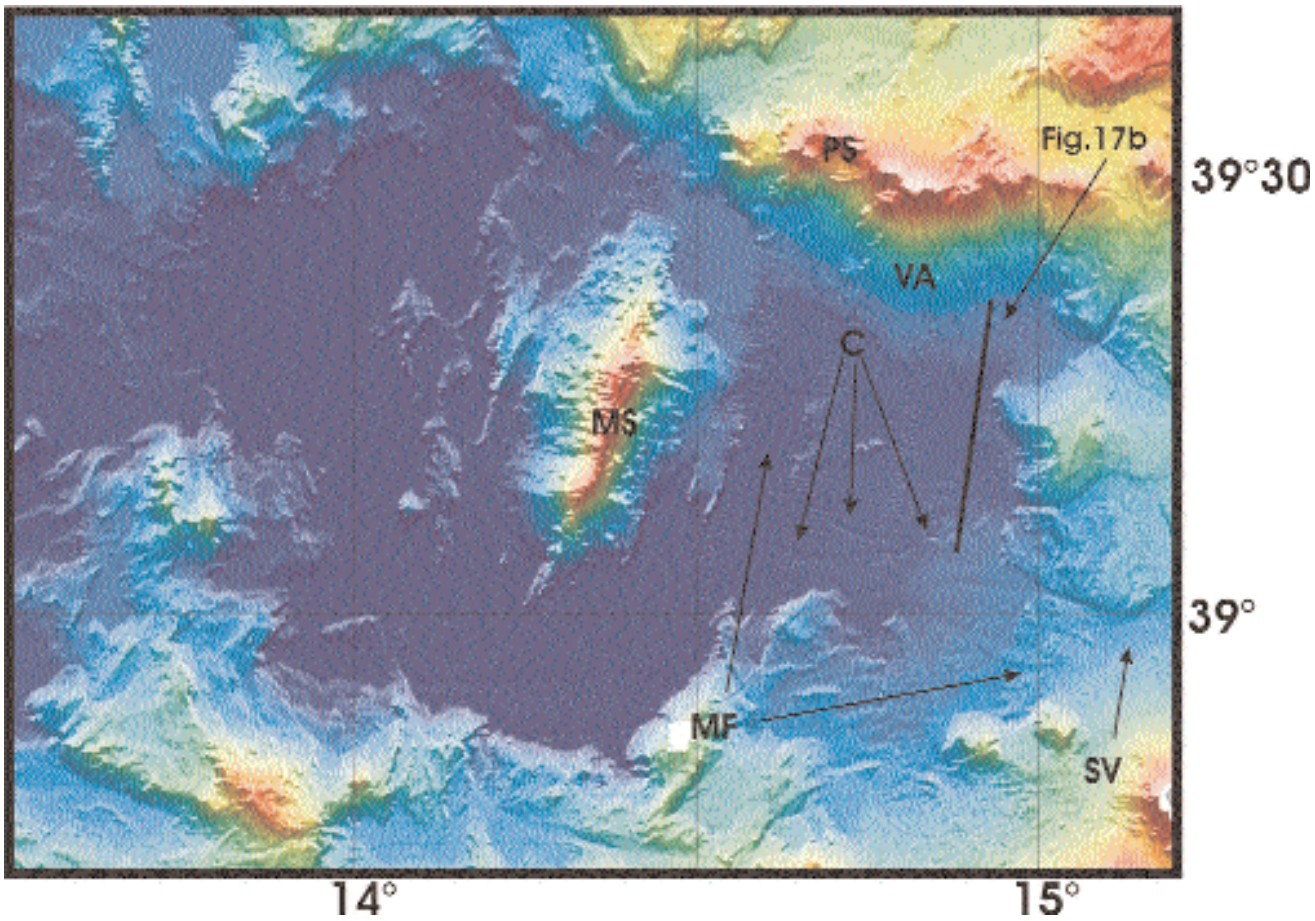

Fig. 18. – *Colour-shaded map of the marsili basin (MF = Marsili fan; SV = Stromboli valley; MS = Marsili seamount; PS = Palinuro seamount; VA = volcaniclastic apron; C = channels).*

while the large Posada and Orosei-Gonone canyon systems are developed at its southern and northern margin. A different stage of slope erosion, with the mature Olbia basin slope canyons and Posada and Orosei-Gonone systems as compared to the younger fairways in the other slope areas can be envisaged to explain the observed differences. In addition, variations in the character of the sediment-gravity flows running within the canyons can be reasonably expected. As a matter of fact, differences in the architecture and dimensions of the base-of-slope fans developed at the canyon mouths can be explained by variations in the efficiency of the sediment-gravity flows delivered to the base-of-slope. The Olbia fan has in fact a proximal leveed channel that passes downslope to a radiating network of distributary channels in the distal fan portions closely matching the architecture of fine-grained fan models. All the other fans, on the contrary, develop a radiating pattern of channels, with diffent planforms and extending directly from the canyon mouth, more akin to coarse-grained fan models.

Markedly different depositional environments characterize even adjacent sectors of single intraslope basins. In the case of the Gioia Basin for example, a constructional slope apron made up of prograding channel-levee deposits is flanked by a destructional slope area In the Orlando basin a prograding apron of channel-levee deposits is present to the west where the basin is directly connected to the emerged areas; to the east an authochtonous slope apron characterizes the slope that is separated by the emerged areas by the Palermo basin.

The deep abyssal plains of the Vavilov and Marsili basins represent the ultimate base level for the sedimentary processes active in the Tyrrhenian region. However, some of the intraslope basins such as the Cefalu and the Olbia basins are completely confined by their seaward bounding structures and represent therefore isolated depositional systems. Other intraslope basins develop, on the contrary, submarine drainage networks resulting in sea valleys that cross the whole margin and are throughoing sedimentary fairways connecting the coastal areas to the deep abyssal plain. The obstacle effect of tectonic and volcanic features control the general course of the sea valleys. This is particularly evident in Latium-Campanian margin where, due to the recent age of the tectonics that has shaped the margin, the Ischia-Magnaghi and the Dhorn Valleys are characterized by sharp bends between fault-parallel and –crosscutting segments. The control

of volcanic features is displayed by the Stromboli valley that in the Gioia basin runs toward the NE parallel to the Aeolian arc and then turns to an E-W direction in correspondence of a breach in the Aeolian arc between the Stromboli and the Lametini volcanic edifices. Tectonic features also promote changes in the sedimentary dynamics within the sea valley. The Ischia-Magnaghi and Dhorn valleys, that have a depositional character in the Ventotene and Capri basins, become highly erosive in the crossing of the Sirene and the Sartori lineaments. Also, the distal portion of the Sardinia valley undergoes a change from depositional to erosional character in the crossing of the Selli line.

In the Calabrian margin and in the Gioia Basin slope deposits have almost completely mantled the basement highs and as a consequence the Gioia-Mesima and the Angitola slope channels follow a more direct downslope route. However, the downslope evolution of the Angitola and the Mesima-Gioia slope channels, from meandering segments running through a wider depositional cahnnel-belt to straight mainly erosional segments, likely reflect changes in slope gradients in turn controlled by basement structures.

The different characteristics of the margins are also basically the major control of the depositional processes in the deep Vavilov and Marsili Basin. The Marsili basin surrounded by the active Sicilian and Calabrian margin and by the Aeolian volcanic arc receives a large sedimentary input mainly through the Stromboli valley. As a consequence it displays a deep-sea fan that occupies the eastern side of the basin with a length of 40 km a a width of 20 km. On the contrary, the Vavilov basin is mainly filled by distal sheet turbidites due to several factors. These include the distance from the Sardinian margin with the Sardinia alley depositing much of its sediment load in the Cornaglia Terrace, and the underfilled nature of the Latium-Campanian margin that stores much of the supplied sediments.

REFERENCES

ARGNANI A. & TRINCARDI F. (1993) – *Growth of a slope ridge and its control on sedimentation: Paola slope basin (eastern Tyrrhenian margin)*. Spec. Publs. Int. Ass. Sediment., **20**: 467-480.

CHIOCCI F.L., MARTORELLI E. & BOSMAN A. (2003) – *Cannibalization of a continental margin by regional scale mass wasting: an example from the central Tyrrhenain Sea*. In LOCAT J. & MIENERT J. (Eds.). Submarine mass movements and their consequences. Kluwer Academic Publishers, 409-416.

COLANTONI P., GENNESSEAUX M., VANNEY J.R., ULZEGA A., MELEGARI G. & TROMBETTA A. (1992) – *Processi dinamici del canyon sottomarino di Gioia tauro (Mare Tirreno)*. Giorn. Geol., **54** (2): 199-213.

CURZI P.V., CASTELLARIN A., VAI G.B. & ZITELLINI N. (2003) – *Raimondo Selli e Renzo Sartori una staffetta generazionale della geologia marina italiana.* In: Convegno in memoria di Raimondo Selli e Renzo Sartori. La geologia del Mar Tirreno e degli Appennini. Bologna, 1-12 December 2003.

FABBRI A., GALLIGNANI P. & ZITELLININI N. (1981) – *Geological evolution of the peri-Tyrrhenian sedimentary basins*. In WEZEL F.C. (Ed.): "*Sedimentary basins of Mediterranean margin*". Tecnoprint Bologna, 101-126.

FABBRI A., GHISETTI F. & VEZZANI L. (1980) – *The Peloritani-Calabria range and the Gioia Basin in the Calabrian arc (southern Italy): relationships between land and marine data*. Geol. Rom., **19**: 131 150.

GALLIGNANI P. (1982) – *Recent sedimentation processes on the Calabria continental shelf and slope (Tyrrhenian Sea, Italy)*. Oceanol. Acta, **5** (4): 493-500.

GALLOWAY W.E. (1998) – *Siliciclastic slope and base-of-slope depositional systems: component facies, stratigraphic architecture and classification*. Am. Ass. Petr. Geol. Bull., **82** (4): 569-595.

GAMBERI F. (1998) – *Volcanic facies associations in a modern volcaniclastic apron (Liparo and Vulcano offshore, Aeolian Island arc)*. Bull. Vulcanol., **63**: 264-273.

GAMBERI F., MARANI M.P. (1998) – *Sedimentary dynamics and pathways on the Gioia forearc basin*. Atti del 79 Congresso della Societa' Geologica Italiana. Palermo, 21-23 settembre 1998, 468-470.

GAMBERI F., MARANI M.P., LANDUZZI V., MAGAGNOLI A, PENITENTI D. & RIVALTA A. (2003) - *Contrasting sedimentation styles in the history of backarc basin: a comparison of recent deposition in the Vavilov and Marsili Basins*. GEOITALIA, 4º Forum FIST, Bellaria, 16-18 settembre 2003, 569-570.

GAMBERI F. & MARANI M. (2003) – *Turbidity currents and aggradational canyon fill: the case of the Stromboli canyon bend*. Atti del Convegno Geosed 2003. Alghero 28 settembre - 2 ottobre 2003, 175-179.

HIEKE W., GLACON G., HASEGAWA S., MULLER C., PEYPOUQUET J.P. (1990) – *Sedimentation in the Marsili Basin during Quaternary (ODP site 650, Tyrrhenian Sea)*. In KASTENS K.A., MASCLE J. (Eds.). Proceedings of the Ocean drilling Program, Scientific Results, **107**: 255-289.

KASTENS K. & MASCLE J. (1990) – *The geological evolution of the Tyrrhenian Sea: an introduction to the scientific results of ODP leg 107*. In KASTENS K.A., MASCLE J. (Eds.). Proceedings of the Ocean drilling Program, Scientific Results, **107**: 3-26.

LOCAT J. & MIENERT J. (2003) – *Submarine mass movements and their consequences*. Kluwer Academic Publishers pp 540.

MILIA A. & TORRENTE M. M. (1999) – *Tectonics and stratigraphic architecture of a peri-Tyrrhenian half-grabe (Bay of Naples, Italy)*. Tectonopysics, **315**: 301-318

NICOLICH R., CITA M.B., FABBRI A., FANUCCI F., TORELLI L. & WEZEL F.C. (1986) – *Bacini sediementari: ricerche geofisiche e di geologia marina nei mari italiano e nel Mediterraneo*. In P.F. Oceanografia e fondi Marini Sottoprogetto Risorse minerarie – Rapporto tecnico finale (Arti Grafiche E. Possidente ROMa 1986) 1- 95.

PEPE F., BERTOTTI G., CELLA F. & MARSELLA E. (2000) – *Rifted margin formation in the south Tyrrhenian Sea: a high-resolution seismic profile across the north Sicily passive continental margin*. Tectonics **19** (2): 241-257.

PEPE F., SULLI A., AGATE M., DI MAIO D., KOK A., LO IACONO C. & CATALANO R. (2003) – *Plio-Pleistocene geological evolotion of the northern Sicily continental margin (southern Tyrrhenian Sea): new insights from high-resolution, multi-electrode sparker profiles*. Geo-Mar. Lett., **23**: 53-63.

POSAMENTIER W. H. (2003) – *Depositional elements associated with a basin floor channel-levee system: case study from the Gulg of Mexico*. Mar. Petr. Geol., **20**: 677-690.

POSAMENTIER W.H. & KOLLA V. (2003) – *Seismic*

geomorphology and stratigraphy of depositional elements in deep-water setting. Journ. Sed. Res., **73** (3): 367-388.

SARTORI R., CARRARA G., TORELLI L. & ZITELLINI N. (2001) – *Neogene evolution of the southwestern Tyrrhenian Sea (Sardinian basin and western bathyal plain)* Mar Geol. **175**: 47-66.

STOCKER M.S., EVANS D & CRAMP A. (1998) – *Geological processes on continental margins: sedimentation, mass-wasting and stability.* Geol. Soc. Spec. Publ. **129**: 355 pp.

WEIMER P., SLATT F.M., COLEMAN J., ROSEN N.C., NELSON. H., BOUMA A.H., STYZEN M.J. & LAWRENCE D.T. (2000). *Deep-water reservoirs of the world:* gulf coast section SEPM foundation, 210th Annual Bob Perkins Reserch Conference.

WEZEL F.C., SAVELLI D., BELLAGAMBA M., TRAMONTANA M. & BARTOLE R. (1981) – *Plio-Quaternary depositional style of sedimentary basins along insular Tyrrhenian margins.* In WEZEL F.C. (Ed.): "*Sedimentary basins of Mediterranean margin*". Tecnoprint, Bologna, 239-26.

Mem. Descr. Carta Geol. d'It.
XLIV (2004), pp.147-164
12 figg.

On the tyrrhenian sea opening
Sull'apertura del Mar Tirreno

DOGLIONI C. (*), INNOCENTI F. (**), MORELLATO C. (*),
PROCACCIANTI D. (*), SCROCCA D. (***)

ABSTRACT - The Tyrrhenian Sea is the easternmost basin of the boudinated backarc lithosphere in the hangingwall of the Late Oligocene to Present Apennines subduction, which started in the Provençal and Valencia troughs and progressively moved to the Algerian and Tyrrhenian basins. All basins and in particular the Tyrrhenian Sea are asymmetric, being more extended and magmatically intruded in the eastern side, as testified also by the higher heat flow. The Apennines slab retreated "eastward", which kinematically requires an eastward mantle flow either to compensate or push the slab rollback.
Corsica and Sardinia represent the major lithospheric boudin in the backarc basin and their crustal and lithospheric roots have an eastward offset with respect to the superficial topography, possibly related to the shear induced by the underlying relative eastward mantle flow. It is interpreted that the mantle that generated the oceanic crust of the Provençal basin was depleted and consequently it became lighter; during its eastward transit below Sardinia and Corsica the depleted mantle could have generated the Miocene uplift of the continental swell.
Fault spacing in the brittle upper crust has an average value of 4-5 km in the Northern Tyrrhenian and 4 km to 16-17 km in the southern part. Internal sub-basins developed at different bathymetries, due to variable stretching and sediment supply in the different parts of the Tyrrhenian Sea. Northern and southern Tyrrhenian basins present respectively as minimum estimates 25 and 253 km of extension, according to the larger subduction of the Ionian heavier lithosphere of the Apennines foreland. The whole Tyrrhenian basin opened obliquely to the pre-existing alpine orogen. Therefore the main Tyrrhenian architecture and magmatism seem to have been primarily controlled by the composition and thickness of the downgoing subducting lithosphere beneath the Apennines, i.e., continental in the Adriatic and oceanic in the Ionian, and the westward motion of the lithosphere relative to the mantle.

KEY WORDS: Tyrrhenian Sea, backarc basin, slab retreat, eastward mantle flow

RIASSUNTO - Il Mar Tirreno è il bacino più orientale del Mediterraneo occidentale, che è considerabile come un unico grande bacino di retroarco della coeva subduzione appenninico-maghrebide, attiva dall'Oligocene superiore all'attuale. L'estensione è iniziata nei bacini Provenzale e di Valenzia, e si è progressivamente spostata nei bacini di Algeria e del Tirreno, generando un diffuso budinaggio della litosfera. Tutti i bacini, e in particolare il Tirreno, sono asimmetrici, essendo più assottigliati sul lato orientale, come confermato anche dal maggior magmatismo e dal più alto flusso di calore. La subduzione appenninica è arretrata verso "est", il che implica cinematicamente un flusso di mantello nella stessa

(*)Dipartimento di Scienze della Terra, Università La Sapienza, Roma
(**)Dipartimento di Scienze della Terra, Università di Pisa
(***)CNR-IGAG, Roma

direzione o a compensare, o a generare l'arretramento stesso. Il blocco sardo-corso rappresenta il più grande "budino" litosferico dell'intero bacino di retroarco; le sue radici crostali e litosferiche sono spostate verso est rispetto alla topografia, probabilmente a causa del flusso relativo del mantello verso est. Si interpreta che il mantello che ha generato la crosta oceanica del bacino Provenzale si sia impoverito, e sia divenuto quindi meno denso; durante il suo movimento verso est, transitando sotto Corsica e Sardegna, questo mantello più leggero potrebbe aver generato il sollevamento Miocenico del blocco continentale.
La spaziatura tra le faglie nella crosta superiore fragile ha una media di circa 4-5 km nel Tirreno settentrionale, e di 4-5 km, e 16-17 km nel Tirreno meridionale. Vi sono sotto-bacini interni minori a batimetria diversificata a causa del diverso grado di assottigliamento, e del variabile apporto sedimentario. Il Tirreno settentrionale e meridionale hanno subito un'estensione minima rispettivamente di 25 e 253 km, in accordo con la maggiore apertura del retroarco dove in avampaese dell'Appennino è subdotta la litosfera oceanica ionica più pesante. L'intero bacino tirrenico si è aperto obliquamente rispetto al pre-esistente orogene alpino. La struttura e il magmatismo del Tirreno sembrano dunque essere stati controllati principalmente dalla composizione e spessore della litosfera in subduzione sotto gli Appennini, cioè continentale in Adriatico e oceanica nello Ionio, e dal movimento verso "ovest" della litosfera rispetto al mantello.

PAROLE CHIAVE: Mar Tirreno, bacino di retroarco, arretramento della subduzione, flusso verso est del mantello

1. - INTRODUCTION

This paper aims to contribute in unravelling the tectonic evolution of the Tyrrhenian Sea (fig. 1), providing a multidisciplinary approach, regarding its structure, magmatology and geodynamics. The Tyrrhenian basin is the easternmost sub-basin of the wider western Mediterranean backarc basin, developed since the Late Oligocene in the hangingwall of the Apennines-Maghrebides "west"-directed subduction zone, which generated the arc running from northwest Italy throughout the Italian peninsula, Sicily and the north-western margin of Africa, from Tunisia to Morocco (REHAULT *et alii*, 1984; GUEGUEN *et alii*, 1998). The other western Mediterranean sub-basins are the Alboran, Valencia, Provençal and Algerian troughs. The Tyrrhenian Sea is the recent most sub-basin, developed from Miocene-to-Present (e.g., SCANDONE, 1980; MALINVERNO & RYAN, 1986). The basin is asymmetric in any respect: the extension is larger in the south; the rifting process and the related magmatism migrated in time from west to east (e.g., KASTENS *et alii*, 1988; BIGI *et alii*, 1992; SARTORI, 1989; DOGLIONI, 1991; SAVELLI, 2002). The extension evolved to oceanization in two main areas, i.e., the Vavilov (7-3.5 Ma) and the Marsili (1.7-1.2 Ma) sub-basins (BIGI *et alii*, 1989). Subduction-related magmatism and OIB basalts coexist in the Tyrrhenian

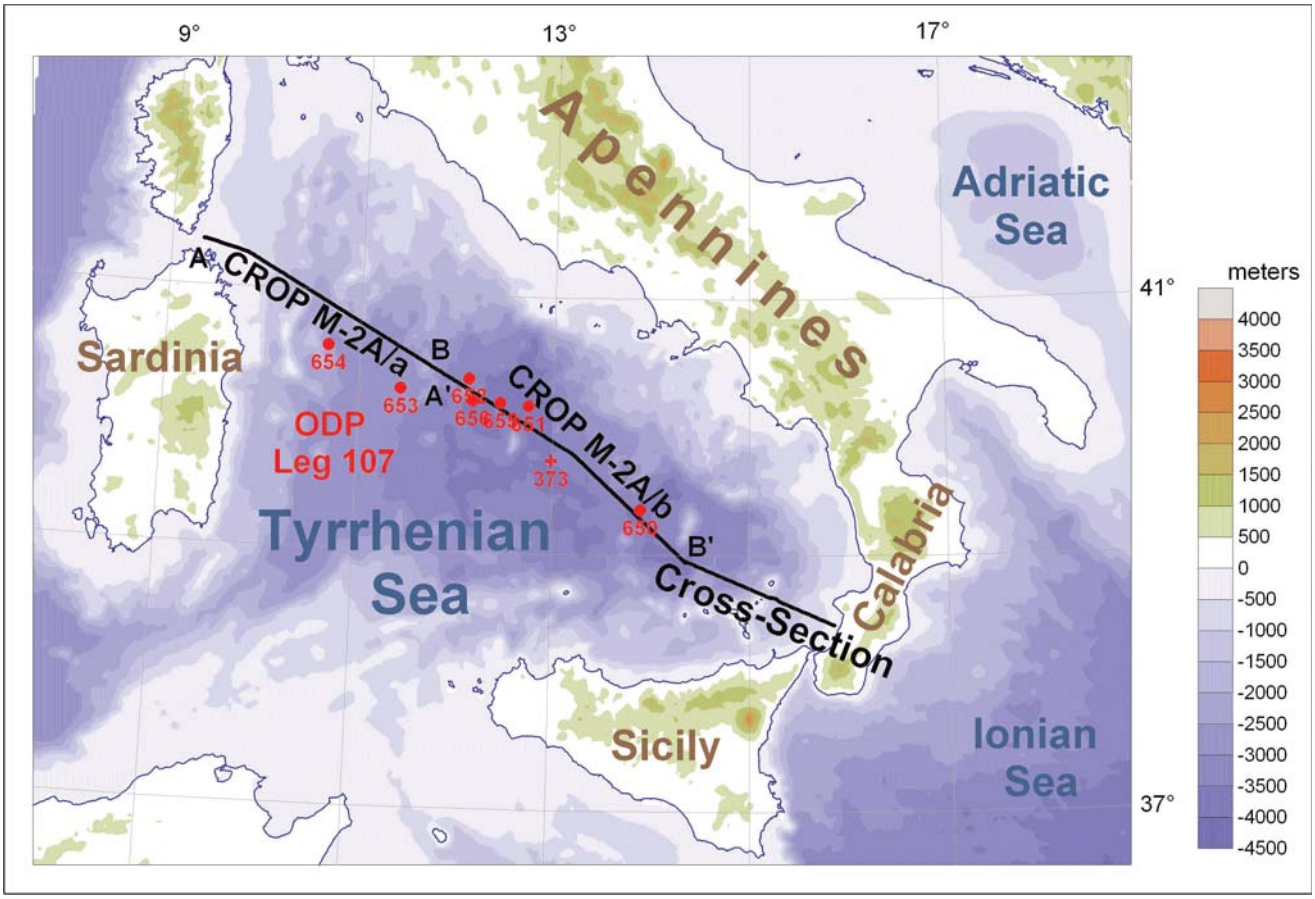

Fig. 1. - *Bathymetric map of the Tyrrhenian Sea and location of the cross-section and of the Crop seismic profiles M-2A/a and M-2A/b, interpreted in figures 3 and 4.*

basin and surrounding areas (e.g., SERRI *et alii*, 1993; SAVELLI, 2002). Researches about the geological history of the Tyrrhenian Sea have greatly improved due to some DSDP and ODP wells, seismic reflection profiles, dragging and volcanological researches (e.g., ZITELLINI *et alii*, 1986; FINETTI & DEL BEN, 1986; ELLAM *et alii*, 1988; KASTENS *et alii*, 1988; FRANCALANCI *et alii*, 1993; PASCUCCI *et alii*, 1999). Several papers proposed geophysical and geodynamic models on the opening of the basin (e.g., SCANDONE, 1980; MALINVERNO *et alii*, 1981; MANTOVANI, 1982; MOUSSAT *et alii*, 1986; FINETTI & DEL BEN, 1986; MALINVERNO & RYAN, 1986; PATACCA & SCANDONE, 1989; MONGELLI & ZITO, 1994; FACCENNA *et alii*, 1997; GUEGUEN *et alii* 1997; CELLA *et alii*, 1998; PANZA, 1998; DOGLIONI *et alii*, 1999; MAUFFRET *et alii*, 1999; PECCERILLO & PANZA, 1999).

There are several questions that are still unsolved in the knowledge of the basin, such as what is the exact relation with the Apennines subduction, what is the total extension in the different parts of the basin, when it opened, how many faults accompanied the opening, why Corsica-Sardinia uplifted during the opening of the western Mediterranean basin, why there are variations in the geochemical signature of magmatism, what is the relationship with respect to the Alpine orogen. In the following, new data are described and a few interpretations of the aforementioned themes are discussed.

2. - GEODYNAMIC SETTING

A number of different models tried to describe the process of the Tyrrhenian Sea opening. Most of them related the basin evolution to the Apennines subduction zone. Subduction of the Adriatic-Ionian plate is demonstrated by the existence of a well-defined Benioff plane under the Tyrrhenian Sea. Many authors (CAPUTO *et alii*, 1970; GASPARINI *et alii*, 1982; GIARDINI & VELONÀ, 1991; AMATO *et alii*, 1991, 1993; SELVAGGI & CHIARABBA, 1995; CIMINI, 1999; DE GORI *et alii*, 2001; SELVAGGI, 2001; PIROMALLO & MORELLI, 2003) have depicted the geometry of the subducted slab with different seismological methods. SELVAGGI & CHIARABBA (1995) have defined a continuous slab having a gentle slope down to 50 km of depth, then a rapid increase at the hinge, where the slope reaches 70° that remains constant down to 500 km. However this dip is partly computed along a section oblique to the slab, measuring a lower apparent dip.

There are a number of evidences indicating that the extension rates in backarc rifts such as the Tyrrhenian or Pannonian basins are related to the rates of subduction. The co-genetic link between the Apennines subduction and the Tyrrhenian backarc is supported by the following evidences, such as the coeval evolution of the two processes, the same "eastward" migration, the largest opening of the southern Tyrrhenian basin in correspondance of the maximum subduction depth of the Calabrian slab segment, where oceanic lithosphere is present in the Ionian foreland and it is supposed to continue northwestward at depth (CATALANO *et alii*, 2001). The co-genesis does not highlight whether the subduction generates the back-arc, or viceversa, where the rift is actively opening and subduction is a consequence of the expanding lithosphere. This last interpretation fails to explain the single polarity of the extension. Alternatively, both backarc rift and subduction are phenomena related to a third common process.

Extensional thinning of the lithosphere is often considered as related to stresses generated by boundary forces related either to slab pull or ridge push, or collapse of the orogen (e.g., FORSYTH & UYEDA, 1975; ROYDEN, 1993; PLATT & VISSERS, 1989; FACCENNA *et alii*, 2003). However, along slab compression focal mechanisms (FREPOLI *et alii*, 1996) are against the slab pull force, and the ridge push effect is too low in the Mediterranean basin. Moreover the rifting is oblique and even located far away from the pre-existing Alpine-Betic belt, supporting an independent origin from the gravitational collapse of the orogen ralated to the convective removal of its roots (DOGLIONI *et alii*, 1997). An alternative model relates rifting to the differential drag exerted by an eastward migrating mantle, providing an horizontal force able to push down also the "west"-directed slab (DOGLIONI *et alii*, 1999).

The Tyrrhenian rifting proceeded through jumps isolating thicker lithospheric swells, generating a sort of boudinage of the lithosphere (GUEGUEN *et alii*, 1997). Episodic backarc extension in the Tyrrhenian basin would suggest either that the subduction rate is not continuous or, alternatively, the stretching in the backarc is not continuous during a steady state subduction process. The average rate of the largest extension deduced by comparing the subducted slab length (>500 km), backarc basin width and its age (about 20 Ma) is in the order of about 2.5 cm/yr. The rifting opened mainly from W to E in most of the basin, but in the south-eastern part it deviated to SE since late Pliocene (?). This could be related to the encroachment of the Adriatic thick continental lithosphere east of the southern Apennines which slowed that segment of the subduction (DOGLIONI *et alii*, 1994). Then the rollback concentrated to the southeast toward the inherited Mesozoic Ionian ocean basin (CATALANO *et alii*, 2001) and to the northeast in the central-northern Adriatic Sea. The Tyrrhenian basin has a triangular shape with a tight angle in the north. The kinematics of the Apennines-Tyrrhenian system predict diffuse right-lateral transtension in the NW-SE-trending central-northern part, and left-lateral transtension in the E-W-trending southern part, north of Sicily. This tectonic setting is conjugate to the diffuse left-lateral transpression in the NW-SE-trending central-northern part of the Apennines, and right-lateral transpression in the E-W-trending southern part (DOGLIONI, 1991). The migration of the Apennines arc during the last 30 Ma has been computed to more than 700 km, a value about five times higher than the contemporaneous N-S convergence (130 km) of Africa (Tunisia) relative to Europe: this indicates that i) the Apennines arc migration and its related Tyrrhenian backarc opening have independent origin from the Africa-Europe

relative motion (GUEGUEN *et alii*, 1998) and ii) the Apennines-Tyrrhenian arc is rather slightly deformed in the southern arm by the Africa impingement.

The Adriatic microplate subduction initiated in the Late Oligocene-Early Miocene and developed to the east of the former Alpine-Betics belt, along its retrobelt. The Apennines accretionary prism formed in sequence at the front of the Alpine retrobelt. The Apenninic back-arc extension migrated eastward and boudinated the former Alpine nappe stack (DOGLIONI *et alii*, 1998). Kinematics and geophysical data support the presence of an eastward migrating asthenospheric wedge at the subduction hinge of the retrating Adriatic plate (DOGLIONI, 1991; GUEGUEN *et alii*, 1997). Mantle tomography and Q values confirmed the presence of a shallow asthenosphere below the western Apennines (PIROMALLO & MORELLI, 2003; MELE *et alii*, 1997).

Rifting initiated in the Upper Oligocene in the Liguro-Provençal basin to the west of the Corsica-Sardinia, floored by oceanic crust 19-15 Ma ago. The rifting jumped east of Corsica and Sardinia proceeding by steps and generating in the southern Tyrrhenian few major sub-basins, marked by homonymous volcanoes, i.e., Magnaghi, Vavilov and Marsili (fig. 2).

Basalts at the Mt Vavilov are OIB-MORB type with an age of 4.1 Ma (SARTORI, 1989), while the basalts of Mt. Marsili are also calc-alkaline (BECCALUVA *et alii*, 1990), and the upper-lying sediments have an age of 1.8 Ma (KASTENS *et alii*, 1988) indicating a young basaltic crust.

The Tyrrhenian Sea shows high Bouguer anomaly (>250 mGal) and heat flow values, both indicating shallow hot mantle and thin crust. The highest values are shifted in the eastern side, indicating asymmetry of the rift and possibly of the underlying mantle (fig. 2).

The map of the depth of the Moho (NICOLICH, 1989, NICOLICH & DAL PIAZ, 1991) shows values lower than 15-20 km for the bathial plane, and two minima of 10 km centered on the Vavilov and Marsili basins. It is worthwhile to note that these minima coincide with the highest values of the heat flow. The lithospheric boudinage proposed by GUEGUEN *et alii* (1997) is also suggested to be asymmetric by the gravimetric reconstruction of CELLA *et alii* (1998), being the continental roots of Corsica-Sardinia shifted to east with respect to the higher topography. This would confirm the presence of a migrating asthenosphere from west to east.

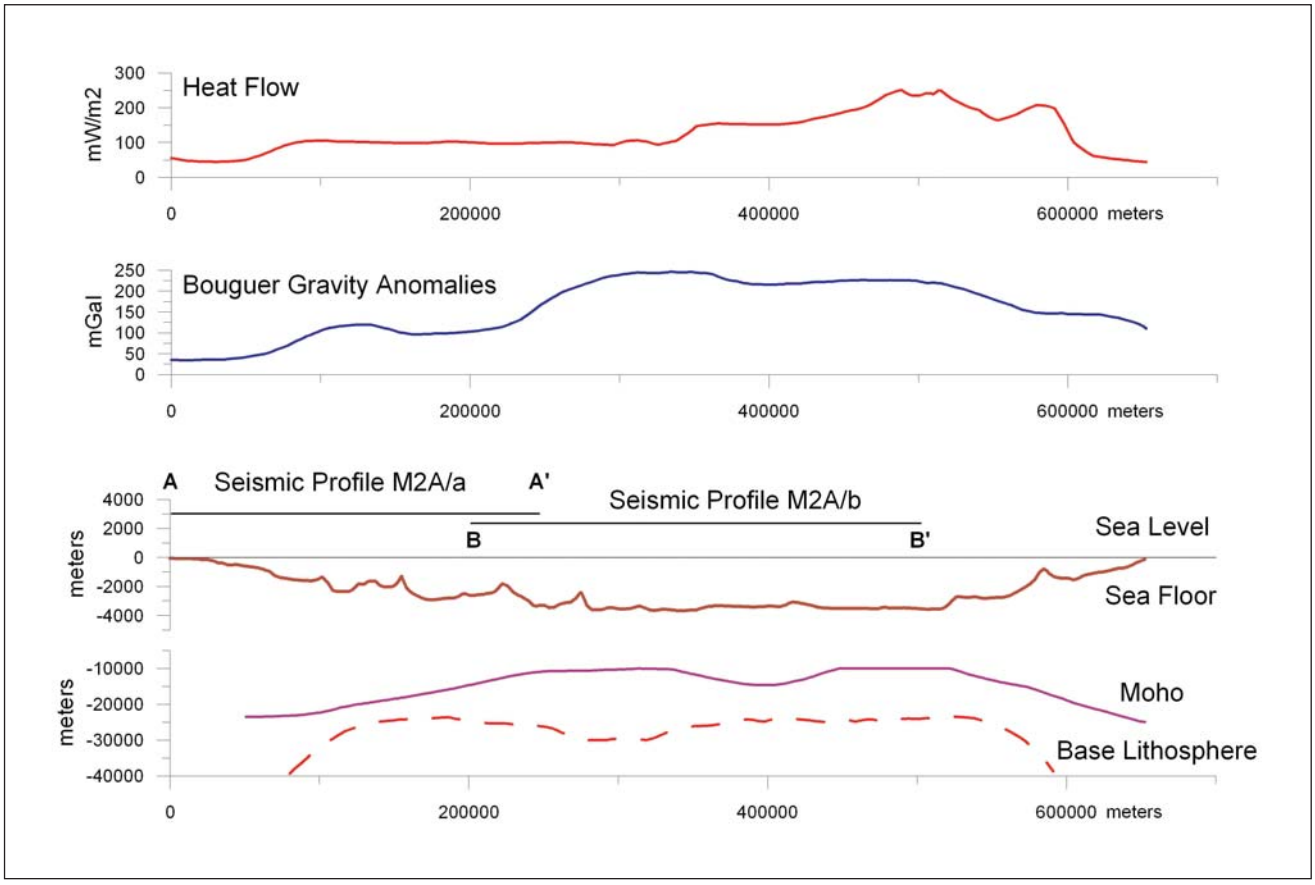

Fig. 2. - *The crustal and lithospheric structure of the Tyrrhenian Sea are shown along a regional cross-section (see fig. 1 for location) built along the* CROP *seismic profiles M2A/a and M2A/b ; heath flow and Bouguer anomalies are shown along the same cross-section.*
Data sources: Moho depth after NICOLICH & DAL PIAZ (1992), NICOLICH *(2001); base Lithosphere after* PANZA *et alii* (1992; 2003)*; Bouguer Gravity Anomalies after* MONGELLI *et alii* (1975)*; Heath Flow data after* DELLA VEDOVA *et alii* (2001). *Note the higher heat flow and gravity values in the eastern side of the basin.*

The Tyrrhenian Sea can be divided into three parts, i.e., northern, central and southern areas. The southern one (fig. 1) is the widest and more stretched area; it is the deepest part of the Tyrrhenian sea (>3500m), being subdivided into the aforementioned sub-basins. It is also the area of highest heat flow values (DELLA VEDOVA *et alii*, 1991; MONGELLI *et alii*, 1991) in some spots of the south-eastern part (>200 mW m^{-2}). The central part of the Tyrrhenian sea is rather characterized by the lowest heat flow values of the basin (~100 mW m^{-2}). Moving into the northern Tyrrhenian sea, close to Tuscany heat flow values are high again (>160 mW m^{-2}). Stretching in the Tyrrhenian sea decreases from south to north, and therefore there seems not to be a linear relation between total extension and heat flow. Asymmetric rifting and heat flow occur also in the Ligurian Sea at the northernmost tip of the Tyrrhenian Sea (PASQUALE *et alii*, 2002).

However there rather appears an evident correlation between active magmatism and heat flow, and the magmatism is directly correlated to the activity of the subduction rate and composition of the slab in the Apennines. In fact the most active part of the Apennines subduction is in the Southern Tyrrhenian-Calabria, where in the foreland there occurs the oceanic Ionian basin. Moving northward, the foreland of the southern Apennines is almost locked by the presence of the Puglia thick lithosphere (CALCAGNILE & PANZA, 1981), which is barely subducting and buckled (DOGLIONI *et alii*, 1994). This area of slow or stopped downgoing of the slab is recorded in the backarc basin where extension seems rather starved, low or absent magmatic activity, and low heat flow. The central northern part of the Apennines subduction is more lively, it generates seismicity and latent magmatism in Latium and Tuscany, and relatively high heat flow.

3. - THE CROP M2A PROFILE

A new picture of the structural setting in the Tyrrhenian Sea is provided by the new data acquired within the framework of the Italian deep crust exploration project (CROP Project). The main goal of the CROP Project was to study the crustal structure by means of near-vertical reflection (NVR) seismic as in similar projects in the USA (COCORP), in Germany (DEKORP), in France (ECORS), and in the UK (BIRPS). With this project, supported by the Italian National Research Council (CNR) and by two leading companies in the energy sector (ENI-AGIP and ENEL), more than 8700 km of seismic profiles off-shore and about 1254 km on-shore have been acquired, in the period 1986-1999.

The Tyrrhenian Sea is crossed by several CROP seismic profiles; two of them, the CROP M2A/a and M2A/b profiles, have been considered in our study (fig. 1). Both these profiles were acquired in 1991 by OGS: the first one was processed by ISMES in 1993 while the second one by OGS in 1991; the two seismic profiles present an overlap of about 30 km.

In this paper, we present only the interpretation of the whole M2A/b profile, located in the central Tyrrhenian Sea, and of the eastern Tyrrhenian half of the M2A/a (a 548 km long seismic profiles that crosses both the eastern side of the Provençal Basin and the western part of the Tyrrhenian Sea). The original seismic profiles, acquired to 17 s TWT, are available in the "CROP Atlas: seismic reflection profiles of the Italian crust", edited by SCROCCA *et alii* (2003).

The seismic profiles interpretation has been calibrated by analysing and compiling the available data related to the seven ODP Leg 107 wells, sites from 650 to 656 (KASTENS *et alii*, 1988, 1990), and by considering the other available geological and geophysical constraints.

Although several studies of the Tyrrhenian Sea have already pointed out the seismic stratigraphy and the main structural features of this peculiar backarc basin (among the others: FINETTI & MORELLI, 1973; MALINVERNO *et alii*, 1981; FABBRI & CURZI, 1979; FINETTI & DEL BEN, 1986; REHAULT *et alii*, 1987; MASCLE & REHAULT, 1990), the CROP seismic profiles provide new information on the structure and tectonic evolution of the Tyrrhenian Sea. Interpretable seismic signals can be recognised down to 9-10 s TWT or more, well below the usual limit of previously acquired seismic data, sometime making available a seismic image of the Moho discontinuity both in the continental and oceanic domains.

3.1. - CROP M2A/A SEISMIC PROFILE

The interpreted segment of this profile starts north of the Sardinia and, running NW-SE, cuts across the whole continental Sardinia margin (fig. 3). In its western side, a Mesozoic sedimentary cover has been interpreted between the Upper Messinian reflector and units that can be ascribed to the Varisican basement and to Late-Post Varisican sedimentary and magmatic rocks (outcropping in Sardinia and Corsica). This Mesozoic sedimentary cover, up to about 600 msh TWT thick, is likely made up of Upper Triassic continental clastic deposits and of Jurassic-Lower Cretaceous shallow water carbonates, as suggested by outcrops in the eastern side of Sardinia around the Orosei Gulf.

The eastern margin of the upper slope of the Sardinia margin is characterised by the presence of several N-S trending basement highs. One of them is the Monte Baronie ridge; a slightly asymmetrical horst bounded by faults of both its sides. Within this block we have tentatively interpreted the position of the western front of the Alpine units based on some seismic evidences and as suggested by dredging (COLANTONI *et alii*, 1981).

In the two basins adjacent to Monte Baronie ridge, below the well known strong reflector that characterises the top of the Messinian evaporitic units,

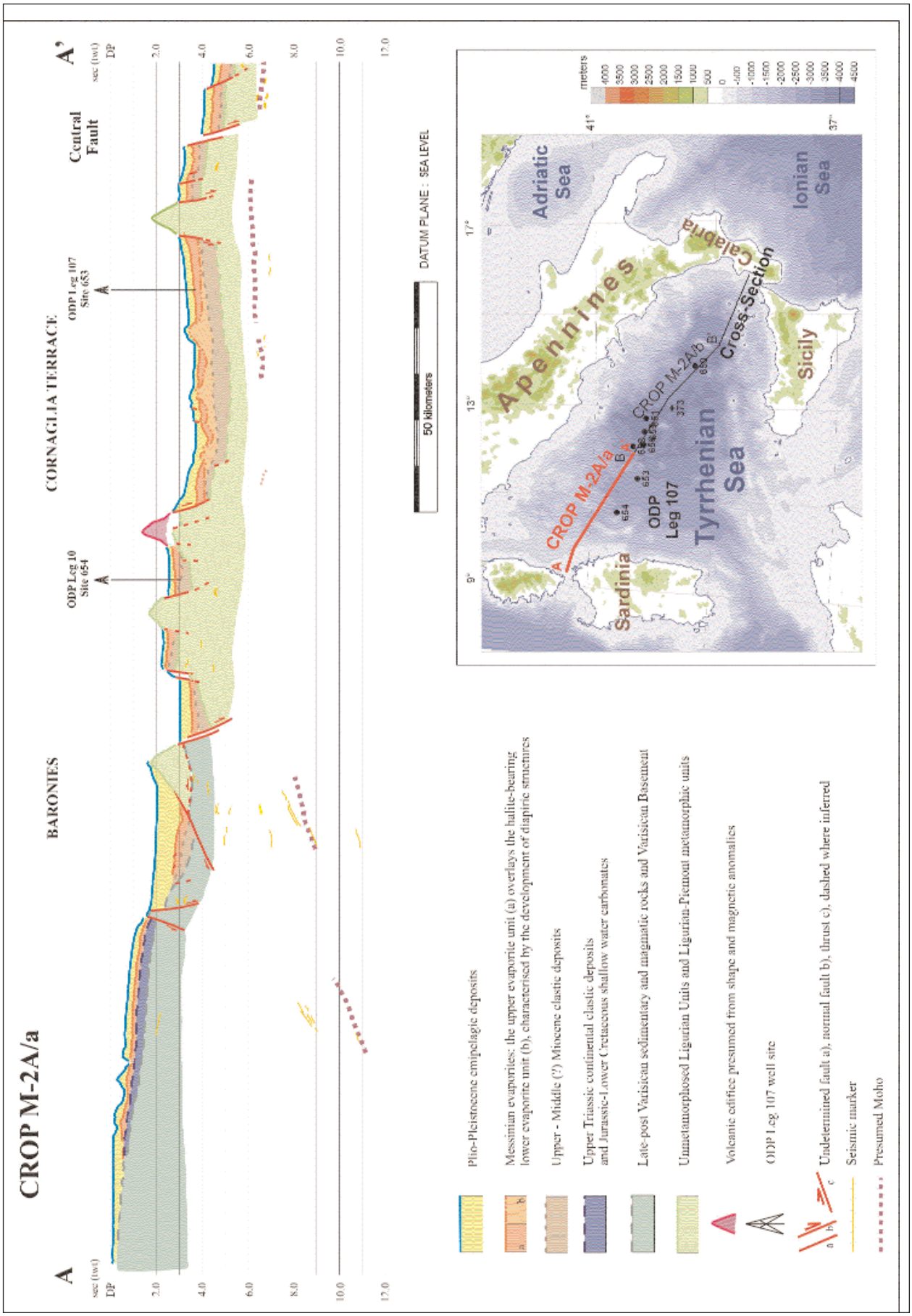

a

Fig. 3. - *Interpretation of the CROP M2A/a profile.*

a large thickness of the "pre-Messinian" sediments can be observed above the acoustic basement. This seismic unit shows quite clear wedge-shaped reflectors arrangement that suggests a syn-rift interpretation.

The onset of the rifting processes on the upper Sardinia slope is a matter of scientific debate. On one side, it is generally accepted (and also well documented) the syn-rift evolution during Upper Tortonian-Messinian times (e.g. MOUSSAT *et alii*, 1986; MASCLE & REHAULT, 1990). On the other side, being the upper Sardinia slope not interested by any ODP drilling, no direct dating is available for these pre-Messinian deposits. As a consequence, a Serravallian-Early Tortonian has been proposed for the rifting process in this area by MALINVERNO *et alii* (1981). In our interpretation, an age older than Upper Tortonian has been considered for the base of these pre-Messinian deposits, taking into account their thickness and in analogy with the correlatable sedimentary cycles on the outcropping Sardinian margin, and the earlier Miocene dating of the rifting to the north (PASCUCCI *et alii*, 1999).

All along the Cornaglia Terrace a strongly reflective horizon is present that represents the top of well-developed Messinian evaporites. According to CURZI *et alii* (1980), an upper evaporite unit overlying a halite-bearing lower evaporite unit have been distinguished (fig. 3); several diapiric structures related to the uplift Messinian salt can be observed.

In the western part of this profile, at about 10-11 s TWT, some strong west-dipping reflectors are recognisable; moving eastward, they became shallower, being at about 8-9 s TWT below Monte Baronie and at 6-7 s TWT in the eastern side of the Cornaglia Terrace. These reflectors have been interpreted as the seismic evidence of the continental Moho and confirm the sharp thinning of the continental crust of the Sardinia margin moving towards the Tyrrhenian basin. Based on our interpretation of these deep reflector on the CROP M2A/a, the crustal thickness decrease might be steeper and slightly shifted westwards than previously imaged (e.g.; RECQ *et alii*, 1984).

3.2. - CROP M2A/B SEISMIC PROFILE

This profile represents the south-eastwards prosecution of the CROP M2A/a (with a 30 km overlap). It intersects the "Central Fault", and runs through the Vavilov Basin, the Issel swell, and the western portion of the Marsili Basin. The interpretation of this profile (fig. 4) offers some further information on the deeper part of the Tyrrhenian Sea.

East of the "Central Fault", there are no evidences of the typical Messinian acoustic facies and, as documented by sites 652 and 656, the Messinian deposits show a sub-aerial and lacustrine facies (KASTENS *et alii*, 1988, 1990).

Further to the southeast, a sharp transition between the stretched continental domain and the oceanic one can be inferred. The top of the acoustic basement, interpreted as the top of the oceanic crust, has been represented; no differentiation has been possible between the serpentinized peridotite and the lava flows and basaltic breccias drilled by the site 651.

The Issel swell shows a faulted acoustic basement made up, according to dredging (COLANTONI *et alii*, 1981; BIGI *et alii*, 1992), of shallow and deep water carbonates, siliciclastic rocks and low- to medium-grade metamorphites; the first one may be Mesozoic while the other are of undefined age.

Moving south-eastwards, a picture of the general structure of the western side of the Marsili Basin, the younger of the basins floored by oceanic crust, is provided.

Although some multiples partially confuse the seismic image, it is worth noting that some scattered deep reflectors, tentatively attributed to the Moho, can be observed also on this profile. In particular, some strong reflectors are recognisable below the eastern margin of the Issel swell; if correctly interpreted, they might show a Moho significantly shallower than usually described (e.g. NICOLICH, 2001).

4. - EXTENSION IN THE TYRRHENIAN SEA

Along the section MS1 of FINETTI & DEL BEN (1986) there are about 162 normal or transtensional faults. The average spacing of the faults is about 4 km, but it raises to about 16-17 when only the most relevant are computed (fig. 5). The extension measured on the faults is around 67 km. Moreover there are 186 km of oceanic crust summing the Vavilov and Marsili interpreted sub-basins. Then the conservative amount of extension measured in the central-southern Tyrrhenian basin in the seismic section MS1 is about 253 km (67+186), along a section 640 km long (fig. 5). This value does not consider the stretching of the pre-existing alpine thickening and it is computed adding the horizontal component of the normal faults plus the oceanic segments. In the northern Tyrrhenian basin and Tuscany, where no oceanic crust crops out, a much smaller extension of about 25 km has been calculated from Corsica to Tuscany, again disregarding Alpine thrusting (fig. 6).

In order to have the entire extension in the backarc basin, these values have to be added to the horizontal stretching of the Provençal basin and of the normal faults in the related conjugate continental margins. It is maintained that moving northward, the extension decreases, like shortening does in the Apennines accretionary prism (BALLY *et alii*, 1986).

Therefore, computing the extension in the Provençal basin to about 300 km, the total stretching in the maximum extended backarc amounts to > 553 km. The variability of the extension in the Tyrrhenian sea is accommodated by frequent transfer zones with different orientation, oblique or normal to the grabens and horts.

Extension in the hangingwall of the Apennines can be differentiated in three different settings: 1) Extension in the Tyrrheanian sea and related conjugate margins, where subsidence is prevailing, and related to

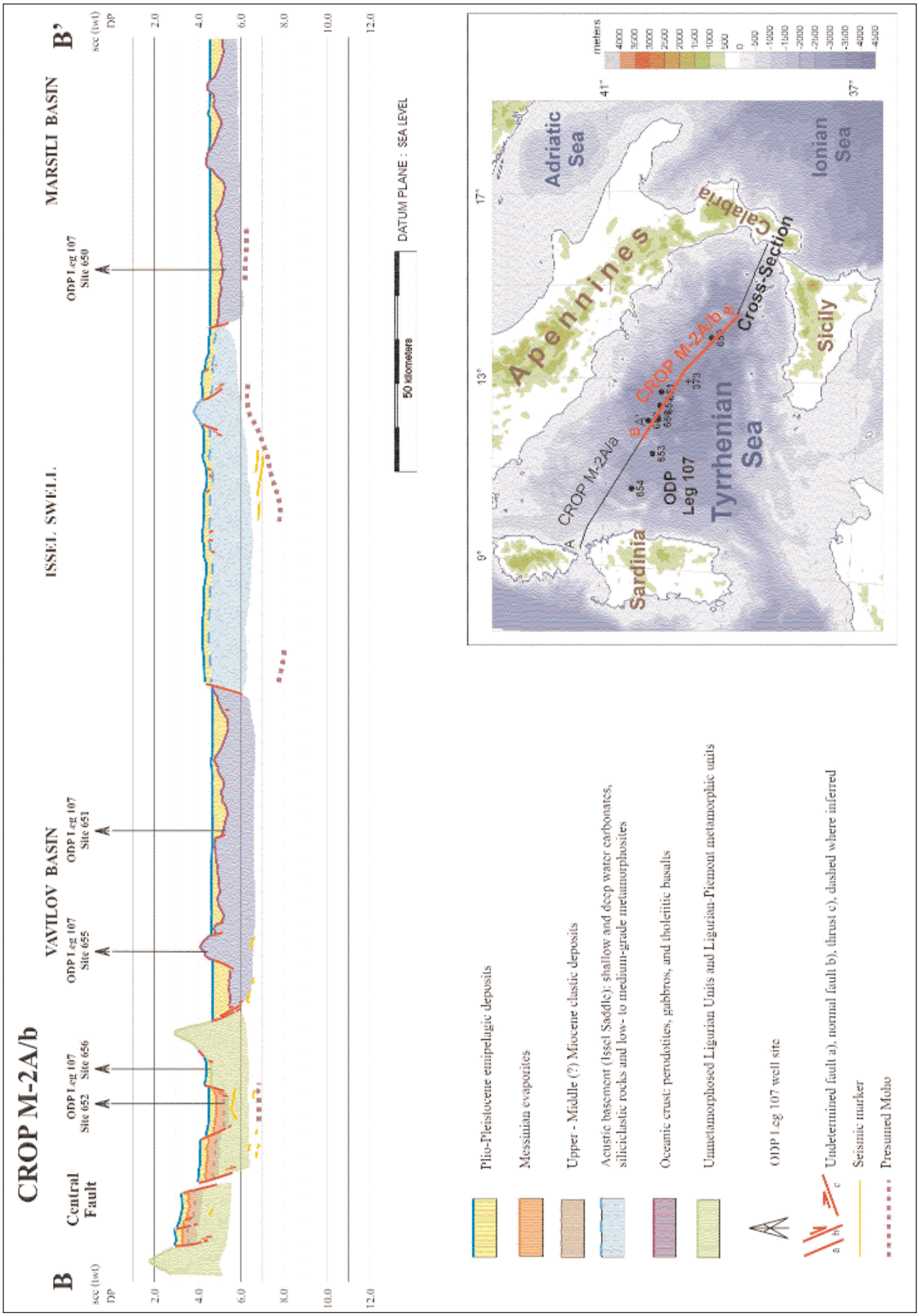

Fig. 4. - *Interpretation of the CROP M2A/b profile.*

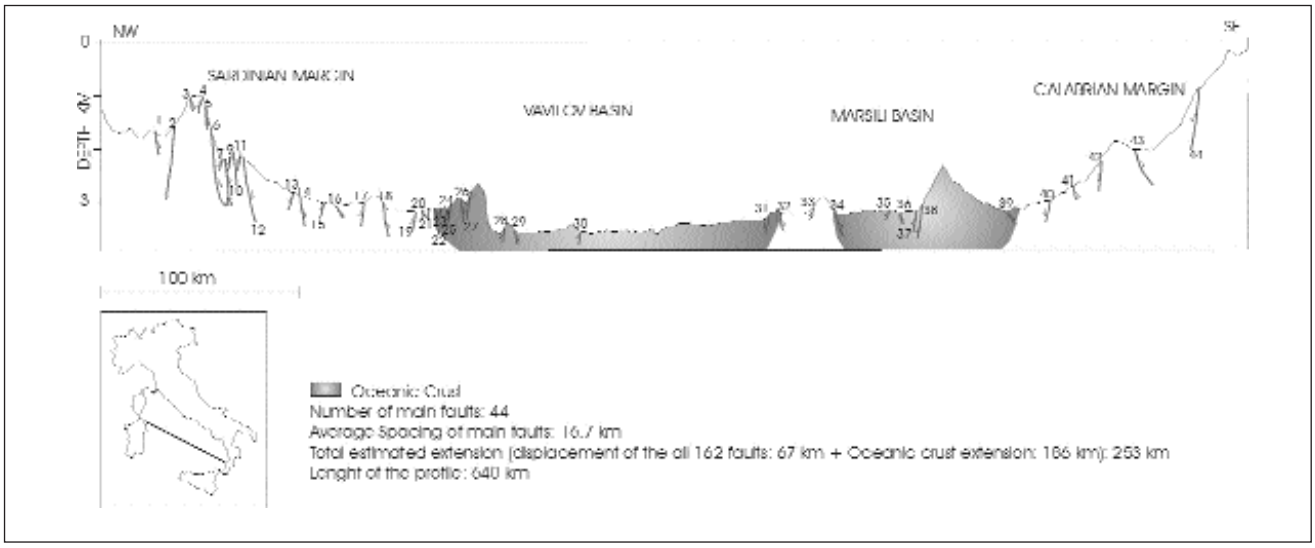

Fig. 5. - *Cross-section of the central-southern Tyrrhenian basin, with location of the main faults and the area where oceanic basement has been inferred. Base profile after* FINETTI & DEL BEN (1986).

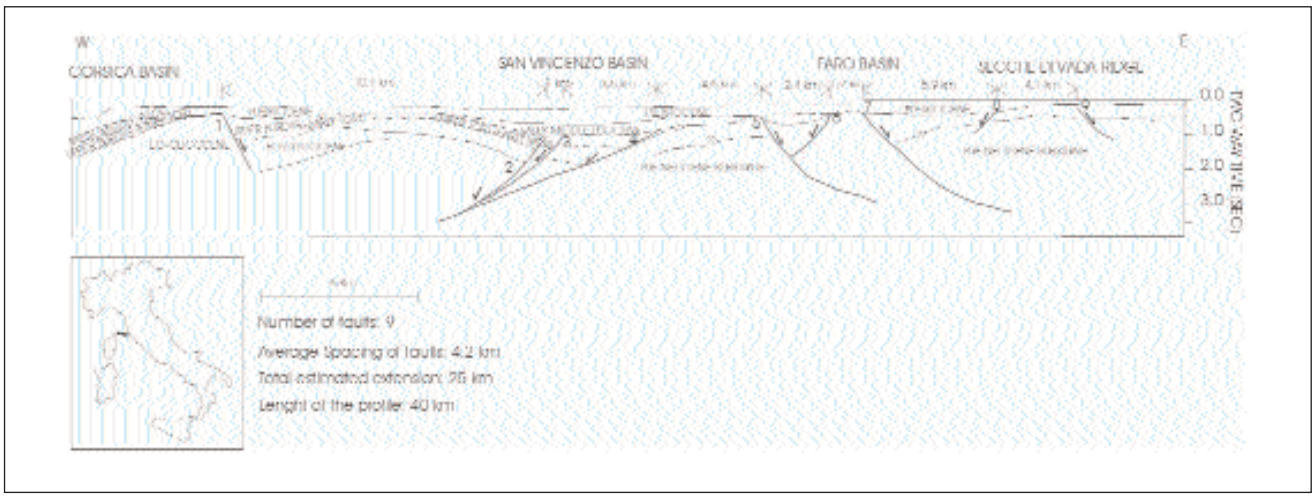

Fig. 6. - *The extension in the northern Tyrrhenian is about 10 km, and it raises to at least 25 km when including Tuscany, disregarding pre-extension thickening related to the Alpine orogen. Fault spacing is also shorter than in the southern Tyrrhenian. Cross-section after* PASCUCCI *et alii* (1999).

leghtening between the backarc margins. 2) Extension along the axis of the Apennines, where uplift is prevailing, with master faults mainly dipping toward the orogen foreland, (i.e., "E"-ward) and associated to the space generated by the slab retreat; this rifting is located in the uplifting area of the belt probably because accretion at the front of the orogen is larger than volume loss for slab rollback. 3) Extension perpendicular to the Apennines, related to the leghtening of the arc (DOGLIONI, 1991). In fig. 7 is proposed the kinematic setting of the Apennines subduction where extension in the hangingwall is generated both by space compensation in the subduction hinge (e.g., along the uplifting Apennines), and the increasing distance between the belt and the conjugate margin of the backarc basin (e.g., in the Tyrrheanian Sea).

In the Apennines, extension generated by hinge rollback is located in an area of regional uplift. This contradictory behaviour could be explained by the competing loss of volume generated by the slab rollback, and the volume added to the accretionary prism and/or by the Tyrrhenian asthenospheric mantle wedging. The uplift in the Apennines appears located where at depth there is the wedge of the active prism, and its thickening should contribute to the uplift. In the meanwhile, the slab retreat is responsible for the loss of volume in the hangingwall of the subduction. Therefore if the accretion is compensating part, but not all of the volume loss, extension might occur.

5. - EASTWARD MANTLE FLOW

Eastward mantle flow in the western Mediterranean is kinematically required by the slab rollback of the Apennines subduction (fig. 8): the

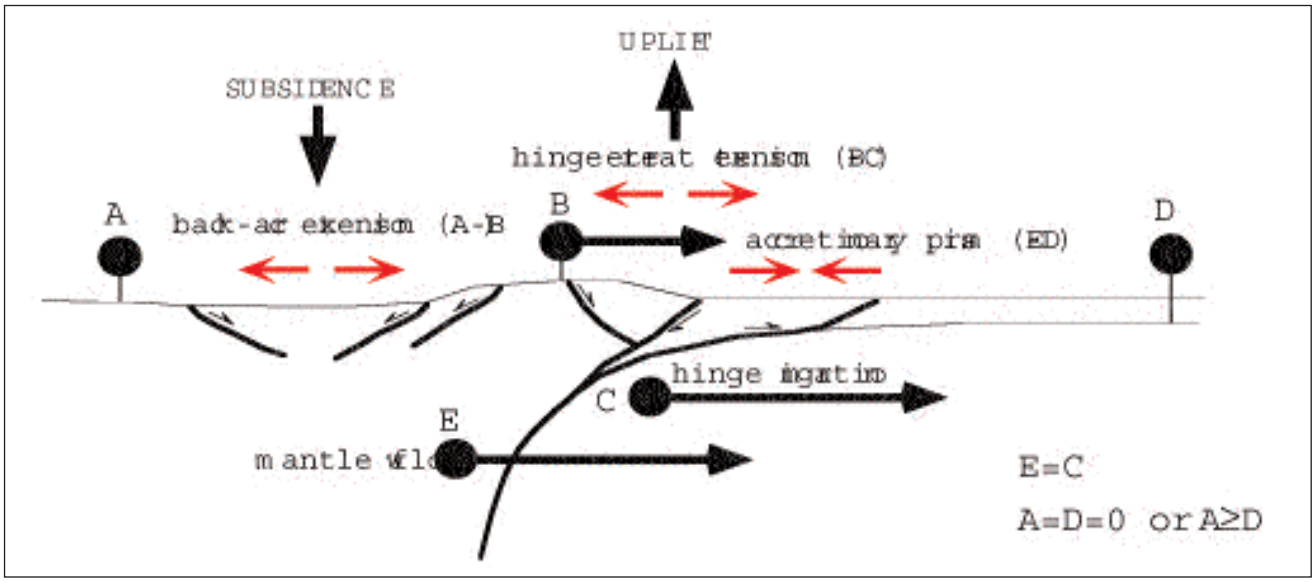

Fig. 7. - *Kinematic model of a west-directed subduction where two extensional settings form between A and B in the area of generalized subsidence (e.g., Tyrrhenian basin), and between B and C, along the uplifting belt (e.g., Apennines). The subduction hinge (C) eastward migration is faster than the convergence rate between D and B. Since C is faster than B, extension occurs also along the belt axis.*

volume left by the slab retreat is in fact necessarily filled by the upper mantle, regardless this mantle flow is the cause or a consequence of the slab rollback. The same kinematics are required for the mantle to the east of the slab: in order to allow the eastward slab retreat, mantle has to move eastward. Independently from this consideration, the relative eastward mantle flow is predicted by the westward drift of the lithosphere (DOGLIONI *et alii*, 1999) detected at the global scale in the hotspot reference frame which has been computed in an average of about 4.9 cm/yr (GRIPP & GORDON, 2002). The slab retreat in the Mediterranean has generally been ascribed to the negative buoyancy of the slab, i.e., the slab pull (ROYDEN, 1993; FACCENNA *et alii*, 2003). However, apart other general issues, this mechanism fails to explain a number of observations such as the along slab compression in the southern Tyrrhenian (FREPOLI *et alii*, 1996), and the subduction of continental lithosphere along the central-northern Apennines.

The eastward mantle flow in the western Mediterranean appears supported by the asymmetry indicated by the polarization of the seismic waves (MARGHERITI *et alii*, 1996) due to the elongation of olivine crystals in the mantle. The anisotropy deviates to an Apenninic trend underneath the belt: these data might be an indication of a flow underneath the Tyrrhenian backarc where the crystals should parallel the direction of mantle movement, and the encroachment with the subduction zone underneath the Apennines where the crystals should reorient due to the obstacle of the subduction.

The eastward mantle flow can account for the progressive eastward rejuvenation and boudinage of the western Mediterranean basins, e.g., from the Provençal to the Tyrrhenian, with the Vavilov, Marsili and Paola sub-basins (GUEGUEN *et alii*, 1997). The boudins and necks are also asymmetric: the base of the crust and of the lithosphere are in fact shifted several tens of km eastward relative to the topography of the basins and swells (CELLA *et alii*, 1998), coherently with a shear between lithosphere and underlying mantle (fig. 9).

6. - ON THE CORSICA-SARDINIA UPLIFT

The micro-continental plate of Corsica and Sardinia uplifted about 2 km as a single block together with the Alpine Corsica thrust sheets during the late Early Miocene (CAVAZZA *et alii*, 2001), and there is not a unique explanation of this phenomenon. It appears to be an uniform upward movement related to isostatic rebound. We discuss here the hypothesis that it is related to the opening of the Provençal basin to the west. Oceanization in the Provençal Basin (ROLLET *et alii*, 2002) occurred between 19-15 Ma, but the rift started during the Late Oligocene (e.g., GUEGUEN *et alii*, 1997).

The mantle uprise along rift zones determines partial melting and a residual lighter mantle (OXBURGH & PARMENTIER, 1977) with lower density of 20-60 kg m^{-3}, than the undepleted mantle. The residual mantle, less dense and containing some fluids, when displaced to the east, should generate a mass deficit with respect to the western limb of the ridge, where this low-density mantle did not propagate. Moving relatively eastward, the depleted mantle, determines asymmetry along oceanic rifts and eventually the uplift of the continent to the east as Africa (DOGLIONI *et alii*, 2003). This model could be applied to the opening of the Provençal basin and the later uplift of the adjacent Corsica-Sardinia continental lithosphere situated to

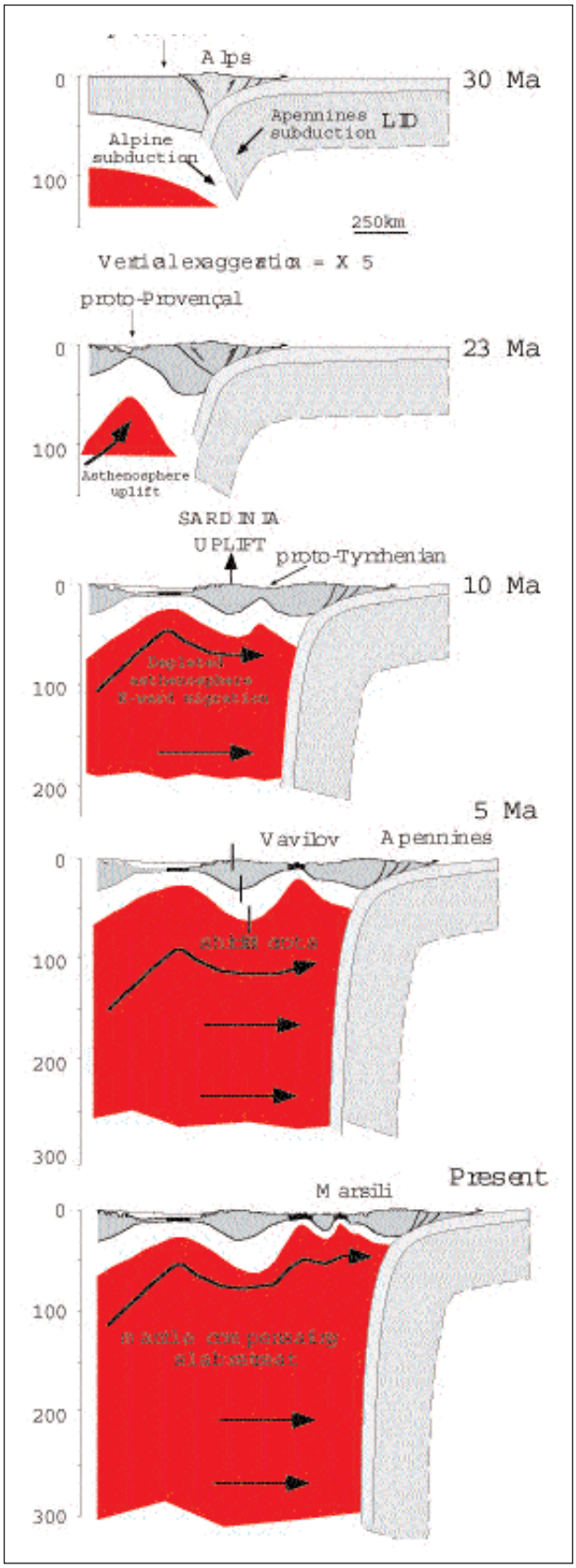

Fig. 8. - *Slab retreat and boudinage of the backarc basin in the hangingwall of the Apennines subduction during the last 30 Ma are interpreted in the central western Mediterranean (modified after* GUEGUEN *et alii*, 1998*). Slab retreat implies mantle compensation, in other words "eastward" mantle flow.*

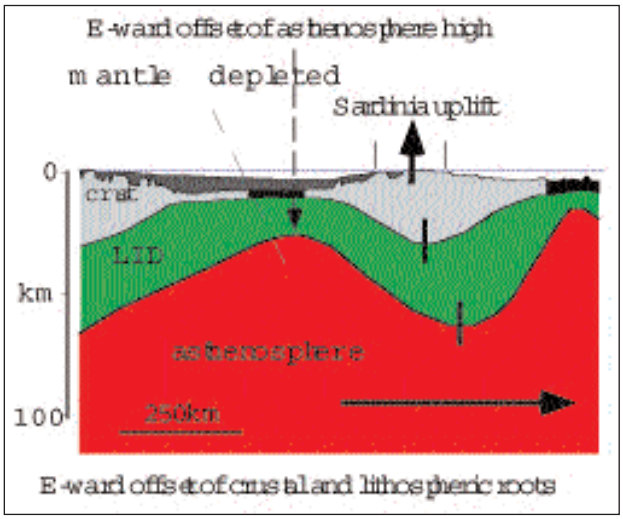

Fig. 9. - *Asthenosphere uplift and depletion associated to the Provençal basin opening (Late Oligocene-Early Miocene) determined a lighter mantle. An eastward mantle flow is inferred for the rollback of the steep Apennines slab, the shear wave splitting, and the westward drift of the lithosphere. The eastward mantle shear could explain the asymmetry of the Sardinia roots (data after* CELLA *et alii*, 1998*) and the Miocene uplift of Corsica-Sardinia due to an isostatic rebound related to the underlying transit of a less dense asthenosphere.*

the east: the substitution of undepleted mantle with depleted lighter mantle underneath Corsica-Sardinia could explain their generalized uplift (fig. 9). A similar model could be invoked for the uplift of the Balearic promontory, due to the opening of the Valencia trough to the west.

7. - SOUTH TYRRHENIAN MAGMATISM

The South Tyrrhenian Area (STA) is located south of 41°N and is bordered in the east by Campania and Calabria, in the west by Sardinia and in the south by Sicily. This domain is characterized by a widespread and very complex magmatism, with different petrogenetic affinities (figures 10 & 11). One common petrogenetic feature of this magmatism is that its ultimate source seems to be the mantle; anatectic magmas derived from the partial melting of continental crust are in fact typically absent in this area, in contrast to the northern Tyrrhenian region where they are conspicuous by their presence (SERRI *et alii*, 2001).

In order to minimize the effects of crustal contamination and shallow fractionation, and considering the petrological and geochemical data for the most primitive products only, we observe some important geochemical heterogeneities in the mantle of the southern Tyrrhenian domain. If we classify the volcanic products according to the geochemical characteristics of the mantle from which they have originated, then three main sources emerge.

Subduction-related source(s), which gave origin to two main suites: the south Tyrrhenian orogenic association (STOA), and the K-rich alkaline association of the

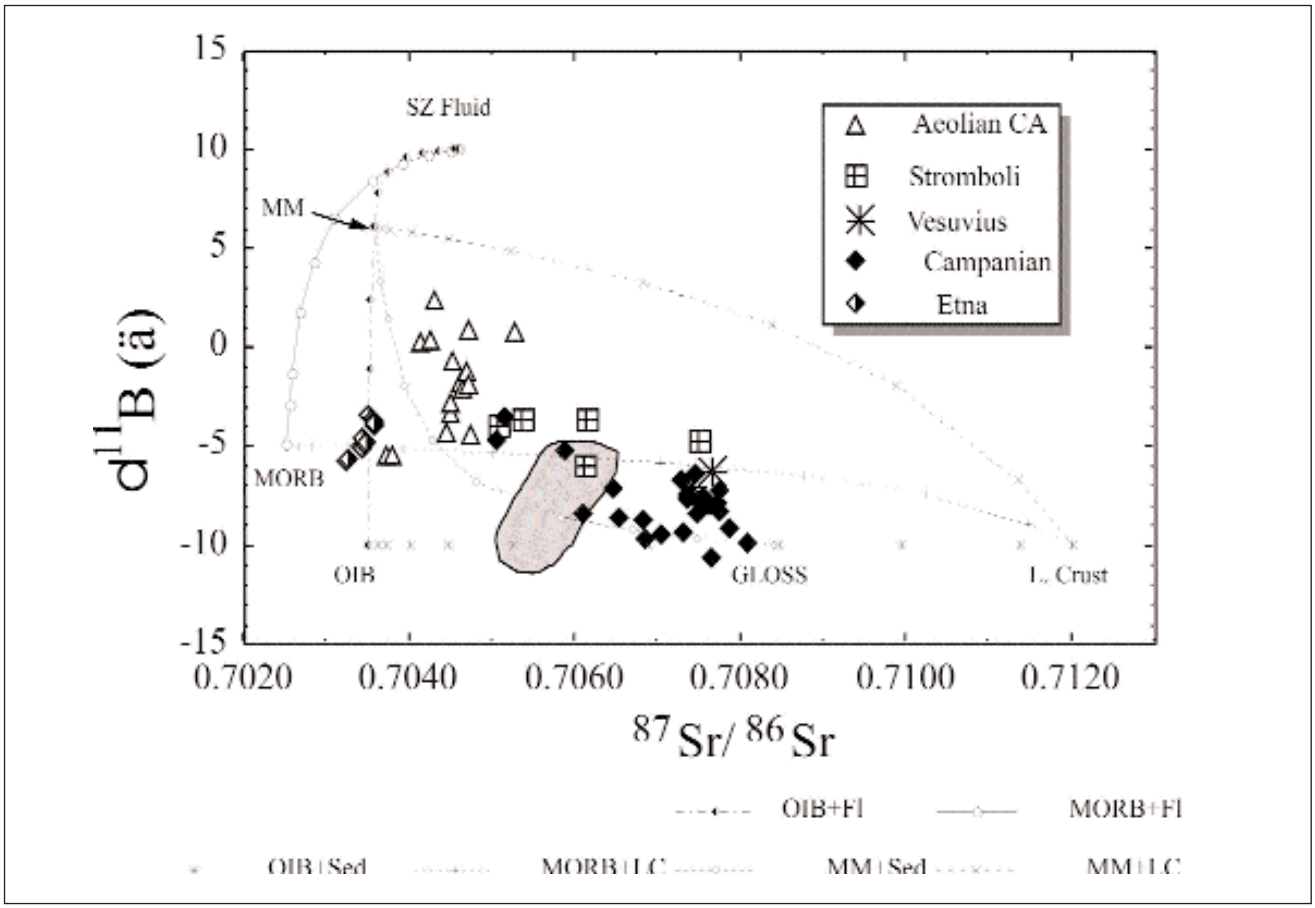

Fig. 10. - *$\delta^{11}B$ vs. 87Sr/86Sr diagram for South Tyrrhenian Quaternary volcanic rocks {$\delta^{11}B=[(11_B/10_B)$sample$/(11_B/10_B)$Std-1]*1000}. Dashed lines represent mixing trajectories between different hypothetical end-members (L.C., lower crust, SZ fluid, subduction-related fluid; MM, OIB-type mantle modified by subduction-related fluids;* GLOSS, (PLANK & LANGMUIR, 1998). G*ray area encircles Mt. Vulture samples. (from ,* TONARINI*, unpubl. Data).*

Central Campanian Province (CCP). The STOA includes the active volcanic arc of Aeolian Islands, made up of seven islands and several seamounts that extend east and west of the emerged arc. The erupted products form a suite with a variable affinity from tholeiitic to shoshonitic through calc-alkaline and high-K calc-alkaline rocks; K-rich alkaline products are also present and characterize the most recent volcanics of Stromboli and Vulcano (eastern sector of the arc). Several seamounts older than the Quaternary Aeolian volcanics and made up of rocks with an evident calc-alkaline affinity have been described in back-arc positions [e.g. Anchise, Sisifo, Marsili, Palinuro, Vavilov Basin (ARGNANI & SAVELLI, 1999; MARANI & TRUA, 2002; TRUA *et alii*, 2002). They are considered as isolated, partially dismembered portions of the oldest arc structures, abandoned as a consequence of the trenchward SE migration of the arc induced by the roll-back of the subducting Ionian slab (MALINVERNO, 1986). The morphotectonic features of the STOA and, in particular, the absence of high-standing cross-arc ridges (MARANI & TRUA, 2002) suggest a high rate of back-arc extension: in these conditions magma production was unable to keep pace with the widening of the back-arc (WRIGHT, 1996).

Evidence of the oldest Tertiary arc related to the westward-oriented subduction still remains in Sardinia, where an orogenic sequence ranging from 32 to 13 Ma is exposed along the western part of the island. The volcanic products show an affinity varying from tholeiite (southernmost sector) to calc-alkaline (northern part, DOWNES *et alii*, 2001; BROTZU, 1997) noteworthy is the eruption during the more extensional phases of the construction of the arc of primitive magmas, such as high-Mg basalts (MORRA *et alii*, 1997; MATTIOLI *et alii*, 2000).

The CCP includes the volcanic centres of the Campi Flegrei, Ischia-Procida and Somma-Vesuvio. The erupted products consist of slightly undersaturated or saturated K-alkaline rocks and ultra-alkaline leucite-bearing undersaturated products. Evolved terms are dominant in Ischia and the Campi Flegrei where significant contamination processes by crustal material in shallow magma chambers have been documented (PAPPALARDO *et alii*, 2002). The geochemical features of the primitive rocks exhibit a subduction-related signature, as indicated by high LILE/HFSE ratios and the negative anomalies of Ta, Nb, Ti and, to a lesser extent, Hf in the trace element profiles, normalized to primordial mantle (fig. 11, CONTICELLI *et alii*, 2002).

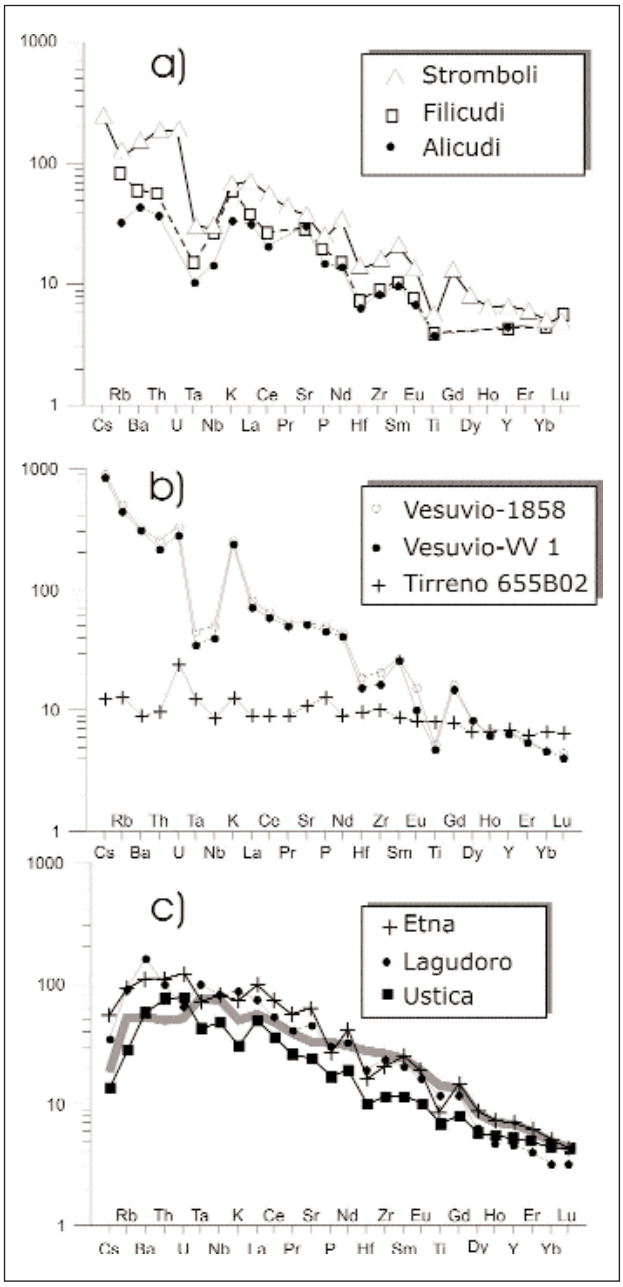

Fig. 11. - *Primordial mantle normalized multi-element patterns for Quaternary selected samples from South Tyrrhenian Area* (METRICH *et alii,* 2001*). Normalizing values are from* (MCDONOUGH & SUN, 1995). *Stromboli: scoria STR 43 (Mg#=61.2)* (METRICH *et alii*, 2001)*; Filicudi: La Canna, STR 197 (Mg#=63.9)* (FRANCALANCI & SANTO, 1993)*; Alicudi, STR185 (Mg# 62.8)* (FRANCALANCI *et alii,* 1993). *Vesuvio: 1868 phonotephrite lava (Mg#55); VV1, S. Maria La Bruna historic phonotephrite lava (Mg#=59.3) (M. D'Orazio unpubl. data); Tyrrhenian Basin,ODP site 655 B02* (BECCALUVA *et alii*, 1990) (GASPERINI *et alii*, 2002). *Etna: 1998 South-East Crater lava (Mg#53.9) (M. D'Orazio unpubl. data); Lagudoro lava (Mg# 65.9)* (GASPERINI *et alii,* 2000)*; Ustica: submarine olivin basalt (Mg#61.4) (M. D'Orazio unpubl. data).*

MORB-type source, which produced the basalts that form the floor of the Vavilov (Late Miocene) and Marsili (Late Pliocene-Early Pleistocene) basins (SERRI *et alii*, 2001), which evolved from the back-arc widening of the hangingwall plate induced by the roll-back of the ongoing subduction of the Ionian plate.

OIB-like sources, (fig. 11) which generated scattered basaltic covers or volcanic complexes in Sardinia and on its eastern off-shore margin (Late Miocene-Pleistocene), some seamounts in the central and south Tyrrhenian basin (e.g. Vavilov, Magnaghi and Aceste), the island of Ustica and the related Prometeo Ridge, and the Etna Volcano (ARGNANI & SAVELLI, 1999; LUSTRINO *et alii*, 2000; SCROCCA *et alii*, 2003).

The tectonic setting of this volcanism shows contrasting features; for example, Sardinian volcanism and the Tyrrhenian seamounts lie within the European continental hinterland or the thinned Tyrrhenian basin, relatively far from the active volcanic arc, whereas Ustica is located on the eastern extension of the active Aeolian volcanic arc, between the calc-alkaline seamounts Sisifo and Enarete to the east and Anchise to the west; finally, Mount Etna is in a peculiar position, in the foreland of the Apennine accretionary wedge (ARGNANI & SAVELLI, 1999; GASPERINI *et alii*, 2001; DOGLIONI *et alii*, 2001).

The distribution and first-order geochemical characteristics of the STA volcanics highlight two main features, the first of which is the predominance of products with a clear orogenic geochemical signature. The composition of the emitted lavas is extremely variable, however, ranging from rocks compositionally akin to the lavas forming the magmatic arcs at destructive margins (Aeolian arc) to K-rich silica, strongly undersaturated and saturated rocks (PC rocks). The other major feature is the occurrence of rocks closely associated with the orogenic suites that have an intraplate or OIB geochemical hallmark.

It is commonly accepted that, in convergent zones, orogenic magmas are generated by a melting in-wedge mantle modified by metasomatizing components (aqueous fluids or silicate melts) derived from a subducting slab (TATSUMI & EGGINS, 1995). Geochemical and isotopic data obtained from STA primitive rocks can be used to constrain the nature of the mantle sources; of particular importance for our comprehension of their geochemical features is the distribution of the incompatible fluid mobile elements, especially B and its isotopic ratio. Boron is, in fact, a strongly incompatible element, like Th and Nb; however, as it shows a marked affinity for the fluid phase, its behaviour is decoupled from that of incompatible immobile trace elements such as Nb, when a fluid phase is present (BRENNAN *et alii*, 1996; LEEMAN, 1996). Furthermore, there are distinct reservoirs of boron: in fact B is relatively enriched in altered oceanic crust (AOC) and pelagic sediments, whereas it is strongly depleted in the upper mantle and lower continental crust (LEEMAN, 1996). The B-isotope composition can further help to constrain the geochemical features of the sources providing components that may modify upper mantle composition. AOC and subduction-related fluids are, for example, characterized by markedly positive $\delta^{11}B$ values, whereas negative values are found in the upper

mantle, continental crust and sediments (RYAN *et alii*, 1995; ISHIKAWA & TERA, 1997).

The efficacy of B in differentiating source components can be strongly enhanced if its isotopic composition is combined with other isotopic ratios (e.g. Sr and Nd) and/or with mobile/immobile incompatible trace element ratios, such as B/Nb. This is shown in fig. 10, where the B isotope ratio is plotted against $87_{Sr}/86_{Sr}$ ratio for the Quaternary volcanic rocks related to the Apen nine subduction. The diagram shows the poles of the main end members contributing to a definition of the upper mantle sources. The plotted data clearly show the distinction between the volcanics of the Aeolian Islands and Campanian Province (TONARINI *et alii*, 2001a; 2004). In fact, the trends defined by the analyzed products of the two associations intersect, suggesting that the dominant component metasomatizing the mantle source in the Aeolian products is represented by fluids related with altered oceanic crust, whereas the Campanian products seem to be related with a source whose geochemical characteristics have been affected by a component of sedimentary origin, along with a subduction-related fluid with an AOC signature. Figure 10 also reports the curves of a binary mixing between the assumed end members to give a semi-quantitative indication of the interacting components. The data can also be used to acquire information on the pristine nature of the mantle before it was affected by metasomatic processes. Although B-isotopes are not particularly adept at discriminating mantle sources (CHAUSSIDON & MARTY, 1995; RYAN *et alii*, 1996), the combined geochemical data of fig. 10 as well as the values of mobile/immobile incompatible element ratios (TONARINI *et alii*, 2004) appear consistent with a model involving a depleted MORB-like mantle for the Aeolian magmas, whereas a more enriched OIB-like mantle source is required for the Campanian rocks; an attenuated OIB-signature for the CP volcanics has also been assumed, on the basis of the incompatible trace element distribution and isotopic data on the most primitive rocks (BECCALUVA *et alii*, 1991; GASPERINI *et alii*, 2002).

8. - GEODYNAMIC INTERPRETATION

The subduction-related Quaternary volcanism of the south Tyrrhenian Basin is characterized by remarkable geochemical and petrological variations that develop along the magmatic arc; they have been attributed to the interaction of mantle wedge with a predominant component linked to AOC in the Aeolian magmas or to sediments in the CP magmatism.

The geological and seismological data indicate that, at least since the Miocene, the Adriatic plate has been subducting westwards beneath the Apenninic arc, NW in the Calabrian arc and N in Sicily (DOGLIONI *et alii*, 1998; AMATO & CIMINI, 2001). The subducting plate shows important lateral variations, appearing oceanic in the Calabrian-Ionian sector, and continental under the Campanian region or in Sicily (CATALANO *et alii*, 2001; CARMINATI *et alii*, 2002). These lateral structural and compositional variations account for the differences in seismicity between the Apennine and Calabrian arcs: underneath the Apennines the earthquake foci have been monitored to a depth of about 90 km, whereas the Calabrian arc is characterized by a well-defined Benioff zone extending for 500 km (AMATO *et alii*, 1997); the differential retreat of the subduction hinge between Puglia, Calabria and Sicily is also considered a consequence of the lateral changes in composition of the subducting slab (DOGLIONI *et alii*, 2001). This geodynamic scenario explains the geochemical features of the main components metasomatizing the mantle sources of the South Tyrrhenian arc magmatism and, in particular, of the AOC-related component in the Aeolian arc and the sedimentary or crustal component in the Campanian magmas. Thus, the geochemical variations observed in erupted products from the Aeolian Islands to the Campanian Province probably reflect the changes in lithosphere from oceanic to continental.

The occurrence of magma with an OIB signature in the general convergence context of the south Tyrrhenian region is a more intriguing question. The existence of intraplate magmatism in a back-arc situation, i.e. Sardinian and Tyrrhenian volcanism, can be explained by mantle decompression melting, triggered both by its movement into the space created by the rollback of the subducting plate and the rifting process that eventually led to the opening of the Tyrrhenian Basin. The isotope characteristics of the erupted products seem to indicate the presence of an EM-1 reservoir linked with ancient oceanic plateau material recycled through a mantle plume (GASPERINI *et alii*, 2001); however, there is no geological and volcanological evidence of a Plio-Quaternary plume in northern Sardinia (e.g. very low eruption rate and absence of regional upwarping).

It is more difficult to explain the presence of the magma with predominant intraplate features along or close to the magmatic arc, such as Ustica and Etna. Geochemical and isotope variations have been detected at Mt. Etna, despite the relatively homogeneous petrological nature of its erupted products. In particular, the good correlation between $\delta^{11}B$ and $87_{Sr}/86_{Sr}$ and the fluid mobile elements (TONARINI *et alii*, 2001b; see also fig. 10), has been interpreted as the result of contamination by subduction-related fluids released by the subducted Ionian slab of the sub-slab mantle (asthenosphere). The relatively deep mantle was able to raise because a major structural discontinuity, considered a vertical slab window, opened in the subducting plate at the transition between the oceanic Ionian and continental Sicilian lithospheres. This geodynamic model can be tentatively extended all along the Apennines subduction zone where a drastic structural change occurs in the nature of the slab, leading to a differential retreating rate of the subduction hinge and, therefore, to the creation of a vertical window. This phenomenon could be applied to the plateau volcanism of Ustica and Prometeo, on the northern prolongation of the Malta

escarpment. Another structural situation of slab discontinuity is expected at the conjugate location with respect to the Etna and Malta escarpment.

Magmatism is likely triggered by fluids released by slabs at around 150-250 km depth. Magmatism is sensitive to composition of the downgoing slab, thermal state of the slab and surrounding mantle, dip of the slab, velocity of the subduction, fluids content of the slab, and possibly the thickness and composition of the hangingwall plate and mantle. In the hangingwall of the Apennines subduction, as an example, there is volcanism fed by subducting both continental and oceanic lithospheres. As a hypothesis, since continental crust melts at lower temperatures than oceanic crust, shallower depth for magma generation is expected for continental crust with respect to oceanic crust; this could explain the closer location of the continental-related volcanism to the subduction hinge in the central-northern Apennines subduction zone with respect to the southern Tyrrhenian Eolian arc (fig. 12).

The Tyrrhenian Sea appears as the area where the asthenosphere and the underlying upper mantle replaced the volumes of the heterogeneous foreland lithosphere that were consumed by the Apennines subduction.

Acknowledgments

Many thanks to Michael MARANI *for inviting us to contribute to the volume.* Sonia TONARINI *and* Massimo D'ORAZIO *are thanked for useful discussions and for providing unpublished isotopic data. Research supported by* Cofin 2001, ASI 2002 and Ateneo La Sapienza 2003.

REFERENCES

AMATO A., ALESSANDRINI B., CIMINI G., FREPOLI A. & SELVAGGI G. (1993) – *Active and remnant subducted slabs beneath Italy: evidence from seismic tomography and seismicity.* Ann. Geofis., **36** (2): 201-214.

AMATO A., CHIARABBA C. & SELVAGGI G. (1997) - *Crustal and deep seismicity in Italy (30 years after).* Ann. Geofis., **40**: 981– 993.

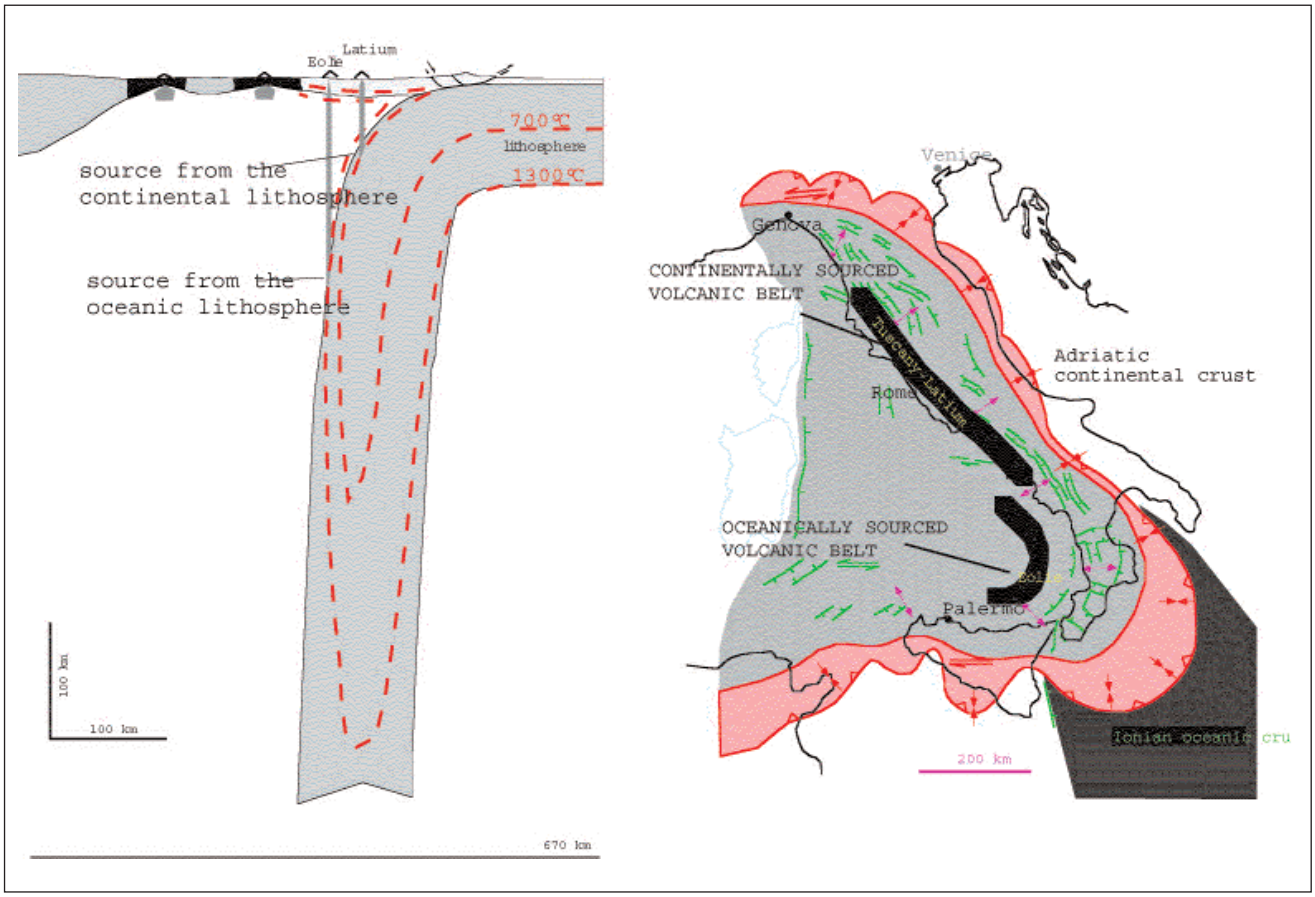

Fig. 12. - *The depth of fluids release and of melt generation along a subduction zone is a function of the composition of the downgoing rocks. Continental crust melts at lower temperature (650-800°C) than oceanic crust (1200-1300°C). As an application, the Apennines have both continental (Adriatic) and oceanic (Ionian) lithosphere subducting toward the west underneath the belt. The related magmatism is likely shallower for the continental subduction than the oceanic one because melting temperature is reached earlier. This could explain the shorter distance to the subduction hinge and the inland location of the subduction-related magmatism in the central-northern Apennines with respect to the Eolian volcanic arc in the southern Tyrrhenian.*

AMATO A. & CIMINI G.B. (2001) - *Deep structure from seismic tomography*. In: VAI G.B. & MARTINI I.P. (Eds.): "*Anatomy of an Orogen: the Apennines and Adjacent mediterranean basins"*. Kluwer Academic Publishers, Dordrecht, The Netherlands, 33-45.

AMATO A., CIMINI C., ALESSANDRINI B. (1991) - *Struttura del sistema litosfera–astenosfera nell'Appennino Settentrionale da dati di tomografia sismica*. Studi Geologici Camerti, Vol. Spec. (1991/1): 83–90.

ARGNANI A. & SAVELLI C. (1999) - *Cenozoic volcanism and tectonics in the southern Tyrrhenian sea: space-time distribution and geodynamic significance*. J. Geodynamics, **27:** 398-321.

BALLY A.W., BURBI L., COOPER C. & GHELARDONI R. (1986) - *Balanced sections and seismic reflection profiles across the central Apennine*. Mem. Soc. Geol. It., **35**: 257-310.

BECCALUVA L., BONATTI E., DUPUY C., FERRARA G., INNOCENTI F., LUCCHINI F., MACERA P., PETRINI R., ROSSI P.L., SERRI G., SEYLER M., SIENA F. (1990) - *Geochemistry and mineralogy of volcanic rocks from ODP sites 650, 651, 655, and 654 in the Tyrrhenian Sea*. In: STEWART: N.J. (Ed.): "*Procedings of the Ocean Drilling Program, Scientific Results"*. U.S. Gov. Print. Off., Washington, D.C., 107, pp. 49-74.

BECCALUVA L., DI GIROLAMO P. & SERRI G. 1991. *Petrogenesis and tectonic setting of the Roman volcanic Province, Italy*. Lithos, **26**: 191-221.

BIGI G., CASTELLARIN A., CATALANO R., COLI M., COSENTINO D., DAL PIAZ G.V., LENTINI F., PAROTTO M., PATACCA E., PRATURLON A., SALVINI F., SARTORI R., SCANDONE P. & VAI G.B. (1989) - *Synthetic structural-kinematic map of Italy, scale 1:2.000.000*. CNR, Progetto Finalizzato Geodinamica, Roma.

BIGI G., COSENTINO D., PAROTTO M., SARTORI R. & SCANDONE P. (1992) - *Structural Model of Italy. Scale 1:500.000*. Quaderni de "La Ricerca Scientifica", 114, Vol. 3. CNR.

BRENNAN J.M., NERODA E., LUNDSTROM C.C., SHAW H.F., RYERSON F.J. & PHINNEY D.L. (1998) - *Behaviour of boron, beryllium, and lithium during melting and crystallization: Constraints from mineral-melts partitioning experiments*. Geochim. Cosmochim. Acta, **62**: 2129-2141.

BROTZU P. (1997) - *The calcalkaline volcanism in Sardinia*. Per. Mineral., **66**: 1-231.

CALCAGNILE G. & PANZA G.F. (1981) – *The main characteristics of the lithosphere-asthenosphere system in Italy and surrounding regions*. Pure Appl. Geophys., **119**: 865-879.

CAPUTO M., PANZA G. F. & POSTPISCHL D. (1970) – *Deep structure of the Mediterranean Basin*. J. Geophys. Res., **75**: 4,919-4,923.

CARMINATI E., GIARDINA F. & DOGLIONI C. (2002) - *Rheological control of subcrustal seismicity in the Apennines subduction (Italy)*. Geophys. Res. Lett., **29**, doi:10.1029/2001GL014084.

CATALANO R., DOGLIONI C. & MERLINI S. (2001): On the Mesozoic Ionian basin. Geophys. J. Int., **144**: 49-64.

CAVAZZA W., ZATTIN M., VENTURA B. & ZUFFA G.G. (2001) - *Apatite fission-track analysis of Neogene exhumation in northern Corsica (France)* Terra Nova, **13**: 51-57.

CELLA F., FEDI F., FLORIO G. & RAPOLLA A. (1998) - *Optimal gravity modelling of the litho-asthenosphere system in Central Mediterranean*. Tectonophysics, **287**: 1-4, 117-138.

CHAUSSIDON M. & MARTY B. (1995) - *Primitive Boron Isotope Composition of the Mantle*. Science, **269** (121): 383-386.

CIMINI G.B. (1999) – *P-wave deep velocity structure of the southern Tyrrhenian subduction zone from non-linear teleseismic travel time tomography*. Geoph. Res. Let., **26** (24): 3709-3712.

COLANTONI P; FABBRI A; GALLIGNANI P., 1981. *Seismic-stratigraphic interpretation of high resolution profiles; some applied examples*. Boll. Geof. Teor. Appl., **23**, 90-91, 89-106.

CONTICELLI S., D'ANTONIO M., PINARELLI L. & CIVETTA L. (2002) - *Source contamination and mantle heterogeneity in the genesis of Italian potassic and ultrapotassic volcanic rocks: Sr-Nd-Pb isotope data from Roman Province and Southern Tuscany*. Mineral. and Petrol., **74**: 189-222.

CURZI P; FABBRI A; NANNI T., 1980. The Messinian evaporitic event in the Sardinia Basin area (Tyrrhenian Sea). Mar. Geol., **34**, 3-4, 157-170.

DE GORI P., CIMINI G.B., CHIARABBA C., DE NATALE G., TROISE C. & DESCHAMPS A. (2001) - *Teleseismic tomography of the Campanian volcanic area and surrounding Apenninic belt*. J. Volc. Geother. Res., **109**: 55-75.

DELLA VEDOVA B., MONGELLI F., PELLIS G. & ZITO G. (1991) – *Campo regionale del flusso di calore nel Tirreno*. Atti 10° Convegno GNGTS, Roma, 817-825.

DELLA VEDOVA B., BELLANI S., PELLIS G. & SQUARCI P. (2001) - *Deep temperatures and surface heat flow distribution*. In: VAI G.B. & MARTINI L.P. (Ed.): *"Anatomy of an orogen: the Apennines and adjacent Mediterranean basins"*. Kluwer Academic Publishers, Dordrecht, The Netherlands, 65-76.

DOGLIONI C. (1991) - *A proposal of kinematic modelling for W-dipping subductions - Possible applications to the Tyrrhenian-Apennines system*. Terra Nova, **3**: 423-434.

DOGLIONI C., CARMINATI E. & BONATTI E. (2003) - *Rift asymmetry and continental uplift*. Tectonics, **22**, 3, 1024, doi:10.1029/2002TC001459.

DOGLIONI C., GUEGUEN E., SABAT F. & FERNANDEZ M. (1997) - *The western Mediterranean extensional basins and the Alpine orogen*. Terra Nova, **9**: 3, 109-112.

DOGLIONI C., GUEGUEN E., HARABAGLIA P. & MONGELLI F. (1999) - *On the origin of W-directed subduction zones and applications to the western Mediterranean*. Geol. Soc. Sp. Publ., **156**: 541-561.

DOGLIONI C., INNOCENTI F. & MARIOTTI G. (2001) – Why Mt. Etna? *Terra Nova*, **13**: 25-31.

DOGLIONI C., MONGELLI F. & PIALLI G.P. (1998) - *Boudinage of the Alpine belt in the Apenninic back-arc*. Mem. Soc. Geol. It., **52**: 457-468.

DOGLIONI C., MONGELLI F. & PIERI P. (1994) - *The Puglia uplift (SE Italy): An anomaly in the foreland of the Apenninic subduction due to buckling of a thick continental lithosphere*. Tectonics, **13**: 1309-1321.

DOWNES H., THIRLWALL M.F. & TRAYHORN S.C. (2001) - *Miocene subduction-related magmatism in southern Sardinia: Sr-Nd- and oxygen isotopic evidence for mantle source enrichment*. J. Volcanol. Geotherm. Res, **106**: 1-21.

ELLAM R.M., MENZIES M.A., HAWKESWORTH C.J., LEEMAN W.P., ROSI M. & SERRI G. (1988) - *The transition from calc-alkaline to potassic orogenic magmatism in the Aeolian Islands, Southern Italy*. Bull. Volcanol., **30**: 386-398.

FABBRI A. & CURZI P. (1979) - *The Messinian of the Tyrrhenian Sea; seismic evidence and dynamic implications*. Giorn. Geol., **43**(1): 215-248.

FACCENNA C., JOLIVET L., PIROMALLO C. & MORELLI A. (2003) - *Subduction and the depth of convection in the Mediterranean mantle*. J. Geophys. Res., 108, doi:10.1029/2001JB001690.

FACCENNA C., MATTEI M., FUNICIELLO R. & JOLIVET L. (1997) - *Styles of back-arc extension in the Central Mediterranean*. Terra Nova, **9**: 126-130.

FINETTI I. & DEL BEN A. (1986) - *Geophysical study of the Tyrrhenian opening*. Boll. Geofis. Teor. ed Appl., **28**: 75-156.

FINETTI I. & MORELLI C. (1973) – *Geophysical exploration of the Mediterranean Sea*. Boll. Geof. Teor. Appl., **15**(60):

263-340.

FORSYTH D. & UYEDA S. (1975) - *On the relative importance of driving forces of plate motion*. Geophys. J. R. Astron. Soc., **43**: 163-200.

FRANCALANCI L. & SANTO A. (1993) - *Magmatological evolution of Filicudi volcanoes, Aeolian Islands, Italy: constraints from mineralogical, geochemical and isotopic data*. Acta Vulcanol., **3**: 203-227.

FRANCALANCI L., TAYLOR S.R., MC CULLOCH M.T. & WOODHEAD J. (1993) - *Petrological and geochemical variations in the calc-alkaline rocks of Aeolian arc (Southern Tyrrhenian Sea, Italy)*. Contrib. Mineral. Petrol., **113**: 300-313.

FREPOLI A., SELVAGGI G., CHIARABBA C. & AMATO A. (1996) - *State of stress in the Southern Tyrrhenian subduction zone from fault-plane solutions*. Geophys. J. Int., **125**: 879-891.

GASPARINI C., IANNACCONE G., SCANDONE P. & SCARPA R. (1982) - *Seismotectonics of the Calabrian Arc*. Tectonophysics, **84**: 267-286.

GASPERINI D., BLICHERT-TOFT J., BOSCH D., DEL MORO A., MACERA P., TELOUK P. & ALBAREDE F. (2000) - *Evidence from Sardinian basalt geochemistry for recycling of plume heads into the Earths mantle*. Nature, **408**: 701-704.

GASPERINI D., BLICHERT-TOFT J., BOSCH D., DEL MORO A., MACERA P. & ALBAREDE F. (2001) - *Upwelling of deep mantle material through a plate window: evidence from the geochemistry of Italian basaltic volcanics*. J. Geophys. Res. **107** (B12) 2367, doi:10.1029/2001JB000418

GIARDINI D. & VELONÀ M. (1991) - *The deep seismicity of the Tyrrhenian Sea*. Terra Nova, **3**: 57-64.

GRIPP A.E. & GORDON R.G. (2002) - *Young tracks of hotspots and current plate velocities*. Geophys. J. Int., **150**: 321–361.

GUEGUEN E., DOGLIONI C. & FERNANDEZ M. (1997) - *Lithospheric boudinage in the Western Mediterranean back-arc basins*. Terra Nova, **9** (4): 184-187.

GUEGUEN F., DOGLIONI C. & FERNANDEZ M. (1998) – *On the post-25 Ma geodynamic evolution of the western Mediterranean*. Tectonophysics, **298**: 259-269.

ISHIKAWA T. & TERA F. (1997) - *Source, composition and distribution of the fluid in Kurile mantle wedge: Constraints from across-arc variations of BINb and B isotopes*. Earth Planet. Sci. Lett., **152**: 123-138.

KASTENS K.A. *et alii* (1988) - *ODP Leg 107 in the Tyrrhenian Sea: Insigths into passive margin and back-arc basin evolution*. Geol. Soc. Am. Bull., **100**: 1140-1156.

KASTENS K.A., MASCLE J. *et alii* (1990) – *Proc. ODP, Sci. Results, 107*: College Station TX (Ocean Drilling Program), 772 pp.

LEEMAN W.P. (1996) - *Boron and other fluid-mobile elements in volcanic arc lavas: Implications for subduction processes*. In: BEBOUT G.E., SCHOLL D.W., KIRBY S.H., PLATT J.P. (Ed.): "*Subduction Top to Bottom*". AGU Monograph, 269-276.

LUSTRINO M., MELLUSO L. & MORRA V. (2000) - *The role of lower continental crust and lithospheric mantle in the genesis of Plio-Pleistocene volcanic rocks from Sardinia (Italy)*. Earth Planet. Sci. Letters, **180**: 259-270.

MALINVERNO A., CAFIERO M., RYAN W.B.F. & CITA M.B. (1981) – *Distribution of Messinian sediments and erosional surfaces beneath the Tyrrhenian Sea: geodynamical implications*. Oceanol. Acta, **4:** 489-496.

MALINVERNO A. & RYAN W.B.F. (1986) - *Extension in the Tyrrhenian Sea and shortening in the Apennines as a result of arc migration driven by sinking of the lithosphere*. Tectonics, **5**: 227-245.

MANTOVANI E. (1982) - *Some remarks on the driving forces in the evolution of the Tyrrhenian basin and Calabrian Arc*. Earth Evol. Sci., **3**: 266-170.

MARANI M. & TRUA T. (2002) - *Thermal constriction and slab tearing at the origin of super-inflated spreading ridge: the Marsili volcano (Tyrrhenian Sea)*. J. Geophys. Res., **107** (B2): 2188 doi:1029/2001JB000285.

MARGHERITI L., NOSTRO C., COCCO M. & AMATO A. (1996) - *Seismic anisotropy beneath the Northern Apennines (Italy) and its tectonic implications*. Geophys. Res. Lett., **23**: 2721-2724.

MASCLE J., REHAULT J.P. (1990) – *A revised seismic stratigraphy of the Tyrrhenian Sea: implications for the basin evolution*. In: KASTENS K.A., MASCLE J. *et alii – Proc. ODP, Sci. Results, 107*: College Station TX (Ocean Drilling Program), 617-636.

MATTIOLI M., GUERRERA F., TRAMONTANA M., RAFFAELLI G. & D'ATRI M. (2000) - *High-Mg Tertiary basalts in Southern Sardinia (Italy)*. Earth Planet. Sci. Letters, **179**: 1-7.

MAUFFRET A., CONTRUCCI I. & BRUNET C. (1999) - *Structural evolution of the Northern Tyrrhenian Sea from new seismic data*. Mar. Petrol. Geol., **16**: 381-407.

MCDONOUGH W.F. & SUN S.S. (1995) - *The composition of the Earth*. Chem. Geol., **120**: 223-253.

MELE G., ROVELLI A., SEBER D. & BARANZAGI M. (1997) - *Shear wave attenuation in the lithosphere beneath Italy and surrounding regions: tectonic implications*. J. Geophys. Res., **102** (6): 11,863-11,875.

METRICH N., BERTAGNINI A., LANDI P. & ROSI M. (2001) - *Cristallization Driven by Decompression and Water Loss at Stromboli Vocano (Aeolian Islands, Italy)*. J. Petrol., **42**: 1471-1490.

MONGELLI F., LODDO M. & CALCAGNILE G. (1975) - *Some observations on the Apennines gravity field*. Earth Planet. Sci. Lett., **24**: 385-393.

MONGELLI F. & ZITO G. (1994) - *Thermal aspects of some geodynamical models of tyrrhenian opening*. Boll. Geof. Teor. ed Appl., **XXXVI** (141-144): 21-28.

MONGELLI F., ZITO G., DELLA VEDOVA B., PELLIS G., SQUARCI P. & TAFFI L. (1991) - *Geothermal Regime of Italy and surrounding Seas*. In: Exploration of the deep continental crust, Springer-Verlag Berlin, 381-394.

MORRA V., SECCHI F.A.G., MELLUSO L. & FRANCIOSI L. (1997) – *High-Mg subduction-related Tertiary basalts in Sardinia, Italy*. Lithos, **40**: 69-91.

MOUSSAT E., REHAULT J.P. & FABBRI A. (1986) - *Rifting et évolution tectono-sédimentaire du Bassin tyrrhenien au cours du Néogène et du Quaternaire*. Giornale Geol., **48** (1/2): 41-62.

NICOLICH R. (1989) - *Crustal structures from seismic studies in the frame of the European Geotraverse (southern segment) and Crop projects*. In: BORIANI A., BONAFEDE M., PICCARDO G.B. & VAI G.B. (Eds.):"*The lithosphere in Italy*". Accad. Naz. Lincei, **80**: 41-61.

NICOLICH R. (2001) - *Deep seismic transects*. In: VAI G.B. & MARTINI I.P. (Eds.): "*Anatomy of an orogen: the Apennines and adjacent Mediterranean basins*". Kluwer Academic Publishers, 47-52, Dordrecht, The Netherlands.

NICOLICH R. & DAL PIAZ G.V. (1992) - *Moho isobaths, Structural Model of Italy. Scale 1:500,000*. Quaderni de "La Ricerca Scientifica", **114** (3): CNR.

OXBURGH E.R. & E.M. PARMENTIER. (1977) - *Compositional and density stratification in oceanic lithosphere; causes and consequences*. J. Geol. Soc. London, **133** (4): 343-355.

PANZA G.F., SCANDONE P., CALCAGNILE G., MUELLER S. & SUHADOLC P. (1992) – *The lithosphere-asthenosphere system in Italy and surrounding regions*. Quaderni de "La Ricerca Scientifica", **114** (3): CNR.

PANZA G.F., PONTEVIVO A., SARAÒ A., AOUDIA A. & PECCERILLO A. (2003) - *Structure of the Lithosphere - Asthenosphere and Volcanism in the Tyrrhenian Sea and surroundings*. This volume.

PAPPALARDO L., PIOCHI M., D'ANTONIO M., CIVETTA L. & PETRINI R. (2002) - *Evidence for Multi-stage Magmatic*

Evolution during the past 60 kyr at campi Flegrei (Italy) Deduced from Sr, Nd, and Pb Isotope Data. J. Petrol., **43**: 1415-1434.

PASCUCCI V., MERLINI S., MARTINI P. (1999) - *Seismic stratigraphy of the Miocene-Pleistocene sedimentary basins of the Northern Tyrrhenian Sea and western Tuscany (Italy).* Basin Res., **11**: 337-356.

PASQUALE V., VERDOYA M. & CHIOZZI P. (2002) - *A possible mechanism for the thermal asymmetry of the Ligurian basin.* Terra Nova, **14** (6): 484-490.

PATACCA E. & SCANDONE P. (1989) - *Post-Tortonian mountain building in the Apennines. The role of the passive sinking of a relic lithospheric slab.* In BORIANI A., BONAFEDE M., PICCARDO G.B. & VAI G.B. (Eds.): "*The Lithosphere in Italy*". Accademia Nazionale Lincei, **80**: 157-176.

PECCERILLO A. (1998) - *Relationships between ultrapotassic and carbonate-rich volcanic rocks in central Italy: petrogenetic and geodynamic implications.* Lithos, **43**(4): 267-279.

PECCERILLO A. & PANZA G. F. (1999) - *Upper mantle domains beneath Central-Southern Italy, Petrological, geochemical and geophysical constraints.* PAGEOPH, **156**: 421-444.

PIROMALLO C. & MORELLI A. (2003) - *P wave tomography of the mantle under the Alpine-Mediterranean area.* J. Geophys. Res., **108**, B2, 2065, doi:10.1029/2002JB001757.

PLANK K.T. & LANGMUIR C.H. (1988) – *The geochimical compoisition of subducting sediment and its consequences for the crust and mantle.* Chem. Geol., **145**: 325-394.

PLATT J.P. & VISSERS R.L.M. (1989) - *Extensional collapse of thickened continental lithosphere: a working hypothesis for the Alboran Sea and Gibraltar Arc.* Geology, **17**: 540-543.

RECQ M., REHAULT J.P., STEINMETZ L. & FABBRI A. (1984) - *Amincissement de la croute et accretion au centre du bassin tyrrhenien d'apres la sismique refraction. Crustal thinning and accretion in the central Tyrrhenian Basin from seismic refraction studies.* Mar. Geol., **55**(3-4): 409-426.

REHAULT J.P., MASCLE J. & BOILLOT G. (1984) - *Evolution geodynamique de la mediterranee depuis l'Oligocene.* Mem. Soc. Geol. It., **27**: 85-96.

ROLLET N., DÉVERCHÈRE J., BESLIER M.O., GUENNOC P., RÉHAULT J.P., SOSSON M. & TRUFFERT C. (2002*) - Back arc extension, tectonic inheritance, and volcanism in the Ligurian Sea, Western Mediterranean.* Tectonics, **21**, 3, 10.1029/2001TC900027.

ROYDEN L.H. (1993) - *The tectonic expression slab pull at continental convergent boundaries.* Tectonics, **12**: 303-325.

RYAN J.G., LEEMAN W.P., MORRIS J.D. & LANGMUIR C.H. (1996*) - The boron systematics of intraplate lavas: Implications for crust and mantle evolution.* Geochim. Cosmochim. Acta, **60**: 415-422.

RYAN J.G., MORRIS J.D., TERA F., LEEMAN W.P. & TSVETKOV A. (1995) - *Cross-arc geochemical variations in the Kurile arc as a function of slab depth.* Science, **270**: 625-627.

SARTORI R. & ODP LEG 107 SCIENTIFIC STAFF (1989) - *Drillings of ODP Leg 107 in the Tyrrhenian Sea: Tentative Basin Evolution Compared to Deformations in the Surroundings Chains.* In BORIANI A., BONAFEDE M., PICCARDO G.B. & VAI G.B. (Eds.): "*The Lithosphere in Italy*". Accademia Nazionale Lincei, **80**: 139-156.

SAVELLI C. (2002) - *Time–space distribution of magmatic activity in the western Mediterranean and peripheral orogens during the past 30 Ma (a stimulus to geodynamic considerations)* J. Geodynamics, **34**: 99-126.

SCANDONE P. (1980) - *Origin of the Tyrrhenian Sea and Calabrian Arc.* Boll. Soc. Geol. It., **98**: 27-34.

SCROCCA D., DOGLIONI C., INNOCENTI F., MANETTI P., MAZZOTTI A., BERTELLI L., BURBI L. & D'OFFIZI S. (Eds.) (2003) – *CROP Atlas: seismic reflection profiles of the Italian crust.* Mem. Descr. Carta Geol. It., **62**.

SCROCCA D., DOGLIONI C. & INNOCENTI F. (2003) - *Constraints for an interpretation of the italian geodynamics: A review.* In: SCROCCA D., DOGLIONI C., INNOCENTI F., MANETI P., MAZZOTTI A., BERTELLI L. & D'OFFIZI S. (Eds.): "*Crop Atlos: seismic reflection profiles of the italian crust*". Mem. Descr. Carta Geol. It., **62**: 15-46

SELVAGGI G. (2001) – *Strain pattern of the Southern Tyrrhenian slab from moment tensors of deep earthquakes: implications on the down-dip velocity.* Ann. Geof., **44** (1): 155-165.

SELVAGGI G. & CHIARABBA C. (1995) - *Seismicity and P-wave velocity image of the Southern Tyrrhenian subduction zone.* Geophys. J. Int., **121** : 818-826.

SERRI G., INNOCENTI F. & MANETTI P. (2001) - Magmatism from Mesozoic to Present: petrogenesis, time-space distribution and geodynamic implications. In: Vai, G.B.and Martini, I.P. (Eds.): *"Anatomy of an Orogen: the Apennines and the adjacent Mediterranean Basins"*. Kluwer Academic Publishers: 77-104, Dordrecht, The Netherlands.

TATSUMI Y. & EGGINS S. (1995) - *Subduction Zone magmatism.* Blackwell, 211 pp.

TONARINI S., LEEMAN W.P. & FERRARA G. (2001a) - *Boron Isotopic Variations in Lavas of the Aeolian Volcanic Arc, South Italy.* J. Volcanol. Geotherm. Res, **110**: 155-170.

TONARINI S., ARMIENTI P., D'ORAZIO M. & INNOCENTI F. (2001b) - *Subduction-like fluids in the genesis of Mt. Etna magmas: evidences from boron isotopes and fluid mobile elements.* Earth Planet. Sci. Lett., **192**: 471-483.

TONARINI S., LEEMAN W.P., CIVETTA L., D'ANTONIO M., FERRARA G. & NECCO A. (2004) - *B/Nb and d11B systematics in the Phlegrean Volcanic District (PVD), Italy.* J. Volcanol. Geoth. Res., **133** (1-4), 123-139.

ZITELLINI N., TRINCARDI F., MARANI M. & FABBRI A. (1986) - *Neogene tectonics of the Northern Tyrrhenian Sea.* Giornale Geol., **48**: 1/2, 25-40.

WRIGHT I.C., PARSON L.M. & GAMBLE J.A. (1996) – *Evolution and interaction of migrating cross-arc volcanism and backarc rifting: An example from the southern Havre through (35°20'-37°S).* J. Geophys. Res., **101**: 22,071-22,088.

Mem. Descr. Carta Geol. d'It.
XLIV (2004), pp.165-184
8 figg.

Subduction and back-arc extension in the Tyrrhenian Sea
Subduzione e distensione di retro-arco nel Mar Tirreno

FACCENNA C. (*), FUNICIELLO F. (**), PIROMALLO C. (***),
ROSSETTI F. (**), GIARDINI D. (****), FUNICIELLO R. (**)

ABSTRACT - This paper is a synthesis of the work we have done in the Central Mediterranean subduction zone. Our effort is to tie together the geological signature of the subduction process and the plate kinematics with the deep images of the mantle to unravel a tectonic model at the scale of the Central Mediterranean mantle. This model is tested by means of laboratory experiments where we simulated the retreat of subducting slab sinking inside a stratified material. Geological data have been mainly collected in the Calabrian orogenic wedge where we can have preserved the trace of the oldest subduction event and in the back-arc region where we can infer the amount of retreat of the Calabrian trench. The amount of subduction in time has been reconstructed by estimating the amount of convergence from plate kinematics model with the amount of back-arc extension. These data have been used to propose a tectonic scenario and to backtrack the evolution of the Calabrian slab, starting from the present-day tomographic images. Finally the tectonic scenario is tested by means of laboratory experiments.
Our results give a dynamic picture of the evolution of the back-arc basins, suggesting that the kinematics and the dynamics of the central Mediterranean system is driven by the subduction of the land-locked oceanic lithosphere and that the episodic and intermittent phase of extension that produced the opening of the Liguro-Provençal first and of the Tyrrhenian basin, after, is the result of the interaction between the subducting slab and the 660-km discontinuity in a restricted convecting mantle.

KEY WORDS: central Mediterranean mantle, subduction kinematics, analogue modeling, episodic back-arc extension

RIASSUNTO - Questo lavoro rappresenta una sintesi del lavoro effettuato sull'evoluzione della zona di subduzione del Mediterraneo centrale. A tal fine sono stati integrati dati geologici, cinematici e sismologici. Il modello prodotto è stato testato utilizzando esperimenti di laboratorio a scala del mantello dove viene simulata l'evoluzione di un piano di subduzione all'interno di un mezzo viscoso stratificato.
I dati geologici analizzati riguardano le unità metamorfiche affioranti in Calabria, dove sono meglio preservate le testimonianze del cuneo orogenico, e nei bacini di retro-arco dove è possibile ricostruire la quantità di estensione e di arretramento della cerniera della placca in subduzione. Questi ultimi dati, sommati ai dati riguardanti la quantità di convergenza delle placche Africa-EurAsia hanno permesso di stimare la quantità di subduzione nel tempo. Questi valori sono stati confrontati con le immagini del modello tomografico al fine di produrre una paleoricostruzione terziaria del piano di subduzione. I risultati di questo esercizio, sono stati poi confrontati con quanto ottenuto in laboratorio.
Il modello proposto suggerisce che l'evoluzione del Mediterraneo Centrale è dinamicamente congruente con un modello di arretramento di una placca in subduzione. In particolare il discontinuo processo di arretramento della placca in subduzione, producendo l'apertura dei due bacini di retro-arco distinti (Liguro-Provenzale e Tirrenico) viene messo in relazione con l'interazione tra la placca in subduzione e la discontinuità posta a 660 km di profondità in un quadro convettivo ristretto al mantello superiore.

PAROLE CHIAVE: mantello Mediterraneo centrale, cinematica della subduzione, modelli analogici, estensione di retro-arco episodica

(*)Università di Roma Tre, Roma, Italy
Corresponding Author: Claudio Faccenna Dipartimento di Scienze Geologiche, Università di Roma Tre, Largo S. L. Murialdo 1, 00146, Roma (Italy). Fax +39-6-54888201 , Tel +39-6-54888029; (faccenna@uniroma3.it).
(**)Università di Roma Tre, Roma, Italy
(***)Istituto Nazionale di Geofisica, INGV, Roma Italy
(****)ETHZ Zurich, Suisse.

1. - INTRODUCTION

The origin of backarc basins represents an important task in plate tectonics. Their formation is somehow problematic as extensional processes and creation of new oceanic crust develop just to the back of convergent margins where oceanic lithosphere is consumed and digested into the mantle. Exploration of backarc basins around the globe, especially along the Western Pacific margin, allow us to define their peculiarities and differences if compared to oceanic basins. One of the striking characteristic of backarc basins is represented by their ephimeral life, which is generally in the order of 1-3 108 years. In some cases, namely to the back of the Izu-Bonin, the Marianas and the Tonga trench, backarc extensional process occurred episodically and the locus of extension jumps trenchward after quiescent periods of stasis. This represents the most enigmatic aspect of backarc extension and give us a complicated image of what can be the driving mechanism for backarc extension. Apart for the classical, Western Pacific examples, other basins around the world have been interpreted in terms of backarc extension. The Aegean and the Tyrrhenian Sea (fig. 1), for example, have been interpreted in terms of backarc extension (MALINVERNO & RYAN, 1986; KASTEN *et alii*, 1988; PATACCA *et alii*, 1990; SARTORI, 1990; DOGLIONI, 1991; ROYDEN, 1993; FACCENNA *et alii*, 1996; GIUNCHI *et alii*, 1996; JOLIVET & FACCENNA, 2000).

If this is the case, they represent rare examples of active back-arc basins developed on continental lithosphere. The Tyrrhenian basin, in particular, has been deeply explored and studied during several geophysical and geological surveys. The huge amount of data available at present on the Tyrrhenian basin structure and on its evolution makes it a unique candidate to analyse plate tectonic processes such as the ones that cause the internal dynamics of a back-arc system.

Here, we address the problem concerning the origin of the Tyrrhenian Sea, testing the hypothesis that its formation is related to the retreat of the Calabrian subducting slab. In this hypothesis, in fact, some questions still need to be answered. For example, it is not clear why did extensional processes take place in an overall convergence regime produced by the Africa-EurAsia relative motion or why did back-arc extension in the central Mediterranean create two different basins which intermittently opened reaching high rates of extension (up to 5-6 cm/y).

Our contribution to the problem is based on a multidisciplinary approach where the internal dynamics of the subduction-back-arc system is analysed using surface geological data in the back-arc region and subduction-accretionary wedge, tomography images at the scale of the mantle below the central Mediterranean, and tectonic reconstructions. The result of this different data set is integrated to set up laboratory experiments at the scale of the mantle with the aim to physically test the different models and hypothesis.

Our results give a dynamic picture of the evolution of the back-arc basins, suggesting that the kinematics and the dynamics of the central Mediterranean system is driven by the subduction of the land-locked oceanic lithosphere and that the episodic and intermittent phase of extension that produced the opening of the Liguro-Provençal first and of the Tyrrhenian basin, later, is the result of the interaction between the subducting slab and the 660-km discontinuity.

In this paper we synthesise the work we have done during the last years, first introducing the geological data, then the tomographic images at upper mantle level. Afterwards, on the base of a revised tectonic reconstruction, we will unravel the kinematics of the subducting system that will be tested using laboratory experiments.

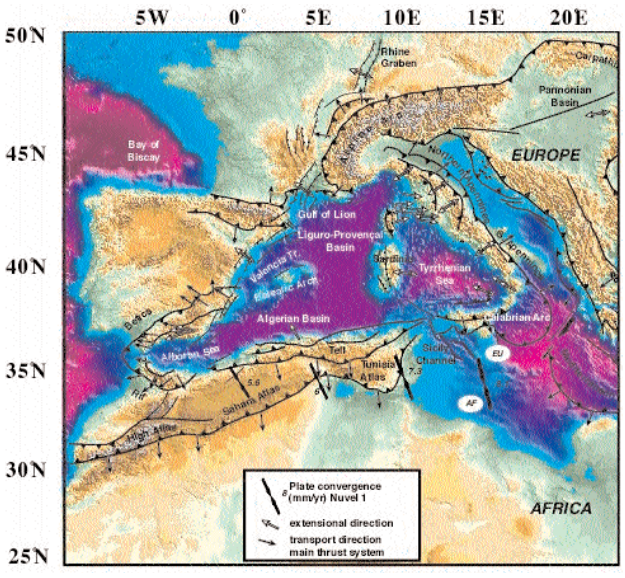

Fig. 1 - *Tectonic map of the western Mediterranean region. Sense of transport along main thrusts fronts (black arrows) and along the main extensional detachments (white arrows) are shown (see text for references).*

2 - THE CENTRAL MEDITERRANEAN SUBDUCTION ZONE: GEOLOGICAL STRUCTURE

Three distinct domains can be distinguished in the Central Mediterranean subduction zone. The inner orogenic domain, outcropping in northern Apennines and Calabria, which is constituted by polymetamorphic units and represents the oldest trace of a subduction process. It separates the extensional back-arc domain (Tyrrhenian, Liguro-Provençal) from the external domain, where slices of the sedimentary cover derived from the paleomargins are piled up (Apennines, Magrebides). Over the whole subduction zone, the extensional back-arc domain deforms contemporaneously with the external domain. Information concerning the evolution and the kinematics of the subduction system of the Tyrrhenian region can be found in the back-arc domain, which gives indications on

the kinematics of subduction (amount and rate of trench retreat) and on the inner orogenic wedge that can give us information about the age of the oldest event and of its geothermal gradient. The external portion also furnishes a lot of information concerning the way the subducting plate is flexed, but often the oldest trace of subduction are digested inside the subduction zone.

2.1. - The backarc system

Figure 2 shows a cross section at the scale of the lithosphere running from the Gulf of Lyon to Calabria. The cross section cuts across the two basins parallel to the direction of extension. In the upper panel of the figure 2 the ages of the syn-rift deposits of the sedimentary basin and of the main magmatic event is projected.

In the Provençal region, an older Late Eocene phase of extension related to the central european rift system is recorded (Seranne, 1999). Extension related to the opening of the Liguro-Provençal basin initiated probably during the Late Oligocene (Cherchi & Montadert, 1982; Gorini *et alii*, 1994; Seranne, 1999) within a Hercynian continental crust, except in the Gulf of Lions, which was previously affected by external Pyrenean thrusting. Extension developed at the back of a NW dipping subducting oceanic lithosphere, as attested by the presence of a volcanic arc (basaltic-andesitic suites, 32-34 Ma to 13 Ma) erupting along the Sardinian and Provençal margins (Beccaluva *et alii,* 1989, and references therein) (fig. 2).

The age of the syn-rift deposits, located along the western Sardinian and Provençal margins, ranges from the Oligocene to the Aquitanian (Cherchi & Montadert, 1982; Gorini *et alii*, 1994). From the late Aquitanian, post-rift deposits unconformably overlie the syn-rift sequence (Gorini *et alii*, 1994; Seranne, 1999), and oceanic crust (probably Burdigalian in age;) was emplaced during the 25°-30° counterclockwise drifting of the Sardinia-Corsica block (Van der Voo, 1993). In southern Sardinia the rate of drifting, according to paleogeographic reconstruction (Burrus, 1984) and to the age of rotation proposed by , can be estimated in the order of 4-5 cm yr^{-1}. As a result, the basin is characterized by oceanic crust within the central abyssal plain surrounded by narrow (except for the Gulf of Lions) older sedimentary basins (fig. 2). Based on this geometry and the pattern of magnetic anomalies the existence of a mid-oceanic ridge has been proposed (Burrus, 1984) even if the characteristics of a spreading ridge relief has not been observed on deep seismic profiles (de Voogd *et alii*, 1990).

In the Tyrrhenian basin, syn-rift deposits are progressively younger (10-12 Ma to 5 Ma) from Sardinia margin towards the Vavilov basin (Kasten *et alii*, 1988; Sartori, 1990). The age of first syn-rift deposition in the Sardinia margin, however is still uncertain, as a Tortonian-Serravallian unit (B3.2 seismic unit, Sartori *et alii*, 1990), has been interpreted as a pre- or syn-rift unit (Mattei *et alii,* 2002). The conjugate, drifted margin of Sardinia is the Calabrian block, where the syn-rift deposits of the Amantea basin are composed by Serravallian coarse-grained conglomerates and sandstone (Mattei *et alii,* 2002). On the western side, the initial rifting phase is followed by an E/ESE migration of the locus of extension and magmatism (fig. 2). The average velocity of extension is in the order of 5-6 cm yr^{-1} (Patacca *et alii*, 1990; Spadini *et alii*, 1995). Formation of oceanic crust occurred since 5 Ma in two separate and rather small basins (Bigi *et alii*, 1990) during the drifting of the Calabria block (figs. 2 c-d). It started first in the Magnaghi-Vavilov (4-5 Ma) and then in the Marsili (2 Ma) basin, getting younger towards the ESE (fig. 2).

The precise timing of formation of the arcuate structure of the Calabria-Sicily region is not precisely

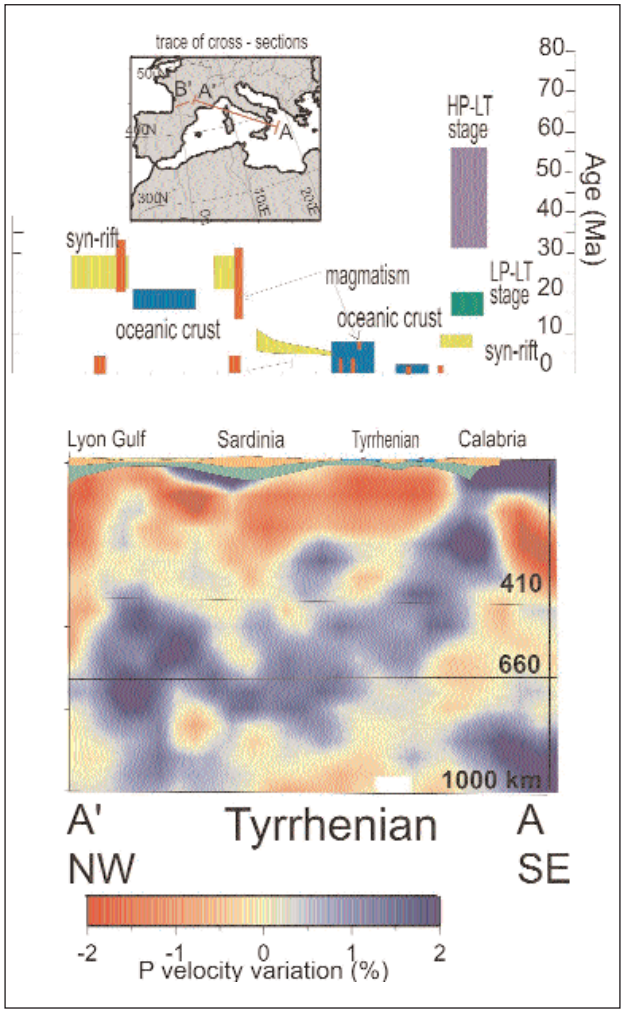

Fig. 2 - *Cross section of the studied area (location in the inset). (AA') From the Gulf of Lyon to Calabria. Crustal structure of section AA' is from from* Finetti & Del Ben (1982), Chamoot Rook *et alii* (1999). *Lithospheric structure is from* Suhaldoc & Panza (1989), Torné *et alii* (2000). *Tomographic cross sections are from model PM0.5* (Piromallo & Morelli, 2002). *The upper panels show the age and distribution of the geological record related to subduction (see text for references): metamorphism (blue and green boxes represent blueschist and greenschist facies, respectively), magmatism (red boxes represent volcanic and intrusive rocks), synrift deposits filling extensional basins (yellow box) and oceanic crust (light blue box).*

defined. Paleomagnetic data indicate that the arcuate shape was attained between the Late Miocene and the Pleistocene, during the opening of the Tyrrhenian sea. Significant counterclockwise rotation of the southern Apennines, in fact, occurred after the opening of the Liguro-Provençal basin (GATTACECA & SPERANZA, 2002), and part of this rotation (25°according to SAGNOTTI, 1992; SCHEEPERS *et alii*, 1993) should have occurred after the early Pleistocene. The Calabrian region itself rotated clockwise about 15°-25° during the Plio-Pleistocene (SCHEEPERS *et alii*, 1993; SCHEEPERS & LANGERAIS, 1994; SPERANZA *et alii*, 2000). Moreover, an overall clockwise rotation has been detected in the Sicilian belt (CHANNELL *et alii,* 1980, 1990**,** AIFA *et alii,* 1988**;** SCHEEPERS & LANGERAIS, 1993), but its timing and magnitude is still uncertain as it can be related to the complex rotational pattern of single thrust sheets (SPERANZA *et alii*, 1999).

In synthesis, the Tyrrhenian basin is characterized by extensional deformation, sedimentary basins, magmatic loci, and spreading centers which are distributed over a wide area (fig. 2). This contrasts with the Liguro-Provençal style of extension which shows a rather narrow margin (with the exception of the Gulf of Lyon), bordering the abyssal plain.

Over the whole, the Central Mediterranean basins show a rapid and intermittent episode of extension as the Tyrrhenian basin opened few million years after the drifting of the Liguro-Provençal basin. At the time extension initiate 30 Ma, we should expect that the subduction system was already developed enough to drive a vigorous retreating process.

2.2. - THE CALABRIA OROGENIC WEDGE

The nappe-structured belt of Calabria (fig. 1) is part of the peri-Mediterranean Alpine system progressively drifted and dispersed during the Neogene to Recent opening of the South Tyrrhenian basin and the subduction of the Ionian slab (DEWEY *et alii*, 1989; FACCENNA *et alii*, 2001a; HACCARD *et alii*, 1972). Here is preserved the oldest trace of the subduction process. However, the origin and tectonic significance of the Calabrian nappe architecture has been debated. In fact, kinematic data from Calabria have been used to support different interpretations of the Alps-Apennines linkage and the polarity of the subduction process in the Apennine region (see e.g. ; AMODIO MORELLI *et alii,* 1976; SCANDONE, 1982; BOULLIN, 1984; DIETRICH, 1988; CELLO *et alii,* 1996; DOGLIONI *et alii,* 1998; ROSSETTI *et alii,* 2001). These contrasting interpretations mainly derive from the kinematic stratification of the nappe pile, where both westward and eastward shear senses have been reported as responsible for nappe stacking (AMODIO MORELLI *et alii*, 1976; FAURE, 1980; DIETRICH, 1988).

The tectonic scheme generally accepted for the nappe architecture of Calabria is based on the synthesis of AMODIO MORELLI *et alii* (1976). In this scheme it is assumed that the Calabrian orogenic pile is the result of the eastward-verging overthrusting of an early westward-verging Alpine structured belt (Alpine Chain of AMODIO MORELLI *et alii,* 1976) onto the dominantly Meso-Cenozoic carbonate sequences that, originally part of the African and Adrian plate margin (Apennine Chain of AMODIO MORELLI *et alii,* 1976), presently constitute the major portions of the southern Apennine and Maghrebide chains. The Alpine Chain consists of the stacking of two main group of units: (i) Calabrian units (Calabride Complex of OGNIBEN, 1969), pre-Alpine (Paleozoic) in age, continental-derived metamorphic and igneous rocks and their Meso-Cenozoic sedimentary or weakly metamorphosed cover; and (ii) ophiolitic units (Liguride Complex of OGNIBEN, 1969), consisting of Cretaceous to late Oligocene ophiolite-bearing flyschoid sequences (BONARDI *et alii,* 1988, 1994) with local high-pressure/low-temperature (HP/LT) metamorphic signature (e.g. DE ROEVER 1972; SPADEA *et alii,* 1976; BECCALUVA *et alii,* 1982). This general picture, with no or few modifications, is also reported in more recent papers (BONARDI *et alii,* 1994; CELLO *et alii*, 1996; DOGLIONI *et alii,* 1998; THOMSON, 1994). In this scheme, it is thus assumed a priori that the present nappe contacts in Calabria are the results of overprinting compressional event, with no or little contribution of post-orogenic extension. In addition, it is also assumed that the high-pressure metamorphism (in both the Calabrian and Liguride complexes) occurred exclusively during the Alpine stage, i.e. during the westward-verging subduction linked to the eo-Alpine (Cretaceous and Paleocene) thickening phase, whereas the Apennine orogenesis produced only a reworking of the already structured high-pressure-belt (see also CELLO *et alii,* 1996, DOGLIONI *et alii,* 1998). This assumption strongly contrasts with the increasing amount of Tertiary ages (Eocene to Oligo-Miocene) that have been recently obtained for the orogenic metamorphism on the oceanic-derived units exposed in the northern Apennines ($^{40}Ar/^{39}Ar$ method on white micas of the Schistes Lustrées Nappe (BRUNET *et alii,* 2000; ROSSETTI *et alii,* 2000); and Calabria itself (ROSSETTI *et alii,* 2001). Fission track data on the Calabrian basement rocks also indicate a rapid un-roofing of this rock group between 30 to 18 Ma (THOMSON, 1994; 1998), once again confirming the Tertiary age of the main contacts within the nappe pile.

Based on coupled structural and petrographical investigations on the nappe stack exposed in the Sila Piccola Massif, we recently proposed an alternative tectonic scenario for the orogenic tectonic evolution of Calabria. ROSSETTI *et alii* (2001) documented the occurrence of a major top-to-the-W/NW semi-brittle to brittle extensional shear zone separating an upper tectonic complex from a lower one, each complex showing different Alpine metamorphic and structural signatures (fig. 3). The upper tectonic complex consists of a nappe-like structure, piling up the Calabrian, ophiolitic and Appenine carbonate rock units and recording a main top-to-the-E compressional shear. The lower tectonic complex consists of a polymetamorphic high-pressure-low-temperature (Mg-carpholite-bearing)

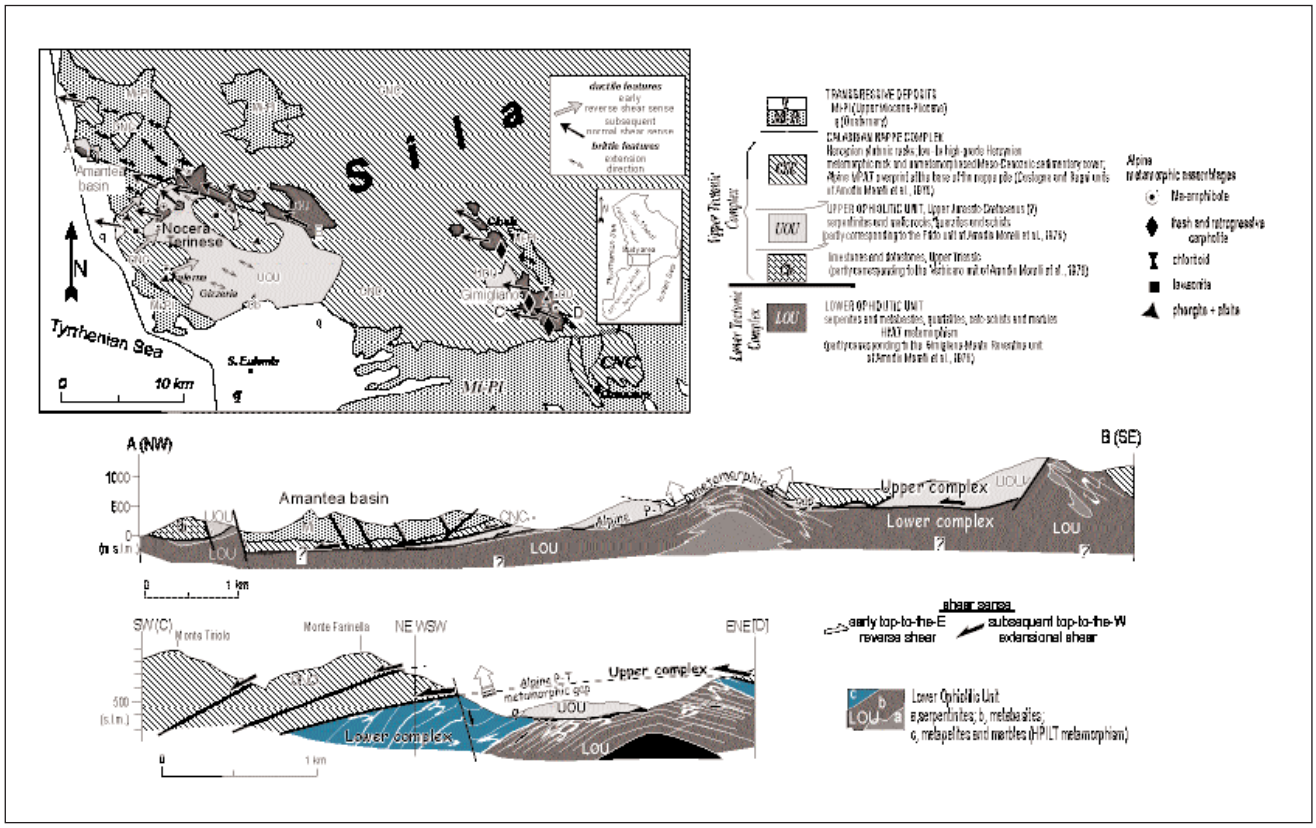

Fig. 3 - *Geological sketch map and related profiles showing the arrangment of the nappe stack of the Calabria orogenic wedge. Note the geometry of the flat-lying extensional detachment fault.*

ophiolite-bearing metamorphic sequence.

P-T estimates range from 0.5 to 0.8 GPa for pressure and less than 350°C for temperature in the continental-derived basement rocks (PICCARRETA, 1981; ROSSETTI *et alii,* 2001) and from 0.9 to 1.2 GPa for pressure and less than 450°C for temperature in the oceanic-derived rocks (SPADEA *et alii*, 1976; CELLO *et alii,* 1991; ROSSETTI *et alii*, 2001). Radiometric ages of the Alpine metamorphism range from Paleocene to Upper Oligocene times for the Calabride continental-derived rocks. BORSI & DUBOIS (1968) obtained ages ranging between 65 and 56 Ma (whole rock K/Ar and Rb/Sr methods), SCHENK (1980) of ~ 43 Ma (Rb/Sr method on pre-alpine biotites), BONARDI *et alii* (1987) of 25-30 Ma (Rb/Sr method on phengites). Ages of Alpine metamorphism for the oceanic-derived units are constrained at the Eocene-Oligocene boundary. ROSSETTI *et alii* (2001) obtained ages of ~35 Ma (Ar^{40}/Ar^{39} method on phengites) BECCALUVA *et alii* (1981) obtained ages ranging from ~ 48 to ~ 30 Ma (K/Ar method whole rock). Fission track data on the Calabride complex indicates a rapid unroofing of these rock types from 30 to 18 Ma (THOMPSON, 1998).

Top-to-the-northeast compressional shearing, syn- to post-kinematic to blueschist metamorphism, has been reported from the Variscan basement rocks of the upper plate (ROSSETTI *et alii,* 2001). These data, coupled with the ones derived from the same units (DIETRICH, 1988) and oceanic-derived units (MONACO, 1993) indicate a major northeastward-directed thickening event, locally experienced under blueschist metamorphic conditions. Ductile to brittle top-to-the west extensional shear (probably active since Late Oligocene) accompanied exhumation of the lower complex rocks, reworking the previous nappe contacts with shear localisation along the upper/lower tectonic complex discontinuity. A similar tectonic configuration has been previously described by PLATT & COMPAGNONI (1990) for the Calabrian units exposed in the Aspromonte region and for the Liguride Complex. Tectonic evolution of Calabria is thus reinterpreted as the effect of superimposed westward-directed extension onto a previously eastward-structured compressional belt.

Finally, domino-like style of extension controls the early tectono-sedimentary evolution of the Middle-Upper Miocene post-orogenic tectonic depressions, lying at the top of the brittle westward extending upper-plate nappe stack (MATTEI *et alii,* 2002). Maximum extension directions as deduced by fault slip data sets are subparallel to the stretching direction of the westward-verging attenuation shear zones (fig. 3).

Summing up, *HP/LT*, subduction-related metamorphism affecting both upper- and lower-plate

rocks is indicative of active underthrusting before and during the back-arc extension, from Paleocene to Early Miocene. The continuous formation of blueschist units thus better supports a model of continuous subduction at least from the beginning of the Tertiary.

3. - THE CENTRAL MEDITERRANEAN SUBDUCTION ZONE: DEEP STRUCTURE

The Calabrian Arc is the only region of the Mediterranean in which crustal, intermediate depth and deep earthquakes are recorded all along an approximately continuous dipping plane. Seismicity is distributed along a narrow (~200 km) and steep (~70°) Benioff plane, SW-NE striking and NW dipping, down to about 500 km (e.g. ANDERSON & JACKSON, 1987; SELVAGGI & CHIARABBA, 1995)

The presence of seismicity on a well defined Benioff zone reveals a direct trace of the past and still active process of lithospheric subduction from the Ionian foreland below the Calabrian Arc and Tyrrhenian Sea. Further information can be supplied by indirect seismological studies, such as seismic tomography, which are able to give insights into the three-dimensional deep structure of the region, providing images of deviation from an average reference velocity profile. This allows to determine the spatial distribution and lateral dimensions of the fast seismic velocity anomalies, in order to assess the extent of subducted lithosphere, and, if any, of an aseismic slab and to detect the presence of low seismic velocity areas.

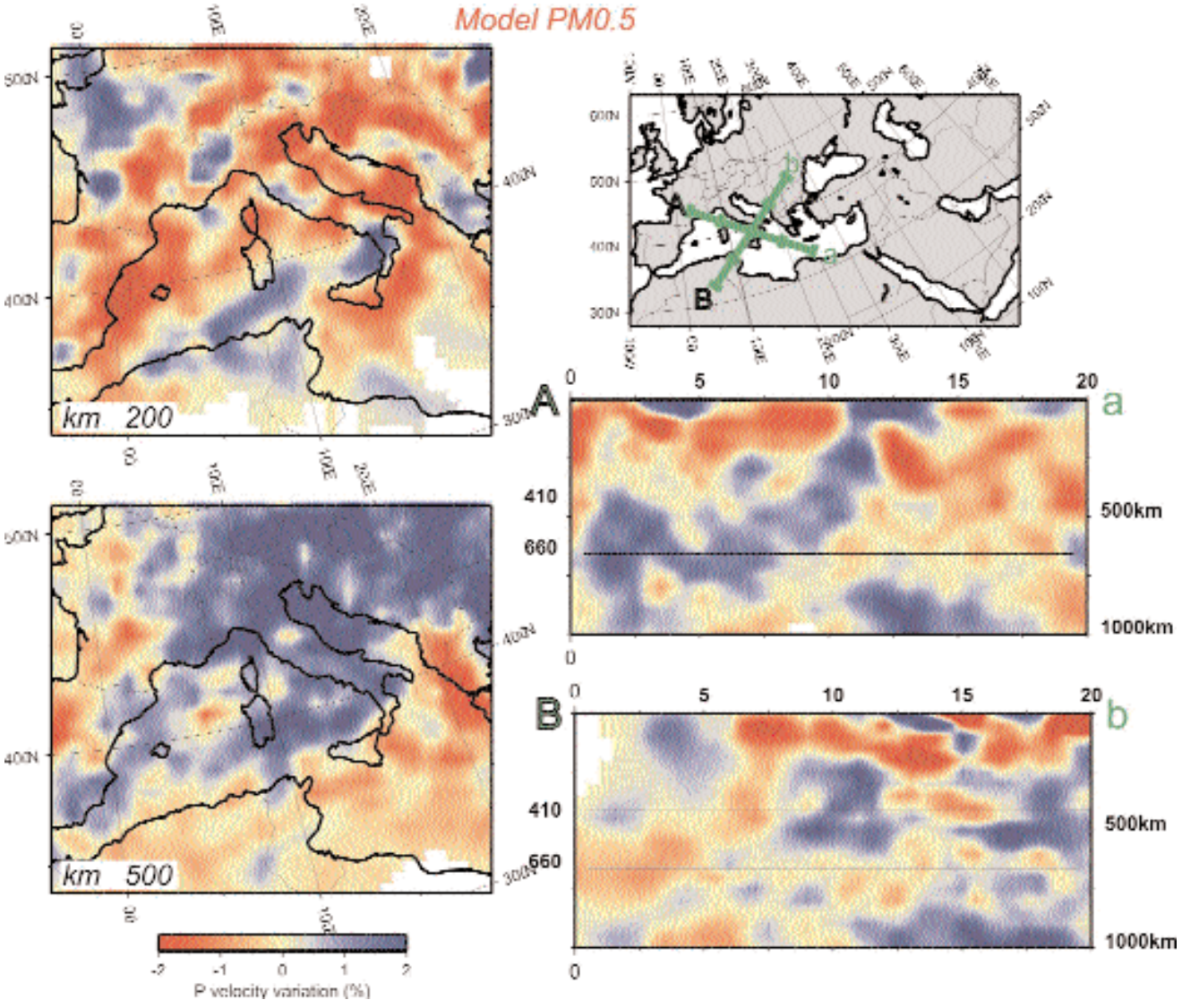

Fig. 4 - *Map views of tomographic results at 200 km and 500 km, and cross-sections (Aa, Bb) from model PM0.5* PIROMALLO & MORELLI (2002). *Velocity anomalies are displayed in percentages with respect to the reference model sp6* (MORELLI & DZIEWONSKI, 1993).

3.1. - Tomographic model PM0.5

We focus here on a limited area of the recent high-resolution, large-scale tomographic model built for the whole Euro-Mediterranean region (Piromallo & Morelli, 2003). The model (PM0.5) is obtained through the inversion of the large dataset constituted by the collection of over 30 years of P-wave delay times by the International Seismological Centre (ISC). After accurate data selection and relocation (52,000 relocated events using more than 5,000,000 observations), first arrival residuals of both regional (epicentral distance $\Delta \leq 28°$) and teleseismic ($\Delta > 28°$) rays from shallow earthquakes (focal depth $h \leq 50$ km) are used to compute summary residuals as input data to the inversion (Piromallo & Morelli, 1997; 2003). The velocity model is parameterized over a three-dimensional cartesian grid, with horizontal node spacing of roughly 55 km in both directions and 50 km vertical spacing, down to 1000 km depth. Standard ray tracing and inverse problem solution techniques are applied. The perturbation to the velocity field is computed and displayed with respect to the global reference velocity model sp6 (Morelli & Dziewonski, 1993).

Resolution sensitivity analyses, performed with input velocity anomalies of different spatial wavelength and shape, indicate that structures with spatial extent ranging from ~100 km to ~600 km are fairly resolved all over large part of the inversion domain. In the best sampled regions, features with size smaller than 100 km (and larger than 55 km, the nominal model resolution) are also detectable. However, smaller-scale details may sometimes result unstable in the inversion. Crustal structure is instead not explicitly modeled and therefore poorly or not resolved at all, implying that features at crustal depths may result unreliable.

3.2. - Images of the Southern Tyrrhenian area

The whole PM0.5 model is displayed by means of maps at different depth layers in Piromallo & Morelli (2003), therefore we refer to this paper for a comprehensive view. We show here in figure 4 a zoom in of the model into the region of interest, the Southern Tyrrhenian area, at two representative horizontal layers, at 200 and 500 km. The layer at 200 km depth roughly marks the limit between two depth ranges in which the seismic velocity of the region is characterised by a different structure. Below 200 km depth, the high velocity anomaly in correspondence of the Calabrian Arc joins into a continuous belt with the southern Apennines to the N and with the Sicily-Maghrebides chain to the SW (Piromallo & Morelli, 2003; Faccenna *et alii,* 2003).

Moving from 200 km depth to the surface, instead, high velocity anomalies along the peninsula appear disconnected from each other, interrupted by wide gaps of low velocity anomalies (below the southern Apennines and the Sicily Channel). Therefore, the Calabrian Arc is the only place where, along a segment whose lateral extent reaches ~300 km, the high velocity structure is vertically continuous all over the depth range, from the surface to the transition zone. The map at 500 km depth of figure 4, located in the middle of the transition zone, shows another representative layer, in which we can clearly see how the Calabrian fast anomaly merges into a broader positive anomaly, spreading all over central Europe and the western Mediterranean. This large-scale high velocity anomaly which characterizes the transition zone (Piromallo *et alii,* 2001), probably gathers the material from different portions of subducted slabs. Below the western Mediterranean we find the traces of Betic-Alboran, Algerian, Apenninic and Calabrian slabs (Faccenna *et alii,* 2003), while below central Europe fast velocity material likely comes from the Alpine-Carpathians subduction.

The vertical profile Aa (figs. 2, 4) cross-cuts the positive anomaly of the Calabrian Arc, approximately parallel to the direction of maximum extension of the Tyrrhenian basin. The high velocity structure can indeed be followed continuously, starting from a shallow horizontal portion, located on the Ionian side of the arc, which connects to a feature that deepens steeply to the NW into the mantle, down to 400 km, and then bends almost horizontal in the transition zone, lying on the 660 km discontinuity. Below the Tyrrhenian Basin a low velocity anomaly is detected, from the surface down to the top of the transition zone at 400 km, overlain by the fast shallow anomaly of the Sardinia-Corse block. In the eastern portion of the cross-section, note also the pronounced slow anomaly at intermediate depths, just behind the slab-like fast one.

Cross-section Bb (fig. 4), orthogonal to the previous profile, intersects the Calabrian fast anomaly along-strike, imaging the slab as a trapezoidal structure and showing its limited lateral extent. On its left side a very strong slow anomaly, is located in the shallower 150 km below the Sicily Channel and western Sicily. On the top right side of the trapezoid, another pronounced slow anomaly, below the Southern Apennines, and, further to the east, the fast slab-like body deepening below the Hellenides are imaged.

Overall, the three-dimensional image that we can derive from tomography for the Calabrian fast anomaly is that of a spoon-like structure, with a handle that is dipping to the NW at a steep angle and the cup which bends almost horizontally in the transition zone.

3.3. - Comparison with other models

All P-wave tomographic models available for the Southern Tyrrhenian area, based upon different datasets and techniques, are consistent in detecting a continuous fast velocity feature, steeply dipping below the Calabrian Arc: joint regional and teleseismic tomography with ISC P first arrivals (Spakman *et alii*, 1993; Piromallo & Morelli, 1997; 2003), teleseismic tomography with Italian National Seismic Network

(RSNC) P and PKP first arrivals (AMATO *et alii*, 1993; LUCENTE *et alii*, 1999), deep earthquake tomography with RSNC plus local networks P arrivals (SELVAGGI & CHIARABBA, 1995), and teleseismic tomography with RSNC P direct and secondary arrivals (CIMINI & DE GORI, 2001). This slab-like feature is unanimously interpreted as the signature of subducted lithosphere. Differences in the imaged structure among these models arise instead moving northward, below the southern Apennines, or in the Tyrrhenian and Ionian domains, mainly due to the combined effect of the ray-sampling/model inversion volume and of the pattern of heterogeneous structures which characterizes the area.

Teleseismic rays have quasi-vertical ray paths in the uppermost mantle and bottoming depths in the lower mantle, while regional ray paths have a larger horizontal component and turning points ranging in the upper mantle (down to 750 km), with discontinuous depth distribution due to the presence of upper mantle velocity interfaces (i.e. PIROMALLO & MORELLI, 1997). For these reasons there is a substantial difference, mainly at shallow depths, in the coverage provided by rays travelling in the two distance ranges, that result somehow complementary in space: teleseismic rays being confined to regions right below stations and events, especially in the shallower layers, while regional rays more extensively sampling the regions in between the ray foci. Therefore, while teleseismic tomography mainly detects features with a vertical extent, joint tomography of regional and teleseismic residuals is able to image, in addition, horizontally lying structures (SPAKMAN *et alii*, 1993; PIROMALLO & MORELLI, 1997; 2003). This explains why results of studies based on teleseismic data alone (see for comparison) fail in imaging features with horizontal rather than vertical extent (for example the fast Ionian lithosphere, fast Adriatic lithosphere, slow Tyrrhenian province of fig. 2). Moreover, below the central Apennines, where model PM0.5 detects a strong positive anomaly in the top 200 km (see fig. 4), teleseismic studies obtain an almost unperturbed/slightly positive model, likely due to limited vertical resolution at these depths.

The power of models built through joint inversion of regional and teleseismic data, like PM0.5 (PIROMALLO & MORELLI, 2003), with respect to tomography performed with teleseismic data alone, resides in that the combination of the two datasets results in the avalability of a large number of criss-crossing rays, with an ample range of incidence angles, which contribute to a more uniform illumination of the investigated volume and better constrain the resulting model.

4. - THE CENTRAL MEDITERRANEAN SUBDUCTION ZONE: KINEMATICS

To calibrate the tectonic evolution of the Central Mediterranean and to reconstruct the rifting and spreading events of the backarc Tyrrhenian and Liguro-Provençal basins we use the geological data illustrated before. In particular, to identify the main tectonic episodes and to estimate the amount of backarc extension, we subtract from the present geological cross-section (fig. 2) the oceanic crust and, using an area balancing technique, we restore the thinned continental crust to the thickness of its shoulders (fig. 2). The restoring technique is based on the assumption that the locus of extension at the surface corresponds to the locus of maximum crustal thickening (pure shear mechanism) and that the pre-rift thickness of the crust was about 30-35 km, as presently observed on the basin shoulders in Sardinia and in Provençal area (~30 km, see FINETTI & DEL BEN, 1986; CHAMOT-ROOKE *et alii*, 1999) where the amount of extension is considerably lower with respect to the basin itself. In addition, we neglect the role of erosion and possible lower crustal flow that might complicate the relationships. For these reasons, large error bars have been adopted. We estimated the amount of back-arc extension by reconstructing the

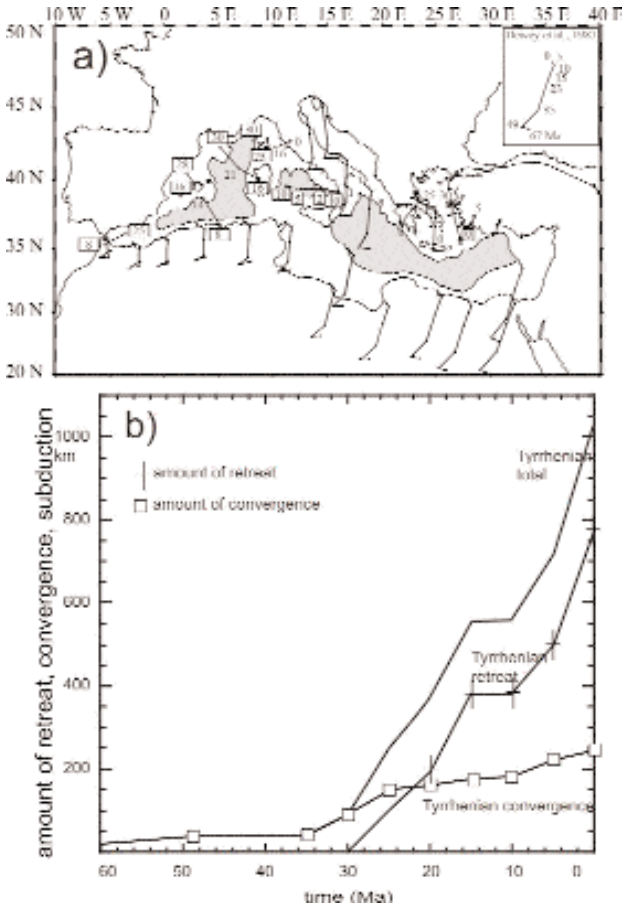

Fig. 5 - *(a) Displacement trajectories of Africa and Apulia motion with respect to stable Eurasia (calculated from* DEWEY *et alii* (1989), *see inset for stages division) and displacement trajectories related to back-arc extension (numbers are million years). (b) Amount of relative convergence, extension and total amount of subduction calculated along the cross-section of figure 2 perpendicular to the trench in the last 64 Ma.*

main tectonic events at the scale of the crust in different steps. Figure 5 shows the amount of extension attained by the Southern Tyrrhenian (steps at 3, 5, 7, and 10 Ma), and the Liguro-Provençal basin (step at 16, 23, and 30 Ma).

We note that the total amount of extension (~780 km) is partitioned roughly equally between the two basins, with alternating episodes of rifting (~7 Ma) and oceanic spreading (~5 Ma). In addition, we note that the rate of extension is reduced at the end of spreading of the Liguro-Provençal basin: rifting in the Tyrrhenian initiated after a small pause of few Ma and progressively accelerated.

We also find that the volcanic arc-trench gap is rather wide (~400 km) in comparison to the present-day. This suggests, in agreement with the paleo-reconstruction of BECCALUVA *et alii*, 1989 and SERANNE, 1999, that the slab attained a shallow dip prior to and after the opening of the Liguro Provençal basin. In addition, slab steepening has been proposed by JOLIVET *et alii*, 1999 and BRUNET *et alii,* 2000 along the northern section of the Tyrrhenian sea to account for the decreasing time gap between the HP compressional event and the onset of extension and magmatism.

The amount and velocity of extension estimated here is in good agreement with previous evaluations. Along the southern section of the Liguro-Provençal basin, the rifting event was estimated to be 150±20 km (CHAMOT-ROOKE *et alii*, 1999) while the amount of spreading was estimated to be 150 km (MAUFFRET *et alii*, 1995), 230 (BURRUS, 1984), and 230 ± 20 km (CHAMOT-ROOKE *et alii*, 1999; fig. 5). For the Tyrrhenian Sea, the total extension evaluated by MALINVERNO & RYAN, 1986 is on the order of 330-350 km. In the southern section of the Tyrrhenian Sea, similar values have been estimated by PATACCA *et alii*, 1990 and SPADINI *et alii*, 1995. Furthermore, the total amount of extension along the whole southern section agrees well with previous studies (GUEGUEN *et alii*, 1998).

The amount of convergence at the trench has been estimated by calculating the component of the Africa-Eurasia convergence perpendicular to the paleo-trench. Several kinematic reconstructions were proposed for the Mediterranean region to define the way the African plate converges toward Eurasia (e.g., DEWEY *et alii*, 1989; DERCOURT *et alii*, 1993). All of these models basically agree that Africa moved slowly relative to stable Eurasia with counterclockwise rotation, moving NE up to ~ 40 Ma, then N-S, and finally NNW (fig. 5). The relative velocity of a point located half way along the northern African coast was probably slower than 3 cm/yr during the last 80 Myrs, halving during the last 20-30 Ma (JOLIVET & FACCENNA, 2000). These numbers agree with another recent estimate of absolute plate motion for Africa (SILVER *et alii*, 1998). Geodetic data indicate that Africa currently moves N20°W at a rate of 0.7 cm/yr in the Central Mediterranean (WARD, 1994).

In order to estimate the net convergence rate (the rate at which the plates moved perpendicularly to the trench), we reconstruct the orientation of the trench in time (fig. 5). Paleomagnetic data indicate that Iberia accomplished a significant rotation (22° ± 14°) with respect to Europe between 132 and 124 Ma (VAN DER VOO, 1993; MOREAU *et alii,* 1997). After this episode, the rotation of the Iberian peninsula slowed down and was followed by translation (~120 Ma) during the initial phase of the opening of the Bay of Biscay (~85 Ma; JOLIVET, 1996, and references therein). At that time, the trench was therefore oriented NE-SW running parallel to the former Iberian passive margin. Subsequently, the trench position remained rather stable, turning to N-S only after the rotation of the Sardinia-Corsica block (~21-16 Ma;), and then turning again to its present-day position during the Southern Tyrrhenian spreading episodes (~5-2 Ma). The trench was therefore oriented roughly parallel to the motion of Africa during most of the subduction process. With the numbers from DEWEY *et alii*, 1989, we can estimate that the total amount of net convergence produced by the motion of Africa since 80 Ma is ~240 km with an average rate of 3 mm/yr. We note that the motion of the Adria microplate cannot contribute significantly to increase the convergence because its Tertiary motion can be assumed to be coherent with Africa (CHANNEL*,* 1986). We therefore observe that the net convergence velocity on the Central Mediterranean trench appears to be very low when compared with other subduction zones worldwide (JARRARD, 1986).

Figure 5 shows that the total amount of subduction during the Tertiary is on the order of 1000 km. This value derives from the sum of the contribution given by the Africa-EurAsia shortening (on the order of 200 km) and of the one given by the retreat of the trench (on the order of 800 km).

5. - THE CENTRAL MEDITERRANEAN SUBDUCTION ZONE: TECTONICS

On the basis of the geological and kinematic constraints, tied with tomographic images, we are able to reconstruct the evolution of the Calabrian slab in six main steps from 35 Ma to present-day (fig. 6). The main assumption behind this model is that the high velocity anomalies, imaged by tomography, are related to cold subducted material. This assumption is supported by the fact that seismicity is lined up over the high velocity anomalies and that the expected amount of subduction is in good agreement with the one measured from the tomographic images. The reconstruction is then performed subtracting from the present-day high velocity anomaly the estimated amount of subduction.

Around 35 Ma, the Calabrian slab constitutes a segment of the wider subducting slab, extending for more than 1500 km from southern Iberia to the Ligurian region (fig. 6). It dips towards NW and consumes the land-locked Jurassic oceanic basin (LE PICHON *et alii*, 1988). The position of the trench,

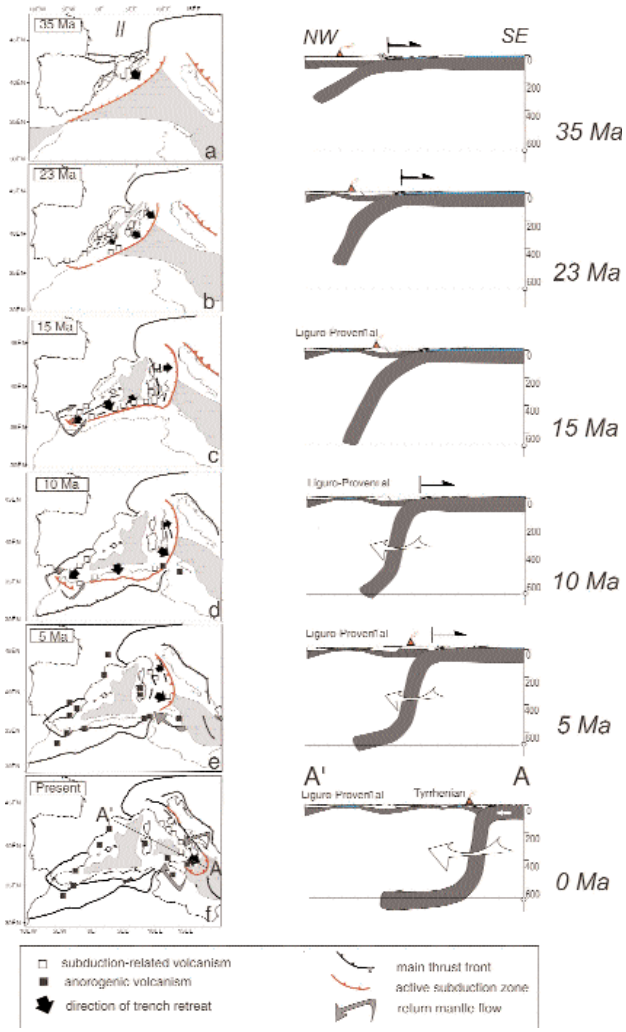

Fig. 6 - *Reconstruction of the evolution of the Mediterranean region in relative (Eurasia fixed) reference frame in six stages, from 35 to present-day. Oceanic domains are marked in grey. The location of the magmatic centers and their bearing with subduction process are marked with black (anorogenic) and white (subduction-related) squares. Cross sections illustrate the evolution of the subduction process along the the Tyrrhenian (inspired from the tomographic cross section AA' of Figure 2). Black arrows indicate the net motion of the trench, large white arrows indicate possible lateral flow of the mantle. Small volcanoes indicate the approximate position of the arc, if any.*

running along the Iberia margin, has been reconstructed by restoring back the amount of back-arc extension. The trench terminates to the north-east in correspondence of the Ligurian region, where subduction flips dipping southward beneath the Alps, and to the south-west in correspondence of the Gibraltar region where the Tethyan seaway gets narrow or even disappears (fig. 6). At this time, the subducting slab was probably continuous and already well developed, reaching a depth of 300-400 km and dipping at rather shallow angle. Therefore, the infant stage of the slab should be traced back at least up to the Paleogene, as attested by evidences of blueschist metamorphism in Calabria.

At about 30 Ma, the back-arc extensional process starts over the Mediterranean (JOLIVET & FACCENNA, 2000). It initiates in the north-eastern sector, in the Liguro-Provençal area. Calc-alkaline volcanism spreads over the region, attesting the efficiency of the subduction process. This large-scale re-organization of the subduction process over the whole Mediterranean region has been related to an increment of the retrograde motion of the slab under the concurrent action of increased slab pull level and of the decrease in the Africa rate of motion (JOLIVET & FACCENNA, 2000).

From 30 to 23 Ma (fig. 6) back-arc extensional processes propagate southward from the Liguro-Provençal basin to the Valencia and to the Alboran basin. Extensional processes localise not only in the backarc region, but also induce the collapse of the previously thickened orogenic wedges with the formation of large-scale flat-lying detachments in Calabria (ROSSETTI *et alii,* 2001). The formation of this structure and the exhumation of the deep-seated units attest a change in the evolution of the subduction wedge. The velocity of subduction, mainly related to the slab retrograde motion, progressively increases, reaching its maximum in southern Sardinia (fig. 6), and produces the formation of a first smooth arc, in front of the oceanic seaway. Calc-alkaline subduction related volcanism is widespread over the whole region from Sardinia to the Valencia and Alboran region.

Between 21 and 16-15 Ma (fig. 6), the Liguro-Provençal basin completes its opening phase with the peak of extension and during the rapid counter-clockwise rotation of the Sardinia block. Around 16-15 Ma, the retrograde migration of the western Mediterranean slab stops. No appreciable extension takes place during this time interval in the central-western Mediterranean basins. The geometry of the trench already attains a sharp curvature in the proto-Calabrian area possibly related with the lateral extent of the Tethyan oceanic seaway. Reconstruction of slab geometry reveals that at that time the subducted lithosphere already reaches and interacts with the deeper part of the transition zone (fig. 6). The interaction and deformation of the slab at its arrival at the 660-km discontinuity is proposed as a primary cause for the sudden decrease in the rate of rollback (FACCENNA *et alii*, 2001b)

Around 12-10 Ma (fig. 6) the locus of extension jumps southward from the Liguro-Provençal to the Tyrrhenian region.

Between 10 and 5 Ma (fig. 6) rifting migrates eastward inside the Tyrrhenian domain. There, the velocity of extension increases leading to the emplacement of an isolated oceanic spreading centres from about 5 Ma onward. From this moment we also observe the opening of the Sicily channel rift system, that can suggest that the Calabrian slab separates from the African one, following different directions: southward in northern African and southeastward in Calabria, where the trench retreats faster, consuming the oceanic seaway lithosphere. The formation of the slab window is marked by a change in the nature of

volcanism, and alkali-basalts are emplaced during the late Miocene- Pliocene in northern Tunisia and in Sardinia.

At present (fig. 6), the remnant of the once vigorous western Mediterranean subduction zone is preserved only in the narrow tongue below Calabria and perhaps in the northern Apennine (SELVAGGI & AMATO, 1992). Despite the presence of a well defined Wadati-Benioff zone (SELVAGGI & CHIARABBA, 1995), some arguments on the morphology of the accretionary prism off Calabria could suggest that the subduction process below Calabria is progressively decaying (CHAMOT-ROOKE, personal comunication).

6. - TESTING IN LABORATORY THE KINEMATICS OF THE CENTRAL MEDITERRANEAN SUBDUCTING SYSTEM

To test the tectonic reconstruction of subduction proposed here and back-arc extension we have performed 3-D laboratory experiments. In particular, the aim of this experimental program is to investigate the kinematics of a retreating subduction during the free sinking of the slab into the mantle and its interaction with the upper/lower mantle boundary.

6.1. - MODELS: ASSUMPTIONS AND LIMITATIONS

Our experiments are set up in the following framework:

1. - Viscous rheology. We model the slab as a viscous body assuming that the lithosphere behaves like a viscous fluid, characterized by large temporal- and spatial-scale, such as is the case for subduction (TAO & O'CONNELL, 1993). We further simplify slab behavior by using a Newtonian fluid whereas laboratory data indicate that upper mantle materials obey a creep power law of deformation (e.g. BRACE & KOHLSTEDT, 1980). Since a Newtonian material has a stronger response to deformations than a power-law fluid (RANALLI, 1995), the velocities observed in laboratory should be considered as a lower bound.

2. - No net plate convergence. The system is driven only by the slab pull force to simulate the Central Mediterranean conditions where the average net convergence of the incoming African plate at the trench has always been very low (DEWEY *et alii*, 1989; DERCOURT *et alii*, 1993)

3. - The system is isothermal. For experimental constraints we consider a simplified system governed only by the negative buoyancy of the subducting lithosphere; no positive buoyancy from plumes is included. The negative buoyancy is implemented chemically. This implies that the mantle is convectively neutral so that the only moment within it is that caused by the lithosphere/slab system. Moreover it is assumed that the density contrast of the slab is preserved during the whole subduction process. This situation is equivalent to quasi-adiabatic conditions. Our velocity of the subduction process is much higher than 1 cm/y. Under these conditions, we effectively neglect temperature changes during subduction (WORTEL, 1982; BUNGE *et alii*, 1997). Another consequence is that we neglect the role of the endothermic phase changes at the transition zone (CHRISTENSEN & YUEN, 1985; TACKLEY, 1993; PYSKLYWEC & MITROVICA, 1998). The possible effect of impediment for the slab to penetrate into the lower mantle is here reproduced only by the increase in viscosity with depth.

4. - The system does not include an overriding plate. This simplification has two consequences. The first consequence is that we assume that the subduction fault is weak with a viscosity comparable with the upper mantle viscosity. This choice is able to reduce the time scale of the subduction process but not its general behavior (KING & HAGER, 1990). The second consequence is that the overriding plate is assumed to passively move with the retreating trench. Therefore, this experimental setting can be considered as appropriate for all the natural cases, including the central Mediterranean, where the motion of the overriding plate towards the trench is lower than the velocity of trench retreat.

6.2. - SETUP

Following the approach used in previous analogue studies**,** the rheology of the lithosphere, upper- and lower mantle is approximated by linear viscous multi-layer regions (KINCAID & OLSON, 1987; GRIFFITHS & TURNER, 1988; GRIFFITHS *et alii*, 1995; GUILLOU-FROTTIER *et alii*, 1995; FACCENNA *et alii*, 1996; FACCENNA *et alii*, 1999). The analogue materials, a silicone putty-honey composite, are selected to scale to the slab–mantle system, as described by FACCENNA *et alii* (1999). A lower mantle layer has been added as a new feature. Silicone putty is a visco-elastic material. For the applied experimental strain-rate the silicone putty can be considered as a quasi-Newtonian fluid where stress increases linearly with strain rate (WEIJERMARS, 1986). It is composed of a pure polymeric substrate (polidimethylsiloxane-PDMS) with galena powder to vary both density and viscosity. The upper mantle has been modeled by honey, which is a Newtonian low-viscosity fluid. The increase in viscosity in the lower mantle has been reproduced by a mixture of pure honey and glucose syrup. The viscosity and density of each layer are constant and are considered as average effective values. Parameters and values for nature and the experimental system are listed in table 1.

The multilayered system is arranged in a rectangular Plexiglas tank (34 cm high, 58 cm long and 14 to 30 cm wide). Vertical walls are lubricated by a homogeneous layer of Vaseline in order to minimize edge effects. Experiments were performed 2-6 times to ensure reproducibility. Each experiment was monitored using a sequence of photographs taken in time intervals (from 1 to 4 minutes) in the lateral and top view.

Tab. 1 - *Scaling of parameters in nature and in laboratory for a reference model.*

PARAMETER			NATURE	REFERENCE MODEL
g	Gravitational acceleration	m s^{-2}	9.81	9.81
Thickness				
h	Oceanic lithosphere	m	70000	0.012
H	Upper mantle		660000	0.11
Scale factor for lenght			$L_{model}/L_{nature}=1.6\ 10^{-7}$	
Density				
ρ_l	Oceanic lithosphere	kg m^{-3}	3300	1482
ρ_{um}	Upper mantle		3220	1383
ρ_{lm}	Lower mantle		3220	1383
Density contrast (ρ_l-ρ_{um})			80	99
Density ratio (ρ_l/ρ_{um})			1.025	1.072
Viscosity				
η_l	Oceanic lithosphere	Pa s	$4\ 10^{23}$	$1.6\ 10^{5}$
η_{um}	Upper mantle		$4\ 10^{21}$	459
η_{lm}	Lower mantle		$1.2\ 10^{23}$	$1.8\ 10^{4}$
Viscosity ratio (η_l/η_{um})			10^{2}	$3\ 10^{2}$
t	**Characteristic time**	s	$3.1*10^{13}$ *(1Ma)*	60 *(1min)*

6.3. – Results

We show here the results of two experiments (out of 50 performed) characterized by the same lithospheric structure but by a different upper/lower mantle condition: experiment 1, with a uniform mantle configuration, and experiment 2 with a layered configuration with a lower mantle 30 times more viscous than the upper mantle (tab. 2 fig. 7).

In both cases we identify a distinct sequences of phases:

Phase I: Subduction initiation

To start the process, the silicone plate is initially manually bent inside the syrup to reach the critical amount of a gravitational unstable wedge corresponding to about 150-200 km in nature. More detailed problems linked to initiation of subduction are beyond the scope of these experiments (McKenzie, 1977; Mueller & Phillips, 1991; Ericksson & Arkani-Hamed, 1993).

Phase II: Free falling slab

Once the subduction instability is formed, the plate starts to sink into the mantle increasing progressively its dip to about 70°-90° while both velocity of trench motion and back-arc opening accelerate. Confirming the laboratory and numerical modeling of Becker *et alii*, 1999, we find that during the free fall descent into the mantle the slab length

Tab. 2 - *Physical parameters used in the selected experiments. The rheogical parameters are measured at room temperature.*

Experiment	Oceanic lithosphere	Upper mantle	Lower mantle
1	h=0.012 m ρ=1482 kg m^{-3} η=1.6×10^{5} Pa s	H=0.11 m ρ=1383 kg m^{-3} η=459 Pa s	ρ=1383 kg m^{-3} η=459 Pa s
2	h=0.012 m ρ=1482 kg m^{-3} η=1.6×10^{5} Pa s	H=0.11 m ρ=1383 kg m^{-3} η=459 Pa s	ρ=1383 kg m^{-3} η=1.5×10^{4} Pa s
3	h=0.012 m ρ=1482 kg m^{-3} η=1.6×10^{5} Pa s (laterally free)	H=0.11 m ρ=1383 kg m^{-3} η=459 Pa s	ρ=1383 kg m^{-3} η=1.5×10^{4} Pa s

H(t) scales exponentially as:

$$H(t) \propto H_0 \exp\left(C \frac{\Delta\rho g r^3}{\eta_o R^2} t\right) \qquad (1)$$

where $\Delta\rho$ is the density contrast between the ocean and the upper mantle, g the gravitational acceleration, r the bending radius, R the width of the plate, H_o the initial length and η_o the viscosity of the oceanic plate. The scaling indicates that the subduction process results mainly from the balance between two opposite actions: the negative buoyancy of the subducted material and the resisting viscous dissipation due to the bending at the trench.

As a kinematic consequence the descending slab has always a retrograde migration which produces a significant mass flow in the mantle directed from region of high pressure to region of lower pressure.

Phase III: Interaction slab/transition zone

When the slab reaches and anchors at the upper/lower mantle discontinuity, it decreases its dip to 50° while subduction and trench migration are temporarily delayed for about 5-10 Ma. The lithospheric system, then, bends laterally attaining an arcuate shape which allows the lateral escape of mantle material. From this moment subduction and trench migration resume while, simultaneously, the lower portion of the subducted lithosphere starts to bend and to lie down on the transition zone, the dip of the slab steepens again to 70° and the locus of back-arc extension jumps trenchward.

Phase IV: Steady-state subduction

The system reaches a steady-state configuration characterized by slab reorganization and a constant trench retreat velocity.

We find that at the observed timescales, the general features of the subduction evolution are relatively insensitive to the choice of viscosity imposed for the 660 km discontinuity. We obtain both the episodicity and the stagnant behavior of the slab lying on the 660 km discontinuity by imposing any viscosity ratio between the lower and the upper mantle higher than 10 (FUNICIELLO *et alii*, 2003). In any case, phase III is strongly dependent on the lateral boundary conditions. To test it, in experiment 3 we double the width of the box leaving constant the width of the plate. It ensures lateral circulation of the mantle during the whole process. As predicted by previous calculation (DVORKIN *et alii*, 1993), the process increases remarkably its velocity (rate similar to experiments 1), but the general picture is preserved. In particular, the subduction process is interrupted only for few Ma during the slab-660 km discontinuity interaction and the final dip of the slab is higher.

7. - REMARKS ON THE DYNAMICS OF THE CENTRAL MEDITERRANEAN SUBDUCTION SYSTEM

The comparison between laboratory simulation and the kinematics of the system permits to drawn some considerations on the dynamics of the Central Mediterranean

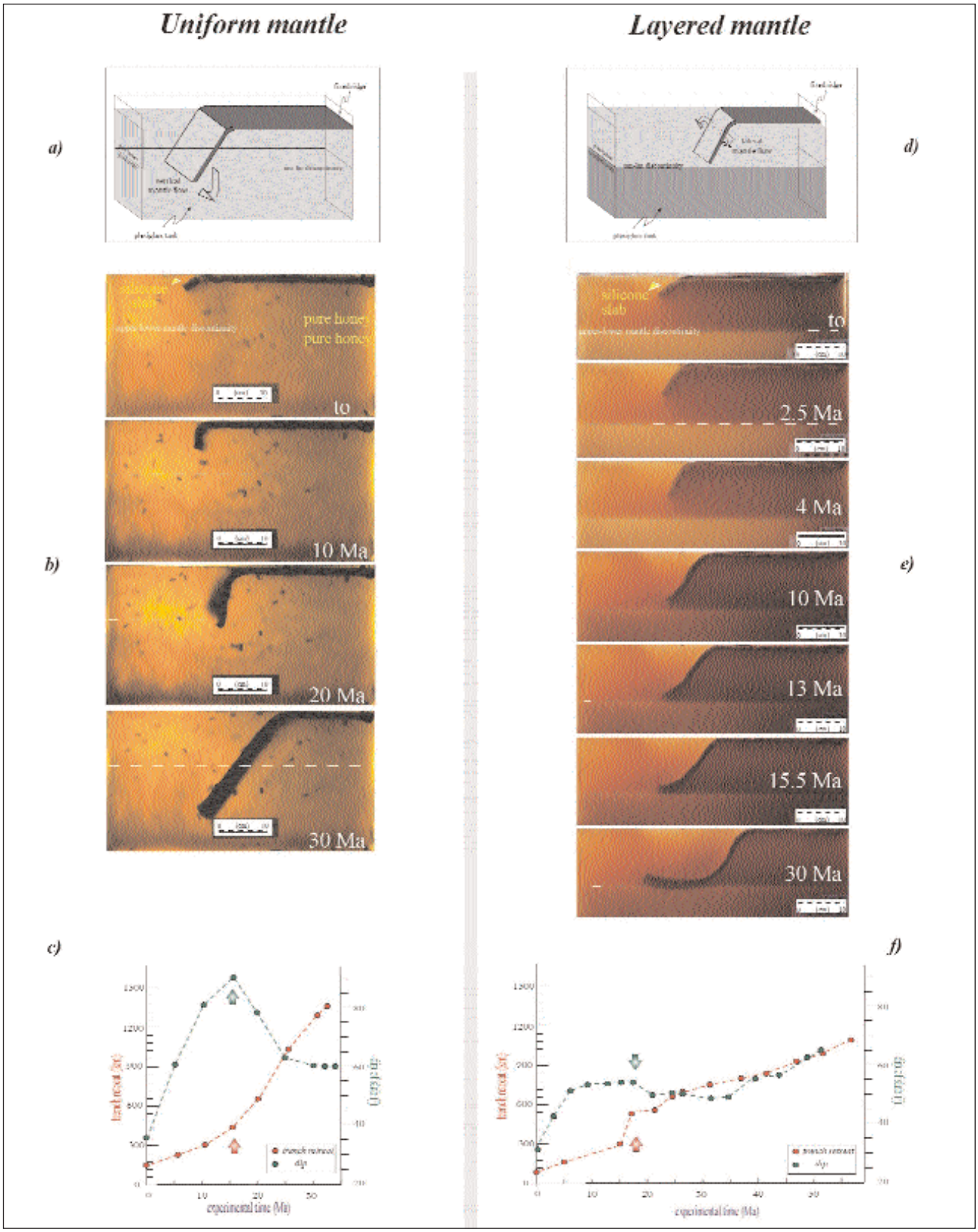

Fig. 7 - *(a) Set up of the experiment 1 characterized by a uniform mantle configuration; (b) lateral view of four stages of evolution of the experiment 1; (c) plot of amount of trench retreat and dip versus time for the experiment 1. The arrow indicates the time of interaction with the 660 km discontinuity. Hereafter 1 minute and 1 centimeter in the experiment correspond to 1 Ma and 60 km; (d) set up of the experiment 2 characterized by a layered configuration with a lower mantle 30 times more viscous than the upper mantle; (e) lateral view of four stages of evolution of the experiment 2; (f) plot of amount of trench retreat and dip versus time for the experiment 2.*

subduction zones, respecting the separation in three different steps, as in the experiments.

Phase I, 60-35 My: subduction initiation. In this initial phase, lithospheric subduction is entirely pushed by the slow plate convergence. About 300-400 km of cold lithosphere subducts at low angle, reaching a depth of 150 km and allowing the development of arc-volcanism. This means that until a critical gravity anomaly is reached, subduction will not be driven by gravity, but only by the incoming plate velocity. During this phase, the orogenic structure in the subduction wedge is dominated by thrusting of the nappe pile at different depth. The strong coupling between the plates prevents the exhumation of the deepest blue-schist units. It is difficult to estimate the velocity of subduction during this phase because it is difficult to define the exact age for the initiation of subduction. Pressure-Temperature estimate for the 35 Ma old blue-schist units gives a quite cold gradient typical of vigorous subduction process.

Phase II, 30-16 My. The presence of arc volcanism signals that a sufficient length of subducted lithosphere is available to allow the gravitational pull to become the driving force of the subduction. Back-arc opening starts, aided by (i) the weakening of the lithosphere due the volcanic activity in the back-arc region, and (ii) the decrease of the confining horizontal compression on the Alpine orogen associated to the decrease in absolute motion of the African plate (JOLIVET & FACCENNA, 2000). Subduction velocity rapidly increases up to 4 cm/y during the rifting and spreading phases of the opening of the Liguro-Provençal basin.

The progressive increase of subduction velocity during phase II (starting at 35 My ago) can be matched by the results of laboratory experiments simulating the free falling of a slab into the mantle under the effect of gravitational pull and can be fit by the equation (1) (FACCENNA *et alii*, 2001a) (fig. 8).

In particular, this result indicates that the time-scale of the process is highly influenced by choice of the viscosity of the slab/mantle system, but the general trend of the process is respected. Our results also show than when the subduction is gravity-driven in an unrestricted upper mantle the pattern is not sensitive to lower mantle conditions. We observe that after the first phase of shallow- dipping subduction initiation, the gravity-driven slab increases its dip to about 70° while both slab sinking and back-arc opening accelerates (fig. 5). Confirming the laboratory and numerical modeling of BECKER *et alii* (1999), we find that during the free fall descent into the upper mantle the slab length *H(t)* scales exponentially with the load exerted by the subducted lithosphere and resisted mainly by the viscous dissipation due to bending of the oceanic lithosphere at the trench.

Phase III, 16 My-present: interaction slab/transition zone. At about 16 My ago in the absolute time scale in figure 7, the slab hits the 660 discontinuity and impinges in the lower mantle. In the simpler case of a whole, undifferentiated mantle (exp.1; fig. 7), the subducting slab sinks freely into the lower mantle, increasing its depth and the rate of back-arc opening. A single exponential scaling reproduces accurately this behavior, but cannot in any way reproduce the reduction of the rate of subduction recorded 16 Ma ago at the end of the Liguro-Provençal opening, nor the second episode of Tyrrhenian opening. Only a restricted upper mantle convection characterized by a viscosity ratio higher than 10 between lower and upper mantle (exp.2 in fig. 7 and 8) can simulate this process. When the slab reaches and anchors at the 660 km boundary subduction and trench migration stop; then, under the pull of its own weight, the slab/lithospheric system starts to bend laterally attaining an arcuate shape allowing lateral escape of mantle material. From this moment, the lower portion of the subducted lithosphere deforms at depth. After 5 My the slab tip lies horizontally in the transition zone, the locus of back-arc extension jumps trenchward following the new, steep configuration of the slab and subduction and trench migration resume. The experimental curve 2 fits well the geologic timing in figure 8, showing that indeed the episodic trench migration in the Mediterranean can be explained by the interaction between the subducting slab and the transition zone.

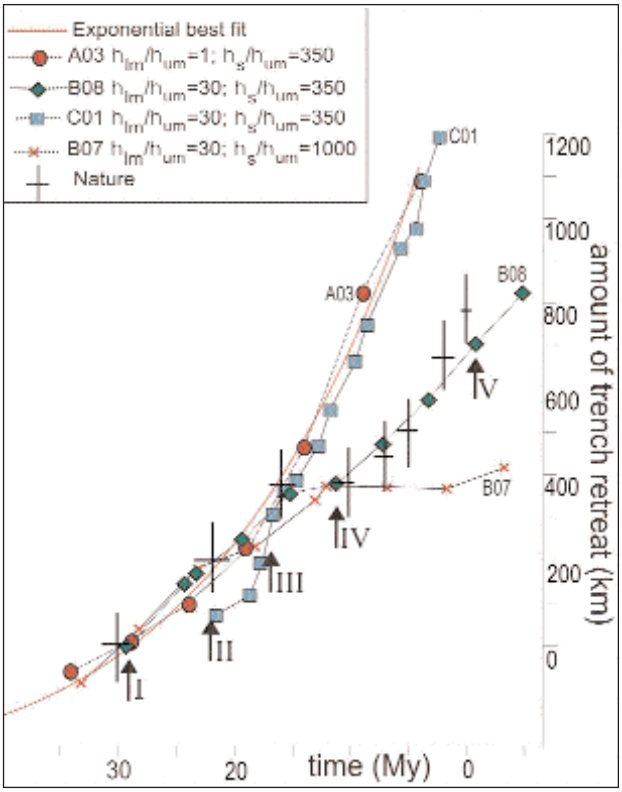

Fig. 8 - *Diagram comparing the geological timing of trench migration in the Central Mediterranean during the last 40 Myr with the results from different models. We show four laboratory experiments (A03, B08, B07, C01) using the scaling rules listed in table 1 (1 Myr corresponds to about 1 min of experiment, and 60 km correspond to 1 cm) and in table 2; the timing of the five snapshots I-V of curve B08 displayed in Figure 7e are marked. We also show the best-fitting exponential curve to experiment A03, simulating a gravity-driven subduction in a homogeneous mantle.*

As illustrated before, the importance of the convection process in restricted mantle configuration is further illustrated by the result of another set of experiments, settled with an unbounded upper mantle circulation: this experiment preserved the general picture but the process increases remarkably its velocity. In particular, the subduction process is interrupted only for few My during the slab-660 km interaction and the final dip of the slab is higher.

In the Central Mediterranean, a partially bounded upper mantle circulation provides a good fit to the timing history of the episodic back-arc opening (exp.2 is marginally slower than the geological curve in figure 8), in agreement with the continuous surface geological signature and with the high-velocity anomaly imaged in the transition zone along the entire Calabrian Arc-Apennine line, but also with the possible partial lateral detachment of the slab proposed for the last evolutionary phase of subduction (WORTEL & SPAKMAN, 2000). We speculate that the formation of the Sicily channel rift zone, for example, could represent the superficial feature of a deep process related to the lateral escape of the mantle material from beneath the slab.

This tectonic model has a number of geological implications.

(i) First, the non-steady evolution of subduction process in the Central Mediterranean founds direct correlation with the evolution of the subduction zone. The phases distinguished here at the scale of the mantle are also reflected in the evolution of the inner orogenic wedge. The exhumation of the high –pressure units are, for example, attained during the maximum acceleration of the extensional process during the opening of the Liguro-Provençal region. This means that the overall re-organization of the subduction process has a direct influence on the evolution of the subduction wedge itself, corroborating previous ideas (JOLIVET *et alii,* 1999). The end of the exhumation event, in fact, corresponds with the stasis of the extensional process that occurred between 16 and 12 Ma. The period of stasis of extension and the re-organisation of subduction process is also recorded by volcanism. The volcanic activity of the arc with a calk-alcaline imprinting, in fact, stopped at the end of the Sardinia-Corsica drifting and is resumed after few million years in the Tyrrhenian region (ARGNANI & SAVELLI, 1999).

(ii) The entrance of the continent at trench, probably attained at 35-40 Ma, did not cause any decrease in the rate of subduction. In fact, soon after the entrance at trench of the small continental margin the subduction process accelerates causing back-arc extension. This fact can be probably justified by the small dimension of the subducting continent compared to the already subducted negatively buoyant oceanic lithosphere. Analytical (RANALLI *et alii,* 2000) and laboratory experiments (REGARD *et alii*, 2003), for example indicate that the only subduction of more than 200-300 km of light continental material material is indeed able to reduce and stop the subduction process.

(iii) The opening of the Sicily channel can be related to the necessity for the mantle to laterally escape from beneath the slab. In fact, the formation (late Messinian-Pliocene) of this rift zone is coeval with the break-up of the Tyrrhenian crust and the acceleration of slab retreat.

The model proposed here bears interesting insights on the way the slab deforms and on the way the mantle convects over the geological time-scale. Our model indicates that the evolution of the subduction process is a non-steady state process punctuated by an intermittent evolution related to the interaction between the slab and the deep mantle layers. In particular, the episodic evolution of back-arc basins is here interpreted as an effect of the restricted convection process related to an increase of viscosity with depth. This idea is in agreement with the finding of different tomographic models that the high velocity anomaly below the Central-Western Mediterranean region is restricted in the upper mantle and lying over the 660-km discontinuity.

The model presented can be used to interpret the gross evolution of the Central Mediterranean slab. We identify the interaction between slab and mantle as the key to interpret the non-steady evolution of the retreating slab and its intermittent behaviour. This model fits the geometry of the slab, as imaged by tomography, and the timescale of the retreating process. In addition, we propose an alternative mechanism to explain the opening of the Sicily channel rift system.

The validity of this model should be tested by other independent data sets. For example, shear wave splitting can shed light on the mantle pathway around the Calabrian slab. In our model, for example, we should expect a strong imprinting of the seismic anisotropy of the mantle with fast polarization that turns around the slab and converges, in western Sicily, towards the Tyrrhenian region. In addition, structural analysis could contribute to constrain the kinematics of the Sicily channel rift system that seems to be characterised by the superimposition of different deformational episodes (CELLO *et alii*, 1985; JONGSMA *et alii*, 1987; GRASSO *et alii,* 1990; ARGNANI, 1993). Finally, testing the different phases of evolution of the model as proposed in figure 6 can be also done by including dynamic topography produced by the motion of the slab and its coupling with the mantle, and this can be compared with the curve of subsidence in the southern Tyrrhenian region.

This model with its inherent semplicity does not account for the very recent evolution of the Calabrian subduction zone. During the last 700 kyr the Calabrian arc, in fact, underwent rapid uplift. The GIUNCHI *et alii* (1996) simulation illustrates that uplift of the calabrian arc can be justified by the unlocking of the subduction zone during its retreat. We believe that the reconstruction of the present-day velocity field can reveal if the Calabrian Arc is indeed still retreating at high rate, as it has done during the Pliocene, or most probably, if we are assisting to its final decay.

Acknowledgements

This research derives from the long-term collaboration between the ETHZ *of Zurich, the University of Roma Tre and the* INGV *of Rome.*

REFERENCES

AIFA T., FEINBERG H. & POZZI J.P. (1988) - *Pliocene-Pleistocene evolution of the Tyrrhenian arc: Paleomagnetic determination of uplift and rotational deformation*, Earth Planetary Sci. Letters, **87**: 438-452.

AMATO A., ALESSANDRINI B., CIMINI G., FREPOLI A. & SELVAGGI G. (1993) - *Active and remanant subducted slabs beneath Italy: evidence from seismic tomography and seismicity*, Annali di Geofisica, **36**: 201-214.

AMODIO-MORELLI L., BONARDI G., PAGLIONICO A., PERRONE V., PICCARETTA G., RUSSO M., SCANDONE P., ZANETTIN LORENZONI E., ZUPPETTA A. (1976) - *L'arco Calabro-Peloritano nell'orogene Appenino-Magrebide*, Mem. Soc. Geol. It., **17**, 1-60.

ANDERSON H. & JACKSON J. (1987) - *Active tectonics of the Adriatic region*, Geophysical Journal of the Royal Astronomical Society, **91**: 937-987.

ARGNANI A. & SAVELLI C. (1999) - *Cenozoic volcanism and tectonics in the southern Tyrrhenian sea: space-time distribution and geodynamic signifiance*, Journal of Geodynamics, **27**: 409-432.

ARGNANI A. (1993) - *Neogene basins in the Strait of sicily (Central Mediterranean): tectonic setting and geodynamic implications.* In: BOSCHI *et alii* (Eds.): *"Recent evolution and seismicity of the Mediterranean region"*, Kluwer Publishers, 173-187.

BECCALUVA L., CHIESA S. & DELALOYE M. (1981) - *K/Ar age determinations on some Tethyan ophiolite*s. Rend. Soc. It. Min. Petr., **37**: 869-880.

BECCALUVA L., MACCIOTTA L. & SPADEA P. (1982) - *Petrology and geodynamic significance of the Calabria-Lucania ophiolites*. Rend. Soc. It. Min. Petr., **38**: 937-982.

BECCALUVA L., BROTZU P., MACCIOTTA G., MORBIDELLI L., SERRI G. & TRAVERSA G. (1989) - *Cainozoic Tectono-magmatic evolution and inferred mantle sources in the Sardo-Tyrrhenian area*, In: VAI G.B. (Ed.): *"The lithosphere in Italy. Advances in science research"*. pp. 229- 248, Accademia Nazionale dei Lincei, Rome.

BECKER T.W., FACCENNA C., O'CONNELL R.J. & GIARDINI D. (1999) - *The development of slabs in the upper mantle: Insights from numerical and laboratory experiments*, Journal of Geophysical Research-Solid Earth, **104** (B7) (15): 207-226.

BIGI G., COSENTINO D., PAROTTO M., SARTORI R. & SCANDONE P. (1990) - *Structural model of Italy*, Consiglio Nazionale delle Richerche, Firenze.

BONARDI G., AMORE F.O., CIAMPO G., DE CAPOA P., MICCONET P. & PERRONE V. (1988) - *Il complesso liguride auct.: stato delle conoscenze e problemi aperti sulla sua evoluzione pre-appenninica ed i suoi rapporti con l'Arco Calabro*. Mem. Soc. Geol. It., **41**: 17-36.

BONARDI G., COMPAGNONI R., DEL MORO A., MESSINA A. & PERRONE V. (1987) - R*iequilibrazioni tettono-metamorfiche alpine nell'Unità dell'Aspromonte (Calabria meridionale)*. Rend. SIMP., **42**: 301.

BONARDI G., DE CAPOA P., FIORETTI B. & OLIVIER P. (1994) - *Some remarks on the Calabria-Peloritani Arc and its relationships with the southern Apennines*. Boll. Geof. Teor. Appl., **36**: 483-492.

BORSI S. & DUBOIS R. (1968). *Données géochronologiques sur l'histoire hercynienne et alpine de la Calabre Centrale*. C.R. Ac. Sci., Paris, **266** (D) : 72-75.

BOULLIN J.P. (1984) - *Interpretation de la liason Apennin-Maghrrébides en Calabre: consequences sur la paléogéographie téthysienne entre Gibraltar e les Alpes*. Rev. Géol. Dynam. Géog. Phys., **25**: 321-338.

BRACE F.W. & KOHLSTEDT D.L. (1980) - *Limits on lithospheric stress imposed by laboratory experiments*, Journal of Geophysical Research, **50**: 6248-6252.

BRUNET C., MONIÉ P., JOLIVET L. & CADET J.P. (2000) - *Migration of compression and extension in the Tyrrhenian Sea, insights from 40 AR/39Ar ages on micas along a transect from Corsica to Tuscany*, Tectonophysics, **321**: 127-155.

BUNGE H.P., RICHARDS M.A., ENGEBRETSON D.C. & BAUMGARDNER J.R. (1997) - *A sensitivity study of three-dimensional spherical mantle convection at 108 Rayleigh number: effects of depth-dependent viscosity, heating mode, and endothermic phase change*. Journal of Geophysical Research, **102**: 11991-12007.

BURRUS J. (1984) - *Contribution to a geodynamic synthesis of the Provencal basin (north-western Mediterranean)*, Marine Geol., **55**: 247-269.

CELLO G., CRISCI G.M., MARABINI S. & TORTORICI L. (1985) - T*ranstensive tectonics in the Strait of Sicily: structural and volcanological evidence from Island Pantelleria*. Tectonics, **4**: 311-322.

CELLO G., INVERNIZZI C. & MAZZOLI S. (1996) - *Structural signigficance of tectonic processes in the Calabrian Arc, southern Italy: Evidence from the oceanic-derived Diamante-Terranova unit*. Tectonics, **15**: 187-200.

CELLO G., MORTEN L. & DE FRANCESCO A.M. (1991) - *The tectonic significance of the Diamante-Terranova unit (Calabria, southern Italy) in the Alpine evolution of the northern sector of the Calabrian Arc*. Boll. Soc. Geol. It., **110**: 685-694, 1991.

CHAMOT-ROOKE N., GAULIER J.-M. & JESTIN F. (1999) - *Constaints on Moho depth and crustal thickness in the Liguro-Provençal basin from a 3D gravity invertion : geodynamic implications.* In: SÉRANNE M. (Ed.): *"The Mediterranean Basins: Tertiary extension within the Alpine orogene"*, pp. 37-61, Geological Society, special publication, London.

CHANNELL J.E.T., OLDOW J.S., CATALANO R. & D'ARGENIO B. (1990) - *Paleomagnetically determined rotations in the western Sicilian fold and thrust belt*, Tectonics **9**: 641-660.

CHANNELL J.E.T., CATALANO R. & D'ARGENIO B. (1980) - *Paleomagnetism and deformation of the Mesozoic continental marginin Sicily,* Tectonophysics, **61**: 91-407.

CHANNELL J.E.T. (1986) - *Paleomagnetism and continental collision in the Alpine belt and the formation of late-tectonic extensional basins* In: COWARD M.P. & REIS A.C. (Eds.): *"Collision Tectonics"*, **19**: pp. 261-284, Geol. Soc. Sp. Pub., London.

CHERCHI A., MONTANDERT L. (1982) - *Oligo-Miocene rift of Sardinia and the early history of the Western Mediterranean basin*, Nature, **298**: 736-739.

CHRISTENSEN U. & YUEN D. (1985) - *Layered convection induced by phase transition*, Journal of Geophysical Research, **89**: 4389-4402.

CIMINI G.B. & DE GORI P. (2001) - *Nonlinear P-wave tomography of subducted lithosphere beneath central-southern Apennines (Italy)* Geophys. Res. Letters, **28**: 4387-4390.

DE VOOGD B., NICOLICH R., OLIVET J.L., FANUCCI F., BURRUS J., MAUFFRET A., PASCAL G., ARGNANI A., AUZENDE J.M., BERNABINI M., BOIS C., CARMIGNANI L., FABBRI A., FINETTI I., GALDEANO A., GORINI C., LABAUME P., LAJAT D., PATRIAT P., PINET B., RAVAT J., RICCI LUCCHI F. & VERNASSA S. (1990) - *Continental lithosphere; First deep seismic reflection transect from the Gulf of Lions to Sardinia (ECORS-CROP) profiles in western Mediterranean)*. In: SEIFERT F. (Ed.): *"International symposium on Deep reflection profiling of the continental lithosphere"*, pp. 265-274, Bayreuth, Federal Republic of Germany.

DE ROEVER E.W.F. (1972) - *Lawsonite-albite facies metamorphism near Fuscaldo, Calabria (southern Italy), its*

*geological significance and petrological aspect*s. GUA Pap. Geol. S., **1**(3): 171pp.

DEWEY J.F., HELMAN M.L., TORCO E., HUTTON D.H.W. & K.S. D. (1989) - *Kinematics of the Western Mediterranean*. In: DIETRICH D. (Ed.): *"Alpine Tectonic"*, pp. 265-283.

DERCOURT J, RICOU L.E. & VRIELYNCK B. (1993) - *Atlas Tethys Palaeoenviromental maps*, 307 pp., Gauthier-Villars, Paris.

DIETRICH D. (1988) - *Sense of overthrust shear in the Alpine nappes of Calabria (southern Italy)*. J. Str. Geol., **10**: 373-381.

DOGLIONI C., MONGELLI F. & PIALLI P. (1998). *Boudinage of the Alpine belt in the Appenninic back-arc*. Mem. Soc. Geol. It., **52**: 457-468.

DOGLIONI C. (1991) - *A proposal for the kinematic modelling of W-dipping subductions - possible applications to the Tyrrhenian-Apennines system*, Terra Nova, **3**: 423-434.

DVORKIN J., NUR A., MAVKO G. & BEN A.Z. (1993) - *Narrow subducting slabs and the origin of backarc basins*, Tectonophysics, **227** (1-4) : 63-79.

ERICKSSON S.G. & ARKANI-HAMED J. (1993) - *Subduction initiation at passive margins: The Scotian Basin, Eastern Canada as a potential example*, Tectonics, **12**: 678-687.

FACCENNA C., JOLIVET L., PIROMALLO C. & MORELLI A. (2003) - *Subduction and the depth of convection in the Mediterranean,* Journal Geophysical Reasearch, **108** (B2): 2099, doi: 10.1029/2001JB001690.

FACCENNA C., DAVY P., BRUN J.-P., FUNICIELLO R., GIARDINI D., MATTEI M. & NALPAS T. (1996) - *The dynamics of back-arc extensions: an experimental approach to the opening of the Tyrrhenian sea*, Geophysical Journal International, **126**: 781-795.

FACCENNA C., GIARDINI D., DAVY P. & ARGENTIERI A. (1999) - *Initiation of subduction at Atlantic-type margins: Insights from laboratory experiments*, Journal of Geophysical Research, **104** (B2): 2749-2766.

FACCENNA C., FUNICIELLO F., GIARDINI D. & LUCENTE P. (2001a) - *Episodic back-arc extension during restricted mantle convection in the Central Mediterranean*, Earth and Planetary Science Letters, **187** (1-2): 105-116.

FACCENNA C., BECKER T.W., LUCENTE F.P., JOLIVET L. & ROSSETTI F. (2001b) - *History of subduction and back-arc extension in the Central Mediterranea*n, Geophysical Journal International, **145** (3): 809-820.

FAURE M. (1980). *Microtectonique et charriage Est-Ouest des nappes alpines profonde de la Sila (calbre, Italie meridionale)*. Rev. Géol. Dynam. Géog. Phys., **22**: 135-146.

FUNICIELLO F., FACCENNA C., GIARDINI D., REGENAUER-LIEB K. (2003 in press.) - *Dynamics of retreating slabs (part 2): Insights from 3-D laboratory experiments*, Journal of Geophysical Research.

FINETTI I. & DEL BEN A. (1986) - *Geophysical study of the Tyrrhenian opening*, Bollettino di Geofisica Teorica ed Applicata, **28** (110): 75-155.

GATTACCECA J. & SPERANZA F. (2002) - *Paleomagnetism of Jurassic to Miocene sediments from the Apenninic carbonate platform (southern Apennines,Italy): evidence for a 60° counterclockwise Miocene rotation*, Earth and Planetary Science Letters, **201**: 19-34.

GIUNCHI C., SABADINI R., BOSCHI E. & GASPERINI P. (1996) - *Dynamic models of subduction: geophysical and geological evidence in the Tyrrhenian Sea*, Geophys. J. Int., **126**: 555-578.

GORINI C., MAUFFRET A., GUENNOC P. & LE MARREC A. (1994) - *Structure of the Gulf of Lions (Northwestern Mediterranean Sea)*, In: MASCLE A. (Ed.): *"Hydrocarbon and Petroleum Geology of France"*. pp. 223-243, Europ. Assoc. Petrol. Geol.

GRASSO M., DE DOMICICIS A. & MAZZOLDI G. (1990) - *Structures and tectonic setting of the western margin of the Hyblean-Malta shelf, Central Mediterranean*, Annales Tectonicae, **4**: 1409-145.

GRIFFITHS R.W., HACKNEY R.I. & VAN DER HILST R.D. (1995) - *A Laboratory Investigation of Effects of Trench Migration on the Descent of Subducted Slabs*, Earth and Planetary Science Letters, **133** (1-2): 1-17.

GRIFFITHS R.W. & TURNER J.S. (1988) - *Folding of viscous plumes impinging on a density or viscosity interface*, Geophysical Journal, **95**: 397-419.

GUEGUEN E., DOGLIONI C. & FERNANDEZ M. (1998) - *On the post-25 Ma geodynamic evolution of the western Mediterranean*, Tectonophysics, **298**: 259-269.

GUILLOU-FROTTIER L., BUTTLES J. & OLSON P.(1995) - *Laboratory experiments on structure of subducted lithosphere*, Earth and Planetary Science Letters, **133**: 19-34,.

HACCARD D., LORENTZ C. & GRANDJACQUET C. (1972) - E*ssai sur l'évolution tectogénétique de la liaison Alpes-Appennins (de la Ligurie à la Calabre)*, Memorie della Società Geologica Italiana, **11**: 309-341.

JARRARD R.D. (1986) - R*elations among Subduction Parameters*, Reviews of Geophysics, **24** (2): 217-284.

JOLIVET L., FACCENNA C., D'AGOSTINO N., FOURNIER M. & WORRALL D. (1999) - *The kinematics of back-arc basins, examples from the Tyrrhenian, Aegean and Japan Seas*, In: SÉRANNE M. (Ed.): *"The Mediterranean Basins: Tertiary extension within the Alpine orogene"*. pp. 21-53, Geological Society, special publication, London.

JOLIVET L. & FACCENNA C. (2000) - *Mediterranean extension and the Africa-Eurasia collision*, Tectonics, **19**: 781-795.

JONGSMA D., WOODSIDE J.M., KING G.C.P. & VAN HINTE J.E. (1987) - *The Medina Wrench: A key to the kinematics of the central and eastern Mediterranean over the past 5 Ma*, Earth Planet. Sci. Lett., **82**: 97-106.

KASTEN K.A., MASCLE J. & PARTY O.L.S.(1988) - *ODP Leg 107 in the Tyrrhenian Sea: insights into passive margin and backarc basin evolution*, Geol. Soc. Amer. Bull., **100**: 1140-1156.

KINCAID C. & OLSON P. (1987) - *An experimental study of subduction and slab migration*, Journal of Geophysical Research, **92**: 13832-13840.

KING S.D. & HAGER B.H. (1990) - *The Relationship between Plate Velocity and Trench Viscosity in Newtonian and Power-Law Subduction Calculations*, Geophysical Research Letters, **17** (13): 2409-2412.

LE PICHON X., BERGERAT F. & ROULET M.-J. (1988) - *Plate kinematics and tectonics leading to the Alpine belt formation; A new analysis*, Geological Society of America Special Paper, **218**: 111-131.

LUCENTE P.F., CHIARABBA C., CIMINI G.B. & GIARDINI D. (1999) - *Tomographic constarints on the geodynamic ezvolution of the Italian region*, Journ. Geophys. Res., **104**: 20307-20327.

MALINVERNO A. & RYAN W. (1986) - *Extension in the Tyrrhenian sea and shortening in the Apennines as result of arc migration driven by sinking of the lithosphere*, Tectonics, **5**: 227-245.

MATTEI M., CIPOLLARI P., COSENTINO D., ARGENTIERI A., ROSSETTI F., SPERANZA F., DE BELLA L. (2002) - *Miocene tectono-sedimentary evolution of the asouthern Tyrrhenian Sea: stratigrapihy, structural and paleomagnetic data from the on-shore Amantea basin 4calabrian Arc, Italy*, Basin Reasearch, **14**: 147-168.

MAUFFRET A., PASCAL G., MAILLARD A. & GORINI C. (1995) - T*ectonics and deep structure of the North-Western Mediterranean Basin*, Marine and Petroleum Geology, **12** (6): 645-666.

MONACO C. (1993) - *Le unità Liguridi nel confine Calabro-Lucano (Appennino meridionale): Revisione dei dati esistenti, nuovi dati ed interpretazione*. Boll. Soc. Geol. It., **112**: 751-769.

MOREAU M. G., BERTHOU J. Y. & MALOD J.-A. (1997) - *New paleomagnetic Mesozoic data from the Algarve (Portugal): fast rotation of Iberia between the Hauterivian and the Aptian*. Earth Planet. Sci. Lett., **146**: 689-701.

MORELLI A. & DZIEWONSKI A. (1993) - *Body wave traveltimes and a spherically symmetric P- and S-wave velocity model*, Geophysical J. Int., **112**: 178-194.

MCKENZIE D.P. (1977) - T*he initiation of trenches: A finite amplitude instability*, In: PITMAN W.C. (Ed): *"Island Arcs Deep Sea Trenches and Back-Arc Basins"* pp. 57-61, Maurice Ewing Ser. Vol. 1.

MUELLER S. & PHILLIPS R. (1991) - *On the initiation of subduction*, Journal of Geophysical Research, **96**: 651-665.

OGNIBEN L. (1969). S*chema introduttivo alla geologia del confine calabro-lucano*. Mem. Soc. Geol. It., **8**: 453-763.

OLIVET J.-L. (1996) - *La cinematique de la plaues Iberique*, Bull. Centres Recherces Expl.-Prod. Elf Aquitaine, **20**: 131-195.

PATACCA E., SARTORI R. & SCANDONE P. (1990) - T*yrrhenian basin and Apenninic arcs : Kinematic relations since late tortonian times*, Memorie della Società Geologica Italiana, **45**: 425-451.

PICCARRETA G. (1981) - *Deep-rooted overthrusting & blueschistic metamorphism in compressive continental margins. An example from Calabria (southern Italy)*. Geol. Mag., **118** (5): 539-544.

PIROMALLO C. & MORELLI A. (1997) - I*maging the Mediterranean upper mantle by P-wave travel time tomography*, Annali di Geofisica, **40**: 963-979.

PIROMALLO C. & MORELLI A. (2003 in press) - *P-wave tomography of the mantle under the Alpine-Mediterranean area*, J. Geophys. Res.

PIROMALLO C., VINCENT A.P., YUEN D.A. & MORELLI A. (2001) - *Dynamics of the transition zone under Europe inferred from wavelet cross-spectra of seismic tomography*, Phys. Earth Planet. Int., **125**: 125-139.

PLATT J.P. & COMPAGNONI R. (1990) - *Alpine ductile deformation and metamorphism in a Calabria basement nappe (Aspromonte, South Italy)*. Ecl. geol. Elv., **83**: 41-58.

PYSKLYWEC R.N. & MITROVICA J.X. (1998) - *Mantle flow mechanisms for the large-scale subsidence of continental interiors*, Geology, **26** (8): 687-690.

RANALLI G. (1995) - *Rheology of the earth*, 413 pp., Chapman and Hall, London.

RANALLI G., PELLEGRINI R. & D'AFFIZI S. (2000) - *Time dependance of negative buoyancy and the subduction of continental lithosphere*, J. Geodyn., **30**: 539-555.

REGARD V., FACCENNA C., MARTINOD J., BELLIER O. & THOMAS JC (2003) - *From Subduction to Collision: control of deep processes on the evolution of convergent plate boundary*, Journ. Geophys. Res., in press.

ROYDEN L.H. (1993) - *Evolution of retreating subduction boundaries formed during continental collision*, Tectonics, **12** (3): 629-638.

ROSSETTI F., FACCENNA C., JOLIVET L., GOFFÉ B., TECCE F., BRUNET C., FUNICIELLO R. & MONIÉ P. (2000) - *Structural signature and exhumation P-T-t paths of the Gorgona blueschist sequence (Tuscan Archipelago, Italy)*. Ofioliti, **26**: 175-186.

ROSSETTI F., FACCENNA C., GOFFÉ B., MONIÉ P., ARGENTIERI A., FUNICIELLO R. & MATTEI M. (2001) - *Alpine tectono-metamorphic evolution of the Sila Piccola Massif (Calabria, Italy): insigths for the tectonic evolution of the Calabrian Arc*. Tectonics, **20**: 112-133.

SAGNOTTI L. (1992) - *Paleomagnetic evidence for a Plio-Pleistocene counterclockwise rotation of the Sant'Arcangelo basin, Southern Italy*, Geophysical Research Letters, **19**: 135-138.

SARTORI R. (1990) - *The main results of ODP Leg 107 in the frame of Neogene to recent geology of peri-tyrrhenian areas*, pp. 715-730.

SCANDONE P. (1982). Structure and evolution of the of the Calabrian Arc. Earth Evol. Sci., 3: 172-180.

SCHEEPERS P.J.J., LANGEREIS C.G. & HILGEN F.J. (1993) - *Counter-clockwise rotations in the southern Apennines during the Pleistocene: paleomagnetic evidences from the Matera area*, Tectonophysics, **225**: 379-410.

SCHEEPERS P.J.J. & LANGEREIS C.G. (1993) - *Analysis of NRM directions from Rossello composite: implication for tectonic rotation of the Caltanisetta basin*, Sicily, Earth Planetary Science Letters, **119**: 243-258.

SCHENK V. (1980) - *U-Pb & Rb-Sr radiometric dates and their correlation with metamorphic events in the granulite facies basement of the Serre, southern Calabria (Italy)*. Contr. Min. Petrol., **73**: 23-38.

SELVAGGI G. & AMATO A. (1992) - *Subcrustal earthquakes in the northern Appennines (Italy) : evidence for a still active subduction?*, Geophys. Res. Lett., **19**: 2127-2130.

SELVAGGI G. & CHIARABBA C. (1995) - *Seismicity and P-wave velocity image of the Southern Tyrrhenian subduction zone*, Geophys. J. Int., **122**: 818-826.

SERANNE M. (1999) - *The Gulf of Lion continental margin (NW Mediterranean) revisited by IBS: an overview*. In: SÉRANNE M. (Ed.): *"The Mediterranean Basins: Tertiary extension within the Alpine orogen"*, pp. 21-53, Geological Society, special publication, London.

SILVER P.G., RUSSO R.M. & LITHGOW-BERTELLONI C. (1998) - *Coupling of South American and African plate motion and plate deformation*, Science, **279**: 60-63.

SPADEA P., TORTORICI L., LANZAFAME G. (1976) - S*erie ofiolitifere nell'area fra Tarsia e Spezzano Albanese (Calabria):stratigrafia, petrografia, rapporti strutturali*. Mem. Soc. Geol. It., **17**: 135-174.

SPADINI G., CLOETINGH S. & BERTOTTI G. (1995) - *Termo-mecanical modeling of the Tyrrhenian sea : lithospheric necking and kinematics of rifting*, Tectonics, **14** (3): 629-644.

SPAKMAN W., VAN DER LEE S. & VAN DER HILST R. (1993) - T*ravel-time tomography of the European-Mediterranean mantle down to 1400 km*, Physic of Earth Planetary Interior, **79** (1-2): 3-74.

SPERANZA F., MATTEI M., SAGNOTTI L. & GRASSO F. (2000) - *Rotational differences between the northern and southern Tyrrhenian domains: paleomagnetic constraints from the Amantea basin (Calabria, Italy)*, Journal Geological Society London, **157**: 327-334.

SPERANZA F., MANISCALCO R., MATTEI M., DI STEFANO A., BUTLER R.W.H. & FUNICIELLO R. (1999) - *Timing and magnitude of rotations in the frontal thrust systems of southwestern Sicily*, Tectonics, **18**: 1178-1197.

TACKLEY P.J. (1993) - *Effects of an endothermic phase transition at 670 km depth in a spherical model of convection in the Earth's mantle*, Nature, **361**: 699-704.

TAO W.C. & O'CONNELL R.J. (1993) - *Deformation of a weak subducted slab and variation od seismicity with depth*, Nature, **361**: 626-628.

THOMSON S.N. (1994) - *Fission track analysis of the crystalline basement rocks of the Calabrian Arc, southern Italy: evidence of Oligo-Miocene late orogenic extension and erosion*. Tectonophysics, **238**: 331-352.

THOMSON S.N. (1998) - *Assessing the nature of tectonic contacts using fission-track thermochronology: an example from the Calabrian Arc*, Southern Italy. Terra Nova, **10**: 32-36.

VAN DER VOO R. (1993) - *Paleomagnetism of the Atlantic Thethys and Iapetus Oceans*, Cambridge University Press,

Cambridge.

WALLIS S.R., PLATT J.P. & KNOTT S.D. (1993) - *Recognition of syn-convergence extension in accretionnary wedges with examples from the Calabrian arc and the Eastern Alps*, American J. Science, **293**: 463-495.

WARD S.N. (1994) - *Constrains on the seismotectonics of the central Mediterranean from Very Long Baseline Interferometry*, Geophys. J. Int., **117**: 441-452.

WEIJERMARS R. (1986) - *Flow behaviour and physical chemistry of bouncing putties and related polymers in view of tectonic laboratory application*, Tectonophysics, **124**: 325-358.

WORTEL R. (1982) - *Seismicity and rheology of subducted slabs*, Nature, **296**: 553-556.

WORTEL M.J.R. & SPAKMAN W. (2000) - *Subduction and slab detachment in the Mediterranean-carpathian region*, Science, **290**: 1910-1917.

Mem. Descr. Carta Geol. d'It.
XLIV (2004), pp.185-194
7 figg.,

Super-inflation of a spreading ridge through vertical accretion
Dilatazione di un centro di espansione attraverso accrezione verticale

MARANI M.P. (*)

ABSTRACT - The 2 Myr-old Marsili basin is the youngest ocean crust floored portion of the Tyrrhenian back-arc basin. A large, ~1400 km^3, N-S elongated volcano is axially positioned in the basin, constituting the only significant relief on the otherwise 3500 m deep, flat lying basin floor.
In this paper, it is suggested that Marsili volcano represents the, super-inflated spreading ridge of the Marsili basin. The morphologically anomalous ridge is considered to result from the up-rise of deep buoyant asthenosphere across lateral tears that develop at the sides of the subducting Ionian lithosphere, making vertical accretion the dominant mechanism acting within a restricted spreading environment.
Onshore and offshore regional data, along with the spreading centre characteristics of the volcano are presented to support this interpretation.

KEY WORDS: Volcano morphology, subduction, lithosphere dynamics, seafloor spreading, Tyrrhenian Sea

RIASSUNTO - Il bacino del Marsili (2 Ma), rappresenta la porzione oceanizzata più recente del bacino di retro-arco del Mar Tirreno. L'omonimo, vulcano, esteso in direzione N-S, con un volume di ~1400 km^3 che occupa la parte assiale del bacino costituisce l'unico elemento topograficamente significativo della piana abissale, profonda 3500 m, del bacino.
In questo lavoro, il vulcano Marsili viene interpretato come un centro di espansione dilatato del bacino Marsili. L'estrema anomalia morfologica del centro di espansione risulta dalla risalita di livelli astenosferici profondi attraverso gli strappi laterali che si sviluppano ai lati della placca Ionica in subduzione. L'accrezione verticale rappresenta il meccanismo dominante nell'ambito di un ambiente di espansione termicamente e spazialmente ristretto.

PAROLE CHIAVE: morfologia vulcanica, subduzione, dinamica dalla litosfera, espansione oceanica, Mar Tirreno

1. - INTRODUCTION

The majority of mid-ocean ridges (MORs) have an established morfological makeup according to whether sea-foor spreading is fast or slow (MACDONALD *et alii,* 1991; MACDONALD *et alii*, 1992; SEMPÉRÉ *et alii*, 1995; SMITH *et alii*, 1995; MAGDE & SMITH, 1995). Their makeup is so distinctive that intermediate velocity spreading ridges have also been described and defined (HOOFT & DETRICK, 1995).

Morphologies of spreading ridges principally depend upon their thermal structure, which is controlled by the magma budget. Moreover, magma supply to the ridge can be taken as a proxy for spreading velocity. Thus, magma oversupply or undersupply relative to the expected for a given spreading rate will result in anomalous MOR morphologies. Well known examples include the Reykjanes Ridge that displays an anomalous slow spreading morphology (MURTON & PARSON, 1993) and the Australian-Antarctic Discordance that has an anomalous fast spreading morphology.

In the southern Tyrrhenian Sea, the recent-most ocean floored Marsili back-arc basin has largely all the geological and geophysical characteristics of oceanic backarc spreading basin (KASTENS *et alii*, 1988). However, it lacks the most evident feature in ocean basins, namely the typical morphology of a spreading centre where new crust is produced. Instead, the axial portion of the basin is occupied by the Marsili seamount, the largest volcano in the Tyrrhenian Sea, 3500 m high and strongly elongated in a NNE-SSW direction. Despite its bulk, the detailed morphology of

(*)ISMAR - CNR, Sezione di Geologia Marina, Via Gobetti 101, 40129 Bologna.

Marsili volcano reveals remarkable similarity to the high order segmentation and volcanic landforms described in the axis and near-axis portions of mid-ocean spreading ridges.

In this paper it is proposed that Marsili volcano exemplifies a morphologically anomalous end-member spreading ridge generated by super-inflation following the model proposed by MARANI & TRUA, 2002. As a consequence, Marsili volcano is here considered the key to understanding the dynamics of spreading and backarc lithosphere formation in the young Marsili basin.

2. - MARSILI BASIN

Marsili basin is the recent-most of two oceanic sub-basins that form the Tyrrhenian Sea. The basin is <2 Myr old, the emplacement of basaltic ocean crust generated by ESE-directed extension (KASTENS *et alii*, 1990) taking place above the presently northwesterly-subducting Ionian oceanic slab (KASTENS *et alii*, 1988,1990; SARTORI, 1990; JOLIVET, 1991). Marsili basin is characterised by a Moho depth of 11 km, matched by thinning of the lithosphere to less than 30 km (SUHALDOC & PANZA, 1989; NICOLICH, 1989; SCARASCIA *et alii*, 1994) and by heat flow values that reach over 200 mWm^{-2} (DELLA VEDOVA *et alii*, 1984; MONGELLI *et alii*, 1992). Average basin basement depth is in the order of 4 km, giving a crustal thickness of ~7 km.

The subducting slab represents a remnant of the Mesozoic oceanic lithosphere that occupied the western and central Mediterranean. Since Early Miocene, most of the ocean domain had been consumed (BECCALUVA *et alii*, 1990), with the exception of the Ionian ocean, delimited to the southwest by its ancient margins, the Malta and Apulian escarpments (fig. 1)

In step with backarc basin expansion, subduction-related island arc volcanism developed in the currently active Aeolian island arc (SERRI 1997 and references therein), generating the present-day arc/backarc configuration of the Marsili basin region (fig. 2).

3. - THE SPREADING RIDGE MORPHOLOGY OF MARSILI VOLCANO

The fine-scale make-up of Marsili seamount displays distinctive volcano-tectonic features closely analogous to those characterising the axial or near-axial zones of MORs, notwithstanding the highly anomalous seamount morphology on which these features develop. Moreover, the available chronology of rocks dredged from the summit and the magnetic anomaly patterns in the region of the volcano are shown to support and to be consistent with the observed morphological characters, suggesting that Marsili volcano represents a spreading ridge, the super-inflated locus of present-day crust accretion in the Marsili basin.

3.1. - BULK MORPHOLOGY OF THE VOLCANO

Marsili volcano rises 3500 metres from the basement level of Marsili basin to a minimum depth of 489 metres, and is elongated 50 km NNE-SSW with mean width of 16 km. A narrow, 1 km wide linear region of lower gradient, approximately bounded by the 1000 metre isobath (fig. 3), marks the summit zone that stretches 20 km along the main axis of the

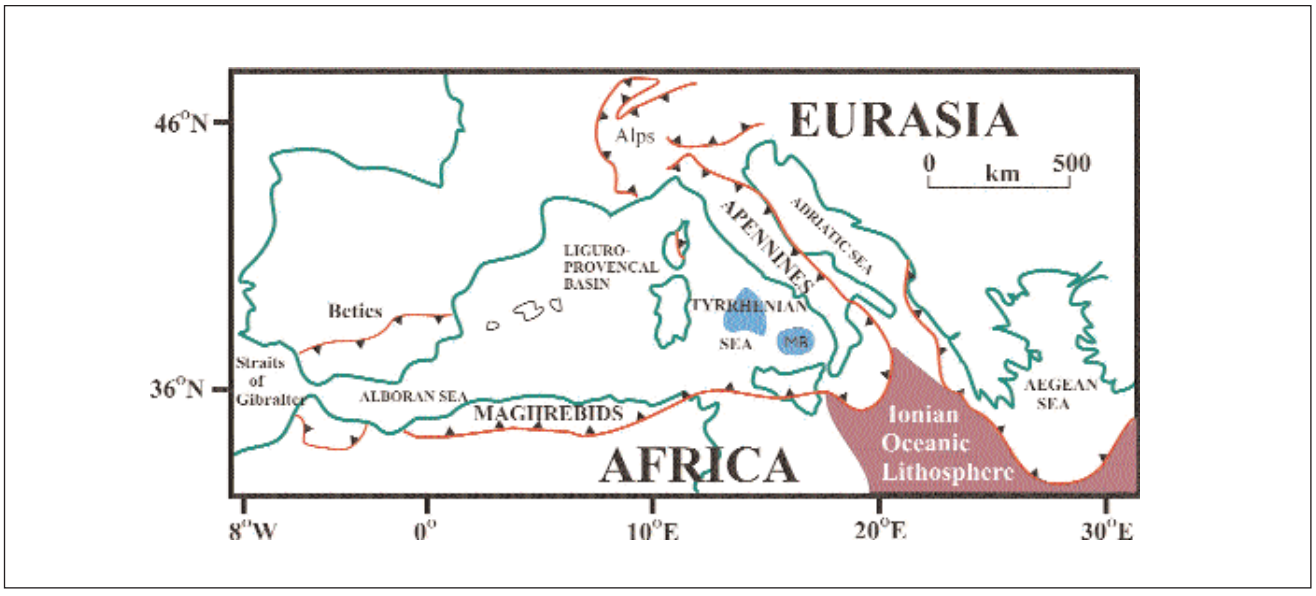

Fig. 1. - *Sketch map displaying remnant Mesozoic Ionian ocean crust in subduction beneath Calabria and the Agean. Surrounding Apennine and Alpine age belts are traced. MB, recent (2 Ma) ocean crust floored Marsili basin.*

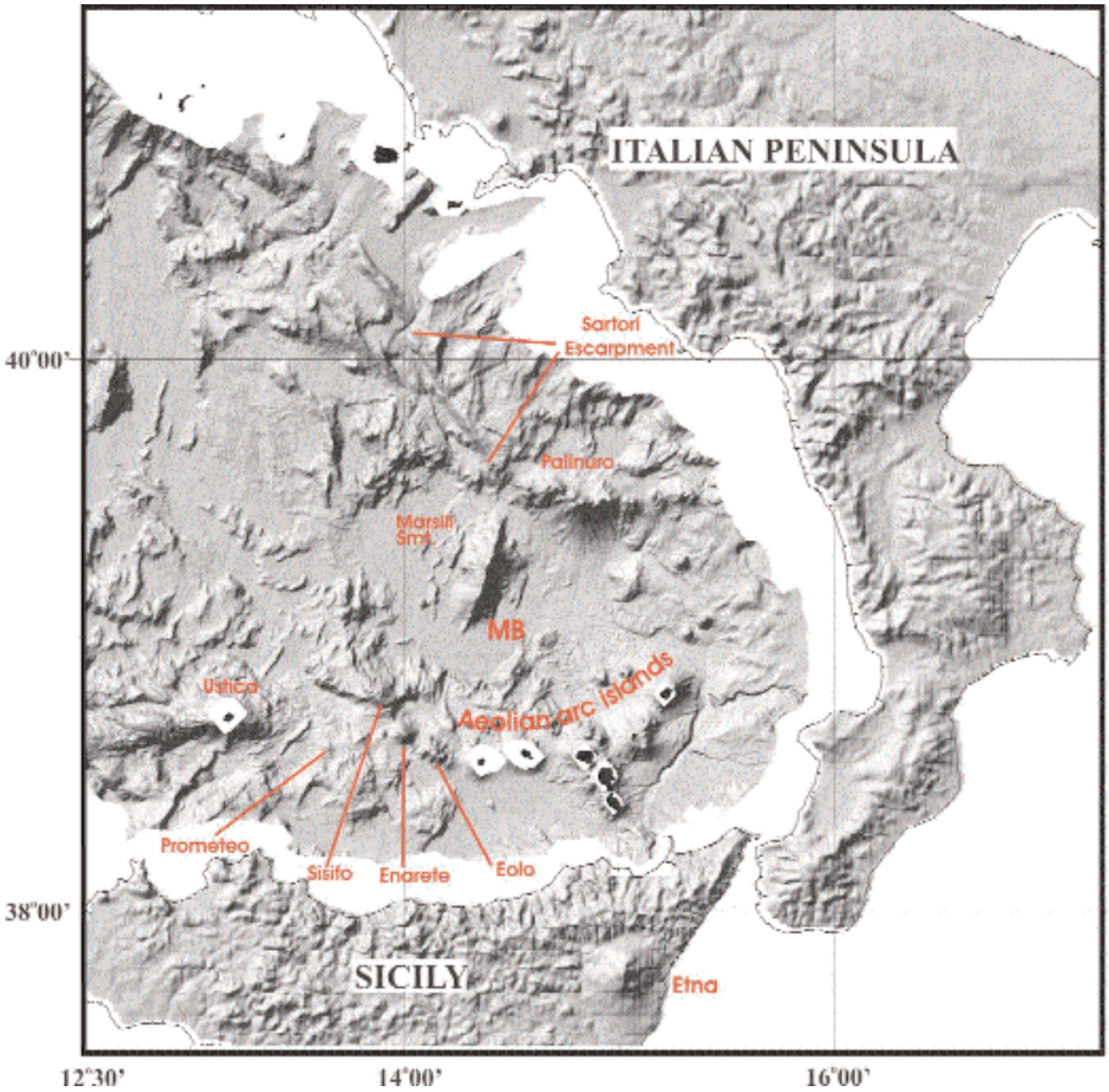

Fig. 2. - *Shaded relief bathymetry (illum from NW) of central and southern Tyrrhenian Sea with feature names discussed in the text. MB, Marsili basin.*

volcano. The summit zone is highlighted (fig. 3) by a region of high gradient relief (>20°) positioned between the axis perimeter and the main slopes (~10°). On the lower flanks of the volcano numerous seamounts develop while the adjacent basin areas to the west and to the east of the Marsili edifice are characterised by large fault scarps (fig. 3).

3.2. – Segmentation

The volcano summit axis zone and tip regions are characterised by the development of linear structures arranged in segments generated mainly by the alignment of contiguous volcanic cones, elongated along-axis to build narrow, linear cone ridges (LCRs), or by the linear arrangement of several circular-based cones (Marani & Trua, 2002). Segment locations show that the central portion of the volcano is the main site of stress release and ensuing volcanic activity.

3.3. - Flank seamounts

Numerous small seamounts grow on the flanks of Marsili volcano (fig. 3), being most developed on its northern tip. The cones have circular bases with

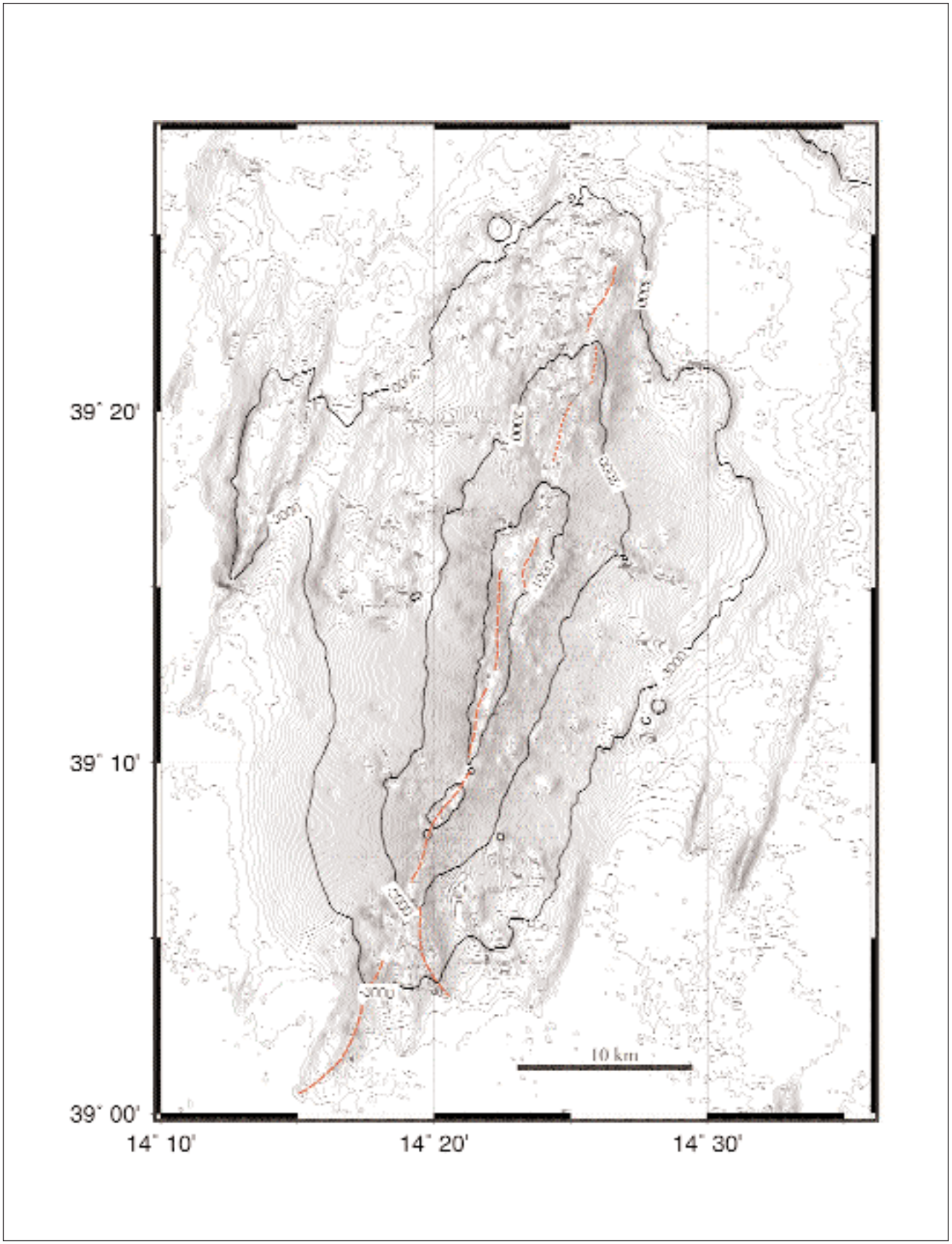

Fig. 3. - *Bathymetry of Marsili volcano (contour interval 25m). In red are traced the linear features that characterise the axial portion of the volcano. Segmentation is given by linear ridges in the northern tip, LCRs along the summit region and circular cone alignments in the southern tip.*

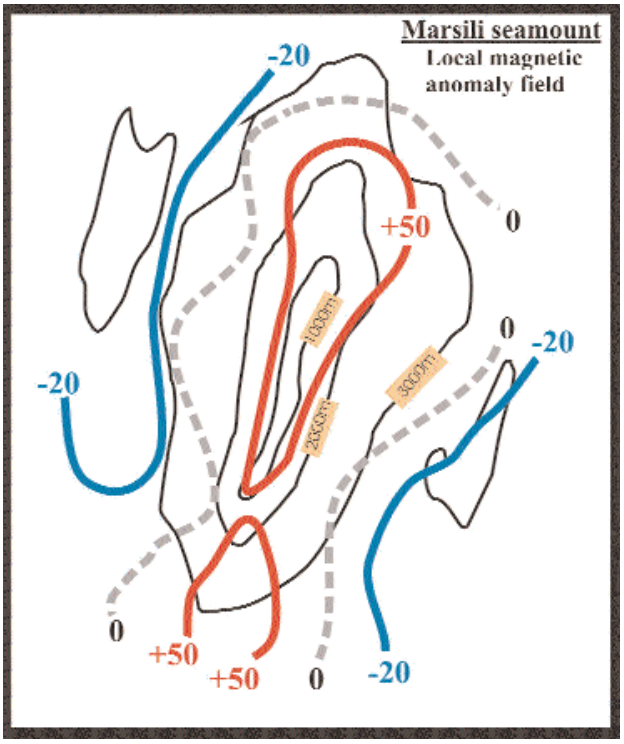

Fig. 4. - *Sketch map of the local magnetic anomaly field centered on Marsili volcano (outlined in black), modified from* FAGGIONI *et alii, 1995. See text for discussion.*

diameters up to 1500 metres and heights up to 300 metres; several are characterised by very low gradient, flat tops (see MARANI & GAMBERI, this volume).

3.4. - BASIN FLOOR FAULTS

Two NNE-SSW-directed (N16°) fault sets, parallel to the general trend of the summit axis, develop symmetrically (fig. 3) in the basin-floor region bounding the south-eastern and north-western flanks of the volcano, forming horst and graben pairs at the sides of Marsili volcano.

3.5. - CHRONOLOGY AND MAGNETIC DATA

Chronological data provide only a partial reconstruction of the volcanic activity of this region: biostratigraphic and magnetostratigraphic constraints indicate that inception of spreading in the western Marsili basin took place between 1.87-1.67 Ma (KASTENS *et alii,* 1988), whereas lavas from the summit of Marsili volcano yield K/Ar ages of 0.1-0.2 Ma (SELLI *et alii*, 1977).

However, this sparse chronological data, in conjunction with the available magnetic anomaly data in the region (FAGGIONI *et alii*, 1995), renders comparative dating possible. Positive anomalies characterise the bulk of Marsili volcano (fig. 4), with highest values distributed along the axis. Locally distinct negative anomalies are positioned on, or in the vicinity of, the basin floor fault zones. The regional anomaly field of the Marsili basin (fig. 5) displays the general spreading setting of the basin.

On the basis of the local and regional magnetic anomaly fields, the 0.1-0.2 Ma summit lavas correlate the positive magnetic anomaly of the volcano to the present-day normal polarity geomagnetic chron C1 (Brunhes, 0.78-0 Ma) (FAGGIONI *et alii*, 1995). The bordering, inversely magnetised basin-floor is attributed to the post Olduvai, late Matuyama chron (1.67-0.78 Ma) (SAVELLI & SCHRIEDER, 1991; FAGGIONI *et alii*, 1995); a time-span which is consistent with the 1.87-1.67 Ma age (positively magnetised Olduvai chron) for inception of spreading in the western Marsili basin based on ODP hole 650 (KASTENS *et alii,* 1988).

Such an arrangement of the anomaly field implies that the bulk structure of Marsili volcano is <0.78 Ma-old and that the off axis, basin floor is older (> 0.78 Ma), indicative of incremental development parallel to the axial elongation of the edifice.

3.6. - SPREADING DIRECTION

The likely direction of the least compressional stress in the Marsili basin region is perpendicular to the basin-floor faults at the time of their formation, and consequently denotes the spreading direction at that time as well. The resulting trend (N106°) is in accordance with the Pleistocene to present-day extensional stress directions (~N100°) that characterise the surrounding land areas (TORTORICI *et alii*, 1993; MAZZUOLI *et alii*, 1995).

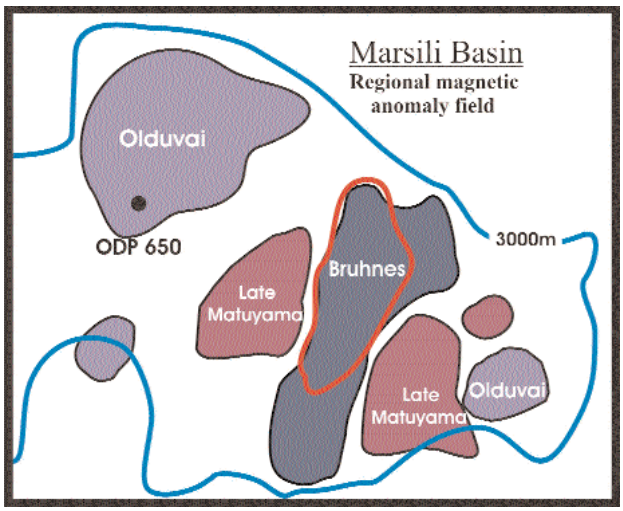

Fig. 5. - *Sketch map of the regional magnetic anomaly field in the Marsili basin (Marsili volcano outlined in red), modified from* FAGGIONI *et alii, 1995, showing interpreted geomagnetic age chrons. For further discussion see text.*

3.7. - Driving force of magma injection

Furthermore, analysis of the discordant directions between segmentation, ridge trend and spreading direction allows the determination of the ratio between the magmatic pressure difference (ΔP) and the regional tectonic stress (ΔS) (Abelson & Agnon, 1997). This results to be 0.33-0.23 for Marsili volcano, a value indicating the dominance of regional stress over magmatic pressure. The fast-spreading East Pacific Rise has a similar ratio, related to the high tensional stress induced by the slab pull forces of subduction at the Pacific active margins. The subduction setting of Marsili ridge is consistent with these observations. Although constructional from a volcanic point of view due to a high melt supply, the low $(\Delta P)/(\Delta S)$ ratio of the Marsili ridge suggests that the driving forces of melt injection are primarily of tectonic origin.

3.8 - Enhanced magma supply rate

An estimate of the added magma flux to the ridge region to produce super-inflation can be made by conservatively considering the 7 km oceanic crust thickness of the basin. The estimated rates of magma supply to produce the -4000 m basement level along the 50 km length of Marsili ridge are 10.5/14 km^3kyr^{-1} at 3/4 $cmyr^{-1}$ full spreading rates respectively. The supplementary accreted volume of crust due to the above-basement construction of Marsili ridge over the last 0.7 Ma is roughly 1500 km^3, giving an added rate of magma supply of ~2.1 km^3kyr^{-1}, involving an increment due to super-inflation of 15-20% respect to the magma flux due to spreading alone.

4. - THE CASE FOR SUPER-INFLATION

In the previous section we have shown that MOR-like 3rd and 4th order (Macdonald, 1998) constructional and tectonic morphologies characterise the Marsili region. Further support for the spreading ridge nature of Marsili volcano derives from the axis-parallel incremental growth, demonstrated by the magnetic anomaly pattern of the region. Moreover, these features develop on and around the 3000 m high Marsili volcano, rendering necessary a 15-20% increase in the rate of magma supply, focused to the site of the volcano.

We propose that a strong increase of melt production, and resultant robust volcanism, within a relatively young (<2Myr) and immature slow spreading backarc environment are the basic components that concurrently are necessary to generate a super-inflated ridge such as Marsili volcano. This model paradoxically involves a thermally restricted young spreading setting simultaneously affected by a strong thermal pulse of increased magmatism.

4.1. - Thermal limitation – focused crust accretion

The young and immature nature of the backarc basin involves an abrupt transition between the oceanic lithosphere and the surrounding, thicker, continental one (fig. 6).

Bordering, cooler continental lithosphere thermally constricts ridge lengthening or propagation through lateral conductive cooling of the newly accreted Marsili crust, in time gradually restricting spreading ridge volcanism to the finite length-scale of Marsili volcano. As a consequence, accretion of new crust principally occurs through eruptive processes along the length of the resulting spatially restricted or "locked" super-inflated ridge. Horizontal plate separation due to the slow-spreading regime of Marsili basin may be effectively obscured, being outpaced by the increased magma supply to the surface resulting in vertical accretion to produce the super-inflated ridge.

4.2. - Thermal resurgence – augmented magma flux

Recently, Gvirtzman & Nur, (1999) linked shallow lateral asthenospheric mantle flow, due to slab tears of the Ionian slab, to the formation of Etna volcano in Sicily and to decoupling of the upper plate in Calabria, resulting in the strong uplift observed there since 0.7 Ma ago.

In developing the Gvirtzman & Nur (1999) model further, by taking into account the back-arc region, it results that the development of the tear faults in the Ionian slab occurred at the time (~0.7 Ma-ago) that we propose the Marsili spreading centre became thermally constricted and functioned as a super-inflated ridge. We relate the increase in melt production in the backarc region to lateral asthenospheric flow induced by the development of the tear faults within the subducting Ionian slab at the time of ridge formation.

At the deep mantle level of the Marsili basin, low pressure produced at the free, torn, boundaries of the moving slab generates lateral flow of asthenospheric mantle along the deep-seated portions of the slab tears, permitting the injection of buoyant high-temperature material upwards (fig. 7). At the time of detachment, when the slab was torn, triggering fast slab sinking and retreat, the concurrent up-welling of deeper, hot asthenosphere would have thermal perturbed the mantle wedge, inducing partial melting to feed the Marsili ridge region. Geophysical confirmation of the presence of "hot" mantle material restricted to beneath the Marsili basin is provided by the attenuation of mantle-earthquake derived S and Sn shear waves (Mele *et alii*, 1997; Mele, 1998), coherent with the high heat flow present over the Marsili basin.

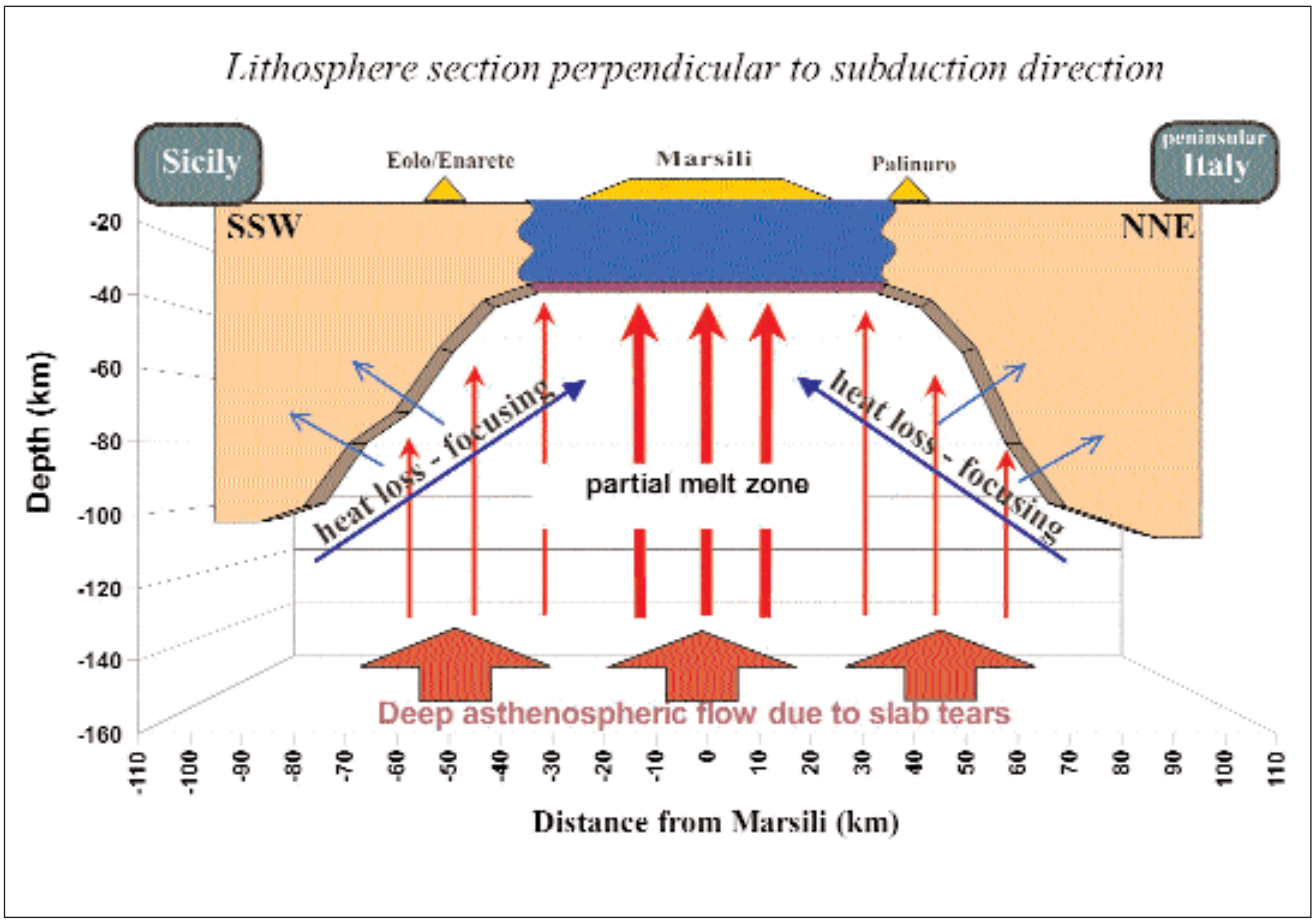

Fig. 6. - *Sketch of lithosphere section perpendicular to the subduction direction showing approximate lithosphere thickness adjacent to the Marsili basin causing focusing of magma supply due to conductive thermal cooling.*

5. - REGIONAL GEOLOGICAL EVIDENCE FOR SLAB TEARING

At the time of formation of the axial part of Marsili volcano (about 0.7 Ma), the central-southern Apennines, formerly undergoing NE-SW shortening, begin to show belt-parallel extension and uplift (Patacca *et alii*, 1990; Hippolyte *et alii*, 1994; Doglioni *et alii,* 1994; Galadini 1999) which is still observable at present (Montone *et alii*, 1997; Mariucci *et alii*, 1999). Contemporaneously, strong uplift is also registered in Calabria and north-eastern Sicily (Westaway, 1993; Robertson & Grasso, 1995; Lentini *et alii*, 1995; Butler *et alii*, 1995).

Tomographic investigations (Lucente *et alii*, 1999; Cimini, 1999) of the Tyrrhenian subduction zone reveal that the ~100 km thick, continuous high velocity mantle anomaly of the slab dips ~70° north-westwards beneath the Marsili basin, to 500 km depth. Shear wave propagation (Mele, 1998) and seismicity (Giardini & Velonà, 1991; Selvaggi & Chiarabba, 1995) demonstrate that the narrow (<200 km) and long (~570 km) Ionian subducting slab is laterally restricted to the terrains of the Calabrian arc and north-eastern Sicily.

The tear faulting event can account for the Early/Middle Pleistocene structural variations, triggering the contemporaneous uplift and extension occurring not only in Calabria, but also in the southern Apennines and Sicily as well. The uplift in the Southern Apennines and Sicily is taken to be the effect of their rebound in response to the release of the lateral stresses that existed prior to tearing.

6. - OFFSHORE VOLCANISM AND TECTONICS RELATED TO SLAB TEARING

The slab tears, detectable by the abrupt NW-SE deep seismicity cutoffs along the south-western margin of peninsular Italy and offshore north-eastern Sicily (Frepoli *et alii*, 1996), are shown to be capable of transmitting their effects to the overlying crustal regions. The region which we interpret to be above the southern slab tear, is characterised by a roughly NW-SE trending belt composed of the Etna and Ustica Island edifices (fig. 2), both with Ocean Island Basalt (OIB)-type activity showing a slight mantle source contamination from subduction related fluids (Beccaluva *et alii*, 1982). Along the same alignment,

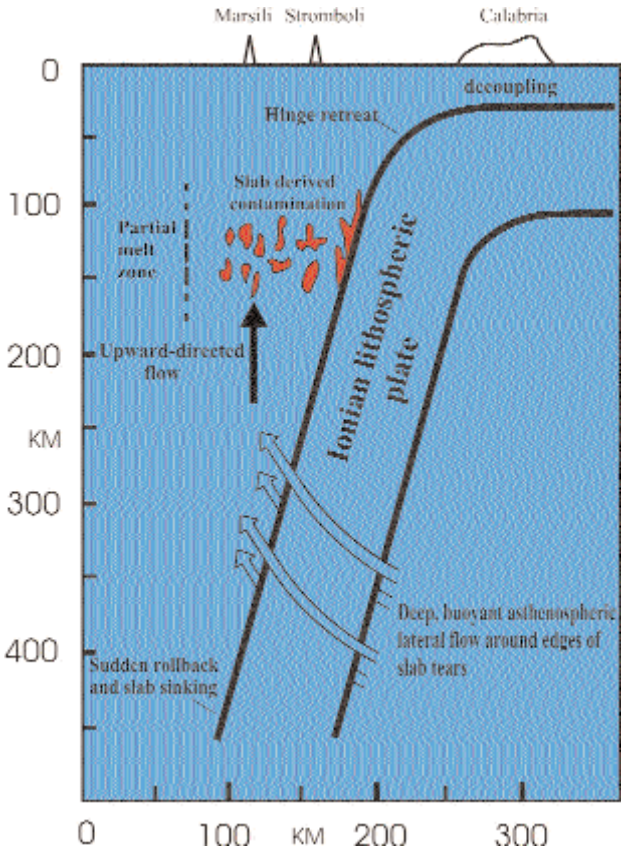

Fig. 7. - *Cartoon representation of the Ionian lithospheric plate with locations of Marsili ridge, Aeolian arc, and Calabria indicated for reference. An abrupt increase of rollback due to the full development of lateral tears in the Ionian slab, between early and middle Pleistocene, generates lateral flow of deep asthenosphere around slab edges, provoking thermal rejuvenation in the previously slab-contaminated partial melting. Kinematics of slab rollback and decoupling are adapted from* GVRITZMAN & NUR (1999a). *See text for discussion.*

samples recovered from the recently discovered Prometeo submarine lava field (MARANI *et alii,* 1999; TRUA *et alii*, 2003), located SE of Ustica Island reveal geochemical characteristics closely resembling those of the hawaiites and mugearites of Ustica island (TRUA *et alii*, 2002; 2003). It is thus suggested that the Prometeo lava field is derived from an intraplate asthenosphere mantle source located at or along the southern boundary of the Ionian slab, as earlier proposed by BECCALUVA *et alii* (1982) for Ustica and Etna volcanoes. This NW-SE trending OIB-type volcanism offers strong evidence supporting the existence of up-welling asthenospheric flow (TRUA *et alii,* 2003) at a location which is aligned with the deep seismicity cut-off tracing the southern tear of the subducting slab, consistent with the model of enhanced melting beneath the super-inflated Marsili ridge. Based on bathymetry data, the offshore NW-SE trending Eolo-Enarete-Sisifo (EES) volcanic alignment (fig. 2), that effectively delimits OIB-type and subduction-affected magmatism, may represent the surface trace of the deep slab tear. The persistence of the EES trend onshore in Sicily, through the Taormina/Tindari-Letojanni tectonic lines (GHISETTI, 1979a; 1979b) which link the Tyrrhenian offshore with the Malta Escarpment, the ancient boundary of the Ionian ocean-floored basin, confirms the structural importance of the composite EES lineament in relation to the Ionian plate (MARANI & TRUA, 2002). In fact, the right-lateral characters of the onshore tectonic lines are in accordance with the expected dextral shearing expected to occur at the southern slab tear.

The deep seismicity cut-off along the northern boundary of the Ionian slab occurs along the central and northern parts of the 1 km scarp of the Sartori Escarpment (SE) system (CURZI *et alii*, 2003) (fig. 2). The left-lateral movement of the SE (MUSACCHIO *et alii*, 1999) is compatible with the shearing sense expected to affect the northern slab tear. These elements point out that perhaps at this boundary of the slab the surface response to tearing is expressed tectonically. Southwards, the NW-SE-trending SE terminates against the E-W structure of Palinuro volcano (fig. 2) essentially outlining the northern limit of the Aeolian arc activity in the region, and thus exerting some form of control on the deep volcanic processes affecting the eastern portion of the volcanic arc.

7. - CONCLUSIONS

The centrally located Marsili volcano is the outstanding feature within the slow-spreading, 2 Ma-year old, Marsili basin. It displays constructional and tectonic features similar to those that characterise MOR spreading centres. Magnetic anomalies in the region show that the bulk of the Marsili volcano developed in the last 0.7 Ma and that incremental growth parallel to the axial elongation of the edifice took place.

It is proposed that Marsili volcano represents a morphologically anomalous, end-member, super-inflated spreading ridge. Increased melt production, and resultant robust volcanism, within the relatively immature (<2Myr) slow spreading Marsili backarc basin is the basic mechanism necessary to generate super-inflation.

Thermal constriction of crust production, due to cool continental lithosphere surrounding the young oceanic basin, restricted spreading-ridge lengthening or propagation to the finite length-scale of Marsili volcano. Emplacement of new crust would thus principally take place through eruptive processes along the length of the spatially restricted "locked" ridge. Slow spreading plate separation at the ridge is outpaced by magma production, resulting in vertical accretion generating the growth of a super-inflated ridge.

Enhanced melt generation in the area of Marsili volcano is provoked by lateral tear faulting of the Ionian slab that occurred in Early/Middle Pleistocene. Sideways flow of asthenosphere developing along the deeper edges of the slab tears causes the injection of

buoyant high-temperature asthenosphere upwards, inducing increased melting in the backarc regions.
Geophysical evidence for the slab tears is furnished by lateral southern and northern cut-offs of the seismicity that traces the subducting slab. Regionally, it is proposed that the Early/Middle Pleistocene extension and uplift of the onshore areas surrounding the Ionian slab, in Calabria, the southern Apennines and north-eastern Sicily, are caused by events of decoupling and rebound, the direct effects of the tearing event.

Surface volcanism and tectonics demonstrate that the effects of the development of slab tears is transmitted to the overlying crust. OIB-type volcanism, trending NW-SE, from the Island of Ustica to Etna volcano by way of the Prometeo submarine lava field offers strong support for the existence of up-welling asthenospheric flow at the southern tear of the subducting slab. Bathymetrically, the surface evidence of the southern tear is suggested to be the submarine alignment of the Eolo and Enarete volcanoes and the Sisifo ridge.
The northern edge of the Ionian slab is marked structurally by an extensive NW-SE-trending sinistral strike-slip fault system that runs along the eastern Tyrrhenian submarine slope. To the south, the fault system ends abruptly at the western edge of the structurally controlled E-W Palinuro volcano alignment, which marks the northernmost limit of Aeolian arc volcanic activity.

REFERENCES

Abelson M. & Agnon A. (1997) - *Mechanics of oblique spreading and ridge segmentation*, Earth Planet. Sci. Lett., **148**: 405–421.

Beccaluva L., Rossi P., Rossi L., Serri G. (1982) - *Neogene to Recent volcanism of the southern Tyrrhenian-Sicilian area: Implications for the geodynamic evolution of the Calabrian arc*, Earth Evol. Sci., **3**: 222– 238.

Beccaluva L. *et alii* (1990) - *Geochemistry and mineralogy of volcanic rocks from ODP sites 650, 651, 655 and 654 in the Tyrrhenian Sea*, Proc. Ocean Drill. Program Sci. Results, **107**: 49–74.

Butler R.W.H., Grasso M. & Lickorish H. (1995) - *Plio-Quaternary megasequence geometry and its tectonic controls within the Maghrebian thrust belt of south-central Sicily*, Terra Nova, **7**: 171– 178.

Cimini G.B. (1999) - *P-wave velocity structure of the southern Tyrrhenian subduction zone from nonlinear teleseismic traveltime tomography*, Geophys. Res. Lett., **26**: 24, 3709– 3712.

Curzi P.V., Castellarin A., Vai G.B., Zitellini N., Selli R. & Sartori R. (2003) - *Una staffetta generazionale della Geologia Marina Italiana*. In: "*Extended Abstracts, Convegno in Memoria di Raimaondo Selli e Renzo Sartori. La Geologia del Mar Tirreno e degli Appennini*". Bologna, 11-12 Dec.

Della Vedova B., Pellis G., Foucher J.P. & Rehault J.P. (1984) - *Geothermal structure of the Tyrrhenian Sea*, Mar. Geol., **55**: 271–289.

Doglioni C., Mongelli F. & Pieri P. (1994) - *The Puglia uplift (SE Italy): An anomaly in the foreland of the Apennine subduction due to buckling of a thick continental lithosphere*, Tectonics, **13**: 1309– 1321.

Faggioni O., Pinna E., Savelli C. & Schreider A.A. (1995) - *Geomagnetism and age study of Tyrrhenian seamounts*, Geophys. J. Int., **123**: 915– 930.

Frepoli A., Selvaggi G., Chiarabba C. & Amato A. (1996) - *State of stress in the southern Tyrrhenian subduction zone from fault-plane solutions*, Geophys. J. Int., **125**: 879– 891.

Galadini F. (1999) - *Pleistocene changes in the central Apennine fault kinematics: A key to decipher active tectonics in central Italy*, Tectonics, **18**: 5, 877– 894.

Ghisetti, F. (1979a) - *Relazioni tra strutture e fasi trascorrenti e distensive lungo i sistemi Messina-Fiumefreddo, Tindari-Letojanni a Alia-Malvagna (Sicilia nord-orientale); uno studio microtettonico,* Geol. Roma, **18**: 23–58.

Ghisetti F. (1979b) - *Evoluzione neotettonica dei principali sistemi di faglie della Calabria centrale*, Boll. Soc. Geol. It., **98**: 387– 430.

Giardini D. & Velona' M. (1991) - *Deep siesmicity of the Tyrrhenian Sea*, Terra Nova, **3**: 57–64.

Gvirtzman Z. & Nur A. (1999) - *The formation of Mount Etna as the consequence of slab rollback*, Nature, **401**: 782– 785.

Hippolyte J.C., Angelier J. & Roure F. (1994) - *A major geodynamic change revealed by Quaternary stress patterns in the southern Apennines (Italy),* Tectonophysics, **230**: 199– 210.

Hooft E.E.E & Detrick R.S. (1995) - *Relationship between axial morphology, crustal thickness and mantle temperature along the Juan de Fuca and Gorda Ridges*, J. Geophys. Res., **100** (22): 499-508.

Jolivet L. (1991) - *Extension of thickened continental crust, from brittle to ductile deformation: Examples from Alpine Corsica and Aegean Sea*, Ann. Geofis., **36**: 139– 153.

Kastens K.A. *et alii* (1988) - *ODP Leg 107 in the Tyrrhenian Sea: Insight into passive margin and backarc basin evolution*, Geol. Soc. Am. Bull., **100**: 1140–1156.

Kastens K.A. *et alii* (1990) - *The geological evolution of the Tyrrhenian Sea: An introduction to the scientific results of ODP Leg 107*, Proc. Ocean Drill. Program Sci, Results, **107**: 3– 26.

Lentini F., Carbone S., Catalano S., Di Stefano A., Garagano C., Romeo M., Straluzza S. & Vinci G. (1995) - *Sedimentary evolution of basins in mobile belts: Examples from the Tertiary terrigenous sequences of the Peloritani mountains (NE Sicily),* Terra Nova, **7**: 161– 170.

Lucente F.P., Chiarabba C. & Cimini G.B. (1999) - *Tomographic constraints on the geodynamic evolution of the Italian region*, J. Geophys. Res., **104** (20): 307–327.

Macdonald K.C. (1998) - *Linkages between faulting, volcanism, hydrothermal activity and segmentation on fast spreading centers*, In W. R. Buck *et alii* (Eds.): "*Faulting and magmatism at Mid-Ocean Ridges"*, Geophys. Monogr. Ser., vol. 106, pp. 27– 58, AGU, Washington, D. C..

Macdonald K.C., Scheirer D.S. & Carbotte S.M. (1991) - *Mid-ocean ridges: Discontunuities, segments and giant cracks*, Science, **253**: 986 – 994.

Macdonald K.C. *et alii* (1992) - *The East Pacific Rise and its flanks 8_–18_N: History of segmentation, propagation and spreading direction based on SeaMARK and Sea Beam studies*, Mar. Geophys. Res., **14**: 299–344.

Magde L.S. & Smith D.K. (1995) - *Seamount volcanism at the Reykjanes Ridge: Relationship to the Iceland hot spot,* J. Geophys. Res., **100**: 8449–8468.

Marani M.P., Gamberi F., Casoni L., Carrara G., Landuzzi V., Musacchio M., Penitenti D., Rossi L. & Trua T. (1999) - *New rock and hydrothermal samples from the southern Tyrrhenian sea: The MAR-98 research cruise*, Giorn. Geol., **61**: 3– 24.

MARANI M.P. & TRUA T. (2002) - *Thermal constriction and slab tearing at the origin of a superinflated spreading ridge: (Marsili volcano (Tyrrhenian Sea)*, J. Geophys. Res., **107**: B9, 2188, doi:10.1029/2001JB000285.

MARIUCCI M.T., AMATO A. & MONTONE P. (1999) - *Recent tectonic evolution and present stress in the Northern Apennines (Italy)*, Tectonics, **18**: 108– 118.

MAZZUOLI R., TORTORICI L. & VENTURA G. (1995) - *Oblique rifting in Salina, Lipari and Vulcano Islands (Aeolian Islands, southern Italy)*, Terra Nova, **7**: 444–452.

MELE G. (1998) - *High-frequency wave propagation from mantle earthquakes in the Tyrrhenian Sea: New contraints for the geometry of the south Tyrrhenain subduction zone*, Geophys. Res. Lett., **25**: 2877– 2880.

MELE G., ROVELLI A., SEBER D. & BARANZAGI M. (1997) - *Shear wave attenuation in the lithosphere beneath Italy and surrounding regions: Tectonic implications*, J. Geophys. Res., **102** (11): 863–875.

MONGELLI F. *et alii (*1992) - *Geothermal regime in Italy*, In: HURTIG E. *et alii* (Eds.): "*Geothermal Atlas of Europe"*, pp. 54– 99, Herman Haak, Gotha, Germany.

MONTONE P., AMATO A., FREPOLI A., MARIUCCI M.T. & CESARO M. (1997) - Crustal stress regime in Italy, Ann. Geofis., **40**: 3, 741–758.

MURTON B.J. & PARSON L.M. (1993) - *Segmentation, volcanism and deformation of oblique spreading centers: A quantitative study of the Reykjanes Ridge*, Tectonophysics, **222**: 237– 257.

MUSACCHIO M., CARRARRA G., GAMBERI F. & MARANI M. (1999) - *Tectonic setting of the eastern Tyrrhenian margin*, Geoitalia, 2 Forum It. Sci. Terra, Riassunti, **1**: 184–185.

NICOLICH R. (1989) - *Crustal structure from seismic studies in the frame of the European Geotraverse (southern segment) and CROP projects*. In BORIANI A. *et alii* "*The Lithosphere in Italy"*, pp. 41 – 62, Accad. Naz. Lincei, Rome.

PATACCA E., SARTORI R. & SCANDONE P.(1990) - *Tyrrhenian and Apenninic arcs: Kinematic relations since Late Tortonian times*, Mem. Soc. Geol. It., **45**: 425–451.

ROBERTSON A.H.F. & GRASSO M. (1995) - *Overview of the late Tertiary-Recent tectonic and palaeo-environmental development of the Mediterranean region*, Terra Nova, **7**: 114–127.

SARTORI R. (1990) - *The main results of ODP Leg 107 in the frame of Neogene to Recent geology of peri-Tyrrhenian areas*, Proc. Ocean Drill. Program Sci. Results, **107**: 715– 730.

SAVELLI C. & SCHRIEDER A.A. (1991) - *The opening processes in the deep Tyrrhenian basins of Marsili and Vavilov, as deduced from magnetic and chronological evidence of their igneous crust*, Tectonophysics, **189**: 1– 13.

SCARASCIA S., LOZEJ A. & CASSINIS R. (1994) - *Crustal structures of the Ligurian, Tyrrhenian and Ionian Seas and adjacent onshore areas interpreted from wide-angle seismic profiles*, Boll. Geof. Teor. Appl., **36**(141– 144): 4– 19.

SELLI R., LUCCHINI F., ROSSI P. L., SAVELLI C. & DEL MONTE M. (1977) - *Dati geologici, petrochimici e radiometrici sui vulcani centro-tirrenici*, Gion. Geol., **42**: 221– 246.

SELVAGGI G. & CHIARABBA C. (1995) - *Seismicity and P-wave velocity image of the southern Tyrrhenian subduction zone*, Geophys. J. Int., **121**: 818– 826.

SEMPE´RE´ J.C., BLONDEL P., BRIAIS A., FUJIWARA T., GE´LI L., ISEZAKI N., PARISO J. E., PARSON L., PATRIAT P. & ROMMEVAUX C. (1995) - *The Mid-Atlantic Ridge between 29_N and 31_ 30'N in the last 10 Ma*, Earth Planet. Sci. Lett., **130**: 45– 55.

SERRI G. (1997) - *Neogene-Quaternary magmatic activity and its geodynamic implications in the central Mediterranean region*, Ann. Geophys., **40**: 681– 703.

SMITH D.K., HUMPHRIS S.E. & BRYAN W.B. (1995) - *A comparison of volcanic edifices at the Reykjanes Ridge and the Mid-Atlantic Ridge at 24_– 30_N,* J. Geophys. Res., **100** (22): 485–498.

SUHALDOC P. & PANZA G.F. (1989) - Physical properties of the lithosphere-asthenosphere system in Europe from geophysical data, in The Lithosphere in Italy, edited by A. Boriani *et alii*, pp. 15–40, Accad. Naz. Lincei, Rome.

TORTORICI L., COCINA O., MONACO C. & TANSI C. (1993) - *Recent and active tectonics of the Calabrian Arc*, Terra Abstr., **5**: 270.

TRUA T., SERRI G., RENZULLI A., MARANI M. & GAMBERI F. (2002) - *Volcanological and petrological evolution of Marsili seamount (southern Tyrrhenian Sea)*, J. Volcanol. Geotherm. Res., **114**: 441– 464.

TRUA T., SERRI G., MARANI M.P. (2003) - Lateral flow of African mantle below the nearby Tyrrhenian plate: geochemical evidence, Terra Nova, 15, 6, 433-440.

WESTAWAY R. (1993) - *Quaternary uplift of southern Italy*, J. Geophys. Res., **98** (21): 741–772.

Included to: **Memorie Descrittive della Carta Geologica d'Italia, vol. XLIV**

PLATE 1

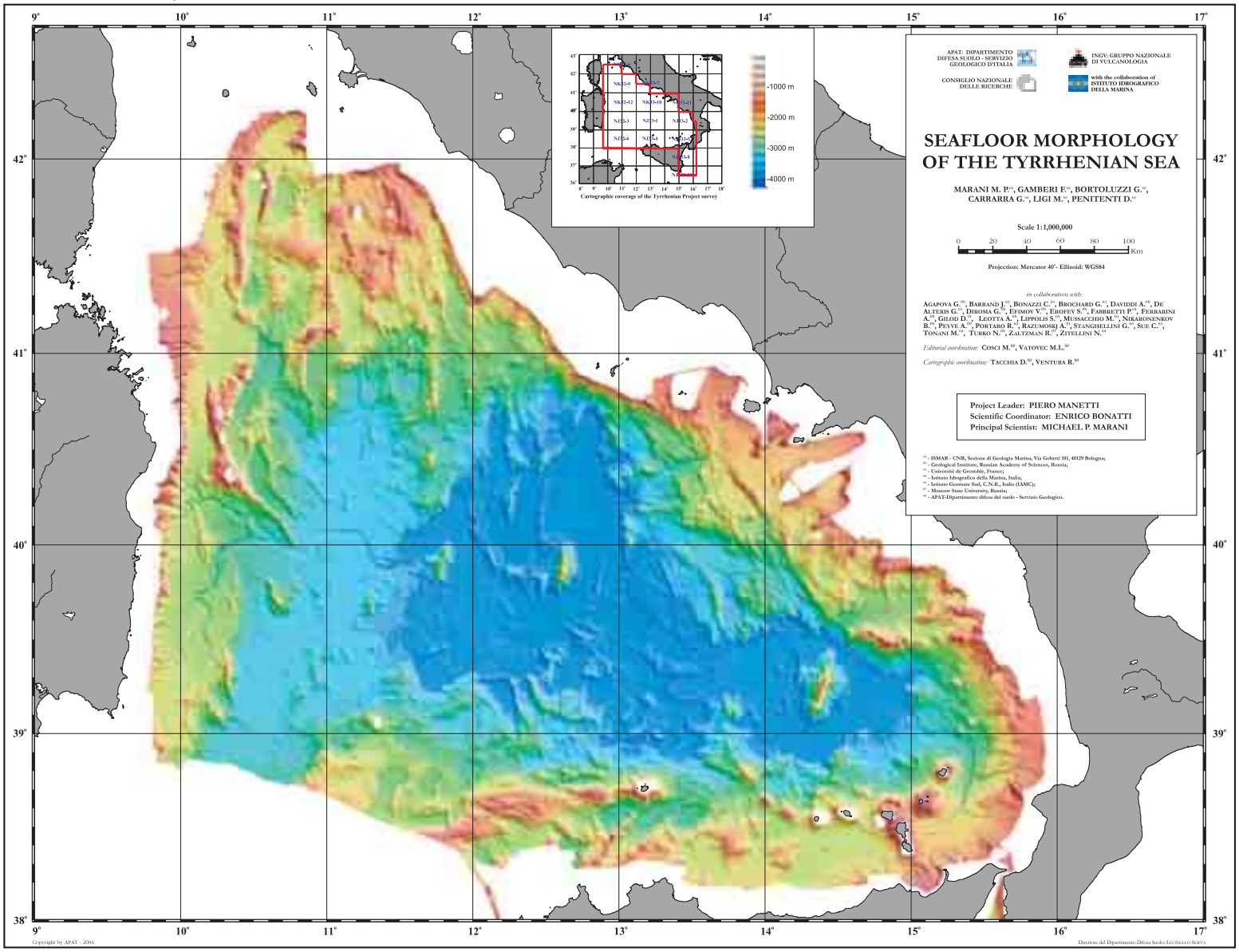

Direttore del Dipartimento Difesa Suolo LEONELLO SERVA

Included to: **Memorie Descrittive della Carta Geologica d'Italia, vol. XLIV**

PLATE 2

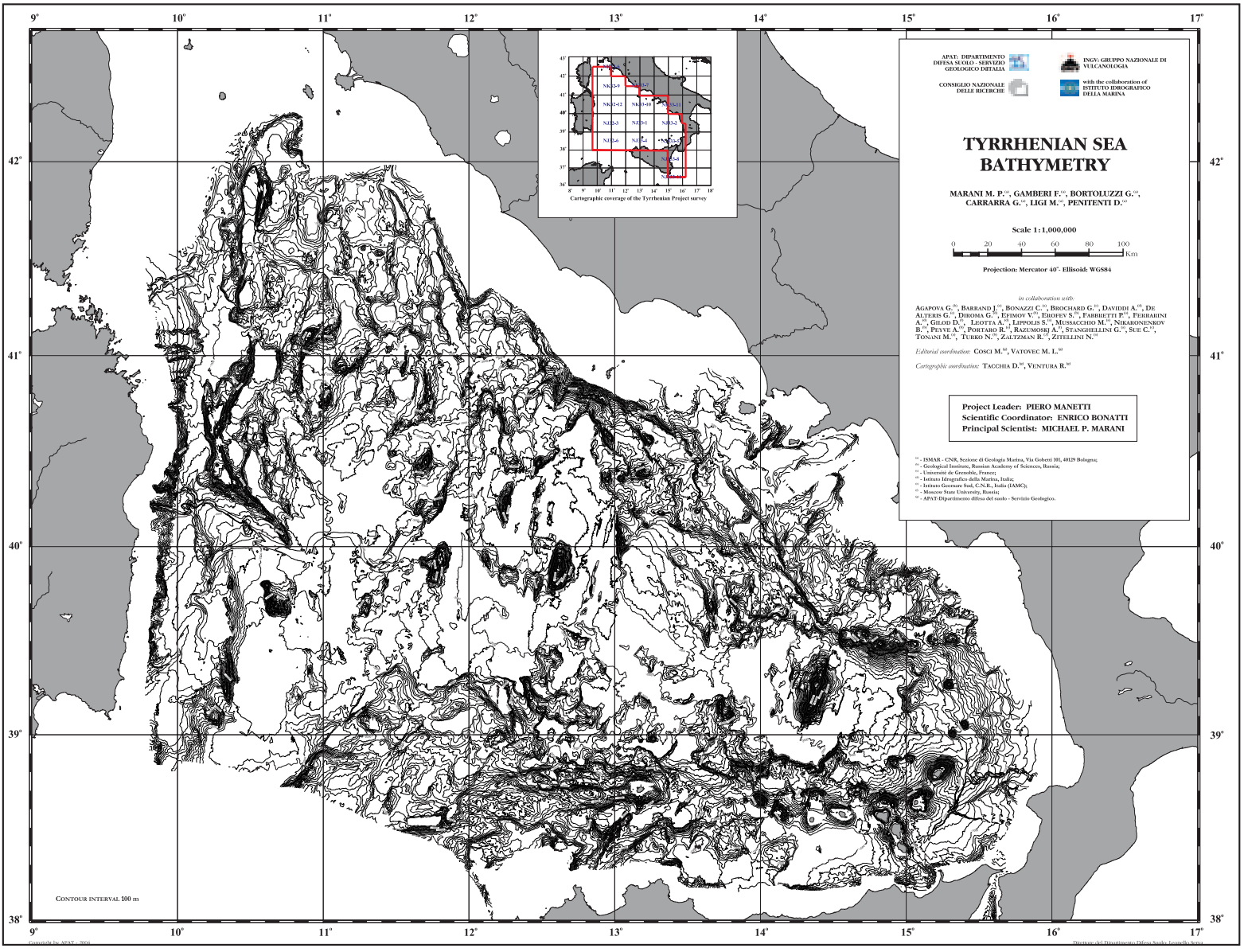

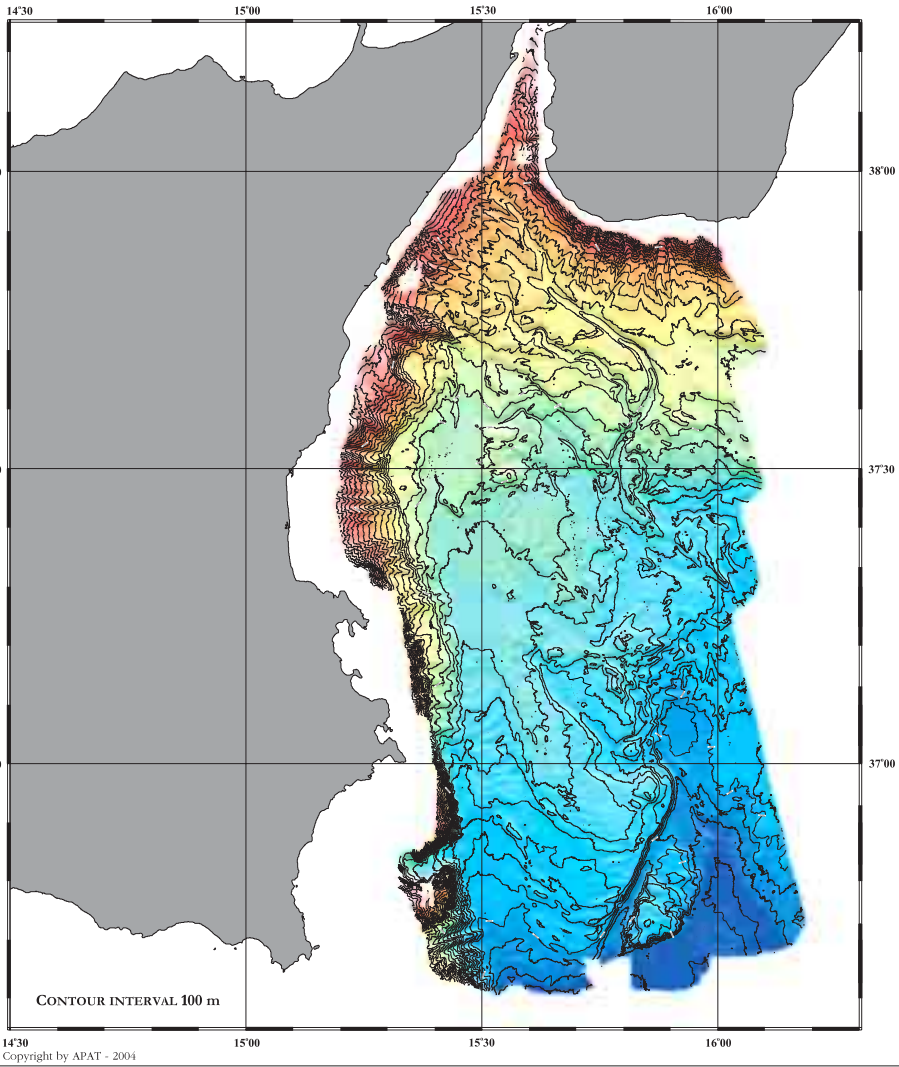

APAT: DIPARTIMENTO DIFESA SUOLO - SERVIZIO GEOLOGICO D'ITALIA

CONSIGLIO NAZIONALE DELLE RICERCHE

INGV: GRUPPO NAZIONALE DI VULCANOLOGIA

with the collaboration of ISTITUTO IDROGRAFICO DELLA MARINA

SEAFLOOR BATHYMETRY OF THE IONIAN SEA

MARANI M. P.[a], GAMBERI F.[a], BORTOLUZZI G.[a], CARRARRA G.[a], LIGI M.[a], PENITENTI D.[a]

0 10 20 30 40 50 Km

Projection: Mercator 38°- Ellisoid: WGS84

in collaboration with:

AGAPOVA G.[b], BARRAND J.[c], BONAZZI C.[c], BROCHARD G.[c], DAVIDDI A.[d], DE ALTERIS G.[e], DIROMA G.[d], EFIMOV V.[b], EROFEV S.[b], FABBRETTI P.[e], FERRARINI A.[e], GILOD D.[f], LEOTTA A.[d], LIPPOLIS S.[e], MUSSACCHIO M.[e], NIKARONENKOV B.[b], PEYVE A.[b], PORTARO R.[e], RAZUMOSKJ A.[f], STANGHELLINI G.[e], SUE C.[c], TONANI M.[e], TURKO N.[b], ZALTZMAN R.[f], ZITELLINI N.[e]

Editorial coordination: **Cosci M.[g], Vatovec M. L.[g]**

Cartographic coordination: **Tacchia D.[g], Ventura R.[g]**

Project Leader: PIERO MANETTI
Scientific Coordinator: ENRICO BONATTI
Principal Scientist: MICHAEL P. MARANI

[a] - ISMAR - CNR, Sezione di Geologia Marina, Via Gobetti 101, 40129 Bologna;
[b] - Geological Institute, Russian Academy of Sciences, Russia;
[c] - Université de Grenoble, France;
[d] - Istituto Idrografico della Marina, Italia;
[e] - Istituto Geomare Sud, C.N.R., Italia (IAMC);
[f] - Moscow State University, Russia;
[g] - APAT-Dipartimento difesa del suolo - Servizio Geologico.

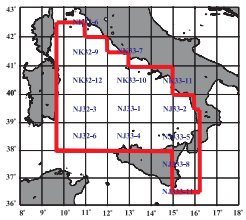

Cartographic coverage of the Tyrrhenian Project survey

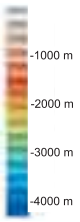

Direttore del Dipartimento Difesa Suolo: Leonello Serva

Included to: **Memorie Descrittive della Carta Geologica d'Italia, vol. XLIV**

FREE AIR ANOMALY OF THE NORTHERN TYRRHENIAN SEA

PLATE 4

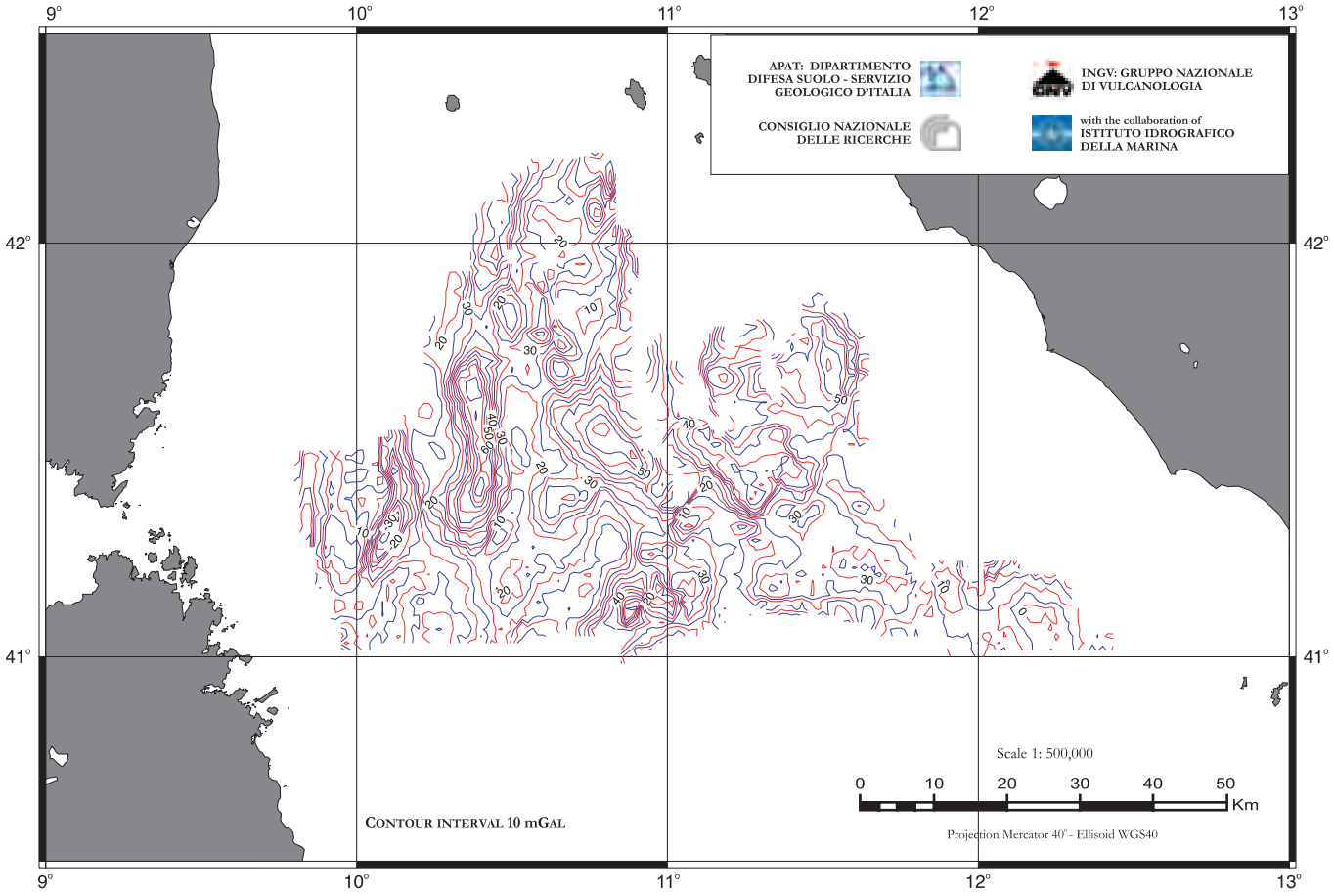

MARANI M. P.(*), GAMBERI F.(*), BORTOLUZZI G.(*), CARRARRA G.(*), LIGI M.(*), PENITENTI D.(*)

(*) - ISMAR - CNR, Sezione di Geologia Marina, Via Gobetti 101, 40129 Bologna.

Direttore del Dipartimento Difesa Suolo: LEONELLO SERVA